

**N A S A T E C H N I C A L
R E P O R T**



NASA TR R-364

C.1

NASA TR R-364

**LOAN COPY: RETURN
AFWL (DOLL)
KIRTLAND AFB, N.**



**GENERAL THEORY OF WALL INTERFERENCE
FOR STATIC STABILITY TESTS
IN CLOSED RECTANGULAR TEST SECTIONS
AND IN GROUND EFFECT**

by Harry H. Heyson

Langley Research Center

Hampton, Va. 23365

NATIONAL AERONAUTICS AND SPACE ADMINISTRATION • WASHINGTON, D. C. • SEPTEMBER 1971



0068446

1. Report No. NASA TR R-364		2. Government Accession No.		3. Recipient's Catalog No.	
4. Title and Subtitle GENERAL THEORY OF WALL INTERFERENCE FOR STATIC STABILITY TESTS IN CLOSED RECTANGULAR TEST SECTIONS AND IN GROUND EFFECT				5. Report Date September 1971	
7. Author(s) Harry H. Heyson				6. Performing Organization Code	
9. Performing Organization Name and Address NASA Langley Research Center Hampton, Va. 23365				8. Performing Organization Report No. L-7549	
12. Sponsoring Agency Name and Address National Aeronautics and Space Administration Washington, D.C. 20546				10. Work Unit No. 760-72-01-05	
15. Supplementary Notes				11. Contract or Grant No.	
16. Abstract A theory is developed which predicts the interference velocities and interference velocity gradients caused by the walls of the tunnel. Large wake deflections are allowed in both the lateral and vertical directions. The theory includes V/STOL and conventional wall-interference theories and ground effect as special cases. Symmetry and interchange relationships between the interference factors are developed and extensive numerical results are presented. Use of the interference factors to correct data depends upon the availability of detailed aerodynamic treatments in nonuniform flow of the model under test. In most tests the available aerodynamic treatments will be found either inadequate or too time consuming for rigorous routine correction of data relating to lateral-directional stability.				13. Type of Report and Period Covered Technical Report	
17. Key Words (Suggested by Author(s)) Static stability tests Wind-tunnel corrections Ground effect				14. Sponsoring Agency Code	
18. Distribution Statement Unclassified - Unlimited					
19. Security Classif. (of this report) Unclassified		20. Security Classif. (of this page) Unclassified		21. No. of Pages 331	
				22. Price* \$6.00	

CONTENTS

	Page
SUMMARY	1
INTRODUCTION	1
SYMBOLS	4
THEORY	8
Momentum Considerations	8
Effective Skew Angles	11
Wake in Free Air	12
Wake in the Wind Tunnel	17
Interference in Case I: Wake Strikes Floor First	18
Interference in Case II: Wake Strikes Wall First	25
Interference in Ground Effect	30
Computer Program	32
Symmetry of Interference Factors	35
Interchange Equivalences	36
APPLICATION OF RESULTS	39
Interference Velocities	40
Interference Gradients	47
NUMERICAL RESULTS	52
Interference at Model	52
Distribution of Interference Factors Over the Principal Axes	53
Effect of Finite Span	55
CONCLUDING REMARKS	57
APPENDIX A – PARTIAL DERIVATIVES OF $\frac{A}{h}$	58
General Case	58
Special Case of $\chi_V = 90^\circ$	60
Special Case of $\chi_H = 90^\circ$	62
Special Case of $\chi_H = \chi_V = 90^\circ$	63
APPENDIX B – PARTIAL DERIVATIVES OF $\frac{A'}{h}$	64
General Case	64
Special Case of $\chi_V = 90^\circ$	64
APPENDIX C – INTERFERENCES AND INTERFERENCE DERIVATIVES AT THE CENTER OF THE LIFTING SYSTEM IN GROUND EFFECT	65
Notation	65

	Page
Method of Derivation	65
Interference Factors for Velocities Caused by Forces in the X-Direction	65
Interference Factors for Velocities Caused by Forces in the Y-Direction	67
Interference Factors for Velocities Caused by Forces in the Z-Direction	68
Interference Factors for the Derivatives of the Velocities Caused by Forces in the X-Direction	69
Interference Factors for the Derivatives of the Velocities Caused by Forces in the Y-Direction	73
Interference Factors for the Derivatives of the Velocities Caused by Forces in the Z-direction	75
APPENDIX D – FORTRAN PROGRAM TO CALCULATE THE INTERFERENCE FACTORS FOR STABILITY TESTS OF A VANISHINGLY SMALL MODEL IN A CLOSED RECTANGULAR TEST SECTION	
	79
APPENDIX E – FLOW CHART FOR FORTRAN PROGRAM OF APPENDIX D	92
REFERENCES	100
TABLES	102
FIGURES	107

GENERAL THEORY OF WALL INTERFERENCE
FOR STATIC STABILITY TESTS IN CLOSED RECTANGULAR
TEST SECTIONS AND IN GROUND EFFECT

By Harry H. Heyson
Langley Research Center

SUMMARY

A theory is developed which predicts the interference velocities and interference velocity gradients caused by the walls of the tunnel. Large wake deflections are allowed in both the lateral and vertical directions. The theory includes V/STOL and conventional wall-interference theories and ground effect as special cases. Symmetry and interchange relationships between the interference factors are developed, and extensive numerical results are presented.

Use of the interference factors to correct data depends upon the availability of detailed aerodynamic treatment in nonuniform flow of the model under test. In most tests the available aerodynamic treatments will be found either inadequate or too time consuming for rigorous routine correction of data relating to lateral-directional stability.

INTRODUCTION

Reference 1 presents a review (published in 1966) of the status of subsonic wall-interference theory. In addition, reference 2 presents a similar review of wall-interference theory as it pertains to models with highly deflected wakes. In general, these reviews find that existing theory is reasonably adequate when used to determine the effect of the walls upon the overall performance of the model. Corrections to longitudinal stability measurements, obtained by calculating the interference at the tail of the model and by examining the gradients of interference over the wing chord, are somewhat less satisfactorily verified. However, provided that the model is reasonably small, generally satisfactory results can be obtained for longitudinal stability tests as well, provided that considerable care is exercised not only in the wall-interference calculations but also in correcting for nonuniformities in the distribution of flow angularities within the basic wind-tunnel flow.

Theoretical treatment of wall interference as applied to lateral-directional stability testing is essentially nonexistent. In a few cases, the asymmetries generated by yawing

a finite wing have been noted by reference 1 to be significant; however, the effect of the side forces generated by the asymmetric model are not considered in the available treatments.

A complete wall-interference theory including lateral-directional stability tests must consider a number of features. First, since the model is asymmetrically disposed in the tunnel, side forces will be present. These side forces will be influenced by the walls and will result in interference velocities just as do the lift and drag forces. Secondly, since lateral-directional testing primarily constitutes a study of the moments rather than the forces on the model, and since it is primarily the gradients of the interference velocities which affect moments, it is necessary to examine all of the possible interference gradients in the tunnel. Observe that the mutual consideration of the above two features is a major complication, since, in order to consider all of the possible wall influences, it becomes necessary to examine the interference velocities in the orthogonal directions as caused individually by forces in these three directions for a total of nine interference velocities, as well as the gradients of these nine interference velocities along each of the three coordinates for a total of 27 interference velocity gradients. Finally, since modern aircraft developments have resulted in the need to test many types capable of extraordinarily large wake deflections, it is desirable to examine the effect of these wake deflections, both vertically and laterally, on the resultant interference factors. That such effects may be large has already been demonstrated by the more limited analyses presented in references 3 to 8.

The present paper presents an analysis which considers all of the foregoing features. In the basic theoretical treatment, the model is assumed to be vanishingly small and located at an arbitrary point within the tunnel test section, and the interference velocities and their gradients are obtained at an equally arbitrary point within the test section. The wake, which actually follows a curved path from the model to infinity downstream in the tunnel, is linearized to consist of a series of straight-line segments which follow approximately the same path. Except for modifications to allow for side forces and for a lateral wake deflection, this wake is essentially the same as that used in references 5 and 6.

The assumption that the model is vanishingly small is less restrictive than appears on the surface. Linear superposition of the results may be used to obtain the appropriate interferences for models of arbitrary size or configuration just as in references 6 and 7. A few sample calculations of this nature are included in the present paper.

In the application of the present theory it is necessary to estimate the wake deflection angles with respect to the tunnel axes. The momentum analysis presented originally in reference 9 is not adequate in the present case because that paper did not consider the possibility of side forces with respect to the coordinate system. The necessary modifications to the theory of reference 9 are derived herein. Furthermore, references 10 and 11

have already noted that it is necessary to modify the wake angles as computed by momentum theory in order to account for wake rollup. A few remarks on useful approximations to the rolled up wake deflection angles are also included.

As presented herein, the theory pertains specifically only to completely closed rectangular wind tunnels. Formal extension to completely open or to closed-on-bottom-only test sections, as in reference 5, is simple. However, it should be observed that the derivation of the usual boundary condition imposed at an open boundary depends upon the use of small perturbation assumptions (ref. 12). If the wake actually impinges upon an open boundary, these assumptions may be severely violated (refs. 3 and 5). Under such conditions the theoretically obtained interference velocities may be grossly in error. It is recommended that such extension should only be attempted with great caution both in the theoretical treatment and in the application of the results to the correction of wind-tunnel data.

Similar concern must be observed when attempting to correct data from closed test sections if the wake deflections are sufficiently great. It was first shown experimentally (refs. 13 and 14) and later theoretically (refs. 8 and 11) that sufficiently large wake deflections can result in such enormous alterations of the flow within the test section that the measured data no longer represent any free-air flight condition (although under certain circumstances they may approximate flight in ground effect (ref. 8)). Reasonably satisfactory correlations of the conditions under which these effects limit testing (ref. 2) have been obtained for tests which involve essentially no lateral wake deflection. The equivalent limiting conditions for wakes with large horizontal as well as vertical deflections are completely unexplored.

The effect of wall interference on the measured data will differ for different models according to the sensitivity of the model characteristics to particular interference velocities or velocity gradients. The corrections to data can be no better than the investigator's ability to calculate the effect of these velocities and velocity gradients on the model characteristics. For some classes of models, particularly many V/STOL types, there is an inadequate theoretical background with which to calculate corrections. For other types of models, theoretical means for these calculations may exist but be too lengthy for practical application to large masses of data. An exploration of actual correction formulas would involve almost all known aerodynamics and is obviously beyond the scope of any one paper or any one author. No such complete treatment is intended herein. Instead, a few remarks on the treatment of wall effects as a problem in similitude are included in the hope that this discussion will point out sources of information presently available for approximate data corrections.

SYMBOLS

In order to arrive at a set of consistent axes and signs in the present analysis, it has been necessary to define certain quantities in a manner in conflict with many stability analyses. The reader is cautioned to consider carefully the definitions, particularly of positive directions, and provide for suitable conversion to his desired standard.

$$A = h \left[R_O C_{HV} - \left(\xi \frac{x}{H} \right) \sin \chi_H \sin \chi_V + \left(\xi \frac{y}{H} \right) \sin \chi_V \cos \chi_H + \left(\xi \frac{z}{H} \right) \sin \chi_H \cos \chi_V \right]$$

$$A' = h \left[R_O C_{HV} - \left(\xi \frac{x}{H} \right) \sin \chi_H \sin \chi_V - \left(\xi \frac{y}{H} \right) \sin \chi_V \cos \chi_H + \left(\xi \frac{z}{H} \right) \sin \chi_H \cos \chi_V \right]$$

A_G reference area in ground effect, $4h^2$

A_m momentum area of lifting system

A_T wind-tunnel cross-sectional area, $4BH$

a_i functions relating length along the wake to the generalized coordinates x_i
(see eqs. (22) to (25))

B semiwidth of wind tunnel

b lateral distance from origin of doublet wake to right-hand (viewed from behind) sidewall of wind tunnel

C_D drag coefficient, $\frac{D}{qS}$

$$C_{HV} = \sqrt{1 - \cos^2 \chi_H \cos^2 \chi_V}$$

C_L lift coefficient, $\frac{L}{qS}$

C_l rolling-moment coefficient, positive when moment tends to roll aircraft to left, $\frac{\text{Rolling moment}}{qS\bar{c}}$

C_m pitching-moment coefficient, positive when moment tends to pitch aircraft nose up, $\frac{\text{Pitching moment}}{qS\bar{c}}$

C_n yawing-moment coefficient, positive when moment tends to yaw aircraft nose left, $\frac{\text{Yawing moment}}{qS\bar{c}}$

\overline{C}_R	resultant-force coefficient, $\frac{\overline{R}}{qS}$
C_Y	lateral-force coefficient, positive along Y-axis, $\frac{Y}{qS}$
C_μ	jet-momentum coefficient, $\frac{\text{Momentum}}{qS}$
\bar{c}	mean aerodynamic chord, or equivalent dimension for nondimensionalizing moments
c_H	$\cos \chi_H$
c_V	$\cos \chi_V$
D	drag, force directed along X-axis
D_i	induced drag, induced force directed along X-axis
H	semiheight of wind tunnel
h	height of model above floor of wind tunnel (or ground)
L	lift
l	distance from origin along wake
m,n,p,q,r	integers
m_i	doublet strength for doublets with axes directed along the i-axis
n	ratio of final to initial induced velocities in wake
q	dynamic pressure, $\frac{1}{2}\rho V^2$
q_t	dynamic pressure at tail
\overline{R}	resultant force
R_O	nondimensional radius to origin, $\sqrt{\left(\xi \frac{x}{H}\right)^2 + \left(\xi \frac{y}{H}\right)^2 + \left(\xi \frac{z}{H}\right)^2}$

S	wing area, or equivalent area for nondimensionalizing forces and moments
s	wing semispan
s_H	$\sin \chi_H$
s_V	$\sin \chi_V$
u, v, w	induced velocities along the X-, Y-, and Z-axes, respectively
u_0, v_0, w_0	mean, or momentum theory, values of induced velocities at the lifting system
V	forward velocity
V_R	resultant velocity
w_h	reference velocity, vertical induced velocity which lifting system would have if it could hover with momentum area A_m , $w_h = -\sqrt{\frac{L}{n\rho A_m}}$
X, Y, Z	Cartesian coordinates, X-axis positive rearward, Y-axis positive to right when viewed from behind, Z-axis positive upward. Unless otherwise noted, the origin is centered in the lifting system of the model.
x, y, z	location of a point with respect to the X-, Y-, and Z-axes, respectively
$\hat{x}, \hat{y}, \hat{z}$	location of a point on the wake with respect to the X-, Y-, and Z-axes, respectively
$\left. \begin{matrix} x_i, x_j, x_k \\ \hat{x}_i, \hat{x}_j, \hat{x}_k \end{matrix} \right\}$	generalized coordinates where i, j , and k may independently take on the values x, y, z (Note, for example, that $x_x = x$, $x_y = y$, and $x_z = z$.)
Y	lateral force
α	angle of attack, positive nose upward
β	sideslip angle

γ	ratio of wind-tunnel width to wind-tunnel height, $\frac{B}{H}$
δ	interference factor (in general terms)
$\delta_{i,j}$	interference factor for finding the interference velocity in the j-direction caused by forces in the i-direction, defined by $\Delta\varphi_{i,j} = \delta_{i,j} \frac{A_m}{A_T} v_i$
$\delta_{i,j,k}$	interference factor for finding the rate of change per semiheight in the k-direction of the interference velocity in the j-direction caused by forces in the i-direction, defined by $\Delta\varphi_{i,j,k} = \delta_{i,j,k} \frac{A_m}{A_T} v_i$
ζ	ratio of wind-tunnel semiheight to height of model lifting system above the floor of the wind tunnel
η	ratio of distance between origin of wake and right-hand (as viewed from behind) sidewall of the wind tunnel to the semiwidth of the wind tunnel, $\frac{b}{B}$
$\dot{\theta}$	rate of pitch, positive nose upward, rad/sec
Λ	wing sweep angle, measured positive rearward from lateral axis of aircraft, deg
μ	helicopter tip-speed ratio, $\frac{V \cos \alpha}{\text{tip speed}}$
v_i	generalized mean induced velocities at lifting system, u_0 when $i = x$, v_0 when $i = y$, w_0 when $i = z$
ρ	mass density of air or other test medium in the wind tunnel
σ	ratio of wingspan to tunnel width, $\frac{s}{B}$
$\Phi_{i,j}$	function related to induced velocity in the j-direction caused by forces in the i-direction
$\Phi_{i,j,k}$	function related to the rate of change in the k-direction of the induced velocity in the j-direction caused by forces in the i-direction
$\Phi'_{i,j}$	$\Phi_{i,j}$ for a mirror-image wake

$\Phi'_{i,j,k}$	$\Phi_{i,j,k}$ for a mirror-image wake
φ_i	potential of wake as produced by forces in the i-direction
$\varphi_{i,j}$	induced velocity in the j-direction as caused by forces in the i-direction
$\varphi_{i,j,k}$	rate of change in the k-direction of the induced velocity in the j-direction as caused by forces in the i-direction
χ_H	horizontal wake skew angle, angle measured positive rearward from the negative Y-axis to the projection of the wake on the X-Y plane
χ_V	vertical wake skew angle, angle measured positive rearward from the negative Z-axis to the projection of the wake on the X-Y plane
ψ	yaw angle, measured positive nose right when viewed from behind
Prefix:	
Δ	change in value caused by boundary interference
Subscripts:	
c	value corrected for boundary interference
M	value from momentum theory
i,j, or k	indices which may independently take on the value x, y, or z, denoting the major axis parallel to which a dimension, force, velocity, or velocity gradient is to be measured.

THEORY

Momentum Considerations

Certain quantities, upon which the interferences will be found to depend, may be found from momentum considerations. The present analysis parallels that of reference 9.

Consider a force-producing system, acting upon the fluid flowing through an area A_m and producing lift, induced drag, and Y-force components, as sketched in figure 1.

Since force is equal to the time rate of change of momentum

$$L = \rho A_m V_R (-nw_o) \quad (1)$$

$$D_i = \rho A_m V_R (-nu_o) \quad (2)$$

$$Y = \rho A_m V_R (-nv_o) \quad (3)$$

where

$$V_R = \sqrt{(V + u_o)^2 + v_o^2 + w_o^2} \quad (4)$$

Dividing equations (2) and (3) by equation (1) yields

$$\frac{D_i}{L} = \frac{u_o}{w_o} \quad (5)$$

$$\frac{Y}{L} = \frac{v_o}{w_o} \quad (6)$$

Expanding equation (4) and substituting equations (5) and (6) into it yields

$$\begin{aligned} V_R &= \sqrt{V^2 + 2V \frac{D_i}{L} w_o + \left(\frac{D_i}{L}\right)^2 w_o^2 + \left(\frac{Y}{L}\right)^2 w_o^2 + w_o^2} \\ &= \sqrt{V^2 + 2V \frac{D_i}{L} w_o + \left[\left(\frac{D_i}{L}\right)^2 + \left(\frac{Y}{L}\right)^2 + 1\right] w_o^2} \end{aligned} \quad (7)$$

Dividing both sides by $-w_o$

$$\frac{V_R}{-w_o} = \sqrt{\left(\frac{V}{-w_o}\right)^2 - 2 \frac{D_i}{L} \left(\frac{V}{-w_o}\right) + \left[1 + \left(\frac{D_i}{L}\right)^2 + \left(\frac{Y}{L}\right)^2\right]} \quad (8)$$

From equation (1)

$$\begin{aligned} w_o &= \frac{-L}{n\rho A_m V_R} \\ w_o^2 &= \frac{-Lw_o}{n\rho A_m V_R} = \frac{L}{n\rho A_m \left(\frac{V_R}{-w_o}\right)} \end{aligned} \quad (9)$$

Now define w_h as the induced velocity w_o when $V = 0$, $D_i = 0$, and $Y = 0$; that is, w_h is the value of w_o in a purely hovering condition. From equation (1)

$$w_h = -\sqrt{\frac{L}{n\rho A_m}} \quad (10)$$

Divide equation (9) by the square of equation (10) to yield

$$\left(\frac{w_o}{w_h}\right)^2 = \frac{\frac{L}{n\rho A_m \left(\frac{V_R}{-w_o}\right)}}{\frac{L}{n\rho A_m}} = \frac{-w_o}{V_R} \quad (11)$$

or

$$\left(\frac{w_o}{w_h}\right)^4 = \frac{1}{1 + \left(\frac{Y}{L}\right)^2 + \left(\frac{V}{w_o} + \frac{D_i}{L}\right)^2} \quad (12)$$

which is best solved for w_o/w_h on digital computing machinery. The desired root is generally the smallest positive real root.

The vertical skew angle $(\chi_V)_M$, from figure 1, is seen to be

$$\tan(\chi_V)_M = \frac{V + u_o}{-w_o} = -\frac{V}{w_o} - \frac{D_i}{L} = -\left(\frac{V}{w_o} + \frac{D_i}{L}\right) \quad (13)$$

$$(\chi_V)_M = -\tan^{-1} \left(\frac{V}{w_o} + \frac{D_i}{L}\right) \quad (14)$$

where V/w_o may be obtained from w_o/w_h by means of the identity

$$\frac{V}{w_o} = \frac{V/w_h}{w_o/w_h} \quad (15)$$

The horizontal skew angle $(\chi_H)_M$ is similarly seen from figure 1 to be

$$\tan(\chi_H)_M = \frac{V + u_O}{-v_O} = -\frac{V}{v_O} - \frac{u_O}{v_O} = -\frac{w_O}{v_O} \left(\frac{V}{w_O} + \frac{u_O}{w_O} \right) = -\frac{\frac{V}{w_O} + \frac{u_O}{w_O}}{\frac{v_O}{w_O}} = -\frac{\frac{V}{w_O} + \frac{D_i}{L}}{\frac{Y}{L}} \quad (16)$$

$$(\chi_H)_M = -\tan^{-1} \left(\frac{\frac{V}{w_O} + \frac{D_i}{L}}{\frac{Y}{L}} \right) \quad (17)$$

or substituting equation (13) into equation (16)

$$\tan(\chi_H)_M = \frac{\tan(\chi_V)_M}{Y/L} \quad (18)$$

Observe from figure 1 that the wake passes downstream with no deflection whatever (as in classical theory) if χ_H and χ_V are both 90° . Note that the hovering case, where the wake must pass directly downward, is given by $\chi_V = 0^\circ$ and $\chi_H = 90^\circ$.

Effective Skew Angles

Reference 10 observes that the inclinations of the mass flow and of the vorticity in the wake differ because of wake rollup. From experimental observations of the wake of a rotor (ref. 15), it was concluded that the wake vorticity would be deflected downward by approximately one-half the deflection indicated by equations (17) and (18). Under this assumption, the effective wake skew angles would be given by

$$\chi_V = \frac{(\chi_V)_M + 90^\circ}{2} \quad (19)$$

$$\chi_H = \frac{(\chi_H)_M + 90^\circ}{2} \quad (20)$$

Equations (19) and (20) suffer from the obvious deficiency that the wake does not assume the proper skew angles in hovering. Reference 11 presents an alternate viewpoint which is more aesthetically pleasing in this regard. However, the practical limitations on very low speed testing (refs. 2, 8, 10, 11, 12, and 14) effectively limit tests to wake angles above which there would be any significant differences between equations (19) and (20) and the alternate form given in reference 11. The wake angles used in the following analysis are completely arbitrary and should be interpreted as being the effective wake angles, however obtained.

Wake in Free Air

The wake is assumed to be a straight line starting at the model and extending to infinity. It is skewed rearward from the vertical axis by an angle χ_V and skewed rearward from the horizontal axis by an angle χ_H (fig. 2). The wake is considered to consist of a string of point doublets whose axes make some constant arbitrary angles with the X-, Y-, and Z-axes.

Since, in the present linearized theory, the effect of the walls on the wake shape is neglected, it is permissible to choose doublets whose axes are parallel to the negative X-, Y-, and Z-axes only. Any arbitrary doublet inclination can then be obtained as a linear superposition of the above three cases.

The potential of a single doublet (fig. 2) of the infinite string comprising the wake caused by forces in the X_i -direction has its axis directed parallel to the negative X_i -axis. Thus, with respect to Cartesian coordinates centered in the point doublet, the potential is

$$d\phi_i = \frac{dm_i x_i}{\left[\sum_i (x_i^2) \right]^{3/2}} \quad (21)$$

The coordinates of the wake may be expressed as a set of parametric equations in l , the length along the wake, as

$$\hat{x} = \frac{\sin \chi_H \sin \chi_V}{\sqrt{1 - \cos^2 \chi_H \cos^2 \chi_V}} l \quad (22)$$

$$\hat{y} = \frac{-\sin \chi_V \cos \chi_H}{\sqrt{1 - \cos^2 \chi_H \cos^2 \chi_V}} l \quad (23)$$

$$\hat{z} = \frac{-\sin \chi_H \cos \chi_V}{\sqrt{1 - \cos^2 \chi_H \cos^2 \chi_V}} l \quad (24)$$

More generally, equations (22) to (24) may be rewritten as

$$\hat{x}_i = a_i l \quad (25)$$

where the a_i are defined implicitly by equations (22) to (24). It will be convenient in the

following derivation to note that $\sum_i (a_i^2) = 1$ since along the wake $l^2 = x^2 + y^2 + z^2$.

Now if the coordinate system of the entire wake is chosen to coincide with the origin of the wake, the wake potentials may be obtained by an integration over the entire length of the wake; that is

$$\varphi_i = -\frac{dm_i}{dl} \int_0^\infty \frac{(x_i - a_i l) dl}{\left\{ \sum_i \left[(x_i - a_i l)^2 \right] \right\}^{3/2}} = -\frac{dm_i}{dl} \int_0^\infty \frac{(x_i - a_i l) dl}{\left[\sum_i (x_i^2) - 2l \sum_i (a_i x_i) + l^2 \right]^{3/2}} \quad (26)$$

where the summations are considered to be carried out over the three values of i .

Equation (26) may be integrated immediately by the use of items 162 and 170 of reference 16 to yield

$$\varphi_i = -\frac{dm_i}{dl} \left(\frac{x_i \left[l - \sum_i (a_i x_i) \right] + a_i \left[-l \sum_i (a_i x_i) + \sum_i (x_i^2) \right]}{\left\{ \sum_i (x_i^2) - \left[\sum_i (a_i x_i) \right]^2 \right\} \sqrt{\sum_i (x_i^2) - 2l \sum_i (a_i x_i) + l^2}} \right) \Bigg|_0^\infty \quad (27)$$

After substituting limits and performing some algebraic simplification, equation (27) becomes

$$\varphi_i = -\frac{dm_i}{dl} \left\{ \frac{x_i - a_i \sqrt{\sum_i (x_i^2)}}{\left[\sqrt{\sum_i (x_i^2)} - \sum_i (a_i x_i) \right] \sqrt{\sum_i (x_i^2)}} \right\} \quad (28)$$

Equation (28) can be written in still more general form as

$$\varphi_i = -\frac{dm_i}{dl} \frac{\frac{\partial A}{\partial x_i}}{A} \quad (29a)$$

where

$$A = \sqrt{(x^2 + y^2 + z^2)(1 - \cos^2 \chi_H \cos^2 \chi_V)} \\ - x \sin \chi_H \sin \chi_V + y \sin \chi_V \cos \chi_H + z \sin \chi_H \cos \chi_V \quad (29b)$$

When the wake is not deflected sideways (that is, when $\chi_H = 90^\circ$ in fig. 2), equation (29) reduces identically to equation (7) of reference 5 for $x_i = x$, and to equation (1) of reference 5 for $x_i = z$. Thus, the theory presented in reference 5 will appear as a subset of the theory developed herein.

The induced velocity in the j -direction is then the partial derivative of equation (29) with respect to x_j , or

$$\frac{\partial \varphi_i}{\partial x_j} = \varphi_{i,j} = -\frac{dm_i}{d\ell} \left[\frac{\frac{\partial^2 A}{\partial x_i \partial x_j}}{A} - \frac{\left(\frac{\partial A}{\partial x_i} \right) \left(\frac{\partial A}{\partial x_j} \right)}{A^2} \right] \quad (30)$$

Similarly, the rate of change in the k -direction of the induced velocity in the j -direction is given by the partial derivative of equation (30) with respect to x_k , or

$$\begin{aligned} \frac{\partial \varphi_{i,j}}{\partial x_k} &= \varphi_{i,j,k} \\ &= -\frac{dm_i}{d\ell} \left[\frac{\frac{\partial^3 A}{\partial x_i \partial x_j \partial x_k}}{A} - \frac{\frac{\partial A}{\partial x_i} \left(\frac{\partial^2 A}{\partial x_j \partial x_k} \right) + \frac{\partial A}{\partial x_j} \left(\frac{\partial^2 A}{\partial x_i \partial x_k} \right) + \frac{\partial A}{\partial x_k} \left(\frac{\partial^2 A}{\partial x_i \partial x_j} \right)}{A^2} + 2 \frac{\left(\frac{\partial A}{\partial x_i} \right) \left(\frac{\partial A}{\partial x_j} \right) \left(\frac{\partial A}{\partial x_k} \right)}{A^3} \right] \end{aligned} \quad (31)$$

Now the values of $\frac{dm_i}{d\ell}$ are obtained, following reference 5, as

$$\frac{dm_i}{d\ell} = \frac{A_m}{2\pi} \nu_i \quad (32)$$

Further, it will, in general, be convenient to nondimensionalize the field points which appear in equations (30) and (31) with respect to $h = \frac{H}{\xi}$. Substituting equation (32) into equations (30) and (31) and performing the indicated nondimensionalization yields

$$\varphi_{i,j} = \frac{A_m}{A_T} \nu_i \left\{ -\frac{2\xi^2 \gamma}{\pi} \Phi_{i,j} \left[\xi \frac{x}{H}, \xi \frac{y}{H}, \xi \frac{z}{H} \right] \right\} \quad (33)$$

and

$$\varphi_{i,j,k} = \frac{A_m}{A_T} \nu_i \left\{ -\frac{2\xi^3 \gamma}{\pi} \Phi_{i,j,k} \left[\xi \frac{x}{H}, \xi \frac{y}{H}, \xi \frac{z}{H} \right] \right\} \quad (34)$$

where

$$\Phi_{i,j} \left[\zeta \frac{x}{H}, \zeta \frac{y}{H}, \zeta \frac{z}{H} \right] = \frac{\frac{\partial^2 \left(\frac{A}{h} \right)}{\partial \left(\frac{x_i}{h} \right) \partial \left(\frac{x_j}{h} \right)}}{\left(\frac{A}{h} \right)} - \frac{\left[\frac{\partial \left(\frac{A}{h} \right)}{\partial \left(\frac{x_i}{h} \right)} \right] \left[\frac{\partial \left(\frac{A}{h} \right)}{\partial \left(\frac{x_j}{h} \right)} \right]}{\left(\frac{A}{h} \right)^2} \quad (35)$$

$$\Phi_{i,j,k} \left[\zeta \frac{x}{H}, \zeta \frac{y}{H}, \zeta \frac{z}{H} \right] = \frac{\left[\frac{\partial^3 \left(\frac{A}{h} \right)}{\partial \left(\frac{x_i}{h} \right) \partial \left(\frac{x_j}{h} \right) \partial \left(\frac{x_k}{h} \right)} \right]}{\left(\frac{A}{h} \right)} - \frac{\frac{\partial \left(\frac{A}{h} \right)}{\partial \left(\frac{x_i}{h} \right)} \left[\frac{\partial^2 \left(\frac{A}{h} \right)}{\partial \left(\frac{x_j}{h} \right) \partial \left(\frac{x_k}{h} \right)} \right] + \frac{\partial \left(\frac{A}{h} \right)}{\partial \left(\frac{x_j}{h} \right)} \left[\frac{\partial^2 \left(\frac{A}{h} \right)}{\partial \left(\frac{x_i}{h} \right) \partial \left(\frac{x_k}{h} \right)} \right] + \frac{\partial \left(\frac{A}{h} \right)}{\partial \left(\frac{x_k}{h} \right)} \left[\frac{\partial^2 \left(\frac{A}{h} \right)}{\partial \left(\frac{x_i}{h} \right) \partial \left(\frac{x_j}{h} \right)} \right]}{\left(\frac{A}{h} \right)^2} + \frac{2 \left[\frac{\partial \left(\frac{A}{h} \right)}{\partial \left(\frac{x_i}{h} \right)} \right] \left[\frac{\partial \left(\frac{A}{h} \right)}{\partial \left(\frac{x_j}{h} \right)} \right] \left[\frac{\partial \left(\frac{A}{h} \right)}{\partial \left(\frac{x_k}{h} \right)} \right]}{\left(\frac{A}{h} \right)^3} \quad (36)$$

and

$$\frac{A}{h} = \sqrt{\left[\left(\zeta \frac{x}{H} \right)^2 + \left(\zeta \frac{y}{H} \right)^2 + \left(\zeta \frac{z}{H} \right)^2 \right] \left(1 - \cos^2 \chi_H \cos^2 \chi_V \right) - \left(\zeta \frac{x}{H} \right) \sin \chi_H \sin \chi_V + \left(\zeta \frac{y}{H} \right) \sin \chi_V \cos \chi_H + \left(\zeta \frac{z}{H} \right) \sin \chi_H \cos \chi_V} \quad (37)$$

For convenience, the partial derivatives of $\frac{A}{h}$ are given in appendix A.

It will be desirable to have the appropriate velocities and slopes for a wake whose position (but not strength) is a mirror image across the X-Z plane of the original wake. Substitution of $180^\circ - \chi_H$ for χ_H in equations (35)

to (37) yields immediately

$$\Phi'_{i,j} \left[\zeta \frac{x}{H}, \zeta \frac{y}{H}, \zeta \frac{z}{H} \right] = \frac{\frac{\partial^2 \left(\frac{A'}{h} \right)}{\partial \left(\frac{x_i}{h} \right) \partial \left(\frac{x_j}{h} \right)}}{\left(\frac{A'}{h} \right)} - \frac{\left[\frac{\partial \left(\frac{A'}{h} \right)}{\partial \left(\frac{x_i}{h} \right)} \right] \left[\frac{\partial \left(\frac{A'}{h} \right)}{\partial \left(\frac{x_j}{h} \right)} \right]}{\left(\frac{A'}{h} \right)^2} \quad (38)$$

and

$$\Phi'_{i,j,k} \left[\zeta \frac{x}{H}, \zeta \frac{y}{H}, \zeta \frac{z}{H} \right] = \frac{\frac{\partial^3 \left(\frac{A'}{h} \right)}{\partial \left(\frac{x_i}{h} \right) \partial \left(\frac{x_j}{h} \right) \partial \left(\frac{x_k}{h} \right)}}{\left(\frac{A'}{h} \right)} - \frac{\frac{\partial \left(\frac{A'}{h} \right)}{\partial \left(\frac{x_i}{h} \right)} \left[\frac{\partial^2 \left(\frac{A'}{h} \right)}{\partial \left(\frac{x_j}{h} \right) \partial \left(\frac{x_k}{h} \right)} \right]}{\left(\frac{A'}{h} \right)^2} + \frac{\frac{\partial \left(\frac{A'}{h} \right)}{\partial \left(\frac{x_j}{h} \right)} \left[\frac{\partial^2 \left(\frac{A'}{h} \right)}{\partial \left(\frac{x_i}{h} \right) \partial \left(\frac{x_k}{h} \right)} \right]}{\left(\frac{A'}{h} \right)^2} + \frac{\frac{\partial \left(\frac{A'}{h} \right)}{\partial \left(\frac{x_k}{h} \right)} \left[\frac{\partial^2 \left(\frac{A'}{h} \right)}{\partial \left(\frac{x_i}{h} \right) \partial \left(\frac{x_j}{h} \right)} \right]}{\left(\frac{A'}{h} \right)^2} + \frac{2 \left[\frac{\partial \left(\frac{A'}{h} \right)}{\partial \left(\frac{x_i}{h} \right)} \right] \left[\frac{\partial \left(\frac{A'}{h} \right)}{\partial \left(\frac{x_j}{h} \right)} \right] \left[\frac{\partial \left(\frac{A'}{h} \right)}{\partial \left(\frac{x_k}{h} \right)} \right]}{\left(\frac{A'}{h} \right)^3} \quad (39)$$

where

$$\frac{A'}{h} = \sqrt{\left[\left(\zeta \frac{x}{H} \right)^2 + \left(\zeta \frac{y}{H} \right)^2 + \left(\zeta \frac{z}{H} \right)^2 \right] (1 - \cos^2 \chi_H \cos^2 \chi_V)} - \left(\zeta \frac{x}{H} \right) \sin \chi_H \sin \chi_V - \left(\zeta \frac{y}{H} \right) \sin \chi_V \cos \chi_H + \left(\zeta \frac{z}{H} \right) \sin \chi_H \cos \chi_V \quad (40)$$

Those partial derivatives of $\frac{A'}{h}$ which differ from the corresponding partial derivatives of $\frac{A}{h}$ are given in appendix B.

Wake in the Wind Tunnel

Consider the model located at the center of the coordinate system as shown in figure 3 with its wake inclined at angles χ_H and χ_V (as in fig. 2).

The wake will intersect the horizontal plane of the floor at a value

$$\left. \frac{x}{H} \right|_{z=-h} = \frac{h}{H} \tan \chi_V = \frac{1}{\xi} \tan \chi_V \quad (41)$$

The wake will intersect the vertical plane of the left-hand wall at

$$\left. \frac{x}{H} \right|_{y=-(2B-b)} = \left(\frac{2B-b}{H} \right) \tan \chi_H = \gamma(2-\eta) \tan \chi_H \quad (42)$$

Within the physical confines of the test section, the wake will intersect either the floor or the wall first. It will be convenient to consider two separate cases: case I, where the wake strikes the floor first; and case II, where the wake strikes the wall first.

Case I: wake strikes floor first. - This case may be distinguished by the fact that

$$\left. \frac{x}{H} \right|_{z=-h} < \left. \frac{x}{H} \right|_{y=-(2B-b)} \quad (43)$$

or

$$\tan \chi_H > \frac{\tan \chi_V}{\xi \gamma (2-\eta)} \quad (44)$$

In this case the wake descends from the model with skew angles χ_H and χ_V until it intercepts the floor. At this point it can no longer pass downward and is assumed to continue along the floor with the original horizontal skew angle of χ_H but with $\chi_V = 90^\circ$. Some distance farther rearward, the wake then intercepts the wall at the corner. From this point on, the wake passes to infinity in the corner with $\chi_H = \chi_V = 90^\circ$.

Case II: wake strikes wall first. - This case may be distinguished by the fact that

$$\left. \frac{x}{H} \right|_{z=-h} > \left. \frac{x}{H} \right|_{y=-(2B-b)} \quad (45)$$

or

$$\tan \chi_H < \frac{\tan \chi_V}{\xi \gamma (2-\eta)} \quad (46)$$

In this case, the wake descends from the model with skew angles χ_H and χ_V until it strikes the wall. At this point it can no longer pass sideward and is assumed to continue along the wall with the original vertical skew angle of χ_V but with $\chi_H = 90^\circ$. Some distance farther rearward, the wake then intercepts the floor at the corner. From this point on, the wake passes to infinity in the corner with $\chi_H = \chi_V = 90^\circ$.

Interference in Case I: Wake Strikes Floor First

The wind-tunnel interference in case I is most easily approached by considering two simple systems before considering the more involved case of the wind tunnel itself.

The first simple system is that of a horizontal floor only (fig. 4). This simple system is, of course, that which applies to ground effect and will be discussed again in a later section as such. For this case, by superposition from the previous results, with the origin centered at the start of the upper wake

$$\begin{aligned} \varphi_{i,j} = \frac{A_m}{A_T} \nu_i \left(-\frac{2\xi^2 \gamma}{\pi} \right) & \left(\Phi_{i,j} \left[\xi \frac{x}{H}, \xi \frac{y}{H}, \xi \frac{z}{H} \right] + \left[\Phi_{i,j} \right]_{\chi_V=90^\circ} - \Phi_{i,j} \right) \left[\xi \frac{x}{H} - \tan \chi_V, \xi \frac{y}{H} + \frac{\tan \chi_V}{\tan \chi_H}, \xi \frac{z}{H} + 1 \right] \\ & + (-1)^{p+q} \left\{ \Phi'_{i,j} \left[\xi \frac{x}{H}, -\xi \frac{y}{H}, -\left(\xi \frac{z}{H} + 2 \right) \right] + \left[\Phi'_{i,j} \right]_{\chi_V=90^\circ} - \Phi'_{i,j} \right\} \left[\xi \frac{x}{H} - \tan \chi_V, -\left(\xi \frac{y}{H} + \frac{\tan \chi_V}{\tan \chi_H} \right), -\left(\xi \frac{z}{H} + 1 \right) \right] \end{aligned} \quad (47)$$

where the following notation has been used

$$\left[\Phi_{i,j} \right]_{\chi_V=90^\circ} - \Phi_{i,j} \left[\bar{x}, \bar{y}, \bar{z} \right] = \Phi_{i,j} \left[\bar{x}, \bar{y}, \bar{z} \right]_{\chi_V=90^\circ} - \Phi_{i,j} \left[\bar{x}, \bar{y}, \bar{z} \right]$$

and where, following in the same line as reference 5, in order to maintain the proper direction of the image strengths and image-induced velocities with respect to the coordinate system of the real wake

$p = 1$ for $i = y$, and $p = 0$ for $i = x$ or $i = z$

$q = 1$ for $j = y$ or $j = z$, and $q = 0$ for $j = x$

The slopes of the induced velocities for this system may be written as

$$\begin{aligned} \varphi_{i,j,k} = \frac{A_m}{A_T} \nu_i \left(-\frac{2\xi^3 \gamma}{\pi} \right) & \left(\Phi_{i,j,k} \left[\xi \frac{x}{H}, \xi \frac{y}{H}, \xi \frac{z}{H} \right] + \left[\Phi_{i,j,k} \right]_{\chi_V=90^\circ} - \Phi_{i,j,k} \left[\xi \frac{x}{H} - \tan \chi_V, \xi \frac{y}{H} + \frac{\tan \chi_V}{\tan \chi_H}, \xi \frac{z}{H} + 1 \right] \right. \\ & \left. + (-1)^{p+q+r} \left\{ \Phi'_{i,j,k} \left[\xi \frac{x}{H}, -\xi \frac{y}{H}, -\left(\xi \frac{z}{H} + 2 \right) \right] + \left[\Phi'_{i,j,k} \right]_{\chi_V=90^\circ} - \Phi'_{i,j,k} \left[\xi \frac{x}{H} - \tan \chi_V, -\left(\xi \frac{y}{H} + \frac{\tan \chi_V}{\tan \chi_H} \right), -\left(\xi \frac{z}{H} + 1 \right) \right] \right\} \right) \end{aligned} \quad (48)$$

where $r = 1$ when $k = y$ or $k = z$, and $r = 0$ when $k = x$.

It is observed that adding slopes by superposition as in equation (48) amounts to adding the tangents of several angles to find the tangent of the sum of the angles. Note that this procedure is valid only if $\varphi_{i,j,k}$ and all of the individual terms summed to obtain $\varphi_{i,j,k}$ are small.

Now consider two such pairs of wakes disposed a distance $2B-b$ to either side of a solid wall as in figure 5. For the four wakes, with the origin at the start of the upper right-hand wake, the induced velocity field of the entire system is found to be

$$\begin{aligned}
\varphi_{i,j} = & \frac{\mathbf{A}_m}{\mathbf{A}_T} \nu_i \left(-\frac{2\xi^2\gamma}{\pi} \right) \left(\Phi_{i,j} \left[\xi \frac{x}{H}, \xi \frac{y}{H}, \xi \frac{z}{H} \right] + \left[\Phi_{i,j} \Big|_{\chi_V=90^\circ} - \Phi_{i,j} \right] \left[\xi \frac{x}{H} - \tan \chi_V, \xi \frac{y}{H} + \frac{\tan \chi_V}{\tan \chi_H}, \xi \frac{z}{H} + 1 \right] \right. \\
& + \left[\Phi_{i,j} \Big|_{\chi_H=\chi_V=90^\circ} - \Phi_{i,j} \Big|_{\chi_V=90^\circ} \right] \left[\xi \frac{x}{H} - \gamma \xi (2 - \eta) \tan \chi_H, \xi \frac{y}{H} + \gamma \xi (2 - \eta), \xi \frac{z}{H} + 1 \right] \\
& + (-1)^{p+q} \left\{ \Phi'_{i,j} \left[\xi \frac{x}{H}, -\xi \frac{y}{H}, -\left(\xi \frac{z}{H} + 2 \right) \right] + \left[\Phi'_{i,j} \Big|_{\chi_V=90^\circ} - \Phi'_{i,j} \right] \left[\xi \frac{x}{H} - \tan \chi_V, -\left(\xi \frac{y}{H} + \frac{\tan \chi_V}{\tan \chi_H} \right), -\left(\xi \frac{z}{H} + 1 \right) \right] \right. \\
& + \left. \left[\Phi'_{i,j} \Big|_{\chi_H=\chi_V=90^\circ} - \Phi'_{i,j} \Big|_{\chi_V=90^\circ} \right] \left[\xi \frac{x}{H} - \gamma \xi (2 - \eta) \tan \chi_H, -\left(\xi \frac{y}{H} + \gamma \xi (2 - \eta) \right), -\left(\xi \frac{z}{H} + 1 \right) \right] \right\} \\
& + (-1)^p \left\{ \Phi'_{i,j} \left[\xi \frac{x}{H}, \xi \frac{y}{H} + 2\gamma \xi (2 - \eta), \xi \frac{z}{H} \right] + \left[\Phi'_{i,j} \Big|_{\chi_V=90^\circ} - \Phi'_{i,j} \right] \left[\xi \frac{x}{H} - \tan \chi_V, \xi \frac{y}{H} + 2\gamma \xi (2 - \eta) - \frac{\tan \chi_V}{\tan \chi_H}, \xi \frac{z}{H} + 1 \right] \right. \\
& + \left. \left[\Phi'_{i,j} \Big|_{\chi_H=\chi_V=90^\circ} - \Phi'_{i,j} \Big|_{\chi_V=90^\circ} \right] \left[\xi \frac{x}{H} - \gamma \xi (2 - \eta) \tan \chi_H, \xi \frac{y}{H} + \gamma \xi (2 - \eta), \xi \frac{z}{H} + 1 \right] \right\} \\
& + (-1)^q \left\{ \Phi_{i,j} \left[\xi \frac{x}{H}, -\left(\xi \frac{y}{H} + 2\gamma \xi (2 - \eta) \right), -\left(\xi \frac{z}{H} + 2 \right) \right] \right. \\
& + \left[\Phi_{i,j} \Big|_{\chi_V=90^\circ} - \Phi_{i,j} \right] \left[\xi \frac{x}{H} - \tan \chi_V, -\left(\xi \frac{y}{H} + 2\gamma \xi (2 - \eta) - \frac{\tan \chi_V}{\tan \chi_H} \right), -\left(\xi \frac{z}{H} + 1 \right) \right] \\
& + \left. \left[\Phi_{i,j} \Big|_{\chi_H=\chi_V=90^\circ} - \Phi_{i,j} \Big|_{\chi_V=90^\circ} \right] \left[\xi \frac{x}{H} - \gamma \xi (2 - \eta) \tan \chi_H, -\left(\xi \frac{y}{H} + \gamma \xi (2 - \eta) \right), -\left(\xi \frac{z}{H} + 1 \right) \right] \right\} \Bigg)
\end{aligned}
\tag{49}$$

Similarly, the slopes of the induced velocities are given by:

$$\begin{aligned}
\varphi_{i,j,k} = \frac{A_m}{A_T} \nu_i \left(\frac{-2\zeta^3\gamma}{\pi} \right) & \left(\Phi_{i,j,k} \left[\zeta \frac{x}{H}, \zeta \frac{y}{H}, \zeta \frac{z}{H} \right] + \left[\Phi_{i,j,k} \Big|_{\chi_V=90^\circ} - \Phi_{i,j,k} \right] \left[\zeta \frac{x}{H} - \tan \chi_V, \zeta \frac{y}{H} + \frac{\tan \chi_V}{\tan \chi_H}, \zeta \frac{z}{H} + 1 \right] \right. \\
& + \left[\Phi_{i,j,k} \Big|_{\chi_H=\chi_V=90^\circ} - \Phi_{i,j,k} \Big|_{\chi_V=90^\circ} \right] \left[\zeta \frac{x}{H} - \gamma \zeta (2 - \eta) \tan \chi_H, \zeta \frac{y}{H} + \gamma \zeta (2 - \eta), \zeta \frac{z}{H} + 1 \right] \\
& + (-1)^{p+q+r} \left\{ \Phi'_{i,j,k} \left[\zeta \frac{x}{H}, -\zeta \frac{y}{H}, -\left(\zeta \frac{z}{H} + 2 \right) \right] + \left[\Phi'_{i,j,k} \Big|_{\chi_V=90^\circ} - \Phi'_{i,j,k} \right] \left[\zeta \frac{x}{H} - \tan \chi_V, -\left(\zeta \frac{y}{H} + \frac{\tan \chi_V}{\tan \chi_H} \right), -\left(\zeta \frac{z}{H} + 1 \right) \right] \right. \\
& + \left. \left[\Phi'_{i,j,k} \Big|_{\chi_H=\chi_V=90^\circ} - \Phi'_{i,j,k} \right] \left[\zeta \frac{x}{H} - \gamma \zeta (2 - \eta) \tan \chi_H, -\left(\zeta \frac{y}{H} + \gamma \zeta (2 - \eta) \right), -\left(\zeta \frac{z}{H} + 1 \right) \right] \right\} \\
& + (-1)^p \left\{ \Phi'_{i,j,k} \left[\zeta \frac{x}{H}, \left(\zeta \frac{y}{H} + 2\gamma \zeta (2 - \eta) \right), \zeta \frac{z}{H} \right] \right. \\
& + \left[\Phi'_{i,j,k} \Big|_{\chi_V=90^\circ} - \Phi'_{i,j,k} \right] \left[\left(\zeta \frac{x}{H} - \tan \chi_V \right), \left(\zeta \frac{y}{H} + 2\gamma \zeta (2 - \eta) - \frac{\tan \chi_V}{\tan \chi_H} \right), \zeta \frac{z}{H} + 1 \right] \\
& + \left. \left[\Phi'_{i,j,k} \Big|_{\chi_H=\chi_V=90^\circ} - \Phi'_{i,j,k} \Big|_{\chi_V=90^\circ} \right] \left[\left(\zeta \frac{x}{H} - \gamma \zeta (2 - \eta) \tan \chi_H \right), \left(\zeta \frac{y}{H} + \gamma \zeta (2 - \eta) \right), \zeta \frac{z}{H} + 1 \right] \right\} \\
& + (-1)^{q+r} \left\{ \Phi_{i,j,k} \left[\zeta \frac{x}{H}, -\left(\zeta \frac{y}{H} + 2\gamma \zeta (2 - \eta) \right), -\left(\zeta \frac{z}{H} + 2 \right) \right] \right. \\
& + \left[\Phi_{i,j,k} \Big|_{\chi_V=90^\circ} - \Phi_{i,j,k} \right] \left[\left(\zeta \frac{x}{H} - \tan \chi_V \right), -\left(\zeta \frac{y}{H} + 2\gamma \zeta (2 - \eta) - \frac{\tan \chi_V}{\tan \chi_H} \right), -\left(\zeta \frac{z}{H} + 1 \right) \right] \\
& + \left. \left[\Phi_{i,j,k} \Big|_{\chi_H=\chi_V=90^\circ} - \Phi_{i,j,k} \Big|_{\chi_V=90^\circ} \right] \left[\left(\zeta \frac{x}{H} - \gamma \zeta (2 - \eta) \tan \chi_H \right), -\left(\zeta \frac{y}{H} + \gamma \zeta (2 - \eta) \right), -\left(\zeta \frac{z}{H} + 1 \right) \right] \right\} \Bigg) \quad (50)
\end{aligned}$$

The arrangement of images required to insure that there is no flow normal to any of the four walls of a closed wind tunnel is shown in figure 6. It will be observed that the repetitive image set which forms the basis for this pattern is that of the four wakes for which the induced flow field is given by equation (50). This image set is merely translated laterally at intervals of $4B = 4\gamma\zeta h$ and vertically at intervals of $4H = 4\zeta h$ in order to form the complete pattern.

Therefore, if the interference velocities caused by the presence of the walls are defined as

$$\Delta\varphi_{i,j} = \delta_{i,j} \frac{A_m}{A_T} v_i \quad (51)$$

the interference factor $\delta_{i,j}$ may be expressed immediately as

$$\begin{aligned} \delta_{i,j} = & -\frac{2\zeta^2\gamma}{\pi} \left[\sum_{m=-\infty}^{\infty} \sum_{\substack{n=-\infty \\ m=n \neq 0}}^{\infty} \Phi_{i,j} \left[\zeta \frac{x}{H}, \zeta \left(\frac{y}{H} - 4m\gamma \right), \zeta \left(\frac{z}{H} - 4n \right) \right] \right. \\ & + \sum_{m=-\infty}^{\infty} \sum_{n=-\infty}^{\infty} \left(\Phi_{i,j} \Big|_{\chi_V=90^\circ} - \Phi_{i,j} \right) \left[\zeta \frac{x}{H} - \tan \chi_V, \zeta \left(\frac{y}{H} - 4m\gamma \right) + \frac{\tan \chi_V}{\tan \chi_H}, \zeta \left(\frac{z}{H} - 4n \right) + 1 \right] \\ & + \left[\Phi_{i,j} \Big|_{\chi_H=\chi_V=90^\circ} - \Phi_{i,j} \Big|_{\chi_V=90^\circ} \right] \left[\zeta \left(\frac{x}{H} - \gamma(2-\eta) \tan \chi_H \right), \zeta \left(\frac{y}{H} + \gamma(2-\eta-4m) \right), \zeta \left(\frac{z}{H} - 4n \right) + 1 \right] \\ & + (-1)^{p+q} \left\{ \Phi'_{i,j} \left[\zeta \frac{x}{H}, -\zeta \left(\frac{y}{H} - 4m\gamma \right), -\zeta \left(\frac{z}{H} - 4n \right) - 2 \right] \right. \\ & + \left[\Phi'_{i,j} \Big|_{\chi_V=90^\circ} - \Phi'_{i,j} \right] \left[\zeta \frac{x}{H} - \tan \chi_V, -\zeta \left(\frac{y}{H} - 4m\gamma \right) - \frac{\tan \chi_V}{\tan \chi_H}, -\zeta \left(\frac{z}{H} - 4n \right) - 1 \right] \\ & + \left[\Phi'_{i,j} \Big|_{\chi_H=\chi_V=90^\circ} - \Phi'_{i,j} \Big|_{\chi_V=90^\circ} \right] \left[\zeta \left(\frac{x}{H} - \gamma(2-\eta) \tan \chi_H \right), -\zeta \left(\frac{y}{H} + \gamma(2-\eta-4m) \right), -\zeta \left(\frac{z}{H} - 4n \right) - 1 \right] \Big\} \\ & + (-1)^p \left\{ \Phi'_{i,j} \left[\zeta \frac{x}{H}, \zeta \left(\frac{y}{H} + 2\gamma(2-\eta-2m) \right), \zeta \left(\frac{z}{H} - 4n \right) \right] \right. \end{aligned}$$

(Equation continued on next page)

$$\begin{aligned}
& + \left[\Phi'_{i,j} \Big|_{\chi_V=90^\circ} - \Phi'_{i,j} \right] \left[\zeta \frac{x}{H} - \tan \chi_V, \zeta \left(\frac{y}{H} + 2\gamma(2 - \eta - 2m) \right) - \frac{\tan \chi_V}{\tan \chi_H}, \zeta \left(\frac{z}{H} - 4n \right) + 1 \right] \\
& + \left[\Phi'_{i,j} \Big|_{\chi_H=\chi_V=90^\circ} - \Phi'_{i,j} \Big|_{\chi_V=90^\circ} \right] \left[\zeta \left(\frac{x}{H} - \gamma(2 - \eta) \tan \chi_H \right), -\zeta \left(\frac{y}{H} + \gamma(2 - \eta - 4m) \right), -\zeta \left(\frac{z}{H} - 4n \right) + 1 \right] \Bigg\} \\
& + (-1)^q \left\{ \Phi_{i,j} \left[\zeta \frac{x}{H}, -\zeta \left(\frac{y}{H} + 2\gamma(2 - \eta - 2m) \right), -\zeta \left(\frac{z}{H} - 4n \right) - 2 \right] \right. \\
& + \left[\Phi_{i,j} \Big|_{\chi_V=90^\circ} - \Phi_{i,j} \right] \left[\zeta \frac{x}{H} - \tan \chi_V, -\zeta \left(\frac{y}{H} + 2\gamma(2 - \eta - 2m) \right) + \frac{\tan \chi_V}{\tan \chi_H}, -\zeta \left(\frac{z}{H} - 4n \right) - 1 \right] \\
& \left. + \left[\Phi_{i,j} \Big|_{\chi_H=\chi_V=90^\circ} - \Phi_{i,j} \Big|_{\chi_V=90^\circ} \right] \left[\zeta \left(\frac{x}{H} - \gamma(2 - \eta) \tan \chi_H \right), -\zeta \left(\frac{y}{H} + \gamma(2 - \eta - 4m) \right), -\zeta \left(\frac{z}{H} - 4n \right) - 1 \right] \right\} \Bigg] \quad (52)
\end{aligned}$$

The rate of change of the interference velocities follows in the same manner. Defining

$$\Delta \varphi_{i,j,k} = \delta_{i,j,k} \frac{A_m}{A_T} \nu_i \quad (53)$$

the equation for $\delta_{i,j,k}$ may be written as

$$\begin{aligned}
\delta_{i,j,k} = & \frac{-2\zeta^3\gamma}{\pi} \left[\sum_{m=-\infty}^{\infty} \sum_{\substack{n=-\infty \\ m=n \neq 0}}^{\infty} \Phi_{i,j,k} \left[\zeta \frac{x}{H}, \zeta \left(\frac{y}{H} - 4m\gamma \right), \zeta \left(\frac{z}{H} - 4n \right) \right] \right. \\
& + \sum_{m=-\infty}^{\infty} \sum_{n=-\infty}^{\infty} \left(\left[\Phi_{i,j,k} \Big|_{\chi_V=90^\circ} - \Phi_{i,j,k} \right] \left[\zeta \frac{x}{H} - \tan \chi_V, \zeta \left(\frac{y}{H} - 4m\gamma \right) + \frac{\tan \chi_V}{\tan \chi_H}, \zeta \left(\frac{z}{H} - 4n \right) + 1 \right] \right. \\
& + \left[\Phi_{i,j,k} \Big|_{\chi_H=\chi_V=90^\circ} - \Phi_{i,j,k} \Big|_{\chi_V=90^\circ} \right] \left[\zeta \left(\frac{x}{H} - \gamma(2 - \eta) \tan \chi_H \right), \zeta \left(\frac{y}{H} + \gamma(2 - \eta - 4m) \right), \zeta \left(\frac{z}{H} - 4n \right) + 1 \right] \\
& \left. + (-1)^{p+q+r} \left\{ \Phi'_{i,j} \left[\zeta \frac{x}{H}, -\zeta \left(\frac{y}{H} - 4m\gamma \right), -\zeta \left(\frac{z}{H} - 4n \right) - 2 \right] \right. \right.
\end{aligned}$$

(Equation continued on next page)

$$\begin{aligned}
& + \left[\Phi'_{i,j,k} \Big|_{\chi_V=90^\circ} - \Phi'_{i,j,k} \right] \left[\zeta \frac{x}{H} - \tan \chi_V, -\zeta \left(\frac{y}{H} - 4m \right) - \frac{\tan \chi_V}{\tan \chi_H}, -\zeta \left(\frac{z}{H} - 4n \right) - 1 \right] \\
& + \left[\Phi'_{i,j,k} \Big|_{\chi_H=\chi_V=90^\circ} - \Phi'_{i,j,k} \Big|_{\chi_V=90^\circ} \right] \left[\zeta \left(\frac{x}{H} - \gamma(2-\eta) \tan \chi_H \right), -\zeta \left(\frac{y}{H} + \gamma(2-\eta-4m) \right), -\zeta \left(\frac{z}{H} - 4n \right) - 1 \right] \Big\} \\
& + (-1)^p \left\{ \Phi'_{i,j,k} \left[\zeta \frac{x}{H}, \zeta \left(\frac{y}{H} + 2\gamma(2-\eta-2m) \right), \zeta \left(\frac{z}{H} - 4n \right) \right] \right. \\
& + \left[\Phi'_{i,j,k} \Big|_{\chi_V=90^\circ} - \Phi'_{i,j,k} \right] \left[\zeta \frac{x}{H} - \tan \chi_V, \zeta \left(\frac{y}{H} + 2\gamma(2-\eta-2m) \right) - \frac{\tan \chi_V}{\tan \chi_H}, \zeta \left(\frac{z}{H} - 4n \right) + 1 \right] \\
& + \left. \left[\Phi'_{i,j,k} \Big|_{\chi_H=\chi_V=90^\circ} - \Phi'_{i,j,k} \Big|_{\chi_V=90^\circ} \right] \left[\zeta \left(\frac{x}{H} - \gamma(2-\eta) \tan \chi_H \right), \zeta \left(\frac{y}{H} + \gamma(2-\eta-4m) \right), \zeta \left(\frac{z}{H} - 4n \right) + 1 \right] \right\} \\
& + (-1)^{q+r} \left\{ \Phi_{i,j,k} \left[\zeta \frac{x}{H}, -\zeta \left(\frac{y}{H} + 2\gamma(2-\eta-2m) \right), -\zeta \left(\frac{z}{H} - 4n \right) - 2 \right] \right. \\
& + \left[\Phi_{i,j,k} \Big|_{\chi_V=90^\circ} - \Phi_{i,j,k} \right] \left[\zeta \frac{x}{H} - \tan \chi_V, -\zeta \left(\frac{y}{H} + 2\gamma(2-\eta-2m) \right) + \frac{\tan \chi_V}{\tan \chi_H}, -\zeta \left(\frac{z}{H} - 4n \right) - 1 \right] \\
& + \left. \left[\Phi_{i,j,k} \Big|_{\chi_H=\chi_V=90^\circ} - \Phi_{i,j,k} \Big|_{\chi_V=90^\circ} \right] \left[\zeta \left(\frac{x}{H} - \gamma(2-\eta) \tan \chi_H \right), -\zeta \left(\frac{y}{H} + \gamma(2-\eta-4m) \right), -\zeta \left(\frac{z}{H} - 4n \right) - 1 \right] \right\} \Bigg\} \quad (54)
\end{aligned}$$

It will be observed that the central image, which represents the wake in free air, has been omitted in equations (52) and (54). This image is removed since it is only the wind-tunnel interferences which are of interest and not the total induced fields of model and wind tunnel.

If χ_H and χ_V are both 90° , the wake passes directly rearward without touching the wind-tunnel boundaries. Thus, equations (47) to (50), (52), and (54) may be simplified by omitting all terms on the right-hand side of the equations except the first, fourth, seventh, and tenth sets of terms. If only χ_H is 90° , the wake will touch the floor, but not the sidewalls of the tunnel. Thus, the third, sixth, ninth, and twelfth sets of terms on the right-hand side of equations (49), (50), (52), and (54) may be omitted. If only χ_V is 90° , the wake touches one of the walls, but not the floor. This set of conditions falls under case II, the equations for which are developed in the following section.

Interference In Case II: Wake Strikes Wall First

The wind-tunnel interference in this case is also most easily approached by considering simpler systems first. The first such simple system (fig. 7) consists of two wakes disposed a distance $2B - b$ to either side of a solid wall. The induced field of this system with the origin centered at the start of the right-hand wake is

$$\begin{aligned} \varphi_{i,j} = \frac{A_m}{A_T} \nu_i \left(-\frac{2\xi^2\gamma}{\pi} \right) & \left(\Phi_{i,j} \left[\xi \frac{x}{H}, \xi \frac{y}{H}, \xi \frac{z}{H} \right] + \left[\Phi_{i,j} \Big|_{\chi_H=90^\circ} - \Phi_{i,j} \right] \left[\xi \left(\frac{x}{H} - \gamma(2-\eta) \tan \chi_H \right), \xi \left(\frac{y}{H} + \gamma(2-\eta) \right), \xi \left(\frac{z}{H} + \gamma(2-\eta) \frac{\tan \chi_H}{\tan \chi_V} \right) \right] \right. \\ & + (-1)^p \left\{ \Phi'_{i,j} \left[\xi \frac{x}{H}, \xi \left(\frac{y}{H} + 2\gamma(2-\eta) \right), \xi \frac{z}{H} \right] \right. \\ & \left. \left. + \left[\Phi'_{i,j} \Big|_{\chi_H=90^\circ} - \Phi'_{i,j} \right] \left[\xi \left(\frac{x}{H} - \gamma(2-\eta) \tan \chi_H \right), \xi \left(\frac{y}{H} + \gamma(2-\eta) \right), \xi \left(\frac{z}{H} + \gamma(2-\eta) \frac{\tan \chi_H}{\tan \chi_V} \right) \right] \right\} \right) \end{aligned} \quad (55)$$

Similarly, the gradients of the induced velocities are given by

$$\begin{aligned} \varphi_{i,j,k} = \frac{A_m}{A_T} \nu_i \left(-\frac{2\xi^3\gamma}{\pi} \right) & \left(\Phi_{i,j,k} \left[\xi \frac{x}{H}, \xi \frac{y}{H}, \xi \frac{z}{H} \right] \right. \\ & + \left[\Phi_{i,j,k} \Big|_{\chi_H=90^\circ} - \Phi_{i,j,k} \right] \left[\xi \left(\frac{x}{H} - \gamma(2-\eta) \tan \chi_H \right), \xi \left(\frac{y}{H} + \gamma(2-\eta) \right), \xi \left(\frac{z}{H} + \gamma(2-\eta) \frac{\tan \chi_H}{\tan \chi_V} \right) \right] \\ & + (-1)^p \left\{ \Phi'_{i,j,k} \left[\xi \frac{x}{H}, \xi \left(\frac{y}{H} + 2\gamma(2-\eta) \right), \xi \frac{z}{H} \right] \right. \\ & \left. \left. + \left[\Phi'_{i,j,k} \Big|_{\chi_H=90^\circ} - \Phi'_{i,j,k} \right] \left[\xi \left(\frac{x}{H} - \gamma(2-\eta) \tan \chi_H \right), \xi \left(\frac{y}{H} + \gamma(2-\eta) \right), \xi \left(\frac{z}{H} + \gamma(2-\eta) \frac{\tan \chi_H}{\tan \chi_V} \right) \right] \right\} \right) \end{aligned} \quad (56)$$

If the two images are now placed below the preceding two images as in figure 8, the induced velocity field, with the origin at the start of the upper right-hand wake, is given by

$$\begin{aligned}
\varphi_{i,j} = & \frac{A_m}{A_T} \nu_i \left(-\frac{2\xi^2\gamma}{\pi} \right) \left(\Phi_{i,j} \left[\xi \frac{x}{H}, \xi \frac{y}{H}, \xi \frac{z}{H} \right] \right. \\
& + \left[\Phi_{i,j} \Big|_{\chi_H=90^\circ} - \Phi_{i,j} \right] \left[\xi \left(\frac{x}{H} - \gamma(2-\eta) \tan \chi_H \right), \xi \left(\frac{y}{H} + \gamma(2-\eta) \right), \xi \left(\frac{z}{H} + \gamma(2-\eta) \frac{\tan \chi_H}{\tan \chi_V} \right) \right] \\
& + \left[\Phi_{i,j} \Big|_{\chi_H=\chi_V=90^\circ} - \Phi_{i,j} \Big|_{\chi_H=90^\circ} \right] \left[\xi \frac{x}{H} - \tan \chi_V, \xi \left(\frac{y}{H} + \gamma(2-\eta) \right), \xi \frac{z}{H} + 1 \right] \\
& + (-1)^p \left\{ \Phi'_{i,j} \left[\xi \frac{x}{H}, \xi \left(\frac{y}{H} + 2\gamma(2-\eta) \right), \xi \frac{z}{H} \right] \right. \\
& + \left[\Phi'_{i,j} \Big|_{\chi_H=90^\circ} - \Phi'_{i,j} \right] \left[\xi \left(\frac{x}{H} - \gamma(2-\eta) \tan \chi_H \right), \xi \left(\frac{y}{H} + \gamma(2-\eta) \right), \xi \left(\frac{z}{H} + \gamma(2-\eta) \frac{\tan \chi_H}{\tan \chi_V} \right) \right] \\
& + \left. \left[\Phi'_{i,j} \Big|_{\chi_H=\chi_V=90^\circ} - \Phi'_{i,j} \Big|_{\chi_H=90^\circ} \right] \left[\xi \frac{x}{H} - \tan \chi_V, \xi \left(\frac{y}{H} + \gamma(2-\eta) \right), \xi \frac{z}{H} + 1 \right] \right\} \\
& + (-1)^{p+q} \left\{ \Phi'_{i,j} \left[\xi \frac{x}{H}, -\xi \frac{y}{H}, -\xi \frac{z}{H} - 2 \right] \right. \\
& + \left[\Phi'_{i,j} \Big|_{\chi_H=90^\circ} - \Phi'_{i,j} \right] \left[\xi \left(\frac{x}{H} - \gamma(2-\eta) \tan \chi_H \right), -\xi \left(\frac{y}{H} + \gamma(2-\eta) \right), -\xi \left(\frac{z}{H} - \gamma(2-\eta) \frac{\tan \chi_H}{\tan \chi_V} \right) - 2 \right] \\
& + \left. \left[\Phi'_{i,j} \Big|_{\chi_H=\chi_V=90^\circ} - \Phi'_{i,j} \Big|_{\chi_H=90^\circ} \right] \left[\xi \frac{x}{H} - \tan \chi_V, -\xi \left(\frac{y}{H} + \gamma(2-\eta) \right), -\xi \frac{z}{H} - 1 \right] \right\} \\
& + (-1)^p \left\{ \Phi_{i,j} \left[\xi \frac{x}{H}, -\xi \left(\frac{y}{H} + 2\gamma(2-\eta) \right), -\xi \frac{z}{H} - 2 \right] \right. \\
& + \left[\Phi_{i,j} \Big|_{\chi_H=90^\circ} - \Phi_{i,j} \right] \left[\xi \left(\frac{x}{H} - \gamma(2-\eta) \tan \chi_H \right), -\xi \left(\frac{y}{H} + \gamma(2-\eta) \right), -\xi \left(\frac{z}{H} - \gamma(2-\eta) \frac{\tan \chi_H}{\tan \chi_V} \right) - 2 \right] \\
& + \left. \left[\Phi_{i,j} \Big|_{\chi_H=\chi_V=90^\circ} - \Phi_{i,j} \Big|_{\chi_H=90^\circ} \right] \left[\xi \frac{x}{H} - \tan \chi_V, -\xi \left(\frac{y}{H} + \gamma(2-\eta) \right), -\xi \frac{z}{H} - 1 \right] \right\}
\end{aligned}$$

and the gradients of the induced velocities are given by

$$\begin{aligned}
\varphi_{i,j,k} = & \frac{\mathbf{A}_m}{\mathbf{A}_T} \nu_i \left(-\frac{2\xi^3\gamma}{\pi} \right) \left(\Phi_{i,j,k} \left[\xi \frac{x}{H}, \xi \frac{y}{H}, \xi \frac{z}{H} \right] \right. \\
& + \left[\Phi_{i,j,k} \Big|_{\chi_H=90^\circ} - \Phi_{i,j,k} \right] \left[\xi \left(\frac{x}{H} - \gamma(2-\eta) \tan \chi_H \right), \xi \left(\frac{y}{H} + \gamma(2-\eta) \right), \xi \left(\frac{z}{H} + \gamma(2-\eta) \frac{\tan \chi_H}{\tan \chi_V} \right) \right] \\
& + \left[\Phi_{i,j,k} \Big|_{\chi_H=\chi_V=90^\circ} - \Phi_{i,j,k} \Big|_{\chi_H=90^\circ} \right] \left[\xi \frac{x}{H} - \tan \chi_V, \xi \left(\frac{y}{H} + \gamma(2-\eta) \right), \xi \frac{z}{H} + 1 \right] \\
& + (-1)^p \left\{ \Phi'_{i,j,k} \left[\xi \frac{x}{H}, \xi \left(\frac{y}{H} + 2\gamma(2-\eta) \right), \xi \frac{z}{H} \right] \right. \\
& + \left[\Phi'_{i,j,k} \Big|_{\chi_H=90^\circ} - \Phi'_{i,j,k} \right] \left[\xi \left(\frac{x}{H} - \gamma(2-\eta) \tan \chi_H \right), \xi \left(\frac{y}{H} + \gamma(2-\eta) \right), \xi \left(\frac{z}{H} + \gamma(2-\eta) \frac{\tan \chi_H}{\tan \chi_V} \right) \right] \\
& + \left[\Phi'_{i,j,k} \Big|_{\chi_H=\chi_V=90^\circ} - \Phi'_{i,j,k} \Big|_{\chi_H=90^\circ} \right] \left[\xi \frac{x}{H} - \tan \chi_V, \xi \left(\frac{y}{H} + \gamma(2-\eta) \right), \xi \frac{z}{H} + 1 \right] \Big\} \\
& + (-1)^{p+q+r} \left\{ \Phi'_{i,j,k} \left[\xi \frac{x}{H}, -\xi \frac{y}{H}, -\xi \frac{z}{H} - 2 \right] \right. \\
& + \left[\Phi'_{i,j,k} \Big|_{\chi_H=90^\circ} - \Phi'_{i,j,k} \right] \left[\xi \left(\frac{x}{H} - \gamma(2-\eta) \tan \chi_H \right), -\xi \left(\frac{y}{H} + \gamma(2-\eta) \right), -\xi \left(\frac{z}{H} - \gamma(2-\eta) \frac{\tan \chi_H}{\tan \chi_V} \right) - 2 \right] \\
& + \left[\Phi'_{i,j,k} \Big|_{\chi_H=\chi_V=90^\circ} - \Phi'_{i,j,k} \Big|_{\chi_H=90^\circ} \right] \left[\xi \frac{x}{H} - \tan \chi_V, -\xi \left(\frac{y}{H} + \gamma(2-\eta) \right), -\xi \frac{z}{H} - 1 \right] \Big\} \\
& + (-1)^{q+r} \left\{ \Phi_{i,j,k} \left[\xi \frac{x}{H}, -\xi \left(\frac{y}{H} + 2\gamma(2-\eta) \right), -\xi \frac{z}{H} - 2 \right] \right. \\
& + \left[\Phi_{i,j,k} \Big|_{\chi_H=90^\circ} - \Phi_{i,j,k} \right] \left[\xi \left(\frac{x}{H} - \gamma(2-\eta) \tan \chi_H \right), -\xi \left(\frac{y}{H} + \gamma(2-\eta) \right), -\xi \left(\frac{z}{H} - \gamma(2-\eta) \frac{\tan \chi_H}{\tan \chi_V} \right) - 2 \right] \\
& + \left[\Phi_{i,j,k} \Big|_{\chi_H=\chi_V=90^\circ} - \Phi_{i,j,k} \Big|_{\chi_H=90^\circ} \right] \left[\xi \frac{x}{H} - \tan \chi_V, -\xi \left(\frac{y}{H} + \gamma(2-\eta) \right), -\xi \frac{z}{H} - 1 \right] \Big\} \Bigg)
\end{aligned} \tag{58}$$

If $\delta_{i,j}$ is defined as in the preceding section, that is, as

$$\Delta\varphi_{i,j} = \delta_{i,j} \frac{A_m}{A_T} \nu_i \quad (59)$$

then $\delta_{i,j}$ may be expressed as

$$\begin{aligned} \delta_{i,j} = & -\frac{2\epsilon^2\gamma}{\pi} \left[\sum_{m=-\infty}^{\infty} \sum_{\substack{n=-\infty \\ n \neq m}}^{\infty} \Phi_{i,j} \left[\zeta \frac{x}{H}, \zeta \left(\frac{y}{H} - 4m\gamma \right), \zeta \frac{z}{H} - 4n \right] \right. \\ & + \sum_{m=-\infty}^{\infty} \sum_{n=-\infty}^{\infty} \left(\left[\Phi_{i,j} \Big|_{\chi_H=90^\circ} - \Phi_{i,j} \right] \left[\zeta \left(\frac{x}{H} - \gamma(2-\eta) \tan \chi_H \right), \zeta \left(\frac{y}{H} + \gamma(2-\eta-4m) \right), \zeta \left(\frac{z}{H} - 4n + \gamma(2-\eta) \frac{\tan \chi_H}{\tan \chi_V} \right) \right] \right. \\ & + \left[\Phi_{i,j} \Big|_{\chi_H=\chi_V=90^\circ} - \Phi_{i,j} \Big|_{\chi_H=90^\circ} \right] \left[\zeta \frac{x}{H} - \tan \chi_V, \zeta \left(\frac{y}{H} + \gamma(2-\eta-4m) \right), \zeta \left(\frac{z}{H} - 4n \right) + 1 \right] \\ & + (-1)^p \left\{ \Phi'_{i,j} \left[\zeta \frac{x}{H}, \zeta \left(\frac{y}{H} + 2\gamma(2-\eta-2m) \right), \zeta \left(\frac{z}{H} - 4n \right) \right] \right. \\ & + \left[\Phi'_{i,j} \Big|_{\chi_H=90^\circ} - \Phi'_{i,j} \right] \left[\zeta \left(\frac{x}{H} - \gamma(2-\eta) \tan \chi_H \right), \zeta \left(\frac{y}{H} + \gamma(2-\eta-4m) \right), \zeta \left(\frac{z}{H} - 4n + \gamma(2-\eta) \frac{\tan \chi_H}{\tan \chi_V} \right) \right] \\ & + \left. \left[\Phi'_{i,j} \Big|_{\chi_H=\chi_V=90^\circ} - \Phi'_{i,j} \Big|_{\chi_H=90^\circ} \right] \left[\zeta \frac{x}{H} - \tan \chi_V, \zeta \left(\frac{y}{H} + \gamma(2-\eta-4m) \right), \zeta \left(\frac{z}{H} - 4n \right) + 1 \right] \right\} \\ & + (-1)^{p+q} \left\{ \Phi'_{i,j} \left[\zeta \frac{x}{H}, -\zeta \left(\frac{y}{H} - 4m\gamma \right), -\zeta \left(\frac{z}{H} - 4n \right) - 2 \right] \right. \\ & + \left[\Phi'_{i,j} \Big|_{\chi_H=90^\circ} - \Phi'_{i,j} \right] \left[\zeta \left(\frac{x}{H} - \gamma(2-\eta) \tan \chi_H \right), -\zeta \left(\frac{y}{H} + \gamma(2-\eta-4m) \right), -\zeta \left(\frac{z}{H} - 4n - \gamma(2-\eta) \frac{\tan \chi_H}{\tan \chi_V} \right) - 2 \right] \\ & + \left. \left[\Phi'_{i,j} \Big|_{\chi_H=\chi_V=90^\circ} - \Phi'_{i,j} \Big|_{\chi_H=90^\circ} \right] \left[\zeta \frac{x}{H} - \tan \chi_V, -\zeta \left(\frac{y}{H} + \gamma(2-\eta-4m) \right), -\zeta \left(\frac{z}{H} - 4n \right) - 1 \right] \right\} \end{aligned}$$

(Equation continued on next page)

$$\begin{aligned}
& + (-1)^q \left\{ \Phi_{i,j} \left[\zeta \frac{x}{H}, -\zeta \left(\frac{y}{H} + 2\gamma(2 - \eta - 2m) \right), -\zeta \left(\frac{z}{H} - 4n \right) - 2 \right] \right. \\
& + \left[\Phi_{i,j} \Big|_{\chi_H=90^\circ} - \Phi_{i,j} \right] \left[\zeta \left(\frac{x}{H} - \gamma(2 - \eta) \tan \chi_H \right), -\zeta \left(\frac{y}{H} + \gamma(2 - \eta - 4m) \right), -\zeta \left(\frac{z}{H} - 4n - \gamma(2 - \eta) \frac{\tan \chi_H}{\tan \chi_V} \right) - 2 \right] \\
& \left. + \left[\Phi_{i,j} \Big|_{\chi_H=\chi_V=90^\circ} - \Phi_{i,j} \Big|_{\chi_H=90^\circ} \right] \left[\zeta \frac{x}{H} - \tan \chi_V, -\zeta \left(\frac{y}{H} + \gamma(2 - \eta - 4m) \right), -\zeta \left(\frac{z}{H} - 4n \right) - 1 \right] \right\} \quad (60)
\end{aligned}$$

If $\delta_{i,j,k}$ is defined as before, that is, as

$$\Delta\varphi_{i,j,k} = \delta_{i,j,k} \frac{A_m}{A_T} \nu_i \quad (61)$$

then $\delta_{i,j,k}$ may be expressed as

$$\begin{aligned}
\delta_{i,j,k} = & -\frac{2\zeta^3\gamma}{\pi} \left[\sum_{m=-\infty}^{\infty} \sum_{\substack{n=-\infty \\ m=n \neq 0}}^{\infty} \Phi_{i,j,k} \left[\zeta \frac{x}{H}, \zeta \left(\frac{y}{H} - 4m\gamma \right), \zeta \left(\frac{z}{H} - 4n \right) \right] \right. \\
& + \sum_{m=-\infty}^{\infty} \sum_{n=-\infty}^{\infty} \left(\left[\Phi_{i,j,k} \Big|_{\chi_H=90^\circ} - \Phi_{i,j,k} \right] \left[\zeta \left(\frac{x}{H} - \gamma(2 - \eta) \tan \chi_H \right), \zeta \left(\frac{y}{H} + \gamma(2 - \eta - 4m) \right), \zeta \left(\frac{z}{H} - 4n + \gamma(2 - \eta) \frac{\tan \chi_H}{\tan \chi_V} \right) \right] \right. \\
& + \left. \left[\Phi_{i,j,k} \Big|_{\chi_H=\chi_V=90^\circ} - \Phi_{i,j,k} \Big|_{\chi_H=90^\circ} \right] \left[\zeta \frac{x}{H} - \tan \chi_V, \zeta \left(\frac{y}{H} + \gamma(2 - \eta - 4m) \right), \zeta \left(\frac{z}{H} - 4n \right) + 1 \right] \right. \\
& + (-1)^p \left\{ \Phi'_{i,j,k} \left[\zeta \frac{x}{H}, \zeta \left(\frac{y}{H} + 2\gamma(2 - \eta - 2m) \right), \zeta \left(\frac{z}{H} - 4n \right) \right] \right. \\
& + \left[\Phi'_{i,j,k} \Big|_{\chi_H=90^\circ} - \Phi'_{i,j,k} \right] \left[\zeta \left(\frac{x}{H} - \gamma(2 - \eta) \tan \chi_H \right), \zeta \left(\frac{y}{H} + \gamma(2 - \eta - 4m) \right), \zeta \left(\frac{z}{H} - 4n + \gamma(2 - \eta) \frac{\tan \chi_H}{\tan \chi_V} \right) \right] \\
& \left. + \left[\Phi'_{i,j,k} \Big|_{\chi_H=\chi_V=90^\circ} - \Phi'_{i,j,k} \Big|_{\chi_H=90^\circ} \right] \left[\zeta \frac{x}{H} - \tan \chi_V, \zeta \left(\frac{y}{H} + \gamma(2 - \eta - 4m) \right), \zeta \left(\frac{z}{H} - 4n \right) + 1 \right] \right\} \quad \text{(Equation continued on next page)}
\end{aligned}$$

$$\begin{aligned}
& + (-1)^{p+q+r} \left\{ \Phi'_{i,j,k} \left[\zeta \frac{x}{H}, -\zeta \left(\frac{y}{H} - 4m \right), -\zeta \left(\frac{z}{H} - 4n \right) - 2 \right] \right. \\
& + \left[\Phi'_{i,j,k} \Big|_{\chi_H=90^\circ} - \Phi'_{i,j,k} \right] \left[\zeta \left(\frac{x}{H} - \gamma(2-\eta) \tan \chi_H \right), -\zeta \left(\frac{y}{H} + \gamma(2-\eta-4m) \right), -\zeta \left(\frac{z}{H} - 4n - \gamma(2-\eta) \frac{\tan \chi_H}{\tan \chi_V} \right) - 2 \right] \\
& + \left[\Phi'_{i,j,k} \Big|_{\chi_H=\chi_V=90^\circ} - \Phi'_{i,j,k} \Big|_{\chi_H=90^\circ} \right] \left[\zeta \frac{x}{H} - \tan \chi_V, -\zeta \left(\frac{y}{H} + \gamma(2-\eta-4m) \right), -\zeta \left(\frac{z}{H} - 4n \right) - 1 \right] \Bigg\} \\
& + (-1)^{q+r} \left\{ \Phi_{i,j,k} \left[\zeta \frac{x}{H}, -\zeta \left(\frac{y}{H} + 2\gamma(2-\eta-2m) \right), -\zeta \left(\frac{z}{H} - 4n \right) - 2 \right] \right. \\
& + \left[\Phi_{i,j,k} \Big|_{\chi_H=90^\circ} - \Phi_{i,j,k} \right] \left[\zeta \left(\frac{x}{H} - \gamma(2-\eta) \tan \chi_H \right), -\zeta \left(\frac{y}{H} + \gamma(2-\eta-4m) \right), -\zeta \left(\frac{z}{H} - 4n - \gamma(2-\eta) \frac{\tan \chi_H}{\tan \chi_V} \right) - 2 \right] \\
& + \left[\Phi_{i,j,k} \Big|_{\chi_H=\chi_V=90^\circ} - \Phi_{i,j,k} \Big|_{\chi_H=90^\circ} \right] \left[\zeta \frac{x}{H} - \tan \chi_V, -\zeta \left(\frac{y}{H} + \gamma(2-\eta-4m) \right), -\zeta \left(\frac{z}{H} - 4n \right) - 1 \right] \Bigg\} \quad (62)
\end{aligned}$$

It will be observed that the central image describing the field of the wake in free air has been omitted from equations (60) and (62). This has been done since it is only the interference due to the walls which is of interest herein.

If χ_H and χ_V are both 90° , the wake passes downstream without touching the wind-tunnel boundaries. Thus, equations (55) to (58), (60), and (62) may be simplified by omitting all terms on the right-hand side of the equations except the first, fourth, seventh, and tenth sets of terms. (Note that under these conditions in each case, the equations are identical in cases I and II.) If only χ_V is 90° , the wake will touch the sidewall but not the floor of the wind tunnel. Thus, the third, sixth, ninth, and twelfth sets of terms on the right-hand side of equations (53), (58), (60), and (62) may be omitted. If only χ_H is 90° , the wake touches the floor but not the sidewall. This set of conditions falls under case I, the equations for which were developed in the preceding section of this paper.

Interference in Ground Effect

As mentioned previously, the initial wake image system considered in developing the wall corrections for case I corresponds to ground effect. Thus, if the interference in ground effect is expressed as

$$\Delta\varphi_{i,j} = \delta_{i,j} \frac{A_m}{A_G} \nu_i \quad (63)$$

where

$$A_G = 4h^2 \quad (64)$$

the interference factor can be determined immediately from equation (47) (by taking $H = h$, so that $\zeta = 1$, and $\gamma = 1$, and so that $A_T = A_G$, and by omitting the term corresponding to the real wake in free air) as

$$\begin{aligned} \delta_{i,j} = -\frac{2}{\pi} & \left(\left[\Phi_{i,j} \Big|_{\chi_V=90^\circ} - \Phi_{i,j} \right] \left[\frac{x}{h} - \tan \chi_V, \frac{y}{h} + \frac{\tan \chi_V}{\tan \chi_H}, \frac{z}{h} + 1 \right] + (-1)^{p+q} \left\{ \Phi'_{i,j} \left[\frac{x}{h}, -\frac{y}{h}, -\frac{z}{h} - 2 \right] \right. \right. \\ & \left. \left. + \left[\Phi'_{i,j} \Big|_{\chi_V=90^\circ} - \Phi'_{i,j} \right] \left[\frac{x}{h} - \tan \chi_V, -\left(\frac{y}{h} + \frac{\tan \chi_V}{\tan \chi_H} \right), -\frac{z}{h} - 1 \right] \right\} \right) \end{aligned} \quad (65)$$

If $\delta_{i,j,k}$ is defined as

$$\Delta\varphi_{i,j,k} = \delta_{i,j,k} \frac{A_m}{A_G} \nu_i \quad (66)$$

Similar treatment of equation (49) yields

$$\begin{aligned} \delta_{i,j,k} = -\frac{2}{\pi} & \left(\left[\Phi_{i,j,k} \Big|_{\chi_V=90^\circ} - \Phi_{i,j,k} \right] \left[\frac{x}{h} - \tan \chi_V, \frac{y}{h} + \frac{\tan \chi_V}{\tan \chi_H}, \frac{z}{h} + 1 \right] + (-1)^{p+q+r} \left\{ \Phi'_{i,j,k} \left[\frac{x}{h}, -\frac{y}{h}, -\frac{z}{h} - 2 \right] \right. \right. \\ & \left. \left. + \left[\Phi'_{i,j,k} \Big|_{\chi_V=90^\circ} - \Phi'_{i,j,k} \right] \left[\frac{x}{h} - \tan \chi_V, -\left(\frac{y}{h} + \frac{\tan \chi_V}{\tan \chi_H} \right), -\frac{z}{h} - 1 \right] \right\} \right) \end{aligned} \quad (67)$$

Note that if χ_V is greater than or equal to 90° the wake does not intersect the ground. Under these conditions, the foregoing equations become simply

$$\delta_{i,j} = -\frac{2}{\pi} (-1)^{p+q} \left\{ \Phi'_{i,j} \left[\frac{x}{h}, -\frac{y}{h}, -\frac{z}{h} - 2 \right] \right\} \quad (68)$$

and

$$\delta_{i,j,k} = -\frac{2}{\pi} (-1)^{p+q+r} \left\{ \Phi'_{i,j,k} \left[\frac{x}{h}, -\frac{y}{h}, -\frac{z}{h} - 2 \right] \right\} \quad (69)$$

As in reference 5, it is possible to express the interference factors at the center of lift in closed form when dealing with ground effect. Because of the vast multiplicity of interference factors involved in the present analysis it is impractical to present complete derivations of these factors as was done in the appendixes of reference 5. Instead, only the final closed-form expressions are presented in appendix C. The specific closed-form expressions for the partial derivatives of $\frac{A}{h}$ and $\frac{A'}{h}$, as used in deriving the results of appendix C, are given in table I.

Computer Program

Program features.- In general, the foregoing equations cannot be evaluated in closed form except for a few isolated special cases. Consequently it is necessary to resort to high-speed digital computing equipment in order to obtain numerical values. A listing of the program used to obtain the values which will be presented in subsequent portions of this paper is presented in appendix D. A flow chart for this program is presented in appendix E. Other programs were evolved in the course of the study which directly obtained values for the average interference, distribution of interference, and interference at the tail for lifting systems which could be represented by arbitrarily swept wings. These latter programs are not presented herein since the modifications to the listing of appendix D in order to obtain the more involved computer programs will be obvious from an examination of references 6 and 7.

The program of appendix D is very flexible. A series of χ_H and χ_V for which values are desired may be inserted as input data. For χ_H not equal to 90° , an additional vertical wake angle is added automatically, this angle being the particular χ_V which provides the borderline value separating cases I and II. This feature may be eliminated by a suitable input character if so desired; it is eliminated automatically if the extra angle is within 0.005° of one of the input angles.

Either ground effect or the closed-tunnel case may be selected by input data. For ground-effect calculations, ξ , η , and γ should be selected as 1.0.

In addition to the complete solution for all interference factors, two limiting options are available. In one, the calculations are limited to only those interference factors which pertain to velocities since these nine terms are those of primary interest in simple performance testing. In the other option, the terms relating to the longitudinal gradients are computed in addition to the aforementioned nine terms. This combination provides the interference factors of primary interest for tests involving only performance and longitudinal stability. The selection of either of these two options will reduce the computing time substantially. These options are not available for ground-effect calculations since the running time is so brief as to be immaterial.

It is obviously not possible to perform the required summations between infinite limits as indicated in the equations of the earlier sections of this paper. After several

trial calculations, it was found that summing over m and n between the limits of ± 3 appeared to achieve a reasonable compromise between speed and accuracy. Since the actual test section occupies one corner of a repetitive group of four images, this choice results in six columns of images to the right and seven columns of images to the left (as viewed from behind) of the real test section. Similarly, there will be six rows of images above and seven rows of images below the real test section. This image pattern differs from that of references 4 to 8 wherein there were only three image sections on each side of the test section, but the vertical arrangement therein is identical to that of the present paper.

Numerical checks.- Within the limits imposed by the different image systems, the interference factors obtained herein (when $\chi_H = 90^\circ$) are identical to those of references 4 to 8 which, in turn, are completely compatible with the values obtained ($\chi_V = \chi_H = 90^\circ$) by more conventional wall-interference calculations. Small residual values are obtained at $\chi_H = \chi_V = 90^\circ$ for certain terms for which symmetry requires that the values be zero. This result occurs because of the lack of complete symmetry in the image systems of the present paper and also in the image systems of references 4 to 8. These residual values could be reduced by increasing the limits of the summations; however, the increased computing time should not be worth the minor increase in numerical accuracy.

Several of the gradients can also be compared with references 5 to 7 by comparing the gradient computed herein with the plotted results for a series of points computed by the procedures of the earlier papers. Numerous such comparisons have been made, and in all cases the slopes agree.

The foregoing checks on numerical accuracy do not encompass cases in which the wake may be deflected to the side as well as downward. There are, however, numerous symmetries and equivalences which must be met in the results. These features will be discussed in the following several sections of the paper. All of these additional tests are met by the present theory as implemented by the program given in appendix D.

In ground effect it is possible to obtain a numerical check of the program accuracy for values of χ_H other than 90° since closed-form solutions for the interference factors at the center of lift have already been presented in appendix C. A comparison of the computed values obtained in both manners indicated complete agreement.

An additional numerical test was performed by calculating the interferences for a small model in the center of a square tunnel and choosing selected equal values of χ_H and χ_V . These choices duplicate the wake and tunnel configuration of the "diamond" test section of reference 17, for which results obtained by a different theoretical treatment are available. After the resolution of interference vectors required by the differing coordinate systems, the present results are identical to those of reference 17.

Skew angles in the second quadrant.- It has already been noted that the image systems in ground effect differ according to whether or not the vertical wake skew angle is greater than 90° . Thus, in ground effect, the program automatically chooses between equations (65) and (67) or equations (68) and (69) according to the value of χ_V .

Although it may not be as evident, the equations developed for the closed tunnel will also lead to an incorrect wake pattern if either χ_H or χ_V is greater than 90° . As will be discussed subsequently, appropriate values, for skew angles exceeding 90° , can be obtained from certain symmetry relations. This procedure is embodied in the computer program, which automatically sets up an equivalent problem in the first quadrant and then converts the results to correspond with the required angles in the second quadrant.

The superposition techniques used herein to obtain the field of wake segments of finite lengths can lead to numerical difficulties (of the nature of overflow and underflow) if the point of interest in the tunnel lies on or near an extension of any of the image wakes. Particular difficulty will be experienced for wake angles near zero. The program as presently constituted excludes values of the skew angles which are less than or equal to zero. Minor modifications to the program at lines (D 108) and (D 111) will allow the use of angles less than but not equal to zero; however, if zero is given as an input value, the execution of the program will terminate at that angle. Since the results of references 8, 10, 13, and 14 indicate that reasonable testing conditions cannot be obtained at very small skew angles, the practical effect of this restriction should be minimal.

Program storage requirements and running time.- The program of appendix D as implemented in the CDC 6600 computers of the Langley Research Center requires $42\,000_8$ (approximately $17\,500_{10}$) spaces in memory in order to compile. Execution of the program requires $24\,000_8$ (approximately $10\,300_{10}$) spaces.

The time required for the calculations varies according to the particular grouping of coefficients desired, the boundary conditions (ground effect or closed tunnel), and, since it is permissible to omit certain terms in those cases, whether χ_H , χ_V , or both are 90° . The following table gives the approximate central processor time (in seconds) required for each combination of one χ_H and one χ_V :

Approximate central processing time, in seconds, in the Langley computer complex				
Boundary conditions	Coefficients	General	$\chi_H = 90^\circ$ or $\chi_V = 90^\circ$	$\chi_H = \chi_V = 90^\circ$
Wind tunnel	All	9.3	5.7	2.1
	$\delta_{i,j}$ and $\delta_{i,j,x}$	5.7	3.5	1.3
	$\delta_{i,j}$ only	1.8	1.1	0.5
Ground effect	All	0.8	0.4	

In addition, when the computer task includes compilation from the FORTRAN listing, approximately 3.7 seconds will be required for the compilation.

Program efficiency.- The present computer program is not particularly efficient, and the computer time required when the program is expanded (by the techniques of ref. 6) to finite-span configurations is clearly excessive for routine application. In a sense, this inefficiency was deliberate in that it was desired to compute all terms in order to obtain a check on the symmetries rather than to use the symmetries to reduce the required running time. Substantial reduction in computer time could be obtained by reprogramming the calculations to take advantage of the symmetries.

Symmetry of Interference Factors

Wake in free air.- Because A and A' are both jointly continuous through at least the third order, as can be seen from equations (37) and (40), transposing the i and j in $\Phi_{i,j}$ (eq. (35)) or $\Phi'_{i,j}$ (eq. (38)), or transposing i , j , and k in any possible permutation in $\Phi_{i,j,k}$ (eq. (36)) or $\Phi'_{i,j,k}$ (eq. (39)) leaves these terms unaltered. Thus, there is a possibility that certain of the interference factors will also be unaltered by such operations. This portion of this report considers these symmetries separately for the cases of the wind tunnel first and then for the case of ground effect.

Wind-tunnel interference.- Examination of equations (52) and (60) indicates that an additional requirement for equality of the correction factors for the interference velocities is that $(-1)^p$, $(-1)^q$, and $(-1)^{p+q}$ must also be unaltered if the correction factors are to be unaltered by transposing i and j . No combinations of i and j exist which satisfy these requirements; therefore, in general, all of the correction factors for interference velocities differ. On the other hand, examination of equations (54) and (62) indicates that the additional requirement for equality of the factors for the slopes of the interference velocities is that $(-1)^p$, $(-1)^{q+r}$, and $(-1)^{p+q+r}$ be unaltered. Because of the way in which p , q , and r are related to the i -, j -, and k -directions, this requirement is far less restrictive than the corresponding requirement for the velocities, and immediately yields

$$\delta_{i,j,k} = \delta_{i,k,j} \quad (70)$$

Ground effect.- In ground effect, conditions for the equality are somewhat less restrictive. For example, for the interference factors describing velocities, it is only necessary that $(-1)^{p+q}$ be unaltered if the factor is to be unaltered by interchanging i and j . Thus,

$$\delta_{x,y} = \delta_{y,x} \quad (71)$$

Similarly for the interference factors describing slopes, it is only necessary that $(-1)^{p+q+r}$ be unaltered by a permutation in i , j , and k . Thus, in addition to equation (70)

$$\delta_{x,y,y} = \delta_{y,y,x} = \delta_{y,x,y} \quad (72a)$$

$$\delta_{x,x,y} = \delta_{y,x,x} = \delta_{x,y,x} \quad (72b)$$

$$\delta_{x,y,z} = \delta_{y,x,z} = \delta_{x,z,y} = \delta_{y,z,x} \quad (72c)$$

The foregoing symmetries are displayed in table II, which reproduces the computer output for one set of conditions.

Interchange Equivalences

Between χ_H and χ_V .- An interesting and sometimes useful set of equivalences may be found by considering the manipulations shown schematically in figure 9. Consider an arbitrary initial wind tunnel as in figure 9(a) with the wake deflected both laterally and vertically, and at arbitrary point (x,y,z) at which the interferences are known. Rotation of the entire picture 90° counterclockwise yields the configuration shown in figure 9(b). Then reverse the configuration to a mirror image as in figure 9(c), and, finally, relabel the configuration to be in accord with the standard symbol nomenclature of this paper. The following table lists the pertinent quantities relating to figure 9(d) in terms of the initial values of figure 9(a).

Initial tunnel	Derived tunnel
χ_H	χ_V
χ_V	χ_H
x/H	$(1/\gamma)(x/H)$
y/H	$(1/\gamma)(z/H)$
z/H	$(1/\gamma)(y/H)$
γ	$1/\gamma$
ζ	$1/(2 - \eta)$
η	$2 - 1/\zeta$

Since it is obvious that there is no essential difference in the physical tunnels if the above conditions are met, the interference factors will be identical in the two cases provided only that in the subscripts of $\delta_{i,j}$, z and y are interchanged for each other wherever they occur. For example, in the final tunnel (fig. 9(d)), $\delta_{x,z}$, $\delta_{y,y}$, and $\delta_{z,y}$ are identical to $\delta_{x,y}$, $\delta_{z,z}$, and $\delta_{y,z}$, respectively, in the initial tunnel.

The gradients are only slightly more involved. In terms of constant unit lengths these quantities would be related in precisely the same manner as the velocities; however,

the gradients as obtained herein are with reference to the nondimensional quantities x_i/H . Thus, regardless of the direction of the gradient, its dimensions are those of a velocity per unit semiheight. Since the semiheight of the original tunnel is interchanged with the semiwidth of the final tunnel, these factors may be corrected to the new semiheight by multiplying the interchanged $\delta_{i,j,k}$ by γ (that is, for example, $\delta_{y,x,z}$ in the final tunnel is equal to $(\gamma) \cdot (\delta_{z,x,y})$ in the initial tunnel).

These relationships are demonstrated in table III by direct reproduction of the computer output for cases meeting the foregoing criteria. These relationships are particularly obvious for a centrally located model in a square test section, and still more obvious when χ_H and χ_V are identical.

The foregoing interchange relationships were very useful in checking the program of appendix D for cases in which the wake is deflected laterally. Not only do they provide a check on consistency of the results, but for $\chi_V = 90^\circ$ the computed interferences may be compared directly with the computed values of reference 5 for the equivalent tunnel.

It is observed that for wind-tunnel stability tests of conventional aircraft configurations, where the wake may generally be considered to be undeflected in either direction, these interchange equivalences may allow one to obtain the correct interference factors for side forces directly from available information (ref. 1) for "lift interference."

Strictly speaking, the interchange equivalences apply only to vanishing small models. If the model had been considered as a finite-span wing lying on the Y-axis of the initial tunnel, figure 9 indicates that the span would be lying on the Z-axis of the final tunnel. The net result would be an entirely different spatial distribution of vorticity in the tunnel. Under such circumstances, there is no reason to expect that the interference factors would follow the rules given here. Several sample calculations indicate that the theorem is not greatly violated for relatively short spans (say $\sigma = 0.25$); however, for large spans, significant differences arise (table IV).

Between values of χ_H in the first and second quadrants.- Now consider figures 9(e) and 9(f). Except for the positive direction of the Y-axis in figure 9(f), these two figures are equivalent provided that the conditions given in the following table are met:

Figure 9(e)	Figure 9(f)
χ_H	$180^\circ - \chi_H$
η	$2 - \eta$
y	$-y$

The effect of changing the positive sense of the Y-axis with respect to the wake depends solely on the number of differentiations with respect to y/H that are implied by the subscripts of $\Phi_{i,j}$, $\Phi_{i,j,k}$, $\delta_{i,j}$, and $\delta_{i,j,k}$ since, for complete equality of the results

between the two figures, it would be necessary to differentiate with respect to $-y/H$ for figure 9(e). Thus, the interference factors in which the subscript y appears an even number of times will be identical in the two cases, and those in which y appears an odd number of times will be identical except for a factor of -1 . As discussed earlier, this interchange is utilized in the FORTRAN program of appendix D to obtain interference factors when χ_H lies in the second quadrant.

If the model is in simple ground effect, or if the model is centered laterally in the closed tunnel, this interchange requires that the interference factors in which the subscript y appears an even number of times be symmetrical with respect to $\chi_H = 90^\circ$. Thus, this group of interference factors will be referred to as the symmetric factors herein. Similarly, if y appears an odd number of times, the interference factors will be antisymmetric about $\chi_H = 90^\circ$; consequently, this group will be referred to as the antisymmetric factors.

Observe that for laterally centered models a symmetric factor may have a substantial value at $\chi_H = 90^\circ$, but that it will vary relatively slowly for small departures from 90° because the rate of change of the factor must be zero at that point in order to allow symmetry. Since most lateral-directional stability testing involves only small lateral deflections of the wake, it may be perfectly acceptable to ignore the effect of χ_H on these factors, using only the values obtained at $\chi_H = 90^\circ$.

Further, in order that antisymmetry be maintained, all of the antisymmetric group of factors must be zero at $\chi_H = 90^\circ$ if the model is laterally centered. On the other hand, the rate of change of any of the factors with respect to χ_H could assume a large value. Thus some caution must be used in applying the present results if it is arbitrarily decided that the lateral deflection of the wake will be ignored.

In the special case of a laterally centered model with $\chi_H = 90^\circ$, the conditions specified in the foregoing table require that the symmetric factors have a symmetric distribution across the Y-axis. Under the same conditions, the antisymmetric factors will have an antisymmetric distribution across the Y-axis.

Between values of χ_V in the first and second quadrants.- Finally, consider figures 9(g) and 9(h). Except for the positive direction of the Z-axis in figure 9(h), these two figures are equivalent provided that the following conditions are met:

Figure 9(g)	Figure 9(h)
χ_V	$180^\circ - \chi_V$
ξ	$\xi/(2\xi - 1)$
z	$-z$

The effect of changing the positive sense of the Z-axis is similar to the effects discussed in the preceding section. The interference factors fall into symmetric and antisymmetric groups depending upon whether z is repeated an even or an odd number of times in the subscripts. Symmetric interference factors will be unaltered by the interchange, and antisymmetric factors will be altered in sign only.

If the model is centered vertically in the tunnel, the symmetric factors will be symmetric about $\chi_V = 90^\circ$ and the antisymmetric factors will be antisymmetric about $\chi_V = 90^\circ$. Again the symmetric factors may have significant values at $\chi_V = 90^\circ$, but these factors will vary only slowly for small deviations from 90° . The antisymmetric factors must be zero when $\chi_V = 90^\circ$, however, there is a possibility that they may be significantly altered for comparatively small vertical deflections of the wake. Furthermore, when $\chi_V = 90^\circ$, the symmetric factors will have symmetric distributions over the Z-axis and the antisymmetric factors will have antisymmetric distributions over the Z-axis.

It is important to observe that this interchange is completely voided in ground effect. The reason, of course, is that there is no restraint on the flow above the model. The only restraint is the ground below the model.

APPLICATION OF RESULTS

Wall-interference theory, in general, is limited to the calculations of the interference velocities and gradients which the walls contribute to the overall flow in the wind tunnel. Ideally, the process of correcting wind-tunnel data involves calculating the effect of these velocities and gradients upon the model and then subtracting these effects to obtain interference-free data. This ideal process is seldom attempted in practice. Indeed, for some of the more exotic V/STOL vehicles, there is no background theory available with which to make such calculations. In other cases, such as wings (for which modern vortex-lattice techniques could be used for relatively accurate calculations), the required computer time for elaborate correction techniques is excessive, and corrections to data are generally made by far more approximate techniques (ref. 1).

An alternative to the direct calculations and removal of wall-interference effects is to consider data correction as a problem in similitude. This is the most generally applied technique. In this manner, the performance as measured in the tunnel becomes simply the correct performance for an altered flight condition, or even for a model slightly altered from that actually tested in the wind tunnel. At times, such similitudes actually lead to alternative means of approximate direct calculations. This portion of the present paper will discuss a number of such techniques which, hopefully, will be of some help in applying the results of the foregoing analysis.

Interference Velocities

The preceding portions of this paper have obtained the interference velocities along each of the three axes of the tunnel as caused by forces along the three axes. The complete interference velocities are therefore given by

$$\Delta u = \sum_i \Delta \varphi_{i,x} \quad (73a)$$

$$\Delta v = \sum_i \Delta \varphi_{i,y} \quad (73b)$$

$$\Delta w = \sum_i \Delta \varphi_{i,z} \quad (73c)$$

Altered flight velocities.- The interference velocities given by equations (73) are superimposed on the main wind-tunnel velocity. Conceptually, the simplest means of accounting for these interference velocities is to assume that the measured data correspond to the performance in free air of a model having a forward speed of $V + \Delta u$ and a sink rate of Δw while it is translating to the left at a velocity of Δv . When the main tunnel velocity is small, this technique may be reasonably satisfactory since it corresponds roughly to the conditions occurring during a landing approach in a cross wind. At speeds corresponding to hovering (or near hovering) conditions it may even be the only reasonable approach; however, in general, in order to obtain meaningful equivalent flight conditions, it will be convenient to express at least one of the interference velocities as an angular change at the model.

Altered yaw angle.- Consider first an equivalent flight condition in which the longitudinal and vertical interferences are still considered as mere alterations in linear speeds, but in which the lateral interference velocity is to be expressed as an alteration of the effective yaw angle of the model. From figure 10, it may be seen that the effective forward speed becomes

$$V_c = \sqrt{(V + \Delta u)^2 + (\Delta v)^2} \quad (74)$$

and the corrected dynamic pressure is

$$q_c = \frac{1}{2} \rho [(V + \Delta u)^2 + (\Delta v)^2] \quad (75)$$

All of the coordinates in the tunnel-based axis system must now be altered to correspond with the new axis system by means of a rotation through an angle $\tan^{-1} [\Delta v / (V + \Delta u)]$ about the Z-axis. In matrix form

$$\begin{vmatrix} x_c \\ y_c \\ z_c \end{vmatrix} = \begin{vmatrix} \frac{V + \Delta u}{\sqrt{(V + \Delta u)^2 + (\Delta v)^2}} & \frac{\Delta v}{\sqrt{(V + \Delta u)^2 + (\Delta v)^2}} & 0 \\ \frac{-\Delta v}{\sqrt{(V + \Delta u)^2 + (\Delta v)^2}} & \frac{V + \Delta u}{\sqrt{(V + \Delta u)^2 + (\Delta v)^2}} & 0 \\ 0 & 0 & 1 \end{vmatrix} \begin{vmatrix} x \\ y \\ z \end{vmatrix} \quad (76)$$

The corrected yaw angle is obtained by transforming a unit vector along the forward axis of the model into the new coordinate system, and then observing that

$$\tan \psi_c = -\frac{y_c}{x_c} \quad (77)$$

Substitution of equation (76) into equation (77) yields

$$\tan \psi_c = \frac{\frac{\Delta v}{V + \Delta u} + \tan \psi}{1 - \frac{\Delta v}{V + \Delta u} \tan \psi} \quad (78)$$

or

$$\psi_c = \psi + \Delta\psi \quad (79a)$$

where

$$\Delta\psi = \tan^{-1} \left(\frac{\Delta v}{V + \Delta u} \right) \quad (79b)$$

It is easily verified that α is unaltered by the rotation since the rotation is about the Z-axis.

In terms of the correction angle $\Delta\psi$, the matrix transformation given by equation (76) becomes

$$\begin{vmatrix} x_c \\ y_c \\ z_c \end{vmatrix} = \begin{vmatrix} \cos \Delta\psi & \sin \Delta\psi & 0 \\ -\sin \Delta\psi & \cos \Delta\psi & 0 \\ 0 & 0 & 1 \end{vmatrix} \begin{vmatrix} x \\ y \\ z \end{vmatrix} \quad (80)$$

In the new coordinate system the force coefficients are obtained by subjecting the resultant-force vector to the same transformation as the simple coordinates (eq. (80)), and then normalizing the force components with respect to the corrected dynamic pressure given by equation (76) to obtain

$$C_{D_c} = (C_D \cos \Delta\psi + C_Y \sin \Delta\psi) \left/ \left(\frac{q_c}{q} \right) \right. \quad (81a)$$

$$C_{Y_c} = (-C_D \sin \Delta\psi + C_Y \cos \Delta\psi) \left/ \left(\frac{q_c}{q} \right) \right. \quad (81b)$$

$$C_{L_c} = C_L \left/ \left(\frac{q_c}{q} \right) \right. \quad (81c)$$

where

$$\frac{q_c}{q} = \left(1 + \frac{\Delta u}{V} \right)^2 + \left(\frac{\Delta v}{V} \right)^2 \quad (81d)$$

In a similar manner, the components of the corrected moment are obtained as

$$C_{l_c} = (C_l \cos \Delta\psi + C_m \sin \Delta\psi) \left/ \left(\frac{q_c}{q} \right) \right. \quad (82a)$$

$$C_{m_c} = (-C_l \sin \Delta\psi + C_m \cos \Delta\psi) \left/ \left(\frac{q_c}{q} \right) \right. \quad (82b)$$

$$C_{n_c} = C_n \left/ \left(\frac{q_c}{q} \right) \right. \quad (82c)$$

Altered yaw angle and angle of attack.— An alternate viewpoint is to consider that the effective axis of the tunnel airstream is altered by the wall interference and that an equivalent flight condition may be obtained by merely resolving all of the data about the corrected stream axis. This is, by far, the most usual manner of dealing with wall effects. Referring to figure 11, it is obvious that the effective forward velocity along the new axis system will be

$$V_c = \sqrt{(V + \Delta u)^2 + (\Delta v)^2 + (\Delta w)^2} \quad (83)$$

or, in terms of dynamic pressure

$$\frac{q_c}{q} = \left(1 + \frac{\Delta u}{V} \right)^2 + \left(\frac{\Delta v}{V} \right)^2 + \left(\frac{\Delta w}{V} \right)^2 \quad (84)$$

All of the coordinates in the old tunnel-based coordinate system must now be altered to correspond with the new effective stream axes. The transformation may be accomplished by rotating the axis system about the Y-axis (fig. 11) through an angle $\tan^{-1} [\Delta w / (V + \Delta u)]$ and then about the new vertical axis through an angle $\tan^{-1} [\Delta v / \sqrt{(V + \Delta u)^2 + (\Delta w)^2}]$. Substantial complications are contributed by the fact that only one of the foregoing axis transformations may be taken about the original wind-tunnel axis system.

In matrix form

$$\begin{bmatrix} x_c \\ y_c \\ z_c \end{bmatrix} = \begin{bmatrix} \frac{\sqrt{(V+\Delta u)^2 + (\Delta w)^2}}{\sqrt{(V+\Delta u)^2 + (\Delta v)^2 + (\Delta w)^2}} & \frac{\Delta v}{\sqrt{(V+\Delta u)^2 + (\Delta v)^2 + (\Delta w)^2}} & 0 \\ \frac{-\Delta v}{\sqrt{(V+\Delta u)^2 + (\Delta v)^2 + (\Delta w)^2}} & \frac{\sqrt{(V+\Delta u)^2 + (\Delta w)^2}}{\sqrt{(V+\Delta u)^2 + (\Delta v)^2 + (\Delta w)^2}} & 0 \\ 0 & 0 & 1 \end{bmatrix} \begin{bmatrix} \frac{V+\Delta u}{\sqrt{(V+\Delta u)^2 + (\Delta w)^2}} & 0 & \frac{\Delta w}{\sqrt{(V+\Delta u)^2 + (\Delta w)^2}} \\ 0 & 0 & 1 \\ 1 & \frac{-\Delta w}{\sqrt{(V+\Delta u)^2 + (\Delta w)^2}} & 0 \end{bmatrix} \begin{bmatrix} x \\ y \\ z \end{bmatrix}$$

(85)

or, after multiplication of the transformation matrices,

$$\begin{bmatrix} x_c \\ y_c \\ z_c \end{bmatrix} = \begin{bmatrix} \frac{V+\Delta u}{\sqrt{(V+\Delta u)^2 + (\Delta v)^2 + (\Delta w)^2}} & \frac{\Delta v}{\sqrt{(V+\Delta u)^2 + (\Delta v)^2 + (\Delta w)^2}} & \frac{\Delta w}{\sqrt{(V+\Delta u)^2 + (\Delta v)^2 + (\Delta w)^2}} \\ \frac{-\Delta v(V+\Delta u)}{\sqrt{(V+\Delta u)^2 + (\Delta w)^2} \sqrt{(V+\Delta u)^2 + (\Delta v)^2 + (\Delta w)^2}} & \frac{\sqrt{(V+\Delta u)^2 + (\Delta w)^2}}{\sqrt{(V+\Delta u)^2 + (\Delta v)^2 + (\Delta w)^2}} & \frac{-\Delta v(\Delta w)}{\sqrt{(V+\Delta u)^2 + (\Delta w)^2} \sqrt{(V+\Delta u)^2 + (\Delta v)^2 + (\Delta w)^2}} \\ \frac{-\Delta w}{\sqrt{(V+\Delta u)^2 + (\Delta w)^2}} & 0 & \frac{V+\Delta u}{\sqrt{(V+\Delta u)^2 + (\Delta w)^2}} \end{bmatrix} \begin{bmatrix} x \\ y \\ z \end{bmatrix}$$

(86)

Expansion of equation (86) into its scalar components yields

$$x_c = \frac{(V + \Delta u) X + \Delta v y + \Delta w z}{\sqrt{(V + \Delta u)^2 + (\Delta v)^2 + (\Delta w)^2}} \quad (87)$$

$$y_c = \frac{-\Delta v(V + \Delta u) X + [(V + \Delta u)^2 + \Delta w^2] y - (\Delta v \Delta w) z}{\sqrt{(V + \Delta u)^2 + (\Delta v)^2 + (\Delta w)^2} \sqrt{(V + \Delta u)^2 + (\Delta w)^2}} \quad (88)$$

$$z_c = \frac{-(\Delta w) X + (V + \Delta u) z}{\sqrt{(V + \Delta u)^2 + (\Delta w)^2}} \quad (89)$$

The corrected angle of attack α_c and yaw angle $\psi_c (= -\beta_c)$ are obtained by transforming a unit vector $(-\cos \alpha \cos \psi) \bar{i} + (\cos \alpha \sin \psi) \bar{j} + (\sin \alpha) \bar{k}$ along the forward longitudinal model axis into the corrected axis system, and then noting that for this unit vector

$$\tan \alpha_c = \frac{z_c}{\sqrt{x_c^2 + y_c^2}} = \frac{z_c}{\sqrt{1 - z_c^2}} \quad (90)$$

and

$$\tan \psi_c = \frac{y_c}{-x_c} \quad (91)$$

Performing the indicated operations on equation (90) yields

$$\tan \alpha_c = \frac{\Delta w \cos \alpha \cos \psi + (V + \Delta u) \sin \alpha}{\sqrt{(V + \Delta u)^2 + (\Delta w)^2} - [\Delta w \cos \alpha \cos \psi + (V + \Delta u) \sin \alpha]^2} \quad (92)$$

which may be simplified by using the relationships of the right triangle to obtain

$$\sin \alpha_c = \frac{\Delta w \cos \alpha \cos \psi + (V + \Delta u) \sin \alpha}{\sqrt{(V + \Delta u)^2 + (\Delta w)^2}} \quad (93)$$

When $\psi = 0$, equation (92) may be reduced to

$$\tan \alpha_c = \frac{\tan \alpha + \frac{\Delta w}{V + \Delta u}}{1 - \frac{\Delta w}{V + \Delta u} \tan \alpha} = \tan \left(\alpha + \tan^{-1} \frac{\Delta w}{V + \Delta u} \right) \quad (94)$$

Therefore, when $\psi = 0$

$$\alpha_c = \alpha + \Delta\alpha \quad (95a)$$

where

$$\Delta\alpha = \tan^{-1} \frac{\Delta w}{V + \Delta u} \quad (95b)$$

Similarly, performing the aforementioned operations on equation (91) yields

$$\tan \psi_c = \frac{\Delta v(V + \Delta u) \cos \alpha \cos \psi + [(V + \Delta u)^2 + \Delta w^2] \cos \alpha \sin \psi - \Delta v \Delta w \sin \alpha}{\sqrt{(V + \Delta u)^2 + (\Delta w)^2} [(V + \Delta u) \cos \alpha \cos \psi - \Delta v \cos \alpha \sin \psi - \Delta w \sin \alpha]} \quad (96)$$

For the special case where $\alpha = \Delta w = 0$, equation (96) reduces to

$$\tan \psi_c = \frac{\frac{\Delta v}{V + \Delta u} + \tan \psi}{1 - \frac{\Delta v}{V + \Delta u} \tan \psi} = \tan \left(\psi + \tan^{-1} \frac{\Delta v}{V + \Delta u} \right) \quad (97)$$

or

$$\psi_c = \psi + \Delta\psi \quad (98a)$$

where

$$\Delta\psi = \tan^{-1} \frac{\Delta v}{V + \Delta u} \quad (98b)$$

Next, the force coefficients must be resolved about the corrected axis system.

This may be accomplished by transforming the resultant-force coefficient

$\bar{C}_R = \bar{i} C_D + \bar{j} C_Y + \bar{k} C_L$ in a manner identical to that of equation (86) and non-dimensionalizing the result with respect to the corrected dynamic pressure

$q_c = \frac{1}{2} \rho [(V + \Delta u)^2 + (\Delta v)^2 + (\Delta w)^2]$; thus,

$$C_{Dc} = \frac{V^2 [(V + \Delta u) C_D + \Delta v C_Y + \Delta w C_L]}{[(V + \Delta u)^2 + (\Delta v)^2 + (\Delta w)^2]^{3/2}} \quad (99)$$

$$C_{Yc} = \frac{V^2 \left\{ -\Delta v (V + \Delta u) C_D + [(V + \Delta u)^2 + (\Delta w)^2] C_Y - \Delta v \Delta w C_L \right\}}{[(V + \Delta u)^2 + (\Delta v)^2 + (\Delta w)^2]^{3/2} \sqrt{(V + \Delta u)^2 + (\Delta w)^2}} \quad (100)$$

$$C_{Lc} = \frac{V^2 [-\Delta w C_D + (V + \Delta u) C_L]}{[(V + \Delta u)^2 + (\Delta v)^2 + (\Delta w)^2] \sqrt{(V + \Delta u)^2 + (\Delta w)^2}} \quad (101)$$

Observe that the lift-drag ratio is also altered; that is, divide equation (101) by equation (99) to obtain

$$\left(\frac{L}{D} \right)_c = \left[\frac{-\Delta w C_D + (V + \Delta u) C_L}{(V + \Delta u) C_D + \Delta v C_Y + \Delta w C_L} \right] \sqrt{\frac{(V + \Delta u)^2 + (\Delta v)^2 + (\Delta w)^2}{(V + \Delta u)^2 + (\Delta w)^2}} \quad (102)$$

In addition, the moments must also be resolved about the corrected axis system. Following the same procedure as for the forces, rotate the resultant moment vector into the new coordinate system and nondimensionalize with respect to q_c to obtain

$$C_{lc} = \frac{V^2 [(V + \Delta u) C_l + \Delta v C_m + \Delta w C_n]}{[(V + \Delta u)^2 + (\Delta v)^2 + (\Delta w)^2]^{3/2}} \quad (103)$$

$$C_{mc} = \frac{V^2 \left\{ -\Delta v (V + \Delta u) C_l + [(V + \Delta u)^2 + (\Delta w)^2] C_m - \Delta v \Delta w C_n \right\}}{[(V + \Delta u)^2 + (\Delta v)^2 + (\Delta w)^2]^{3/2} \sqrt{(V + \Delta u)^2 + (\Delta w)^2}} \quad (104)$$

$$C_{nc} = \frac{V^2 [-\Delta w C_l + (V + \Delta u) C_n]}{[(V + \Delta u)^2 + (\Delta v)^2 + (\Delta w)^2] \sqrt{(V + \Delta u)^2 + (\Delta w)^2}} \quad (105)$$

Scalar qualities.— Scalar quantities such as power are unaltered by the foregoing axis transformations; however, if such quantities are formed into nondimensional terms by dividing by V or q , then the nondimensional parameter must be corrected to correspond to the corrected V or q . Thus, for example, if

$$C_{\mu} = \frac{\text{Momentum}}{qS} \quad (106a)$$

then

$$C_{\mu c} = \frac{C_{\mu} V^2}{[(V + \Delta u)^2 + (\Delta v)^2 + (\Delta w)^2]} \quad (106b)$$

Particular caution is required in correcting certain other parameters; for example, the tip-speed ratio used in helicopter tests

$$\mu = \frac{V \cos \alpha}{\text{Tip speed}} \quad (107)$$

requires corrections to both velocity (eq. (83)) and angle of attack (eq. (92) or (93)).

Interference Gradients

General comments.- If the interference velocities were completely uniform over the model, there would be little difficulty in correcting wind-tunnel data; indeed, the foregoing several sections of this paper would suffice for an almost complete treatment. If the model was extraordinarily small, the deviation of the interferences from the average values would be negligible, and thus, in combination with the small ratio of model to tunnel sizes, it would be permissible to neglect the effect of the interference velocity differences over the model. Unfortunately, in the usual wind-tunnel tests, the model has significant dimensions compared to the wind-tunnel test section, and significant variations in wall-induced interference velocities occur over the extent of the model. Thus, it is necessary to account for the effect of these differences in interference velocity over the model.

The actual techniques by which corrections for interference nonuniformity could be calculated depend entirely upon the available theoretical aerodynamic treatments in non-uniform flow for the particular model under test. For a conventional airplane configuration, the powerful numerical techniques of vortex-lattice theory, at least in principle, could be used to estimate the effects of interference nonuniformity and to develop corrections to the measured data. Unfortunately, this approach might possibly involve such excessive amounts of computer time that it would be uneconomic for routine use, and even then would not account for the possibility that the nonuniform wall-induced interference might alter flow separations occurring as the model conditions approach either complete or local stall. For less conventional models, this technique is not generally available, and for many of the profusion of V/STOL aircraft types, there is no truly adequate theory

at all. Thus, in most cases, it will be necessary to use correction treatments which are only crude approximations of the actual effect of flow nonuniformity.

Even if the most rigorous type of theoretical treatment were available for correcting data, a certain amount of caution would be required. If the size of the corrections becomes comparable to the magnitude of the measured data, it is obvious that the corrected data are as much a product of theory as of the wind-tunnel measurements. At this point it becomes questionable as to whether or not the wind-tunnel tests have contributed significantly to the determination of the model characteristics.

The surest procedure which avoids the problems inherent in large corrections for flow nonuniformity is to avoid testing models which are large relative to the test-section dimensions. Many rules of thumb have been offered as to allowable model sizes; however, none of these rules is failure free. This trend is enforced by recent studies which indicate limits to theoretical calculations because of wake deformation (ref. 18) and the need for a reduction in allowable correction size when testing swept wings (ref. 19). When the primary concern is nonuniformity, a reduction in model size is doubly helpful: first, the reduction in area ratio reduces the overall corrections immediately; second, the model does not extend as far in any direction and thus, for a given rate of change of interference in that direction, will experience a lesser nonuniformity.

If the model size is reasonably small, many of the interference gradients are relatively uniform across the model. Thus, some simple concepts can be used to develop comparatively simple first-order corrections. Thus, it is profitable to discuss a few of these concepts in the following pages. For the sake of convenience in the discussion, the model axes will be considered to be coincident with the principal axes of the tunnel. Similar considerations would apply for any other model orientation, although considerable resolution of the interference vectors might be required to obtain an equivalent frame of reference.

The direct gradients.- Consider first the rates of change along each axis of the interference velocities directed along those axes; that is,

$$\frac{\partial(\Delta u)}{\partial(x/H)} = \sum_i \Delta\varphi_{i,x,x} \quad (108a)$$

$$\frac{\partial(\Delta v)}{\partial(y/H)} = \sum_i \Delta\varphi_{i,y,y} \quad (108b)$$

$$\frac{\partial(\Delta w)}{\partial(z/H)} = \sum_i \Delta\varphi_{i,z,z} \quad (108c)$$

A positive value of any of these three derivatives indicates that the interference velocity increases with positive distance along the axis. Compared to a uniform stream

in free flight the equivalent free-air model would have a velocity field which would expand along these axes. While such a concept seems difficult, it is precisely equivalent in the X-direction to the q_t/q term applied to tail forces in most stability analyses. For conventional models, it would be expected that the largest effect of these derivatives would be an alteration in the effective dynamic pressure at the tail.

The gradients $\frac{\partial(\Delta w)}{\partial(x/H)}$ and $\frac{\partial(\Delta u)}{\partial(z/H)}$.- Consider next the gradients

$$\frac{\partial(\Delta w)}{\partial(x/H)} = \sum_i \Delta \varphi_{i,z,x} \quad (109a)$$

$$\frac{\partial(\Delta u)}{\partial(z/H)} = \sum_i \Delta \varphi_{i,x,z} \quad (109b)$$

The positive sense of these gradients is indicated in figure 12(a). Along the X-axis the distortions in the vertical components of the interference velocities are the same as if the model in free air were rotating about the Y-axis in a nose-up direction. On the other hand, the horizontal velocities along the Z-axis are those that a model in free air would experience if it were rotating about the Y-axis in a nose-down direction. Furthermore, in consequence of the symmetries of the interference factors ($\delta_{i,j,k} = \delta_{i,k,j}$), the two equivalent rotational rates must be identical except for their opposing directions.

If the model was spherically symmetrical, and if there was no forward velocity, such a distortion of the flow field might have little or no effect on the observed performance. Such conditions are seldom met, however, and the effects encountered in practice may be approximated by considering separately the different portions of the model. If the model was a conventional aircraft and lay in the X-Y plane, the effect would be primarily that of an effective pitch rate at constant angle of attack; that is (from ref. 2),

$$\dot{\theta} = \frac{1}{H} \frac{\partial(\Delta w)}{\partial(x/H)} \quad (110)$$

The concept of an equivalent rotational rate may be helpful in developing corrections since a large number of studies exist in aerodynamic stability theory for the estimation of the effects of such rates of rotation. (See, for example, the survey presented in ref. 20.) An alternate viewpoint might be to try to account for the combined effects of an altered wing camber, tail height, and tail incidence (ref. 2) without any rotation rate.

If the model had a significant vertical extent (for example, a biplane of large gap), it might well be necessary to consider separately the effects of the tail system rotating at $\dot{\theta}$ and a biplane cell rotating at $-\dot{\theta}$. Further, if the model had a high T-tail, it might

be necessary to consider the additional alteration in the effective longitudinal velocity at the tail which would result from the vertical displacement above the plane of the lifting system.

For some simple systems, a search of older studies may even produce means of calculating the effects of these gradients directly. For example, reference 21 examines directly the effects of a linear gradient of induced velocity normal to the plane of a centrally hinged rotor and finds that the effect is largely that of an altered lateral flapping. Observe that if such a rotor is tested at extreme negative angle of attack the direction of the effects will change as the rotor plane approaches the vertical. It should also be observed that if the rotor hinges are eliminated and the blades are very rigid, that the effect of this gradient changes from a relatively innocuous lateral tilt to a very powerful pitching moment (ref. 22).

It is important to observe that entirely different corrections are appropriate to different configurations. For some models many of the interference velocities and gradients calculated herein will have no significant effect whatever and thus can be ignored. This does not necessarily mean that they can always be ignored safely since comparatively simple changes in configuration may affect the relative magnitudes of the different effects.

The gradients $\partial(\Delta u)/\partial(y/H)$ and $\partial(\Delta v)/\partial(x/H)$. - The gradients

$$\frac{\partial(\Delta u)}{\partial(y/H)} = \sum_i \varphi_{i,x,y} \quad (111a)$$

and

$$\frac{\partial(\Delta v)}{\partial(x/H)} = \sum_i \varphi_{i,y,x} \quad (111b)$$

are shown schematically in their positive senses in figure 12(b). Again the two effective rotations are equal but in opposite directions because of symmetry.

If the model was a conventional aircraft, the effects would be much the same as if the wings were experiencing a constant rate of yaw while the fuselage and tail would be experiencing the same rate of yaw in the opposite direction. The overall effect on the yawing moment corrections would depend upon the balance of these two effects.

If the model is a helicopter rotor, the effective rotational speed is increased when a blade lies along one axis and decreased when it lies along the other. There is no change in the average effective rotational speed of the rotor even though a small ripple is imposed on this rotational speed.

The gradients $\partial(\Delta v)/\partial(z/H)$ and $\partial(\Delta w)/\partial(y/H)$. - These gradients, shown schematically in figure 12(c) are given by

$$\frac{\partial(\Delta v)}{\partial(z/H)} = \sum_i \varphi_{i,y,z} \quad (112a)$$

$$\frac{\partial(\Delta w)}{\partial(y/H)} = \sum_i \varphi_{i,z,y} \quad (112b)$$

Again because of the symmetry of the interferences the two gradients are equal but opposite in direction. Thus, an axisymmetric model, such as a propeller, located in this plane would have no effective change in rotational rate. On the other hand, a wing lying along the Y-axis would be subjected to a wall-induced flow which would be the equivalent of a constant rate of roll in free air.

One aspect of dealing with distortions on the basis of a simple gradient should be noted carefully. Observe that for the wing on the Y-axis, only the antisymmetric part of the distortion can be described by a single gradient at the center of lift. Symmetrical distortions are entirely lost. Thus, if the interference increases or decreases symmetrically outward from the center of lift (as is usually the case with at least part of the interference in the lateral direction) this information will be lost. Such symmetric vertical interference along the Y-axis is equivalent to an effective alteration (with respect to free air) of the wash-in or wash-out of a wing (ref. 2). Similarly, a lateral gradient of $\partial(\Delta w)/\partial(y/H)$ would be equivalent to an effective alteration of the spanwise distribution of airfoil-section camber. Such wall-induced distortions can have significant effects on several observed quantities (such as the stall angle) and if the wing is swept can have significant effects on the longitudinal pitching moment as well (ref. 6). In correlation studies in which tests of the same model in different tunnels are compared (such as ref. 23) the pitching moments often correlate less well than the lifts and drags. The reason for the poorer correlation of moment can often be found in the failure to account for the effect of wall interference on the spanwise load distribution of a swept wing or a failure to account for the differences in wall interference at the wing and the tail (as in ref. 24).

If the model has any significant size with respect to the tunnel dimensions, it will be necessary to account for this size both by superposition of the present results to obtain interference factors corresponding to the actual finite-size configuration and by using the actual distributions of interference over the model in order to develop proper corrections from the interference velocity calculations. Some aspects of this problem will be examined in a later portion of this paper.

NUMERICAL RESULTS

Since the interference factors are expressed herein in an open form, it is difficult to determine the effect of changes in the input variables by examination of the equations themselves. Consequently, numerical results obtained from the previously described computer program will be presented to illustrate certain effects on the interference factors.

The only wind-tunnel configuration for which the present numerical results were obtained has a width-height ratio γ of 1.5. This width-height ratio approximates that of many operational wind tunnels. The interchange symmetries discussed earlier allow an immediate conversion of these values to correspond to a tunnel having a width-height ratio of 2/3. The model is centered in the tunnel at all times.

Interference at Model

Effect of χ_V . Figure 13 compares the interference factors in the wind tunnel and in ground effect for a wake which is laterally undeflected ($\chi_H = 90^\circ$). As predicted by the prior consideration of the effect of interchanging horizontal skew angles between the first and second quadrants, all of the interference factors for which the subscript y is repeated an odd number of times (the antisymmetric group with respect to y) are zero throughout the entire range of vertical skew angles. The remaining group (or the symmetric group with respect to y) displays a pronounced dependence upon the vertical skew angle with large values being obtained at low vertical skew angles.

The trends of the symmetric group of factors are similar in both the wind tunnel and in ground effect. Note that the factors for ground effect are defined with respect to an area ($A_G = 4h^2$) which is only two-thirds the reference area ($A_T = 4BH = 4\gamma H^2$) with respect to which the factors for the wind tunnel are defined. For small vertical skew angles, this factor is the largest part of the difference between the corresponding factors in the tunnel and in ground effect. Thus, at low wake angles, the floor of the tunnel provides the major contribution to the level of interference at the model. (This situation might be altered if the model were placed differently in the tunnel. The correspondence would be greater if the model were below the centerline of the tunnel; however, if the model were placed well above the centerline the ceiling would assume greater importance.) At higher wake angles, this relationship fails (for example, $\delta_{x,x,x}$ in fig. 13(a)) reflecting a much greater effect of the walls and ceiling on the interference factors.

If a lateral wake deflection is superimposed on the vertical deflection, as in figure 14 ($\chi_H = 60^\circ$) and in figure 15 ($\chi_H = 30^\circ$), significant changes are observed in the interference factors. First, the antisymmetric group of factors are no longer zero and may assume substantial values (for example, $\delta_{x,y,z}$ in figs. 14(b) and 15(b)). Secondly, because the wake strikes the wall first (case II) for $\chi_V > 68.95^\circ$ at $\chi_H = 60^\circ$ and for $\chi_V > 40.89^\circ$

at $\chi_H = 30^\circ$ (eqs. (44) and (46)), significant changes in the trend of several of the factors may be observed at these points (for example, $\delta_{z,z,y}$ in figs. 14(i) and 15(i)). No similar alteration is observed in the ground-effect interference factors since there is no wall present to alter the wake pattern in ground effect. In general, it will be observed that there is some increase in almost all of the interference factors as the horizontal skew angle decreases.

Effect of χ_H .- Similar presentations of the interference factors in figures 16 to 18 directly illustrate the variation of the interference factors with χ_H . Figure 16 has been prepared for $\chi_V = 90^\circ$ where the wake never reaches the floor. Figure 17 treats a vertical skew angle of 60° where the wake strikes the wall first for all $\chi_H < 49.11^\circ$, and figure 18 treats $\chi_V = 30^\circ$ where the wake strikes the wall first for all $\chi_H < 21.05^\circ$. In ground effect, varying χ_H produces relatively mild changes. This would be expected since with suitable resolutions of the axis system, the same results could be obtained from the $\chi_H = 90^\circ$ calculations. There is little correlation between the interference factors for ground effect and for the wind tunnel since the predominant effects on the variation of the factors with χ_H in the tunnel are caused by the walls in this case, and these walls are not present in ground effect. Some noticable changes in slope with respect to χ_H may be observed as the wake changes between striking the wall first and striking the floor first (for example, $\delta_{x,x,x}$ in fig. 18(a)). Note that in figure 16 where $\chi_H = 90^\circ$, the antisymmetric group of factors with respect to z (those in which the subscripts contain z an odd number of times) are zero in the wind tunnel. They are not zero in ground effect because the boundaries are not symmetric with respect to the X-Y plane.

Distribution of Interference Factors Over the Principal Axes

Longitudinal axis.- Figures 19 to 24 show the distribution over the X-axis of the factors representing the interference velocities for vertical skew angles of 90° , 60° , and 30° in combination with horizontal skew angles of 90° and 60° .

The physical concepts of nonuniform interference as rotational rates require that the interference velocities be simple linear functions of distance along a given direction. If this relationship is valid, at least approximately, in the region occupied by the model, it may be possible to obtain relatively simple closed-form expressions for the corrections resulting from the nonuniformity of the wall effects. Figures 19 to 24 examine the degree of approximation involved in such a linearization by comparing the values obtained by a direct calculation at a series of points along the X-axis with those obtained by using the interference gradients in the linear relationship

$$\delta_{i,j} = \delta_{i,j} \Big|_{\frac{x}{H}=0} + \frac{x}{H} \delta_{i,j,x} \Big|_{\frac{x}{H}=0} \quad (113)$$

Except for the combinations of skew angles which require certain factors and their gradients to be zero, it will be observed that very significant differences are obtained between the values at the model and the values corresponding to other points along this axis. These differences will affect measured pitching moments, particularly if the model has a long tail length. In most cases, the linear relationship using the interference gradients (eq. (113)) yields a reasonable approximation to the directly calculated interference factors for a distance on the order of one-third of a semiheight along the axis. This usable distance may shrink dramatically for wakes which have large deflections in either direction. A noticeable example of this trend is $\delta_{z,x}$ (figs. 21(c) and 24(c)), where the model must be relatively small longitudinally if equation (113) is to be used.

Lateral axis.- A similar comparison over the lateral axis is given in figures 25 to 30. Observe that the y-distance is nondimensionalized with respect to the semi-width B in these figures. Thus, the lateral analog of equation (113) becomes

$$\delta_{i,j} = \delta_{i,j} \Big|_{\frac{y}{H}=0} + \gamma \frac{y}{B} \delta_{i,j,y} \Big|_{\frac{y}{H}=0} \quad (114)$$

The interference distribution over the Y-axis is far from uniform. For the interference factors which are antisymmetric with respect to y, the linear relationship given by equation (114) will yield reasonable results over about the central quarter of the tunnel. The situation is far worse with respect to the symmetric interferences. The lateral variation of these interferences may be totally lost if represented by equation (114). (See, for example, $\delta_{z,x}$ and $\delta_{z,z}$ in fig. 27(c).) These interferences, being symmetric, cannot be represented as equivalent rates of rotation. Instead, their interaction with the model must be studied in detail. The effect on the measured data may be only a change in stall angle for an unswept wing; however, these symmetric interferences can produce significant pitching moments on a swept wing.

Vertical axis.- A similar comparison along the vertical axis is presented in figures 31 to 36. In this presentation, the interference factors are obtained from the gradients as

$$\delta_{i,j} = \delta_{i,j} \Big|_{\frac{z}{H}=0} + \frac{z}{H} \delta_{i,j,z} \Big|_{\frac{z}{H}=0} \quad (115)$$

As might be expected, the behavior over this axis is similar to that over the Y-axis since both axes are transverse to the tunnel stream axis. The antisymmetric factors with respect to z are represented reasonably well by the linear relationship for about the central quarter of the tunnel height; however, linear representation of the symmetric interference components is satisfactory. The rapid increase of interference near the floor when the wake is sharply deflected might be expected to lead to a reversed flow at the floor

itself as in references 8 and 11 with limitations on the maximum wake deflection (or minimum forward speed) which can be tolerated in the wind tunnel (refs. 2, 10, 13, and 14).

Effect of Finite Span

The preceding results, and the theoretical treatment given in the present paper, are all obtained by assuming that the model is vanishingly small. This artifice considerably simplifies the mathematical treatment and yields reasonably accurate interference factors for models which are quite small with respect to the wind tunnel. In practice, models tend to be rather too large for such a simplistic treatment, and the interference factors may be significantly altered for models of different sizes or of different configurations (refs. 1, 3, 5, and 6). In such cases, the theoretical treatment of the vanishingly small model can be used as a building block to obtain the appropriate results (by superposition) for models of large size. Reference 6 presents a systematic means of accomplishing these superpositions, and reference 7 provides specific FORTRAN programs (based on the theory of ref. 5) for a wide variety of configurations. The identical treatment has been applied herein to develop interference factors for an arbitrary swept wing of finite size. Since the one significant difference between the present programs and those given in appendixes B, C, and D of reference 7 is the provision of an arbitrary yaw angle, these programs are not reproduced herein; however, a few sample calculated results are now presented. These results should indicate the nature and magnitude of some of the effects of finite size.

Effect at model.- Figures 37 to 40 illustrate the effect of the ratio of model span to tunnel width on the interference factors. In all cases, the model is assumed to be an unswept wing, centered in the wind tunnel, and mounted at zero angle of yaw. While there are a few exceptions (for example, in fig. 38(g) for $\delta_{z,x,x}$ when $\chi_V > 35^\circ$), as a general rule the interference factors decrease continuously as the span-width ratio σ increases. This should not be construed as a decrease in the interference, for the actual interference depends on the product of the interference factor and the area ratio

$$\frac{A_m}{A_T} = \frac{\pi s^2}{4BH} = \frac{\pi}{4} \left(\frac{s}{B}\right)^2 \frac{B}{H} = \frac{\pi}{4} \sigma^2 \gamma \quad (116)$$

where A_m has been taken as the area of a circle circumscribing the wingtips. Examination of figures 38 to 49 indicates that the reduction in the interference factors is seldom of sufficient size to overcome the large increase in the area ratio $\frac{A_m}{A_T}$. Thus, the interference in the tunnel will increase with increases in model size, but not quite in proportion to σ^2 . The effect of σ is sufficiently great that finite span should certainly be included in the calculations whenever the model span exceeds about 10 percent of the wind-tunnel width.

Effect on distribution over the principal axes.- The distributions of interference factors over the principal axes have been obtained for a centered unswept wing with zero yaw when the wing spans half of the tunnel width ($\sigma = 0.5$). These distributions are presented in figures 41 to 58. The directly calculated distributions are compared with those obtained from the gradient using the values calculated at the center of the wing and also using the values obtained by averaging over the span of the entire wing. The lateral distributions (figs. 47 to 52) are presented in terms of y/s where s is the semispan of the wing. In terms of this parameter, equation (114) may be rewritten as

$$\delta_{i,j} = \delta_{i,j} \Big|_{\frac{y}{H}=0} + \sigma \gamma \frac{y}{s} \delta_{i,j,y} \Big|_{\frac{y}{H}=0} \quad (117)$$

Examination of figures 41 to 58 indicates that the extent of agreement between the direct and linearized $\delta_{i,j}$ is about the same as for the vanishingly small model. Along the lateral axis there is actually some small improvement presumably because the wake itself is spread over this axis. As might be expected, using the average values of the slope and intercept in equation (117) yields a better approximation to the distribution over the Y-axis; however, there is still a substantial loss of information if the symmetric factors (with respect to y) are represented by the linearized form. The values along the X- and Z-axes are represented better by using the centerline values in equations (113) and (115) since the directly computed values are not averages over a finite span but represent only the value on the axis itself.

Effect of differences in configuration.- The effect of differences in configuration is briefly examined in figures 59 to 62 for two combinations of wake skew angles ($\chi_H = \chi_V = 90^\circ$ and $\chi_H = \chi_V = 60^\circ$). As before, the span of the wings is half the width of the tunnel, and the apex of the wing lifting line is centered in the tunnel. Only the factors yielding the velocities and their gradients in the X-direction are presented. The configurations compared have either 0° or 45° of sweep and a yaw angle of either 0° or 45° . In all cases, the distribution shown is along the lifting line of the wing.

These figures indicate substantial differences in the gradient interference over the span. Conversion of these interference velocities into their effect on the span loading would result in corrections to both pitching and rolling moments. Observe that the gradients in the X-direction are often thought of as an effective camber, but that for the 45° swept wing with 45° of yaw the effect on one half of the wing is more nearly of the nature of an altered dihedral angle since that side of the wing lies along the X-axis.

Even though the effects of interference distributions such as these can be large, it is somewhat difficult to envision complete corrections being made in a routine fashion. Even though reasonably complete treatments of spanwise loading are available for wings, it would appear that the required expenditure of effort and computer time would be excessive.

It might be considerably more effective to examine the interferences prior to test and to choose a model size such as to minimize the corrections to the point where cruder approximations to the actual corrections may suffice. Such a pre-examination will most likely indicate that models intended for lateral-directional stability testing should be somewhat smaller than models intended solely for symmetrical tests (such as performance or longitudinal stability).

CONCLUDING REMARKS

A theory has been presented which predicts the interference velocities caused by the walls of a wind tunnel as well as the gradients of these interference velocities over the principal axes of the tunnel. The theory allows for large wake deflections in both the lateral and vertical directions. It includes available V/STOL interference theory, where the wake is deflected only in the vertical direction, and conventional interference theory, where the wake is completely undeflected, as special cases. Various symmetry and interchange relationships are developed which by themselves, provide significant restraints on the interferences, and a large number of numerical results typifying the behavior of the interference factors have been presented. The equivalent results for ground effect appear as a degenerate case of wall interference.

Although the application of this interference study to the correction of data has been discussed in general terms, its immediate application depends upon the availability of adequate theoretical aerodynamic treatments of the effects of a nonuniform flow field on the model. Even for conventional configurations, where numerical vortex-lattice theory could, in principle, be used, such corrections may possibly be uneconomically time consuming. For more unconventional aircraft, adequate theoretical treatments often do not exist and rigorous corrections are not possible.

Langley Research Center,
National Aeronautics and Space Administration,
Hampton, Va., April 6, 1971.

APPENDIX A

PARTIAL DERIVATIVES OF $\frac{A}{h}$

Let

$$R_O = \sqrt{\left(\xi \frac{x}{H}\right)^2 + \left(\xi \frac{y}{H}\right)^2 + \left(\xi \frac{z}{H}\right)^2}$$

and

$$C_{HV} = \sqrt{1 - \cos^2 \chi_H \cos^2 \chi_V}$$

General Case

From equation (29b) and the above definitions, $\frac{A}{h}$ is

$$\frac{A}{h} = R_O C_{HV} - \left(\xi \frac{x}{H}\right) \sin \chi_H \sin \chi_V + \left(\xi \frac{y}{H}\right) \sin \chi_V \cos \chi_H + \left(\xi \frac{z}{H}\right) \sin \chi_H \cos \chi_V \quad (A1.1)$$

From equation (A1.1), the partial derivatives of the first order are

$$\frac{\partial \left(\frac{A}{h}\right)}{\partial \left(\frac{x}{h}\right)} = \frac{\left(\xi \frac{x}{H}\right) C_{HV}}{R_O} - \sin \chi_H \sin \chi_V \quad (A1.2)$$

$$\frac{\partial \left(\frac{A}{h}\right)}{\partial \left(\frac{y}{h}\right)} = \frac{\left(\xi \frac{y}{H}\right) C_{HV}}{R_O} + \sin \chi_V \cos \chi_H \quad (A1.3)$$

$$\frac{\partial \left(\frac{A}{h}\right)}{\partial \left(\frac{z}{h}\right)} = \frac{\left(\xi \frac{z}{H}\right) C_{HV}}{R_O} + \sin \chi_H \cos \chi_V \quad (A1.4)$$

From equations (A1.2) to (A1.4), the partial derivatives of the second order are

$$\frac{\partial^2 \left(\frac{A}{h}\right)}{\partial \left(\frac{x}{h}\right)^2} = \frac{C_{HV}}{R_O} \left[1 - \frac{\left(\xi \frac{x}{H}\right)^2}{R_O^2} \right] \quad (A1.5)$$

$$\frac{\partial^2 \left(\frac{A}{h}\right)}{\partial \left(\frac{y}{h}\right)^2} = \frac{C_{HV}}{R_O} \left[1 - \frac{\left(\xi \frac{y}{H}\right)^2}{R_O^2} \right] \quad (A1.6)$$

APPENDIX A – Continued

$$\frac{\partial^2 \left(\frac{A}{h} \right)}{\partial \left(\frac{z}{h} \right)^2} = \frac{C_{HV}}{R_O} \left[1 - \frac{\left(\zeta \frac{z}{H} \right)^2}{R_O^2} \right] \quad (A1.7)$$

$$\frac{\partial^2 \left(\frac{A}{h} \right)}{\partial \left(\frac{x}{h} \right) \partial \left(\frac{y}{h} \right)} = - \frac{\left(\zeta \frac{x}{H} \right) \left(\zeta \frac{y}{H} \right) C_{HV}}{R_O^3} \quad (A1.8)$$

$$\frac{\partial^2 \left(\frac{A}{h} \right)}{\partial \left(\frac{x}{h} \right) \partial \left(\frac{z}{h} \right)} = - \frac{\left(\zeta \frac{x}{H} \right) \left(\zeta \frac{z}{H} \right) C_{HV}}{R_O^3} \quad (A1.9)$$

$$\frac{\partial^2 \left(\frac{A}{h} \right)}{\partial \left(\frac{y}{h} \right) \partial \left(\frac{z}{h} \right)} = - \frac{\left(\zeta \frac{y}{H} \right) \left(\zeta \frac{z}{H} \right) C_{HV}}{R_O^3} \quad (A1.10)$$

From equations (A1.5) to (A1.10), the partial derivatives of the third order are

$$\frac{\partial^3 \left(\frac{A}{h} \right)}{\partial \left(\frac{x}{h} \right)^3} = \frac{3 \left(\zeta \frac{x}{H} \right) C_{HV}}{R_O^3} \left[\frac{\left(\zeta \frac{x}{H} \right)^2}{R_O^2} - 1 \right] \quad (A1.11)$$

$$\frac{\partial^3 \left(\frac{A}{h} \right)}{\partial \left(\frac{y}{h} \right)^3} = \frac{3 \left(\zeta \frac{y}{H} \right) C_{HV}}{R_O^3} \left[\frac{\left(\zeta \frac{y}{H} \right)^2}{R_O^2} - 1 \right] \quad (A1.12)$$

$$\frac{\partial^3 \left(\frac{A}{h} \right)}{\partial \left(\frac{z}{h} \right)^3} = \frac{3 \left(\zeta \frac{z}{H} \right) C_{HV}}{R_O^3} \left[\frac{\left(\zeta \frac{z}{H} \right)^2}{R_O^2} - 1 \right] \quad (A1.13)$$

$$\frac{\partial^3 \left(\frac{A}{h} \right)}{\partial \left(\frac{x}{h} \right)^2 \partial \left(\frac{y}{h} \right)} = \frac{\left(\zeta \frac{y}{H} \right) C_{HV}}{R_O^3} \left[\frac{3 \left(\zeta \frac{x}{H} \right)^2}{R_O^2} - 1 \right] \quad (A1.14)$$

$$\frac{\partial^3 \left(\frac{A}{h} \right)}{\partial \left(\frac{x}{h} \right)^2 \partial \left(\frac{z}{h} \right)} = \frac{\left(\zeta \frac{z}{H} \right) C_{HV}}{R_O^3} \left[\frac{3 \left(\zeta \frac{x}{H} \right)^2}{R_O^2} - 1 \right] \quad (A1.15)$$

$$\frac{\partial^3 \left(\frac{A}{h} \right)}{\partial \left(\frac{y}{h} \right)^2 \partial \left(\frac{x}{h} \right)} = \frac{\left(\zeta \frac{x}{H} \right) C_{HV}}{R_O^3} \left[\frac{3 \left(\zeta \frac{y}{H} \right)^2}{R_O^2} - 1 \right] \quad (A1.16)$$

APPENDIX A – Continued

$$\frac{\partial^3 \left(\frac{A}{h} \right)}{\partial \left(\frac{y}{h} \right)^2 \partial \left(\frac{z}{h} \right)} = \frac{\left(\xi \frac{z}{H} \right) C_{HV}}{R_O^3} \left[\frac{3 \left(\xi \frac{y}{H} \right)^2}{R_O^2} - 1 \right] \quad (A1.17)$$

$$\frac{\partial^3 \left(\frac{A}{h} \right)}{\partial \left(\frac{z}{h} \right)^2 \partial \left(\frac{x}{h} \right)} = \frac{\left(\xi \frac{x}{H} \right) C_{HV}}{R_O^3} \left[\frac{3 \left(\xi \frac{z}{H} \right)^2}{R_O^2} - 1 \right] \quad (A1.18)$$

$$\frac{\partial^3 \left(\frac{A}{h} \right)}{\partial \left(\frac{z}{h} \right)^2 \partial \left(\frac{y}{h} \right)} = \frac{\left(\xi \frac{y}{H} \right) C_{HV}}{R_O^3} \left[\frac{3 \left(\xi \frac{z}{H} \right)^2}{R_O^2} - 1 \right] \quad (A1.19)$$

$$\frac{\partial^3 \left(\frac{A}{h} \right)}{\partial \left(\frac{x}{h} \right) \partial \left(\frac{y}{h} \right) \partial \left(\frac{z}{h} \right)} = \frac{3 \left(\xi \frac{x}{H} \right) \left(\xi \frac{y}{H} \right) \left(\xi \frac{z}{H} \right)}{R_O^5} C_{HV} \quad (A1.20)$$

Special Case of $\chi_V = 90^\circ$

Setting $\chi_V = 90^\circ$ in equations (A1.1) to (A1.20) yields

$$\frac{A}{h} = R_O - \left(\xi \frac{x}{H} \right) \sin \chi_H + \left(\xi \frac{y}{H} \right) \cos \chi_H \quad (A2.1)$$

The partial derivatives of the first order are

$$\frac{\partial \left(\frac{A}{h} \right)}{\partial \left(\frac{x}{h} \right)} = \frac{\left(\xi \frac{x}{H} \right)}{R_O} - \sin \chi_H \quad (A2.2)$$

$$\frac{\partial \left(\frac{A}{h} \right)}{\partial \left(\frac{y}{h} \right)} = \frac{\left(\xi \frac{y}{H} \right)}{R_O} + \cos \chi_H \quad (A2.3)$$

$$\frac{\partial \left(\frac{A}{h} \right)}{\partial \left(\frac{z}{h} \right)} = \frac{\left(\xi \frac{z}{H} \right)}{R_O} \quad (A2.4)$$

The partial derivatives of the second order are

$$\frac{\partial^2 \left(\frac{A}{h} \right)}{\partial \left(\frac{x}{h} \right)^2} = \frac{1}{R_O} \left[1 - \frac{\left(\xi \frac{x}{H} \right)^2}{R_O^2} \right] \quad (A2.5)$$

APPENDIX A – Continued

$$\frac{\partial^2 \left(\frac{A}{h} \right)}{\partial \left(\frac{y}{h} \right)^2} = \frac{1}{R_O} \left[1 - \frac{\left(\zeta \frac{y}{H} \right)^2}{R_O^2} \right] \quad (A2.6)$$

$$\frac{\partial^2 \left(\frac{A}{h} \right)}{\partial \left(\frac{z}{h} \right)^2} = \frac{1}{R_O} \left[1 - \frac{\left(\zeta \frac{z}{H} \right)^2}{R_O^2} \right] \quad (A2.7)$$

$$\frac{\partial^2 \left(\frac{A}{h} \right)}{\partial \left(\frac{x}{h} \right) \partial \left(\frac{y}{h} \right)} = - \frac{\left(\zeta \frac{x}{H} \right) \left(\zeta \frac{y}{H} \right)}{R_O^3} \quad (A2.8)$$

$$\frac{\partial^2 \left(\frac{A}{h} \right)}{\partial \left(\frac{x}{h} \right) \partial \left(\frac{z}{h} \right)} = - \frac{\left(\zeta \frac{x}{H} \right) \left(\zeta \frac{z}{H} \right)}{R_O^3} \quad (A2.9)$$

$$\frac{\partial^2 \left(\frac{A}{h} \right)}{\partial \left(\frac{y}{h} \right) \partial \left(\frac{z}{h} \right)} = - \frac{\left(\zeta \frac{y}{H} \right) \left(\zeta \frac{z}{H} \right)}{R_O^3} \quad (A2.10)$$

The partial derivatives of the third order are

$$\frac{\partial^3 \left(\frac{A}{h} \right)}{\partial \left(\frac{x}{h} \right)^3} = \frac{3 \left(\zeta \frac{x}{H} \right)}{R_O^3} \left[\frac{\left(\zeta \frac{x}{H} \right)^2}{R_O^2} - 1 \right] \quad (A2.11)$$

$$\frac{\partial^3 \left(\frac{A}{h} \right)}{\partial \left(\frac{y}{h} \right)^3} = \frac{3 \left(\zeta \frac{y}{H} \right)}{R_O^3} \left[\frac{\left(\zeta \frac{y}{H} \right)^2}{R_O^2} - 1 \right] \quad (A2.12)$$

$$\frac{\partial^3 \left(\frac{A}{h} \right)}{\partial \left(\frac{z}{h} \right)^3} = \frac{3 \left(\zeta \frac{z}{H} \right)}{R_O^3} \left[\frac{\left(\zeta \frac{z}{H} \right)^2}{R_O^2} - 1 \right] \quad (A2.13)$$

$$\frac{\partial^3 \left(\frac{A}{h} \right)}{\partial \left(\frac{x}{h} \right)^2 \partial \left(\frac{y}{h} \right)} = \frac{\left(\zeta \frac{y}{H} \right)}{R_O^3} \left[3 \frac{\left(\zeta \frac{x}{H} \right)^2}{R_O^2} - 1 \right] \quad (A2.14)$$

$$\frac{\partial^3 \left(\frac{A}{h} \right)}{\partial \left(\frac{x}{h} \right)^2 \partial \left(\frac{z}{h} \right)} = \frac{\left(\zeta \frac{z}{H} \right)}{R_O^3} \left[3 \frac{\left(\zeta \frac{x}{H} \right)^2}{R_O^2} - 1 \right] \quad (A2.15)$$

APPENDIX A – Continued

$$\frac{\partial^3 \left(\frac{A}{h} \right)}{\partial \left(\frac{Y}{h} \right)^2 \partial \left(\frac{X}{h} \right)} = \frac{\left(\zeta \frac{X}{H} \right)}{R_O^3} \left[\frac{3 \left(\zeta \frac{Y}{H} \right)^2}{R_O^2} - 1 \right] \quad (A2.16)$$

$$\frac{\partial^3 \left(\frac{A}{h} \right)}{\partial \left(\frac{Y}{h} \right)^2 \partial \left(\frac{Z}{h} \right)} = \frac{\left(\zeta \frac{Z}{H} \right)}{R_O^3} \left[\frac{3 \left(\zeta \frac{Y}{H} \right)^2}{R_O^2} - 1 \right] \quad (A2.17)$$

$$\frac{\partial^3 \left(\frac{A}{h} \right)}{\partial \left(\frac{Z}{h} \right)^2 \partial \left(\frac{X}{h} \right)} = \frac{\left(\zeta \frac{X}{H} \right)}{R_O^3} \left[\frac{3 \left(\zeta \frac{Z}{H} \right)^2}{R_O^2} - 1 \right] \quad (A2.18)$$

$$\frac{\partial^3 \left(\frac{A}{h} \right)}{\partial \left(\frac{Z}{h} \right)^2 \partial \left(\frac{Y}{h} \right)} = \frac{\left(\zeta \frac{Y}{H} \right)}{R_O^3} \left[\frac{3 \left(\zeta \frac{Z}{H} \right)^2}{R_O^2} - 1 \right] \quad (A2.19)$$

$$\frac{\partial^3 \left(\frac{A}{h} \right)}{\partial \left(\frac{X}{h} \right) \partial \left(\frac{Y}{h} \right) \partial \left(\frac{Z}{h} \right)} = \frac{3 \left(\zeta \frac{X}{H} \right) \left(\zeta \frac{Y}{H} \right) \left(\zeta \frac{Z}{H} \right)}{R_O^5} \quad (A2.20)$$

Special Case of $\chi_H = 90^\circ$

Setting $\chi_H = 90^\circ$ in equations (A1.1) to (A1.20) yields

$$\frac{A}{h} = R_O - \left(\zeta \frac{X}{H} \right) \sin \chi_V + \left(\zeta \frac{Z}{H} \right) \cos \chi_V \quad (A3.1)$$

The partial derivatives of the first order are

$$\frac{\partial \left(\frac{A}{h} \right)}{\partial \left(\frac{X}{h} \right)} = \frac{\left(\zeta \frac{X}{H} \right)}{R_O} - \sin \chi_V \quad (A3.2)$$

$$\frac{\partial \left(\frac{A}{h} \right)}{\partial \left(\frac{Y}{h} \right)} = \frac{\left(\zeta \frac{Y}{H} \right)}{R_O} \quad (A3.3)$$

$$\frac{\partial \left(\frac{A}{h} \right)}{\partial \left(\frac{Z}{h} \right)} = \frac{\left(\zeta \frac{Z}{H} \right)}{R_O} + \cos \chi_V \quad (A3.4)$$

APPENDIX A – Concluded

The partial derivatives of the second and third orders are as given in equations (A2.5) to (A2.20).

Special Case of $\chi_H = \chi_V = 90^\circ$

Setting $\chi_H = \chi_V = 90^\circ$ in equation (A1.1) yields

$$\frac{A}{h} = R_O - \left(\zeta \frac{x}{H} \right) \quad (A4.1)$$

The partial derivatives of the first order are

$$\frac{\partial \left(\frac{A}{h} \right)}{\partial \left(\frac{x}{h} \right)} = \frac{\left(\zeta \frac{x}{H} \right)}{R_O} - 1 \quad (A4.2)$$

$$\frac{\partial \left(\frac{A}{h} \right)}{\partial \left(\frac{y}{h} \right)} = \frac{\left(\zeta \frac{y}{H} \right)}{R_O} \quad (A4.3)$$

$$\frac{\partial \left(\frac{A}{h} \right)}{\partial \left(\frac{z}{h} \right)} = \frac{\left(\zeta \frac{z}{H} \right)}{R_O} \quad (A4.4)$$

The partial derivatives of the second and third order are as given in equations (A2.5) to (A2.20).

APPENDIX B

PARTIAL DERIVATIVES OF $\frac{A'}{h}$

In this appendix, the equation numbers are chosen to correspond with appendix A.

General Case

From equation (40), $\frac{A'}{h}$ is

$$\frac{A'}{h} = R_O C_{HV} - \left(\zeta \frac{x}{H} \right) \sin \chi_H \sin \chi_V - \left(\zeta \frac{y}{H} \right) \sin \chi_V \cos \chi_H + \left(\zeta \frac{z}{H} \right) \sin \chi_H \cos \chi_V \quad (B1.1)$$

so that

$$\frac{\partial \left(\frac{A'}{h} \right)}{\partial \left(\frac{y}{h} \right)} = \frac{\left(\zeta \frac{y}{H} \right) C_{HV}}{R_O} - \sin \chi_V \cos \chi_H \quad (B1.2)$$

Special Case of $\chi_V = 90^\circ$

$$\frac{A'}{h} = R_O - \left(\zeta \frac{x}{H} \right) \sin \chi_H - \left(\zeta \frac{y}{H} \right) \cos \chi_H \quad (B2.1)$$

so that

$$\frac{\partial \left(\frac{A'}{h} \right)}{\partial \left(\frac{y}{h} \right)} = \frac{\left(\zeta \frac{y}{H} \right)}{R_O} - \cos \chi_H \quad (B2.2)$$

All other values of the partial derivatives of $\frac{A'}{h}$ are identical with those in appendix A.

APPENDIX C

INTERFERENCES AND INTERFERENCE DERIVATIVES AT THE CENTER OF THE LIFTING SYSTEM IN GROUND EFFECT

Notation

Because of the length of many of the expressions derived herein, the following abbreviations are used both in this appendix and in table I:

$$c_H = \cos \chi_H \quad s_H = \sin \chi_H$$

$$c_V = \cos \chi_V \quad s_V = \sin \chi_V$$

$$C_{HV} = \sqrt{1 - \cos^2 \chi_H \cos^2 \chi_V}$$

Method of Derivation

The interference factors for the velocities are obtained by a straightforward substitution of $\Phi_{i,j}$ and $\Phi'_{i,j}$ into equation (65). Similarly, the interference factors for the derivatives of the velocities are obtained from equation (67). The values of A and A' and the derivatives thereof are given in table I. Substantial manipulation of the trigonometric terms is required to obtain the final results.

The symmetries discussed earlier (eqs. (70), (71), and (72)) are of substantial value. One velocity interference factor and 12 interference factors for the gradients are obtained directly from the remaining factors.

The expressions presented herein are valid only for $\chi_V \leq 90^\circ$. Simpler expressions for $\chi_V > 90^\circ$ may be derived from equations (68) and (69) in the main text.

Interference Factors for Velocities Caused by Forces in the X-Direction

$\delta_{x,x}$ -

$$\begin{aligned} \delta_{x,x} = \frac{1}{\pi} & \left[\frac{3s_H^6 c_V^4}{C_{HV}^4} - \frac{s_H^4 c_V^4}{s_V^2 C_{HV}^2} + \frac{2s_H^2 c_H^2 c_V^2}{s_V^2} - \frac{4(C_{HV} - s_V)}{C_{HV}} \right. \\ & \left. + \frac{4s_H^2 s_V^2 (C_{HV} - s_V)}{C_{HV}^3} - \frac{1}{2} \frac{c_H^2 C_{HV} - s_H^3 c_V}{C_{HV} - s_H c_V} \right] \end{aligned} \quad (C1a)$$

APPENDIX C - Continued

When χ_H is 90°

$$\delta_{x,x} = \frac{1}{\pi} \left(4s_V c_V^2 - 3s_V^2 c_V^2 + \frac{1}{2} \frac{c_V}{1 + c_V} \right) \quad (C1b)$$

Equation (C1b) is identical, except for notation, with the equivalent expression given as equation (A16) of reference 5.

When χ_V is 90°

$$\delta_{x,x} = - \frac{c_H^2}{2\pi} \quad (C1c)$$

When χ_H and χ_V are 90°

$$\delta_{x,x} = 0 \quad (C1d)$$

$\delta_{x,y}$

$$\delta_{x,y} = \frac{s_H c_H}{\pi} \left[\frac{3s_H^2 c_V^2 s_V^2}{C_{HV}^4} - \frac{4s_H^2 c_V^2 s_V^2}{C_{HV}^3 (C_{HV} + s_V)} - \frac{s_H^2 c_V^2}{C_{HV}^2} + \frac{2s_H^4 c_V^4}{s_V^2 C_{HV}^2} - \frac{1}{2} \frac{C_{HV} + s_H c_V}{C_{HV} - s_H c_V} \right] \quad (C2a)$$

When χ_H is 90°

$$\delta_{x,y} = 0 \quad (C2b)$$

When χ_V is 90°

$$\delta_{x,y} = \frac{s_H c_H}{2\pi} \quad (C2c)$$

$\delta_{x,z}$

$$\delta_{x,y} = \frac{s_H}{\pi} \left(\frac{3s_H^3 s_V c_V^3}{C_{HV}^4} - \frac{4s_H^3 c_V^3}{C_{HV}^3} + \frac{s_H^3 c_V^3}{s_V C_{HV}^2} - \frac{1}{2} \frac{s_V}{C_{HV} - s_H c_V} \right) \quad (C3a)$$

When χ_H is 90°

$$\delta_{x,y} = \frac{1}{\pi} \left(3s_V c_V^3 - 4c_V^3 - s_V c_V - \frac{1}{2} \tan \frac{\chi_V}{2} \right) \quad (C3b)$$

which is identical, except for notation, with the equivalent expression given as equation (A12) of reference 5.

APPENDIX C - Continued

When χ_V is 90°

$$\delta_{x,z} = -\frac{s_H}{2\pi} \quad (C3c)$$

When both χ_H and χ_V are 90°

$$\delta_{x,z} = -\frac{1}{2\pi} \quad (C3d)$$

Interference Factors for Velocities Caused by Forces in the Y-Direction

$\delta_{y,x}$ - See equations (C2).

$\delta_{y,y}$ -

$$\delta_{y,y} = \frac{1}{\pi} \left[\frac{s_H^4 c_V^2}{C_{HV}^4} - \frac{2s_H^2 s_V^2 c_H^2 c_V^2}{C_{HV}^4} - \frac{4s_H^4 c_V^2}{C_{HV}^3 (C_{HV} + s_V)} + \frac{4s_H^2 c_H^2 c_V^2}{C_{HV}^2} \right. \\ \left. - \frac{C_{HV}}{2(C_{HV} - s_H c_V)} + \frac{s_V^2 c_H^2}{2(C_{HV} - s_H c_V)^2} + \frac{s_H^4 c_V^2}{s_V^2 C_{HV}^2} - \frac{2s_H^2 c_H^2 c_V^2}{s_V^2} \right] \quad (C4a)$$

When χ_H is 90°

$$\delta_{y,y} = -\frac{1}{\pi} \left[(s_V - 3)(s_V - 1) + \frac{1}{2} \frac{1 + 2C_V}{1 + c_V} \right] \quad (C4b)$$

When χ_V is 90°

$$\delta_{y,y} = -\frac{s_H^2}{2\pi} \quad (C4c)$$

When both χ_H and χ_V are 90°

$$\delta_{y,y} = -\frac{1}{2\pi} \quad (C4d)$$

$\delta_{y,z}$ -

$$\delta_{y,z} = -\frac{c_H}{\pi} \left(\frac{3s_H^3 s_V c_V^3}{C_{HV}^4} - \frac{4s_H^3 c_V^3}{C_{HV}^3} + \frac{s_H^3 c_V^3}{s_V C_{HV}^2} - \frac{1}{2} \frac{s_V}{C_{HV} - s_H c_V} \right) \quad (C5a)$$

APPENDIX C – Continued

When χ_H is 90°

$$\delta_{y,z} = 0 \quad (C5b)$$

When χ_V is 90°

$$\delta_{y,z} = \frac{c_H}{2\pi} \quad (C5c)$$

Interference Factors for Velocities Caused by Forces in the Z-Direction

$\delta_{z,x}$

$$\delta_{z,x} = \frac{s_H}{\pi} \left(\frac{3s_H^3 s_V c_V^3}{C_{HV}^4} - \frac{s_H^3 c_V^3}{s_V C_{HV}^2} + \frac{1}{2} \frac{s_V}{C_{HV} - s_H c_V} \right) \quad (C6a)$$

When χ_H is 90°

$$\delta_{z,x} = \frac{1}{\pi} \left(3s_V c_V^3 + s_V c_V + \frac{1}{2} \tan \frac{\chi_V}{2} \right) \quad (C6b)$$

Equation (C6b) is identical, except for notation, with the equivalent expression given as equation (A8) of reference 5.

When χ_V is 90°

$$\delta_{z,x} = \frac{s_H}{2\pi} \quad (C6c)$$

When both χ_H and χ_V are 90°

$$\delta_{z,x} = \frac{1}{2\pi} \quad (C6d)$$

$\delta_{z,y}$

$$\delta_{z,y} = \frac{c_H}{\pi} \left(\frac{3s_H^3 s_V c_V^3}{C_{HV}^4} - \frac{s_H^3 c_V^3}{s_V C_{HV}^2} + \frac{1}{2} \frac{s_V}{C_{HV} - s_H c_V} \right) \quad (C7a)$$

When χ_H is 90°

$$\delta_{z,y} = 0 \quad (C7b)$$

APPENDIX C - Continued

When χ_V is 90°

$$\delta_{z,y} = -\frac{c_H}{2\pi} \quad (C7c)$$

$\delta_{z,z}$

$$\delta_{z,z} = -\frac{1}{\pi} \left(\frac{3s_H^4 c_V^4}{C_{HV}^4} + \frac{1}{2} \right) \quad (C8a)$$

When χ_H is 90°

$$\delta_{z,z} = -\frac{1}{\pi} \left(3c_V^4 + \frac{1}{2} \right) \quad (C8b)$$

Equation (C8b) is identical, except for notation, with the equivalent expression given as equation (A4) of reference 5.

When χ_V is 90°

$$\delta_{z,z} = -\frac{1}{2\pi} \quad (C8c)$$

When both χ_H and χ_V are 90°

$$\delta_{z,z} = -\frac{1}{2\pi} \quad (C8d)$$

Interference Factors for the Derivatives of the Velocities Caused by Forces in the X-Direction

$\delta_{x,x,x}$

$$\begin{aligned} \delta_{x,x,x} = \frac{s_H}{\pi} & \left[\frac{6s_H^3 s_V c_V^3 (C_{HV}^2 - s_H^2 s_V^2)}{C_{HV}^6} - \frac{4s_H^5 s_V^3 c_V^3}{C_{HV}^6} \right. \\ & - \frac{12s_H^3 c_V^3 (C_{HV}^2 - s_H^2 s_V^2)}{C_{HV}^5} + \frac{8s_H^5 c_V^3}{C_{HV}^3} - \frac{3s_V C_{HV}}{4(C_{HV} - s_H c_V)^2} \\ & + \frac{s_H^2 s_V^3}{2(C_{HV} - s_H c_V)^3} + \frac{3s_H^3 c_V^3 (C_{HV}^2 - s_H^2 s_V^2)}{s_V C_{HV}^4} \\ & \left. + \frac{3s_H^3 c_V^3 (C_{HV}^2 - s_H^2 s_V^2)}{s_V^3 C_{HV}^2} - \frac{4s_H^5 c_V^3}{s_V^3} \right] \quad (C9a) \end{aligned}$$

APPENDIX C - Continued

When χ_H is 90°

$$\delta_{x,x,x} = \frac{1}{\pi} \left[10s_V c_V^5 - 7s_V c_V^3 - 12c_V^5 + 8c_V^3 - \frac{1}{4} \left(\frac{1 + 2c_V}{1 + c_V} \right) \tan \frac{\chi_V}{2} \right] \quad (C9b)$$

When χ_V is 90°

$$\delta_{x,x,x} = -\frac{s_H}{2\pi} \left(c_H^2 + \frac{1}{2} \right) \quad (C9c)$$

When both χ_H and χ_V are 90°

$$\delta_{x,x,x} = -\frac{1}{4\pi} \quad (C9d)$$

$\delta_{x,x,y}$

$$\begin{aligned} \delta_{x,x,y} = & -\frac{c_H}{\pi} \left[\frac{2s_H^3 s_V c_V^3 (C_{HV}^2 - 5s_H^2 s_V^2)}{C_{HV}^6} - \frac{4s_H^3 c_V^3 (C_{HV}^2 - 3s_H^2 s_V^2)}{C_{HV}^5} \right. \\ & + \frac{8s_H^5 c_V^3}{C_{HV}^3} - \frac{s_V C_{HV}}{4(C_{HV} - s_H c_V)^2} + \frac{s_H^2 s_V^3}{2(C_{HV} - s_H c_V)^3} \\ & + \frac{s_H^3 c_V^3 (C_{HV}^2 - 3s_H^2 s_V^2)}{s_V C_{HV}^4} + \frac{s_H^3 c_V^3 (C_{HV}^2 - s_H^2 s_V^2)}{s_V^3 C_{HV}^2} \\ & \left. - \frac{2s_H^5 c_V^3}{s_V C_{HV}^2} - \frac{4s_H^5 c_V^3}{s_V^3} \right] \quad (C10a) \end{aligned}$$

When χ_H is 90°

$$\delta_{x,x,y} = 0 \quad (C10b)$$

When χ_V is 90°

$$\delta_{x,x,y} = -\frac{c_H}{2\pi} \left(\frac{1}{2} - c_H^2 \right) \quad (C10c)$$

APPENDIX C – Continued

$\delta_{x,x,z}$:-

$$\begin{aligned} \delta_{x,x,z} = & \frac{1}{\pi} \left[\frac{2s_H^4 c_V^4}{C_{HV}^6} (5s_H^2 s_V^2 - C_{HV}^2) - \frac{4s_H^4 c_V^4 (3s_H^2 s_V^2 - C_{HV}^2)}{C_{HV}^5 (C_{HV} + s_V)} - \frac{8s_H^6 c_V^4}{C_{HV}^4} \right. \\ & + \frac{4s_H^4 c_V^4 (C_{HV}^2 - s_H^2 s_V^2)}{C_{HV}^4 (C_{HV} + s_V)^2} + \frac{s_H^4 c_V^4 (C_{HV}^2 - 3s_H^2 s_V^2)}{s_V^2 C_{HV}^4} \\ & \left. - \frac{c_H^2 C_{HV} - s_H^3 c_V}{2(C_{HV} - s_H c_V)} - \frac{2s_H^6 c_V^4}{s_V^2 C_{HV}^2} \right] \end{aligned} \quad (C11a)$$

When χ_H is 90°

$$\delta_{x,x,z} = \frac{1}{\pi} \left(10s_V^6 - 12s_V^5 - 19s_V^4 + 24s_V^3 + 9s_V^2 - 12s_V - 1 + \frac{1}{2} \frac{c_V + 2}{c_V + 1} \right) \quad (C11b)$$

When χ_V is 90°

$$\delta_{x,x,z} = \frac{c_H^2}{2\pi} \quad (C11c)$$

When both χ_H and χ_V are 90°

$$\delta_{x,x,z} = 0 \quad (C11d)$$

$\delta_{x,y,x}$:- See equations (C10).

$\delta_{x,y,y}$:-

$$\begin{aligned} \delta_{x,y,y} = & \frac{s_H}{\pi} \left[\frac{2s_H^3 s_V c_V^3 (s_H^2 - 4s_V^2 c_H^2)}{C_{HV}^6} - \frac{4s_H^3 c_V^3 (s_H^2 - 2s_V^2 c_H^2)}{C_{HV}^5} \right. \\ & + \frac{s_H^3 c_V^3 (s_H^2 - 2s_V^2 c_H^2)}{s_V C_{HV}^4} + \frac{8s_H^3 c_H^2 c_V^3}{C_{HV}^3} - \frac{2s_H^3 c_H^2 c_V^3}{s_V C_{HV}^2} \\ & \left. + \frac{s_H^5 c_V^3}{s_V^3 C_{HV}^2} - \frac{4s_H^3 c_H^2 c_V^3}{s_V^3} - \frac{s_V C_{HV}}{4(C_{HV} - s_H c_V)^2} + \frac{s_V^3 c_H^2}{2(C_{HV} - s_H c_V)^3} \right] \end{aligned} \quad (C12a)$$

APPENDIX C – Continued

When χ_H is 90°

$$\delta_{x,y,y} = \frac{1}{\pi} \left[s_V c_V^3 - s_V^3 c_V - 4c_V^3 - \frac{1}{4(1+c_V)} \tan \frac{\chi_V}{2} \right] \quad (C12b)$$

When χ_V is 90°

$$\delta_{x,y,y} = -\frac{s_H}{4\pi} (1 - 2c_H^2) \quad (C12c)$$

When both χ_H and χ_V are 90°

$$\delta_{x,y,y} = -\frac{1}{4\pi} \quad (C12d)$$

$\delta_{x,y,z}$

$$\begin{aligned} \delta_{x,y,z} = & -\frac{s_H c_H}{\pi} \left[\frac{10s_H^4 c_V^4 s_V^2}{C_{HV}^6} - \frac{8s_H^4 c_V^4 s_V}{C_{HV}^5} + \frac{3s_H^4 c_V^4}{C_{HV}^4} + \frac{2s_H^4 c_V^4}{s_V^2 C_{HV}^2} \right. \\ & - \frac{4s_H^4 s_V^2 c_V^4}{C_{HV}^5 (C_{HV} + s_V)} - \frac{4s_H^4 s_V^2 c_V^4}{C_{HV}^4 (C_{HV} + s_V)^2} - \frac{8s_H^4 c_V^4}{C_{HV}^3 (C_{HV} + s_V)} \\ & \left. - \frac{s_V^2}{2(C_{HV} - s_H c_V)^2} \right] \quad (C13a) \end{aligned}$$

When χ_H is 90°

$$\delta_{x,y,z} = 0 \quad (C13b)$$

When χ_V is 90°

$$\delta_{x,y,z} = \frac{s_H c_H}{2\pi} \quad (C13c)$$

$\delta_{x,z,x}$ – See equations (C11).

$\delta_{x,z,y}$ – See equations (C13).

$\delta_{x,z,z}$ –

$$\begin{aligned} \delta_{x,z,z} = & \frac{s_H}{\pi} \left[\frac{2s_H^3 s_V c_V^3 (s_V^2 - 4s_H^2 c_V^2)}{C_{HV}^6} - \frac{4s_H^3 c_V^3 (s_V^2 - 2s_H^2 c_V^2)}{C_{HV}^5} \right. \\ & \left. + \frac{s_H^3 s_V c_V^3}{C_{HV}^4} - \frac{2s_H^5 c_V^5}{s_V C_{HV}^4} + \frac{s_H^3 c_V^3}{s_V C_{HV}^2} + \frac{1}{2} \frac{s_V}{C_{HV} - s_H c_V} \right] \quad (C14a) \end{aligned}$$

APPENDIX C – Continued

When χ_H is 90°

$$\delta_{x,z,z} = \frac{1}{\pi} \left(12c_V^5 - 10s_Vc_V^5 - 4c_V^3 + 5s_Vc_V^3 + s_Vc_V + \frac{1}{2} \tan \frac{\chi_V}{2} \right) \quad (C14b)$$

When χ_V is 90°

$$\delta_{x,z,z} = \frac{s_H}{2\pi} \quad (C14c)$$

When both χ_H and χ_V are 90°

$$\delta_{x,z,z} = \frac{1}{2\pi} \quad (C14d)$$

Interference Factors for the Derivatives of the Velocities Caused by Forces in the Y-Direction

$\delta_{y,x,x}$ - See equations (C10).

$\delta_{y,x,y}$ - See equations (C10).

$\delta_{y,x,z}$ - See equations (C13).

$\delta_{y,y,x}$ - See equations (C12).

$\delta_{y,y,y}$ -

$$\begin{aligned} \delta_{y,y,y} = \frac{c_H}{\pi} & \left[\frac{2s_H^3s_Vc_V^3(2s_V^2c_H^2 - 3s_H^2)}{C_{HV}^6} + \frac{12s_H^5c_V^3}{C_{HV}^5} - \frac{8s_H^3c_H^2c_V^3}{C_{HV}^3} - \frac{3s_H^5c_V^3}{s_VC_{HV}^4} \right. \\ & \left. - \frac{3s_H^5c_V^3}{s_V^3C_{HV}^2} + \frac{4s_H^3c_H^2c_V^3}{s_V^3} + \frac{3}{4} \frac{s_VC_{HV}}{(C_{HV} - s_Hc_V)^2} - \frac{s_V^3c_H^2}{2(C_{HV} - s_Hc_V)^3} \right] \quad (C15a) \end{aligned}$$

When χ_H is 90°

$$\delta_{y,y,y} = 0 \quad (C15b)$$

When χ_V is 90°

$$\delta_{y,y,y} = \frac{c_H}{2\pi} \left(s_H^2 + \frac{1}{2} \right) \quad (C15c)$$

APPENDIX C – Continued

$\delta_{y,y,z}$ •-

$$\begin{aligned} \delta_{y,y,z} = \frac{1}{\pi} & \left[\frac{2s_H^4 c_V^4 (4s_V^2 c_H^2 - s_H^2)}{C_{HV}^6} - \frac{8s_H^4 s_V c_H^2 c_V^4}{C_{HV}^5} + \frac{4s_H^6 c_V^4}{C_{HV}^5 (C_{HV} + s_V)} \right. \\ & + \frac{4s_H^6 c_V^4}{C_{HV}^4 (C_{HV} + s_V)^2} - \frac{8s_H^4 c_H^2 c_V^4}{C_{HV}^3 (C_{HV} + s_V)} + \frac{2s_H^4 c_H^2 c_V^4}{C_{HV}^4} - \frac{s_H^6 c_V^4}{s_V^2 C_{HV}^4} \\ & \left. + \frac{2s_H^4 c_H^2 c_V^4}{s_V^2 C_{HV}^2} + \frac{C_{HV}}{2(C_{HV} - s_H c_V)} - \frac{s_V^2 c_H^2}{2(C_{HV} - s_H c_V)^2} \right] \end{aligned} \quad (C16a)$$

When χ_H is 90°

$$\delta_{y,y,z} = \frac{1}{\pi} \left(8 - 12s_V + 3s_V^2 + 4s_V^3 - 2s_V^4 - \frac{1}{2} \frac{1}{1 + c_V} \right) \quad (C16b)$$

When χ_V is 90°

$$\delta_{y,y,z} = \frac{s_H^2}{2\pi} \quad (C16c)$$

When both χ_H and χ_V are 90°

$$\delta_{y,y,z} = \frac{1}{2\pi} \quad (C16d)$$

$\delta_{y,z,x}$ •- See equations (C13).

$\delta_{y,z,y}$ •- See equations (C16).

$\delta_{y,z,z}$ •-

$$\begin{aligned} \delta_{y,z,z} = \frac{c_H}{\pi} & \left[\frac{2s_H^3 s_V c_V^3 (4s_H^2 c_V^2 - s_V^2)}{C_{HV}^6} - \frac{4s_H^3 c_V^3 (2s_H^2 c_V^2 - s_V^2)}{C_{HV}^5} - \frac{s_H^3 s_V c_V^3}{C_{HV}^4} \right. \\ & \left. - \frac{1}{2} \frac{s_V}{C_{HV} - s_H c_V} + \frac{2s_H^5 c_V^5}{s_V C_{HV}^4} - \frac{s_H^3 c_V^3}{s_V C_{HV}^2} \right] \end{aligned} \quad (C17a)$$

APPENDIX C – Continued

When χ_H is 90°

$$\delta_{y,z,z} = 0 \quad (C17b)$$

When χ_V is 90°

$$\delta_{y,z,z} = -\frac{c_H}{2\pi} \quad (C17c)$$

Interference Factors for the Derivatives of the Velocities Caused by Forces in the Z-Direction

$\delta_{z,x,x}$

$$\delta_{z,x,x} = \frac{1}{\pi} \left[\frac{10s_H^6 s_V^2 c_V^4}{C_{HV}^6} - \frac{s_H^4 c_V^4 (5 - 3c_H^2)}{C_{HV}^4} - \frac{s_H^4 c_V^4 (1 - 2c_H^2)}{s_V^2 C_{HV}^2} \right. \\ \left. - \frac{C_{HV}}{2(C_{HV} - s_H c_V)} + \frac{s_H^2 s_V^2}{2(C_{HV} - s_H c_V)^2} \right] \quad (C18a)$$

When χ_H is 90°

$$\delta_{z,x,x} = \frac{1}{\pi} \left(10c_V^6 - 5c_V^4 - c_V^2 - \frac{1}{2} \frac{1}{1 + c_V} \right) \quad (C18b)$$

When χ_V is 90°

$$\delta_{z,x,x} = -\frac{c_H^2}{2\pi} \quad (C18c)$$

When both χ_H and χ_V are 90°

$$\delta_{z,x,x} = 0 \quad (C18d)$$

$\delta_{z,x,y}$

$$\delta_{z,x,y} = -\frac{s_H c_H}{\pi} \left(\frac{10s_H^4 s_V^2 c_V^4}{C_{HV}^6} - \frac{3s_H^4 c_V^4}{C_{HV}^4} - \frac{2s_H^4 c_V^4}{s_V^2 C_{HV}^2} + \frac{1}{2} \frac{C_{HV} + s_H c_V}{C_{HV} - s_H c_V} \right) \quad (C19a)$$

APPENDIX C – Continued

When χ_H is 90°

$$\delta_{z,x,y} = 0 \quad (C19b)$$

When χ_V is 90°

$$\delta_{z,x,y} = -\frac{s_H c_H}{2\pi} \quad (C19c)$$

$\delta_{z,x,z}$

$$\delta_{z,x,z} = \frac{s_H}{\pi} \left[\frac{2s_H^3 s_V c_V^3 (s_V^2 - 4s_H^2 c_V^2)}{C_{HV}^6} + \frac{2s_H^5 c_V^5}{s_V C_{HV}^4} - \frac{2s_H^5 c_V^3}{s_V C_{HV}^2} \right. \\ \left. - \frac{s_H^3 s_V c_V^3}{C_{HV}^4} - \frac{1}{2} \frac{s_V}{C_{HV} - s_H c_V} \right] \quad (C20a)$$

When χ_H is 90°

$$\delta_{z,x,z} = -\frac{1}{\pi} \left(10s_V c_V^5 + s_V c_V^3 + s_V c_V + \frac{1}{2} \tan \frac{\chi_V}{2} \right) \quad (C20b)$$

When χ_V is 90°

$$\delta_{z,x,z} = -\frac{s_H}{2\pi} \quad (C20c)$$

When both χ_H and χ_V are 90°

$$\delta_{z,x,z} = -\frac{1}{2\pi} \quad (C20d)$$

$\delta_{z,y,x}$ See equations (C19).

$\delta_{z,y,y}$

$$\delta_{z,y,y} = \frac{1}{\pi} \left[\frac{2s_H^4 c_V^4 (4s_V^2 c_H^2 - s_H^2)}{C_{HV}^6} - \frac{2s_H^4 c_H^2 c_V^4}{C_{HV}^4} + \frac{s_H^6 c_V^4}{s_V^2 C_{HV}^4} - \frac{2s_H^4 c_H^2 c_V^4}{s_V^2 C_{HV}^2} \right. \\ \left. - \frac{C_{HV}}{2(C_{HV} - s_H c_V)} + \frac{s_V^2 c_H^2}{2(C_{HV} - s_H c_V)^2} \right] \quad (C21a)$$

APPENDIX C – Continued

When χ_H is 90°

$$\delta_{z,y,y} = -\frac{1}{\pi} \left(2c_V^4 + c_V^2 + 1 - \frac{1}{2} \frac{1}{1 + c_V} \right) \quad (C21b)$$

When χ_V is 90°

$$\delta_{z,y,y} = -\frac{s_H^2}{2\pi} \quad (C21c)$$

When both χ_H and χ_V are 90°

$$\delta_{z,y,y} = -\frac{1}{2\pi} \quad (C21d)$$

$\delta_{z,y,z}$

$$\delta_{z,y,z} = \frac{c_H}{\pi} \left[\frac{2s_H^3 s_V c_V^3 (4s_H^2 c_V^2 - s_V^2)}{C_{HV}^6} + \frac{s_H^3 s_V c_V^3}{C_{HV}^4} - \frac{2s_H^5 c_V^5}{s_V C_{HV}^4} + \frac{s_H^3 c_V^3}{s_V C_{HV}^2} + \frac{1}{2} \frac{s_V}{C_{HV} - s_H c_V} \right] \quad (C22a)$$

When χ_H is 90°

$$\delta_{z,y,z} = 0 \quad (C22b)$$

When χ_V is 90°

$$\delta_{z,y,z} = \frac{c_H}{2\pi} \quad (C22c)$$

$\delta_{z,z,x}$ - See equations (C20).

$\delta_{z,z,y}$ - See equations (C22).

APPENDIX C – Concluded

$\delta_{z,z,z}$:-

$$\delta_{z,z,z} = \frac{1}{\pi} \left(\frac{7s_H^6 c_V^6}{C_{HV}^6} - \frac{3s_H^4 s_V^2 c_V^4}{C_{HV}^6} + \frac{1}{2} \right) \quad (C23a)$$

When χ_H is 90°

$$\delta_{z,z,z} = \frac{1}{\pi} \left(10c_V^6 - 3c_V^4 + \frac{1}{2} \right) \quad (C23b)$$

When χ_V is 90°

$$\delta_{z,z,z} = \frac{1}{2\pi} \quad (C23c)$$

When both χ_H and χ_V are 90°

$$\delta_{z,z,z} = \frac{1}{2\pi} \quad (C23d)$$

APPENDIX D

FORTRAN PROGRAM TO CALCULATE THE INTERFERENCE FACTORS FOR STABILITY TESTS OF A VANISHINGLY SMALL MODEL IN A CLOSED RECTANGULAR TEST SECTION

THIS PROGRAM WAS WRITTEN IN CDC FORTRAN, VERSION 2.1, TO RUN ON CDC 6000 SERIES COMPUTERS WITH THE SCOPE 3.0 OPERATING SYSTEM AND LIBRARY TAPE. MINOR MODIFICATIONS MAY BE REQUIRED PRIOR TO USE IN OTHER COMPUTERS. THIS PROGRAM HAS BEEN FOUND TO BE SATISFACTORY ON THE AFOREMENTIONED COMPUTERS WHICH CARRY THE EQUIVALENT OF APPROXIMATELY 15 DECIMAL DIGITS. COMPUTERS OF LESSER PRECISION MAY REQUIRE MODIFICATION TO DOUBLE PRECISION IN ORDER TO OBTAIN RESULTS OF EQUAL ACCURACY.

INPUT IS REQUIRED AT LINE (D77) AND EITHER LINE (D 89) OR (D 92). THE FIRST CARD MUST STATE, IN NAMELIST FORMAT, THE HORIZONTAL (CHI(H)) AND VERTICAL (CHI(V)) SKEW ANGLES FOR WHICH THE INTERFERENCE FACTORS ARE REQUIRED. AS MANY AS 11 HORIZONTAL AND 10 VERTICAL SKEW ANGLES MAY BE SUPPLIED, AND THE OUTPUT WILL BE FOR ALL VERTICAL SKEW ANGLES AT EACH HORIZONTAL SKEW ANGLE. THE SECOND CARD SPECIFIES (IN AN A FORMAT) THE DESIRED BOUNDARY CONDITION AND THE DESIRED COMBINATION OF INTERFERENCE FACTORS, THAT IS: STARTING IN COLUMN 1, THIS CARD WILL READ EITHER CLOSED TUNNEL CASE, OR GROUND EFFECT CASE; AND STARTING IN COLUMN 25, THE CARD WILL READ EITHER VELOCITIES ONLY, VELOCITIES AND LONGITUDINAL DERIVATIVES ONLY, OR VELOCITIES AND DERIVATIVES. THE THIRD CARD SPECIFIES I(XTRA), F(TA), E(TA), G(A)MMA, X(O)VERH, Y(O)VERH, AND Z(O)VERH IN FORMAT NO. 80 (LINE (D 251)). I(XTRA) IS DEFINED IN A SUBSEQUENT LIST OF STATUS INDICATORS. THE REMAINING QUANTITIES ARE MERELY THE SPELLED OUT VERSIONS OF QUANTITIES DEFINED IN THE MAIN TEXT. AS MANY SUCH CARDS AS DESIRED MAY BE INSERTED AT THIS POINT PROVIDED THAT THE PREVIOUSLY SUPPLIED QUANTITIES ARE UNALTERED. A SET OF SAMPLE DATA CARDS FOLLOWS THE PROGRAM LISTING.

C	PROGRAM STABIL	(INPUT,OUTPUT,TAPE5=INPUT,TAPE6=OUTPUT)	(D 1)
C			(D 2)
C			(D 3)
C	THIS PROGRAM COMPUTES INTERFERENCE FACTORS FOR STABILITY WORK		(D 4)
C	AT A POINT NEAR A VANISHINGLY SMALL MODEL		(D 5)
C			(D 6)
C			(D 7)
C	***DEFINITIONS OF STATUS INDICATORS***		(D 8)
C			(D 9)
C	*VARIABLE*	*DEFINITION*	(D 10)
C			(D 11)
C	IHV90	1 NEITHER CHI(H) NOR CHI(V) SET TO 90 DEG BEFORE	(D 12)
C		SUBSTITUTION	(D 13)
C		2 EITHER CHI(H) OR CHI(V) SET TO 90 DEG BEFORE SUB-	(D 14)
C		STITUTION	(D 15)
C			(D 16)
C	ICH(H)	1 CHI(H) NOT SET TO 90 DEG BEFORE SUBSTITUTION	(D 17)
C		2 CHI(H) SET TO 90 DEG BEFORE SUBSTITUTION	(D 18)
C			(D 19)
C	ICH(V)	1 CHI(V) NOT SET TO 90 DEG BEFORE SUBSTITUTION	(D 20)
C		2 CHI(V) SET TO 90 DEG BEFORE SUBSTITUTION	(D 21)
C			(D 22)

APPENDIX D - Continued

```

C  AHPRIM      1.0  PHI TO BE EVALUATED (D 23)
C              -1.0  PHI PRIME TO BE EVALUATED (D 24)
C (D 25)
C  IH90        1    CHI(H) NOT EQUAL TO 90 DEG (D 26)
C              2    CHI(H) EQUAL TO 90 DEG (D 27)
C (D 28)
C  IV90        1    CHI(V) NOT EQUAL TO 90 DEG (D 29)
C              2    CHI(V) EQUAL TO 90 DEG (D 30)
C (D 31)
C  IBOTH       1    EITHER CHI(H) OR CHI(V) NOT EQUAL TO 90 DEG (D 32)
C              2    BOTH CHI(H) AND CHI(V) EQUAL TO 90 DEG (D 33)
C (D 34)
C  ICASF       1    CASE I EQUATIONS TO BE USED (D 35)
C              2    CASE II EQUATIONS TO BE USED (D 36)
C (D 37)
C  ITYPE       1    CLOSED TUNNEL (D 38)
C              2    GROUND EFFECT (D 39)
C (D 40)
C  IEXTRA      1    ADD EXTRA CHI(V) DIVIDING CASES I AND II (D 41)
C              2    OMTS EXTRA CHI(V) (D 42)
C              3    ALTER ANGLES, BOUNDARY CONDITIONS, OR REQUIRED (D 43)
C                  INTERFERENCE FACTORS (D 44)
C (D 45)
C  ICH         1    CHI(H) NOT GREATER THAN 90 DEG OR ITYPE EQUALS 2 (D 46)
C              2    CHI(H) GREATER THAN 90 DEG AND ITYPE EQUALS 1 (D 47)
C (D 48)
C  ICV         1    CHI(V) NOT GREATER THAN 90 DEG (D 49)
C              2    CHI(V) GREATER THAN 90 DEG (D 50)
C (D 51)
C (D 52)
COMMON RSUBO, ANOVERH, CHV(2), SINXH(2), COSXH(2), (D 53)
1 SINXV(2), COSXV(2), IHV90, ICHH, CHIV, (D 54)
2 CONRD(3), PHI(2), I, J, K, AHPRIM (D 55)
COMMON XOVERH, YOVERH, ZOVERH, ZETA, ETA, GAMMA, TANXH, (D 56)
1 TANXV, IBOTH, IH90, IV90, ICASE, XSET1, XSET2, (D 57)
2 XSET3, PI, IP(3), IQ(3), IR(3), TERM1(2), TERM2(2), (D 58)
3 TERM3(2), TERM4(2), TERM5(2), TERM6(2), TERM7(2), (D 59)
4 TERM8(2), TERM9(2), TERM10(2), TERM11(2), TERM12(2), (D 60)
5 ANSFR(2), DELTA(3,3), DELTAD(3,3,3), FACTYP(6), ICV (D 61)
DIMENSION CHIH(1), CHIV(1), VHOLD(1), RUNTYP(4), (D 62)
1 PRTXY7(3), PTXYZ(9) (D 63)
DATA PRTXYZ/1HX,1HY,1HZ/,GRNTST,FACTST/6HGROUND,6H /, (D 64)
1 PTXY7/4HX,X),4HX,Y),4HX,Z),4HY,X),4HY,Y),4HY,Z), (D 65)
2 4H7,X),4H7,Y),4H7,Z)/ (D 66)
NAMFI ST /ANGLES/CHIH,CHIV (D 67)
CHV(2)=SINXV(2)=SINXH(2)=1.0 (D 68)
COSXV(2)=COSXH(2)=0.0 (D 69)
IP(1)=IP(3)=IQ(1)=IR(1)=2 (D 70)
IP(2)=IQ(2)=IQ(3)=IR(2)=IR(3)=1 (D 71)
PI=3.14159265358979 (D 72)
RADVSN=PI/180.0 (D 73)
49 IFIRST=0 (D 74)
DO 48 I=1,11 (D 75)
48 CHIH(I)=CHIV(I)=VHOLD(I)=0.0 (D 76)
READ (5,ANGLES) (D 77)
IF (FNF,5) 375,50 (D 78)
50 AHPRIM=1.0 (D 79)
IEXTRA=2 (D 80)
IHV90=ICHH=ICHIV=IH90=IV90=ICH=ICV=1 (D 81)
NOHNR7=NOVERT=NOVSAV=0 (D 82)

```

APPENDIX D - Continued

```

      DO 51 I=1,3                                (D 83)
      DO 51 J=1,3                                (D 84)
      DELTA(I,J)=0.0                             (D 85)
      DO 51 K=1,3                                (D 86)
51  DELTAD(I,J,K)=0.0                             (D 87)
      IF(IFIRST.EQ.0) GO TO 90                    (D 88)
      READ (5,80) IXTRA,ZETA,ETA,GAMMA,XOVERH,YOVERH,ZOVERH
      IF (IXTRA.EQ.3) GO TO 49                     (D 89)
      IF (EOF.5) 375,109                          (D 91)
90  READ (5,100) RUNTYP,FACTYP,IXTRA,ZETA,ETA.    (D 92)
      1  GAMMA,XOVERH,YOVERH,ZOVERH               (D 93)
      IF (EOF.5) 375,101                          (D 94)
101 IFIRST=1                                      (D 95)
102 DO 105 M=1,11                                (D 96)
105 VHOLD(M)=CHIV(M)                             (D 97)
106 IF(RUNTYP(1)-GRNTST)108,107,108              (D 98)
107 ITYPE=2                                       (D 99)
      ZFTA=1.                                     (D 100)
      FTA=1.                                     (D 101)
      GAMMA=2.                                    (D 102)
      GO TO 109                                   (D 103)
108 ITPF=1                                       (D 104)
109 A7FTA=ZFTA                                   (D 105)
      AFTA=ETA                                    (D 106)
      DO 110 M=1,10                              (D 107)
      IF(CHIH(M))130,130,110                      (D 108)
110 NOHORZ=NOHORZ+1                             (D 109)
130 DO 140 M=1,10                              (D 110)
      IF(CHIV(M))160,160,140                      (D 111)
140 NOVERT=NOVERT+1                             (D 112)
160 NOVSAV=NOVERT                               (D 113)
      DO 165 IANGLH=1,NOHORZ                     (D 114)
      ACHIH=CHIH(IANGLH)                         (D 115)
      NOVERT=NOVSAV                              (D 116)
      IF (ITYPE.EQ.2) GO TO 161                   (D 117)
      WRITE (6,903) GAMMA,AZETA,AETA,XOVERH,YOVERH,ZOVERH
      GO TO 162                                    (D 118)
161 WRITE (6,904) XOVERH,YOVERH,ZOVERH          (D 119)
162 ICH=1                                        (D 120)
      IF (CHIH(IANGLH).LE.90..OR.ITYPE.EQ.2) GO TO 164
      ICH=2                                       (D 121)
      FTA=2.0-AFTA                              (D 122)
      CHIH(IANGLH)=180.0-ACHIH                   (D 123)
      YOVERH=-YOVERH                             (D 124)
164 DO 165 M=1,11                                (D 125)
165 CHIV(M)=VHOLD(M)                             (D 126)
      IF (CHIH(IANGLH).EQ.90.0) GO TO 220         (D 127)
170 SINXH(1)=SIN(CHIH(IANGLH)*RADVSN)           (D 128)
      COSXH(1)=COS(CHIH(IANGLH)*RADVSN)          (D 129)
      TANXH=SINXH(1)/COSXH(1)                    (D 130)
      IH90=1                                      (D 131)
      IF (ITPF.EQ.2.OR.IXTRA.EQ.2) GO TO 230      (D 132)
C      (D 133)
C      (D 134)
C      (D 135)
C      (D 136)
C      (D 137)
C      (D 138)
C      (D 139)
      VMID=ATAN(TANXH*ZETA*GAMMA*(2.0-ETA))/RADVSN
      DO 185 M=1,NOVERT                           (D 140)
      IF (ABS(VMID-CHIV(M)).LT.0.005) GO TO 230   (D 141)
      (D 142)

```

APPENDIX D - Continued

185	CONTINUE	(D 143)
	DO 190 M=1,NOVFRT	(D 144)
	IF (VMID.LT.CHIV(M)) GO TO 200	(D 145)
190	CONTINUE	(D 146)
	CHIV(NOVFRT+1)=VMID	(D 147)
	GO TO 215	(D 148)
200	MOVLOC=NOVFRT+1	(D 149)
	MOVF=MOVLOC-M	(D 150)
	DO 210 M=1,MOVF	(D 151)
	CHIV(MOVLOC)=CHIV(MOVLOC-1)	(D 152)
210	MOVLOC=MOVLOC-1	(D 153)
	CHIV(MOVLOC)=VMID	(D 154)
215	NOVFRT=NOVSAV+1	(D 155)
	GO TO 230	(D 156)
220	SINXH(1)=1.0	(D 157)
	COSXH(1)=0.0	(D 158)
	TANXH=10.0E10	(D 159)
	CHV(1)=1.0	(D 160)
	TH90=2	(D 161)
230	DO 364 IANGLV=1,NOVERT	(D 162)
	ICV=1	(D 163)
	IF (CHIV(IANGLV).EQ.90.0) GO TO 240	(D 164)
	IF (CHIV(IANGLV).LT.90.0) GO TO 241	(D 165)
	ICV=2	(D 166)
	IF (ITYPE.EQ.2) GO TO 241	(D 167)
	ZFTA=AZFTA/(2.0*AZETA-1.0)	(D 168)
	ZOVERH=-ZOVERH	(D 169)
	CHIV(IANGLV)=180.0-CHIV(IANGLV)	(D 170)
241	SINXV(1)=SIN(CHIV(IANGLV)*RADVSN)	(D 171)
	COSXV(1)=COS(CHIV(IANGLV)*RADVSN)	(D 172)
	TANXV=SINXV(1)/COSXV(1)	(D 173)
	CHV(1)=SQRT((1.0-((COSXH(1)**2)*(COSXV(1)**2)))	(D 174)
	IV90=1	(D 175)
	IBOTH=1	(D 176)
	IF (TANXH.GE.TANXV/(ZETA*GAMMA*(2.0-ETA))) GO TO 260	(D 177)
	GO TO 250	(D 178)
240	SINXV(1)=1.0	(D 179)
	COSXV(1)=0.0	(D 180)
	TANXV=10.0F10	(D 181)
	CHV(1)=1.0	(D 182)
	IV90=2	(D 183)
	IBOTH=2	(D 184)
	IF (TH90.NE.2) IBOTH=1	(D 185)
250	ICASF=2	(D 186)
	GO TO 270	(D 187)
260	ICASF=1	(D 188)
270	XSFT1=ZFTA*XOVERH	(D 189)
	XSFT2=XSFT1-TANXV	(D 190)
	XSFT3=ZFTA*(XOVERH-GAMMA*(2.0-ETA)*TANXH)	(D 191)
		(D 192)
C		(D 193)
C	COORDINATE PERMUTATION LOOPS	(D 194)
C		(D 195)
	DO 310 I=1,3	(D 196)
	DO 310 J=1,3	(D 197)
	DO 310 K=1,3	(D 198)
	IF (ABS(CHIV(IANGLV)).LT.0.005) GO TO 364	(D 199)
	IF (K.EQ.1.OR.ITYPE.EQ.2) GO TO 279	(D 200)
	IF (FACTYP(4).EQ.FACTST) GO TO 310	(D 201)
	IF (J.NE.1.AND.FACTYP(6).NE.FACTST) GO TO 310	(D 202)
279	DO 280 ITERM=1,24	

APPENDIX D - Continued

```

280 TFRM1(ITFRM)=0.0 (D 203)
GO TO (290,300),ITYPE (D 204)
290 CALL WAFFFF (D 205)
GO TO 310 (D 206)
300 CALL GRNFFF (D 207)
310 CONTINUE (D 208)
IF(ICH.EQ.1) GO TO 3000 (D 209)
DO 2092 I=1,3 (D 210)
DO 2092 J=1,3 (D 211)
IX=IY=2 (D 212)
IF (I.FQ.2) IX=1 (D 213)
IF (J.FQ.2) IY=1 (D 214)
DELTA(I,J)=((-1.)*(IX+IY))*DELTA(I,J) (D 215)
DO 2092 K=1,3 (D 216)
I7=2 (D 217)
IF (K.FQ.2) IZ=1 (D 218)
2092 DELTAD(I,J,K)=((-1.)*(IX+IY+IZ))*DELTAD(I,J,K) (D 219)
3000 IF (ICV.FQ.1.OR.ITYPE.EQ.2) GO TO 3001 (D 220)
DO 2094 I=1,3 (D 221)
DO 2094 J=1,3 (D 222)
IX=IY=2 (D 223)
IF (I.FQ.3) IX=1 (D 224)
IF (J.FQ.3) IY=1 (D 225)
DELTA(I,J)=((-1.)*(IX+IY))*DELTA(I,J) (D 226)
DO 2094 K=1,3 (D 227)
I7=2 (D 228)
IF (K.FQ.3) IZ=1 (D 229)
2094 DELTAD(I,J,K)=((-1.)*(IX+IY+IZ))*DELTAD(I,J,K) (D 230)
CHIV(IANGLV)=180.0-CHIV(IANGLV) (D 231)
YOVRH=-YOVRH (D 232)
ZETA=AZETA (D 233)
3001 WRITE (6,330) ACHI,CHIV(IANGLV) (D 234)
WRITE (6,340) PTXYZ (D 235)
WRITE (6,350) ((DELTA(I,J),J=1,3),I=1,3) (D 236)
IF (FACTYP(6).NE.FACTST.AND.ITYPE.EQ.1) GO TO 361 (D 237)
IF (FACTYP(4).EQ.FACTST.AND.ITYPE.EQ.1) GO TO 364 (D 238)
DO 362 J=1,3 (D 239)
362 WRITE (6,370) PRTXYZ(J),((DELTAD(I,J,K),K=1,3),I=1,3) (D 240)
GO TO 364 (D 241)
361 WRITE (6,370) PRTXYZ(1),((DELTAD(I,1,K),K=1,3),I=1,3) (D 242)
364 CONTINUE (D 243)
IF (ICH.FQ.1) GO TO 365 (D 244)
CHIH(IANGLH)=ACHI (D 245)
ETA=AETA (D 246)
YOVRH=-YOVRH (D 247)
365 CONTINUE (D 248)
GO TO 50 (D 249)
375 STOP (D 250)
80 FORMAT (I1,F9.3,5F10.3) (D 251)
100 FORMAT (I0A6/I1,F9.3,5F10.3) (D 252)
330 FORMAT (//14X,9HCHI(H) = ,F6.2,5X,9HCHI(V) = ,F6.2/) (D 253)
340 FORMAT(19X,9(1H(,A4,8X))) (D 254)
350 FORMAT(1X,10HDELTA(-,-),9F13.4) (D 255)
370 FORMAT (11H DELTA(-,-,A1,1H),F11.4,8F13.4) (D 256)
903 FORMAT (1H1// 35X*INTERFERENCE FACTORS FOR STABILITY WORK IN A CLO (D 257)
15FD TUNNEL*//43X*AT A POINT NEAR A VANISHINGLY SMALL MODEL*/// (D 258)
235X*GAMMA =*F7.3,10X*ZETA =*F6.3,11X*ETA =*F6.3// (D 259)
335X*X/H =*F7.3,10X*Y/H =*F6.3,11X*Z/H =*F6.3// (D 260)
904 FORMAT (1H1//39X*INTERFERENCE FACTORS FOR STABILITY WORK IN GROUND (D 261)
1D EFFECT*//47X*AT A POINT NEAR A VANISHINGLY SMALL MODEL*/// (D 262)
240X*X/H =*F7.3,10X*Y/H =*F6.3,10X*Z/H =*F6.3// (D 263)
END (D 264)

```

APPENDIX D – Continued

SUBROUTINE GRNEFF	(D 265)
COMMON RSUBD,ADVERH,CHV(2),SINXH(2),COSXH(2),	(D 266)
1 SINXV(2),COSXV(2),IHV90,ICHIH,ICHIV,	(D 267)
2 COORD(3),PHI(2),I,J,K,AHPRIM	(D 268)
COMMON XOVERH,YOVERH,ZOVERH,ZETA,ETA,GAMMA,TANXH,	(D 269)
1 TANXV,IBOTH,IH90,IV90,ICASE,XSET1,XSET2,	(D 270)
2 XSFT3,PI,IP(3),IQ(3),IR(3),TERM1(2),TERM2(2),	(D 271)
3 TERM3(2),TERM4(2),TERM5(2),TERM6(2),TERM7(2),	(D 272)
4 TERM8(2),TERM9(2),TERM10(2),TERM11(2),TERM12(2),	(D 273)
5 ANSFR(2),DELTA(3,3),DELTAD(3,3,3),FACTYP(6),ICV	(D 274)
IF (IV90.EQ.2.OR.ICV.EQ.2) GO TO 200	(D 275)
COORD(1)=XOVERH-TANXV	(D 276)
COORD(2)=YOVERH+TANXV/TANXH	(D 277)
COORD(3)=ZOVERH+1.0	(D 278)
IHV90=2	(D 279)
ICHIV=2	(D 280)
AHPRIM=1.0	(D 281)
IF(K.NF.1)GO TO 100	(D 282)
CALL PHIIJ	(D 283)
100 CALL PHIIJK	(D 284)
DO 110 ITERM=1,2	(D 285)
110 TERM1(ITERM)=PHI(ITERM)	(D 286)
IHV90=1	(D 287)
ICHIV=1	(D 288)
IF(K.NF.1)GO TO 120	(D 289)
CALL PHIIJ	(D 290)
120 CALL PHIIJK	(D 291)
DO 125 ITERM=1,2	(D 292)
125 TERM1(ITERM)=TERM1(ITERM)-PHI(ITERM)	(D 293)
AHPRIM=-1.0	(D 294)
ICHIV=2	(D 295)
IHV90=2	(D 296)
COORD(2)=-COORD(2)	(D 297)
COORD(3)=-COORD(3)	(D 298)
IF(K.NF.1)GO TO 130	(D 299)
CALL PHIIJ	(D 300)
130 CALL PHIIJK	(D 301)
DO 140 ITERM=1,2	(D 302)
140 TERM3(ITERM)=PHI(ITERM)	(D 303)
ICHIV=1	(D 304)
IHV90=1	(D 305)
IF(K.NF.1)GO TO 150	(D 306)
CALL PHIIJ	(D 307)
150 CALL PHIIJK	(D 308)
DO 160 ITERM=1,2	(D 309)
160 TERM3(ITERM)=TERM3(ITERM)-PHI(ITERM)	(D 310)
200 AHPRIM=-1.0	(D 311)
IHV90=1	(D 312)
ICHIV=1	(D 313)
COORD(1)=XOVERH	(D 314)
COORD(2)=-YOVERH	(D 315)
COORD(3)=-ZOVERH-2.0	(D 316)
IF(K.NF.1)GO TO 210	(D 317)
CALL PHIIJ	(D 318)
210 CALL PHIIJK	(D 319)
TERM2(1)=PHI(1)	(D 320)
TERM2(2)=PHI(2)	(D 321)
DO 215 ITERM=1,2	(D 322)
215 ANSFR(ITERM)=(-2.0/PI)*((TERM1(ITERM)+	(D 323)
1 ((-1.0)**(IP(I)+IQ(J)+IR(K)))*(TERM2(ITERM)	(D 324)
2 +TERM3(ITERM)))	(D 325)
IF(K.NE.1)GO TO 220	(D 326)
DELTA(I,J)=ANSFR(1)	(D 327)
220 DELTAD(I,J,K)=ANSFR(2)	(D 328)
RETURN	(D 329)
END	(D 330)

APPENDIX D – Continued

```

SUBROUTINE WALEFF                                (D 331)
REAL KORD                                         (D 332)
DIMENSION TFRM(12,2),KORD(12,3)                 (D 333)
COMMON RSUBO,ADVERH,CHV(2),SINXH(2),COSXH(2).    (D 334)
1 SINXV(2),COSXV(2),IHV90,ICHIH,ICHIV.          (D 335)
2 COORD(3),PHI(2),I,J,K,AHPRIM                  (D 336)
COMMON XOVERH,YOVERH,ZOVERH,ZETA,ETA,GAMMA,TANXH. (D 337)
1 TANXV,IBOTH,IH90,IV90,ICASE,XSET1,XSET2.      (D 338)
2 XSET3,PI,IP(3),IQ(3),IR(3),TERM1(2),TERM2(2). (D 339)
3 TFRM3(2),TFRM4(2),TERM5(2),TERM6(2),TERM7(2). (D 340)
4 TERM8(2),TFRM9(2),TERM10(2),TFRM11(2),TFRM12(2). (D 341)
5 ANSWER(2),DFLTA(3,3),DELTA0(3,3,3),FACTYP(6),ICV (D 342)
EQUIVALENCE (TFRM(1,1),TERM1(1))               (D 343)
DATA FACTST/6H /                                (D 344)
PHI(1)=PHI(2)=0.0                               (D 345)
IHV90 = 1                                         (D 346)
ICHIH = 1                                         (D 347)
ICHIV = 1                                         (D 348)
AHPRIM=1.0                                        (D 349)
COORD (1) = XSET1                                (D 350)
DO 130 M = 1,7                                   (D 351)
AM = M-4                                          (D 352)
DO 130 N = 1,7                                   (D 353)
AN = N-4                                          (D 354)
IF (M.EQ.N.AND.N.EQ.4) GO TO 130                (D 355)
COORD (2) = ZETA*(YOVERH-4.0*AM*GAMMA)          (D 356)
COORD (3) = ZETA*(ZOVERH-4.0*AN)                (D 357)
IF (K.NF.1) GO TO 100                           (D 358)
CALL PHIIJ                                       (D 359)
IF (FACTYP(4).EQ.FACTST) GO TO 110              (D 360)
100 CALL PHIIJK                                  (D 361)
110 DO 120 IDV = 1,2                             (D 362)
120 TERM (1,IDV) = TERM (1,IDV) + PHI (IDV)     (D 363)
130 CONTINUE                                     (D 364)
C.                                                (D 365)
C SUMMATION LOOPS AND COORDINATE SET-UPS        (D 366)
DO 1295 M = 1,7                                   (D 367)
AM = M - 4                                       (D 368)
DO 1295 N = 1,7                                   (D 369)
AN = N-4                                       (D 370)
YSFT1 = ZETA*(YOVERH-4.0*AM*GAMMA)              (D 371)
YSFT2 = ZETA*(YOVERH+GAMMA*(2.0-ETA-4.0*AM))    (D 372)
YSFT3 = ZETA*(YOVERH+2.0*GAMMA*(2.0-ETA-2.0*AM)) (D 373)
ZSFT1 = ZETA*(ZOVERH-4.0*AN)                   (D 374)
ZSET2 = ZETA*((ZOVERH-4.0*AN)+GAMMA*(2.0-ETA)*(TANXH/TANXV)) (D 375)
ZSFT3 = ZETA*((ZOVERH-4.0*AN)-GAMMA*(2.0-ETA)*(TANXH/TANXV)) (D 376)
C.                                                (D 377)
C * INITIALIZE TERM COUNTER *                   (D 378)
C.                                                (D 379)
ITERM = 1                                        (D 380)
C.                                                (D 381)
C * SET-UP COORDINATES *                       (D 382)
C.                                                (D 383)
IF(ICASE.EQ.2) GO TO 140                        (D 384)
IXVSFT = 2                                       (D 385)
IXHSET = 1                                       (D 386)
KORD ( 2,1) = XSET2                             (D 387)
KORD ( 2,2) = YSET1+TANXV/TANXH                 (D 388)
KORD ( 2,3) = ZSFT1+1.0                         (D 389)
KORD ( 3,1) = XSET3                             (D 390)

```

APPENDIX D – Continued

KORD (3.2) = YSET2	(D 391)
KORD (3.3) = ZSET1+1.0	(D 392)
KORD (4.1) = XSET1	(D 393)
KORD (4.2) = -YSET1	(D 394)
KORD (4.3) = -ZSET1-2.0	(D 395)
KORD (5.1) = XSET2	(D 396)
KORD (5.2) = -YSET1-TANXV/TANXH	(D 397)
KORD (5.3) = -ZSET1-1.0	(D 398)
KORD (6.1) = XSET3	(D 399)
KORD (6.2) = -YSET2	(D 400)
KORD (6.3) = -ZSET1-1.0	(D 401)
KORD (7.1) = XSET1	(D 402)
KORD (7.2) = YSET3	(D 403)
KORD (7.3) = ZSET1	(D 404)
KORD (8.1) = XSFT2	(D 405)
KORD (8.2) = YSET3-TANXV/TANXH	(D 406)
KORD (8.3) = ZSET1+1.0	(D 407)
KORD (9.1) = XSFT3	(D 408)
KORD (9.2) = YSET2	(D 409)
KORD (9.3) = ZSET1+1.0	(D 410)
KORD (10.1) = XSET1	(D 411)
KORD (10.2) = -YSET3	(D 412)
KORD (10.3) = -ZSET1-2.0	(D 413)
KORD (11.1) = XSET2	(D 414)
KORD (11.2) = -YSET3+TANXV/TANXH	(D 415)
KORD (11.3) = -ZSET1-1.0	(D 416)
KORD (12.1) = XSET3	(D 417)
KORD (12.2) = -YSET2	(D 418)
KORD (12.3) = -ZSET1-1.0	(D 419)
GO TO 200	(D 420)
140 IXVSFT = 1	(D 421)
IXHSFT = 2	(D 422)
KORD (2.1) = XSFT3	(D 423)
KORD (2.2) = YSET2	(D 424)
KORD (2.3) = ZSET2	(D 425)
KORD (3.1) = XSFT2	(D 426)
KORD (3.2) = YSET2	(D 427)
KORD (3.3) = ZSET1+1.0	(D 428)
KORD (4.1) = XSET1	(D 429)
KORD (4.2) = YSET3	(D 430)
KORD (4.3) = ZSET1	(D 431)
KORD (5.1) = XSET3	(D 432)
KORD (5.2) = YSET2	(D 433)
KORD (5.3) = ZSET2	(D 434)
KORD (6.1) = XSFT2	(D 435)
KORD (6.2) = YSET2	(D 436)
KORD (6.3) = ZSET1+1.0	(D 437)
KORD (7.1) = XSFT1	(D 438)
KORD (7.2) = -YSET1	(D 439)
KORD (7.3) = -ZSET1-2.0	(D 440)
KORD (8.1) = XSFT3	(D 441)
KORD (8.2) = -YSET2	(D 442)
KORD (8.3) = -ZSET3-2.0	(D 443)
KORD (9.1) = XSET2	(D 444)
KORD (9.2) = -YSET2	(D 445)
KORD (9.3) = -ZSET1-1.0	(D 446)
KORD (10.1) = XSFT1	(D 447)
KORD (10.2) = -YSET3	(D 448)
KORD (10.3) = -ZSET1-2.0	(D 449)
KORD (11.1) = XSFT3	(D 450)

APPENDIX D - Continued

	KORD (11,2) = -YSET2	(D 451)
	KORD (11,3) = -ZSET3-2.0	(D 452)
	KORD (12,1) = XSET2	(D 453)
	KORD (12,2) = -YSET2	(D 454)
	KORD (12,3) = -ZSET1-1.0	(D 455)
C		(D 456)
C	* TERMS TWO, FIVE, EIGHT, AND ELEVEN *	(D 457)
C		(D 458)
200	ITERM = ITERM+1	(D 459)
	IF (IBOTH.NE.2) GO TO 205	(D 460)
	IF (ITERM.EQ.11) GO TO 1295	(D 461)
	ITERM = ITERM+1	(D 462)
	GO TO 400	(D 463)
205	IHV90 = 2	(D 464)
	ICHIV = IXVSET	(D 465)
	ICHIH = IXHSET	(D 466)
	CORRD (1) = KORD (ITERM,1)	(D 467)
	CORRD (2) = KORD (ITERM,2)	(D 468)
	CORRD (3) = KORD (ITERM,3)	(D 469)
	IF (K.NE.1) GO TO 210	(D 470)
	CALL PHIIJ	(D 471)
	IF (FACTYP(4).EQ.FACTST) GO TO 220	(D 472)
210	CALL PHIIJK	(D 473)
220	DO 230 IDV = 1,2	(D 474)
230	TERM (ITERM,IDV) = TERM (ITERM,IDV)+PHI (IDV)	(D 475)
	IHV90 = 1	(D 476)
	ICHIV = 1	(D 477)
	ICHIH = 1	(D 478)
	IF (K.NE.1) GO TO 240	(D 479)
	CALL PHIIJ	(D 480)
	IF (FACTYP(4).EQ.FACTST) GO TO 250	(D 481)
240	CALL PHIIJK	(D 482)
250	DO 260 IDV = 1,2	(D 483)
260	TERM (ITERM,IDV) = TERM (ITERM,IDV) - PHI (IDV)	(D 484)
C		(D 485)
C	* TERMS THREE, SIX, NINE, AND TWELVE *	(D 486)
C		(D 487)
	ITERM = ITERM + 1	(D 488)
	IHV90 = 2	(D 489)
	ICHIV = 2	(D 490)
	ICHIH = 2	(D 491)
	IF (ICASE.EQ.2) GO TO 300	(D 492)
	IF (IH90.EQ.2) GO TO 450	(D 493)
	GO TO 305	(D 494)
300	IF (IV90.EQ.2) GO TO 450	(D 495)
305	CORRD (1) = KORD (ITERM,1)	(D 496)
	CORRD (2) = KORD (ITERM,2)	(D 497)
	CORRD (3) = KORD (ITERM,3)	(D 498)
	IF (K.NE.1) GO TO 310	(D 499)
	CALL PHIIJ	(D 500)
	IF (FACTYP(4).EQ.FACTST) GO TO 320	(D 501)
310	CALL PHIIJK	(D 502)
320	DO 330 IDV = 1,2	(D 503)
330	TERM (ITERM,IDV) = TERM (ITERM,IDV) + PHI (IDV)	(D 504)
	IF (ICASE.EQ.2) GO TO 340	(D 505)
	ICHIV = 1	(D 506)
	GO TO 350	(D 507)
340	ICHIV = 1	(D 508)
350	IF (K.NE.1) GO TO 360	(D 509)
	CALL PHIIJ	(D 510)

APPENDIX D – Continued

```

      IF (FACTYP(4).EQ.FACTST) GO TO 370 (D 511)
360 CALL PHIJK (D 512)
370 DO 380 IDV = 1,2 (D 513)
380 TFRM (ITERM,IDV) = TERM (ITERM,IDV) - PHI (IDV) (D 514)
C (D 515)
C      * EXIT IF TERM NUMBER IS TWELVE * (D 516)
C (D 517)
      IF (ITERM.EQ.12) GO TO 1295 (D 518)
C (D 519)
C      * TERMS FOUR, SEVEN, AND TEN * (D 520)
C (D 521)
400 ITERM = ITERM+1 (D 522)
      IF (ITERM.EQ.4.OR.ITERM.EQ.7) GO TO 405 (D 523)
      AHPRIM = 1.0 (D 524)
      GO TO 410 (D 525)
405 AHPRIM = -1.0 (D 526)
410 IHV90 = 1 (D 527)
      ICHIV = 1 (D 528)
      ICHIH = 1 (D 529)
      COORD (1) = KORD (ITERM,1) (D 530)
      COORD (2) = KORD (ITERM,2) (D 531)
      COORD (3) = KORD (ITERM,3) (D 532)
      IF (K.NE.1) GO TO 420 (D 533)
      CALL PHIJK (D 534)
      IF (FACTYP(4).EQ.FACTST) GO TO 430 (D 535)
420 CALL PHIJK (D 536)
430 DO 440 IDV = 1,2 (D 537)
440 TERM (ITERM,IDV) = TERM (ITERM,IDV) + PHI (IDV) (D 538)
      GO TO 200 (D 539)
450 IF (ITERM.NE.12) GO TO 400 (D 540)
1295 CONTINUE (D 541)
1300 IF (ICASE.EQ.2) GO TO 1305 (D 542)
      IPOWR1 = IP(I)+IQ(J)+IR(K) (D 543)
      IPOWR2 = IP(I) (D 544)
      GO TO 1310 (D 545)
1305 IPOWR1 = IP(I) (D 546)
      IPOWR2 = IP(I)+IQ(J)+IR(K) (D 547)
1310 DO 1315 IDV = 1,2 (D 548)
      SADA=(-2.*7*ETA** (IDV+1)*GAMMA/PI) (D 549)
      SADB=TERM(1,IDV)+TERM(2,IDV)+TERM(3,IDV)+ (D 550)
      1 ((-1.)* IPOWR1)*(TERM(4,IDV)+TERM(5,IDV)+TERM(6,IDV)) (D 551)
      SADC=((-1.)* IPOWR2)*(TERM(7,IDV)+TERM(8,IDV)+TERM(9,IDV))+ (D 552)
      1 ((-1.)* (IQ(J)+IR(K)))*(TERM(10,IDV)+TERM(11,IDV)+ (D 553)
      2 TERM(12,IDV)) (D 554)
1315 ANSWR(IDV)=SADA*(SADB+SADC) (D 555)
      IF (K.NE.1) GO TO 1320 (D 556)
      DELTA (I,J) = ANSWR (1) (D 557)
1320 DELTAD (I,J,K) = ANSWR (2) (D 558)
      RETURN (D 559)
      END (D 560)

```

APPENDIX D – Continued

```

SUBROUTINE PHI1J                                     (D 561)
COMMON RSUBO, AOVERH, CHV(2), SINXH(2), COSXH(2),   (D 562)
1 SINXV(2), COSXV(2), IHV90, ICHIH, ICHIV,         (D 563)
2 COORD(3), PHI(2), I, J, K, AHPRIM               (D 564)
RSUBO=SQRT(COORD(1)**2+COORD(2)**2+COORD(3)**2)      (D 565)
AOVERH=RSUBO*CHV(IHV90)-COORD(1)*SINXH(ICHIH)*SINXV(ICHIV)+
1 AHPRIM*COORD(2)*SINXV(ICHIV)*COSXH(ICHIH)+      (D 566)
2 COORD(3)*SINXH(ICHIH)*COSXV(ICHIV)               (D 567)
CALL PARTLS(1,I,0,PTL1I)                           (D 568)
IF(I.EQ.J)GO TO 100                                (D 569)
CALL PARTLS(1,J,0,PTL1J)                           (D 570)
CALL PARTLS(3,I,J,PTL2IJ)                          (D 571)
GO TO 200                                           (D 572)
100 PTL1J=PTL1I                                     (D 573)
CALL PARTLS(2,I,0,PTL2IJ)                          (D 574)
200 PHI(1)=PTL2IJ/AOVERH-PTL1I*PTL1J/AOVERH**2     (D 575)
RETURN                                             (D 576)
END                                              (D 577)

SUBROUTINE PHI1JK                                     (D 579)
COMMON RSUBO, AOVERH, CHV(2), SINXH(2), COSXH(2),   (D 580)
1 SINXV(2), COSXV(2), IHV90, ICHIH, ICHIV,         (D 581)
2 COORD(3), PHI(2), I, J, K, AHPRIM               (D 582)
IF(K.EQ.1)GO TO 100                                (D 583)
RSUBO=SQRT(COORD(1)**2+COORD(2)**2+COORD(3)**2)      (D 584)
AOVERH=RSUBO*CHV(IHV90)-COORD(1)*SINXH(ICHIH)*SINXV(ICHIV)+
1 AHPRIM*COORD(2)*SINXV(ICHIV)*COSXH(ICHIH)+      (D 585)
2 COORD(3)*SINXH(ICHIH)*COSXV(ICHIV)               (D 586)
100 CALL PARTLS(1,I,0,PTL1I)                        (D 587)
IF(I.EQ.J)GO TO 200                                (D 588)
CALL PARTLS(1,J,0,PTL1J)                           (D 589)
GO TO 300                                           (D 590)
200 PTL1J=PTL1I                                     (D 591)
CALL PARTLS(2,I,0,PTL2IJ)                          (D 592)
IF(I.EQ.K)GO TO 600                                (D 593)
GO TO 700                                           (D 594)
300 IF(I.EQ.K)GO TO 500                             (D 595)
IF(J.EQ.K)GO TO 400                                (D 596)
CALL PARTLS(1,K,0,PTL1K)                           (D 597)
CALL PARTLS(3,J,K,PTL2JK)                          (D 598)
CALL PARTLS(3,I,K,PTL2IK)                          (D 599)
CALL PARTLS(3,I,J,PTL2IJ)                          (D 600)
CALL PARTLS(6,0,0,PTL1JK)                          (D 601)
GO TO 800                                           (D 602)
400 PTL1K=PTL1J                                     (D 603)
CALL PARTLS(2,J,0,PTL2JK)                          (D 604)
CALL PARTLS(3,I,K,PTL2IK)                          (D 605)
PTL2IJ=PTL2IK                                       (D 606)
CALL PARTLS(5,J,I,PTL1JK)                          (D 607)
GO TO 800                                           (D 608)
500 PTL1K=PTL1I                                     (D 609)
CALL PARTLS(2,I,0,PTL2IK)                          (D 610)
CALL PARTLS(3,J,K,PTL2JK)                          (D 611)
PTL2IJ=PTL2JK                                       (D 612)
CALL PARTLS(5,I,J,PTL1JK)                          (D 613)
GO TO 800                                           (D 614)
600 PTL1K=PTL1J                                     (D 615)
PTL2IK=PTL2IJ                                       (D 616)
PTL2JK=PTL2IJ                                       (D 617)
CALL PARTLS(4,I,0,PTL1JK)                          (D 618)
GO TO 800                                           (D 619)
700 CALL PARTLS(1,K,0,PTL1K)                        (D 620)
CALL PARTLS(3,J,K,PTL2JK)                          (D 621)
PTL2IK=PTL2JK                                       (D 622)
CALL PARTLS(5,J,K,PTL1JK)                          (D 623)
800 PHI(2)=PTL1JK/AOVERH-(PTL1I*PTL2JK+PTL1J*PTL2IK
1 +PTL1K*PTL2IJ)/AOVERH**2+                        (D 624)
2 2.0*PTL1I*PTL1J*PTL1K/AOVERH**3                 (D 625)
RETURN                                             (D 626)
END                                              (D 627)

```

APPENDIX D – Continued

```

SUBROUTINE PARTLS(IORDER,M,N,DERIV) (D 630)
COMMON RSUBO,ADVERH,CHV(2),SINXH(2),COSXH(2), (D 631)
1 SINXV(2),COSXV(2),IHV90,ICHIH,ICHIV, (D 632)
2 COORD(3),PH (2),I,J,K,AHPRIM (D 633)
GO TO (100,200,300,400,500,600),IORDER (D 634)
C (D 635)
C FIRST ORDER PARTIALS WITH RESPECT TO COORDINATE M (D 636)
C (D 637)
100 GO TO(110,120,130),M (D 638)
110 DERIV=(COORD(1)*CHV(IHV90))/RSUBO-SINXH(ICHIH)* (D 639)
1 SINXV(ICHIV) (D 640)
GO TO 700 (D 641)
120 DERIV=(COORD(2)*CHV(IHV90))/RSUBO+AHPRIM* (D 642)
1 SINXV(ICHIV)*COSXH(ICHIH) (D 643)
GO TO 700 (D 644)
130 DERIV=(COORD(3)*CHV(IHV90))/RSUBO+SINXH(ICHIH)* (D 645)
1 COSXV(ICHIV) (D 646)
GO TO 700 (D 647)
C (D 648)
C SECOND ORDER PARTIAL WITH RESPECT TO COORDINATE M (D 649)
C (D 650)
200 DERIV=(CHV(IHV90)/RSUBO)* (1.0-(COORD(M)**2)/ (D 651)
1 (RSUBO**2)) (D 652)
GO TO 700 (D 653)
C (D 654)
C SECOND ORDER PARTIAL WITH RESPECT TO COORDINATES M AND N (D 655)
C (D 656)
300 DERIV=-COORD(M)*COORD(N)*CHV(IHV90)/RSUBO**3 (D 657)
GO TO 700 (D 658)
C (D 659)
C THIRD ORDER PARTIAL WITH RESPECT TO COORDINATE M (D 660)
C (D 661)
400 DERIV=(3.0*COORD(M)*CHV(IHV90)/RSUBO**3)* (D 662)
1 (COORD(M)**2/RSUBO**2-1.0) (D 663)
GO TO 700 (D 664)
C (D 665)
C THIRD ORDER PARTIAL WITH RESPECT TO COORDINATES M AND N (D 666)
C (D 667)
500 DERIV=(COORD(N)*CHV(IHV90)/RSUBO**3)*(3.0* (D 668)
1 COORD(M)**2/RSUBO**2-1.0) (D 669)
GO TO 700 (D 670)
C (D 671)
C THIRD ORDER PARTIAL WITH RESPECT TO THREE VARIABLES (D 672)
C (D 673)
600 DERIV=3.0*COORD(1)*COORD(2)*COORD(3)*CHV(IHV90)/ (D 674)
1 RSUBO**5 (D 675)
700 RETURN (D 676)
END

```

APPENDIX D - Concluded

THE FOLLOWING DATA CARDS WERE USED TO OBTAIN THE COMPUTED RESULTS PRESENTED IN TABLES II AND III:

COLUMN NUMBER

0000000001111111112222222222333333333344444444445555555555666666666677777777778
1234567890123456789012345678901234567890123456789012345678901234567890

\$ANGLES CHIH(1)=60.,CHIV(1)=30.\$
CLOSED TUNNEL CASE VELOCITIES AND DERIVATIVES
2 1.000 1.000 1.000 0.375 0.250 0.125
2 2.000 0.750 2.000 0.750 0.250 0.500
2 1.000 1.000 1.000 0.000 0.000 0.000
3

\$ANGLES CHIH(1)=30.,CHIV(1)=60.\$
CLOSED TUNNEL CASE VELOCITIES AND DERIVATIVES
2 1.000 1.000 1.000 0.375 0.125 0.250
2 0.800 1.500 0.500 0.375 0.250 0.125
2 1.000 1.000 1.000 0.000 0.000 0.000
3

\$ANGLES CHIH(1)=45.,CHIV(1)=45.\$
CLOSED TUNNEL CASE VELOCITIES AND DERIVATIVES
2 1.000 1.000 1.000 0.000 0.000 0.000
3

\$ANGLES CHIH(1)=60.,CHIV(1)=30.\$
GROUND EFFECT CASE VELOCITIES AND DERIVATIVES
2 2.000 0.750 2.000 0.750 0.250 0.500

MORE TYPICALLY, WHEN MULTIPLE SKEW ANGLES ARE REQUIRED, THE FIRST CARD OF EACH GROUP MIGHT ASSUME A FORM SIMILAR TO THE FOLLOWING CARD:

\$ANGLES CHIH(1)=50.,60.,70.,80.,90.,CHIV(1)=45.,60.,75.,90.\$

THE SECOND CARD OF EACH GROUP MIGHT ASSUME ANY OF THE FOUR FOLLOWING FORMS:

CLOSED TUNNEL CASE VELOCITIES ONLY
CLOSED TUNNEL CASE VELOCITIES AND LONGITUDINAL DERIVATIVES ONLY
CLOSED TUNNEL CASE VELOCITIES AND DERIVATIVES
GROUND EFFECT CASE VELOCITIES AND DERIVATIVES

COLUMN NUMBER

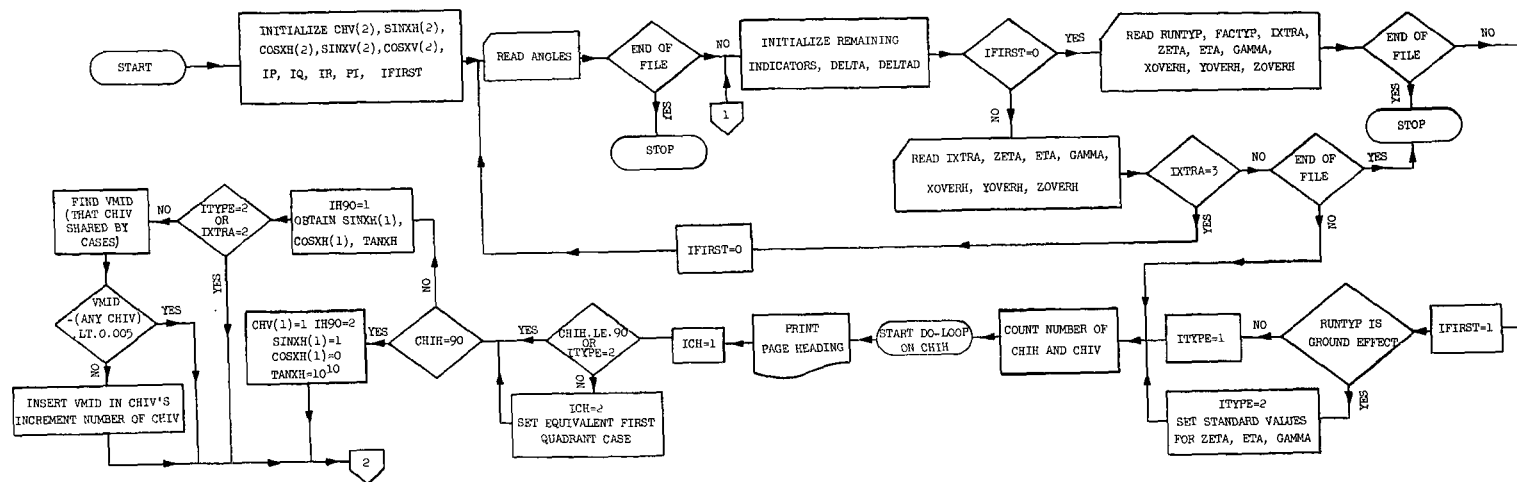
0000000001111111112222222222333333333344444444445555555555666666666677777777778
1234567890123456789012345678901234567890123456789012345678901234567890

APPENDIX E

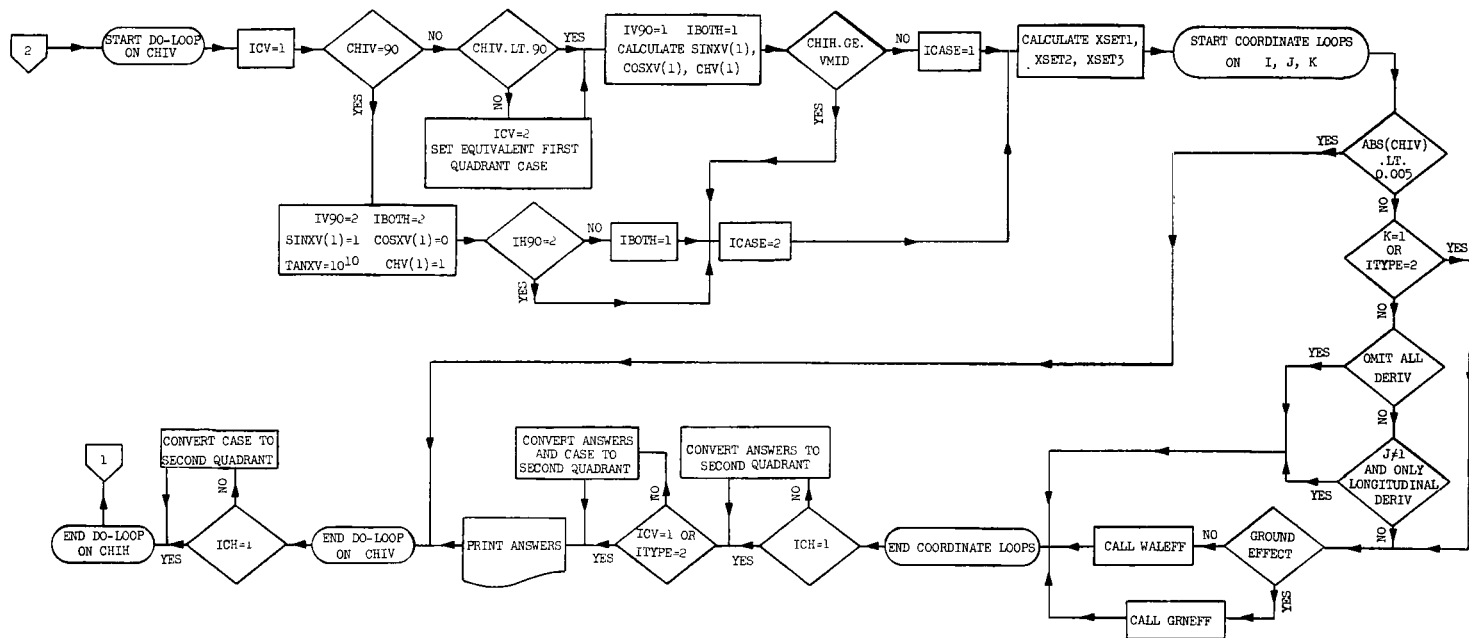
FLOW CHART FOR FORTRAN PROGRAM OF APPENDIX D

Program STABIL

Function: Main Program



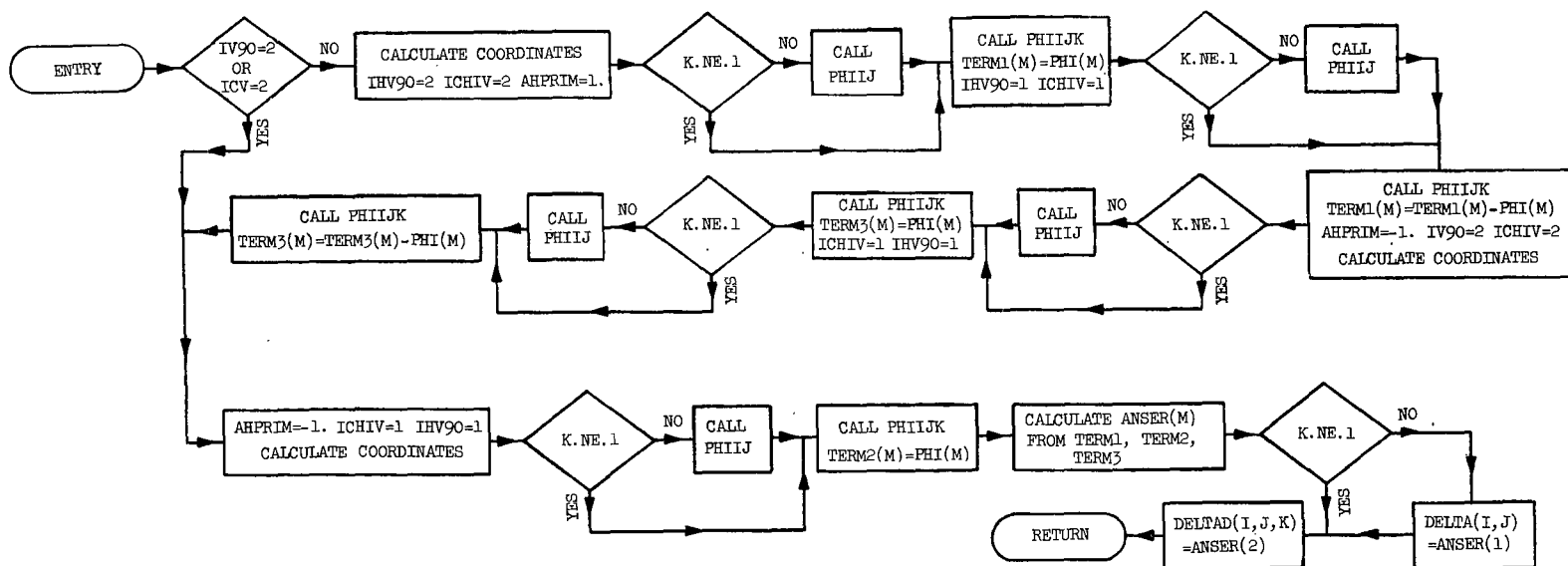
Program STABIL - Concluded.



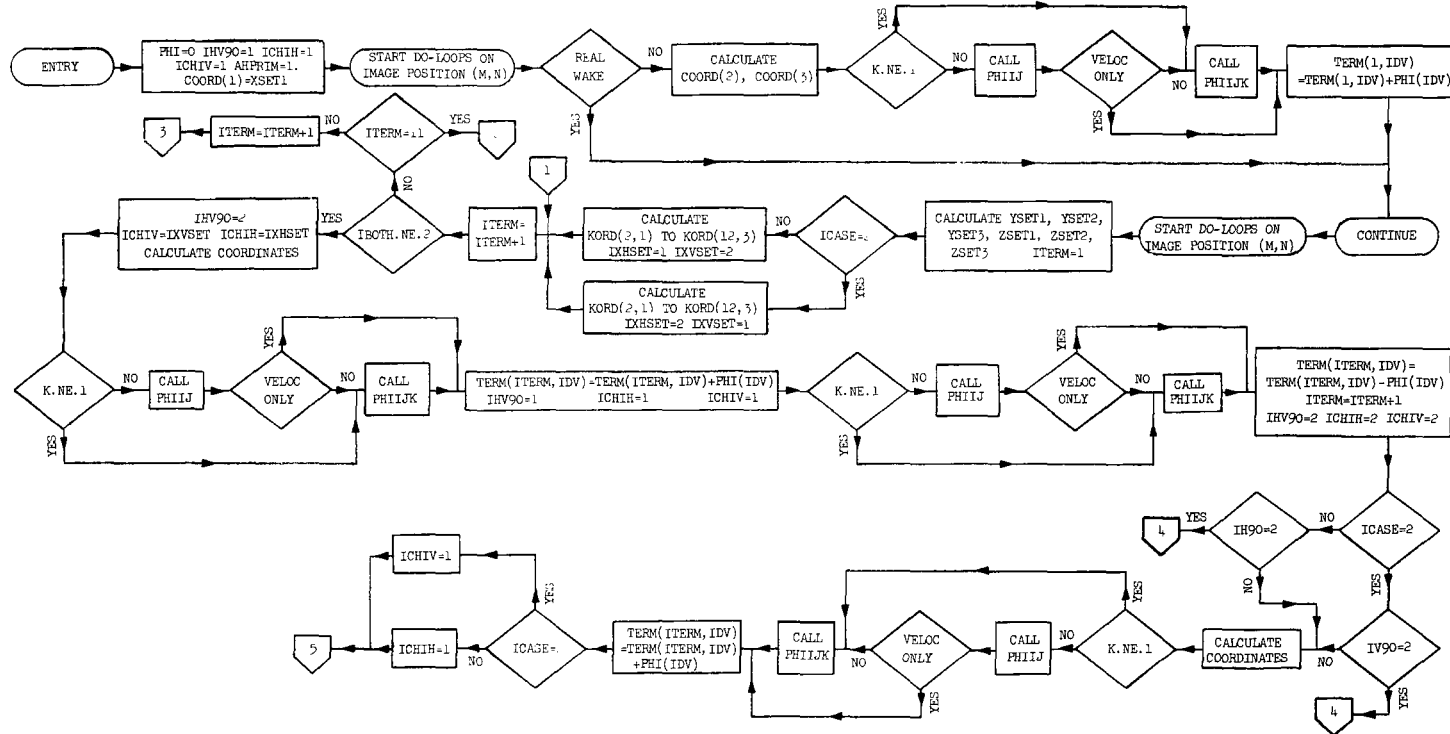
APPENDIX E - Continued

Subroutine GRNEFF

Function: Calculate interference factors in ground effect



Function: Calculate interference factors in a closed wind-tunnel



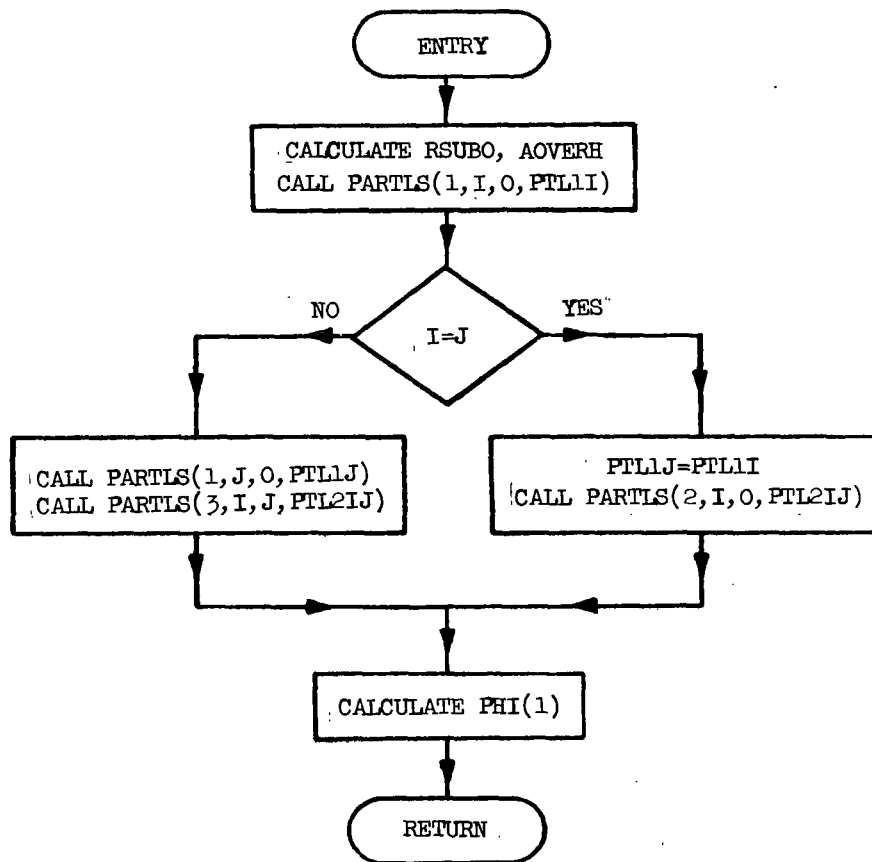

```

graph TD
    Start([Start]) --> KNE1{K.NE.1}
    KNE1 -- YES --> KNE1
    KNE1 -- NO --> CALLPHIJ[CALL PHIJ]
    CALLPHIJ --> VELOCONLY{VELOC ONLY}
    VELOCONLY -- YES --> KNE1
    VELOCONLY -- NO --> CALLPHIJK[CALL PHIJK]
    CALLPHIJK --> TERMIDV1[TERM(ITERM, IDV)  
=TERM(ITERM, IDV)-PHI(IDV)]
    TERMIDV1 --> ITERM12{ITERM=12}
    ITERM12 -- YES --> Exit2{2}
    ITERM12 -- NO --> ITERMplus1[ITERM=ITERM+1]
    ITERMplus1 --> ITERM4OR7{ITERM=4  
OR  
ITERM=7}
    ITERM4OR7 -- YES --> AHPRIMminus1[AHPRIM=-1.]
    ITERM4OR7 -- NO --> AHPRIM1[AHPRIM=1.]
    AHPRIM1 --> KNE1
    AHPRIMminus1 --> KNE1
    KNE1 --> IHV90ICHIV[ITHV90=1 ICHIV=1  
ICHIH=1  
CALCULATE  
COORDINATES]
    IHV90ICHIV --> KNE1
    KNE1 --> CALLPHIJK
    CALLPHIJK --> VELOCONLY
    VELOCONLY -- YES --> KNE1
    VELOCONLY -- NO --> CALLPHIJ
    CALLPHIJ --> ENDLOOP([END DO-LOOP ON  
IMAGE POSITION])
    ENDLOOP --> ITERM12
    ITERM12 -- YES --> Exit3{3}
    ITERM12 -- NO --> Exit2
    Exit2 --> KNE1
    Exit3 --> KNE1
    KNE1 --> ICASE2{ICASE=2}
    ICASE2 -- YES --> CALCIPOWR1_2_1[CALCULATE IPOWR1, IPOWR2]
    ICASE2 -- NO --> CALCIPOWR1_2_2[CALCULATE IPOWR1, IPOWR2]
    CALCIPOWR1_2_1 --> CALCANSERIDV[CALCULATE  
ANSER(IDV)]
    CALCIPOWR1_2_2 --> CALCANSERIDV
    CALCANSERIDV --> KNE1
    KNE1 -- YES --> DELTAD[DELTA(I, J, K)=ANSER(2)]
    DELTAD --> RETURN([RETURN])
    KNE1 -- NO --> DELTAIJ[DELTA(I, J)=ANSER(1)]
    DELTAIJ --> DELTAD
  
```

APPENDIX E - Continued

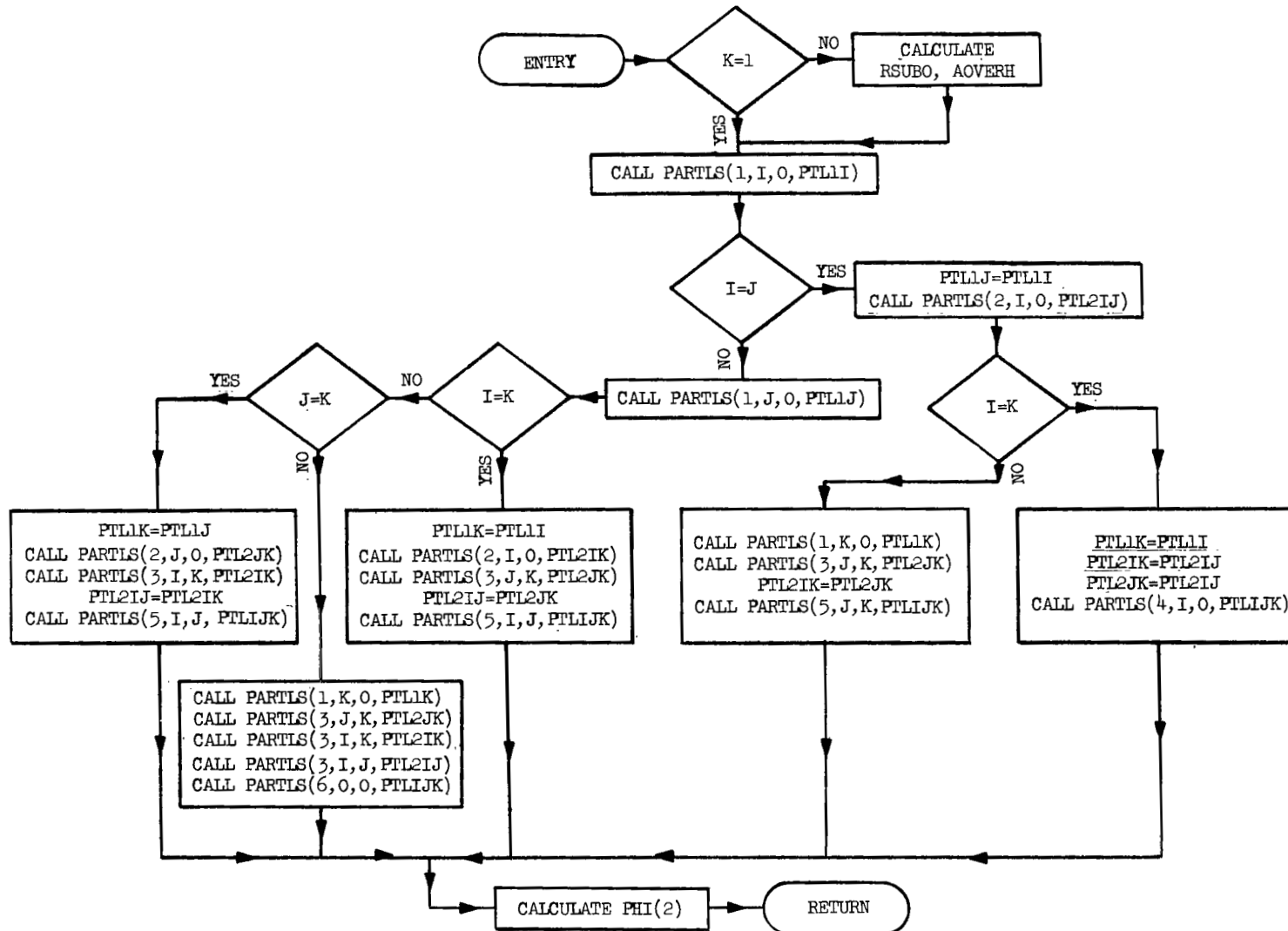
Subroutine PHIJ

Function: Calculate interference velocities in free air



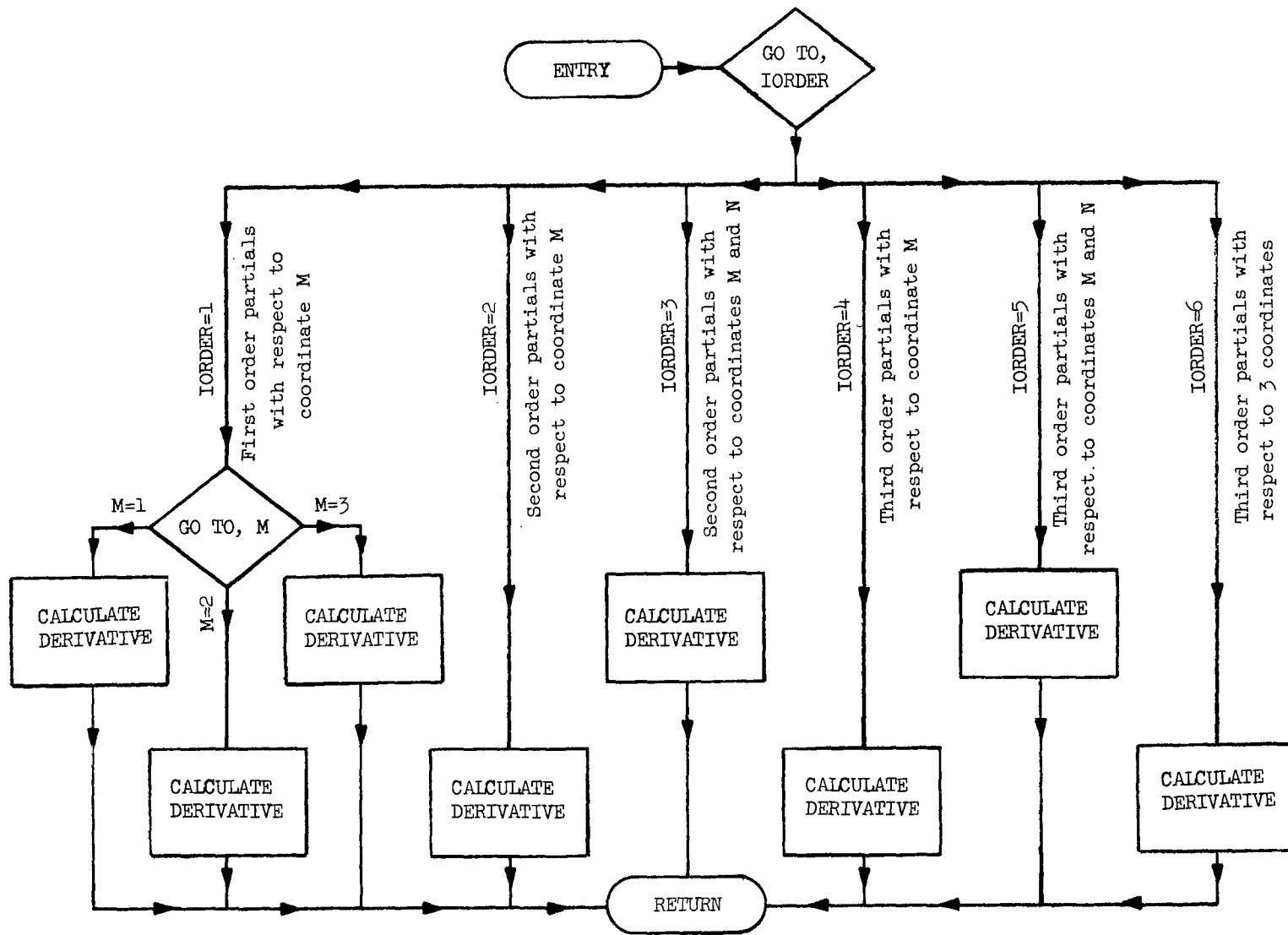
Subroutine PHIIJK

Function: Calculate interference gradients in free air



Subroutine PARTLS(IORDER,M,N,DERIV)

Function: To obtain the partial derivatives of PHI



REFERENCES

1. Garner, H. C.; Rogers, E. W. E.; Acum, W. E. A.; and Maskell, E. C.: Subsonic Wind Tunnel Wall Corrections. *Agardograph* 109, 1966.
2. Heyson, Harry H.: Wind-Tunnel Wall Effects at Extreme Force Coefficients. *Ann. N. Y. Acad. Sci.*, vol 154, art. 2, Nov. 22, 1968, pp. 1074-1093.
3. Heyson, Harry H.: Jet-Boundary Corrections for Lifting Rotors Centered in Rectangular Wind Tunnels. *NASA TR R-71*, 1960.
4. Heyson, Harry H.: Wind-Tunnel Wall Interference and Ground Effect for VTOL-STOL Aircraft. *J. Amer. Helicopter Soc.*, vol. 6, no. 1, Jan 1961, pp. 1-9.
5. Heyson, Harry H.: Linearized Theory of Wind-Tunnel Jet-Boundary Corrections and Ground Effect for VTOL-STOL Aircraft. *NASA TR R-124*, 1962.
6. Heyson, Harry H.: Use of Superposition in Digital Computers to Obtain Wind-Tunnel Interference Factors for Arbitrary Configurations, With Particular Reference to V/STOL Models. *NASA TR R-302*, 1969.
7. Heyson, Harry H.: Fortran Programs for Calculating Wind-Tunnel Boundary Interference. *NASA TM X-1740*, 1969.
8. Heyson, Harry H.: Theoretical Study of Conditions Limiting V/STOL Testing in Wind Tunnels With Solid Floor. *NASA TN D-5819*, 1970.
9. Heyson, Harry H.: Nomographic Solution of the Momentum Equation for VTOL-STOL Aircraft. *NASA TN D-814*, 1961. (Also available as V-STOL Momentum Equation, *Space/Aeronaut.* vol. 38, no. 2, July 1962, pp. B-18 - B-20.)
10. Heyson, Harry H.; and Grunwald, Kalman J.: Wind-Tunnel Boundary Interference for V/STOL Testing. *Conference on V/STOL and STOL Aircraft*, *NASA SP-116*, 1966, pp. 409-434.
11. Heyson, Harry H.: The Flow Throughout a Wind Tunnel Containing a Rotor With a Sharply Deflected Wake. *Proceedings Third CAL/AVLABS Symposium Aerodynamics of Rotary Wing and V/STOL Aircraft. Vol II*, June 1969.
12. Prandtl, L.: Applications of Modern Hydrodynamics to Aeronautics. *NACA Rep. 116*, 1921.
13. Rae, William H., Jr.: Limits on Minimum-Speed V/STOL Wind-Tunnel Tests. *J. Aircraft*, vol. 4, no. 3, May-June 1967, pp. 249-254.
14. Rae, William H., Jr.; and Shindo, Shojiro: Comments on V/STOL Wind Tunnel Data at Low Forward Speeds. *Proceedings Third CAL/AVLABS Symposium, Aerodynamics of Rotary Wing and V/STOL Aircraft. Vol. II*, June, 1969.

15. Heyson, Harry H.; and Katzoff, S.: Induced Velocities Near a Lifting Rotor with Non-uniform Disk Loading. NACA Rep. 1319, 1957. (Supersedes NACA TN 3690 by Heyson and Katzoff and TN 3691 by Heyson.)
16. Peirce, B. O.: A Short Table of Integrals. Third rev. ed., Ginn and Co., 1929.
17. Heyson, Harry H.: Approximate Treatment of V/STOL Wall Interference for Closed Circular Tunnels. NASA TN D-6127, 1971.
18. Joppa, Robert G.: Wall Interference Effects in Wind-Tunnel Testing of STOL Aircraft. J. Aircraft, vol. 6, no. 3, May-June 1969, pp. 209-214.
19. Vayssaire, J. C.: Nouvelle Méthode de Calcul de Correction des Résultats d'essais en Soufflerie Basse-Vitesse. 1re Partie - Corrections de Blocage et Corrections de Parois. (New Method of Calculating Corrections of Test Results in a Low-Speed Wind Tunnel. 1st Part - Blockage Corrections and Wall Corrections.) L'Aeronautique et l'Astronautique, vol. 15, no. 8, 1969, pp. 55-67.
20. Ellison, Don E.; and Hoak, Donald E.: Stability Derivative Estimation at Subsonic Speeds. Ann. N. Y. Acad. Sci., vol. 154, art. 2, No. 22, 1968, pp. 367-396.
21. Wheatley, John B.: An Aerodynamic Analysis of the Autogiro Rotor With a Comparison Between Calculated and Experimental Results. NACA Rep. 487, 1934.
22. Sweet, George E.: Static-Stability Measurements of a Stand-On Type Helicopter With Rigid Blades, Including a Comparison With Theory. NASA TN D-189, 1960.
23. Luoma, Arvo A.; Re, Richard J.; and Loving, Donald L.: Subsonic Longitudinal Aerodynamic Measurements on a Transport Model in Two Slotted Tunnels Differing in Size. NASA TM X-1660, 1968.
24. Heyson, Harry H.: Equations for the Application of Wind-Tunnel Wall Corrections to Pitching Moments Caused by the Tail of an Aircraft Model. NASA TN D-3738, 1966.

TABLE I
VALUES OF $\frac{A}{h}$, $\frac{A'}{h}$, AND THEIR DERIVATIVES FOR THE CENTER OF LIFT IN GROUND EFFECT

[For conciseness, the following abbreviations are used in this table and in appendix C:
 $s_H = \sin \chi_H$, $s_V = \sin \chi_V$, $c_H = \cos \chi_H$, $c_V = \cos \chi_V$, $C_{HV} = \sqrt{1 - \cos^2 \chi_H \cos^2 \chi_V}$]

Function of $\frac{A}{h}$ or $\frac{A'}{h}$	Values for use in determining -				
	$\phi \left[-\tan \chi_V, \frac{\tan \chi_V}{\tan \chi_H}, 1 \right]$	$\phi _{\chi_V=90^\circ} \left[-\tan \chi_V, \frac{\tan \chi_V}{\tan \chi_H}, 1 \right]$	$\phi' [0, 0, -2]$	$\phi' \left[-\tan \chi_V, \frac{\tan \chi_V}{\tan \chi_H}, -1 \right]$	$\phi' _{\chi_V=90^\circ} \left[-\tan \chi_V, \frac{\tan \chi_V}{\tan \chi_H}, -1 \right]$
$\frac{A}{h}$ or $\frac{A'}{h}$	$2 \frac{C_{HV}^2}{s_H c_V}$	$\frac{C_{HV} + s_V}{s_H c_V}$	$2(C_{HV} - s_H c_V)$	$\frac{2s_V^2}{s_H c_V}$	$\frac{C_{HV} + s_V}{s_H c_V}$
$\frac{\partial}{\partial \frac{x}{h}}$	$-2s_H s_V$	$-\frac{s_H}{C_{HV}}(C_{HV} + s_V)$	$-s_H s_V$	$-2s_H s_V$	$-\frac{s_H}{C_{HV}}(C_{HV} + s_V)$
$\frac{\partial}{\partial \frac{y}{h}}$	$2s_V c_H$	$\frac{c_H}{C_{HV}}(C_{HV} + s_V)$	$-s_V c_H$	$-2s_V c_H$	$-\frac{c_H}{C_{HV}}(C_{HV} + s_V)$
$\frac{\partial}{\partial \frac{z}{h}}$	$2s_H c_V$	$\frac{s_H c_V}{C_{HV}}$	$-(C_{HV} - s_H c_V)$	0	$-\frac{s_H c_V}{C_{HV}}$
$\frac{\partial^2}{\partial \frac{x^2}{h}}$	$\frac{s_H c_V}{C_{HV}^2}(C_{HV}^2 - s_H^2 s_V^2)$		$\frac{C_{HV}}{2}$	$\frac{s_H c_V}{C_{HV}^2}(C_{HV}^2 - s_H^2 s_V^2)$	
$\frac{\partial^2}{\partial \frac{y^2}{h}}$	$\frac{s_H^3 c_V}{C_{HV}^2}$		$\frac{C_{HV}}{2}$	$\frac{s_H^3 c_V}{C_{HV}^2}$	
$\frac{\partial^2}{\partial \frac{z^2}{h}}$	$\frac{s_H s_V^2 c_V}{C_{HV}^2}$		0	$\frac{s_H s_V^2 c_V}{C_{HV}^2}$	
$\frac{\partial^2}{\partial \frac{x}{h} \partial \frac{y}{h}}$	$\frac{s_H^2 s_V^2 c_H c_V}{C_{HV}^2}$		0	$-\frac{s_H^2 s_V^2 c_H c_V}{C_{HV}^2}$	
$\frac{\partial^2}{\partial \frac{x}{h} \partial \frac{z}{h}}$	$\frac{s_H^3 s_V c_V^2}{C_{HV}^2}$		0	$-\frac{s_H^3 s_V c_V^2}{C_{HV}^2}$	
$\frac{\partial^2}{\partial \frac{y}{h} \partial \frac{z}{h}}$	$-\frac{s_H^2 s_V c_H c_V^2}{C_{HV}^2}$		0	$-\frac{s_H^2 s_V c_H c_V^2}{C_{HV}^2}$	
$\frac{\partial^3}{\partial \frac{x^3}{h}}$	$\frac{3s_H^3 s_V c_V^2}{C_{HV}^4}(C_{HV}^2 - s_H^2 s_V^2)$		0	$\frac{3s_H^3 s_V c_V^2}{C_{HV}^4}(C_{HV}^2 - s_H^2 s_V^2)$	
$\frac{\partial^3}{\partial \frac{y^3}{h}}$	$-\frac{3s_H^4 s_V c_H c_V^2}{C_{HV}^4}$		0	$\frac{3s_H^4 s_V c_H c_V^2}{C_{HV}^4}$	
$\frac{\partial^3}{\partial \frac{x}{h} \partial \frac{y}{h}}$	$-\frac{3s_H^3 s_V^2 c_V^3}{C_{HV}^4}$		0	$\frac{3s_H^3 s_V^2 c_V^3}{C_{HV}^4}$	
$\frac{\partial^3}{\partial \frac{x^2}{h} \partial \frac{z}{h}}$	$-\frac{s_H^2 s_V c_H c_V^2}{C_{HV}^4}(C_{HV}^2 - 3s_H^2 s_V^2)$		0	$\frac{s_H^2 s_V c_H c_V^2}{C_{HV}^4}(C_{HV}^2 - 3s_H^2 s_V^2)$	
$\frac{\partial^3}{\partial \frac{x^2}{h} \partial \frac{y}{h}}$	$-\frac{s_H^3 c_V^3}{C_{HV}^4}(C_{HV}^2 - 3s_H^2 s_V^2)$		$\frac{C_{HV}}{4}$	$\frac{s_H^3 c_V^3}{C_{HV}^4}(C_{HV}^2 - 3s_H^2 s_V^2)$	
$\frac{\partial^3}{\partial \frac{y^2}{h} \partial \frac{x}{h}}$	$\frac{s_H^3 s_V c_V^2}{C_{HV}^4}(s_H^2 - 2s_V^2 c_H^2)$		0	$\frac{s_H^3 s_V c_V^2}{C_{HV}^4}(s_H^2 - 2s_V^2 c_H^2)$	
$\frac{\partial^3}{\partial \frac{y^2}{h} \partial \frac{z}{h}}$	$-\frac{s_H^3 c_V^3}{C_{HV}^4}(s_H^2 - 2s_V^2 c_H^2)$		$\frac{C_{HV}}{4}$	$\frac{s_H^3 c_V^3}{C_{HV}^4}(s_H^2 - 2s_V^2 c_H^2)$	
$\frac{\partial^3}{\partial \frac{z^2}{h} \partial \frac{x}{h}}$	$\frac{s_H^3 s_V c_V^2}{C_{HV}^4}(s_V^2 - 2s_H^2 c_V^2)$		0	$\frac{s_H^3 s_V c_V^2}{C_{HV}^4}(s_V^2 - 2s_H^2 c_V^2)$	
$\frac{\partial^3}{\partial \frac{z^2}{h} \partial \frac{y}{h}}$	$-\frac{s_H^2 s_V c_H c_V^2}{C_{HV}^4}(s_V^2 - 2s_H^2 c_V^2)$		0	$\frac{s_H^2 s_V c_H c_V^2}{C_{HV}^4}(s_V^2 - 2s_H^2 c_V^2)$	
$\frac{\partial^3}{\partial \frac{x}{h} \partial \frac{y}{h} \partial \frac{z}{h}}$	$-\frac{3s_H^4 s_V^2 c_H c_V^3}{C_{HV}^4}$		0	$-\frac{3s_H^4 s_V^2 c_H c_V^3}{C_{HV}^4}$	

Remaining items are $\frac{1}{C_{HV}}$ times preceding column

Remaining items are $\frac{1}{C_{HV}}$ times preceding column

TABLE II

NUMERICAL DEMONSTRATION OF SYMMETRY OF INTERFERENCE FACTORS

(a) In wind tunnel

INTERFERENCE FACTORS FOR STABILITY WORK IN A CLOSED TUNNEL
AT A POINT NEAR A VANISHINGLY SMALL MODEL

GAMMA = 2.000 ZETA = 2.000 ETA = .750
X/H = .750 Y/H = .250 Z/H = .500

	CHI(H) = 60.00	CHI(V) = 30.00							
	(X,X)	(X,Y)	(X,Z)	(Y,X)	(Y,Y)	(Y,Z)	(Z,X)	(Z,Y)	(Z,Z)
DEFI TA(---)	-1.3957	-.8978	-.1094	-.5998	-.6524	2.0500	-.4285	-.7258	-1.2166
DEFI TA(---X)	-.3771	.8491	1.4427	1.1989	.8414	.4786	-.7179	.5457	1.1923
DEFI TA(---Y)	.8491	1.1433	.5122	.8414	3.0425	-1.7695	.5457	-.6569	1.5429
DEFI TA(---Z)	1.4427	.5122	-.7662	.4786	-1.7695	-4.2414	1.1923	1.5429	1.3747

(b) In ground effect

INTERFERENCE FACTORS FOR STABILITY WORK IN GROUND EFFECT
AT A POINT NEAR A VANISHINGLY SMALL MODEL

X/H = .750 Y/H = .250 Z/H = .500

	CHI(H) = 60.00	CHI(V) = 30.00							
	(X,X)	(X,Y)	(X,Z)	(Y,X)	(Y,Y)	(Y,Z)	(Z,X)	(Z,Y)	(Z,Z)
DEFI TA(---)	-.1647	-.2271	-.1595	-.2271	-.0732	.4127	-.0153	-.1898	-.3645
DEFI TA(---X)	-.1851	.0712	.2345	.0712	.1183	.2463	-.2538	.0167	.0662
DEFI TA(---Y)	.0712	.1183	.2463	.1183	.4851	-.0771	.0167	-.1502	.3173
DEFI TA(---Z)	.2345	.2463	.0662	.2463	-.0771	-.5563	.0662	.3173	.4039

TABLE III

NUMERICAL DEMONSTRATION OF INTERCHANGE EQUIVALENCES FOR A VANISHINGLY SMALL MODEL

(a) Arbitrary point in arbitrary tunnel

INTERFERENCE FACTORS FOR STABILITY WORK IN A CLOSED TUNNEL
AT A POINT NEAR A VANISHINGLY SMALL MODEL

GAMMA = 2.000 ZETA = 2.000 ETA = .750
X/H = .750 Y/H = .750 Z/H = .500

CHI(H) = 60.00 CHI(V) = 30.00

	(X,X)	(X,Y)	(X,Z)	(Y,X)	(Y,Y)	(Y,Z)	(Z,X)	(Z,Y)	(Z,Z)
DELTA(-,-)	-1.3957	-.8978	-.1094	-.5998	-.6524	2.0500	-.4285	-.7258	-1.2166
DELTA(-,-,X)	-.3771	.8491	1.4427	1.1989	.8414	.4786	-.7179	.5457	1.1923
DELTA(-,-,Y)	-.8491	1.1433	.5122	.8414	3.0425	-1.7695	.5457	-.6569	1.5429
DELTA(-,-,Z)	1.4427	.5122	-.7662	.4786	-1.7695	-4.2414	1.1923	1.5429	1.3747

INTERFERENCE FACTORS FOR STABILITY WORK IN A CLOSED TUNNEL
AT A POINT NEAR A VANISHINGLY SMALL MODEL

GAMMA = .500 ZETA = .800 ETA = 1.500
X/H = .375 Y/H = .750 Z/H = .125

CHI(H) = 30.00 CHI(V) = 60.00

	(X,X)	(X,Y)	(X,Z)	(Y,X)	(Y,Y)	(Y,Z)	(Z,X)	(Z,Y)	(Z,Z)
DELTA(-,-)	-1.3957	-.1094	-.8978	-.4285	-1.2166	-.7258	-.5998	2.0500	-.6524
DELTA(-,-,X)	-.7541	2.8855	1.4981	-1.4358	2.3847	1.0915	2.3978	-.9571	1.6828
DELTA(-,-,Y)	2.8855	-1.5325	1.0244	2.3847	2.7495	3.0858	.9571	-8.4828	-3.5389
DELTA(-,-,Z)	1.4981	1.0244	2.2866	1.0915	3.0858	-1.3137	1.6828	-3.5389	6.0849

(b) Arbitrary point with centrally located model in square tunnel

INTERFERENCE FACTORS FOR STABILITY WORK IN A CLOSED TUNNEL
AT A POINT NEAR A VANISHINGLY SMALL MODEL

GAMMA = 1.000 ZETA = 1.000 ETA = 1.000
X/H = .375 Y/H = .125 Z/H = .250

CHI(H) = 30.00 CHI(V) = 60.00

	(X,X)	(X,Y)	(X,Z)	(Y,X)	(Y,Y)	(Y,Z)	(Z,X)	(Z,Y)	(Z,Z)
DELTA(-,-)	-.6061	-.4826	-.5072	.1588	-.7637	-.3555	-.0791	.2414	-.6279
DELTA(-,-,X)	-.8988	.0958	-.1753	-.4212	-.1837	-.1564	.1357	.3045	.0363
DELTA(-,-,Y)	.0958	.4388	.7309	-.1837	.6796	.7169	.3045	-.7749	.3787
DELTA(-,-,Z)	-.1753	.7309	.4599	-.1564	.7169	-.2584	.0363	.3787	.6796

INTERFERENCE FACTORS FOR STABILITY WORK IN A CLOSED TUNNEL
AT A POINT NEAR A VANISHINGLY SMALL MODEL

GAMMA = 1.000 ZETA = 1.000 ETA = 1.000
X/H = .375 Y/H = .250 Z/H = .125

CHI(H) = 60.00 CHI(V) = 30.00

	(X,X)	(X,Y)	(X,Z)	(Y,X)	(Y,Y)	(Y,Z)	(Z,X)	(Z,Y)	(Z,Z)
DELTA(-,-)	-.6061	-.5072	-.4876	-.0791	-.6279	-.1588	-.1588	-.3555	-.7637
DELTA(-,-,X)	-.8988	-.1753	.0558	.1357	.0363	.3045	-.4212	-.1564	-.1837
DELTA(-,-,Y)	-.1753	.4599	.7309	.0363	.6796	.3787	-.1564	-.2584	.7169
DELTA(-,-,Z)	.0558	.7309	.4388	.3045	.3787	-.7749	-.1837	.7169	.6796

TABLE III. - CONCLUDED.

(c) At centrally located model in square tunnel

INTERFERENCE FACTORS FOR STABILITY WORK IN A CLOSED TUNNEL
AT A POINT NEAR A VANISHINGLY SMALL MODEL

GAMMA = 1.000 ZETA = 1.000 ETA = 1.000
X/H = 0.000 Y/H = 0.000 Z/H = 0.000

	CHI(H) = 60.00	CHI(V) = 30.00							
	(X,X)	(X,Y)	(X,Z)	(Y,X)	(Y,Y)	(Y,Z)	(Z,X)	(Z,Y)	(Z,Z)
DEI TA(-,-)	-.0995	-.5752	-.7184	-.0461	-.7899	.0299	.4210	-.2350	-.8231
DEI TA(-,-,X)	-1.0978	-.4978	-.5092	-.2334	-.5315	.3050	-.1301	-.3184	-.9078
DEI TA(-,-,Y)	-.4978	.2308	.8732	-.5315	.6034	.8249	-.3184	-.5837	.5570
DELTA(-,-,Z)	-.5092	.8732	.8670	.3050	.8249	-.3700	-.9078	.5570	.7138

INTERFERENCE FACTORS FOR STABILITY WORK IN A CLOSED TUNNEL
AT A POINT NEAR A VANISHINGLY SMALL MODEL

GAMMA = 1.000 ZETA = 1.000 ETA = 1.000
X/H = 0.000 Y/H = 0.000 Z/H = 0.000

	CHI(H) = 30.00	CHI(V) = 60.00							
	(X,X)	(X,Y)	(X,Z)	(Y,X)	(Y,Y)	(Y,Z)	(Z,X)	(Z,Y)	(Z,Z)
DEI TA(-,-)	-.0995	-.7184	-.5752	.4210	-.8231	-.2350	-.0461	.0299	-.7899
DEI TA(-,-,X)	-1.0978	-.5092	-.4978	-.1301	-.9078	-.3184	-.2334	.3050	-.5315
DEI TA(-,-,Y)	-.5092	.8670	.8732	-.9078	.7138	.5570	.3050	-.3700	.8249
DELTA(-,-,Z)	-.4978	.8732	.2308	-.3184	.5570	-.5837	-.5315	.8249	.6034

(d) At centrally located model in square tunnel with equal vertical and horizontal skew angles

INTERFERENCE FACTORS FOR STABILITY WORK IN A CLOSED TUNNEL
AT A POINT NEAR A VANISHINGLY SMALL MODEL

GAMMA = 1.000 ZETA = 1.000 ETA = 1.000
X/H = 0.000 Y/H = 0.000 Z/H = 0.000

	CHI(H) = 45.00	CHI(V) = 45.00							
	(X,X)	(X,Y)	(X,Z)	(Y,X)	(Y,Y)	(Y,Z)	(Z,X)	(Z,Y)	(Z,Z)
DELTA(-,-)	-.1369	-.5555	-.5555	.2784	-.5826	-.2016	.2284	-.2016	-.5826
DEI TA(-,-,X)	-.9847	-.3277	-.3277	-.0240	-.4351	-.2219	-.0240	-.2219	-.4351
DEI TA(-,-,Y)	-.3277	.4924	.7522	-.4351	.2152	.5286	-.2219	-.1912	.5286
DEI TA(-,-,Z)	-.3277	.7522	.4924	-.2219	.5286	-.1912	-.4351	.5286	.2152

TABLE IV

NUMERICAL DEMONSTRATION OF FAILURE OF INTERCHANGE EQUIVALENCES FOR A WING OF FINITE SPAN

(a) Arbitrary wake skew angles

INTERFERENCE FACTORS FOR STABILITY TESTS IN A CLOSED TUNNEL
AVERAGE INTERFERENCE OVER A SWEEP WING OF FINITE SPAN

UNIFORM LOADING		
ETA= 1.000	ZETA= 1.000	GAMMA= 1.000
SIGMA= .750	ALPHA= 0.000	LAMBDA= 0.000
BETA= 0.000		

$$CHI(H) = 60.00 \quad CHI(V) = 30.00$$

	(X,X)	(X,Y)	(X,Z)	(Y,X)	(Y,Y)	(Y,Z)	(Z,X)	(Z,Y)	(Z,Z)
DELTA(-,-)	-.1799	-.4081	-.7790	.0819	-.7885	-.1506	.3100	-.0566	-.7749
DELTA(-,-,X)	-1.2500	-.2477	-.4959	-.1467	-.7341	-.1537	-.0346	-.0209	-.6877
DELTA(-,-,Y)	-.2477	.3876	.6169	-.7041	.0752	1.0358	-.0209	-.7291	.1853
DELTA(-,-,Z)	-.4959	.6169	.8724	-.1537	1.0358	.0715	-.6977	.1853	.7637

INTERFERENCE FACTORS FOR STABILITY TESTS IN A CLOSED TUNNEL
AVERAGE INTERFERENCE OVER A SWEEP WING OF FINITE SPAN

UNIFORM LOADING		
ETA= 1.000	ZETA= 1.000	GAMMA= 1.000
SIGMA= .750	ALPHA= 0.000	LAMBDA= 0.000
BETA= 0.000		

$$CHI(H) = 30.00 \quad CHI(V) = 60.00$$

	(X,X)	(X,Y)	(X,Z)	(Y,X)	(Y,Y)	(Y,Z)	(Z,X)	(Z,Y)	(Z,Z)
DELTA(-,-)	-.0321	-.0419	-.8724	.6348	-1.0274	-.3844	-.2292	.1852	-.9873
DELTA(-,-,X)	-1.6114	-.9757	-1.1591	.7671	-1.8871	-.9156	-.8274	1.0977	-.7607
DELTA(-,-,Y)	-.0757	1.4936	1.5590	-1.8971	.9415	1.1250	1.0977	-.8390	1.0499
DELTA(-,-,Z)	-1.1591	1.5590	.1182	-.9156	1.1250	-1.0086	-.7607	1.0499	1.6664

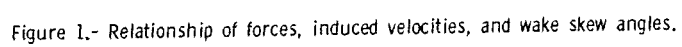
(b) Equal wake skew angles

INTERFERENCE FACTORS FOR STABILITY TESTS IN A CLOSED TUNNEL
AVERAGE INTERFERENCE OVER A SWEEP WING OF FINITE SPAN

UNIFORM LOADING		
ETA= 1.000	ZETA= 1.000	GAMMA= 1.000
SIGMA= .750	ALPHA= 0.000	LAMBDA= 0.000
BETA= 0.000		

$$CHI(H) = 45.00 \quad CHI(V) = 45.00$$

	(X,X)	(X,Y)	(X,Z)	(Y,X)	(Y,Y)	(Y,Z)	(Z,X)	(Z,Y)	(Z,Z)
DELTA(-,-)	-.1487	-.5373	-.7278	.3088	-.7173	-.3057	.1394	-.0192	-.6728
DELTA(-,-,X)	-1.4263	-.3061	-.5702	-.0628	-.8667	-.5662	-.0490	.2382	-.4162
DELTA(-,-,Y)	-.3061	.7082	.9598	-.8662	.1448	.9284	.2382	-.6664	.3368
DELTA(-,-,Z)	-.5702	.9598	.6981	-.5662	.9284	-.0819	-.4162	.3368	.7154



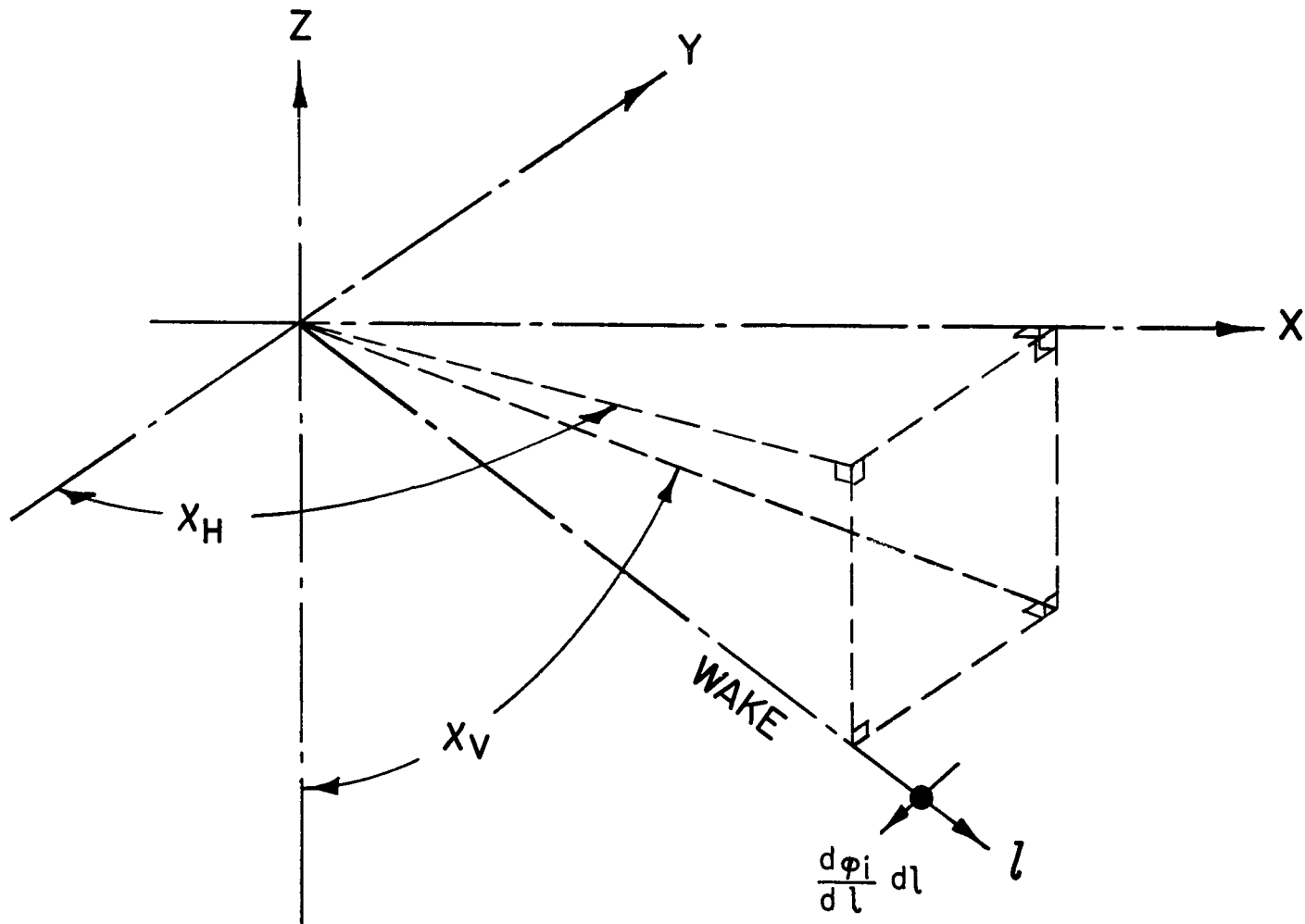


Figure 2.- Wake in free air.

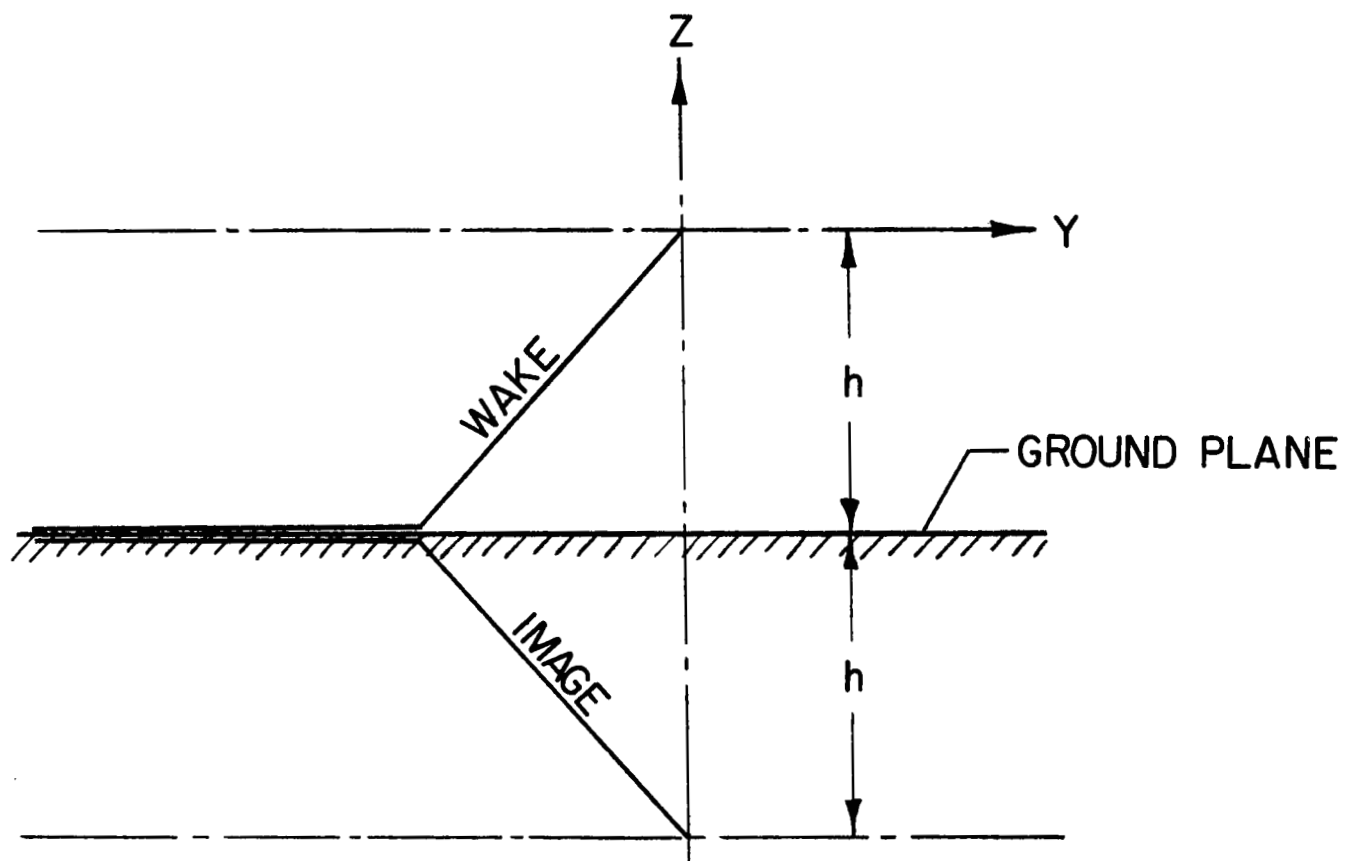


Figure 4.- Wake and image near simple ground plane.

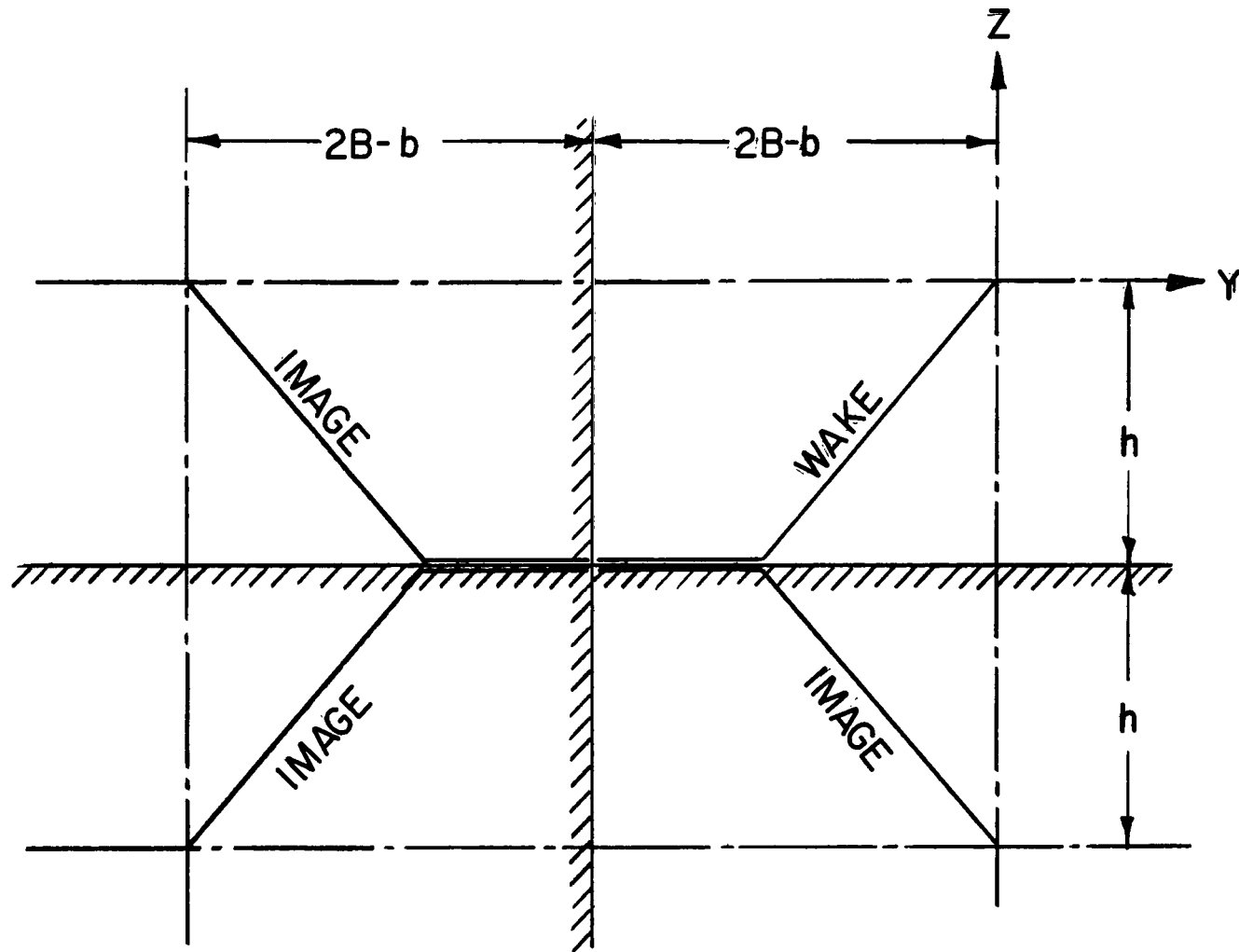


Figure 5.- Wake and images near intersection of simple ground plane and wall.

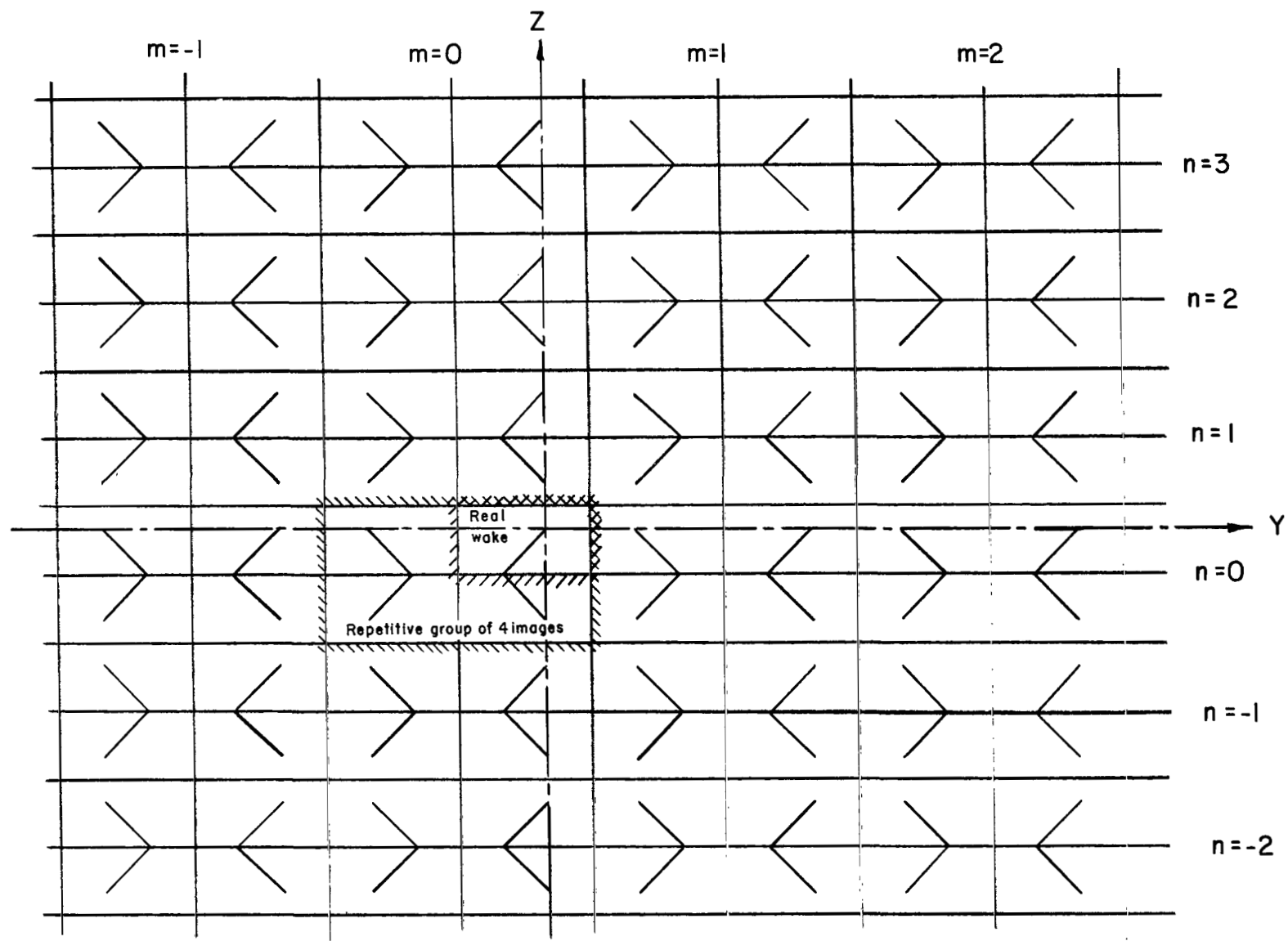


Figure 6.- Wake and central portion of doubly infinite image system used to represent the wind-tunnel walls.

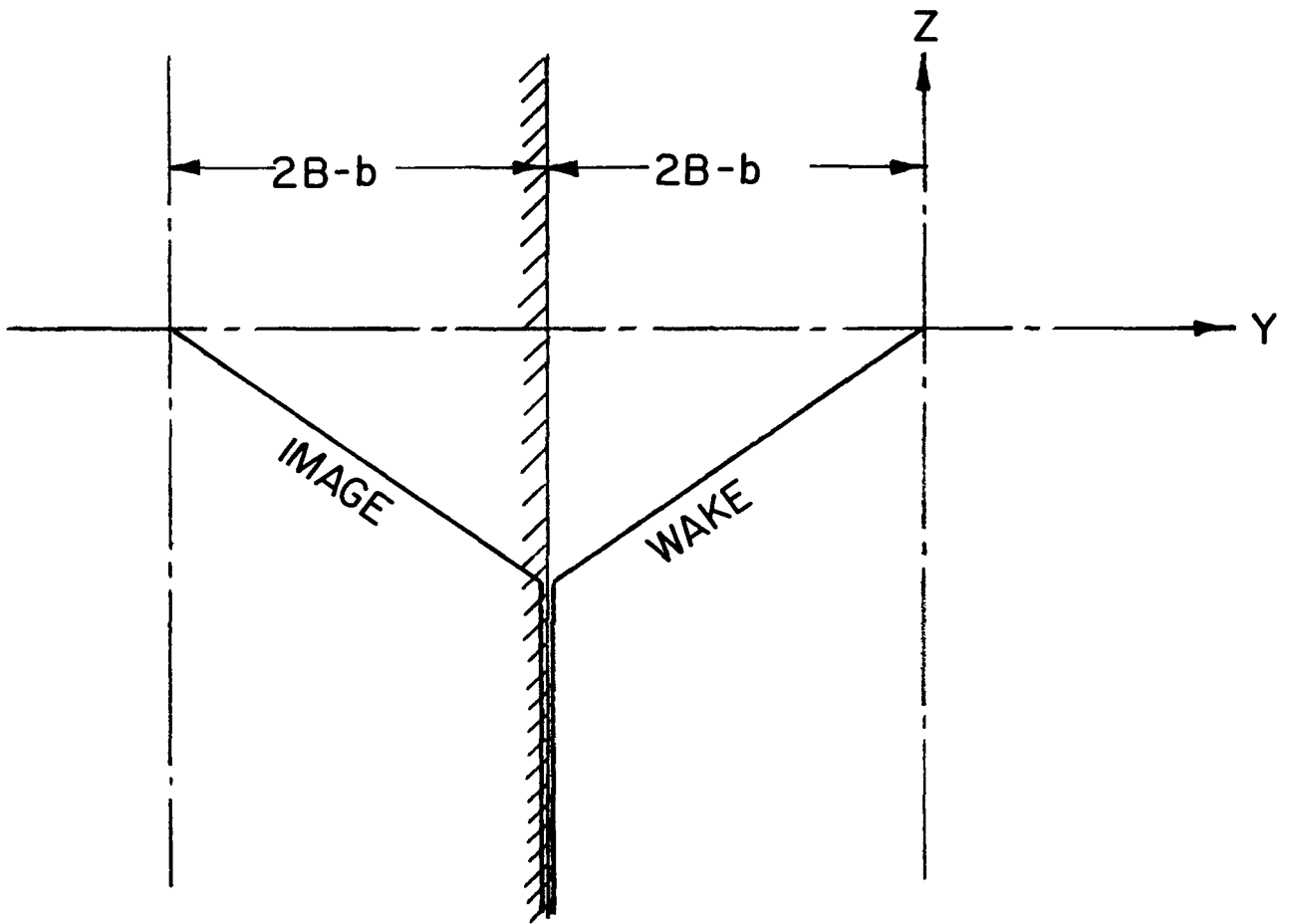


Figure 7.- Wake and image with single sidewall.

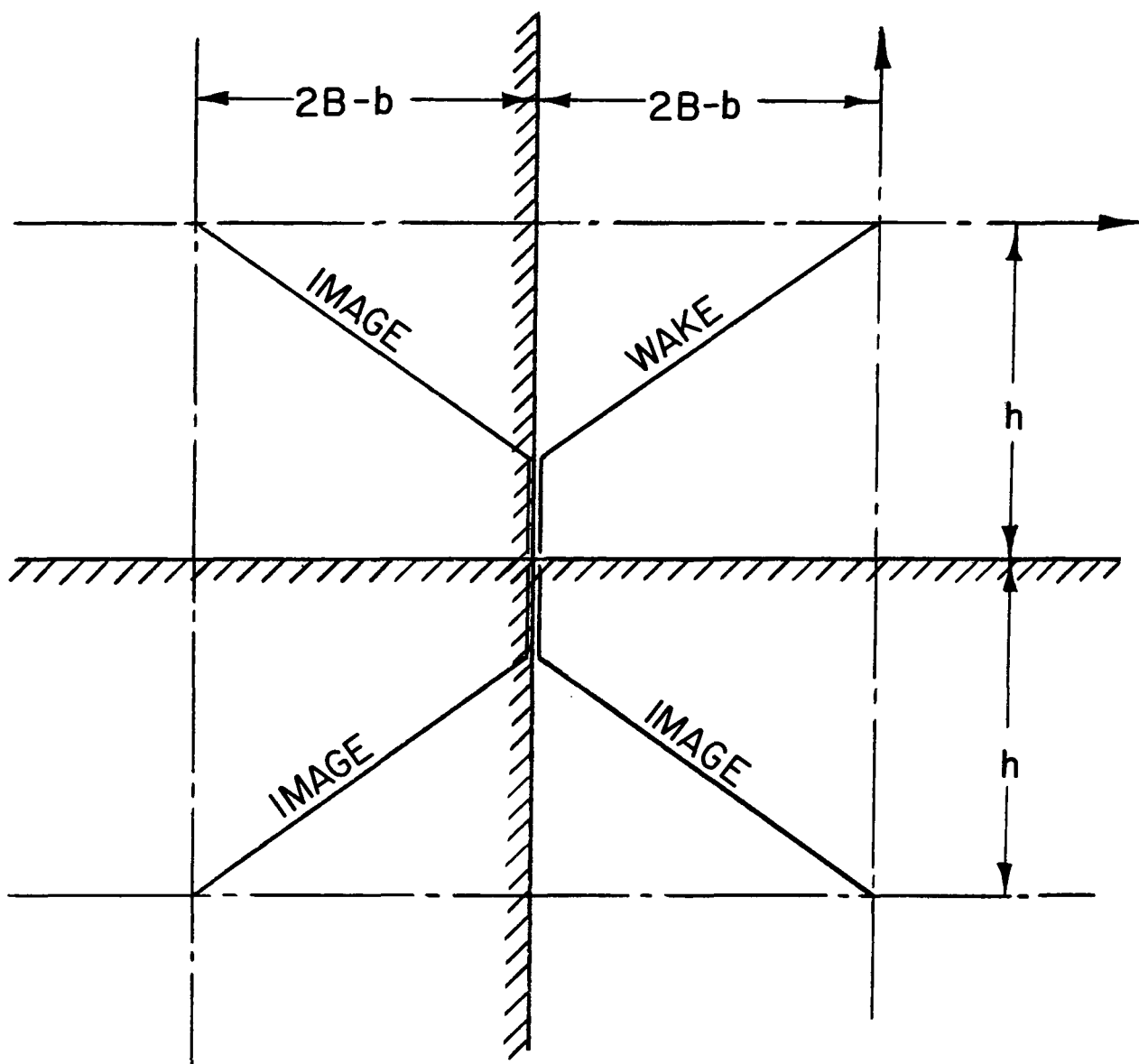
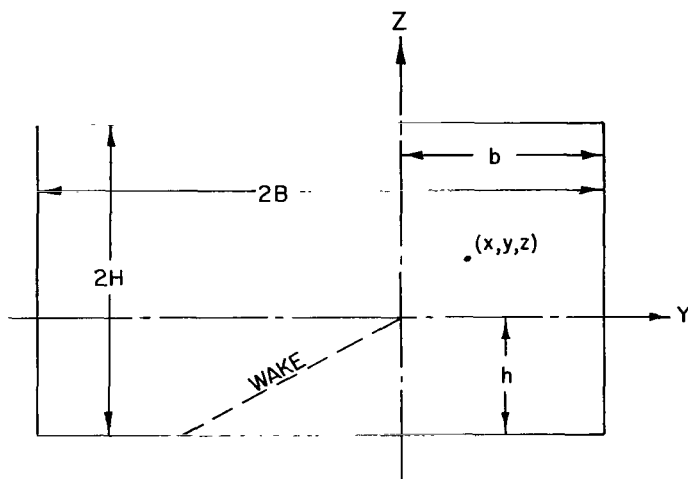
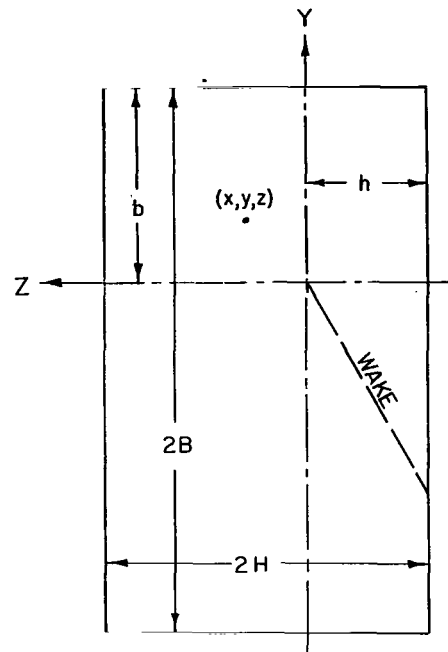


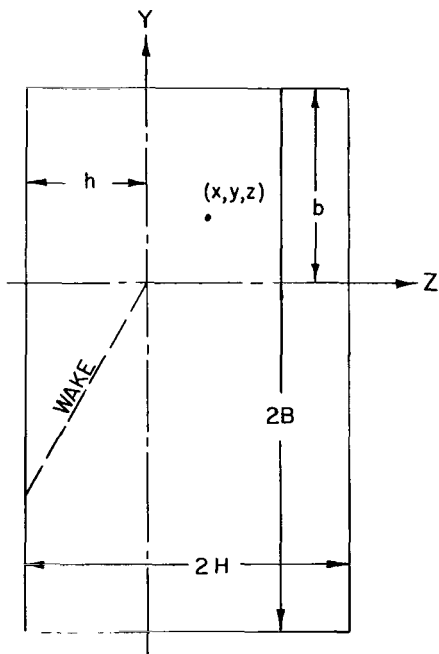
Figure 8.- Wake and images near intersection of single sidewall and ground plane.



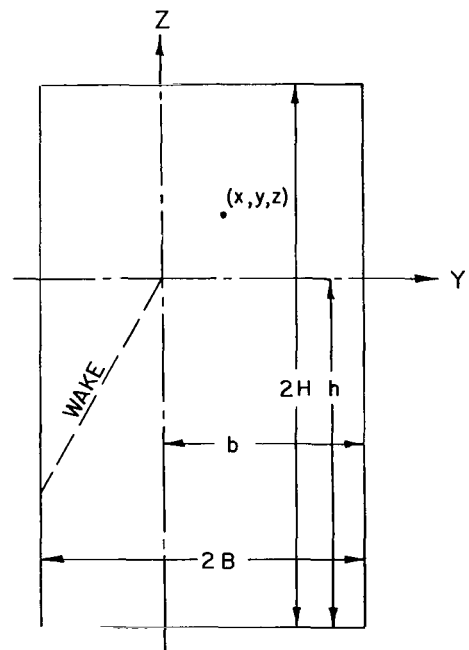
(a) Initial wind tunnel.



(b) Rotate 90° counterclockwise.

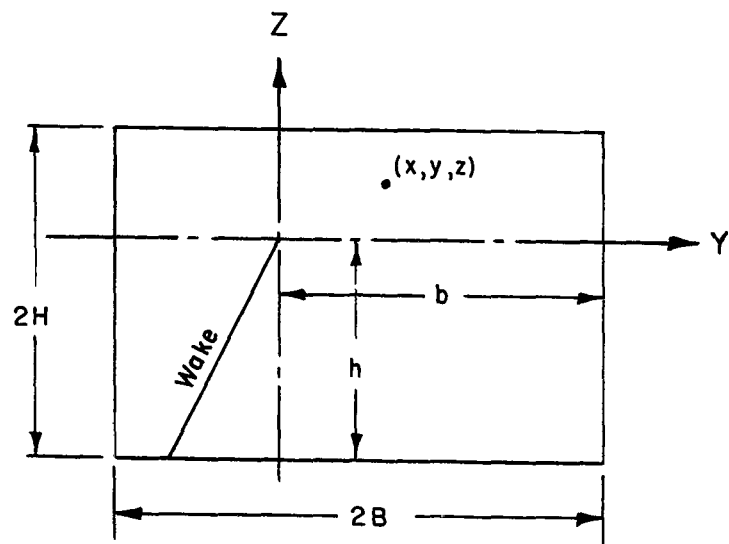
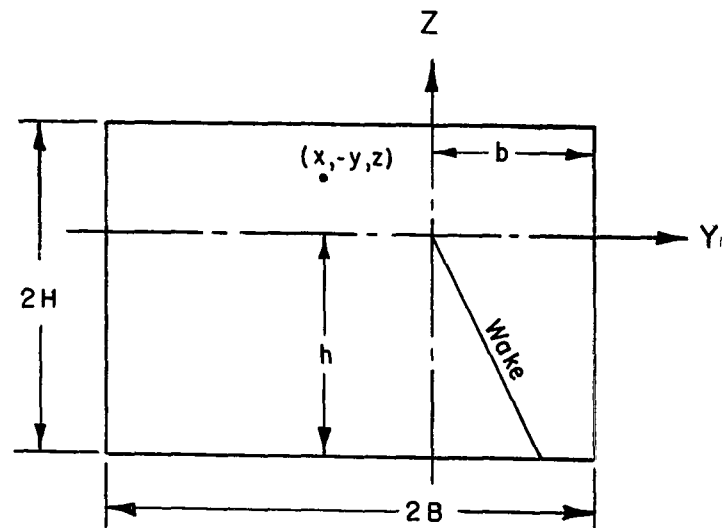
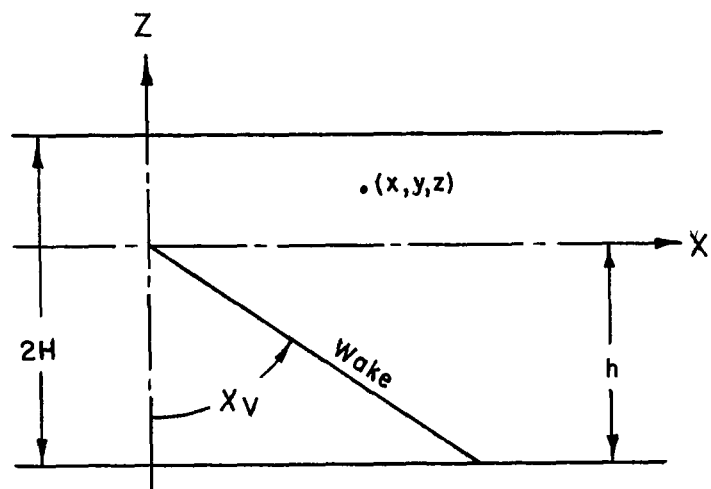
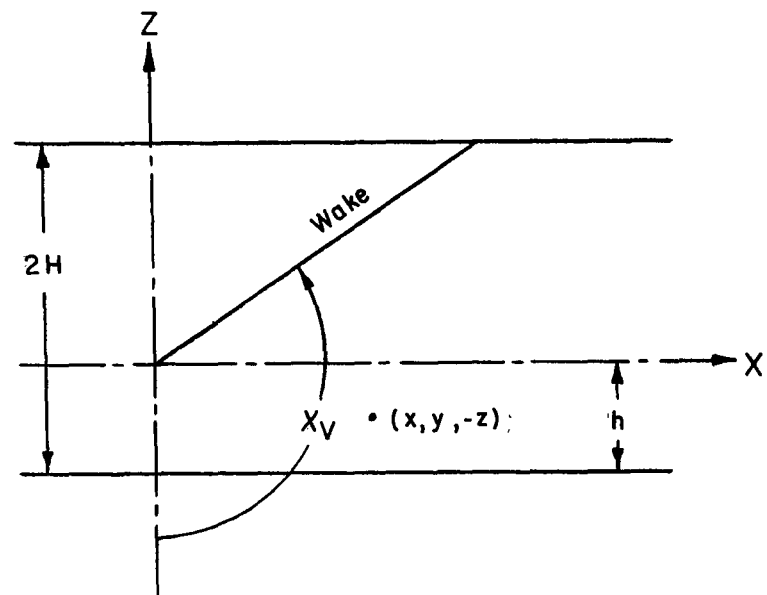


(c) Reverse to mirror image.



(d) Revert to standard nomenclature.

Figure 9.- Steps in developing interchange equivalences.

(e) X_H in first quadrant.(f) X_H in second quadrant.(g) X_V in first quadrant.(h) X_V in second quadrant.

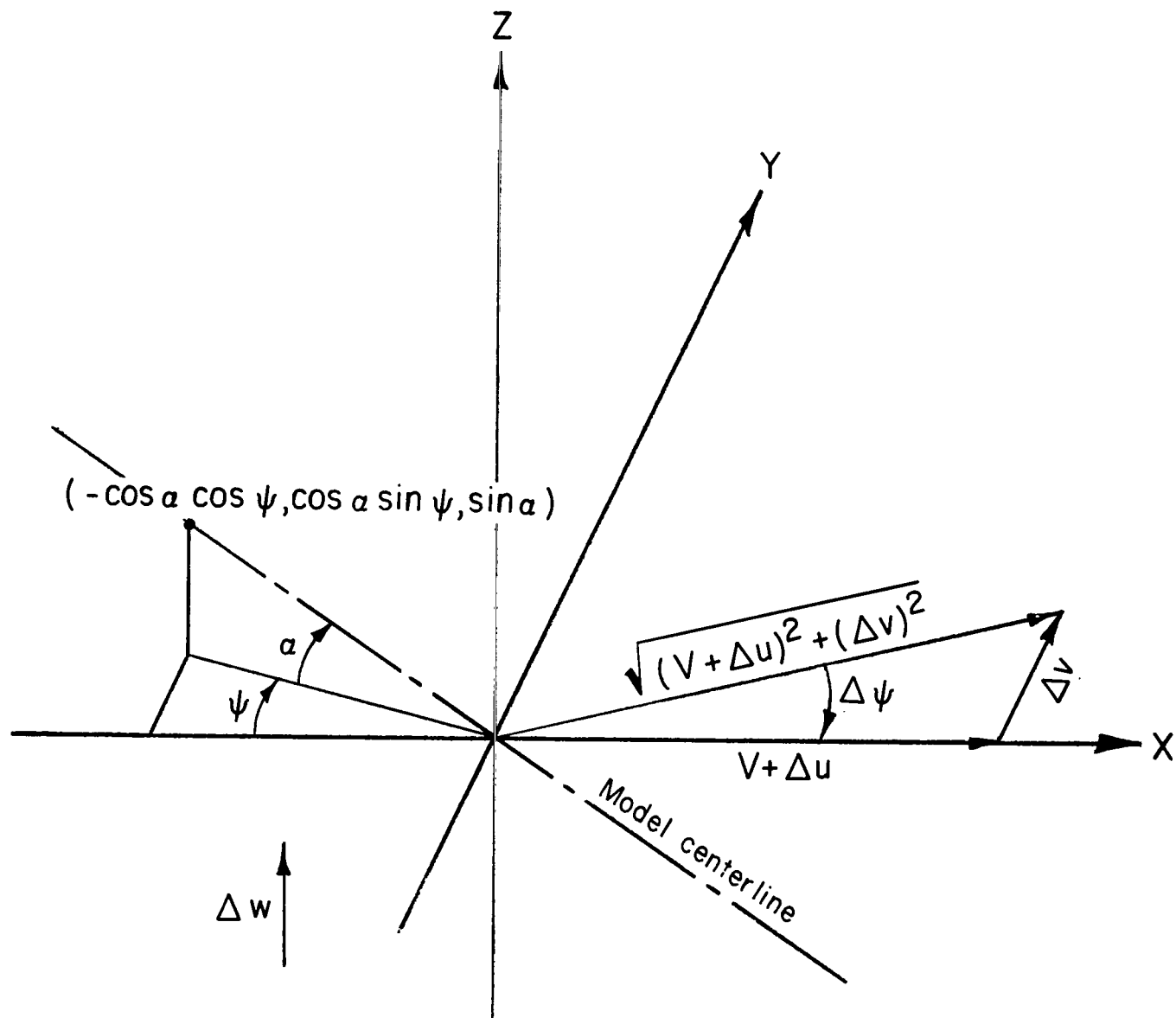


Figure 10.- Vector diagram for correcting yaw angle while retaining a rate of sink.

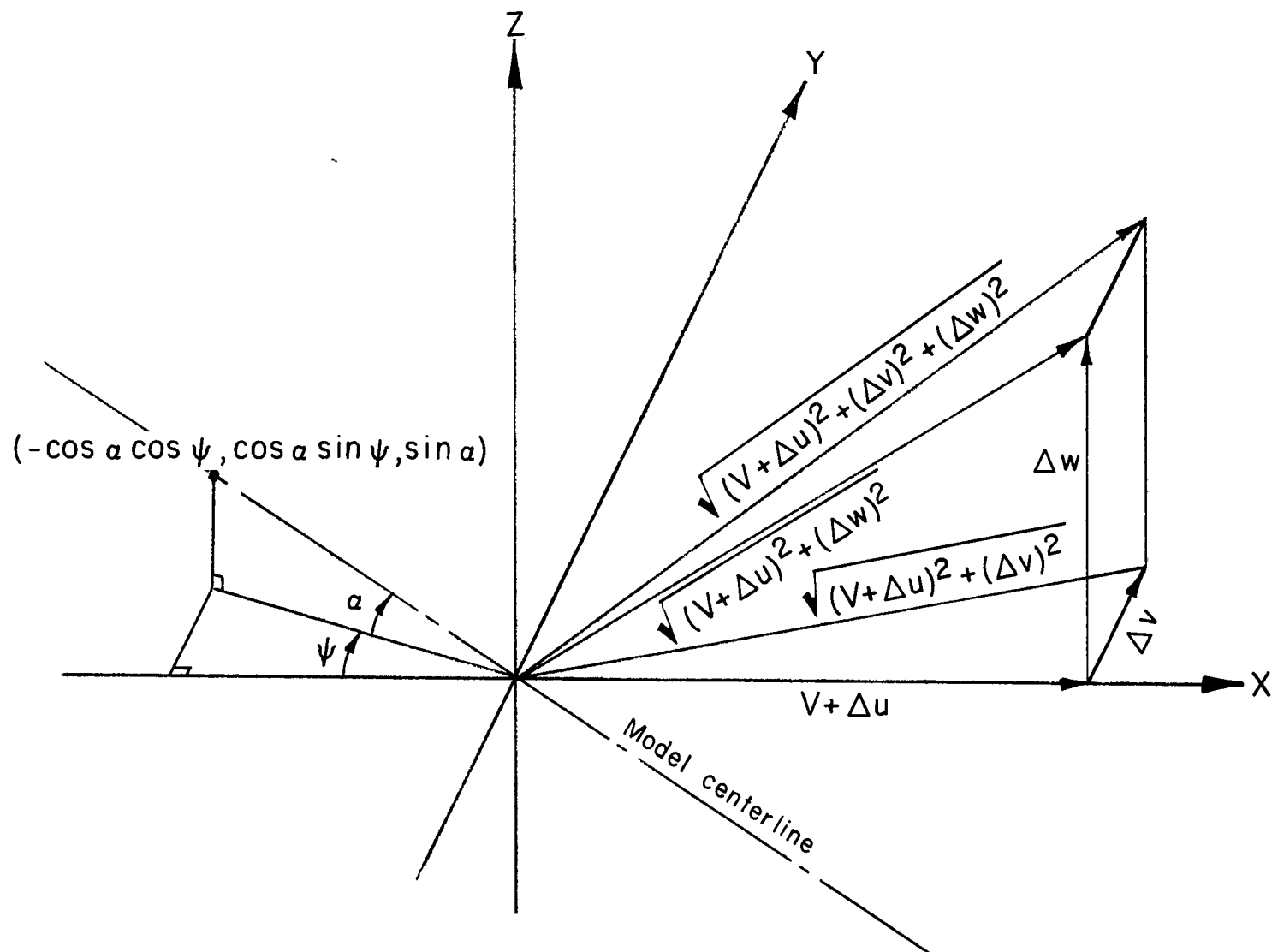
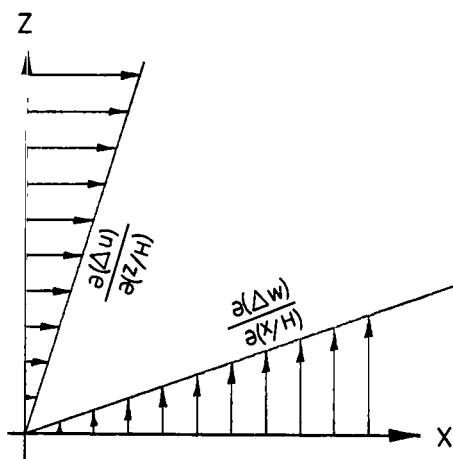
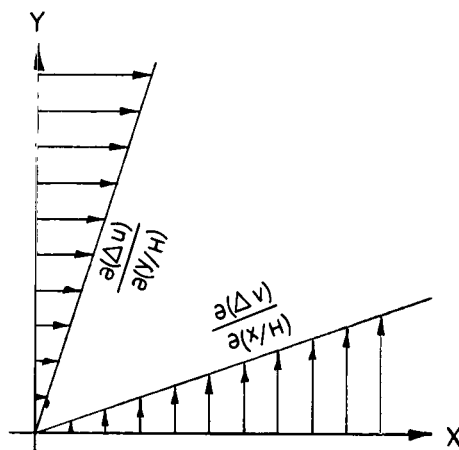


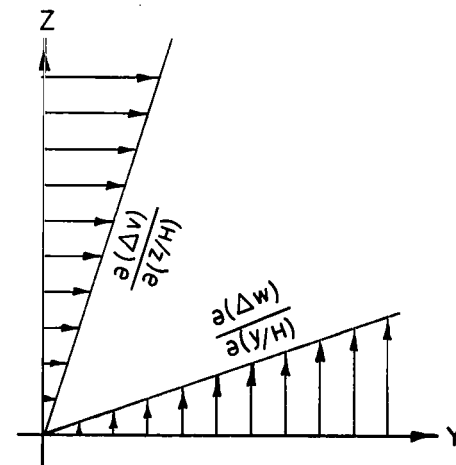
Figure 11.- Vector diagram for correcting both yaw angle and angle of attack.



(a) $\frac{\partial(\Delta u)}{\partial(z/H)}$ and $\frac{\partial(\Delta w)}{\partial(x/H)}$

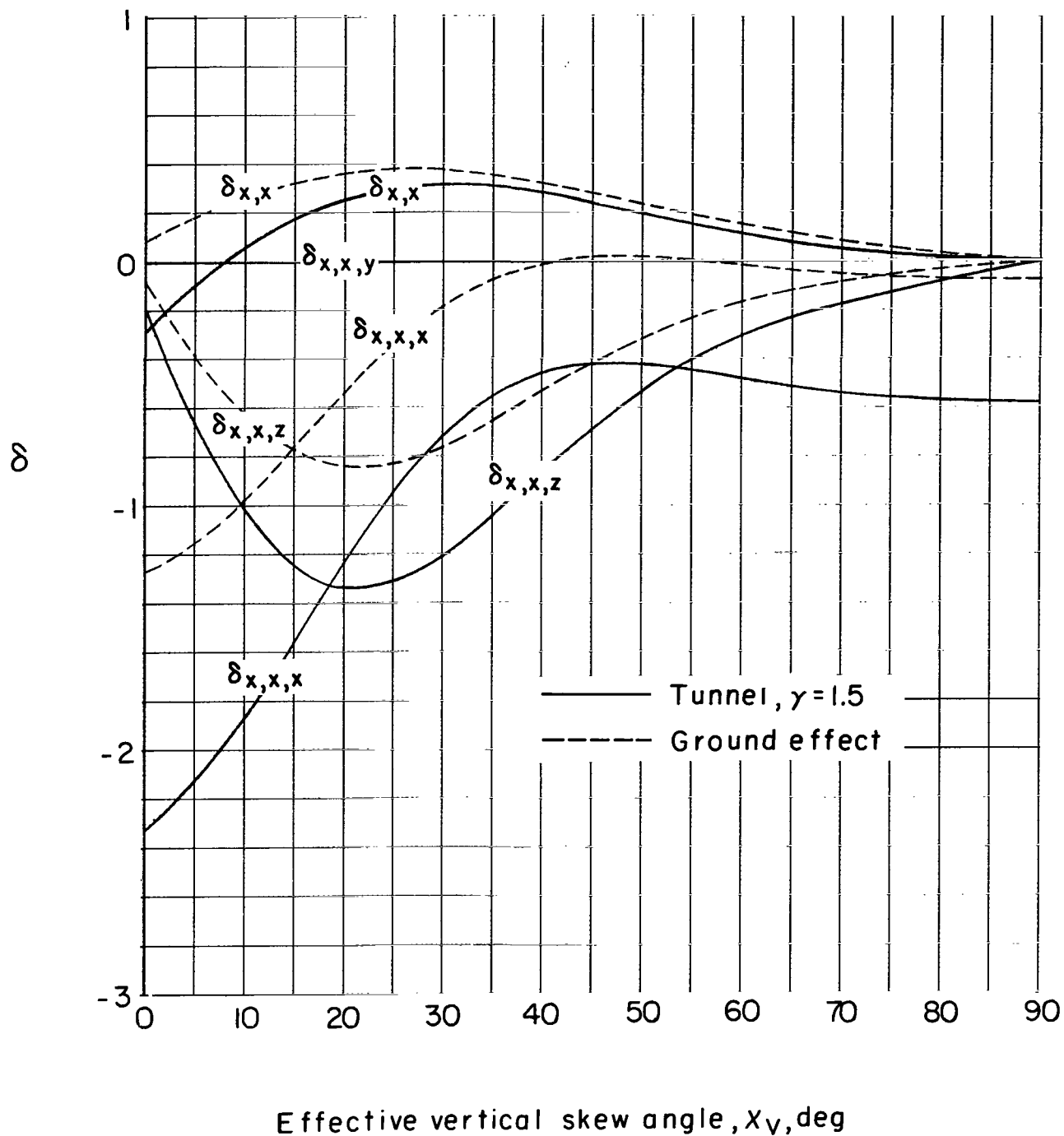


(b) $\frac{\partial(\Delta u)}{\partial(y/H)}$ and $\frac{\partial(\Delta v)}{\partial(x/H)}$



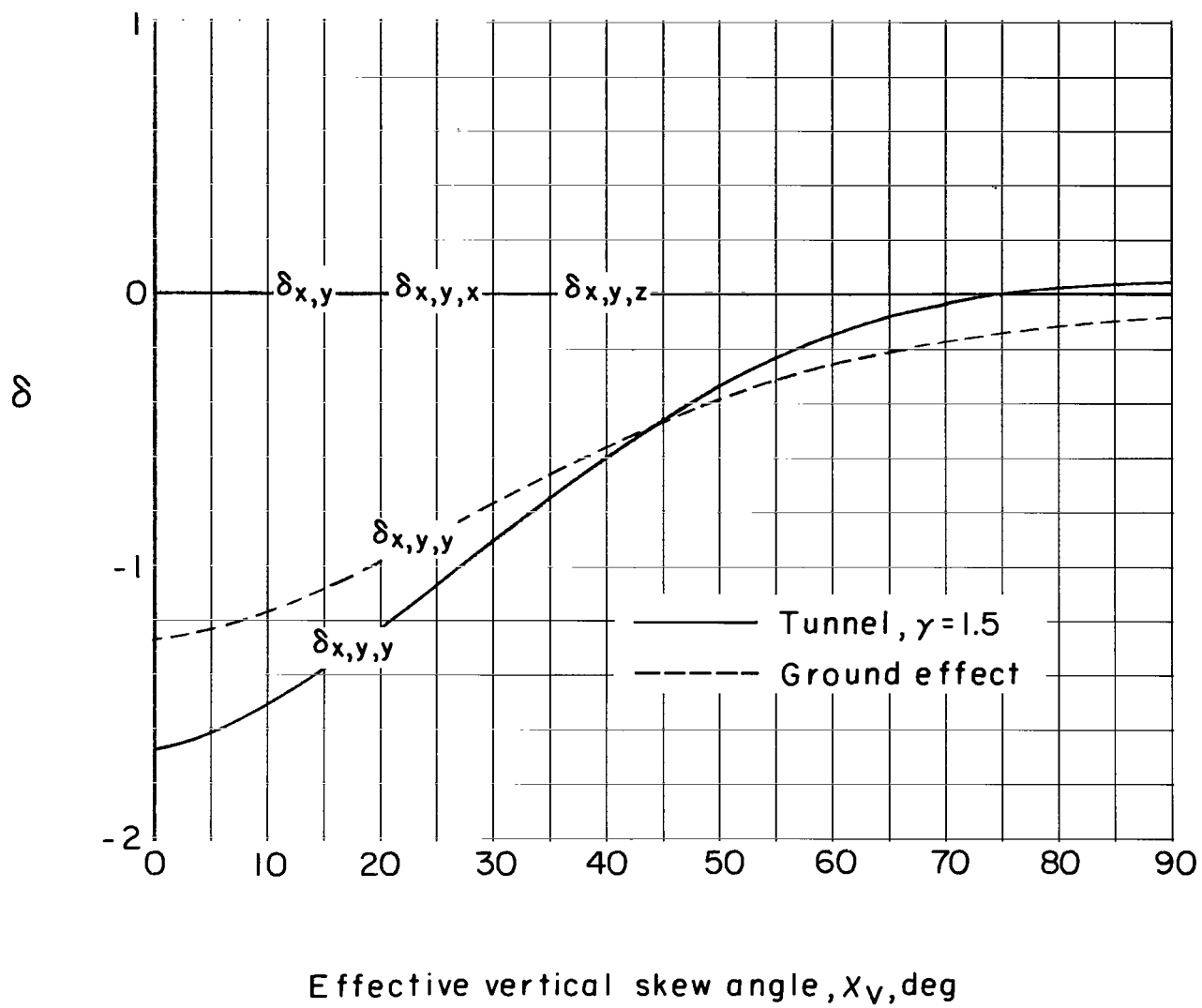
(c) $\frac{\partial(\Delta v)}{\partial(z/H)}$ and $\frac{\partial(\Delta w)}{\partial(y/H)}$

Figure 12.- Effects of the gradients of the wall-induced interference velocities.



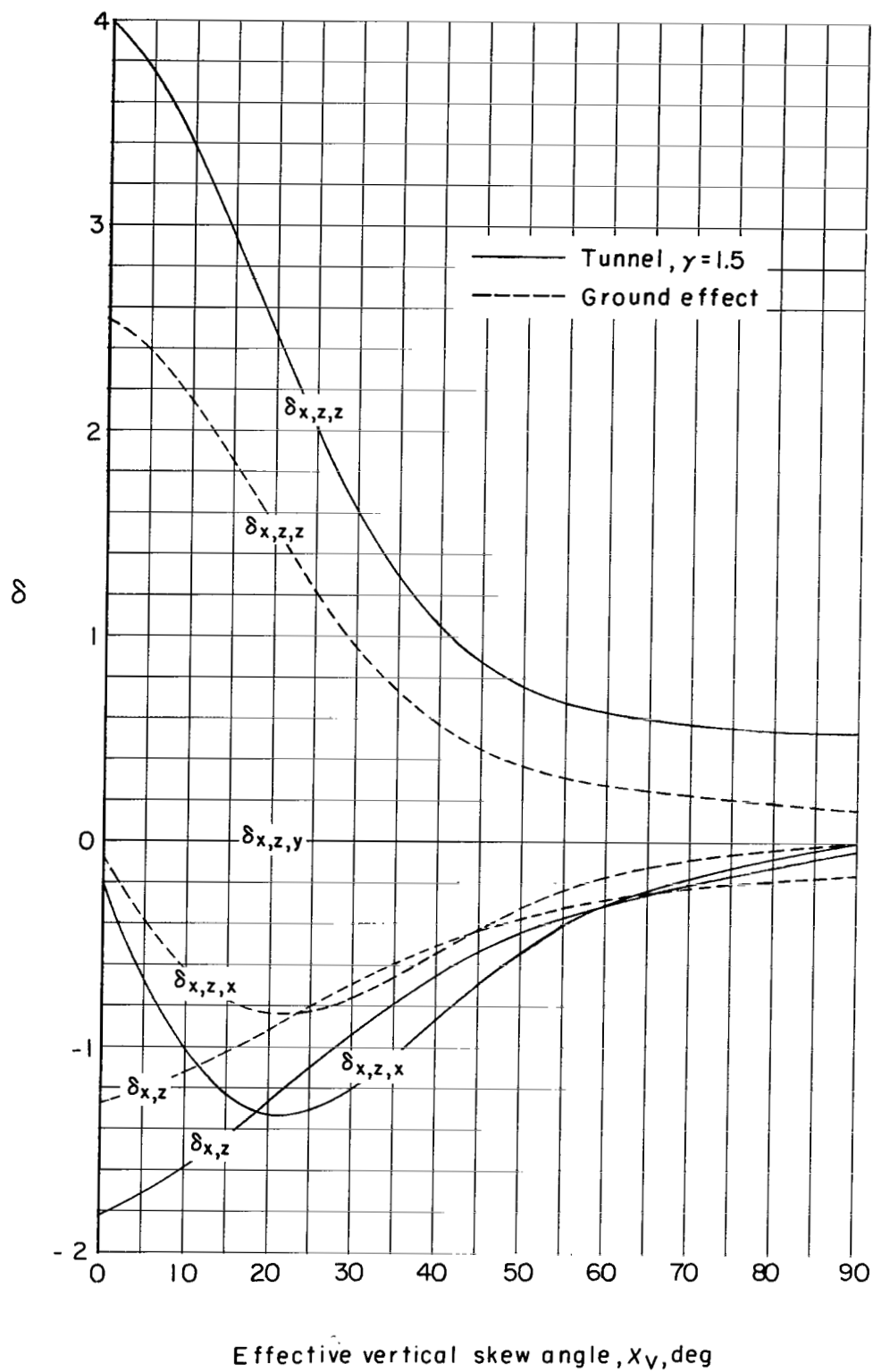
(a) $\delta_{x,x}$ and its gradients.

Figure 13.- Interference factors as a function of X_V for a vanishingly small model in ground effect and centered in a closed rectangular tunnel having a width-height ratio of 1.5. $X_H = 90^\circ$.



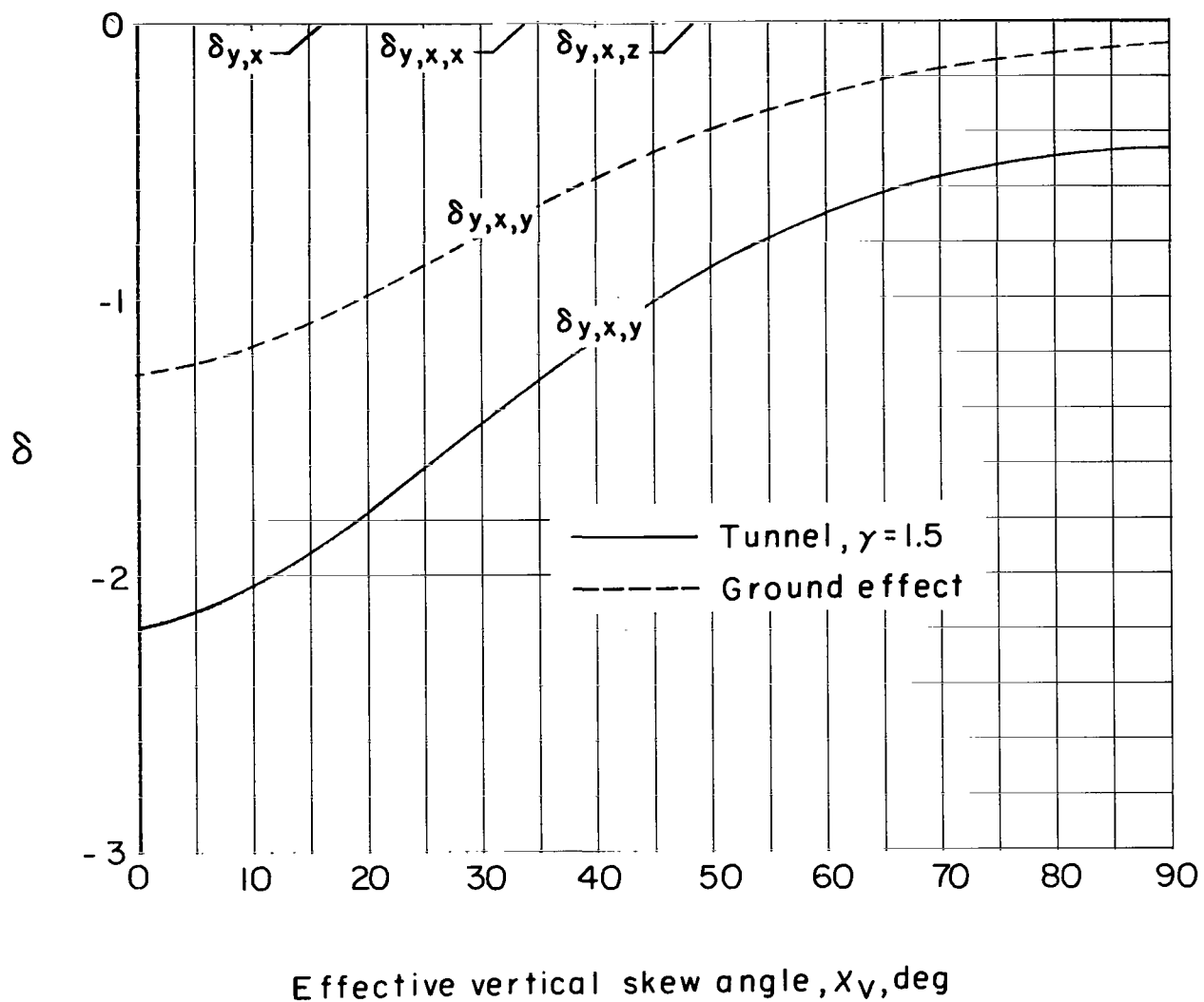
(b) $\delta_{x,y}$ and its gradients.

Figure 13.- Continued.



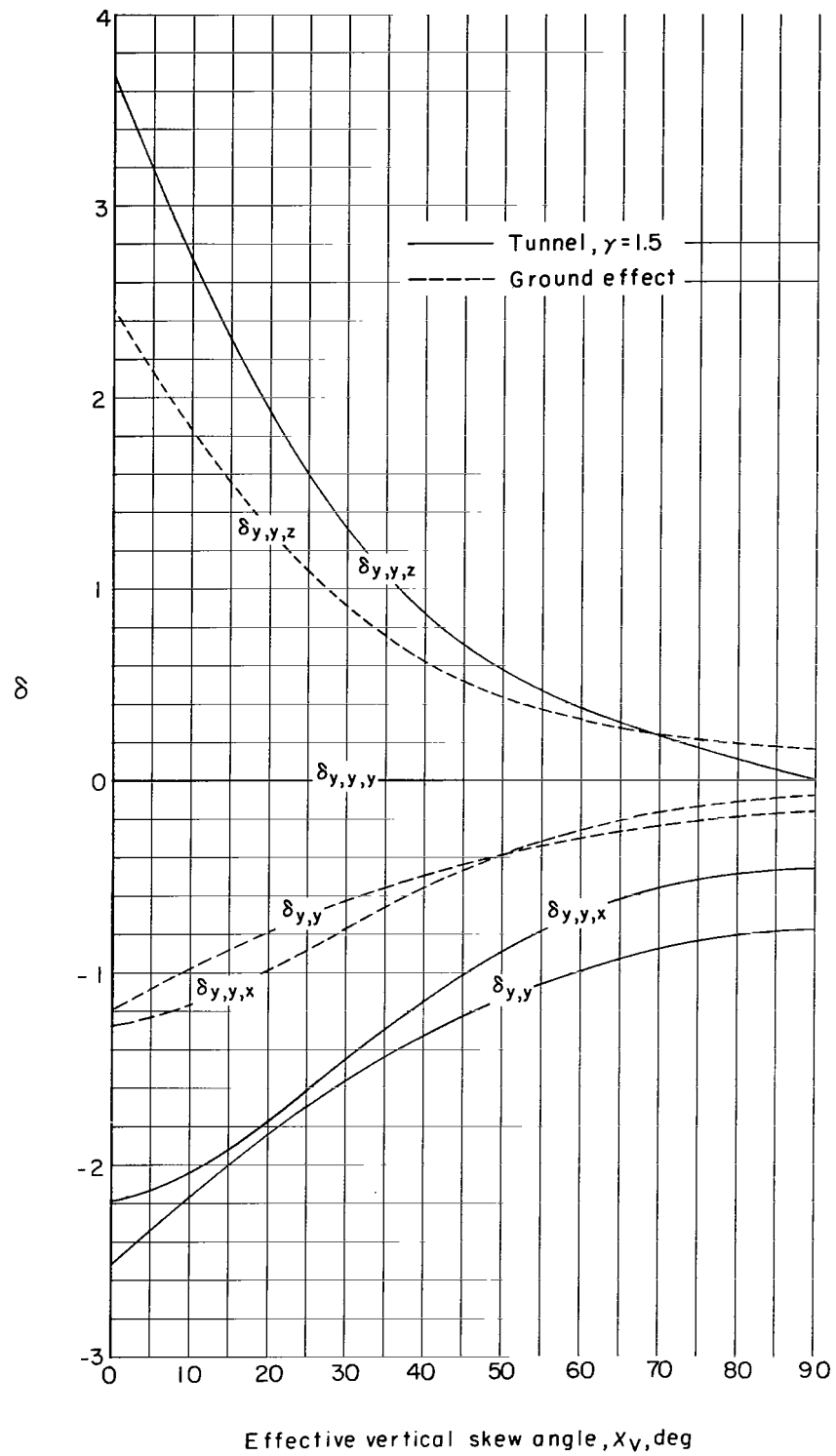
(c) $\delta_{x,z}$ and its gradients.

Figure 13.- Continued.



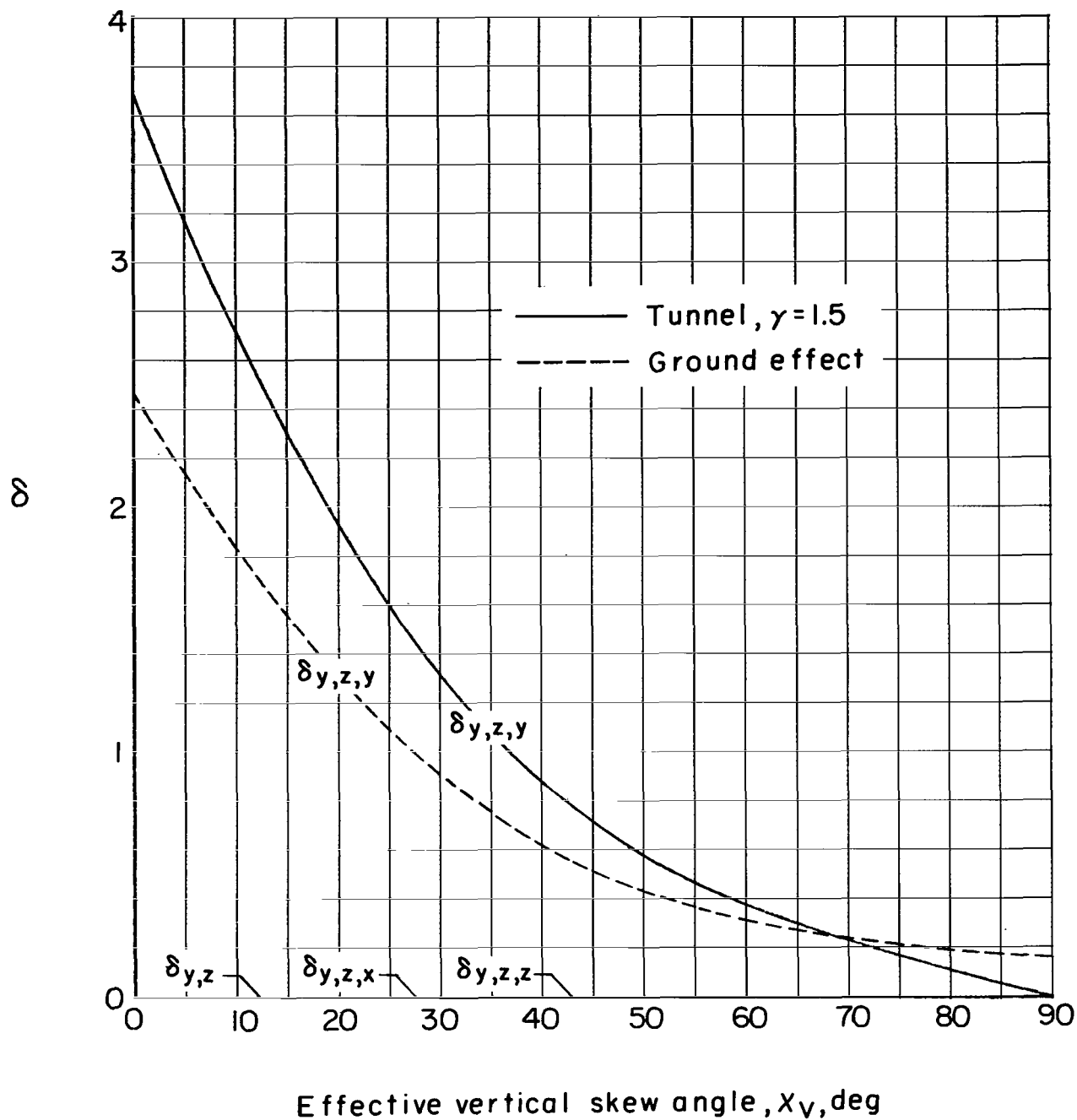
(d) $\delta_{y,x}$ and its gradients.

Figure 13.- Continued.



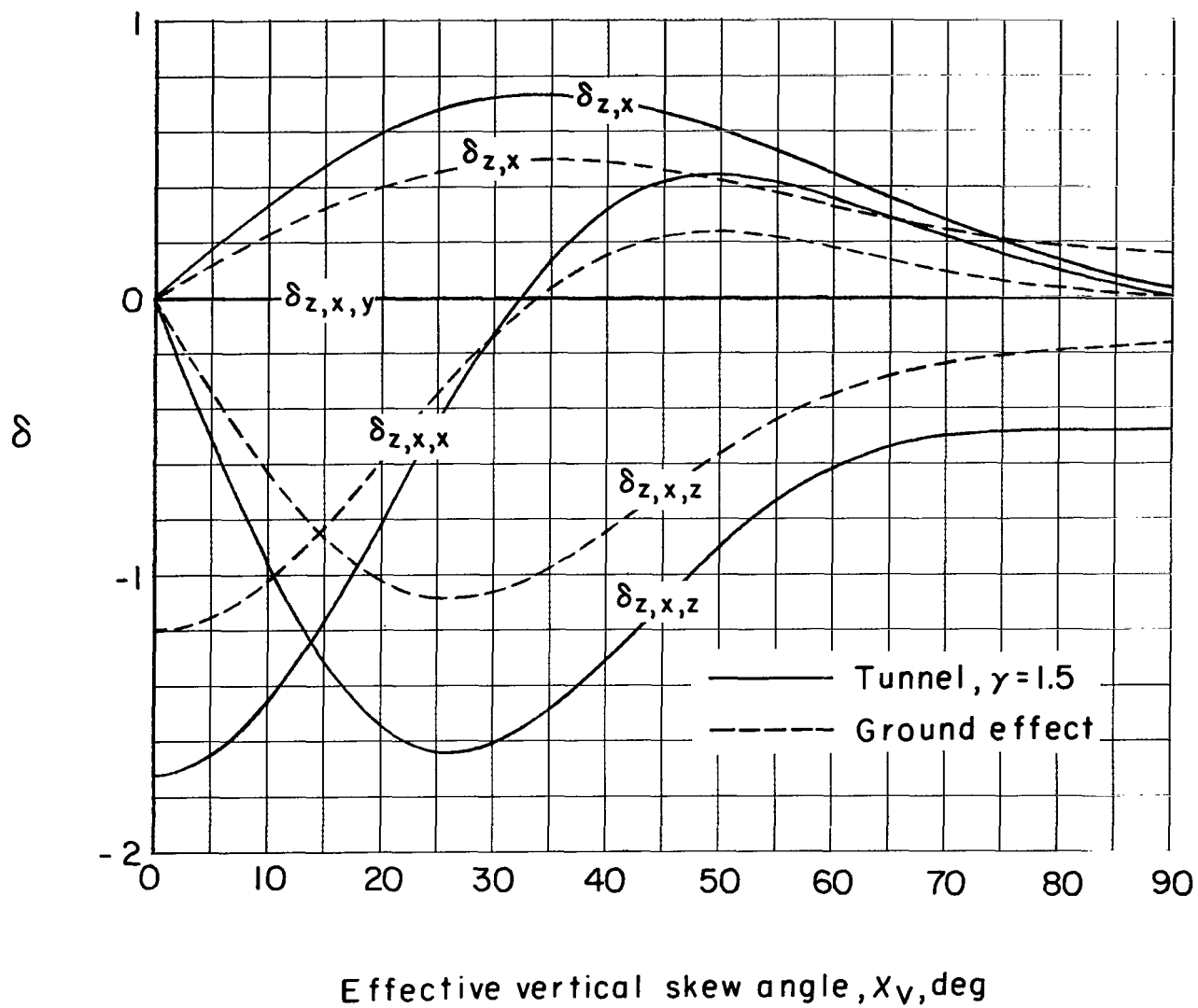
(e) $\delta_{y,y}$ and its gradients.

Figure 13.- Continued.



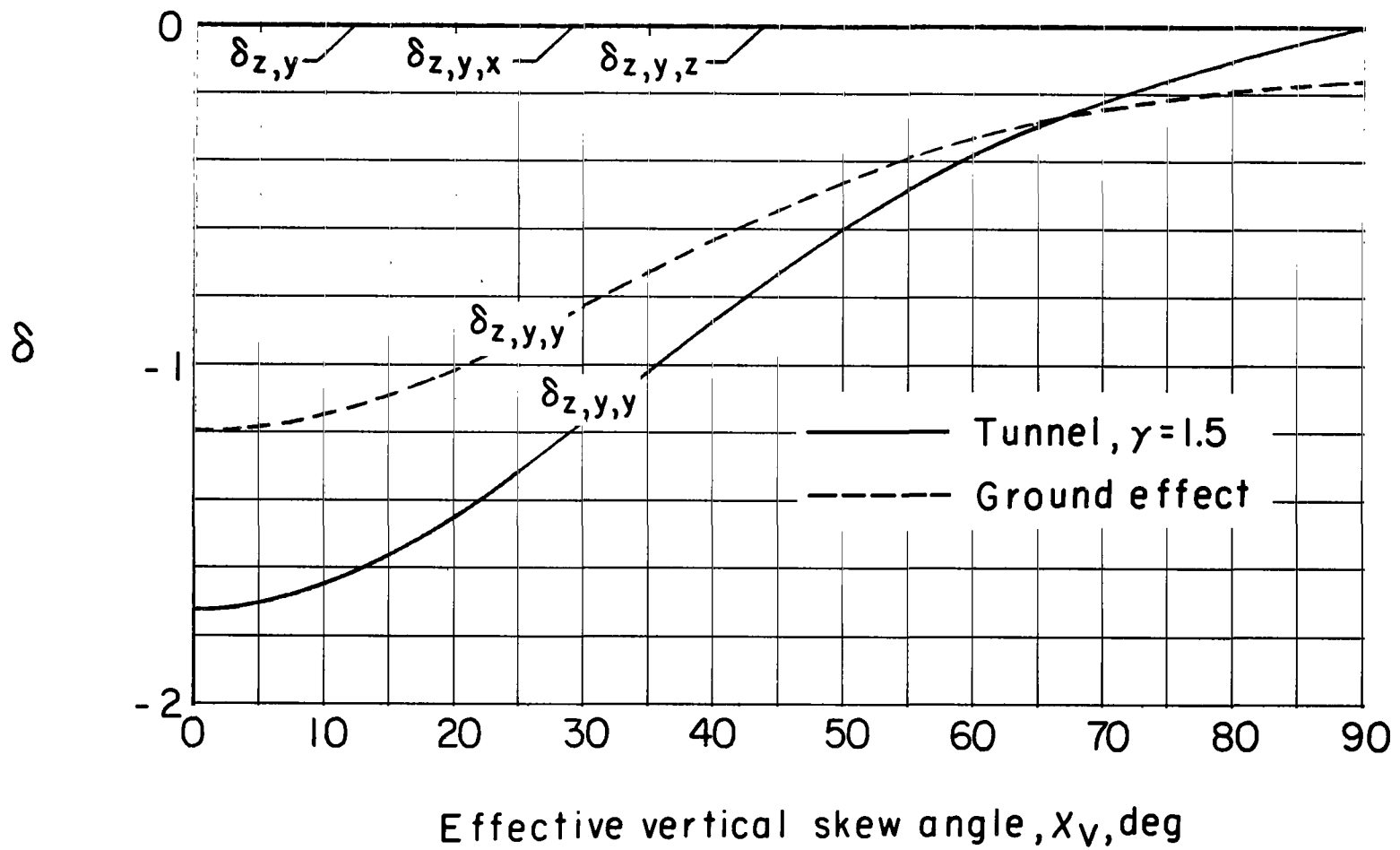
(f) $\delta_{y,z}$ and its gradients.

Figure 13.- Continued.



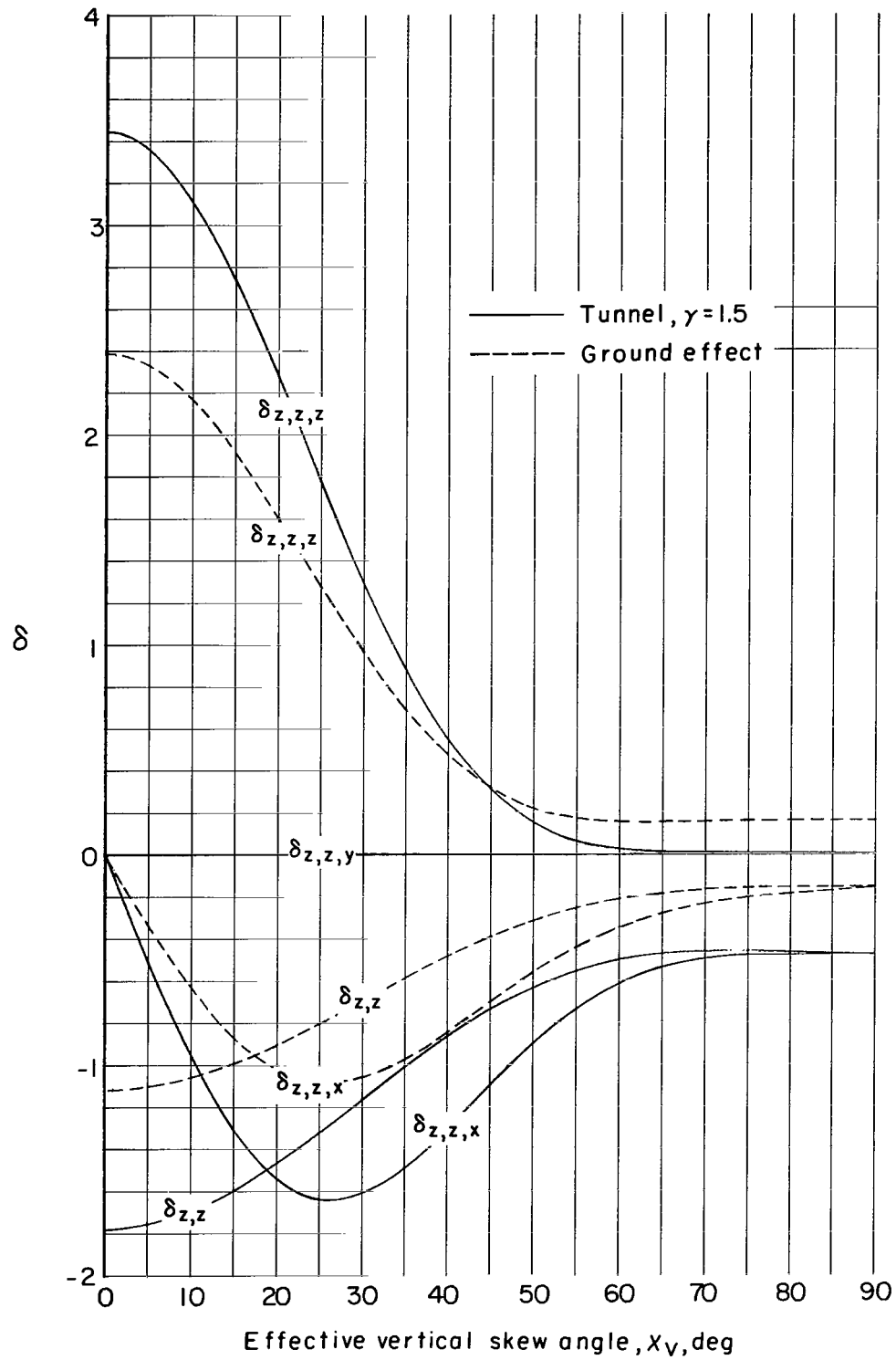
(g) $\delta_{z,x}$ and its gradients.

Figure 13.- Continued.



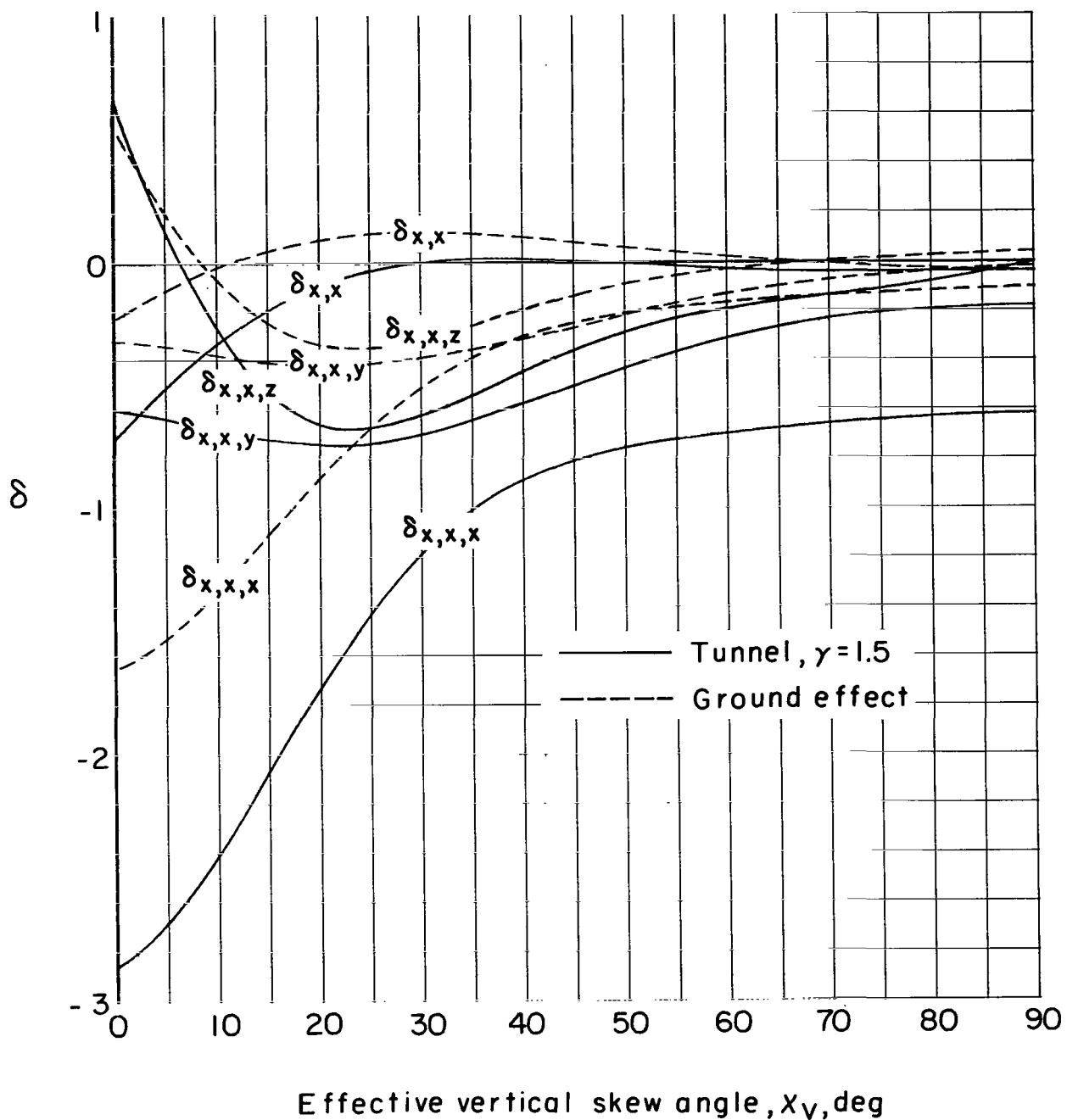
(h) $\delta_{z,y}$ and its gradients.

Figure 13.- Continued.



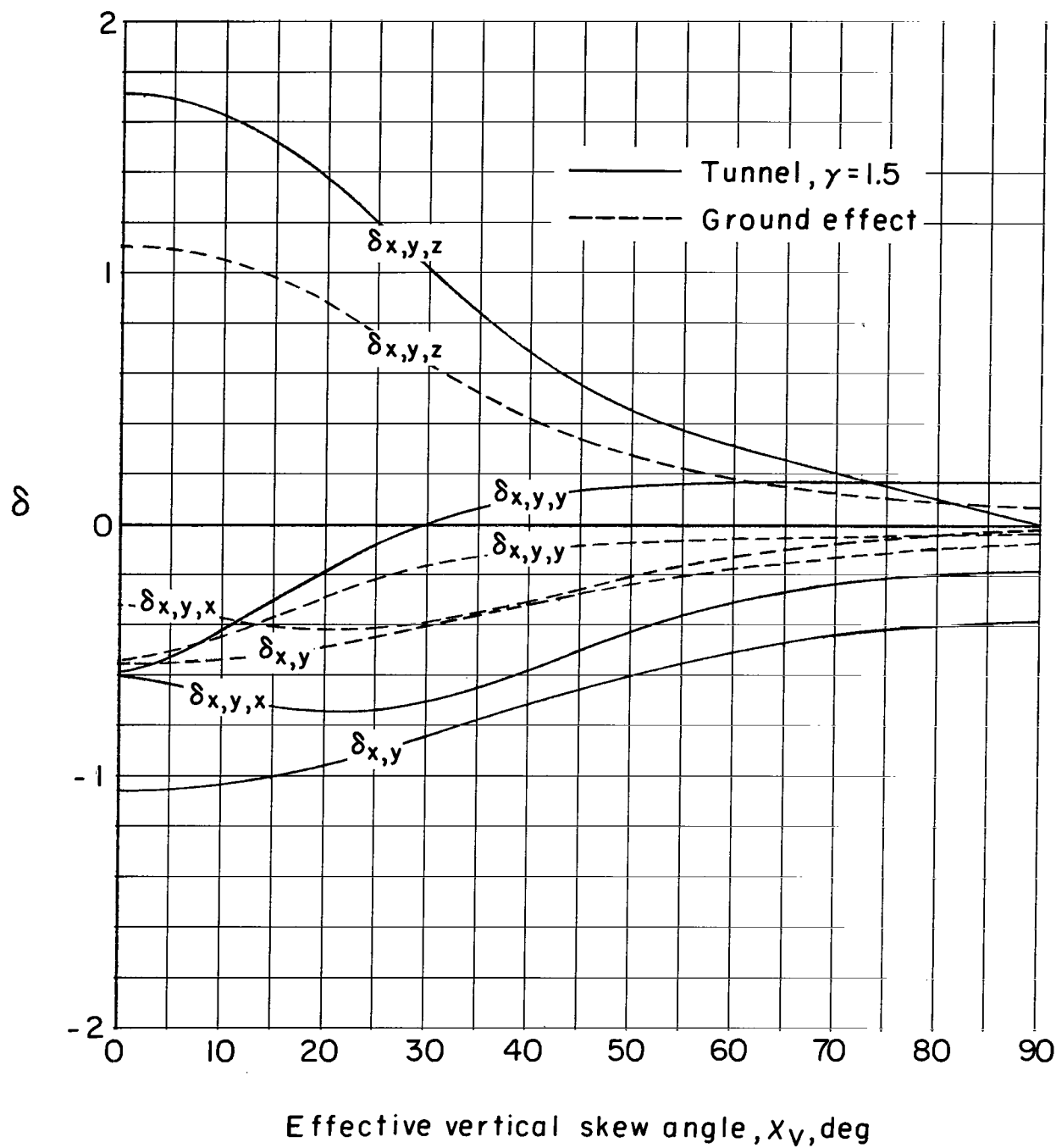
(ii) $\delta_{z,z}$ and its gradients.

Figure 13.- Concluded.



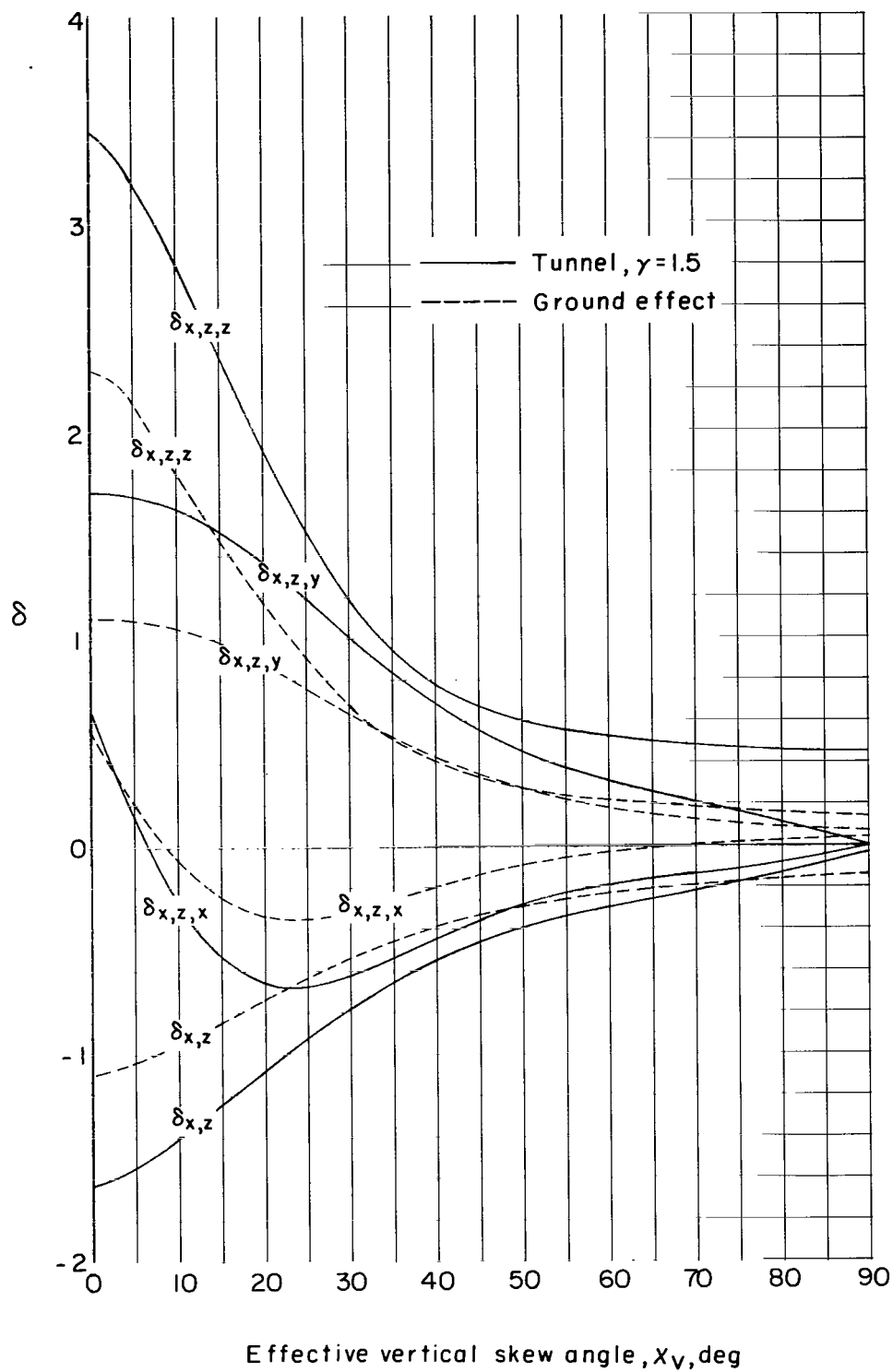
(a) $\delta_{x,x}$ and its gradients.

Figure 14.- Interference factors as a function of X_V for a vanishingly small model in ground effect and centered in a closed rectangular tunnel having a width-height ratio of 1.5. $X_H = 60^\circ$.



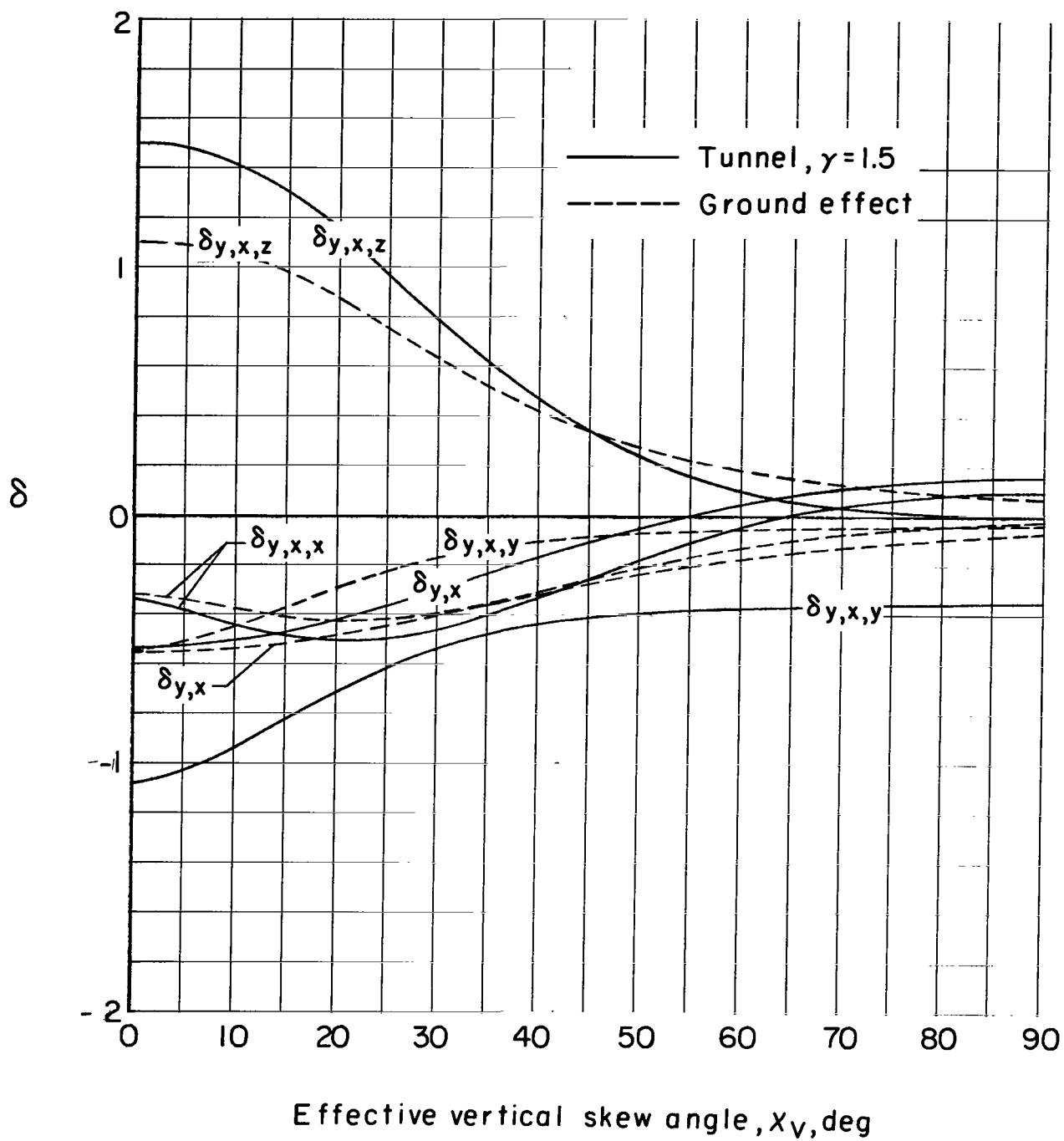
(b) $\delta_{x,y}$ and its gradients.

Figure 14.- Continued.



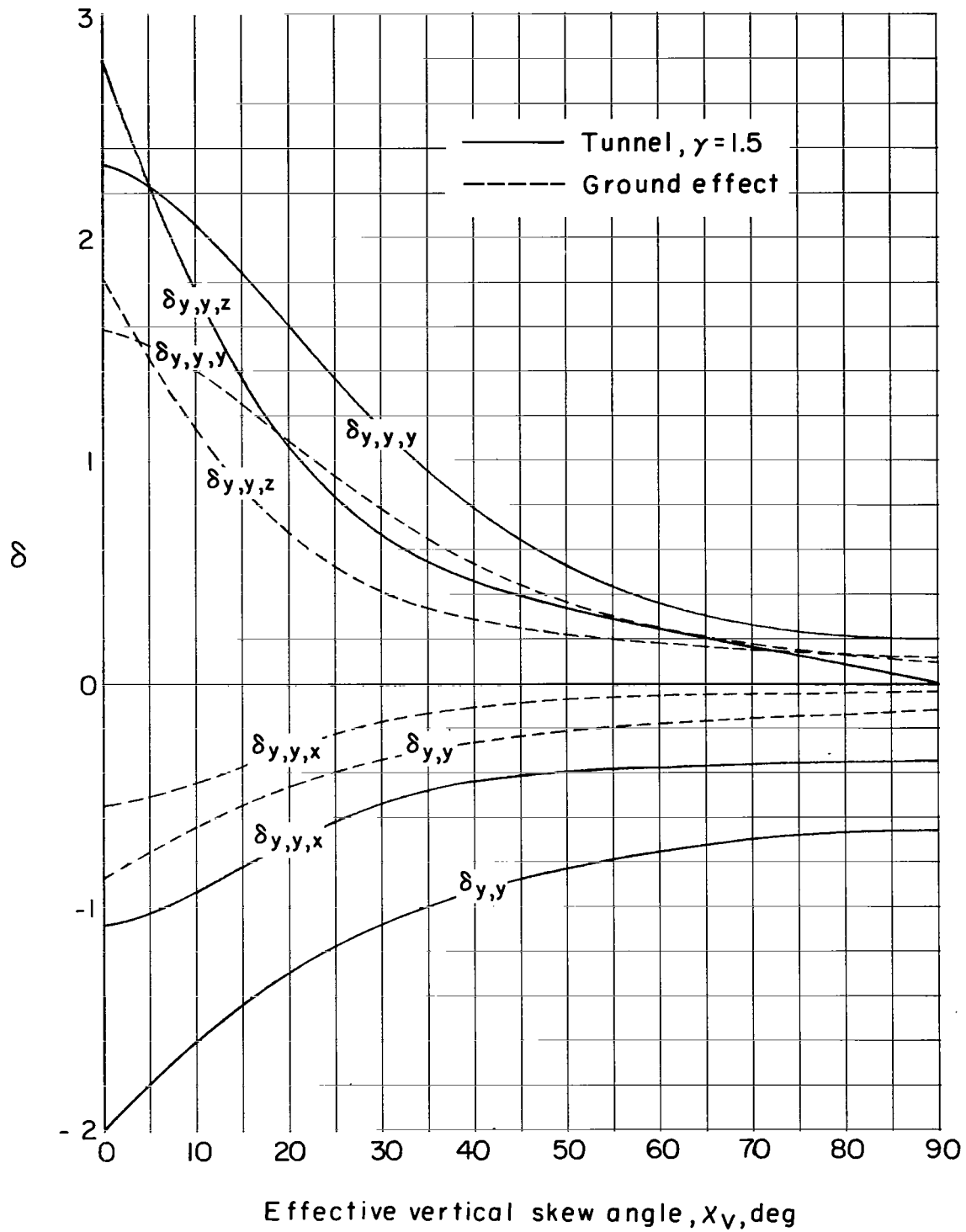
(c) $\delta_{x,z}$ and its gradients.

Figure 14.- Continued.



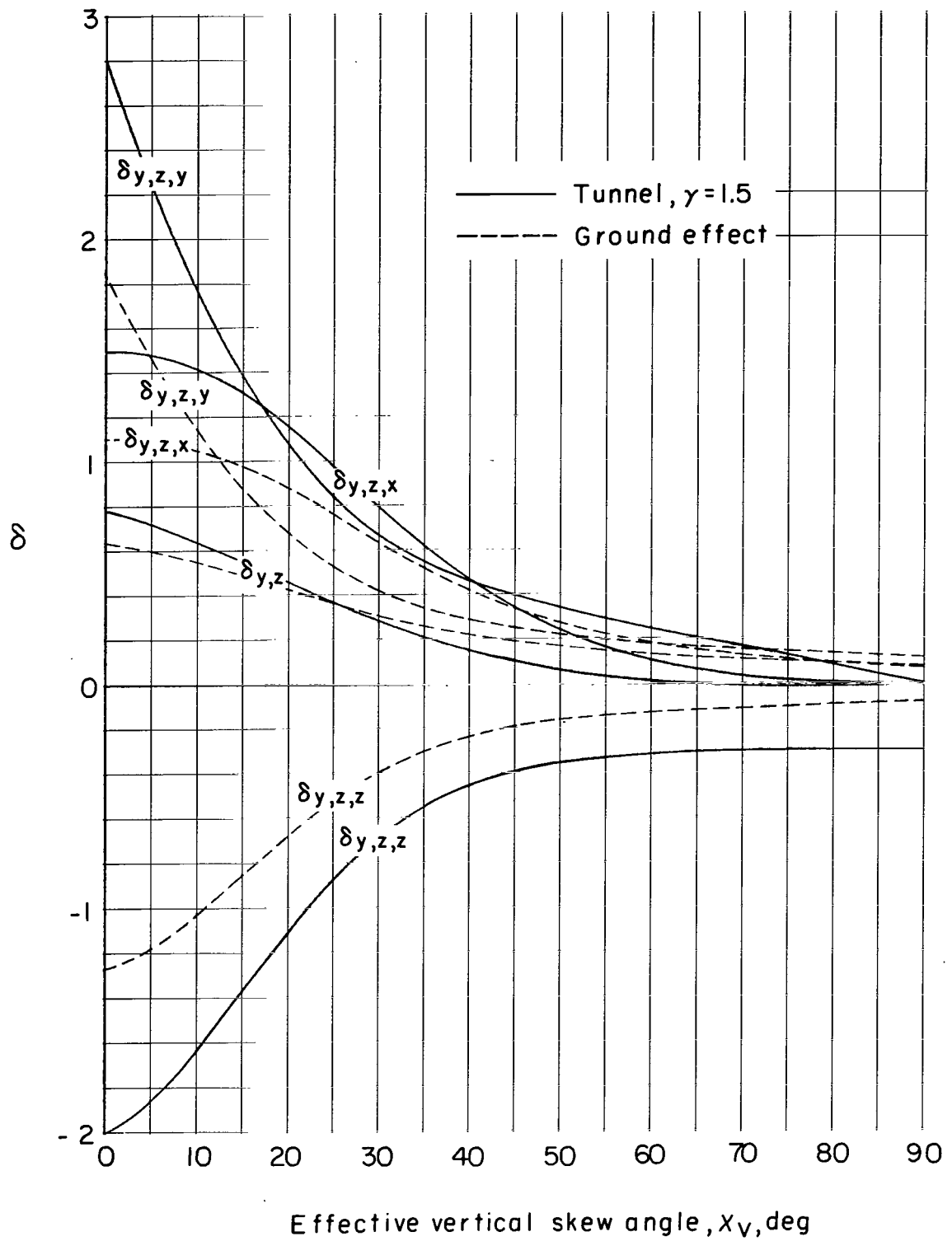
(d) $\delta_{y,x}$ and its gradients.

Figure 14.- Continued.



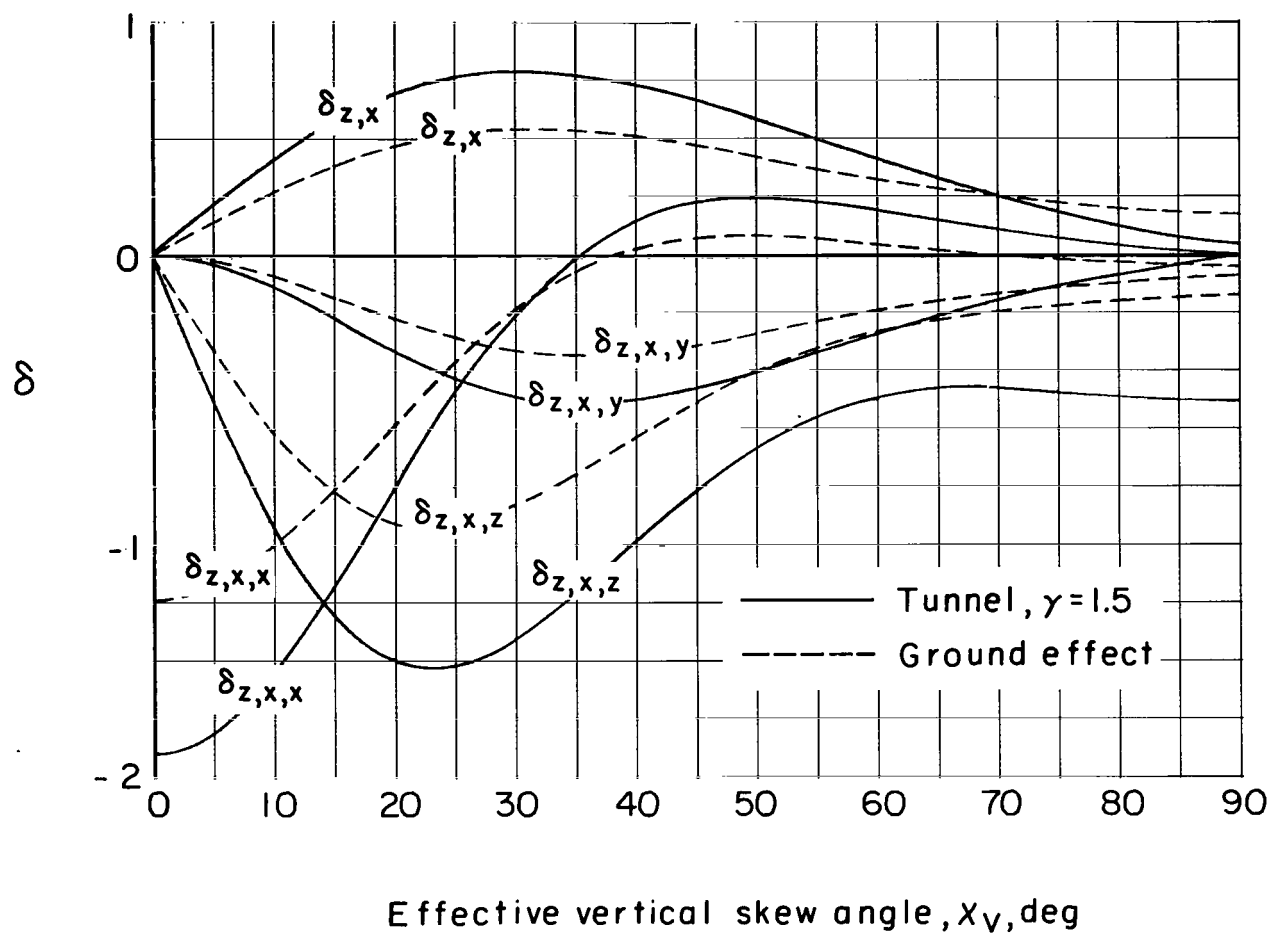
(e) $\delta_{y,y}$ and its gradients.

Figure 14.- Continued.



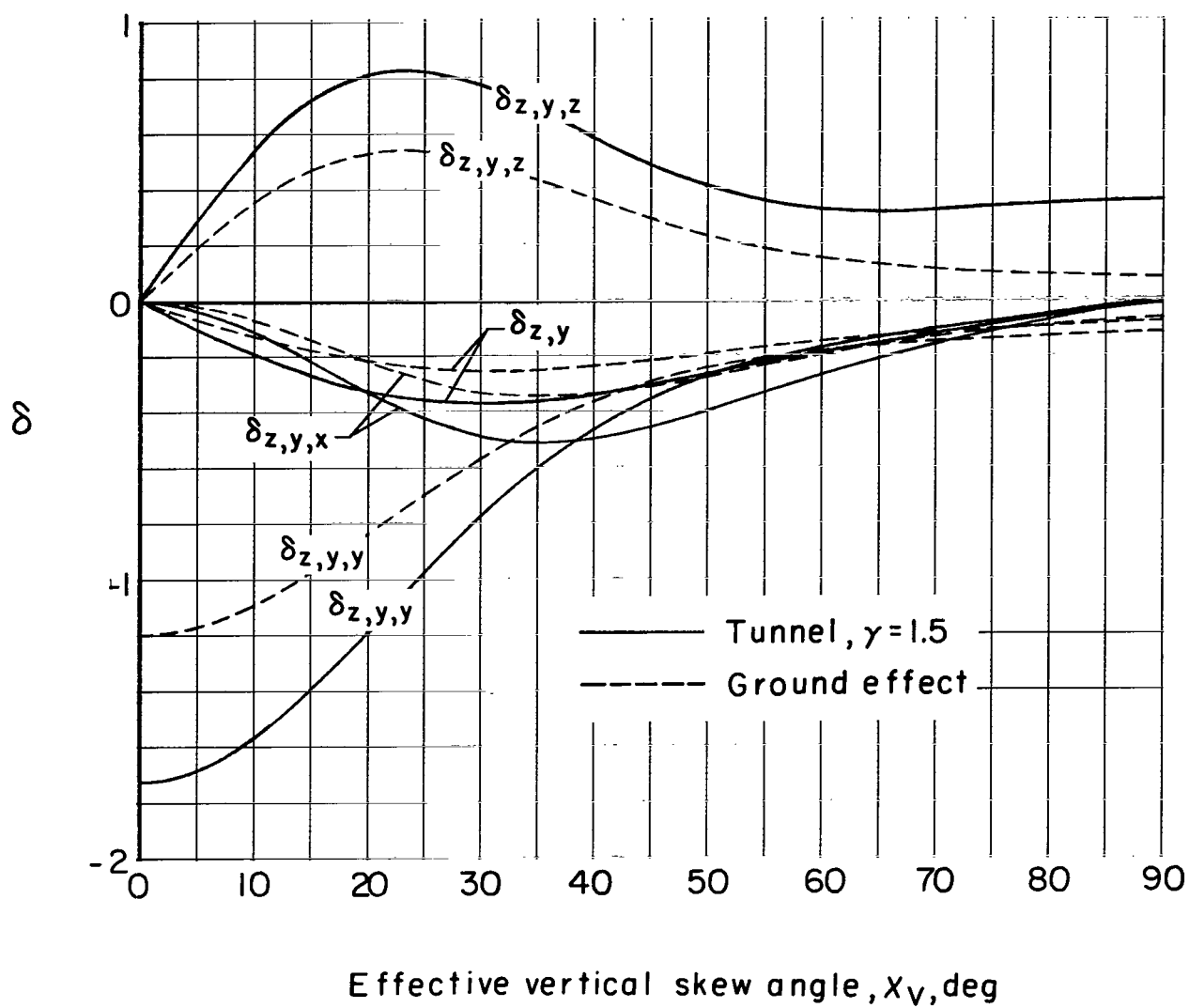
(f) $\delta_{y,z}$ and its gradients.

Figure 14.- Continued.



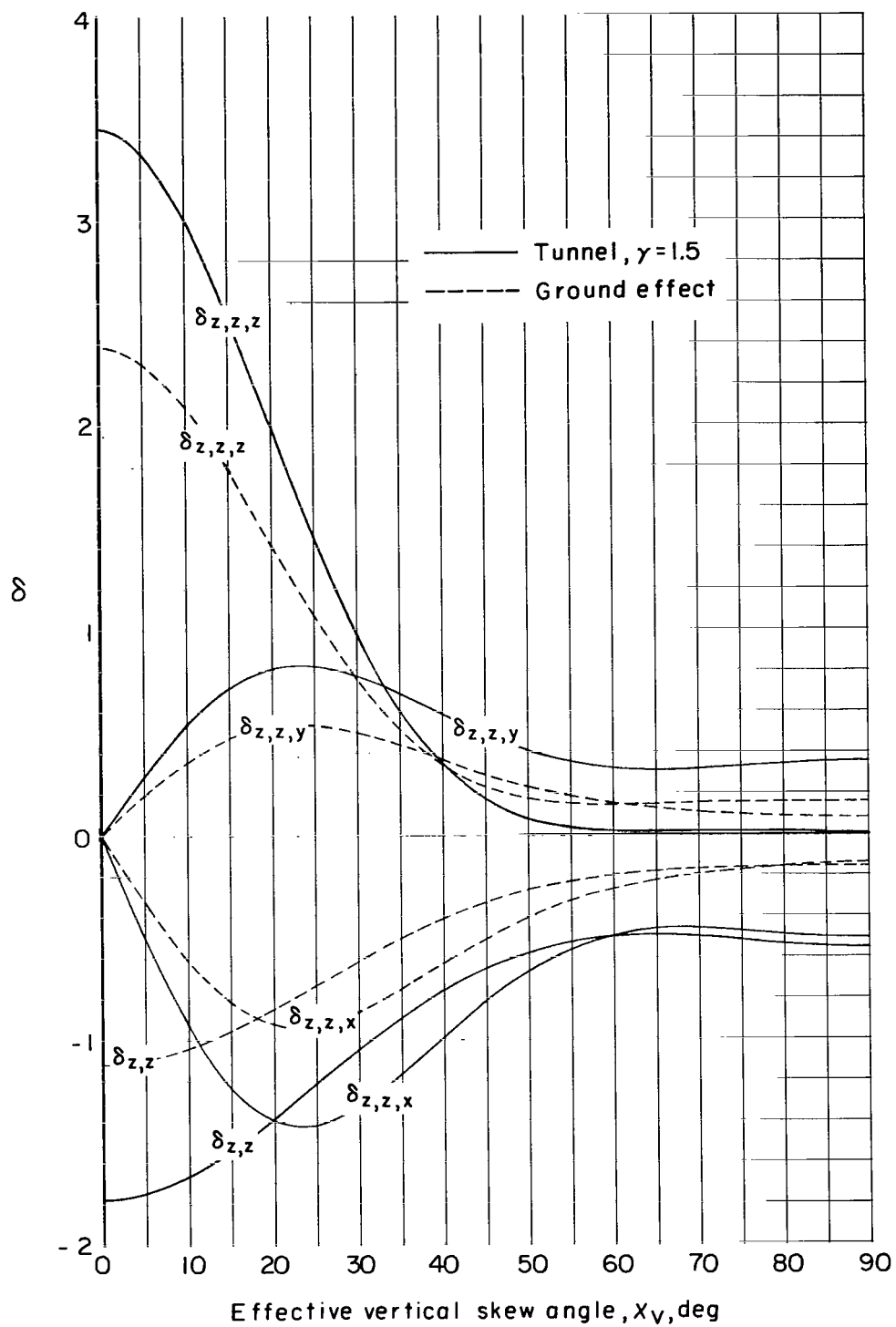
(g) $\delta_{z,x}$ and its gradients.

Figure 14.- Continued.



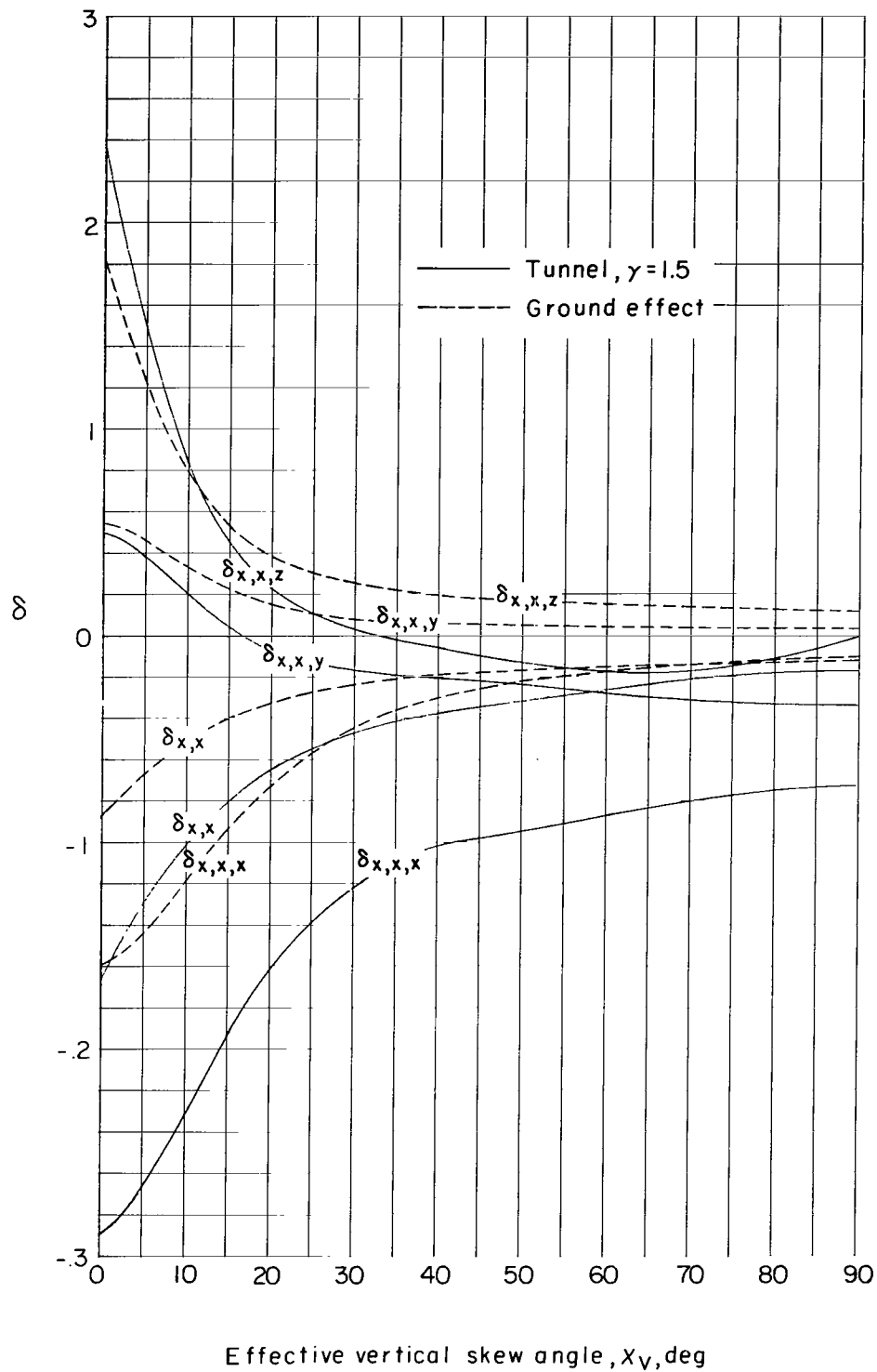
(h) $\delta_{z,y}$ and its gradients.

Figure 14.- Continued.



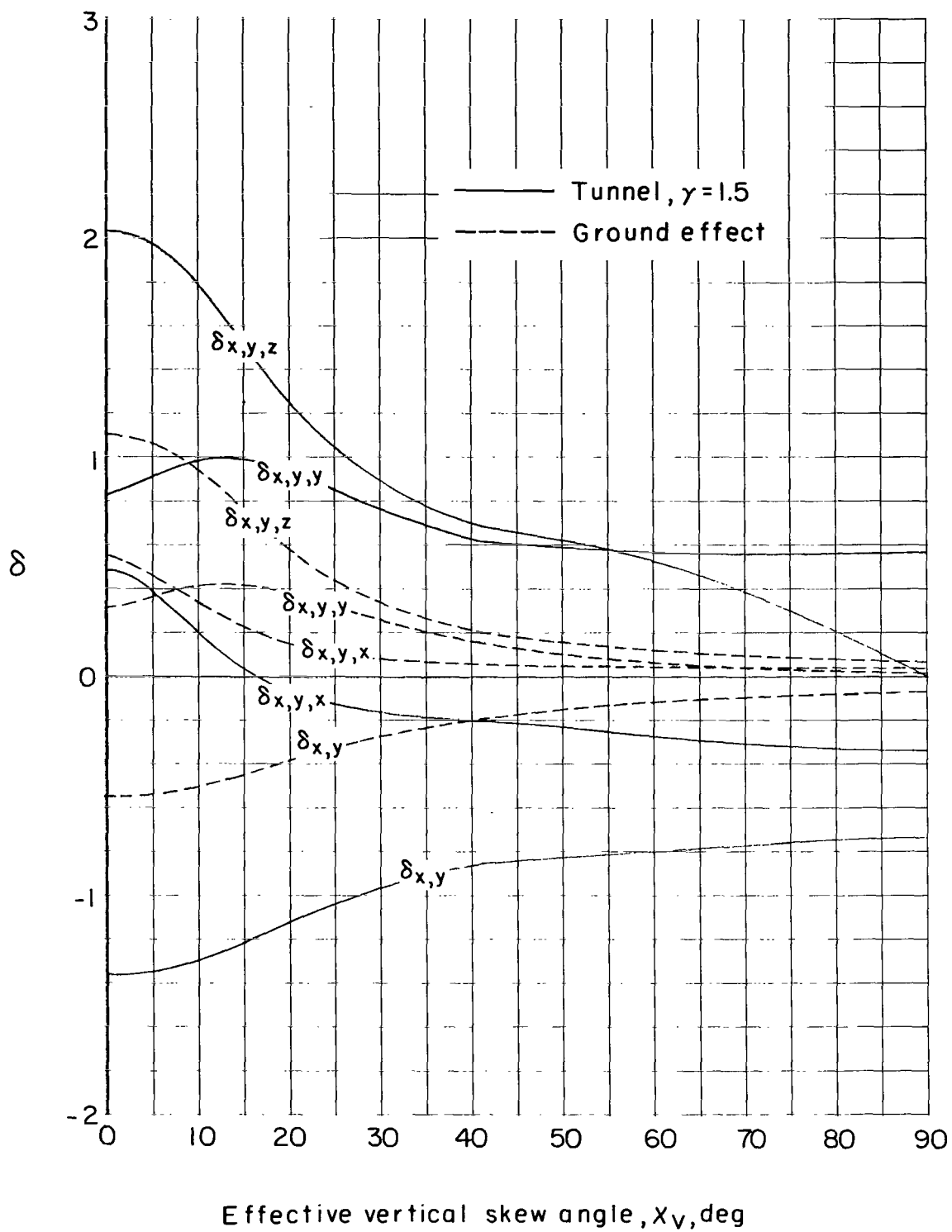
(i) $\delta_{z,z}$ and its gradients.

Figure 14.- Concluded.



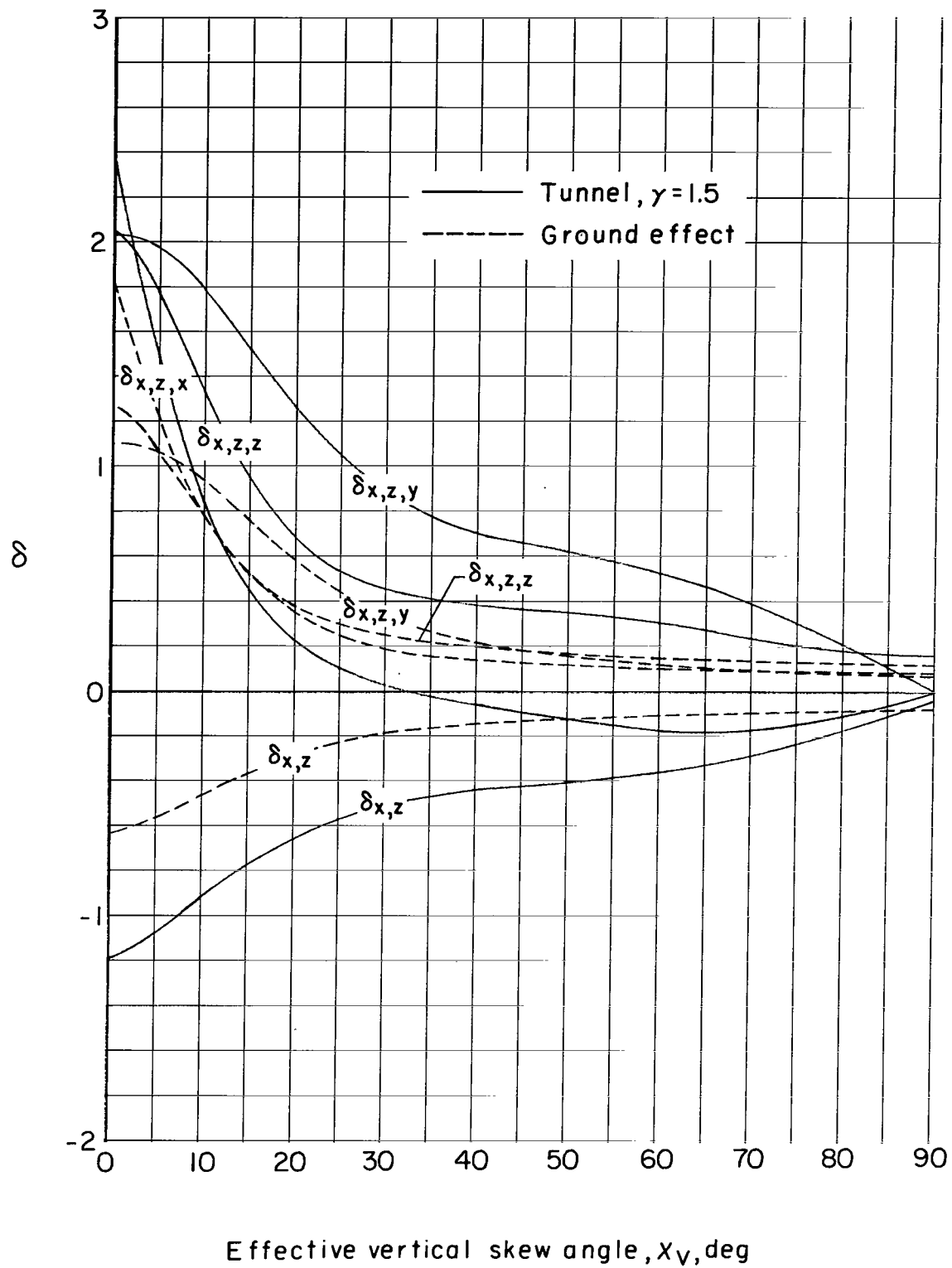
(a) $\delta_{x,x}$ and its gradients.

Figure 15.- Interference factors as a function of X_V for a vanishingly small model in ground effect and centered in a closed rectangular tunnel having a width-height ratio of 1.5. $X_H = 30^\circ$.



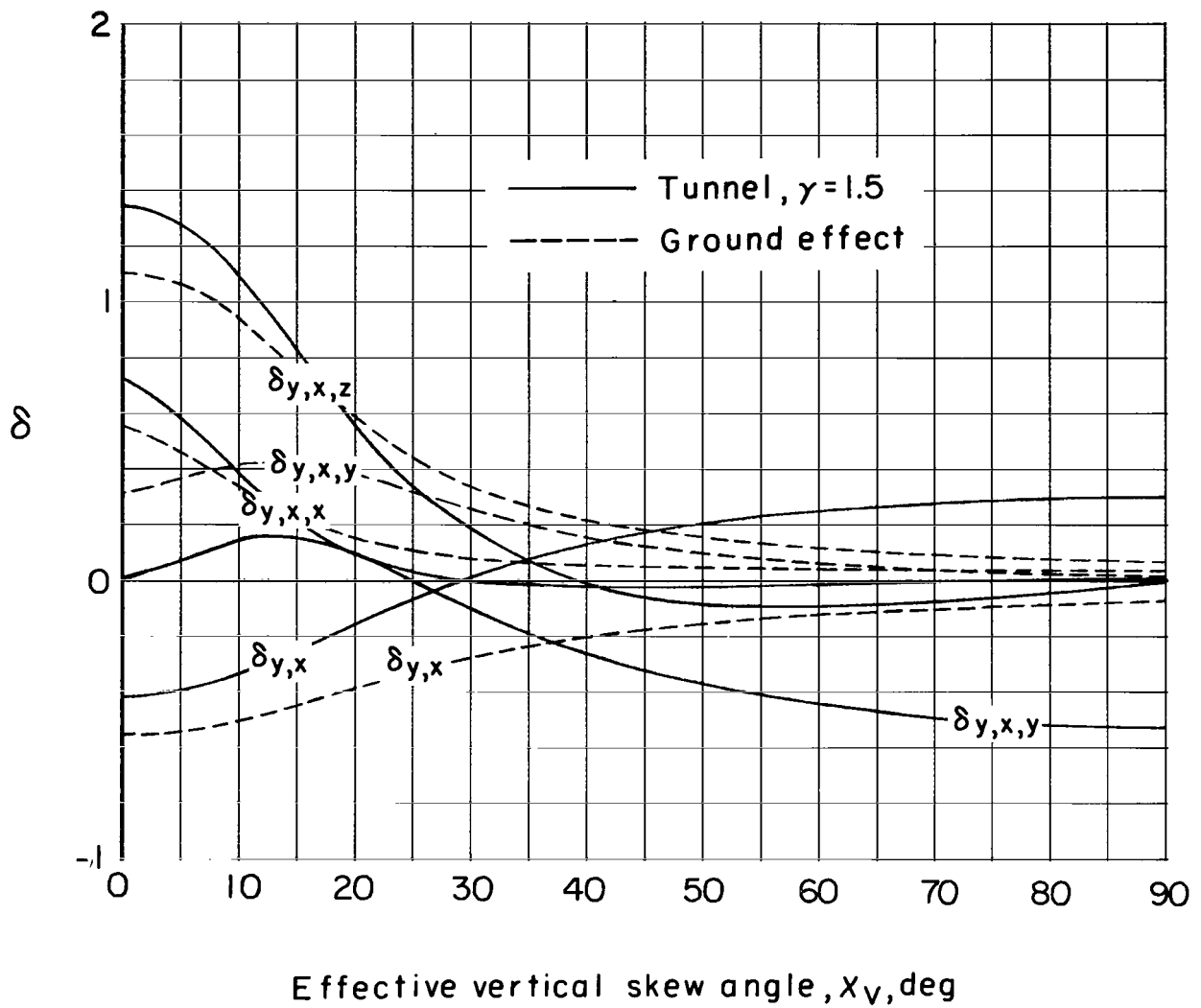
(b) $\delta_{x,y}$ and its gradients.

Figure 15.- Continued.



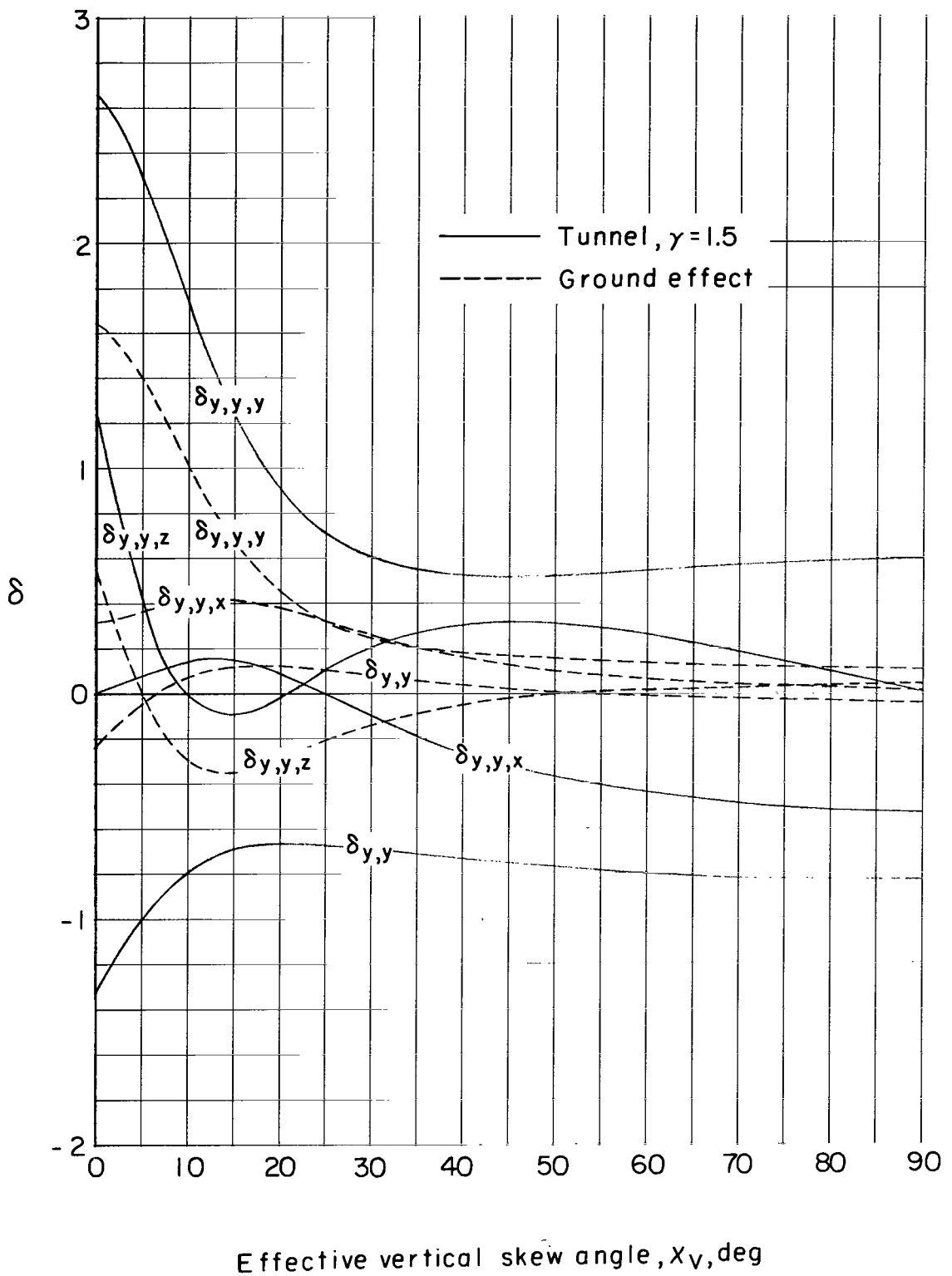
(c) $\delta_{x,z}$ and its gradients.

Figure 15.- Continued.



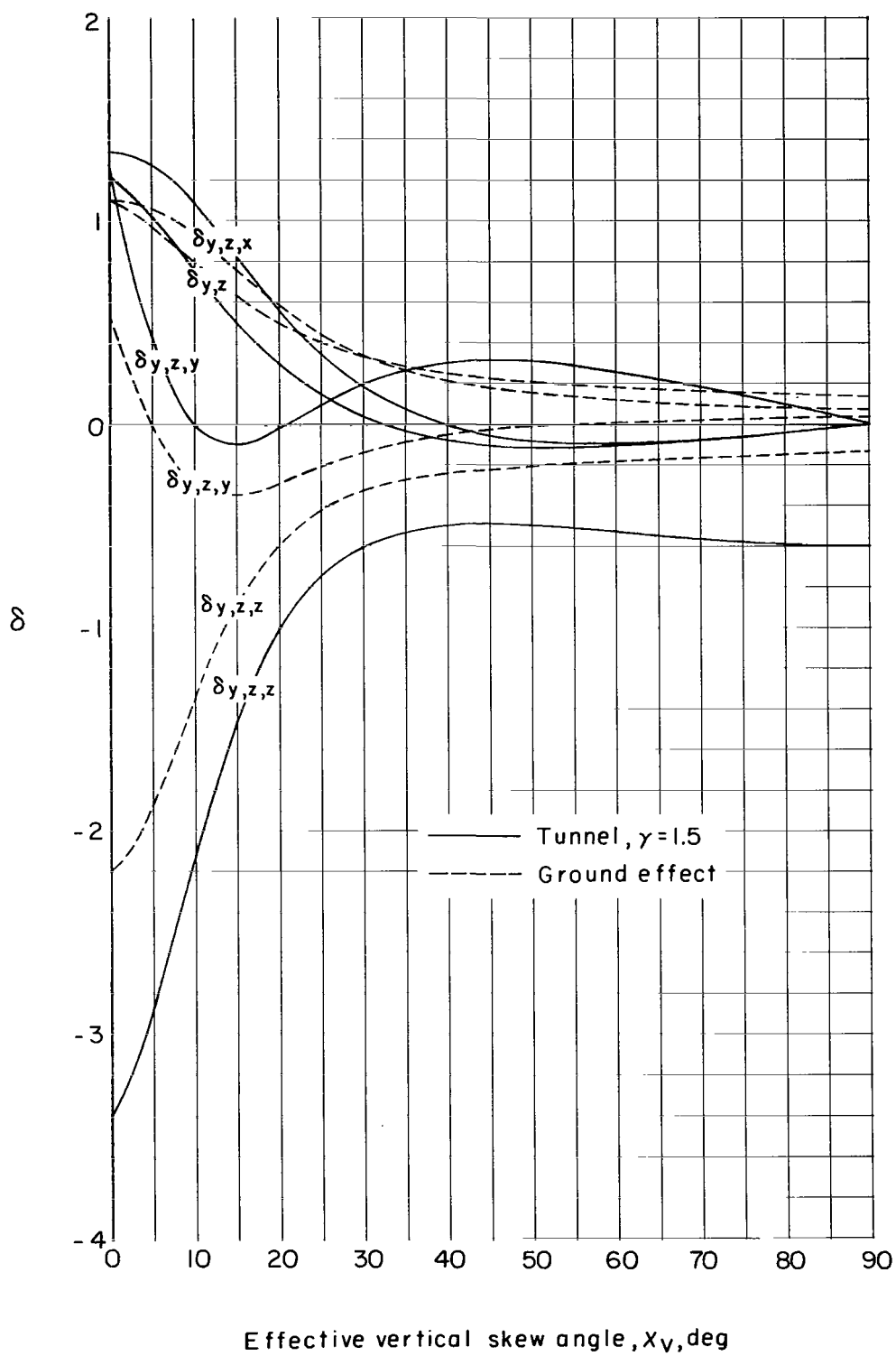
(d) $\delta_{y,x}$ and its gradients.

Figure 15.- Continued.



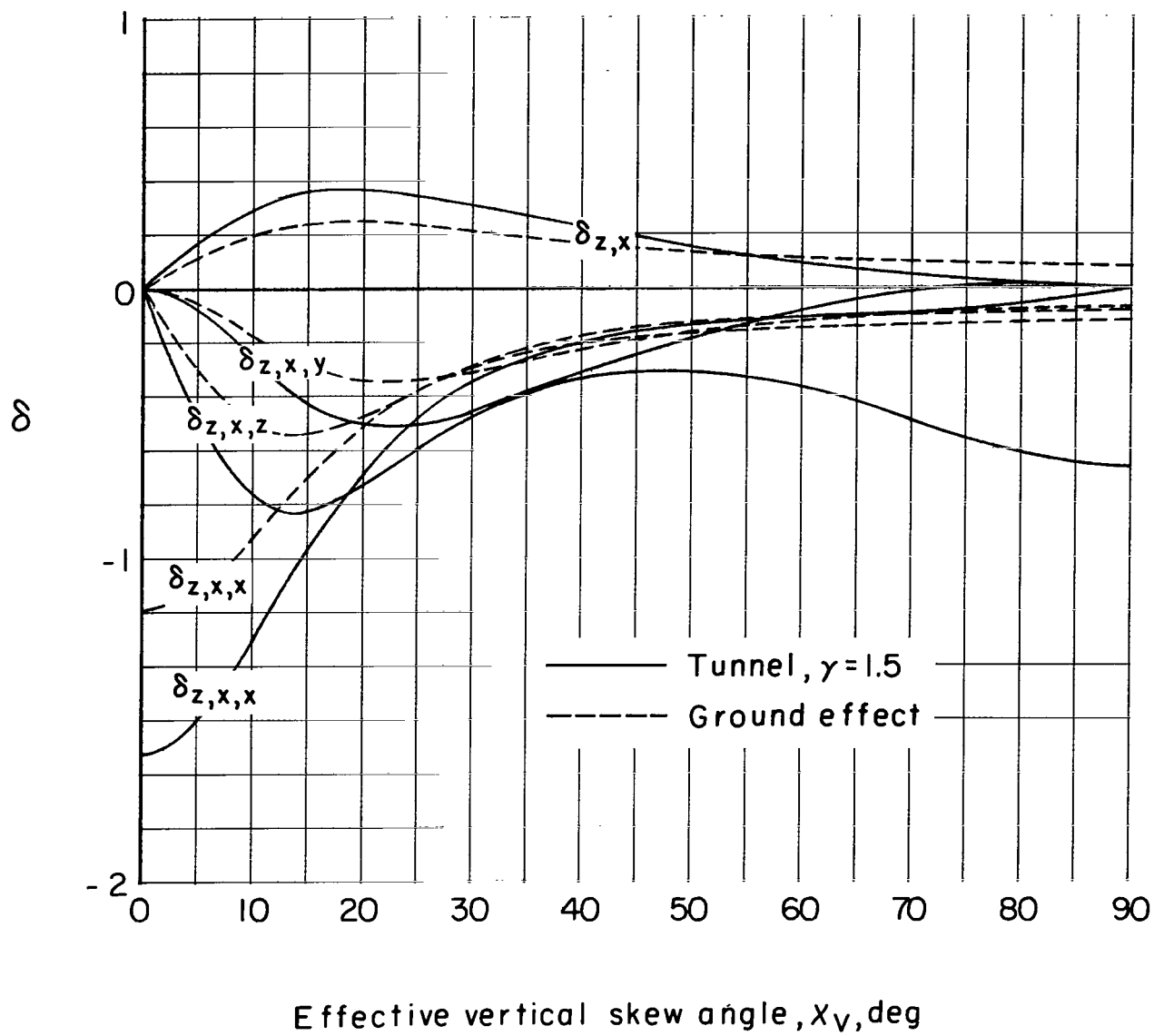
(e) $\delta_{y,y}$ and its gradients.

Figure 15.- Continued.



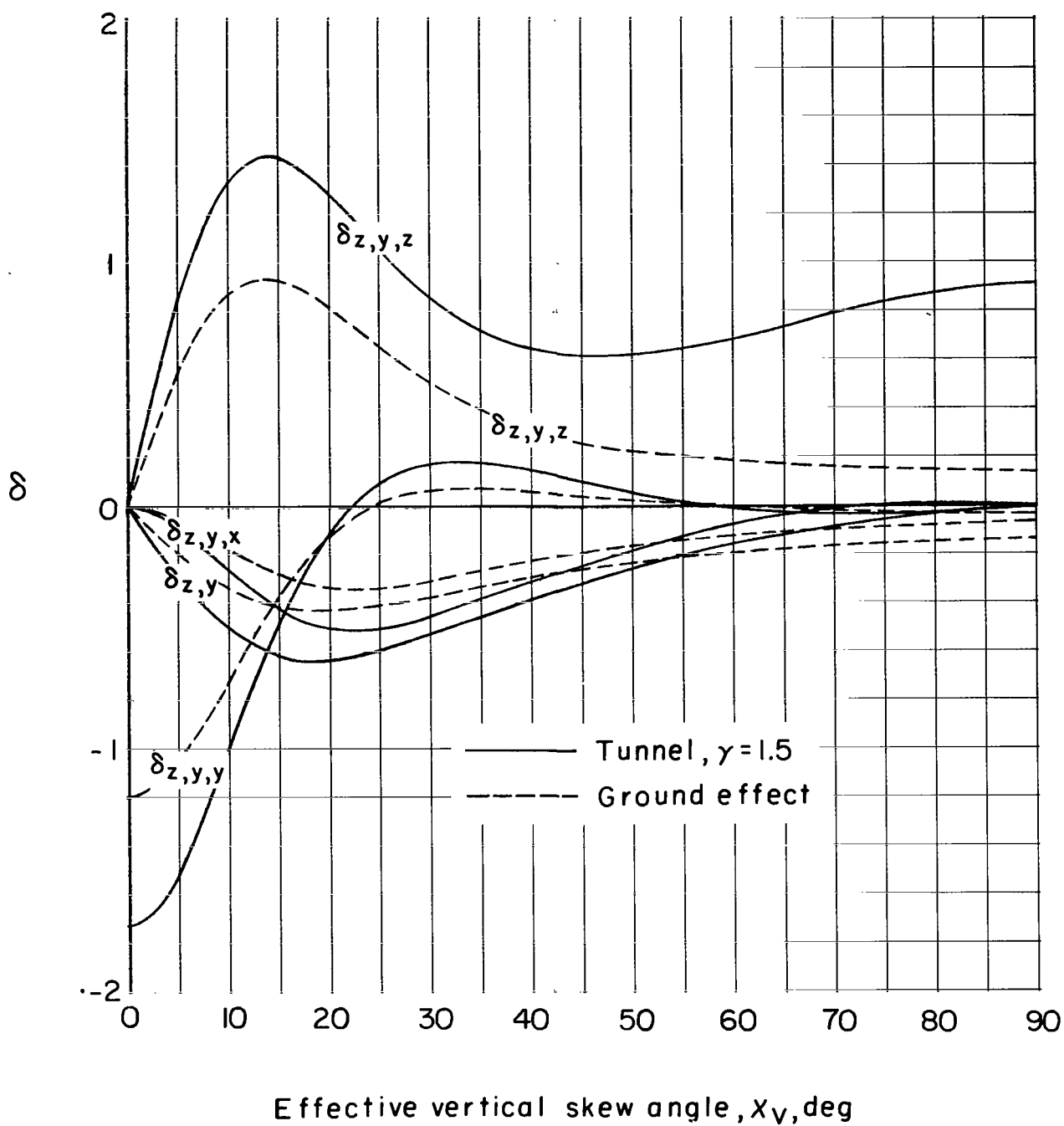
(f) $\delta_{y,z}$ and its gradients.

Figure 15.- Continued.



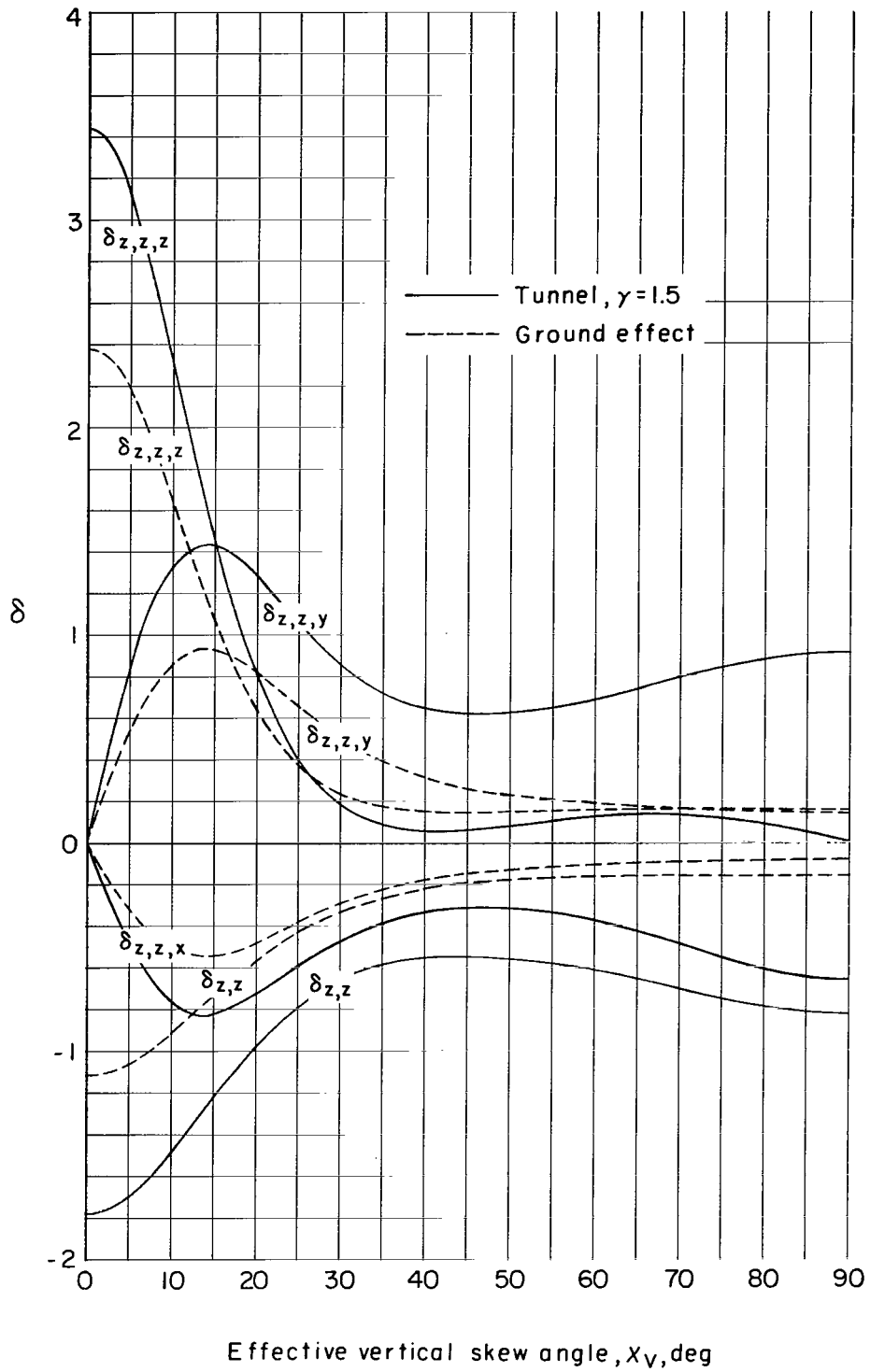
(g) $\delta_{z,x}$ and its gradients.

Figure 15.- Continued.



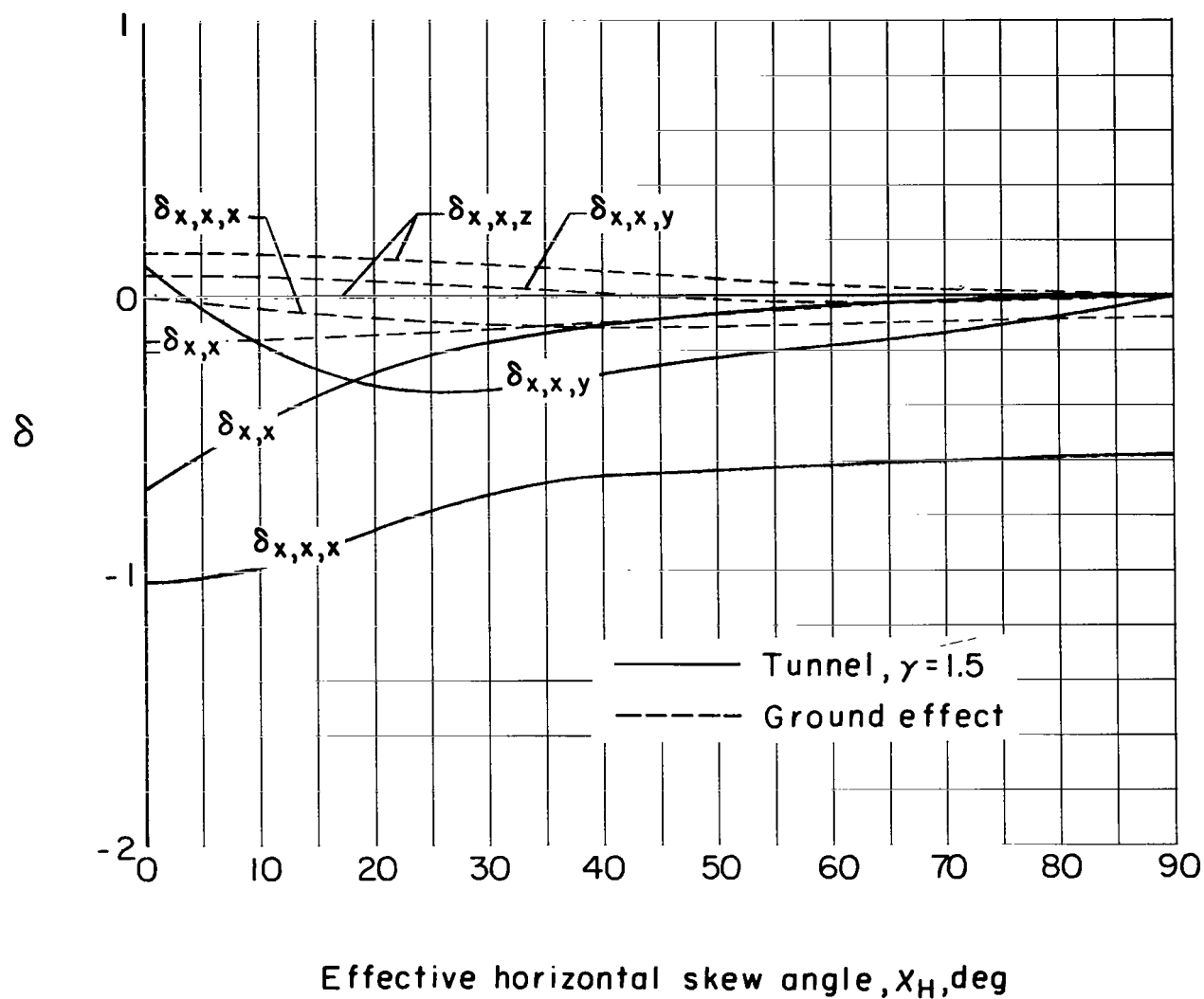
(h) $\delta_{z,y}$ and its gradients.

Figure 15.- Continued.



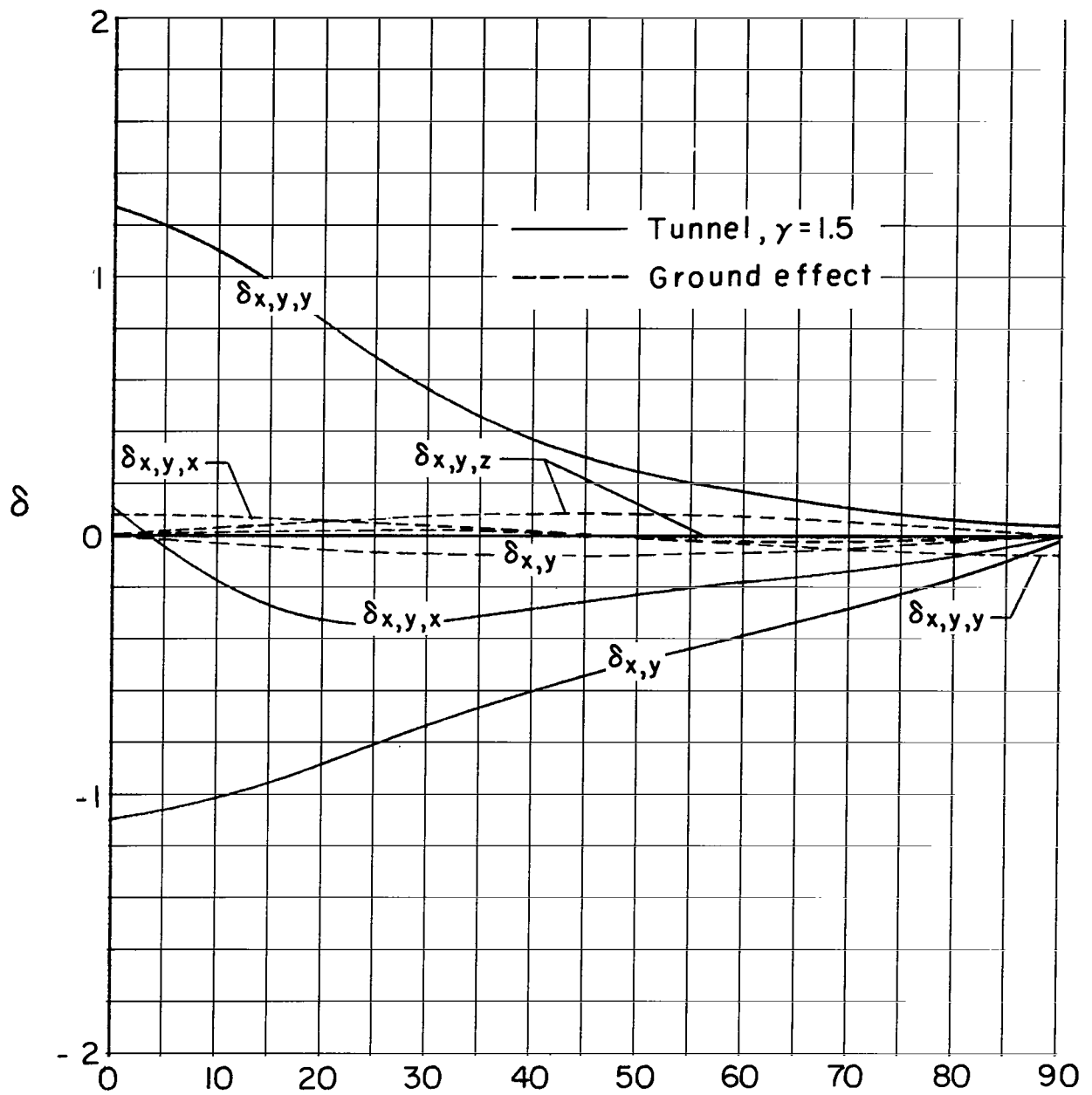
(i) $\delta_{z,z}$ and its gradients.

Figure 15.- Concluded.



(a) $\delta_{x,x}$ and its gradients.

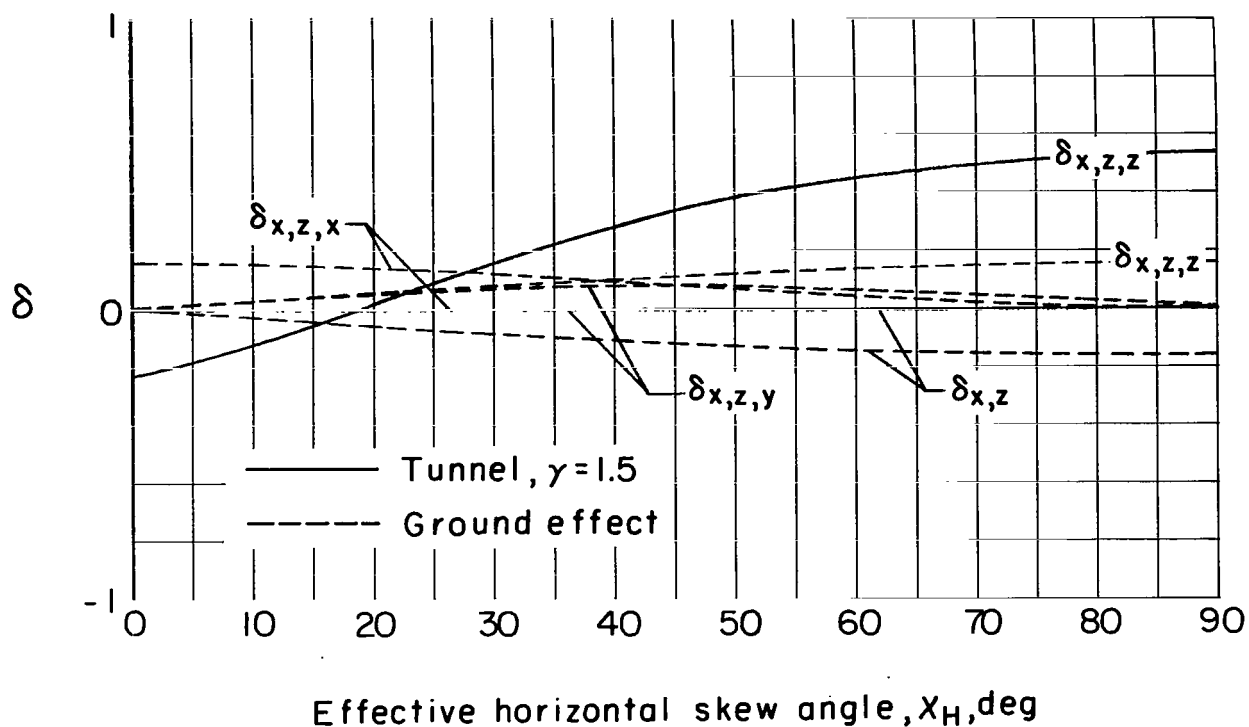
Figure 16.- Interference factors as a function of X_H for a vanishingly small model in ground effect and centered in a closed rectangular tunnel having a width-height ratio of 1.5. $X_V = 90^\circ$.



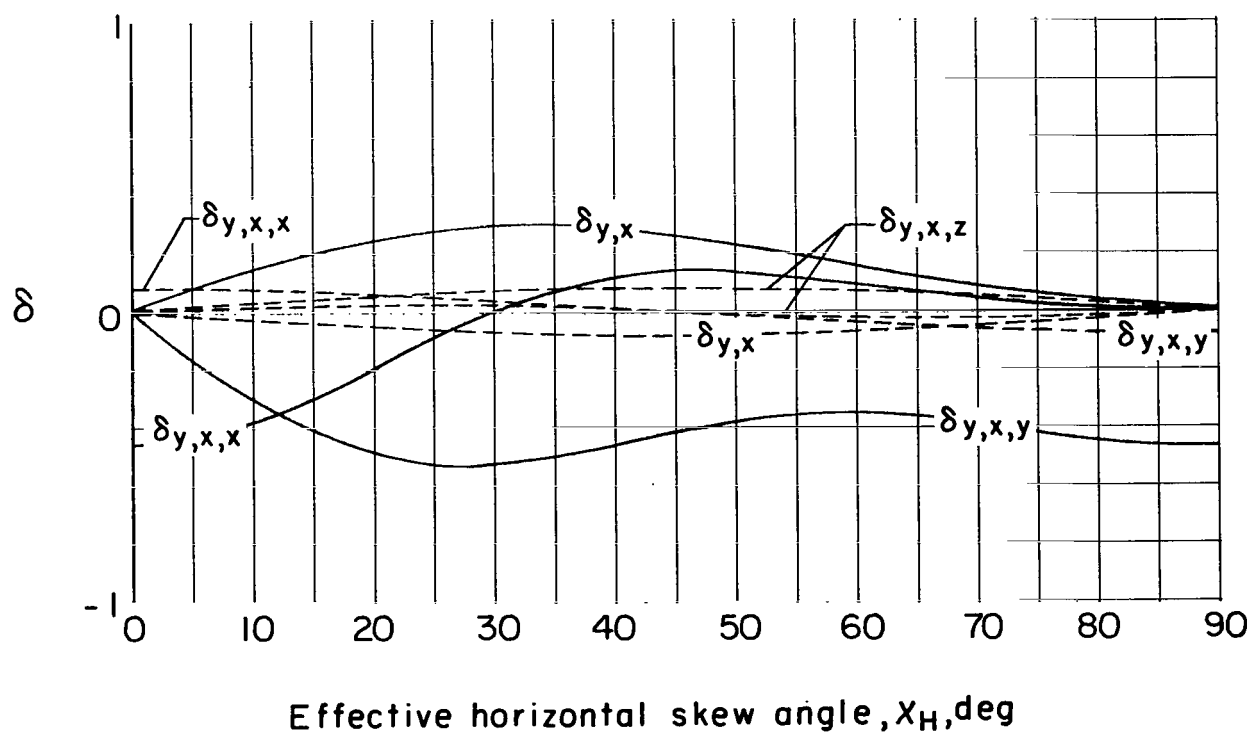
Effective horizontal skew angle, X_H , deg

(b) $\delta_{x,y}$ and its gradients.

Figure 16.- Continued.

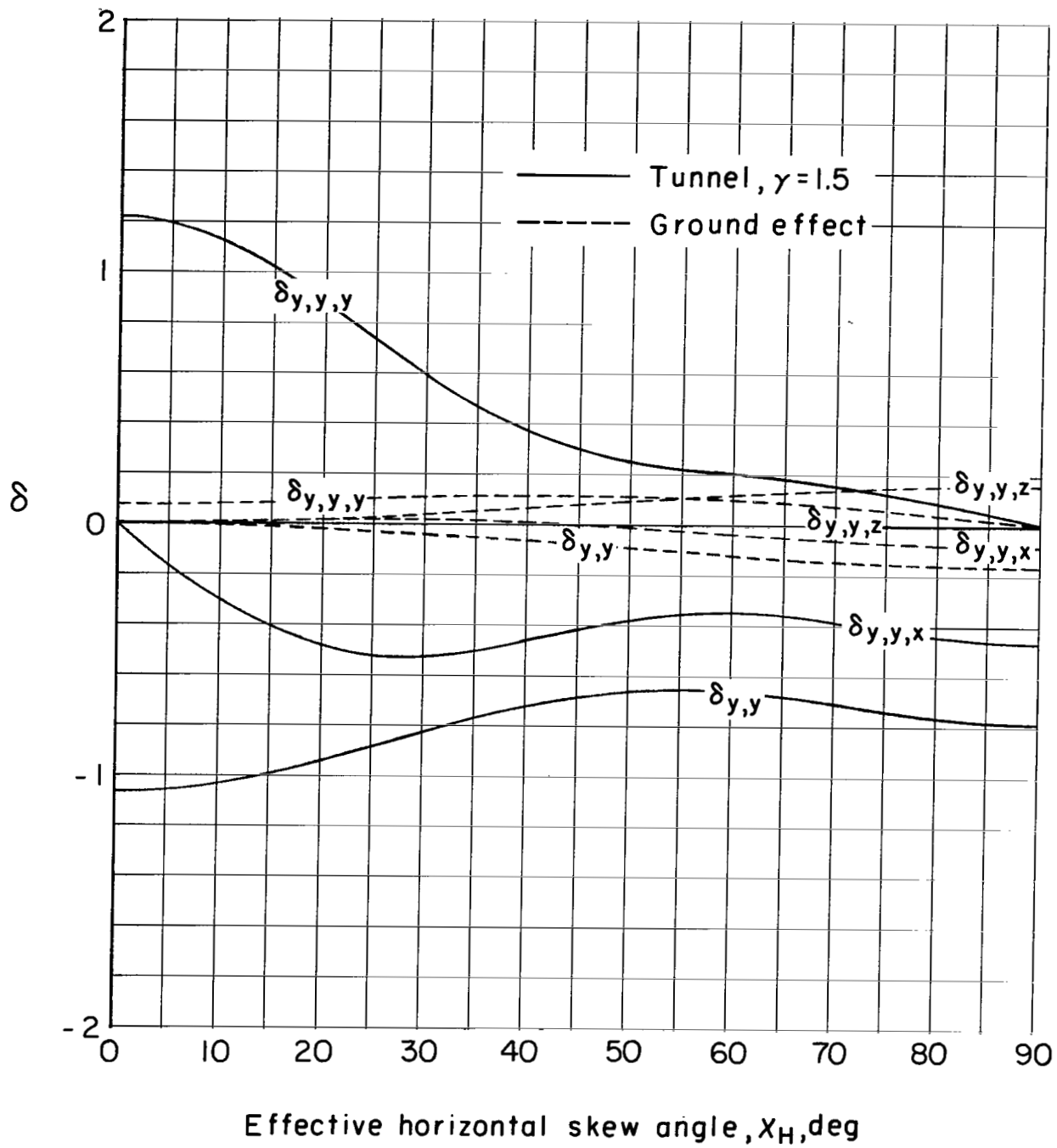


(c) $\delta_{x,z}$ and its gradients.



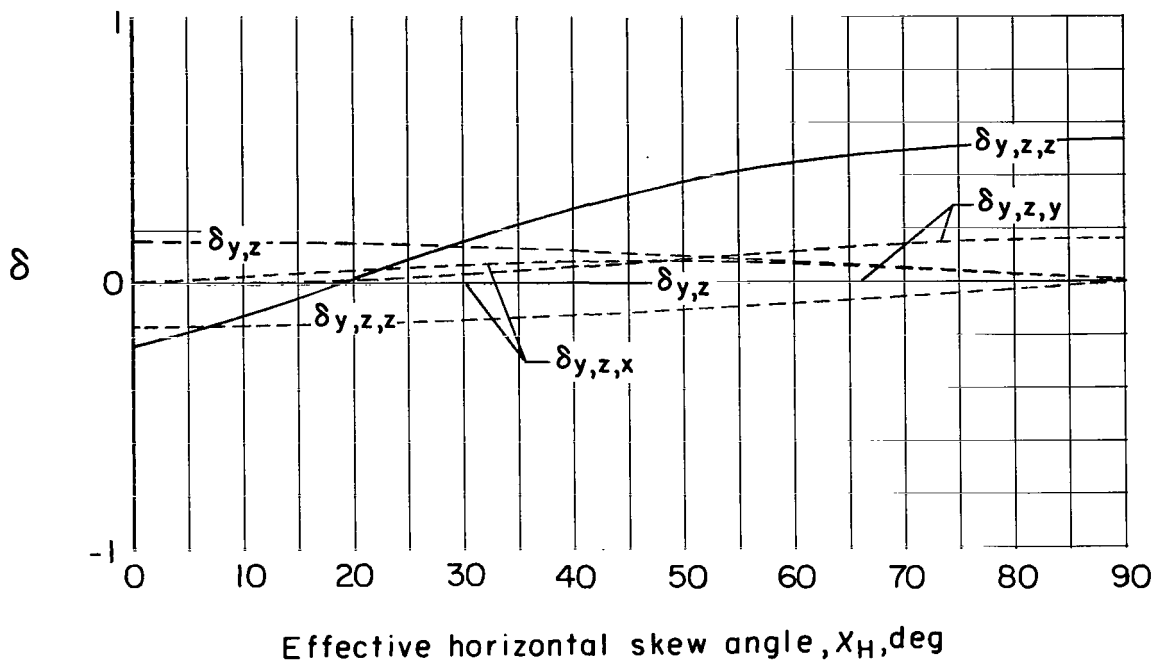
(d) $\delta_{y,x}$ and its gradients.

Figure 16.- Continued.

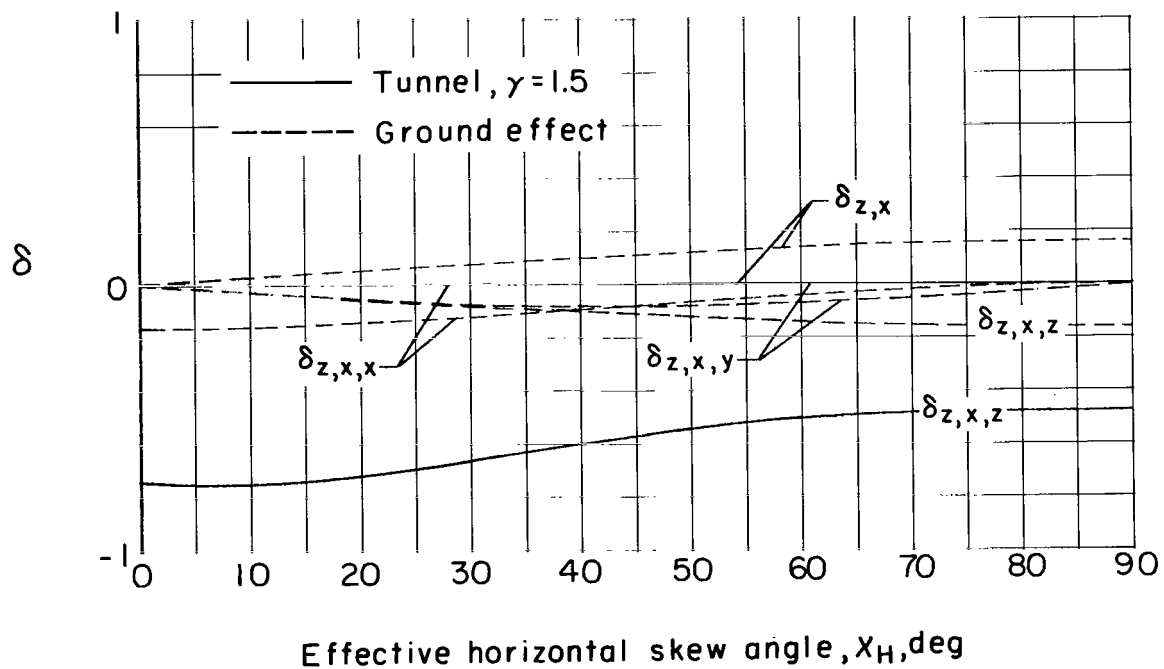


(e) $\delta_{y,y}$ and its gradients.

Figure 16.- Continued.

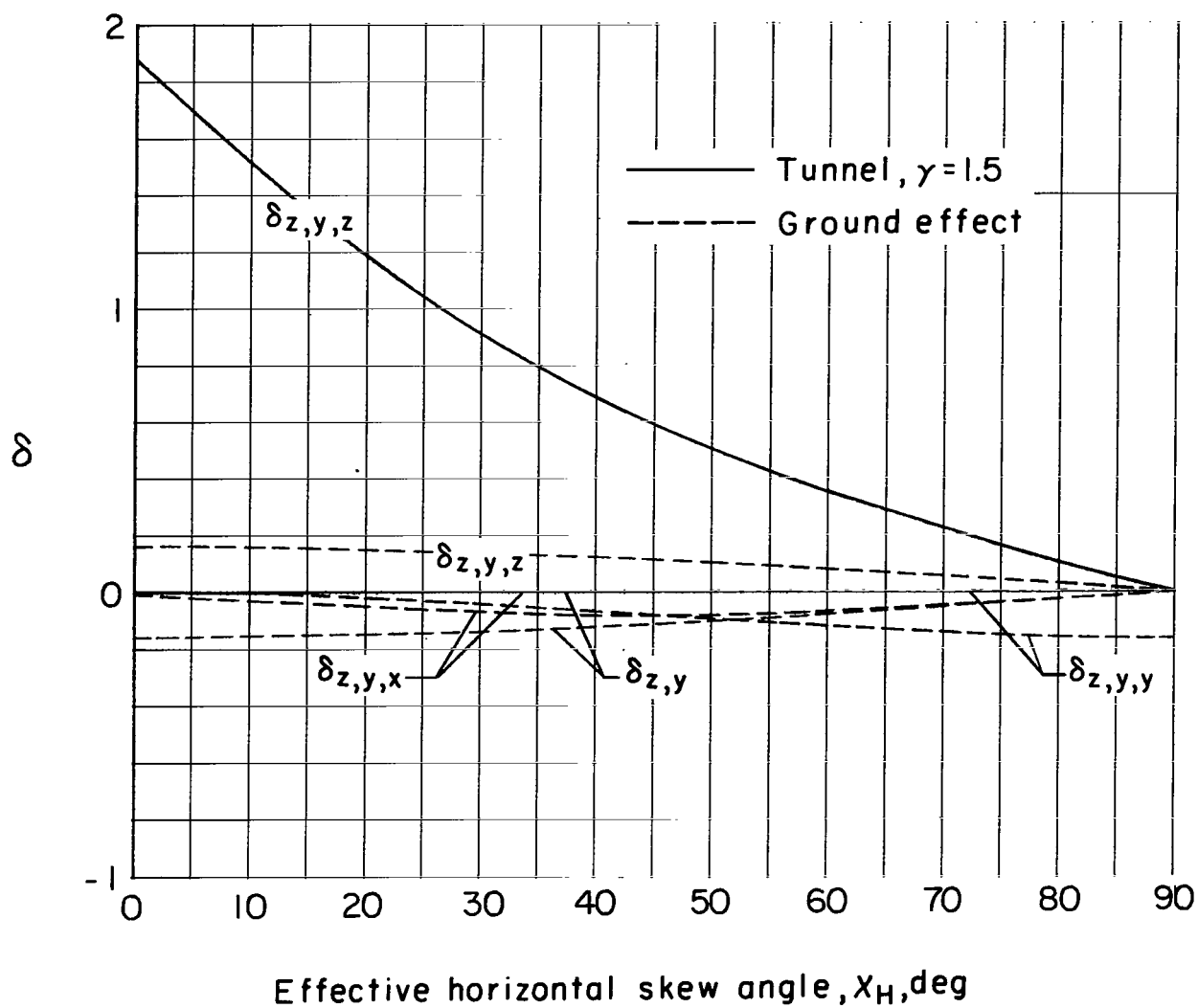


(f) $\delta_{y,z}$ and its gradients.



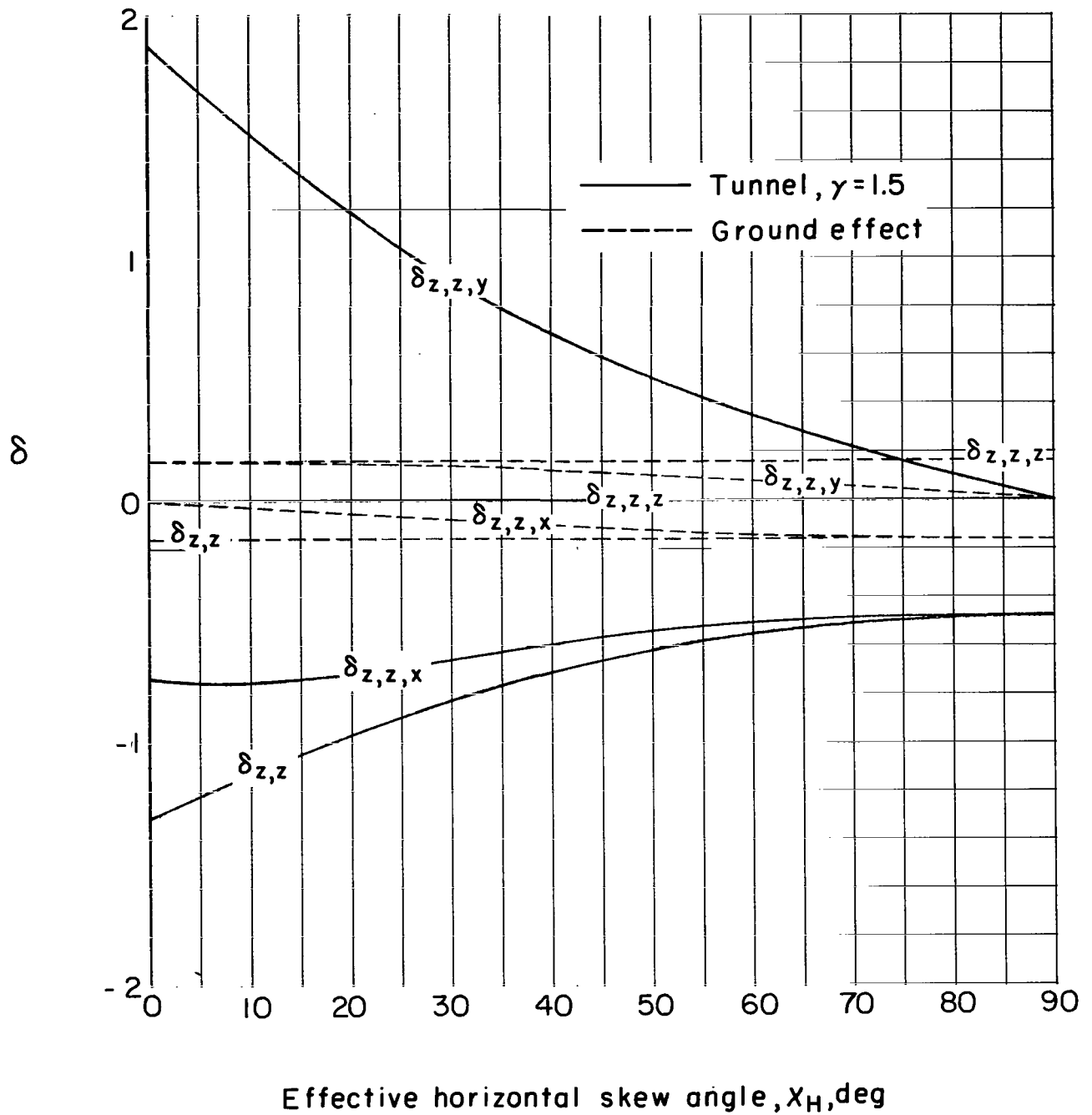
(g) $\delta_{z,x}$ and its gradients.

Figure 16.- Continued.



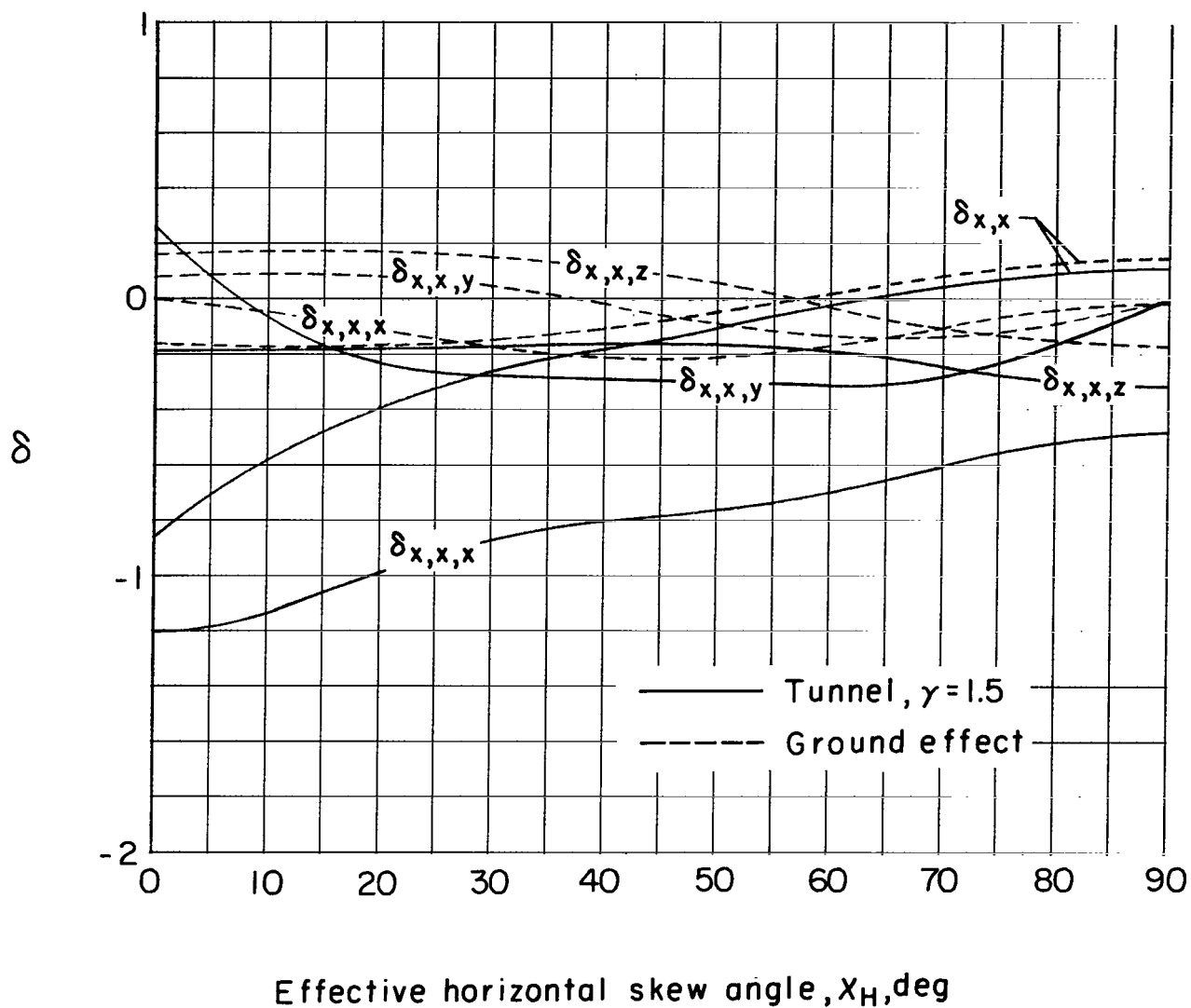
(h) $\delta_{z,y}$ and its gradients.

Figure 16.- Continued.



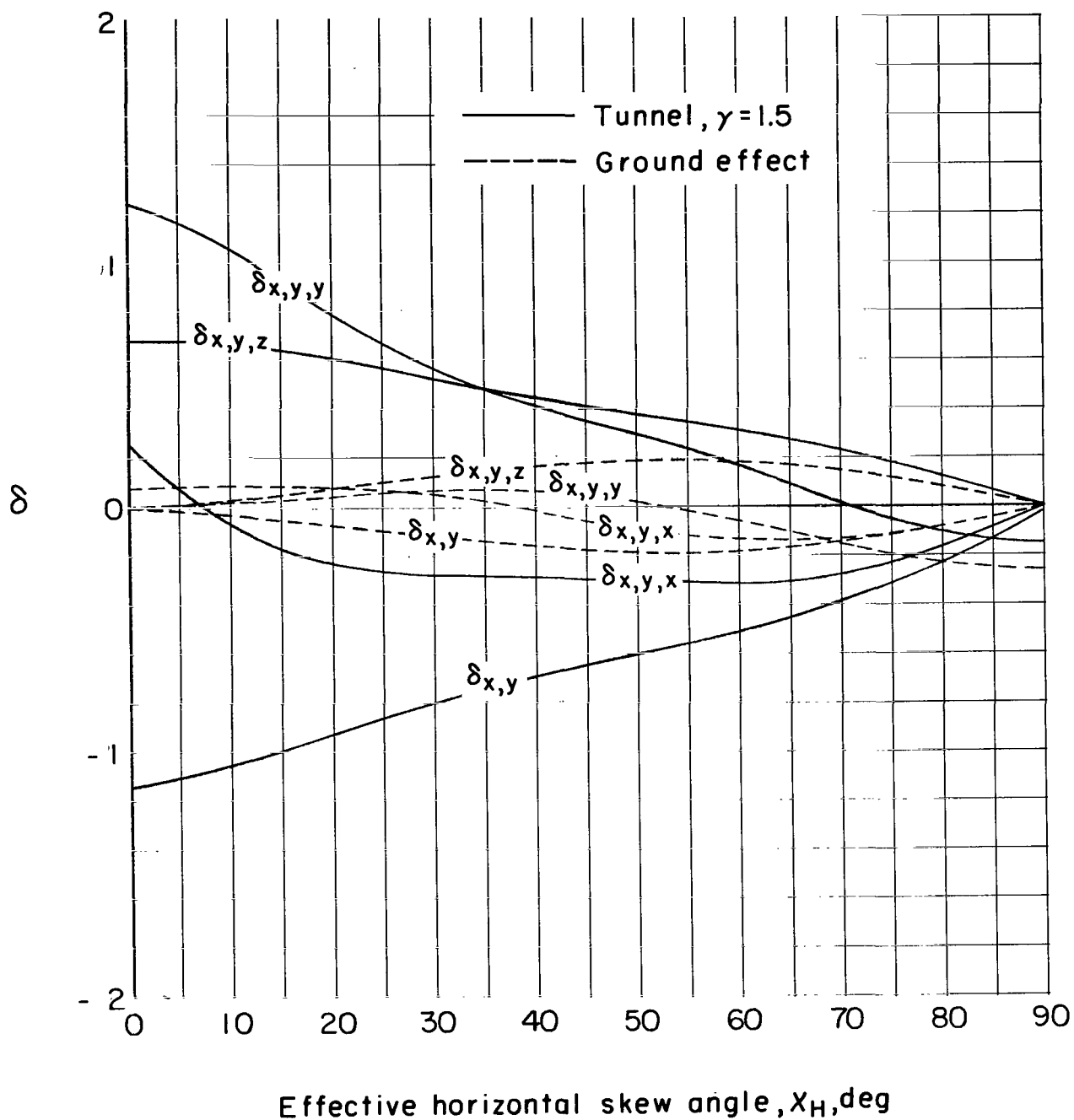
(ii) $\delta_{z,z}$ and its gradients.

Figure 16.- Concluded.



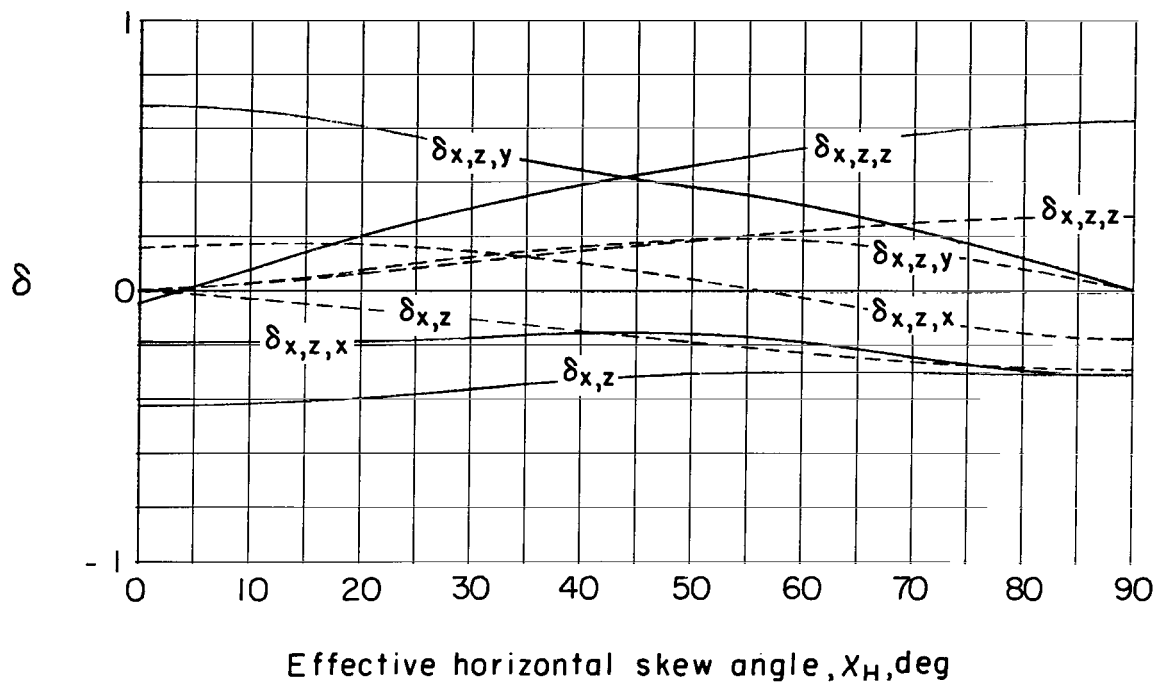
(a) $\delta_{x,x}$ and its gradients.

Figure 17.- Interference factors as a function of X_H for a vanishingly small model in ground effect and centered in a closed rectangular tunnel having a width-height ratio of 1.5. $X_V = 60^\circ$.

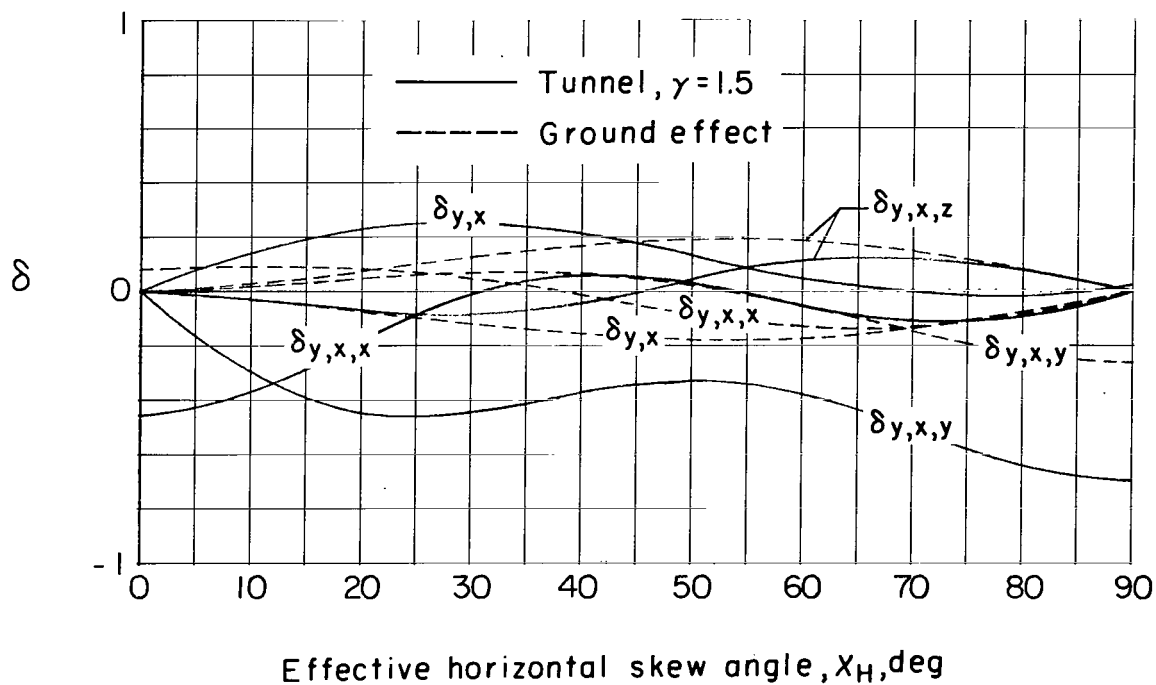


(b) $\delta_{x,y}$ and its gradients.

Figure 17.- Continued.

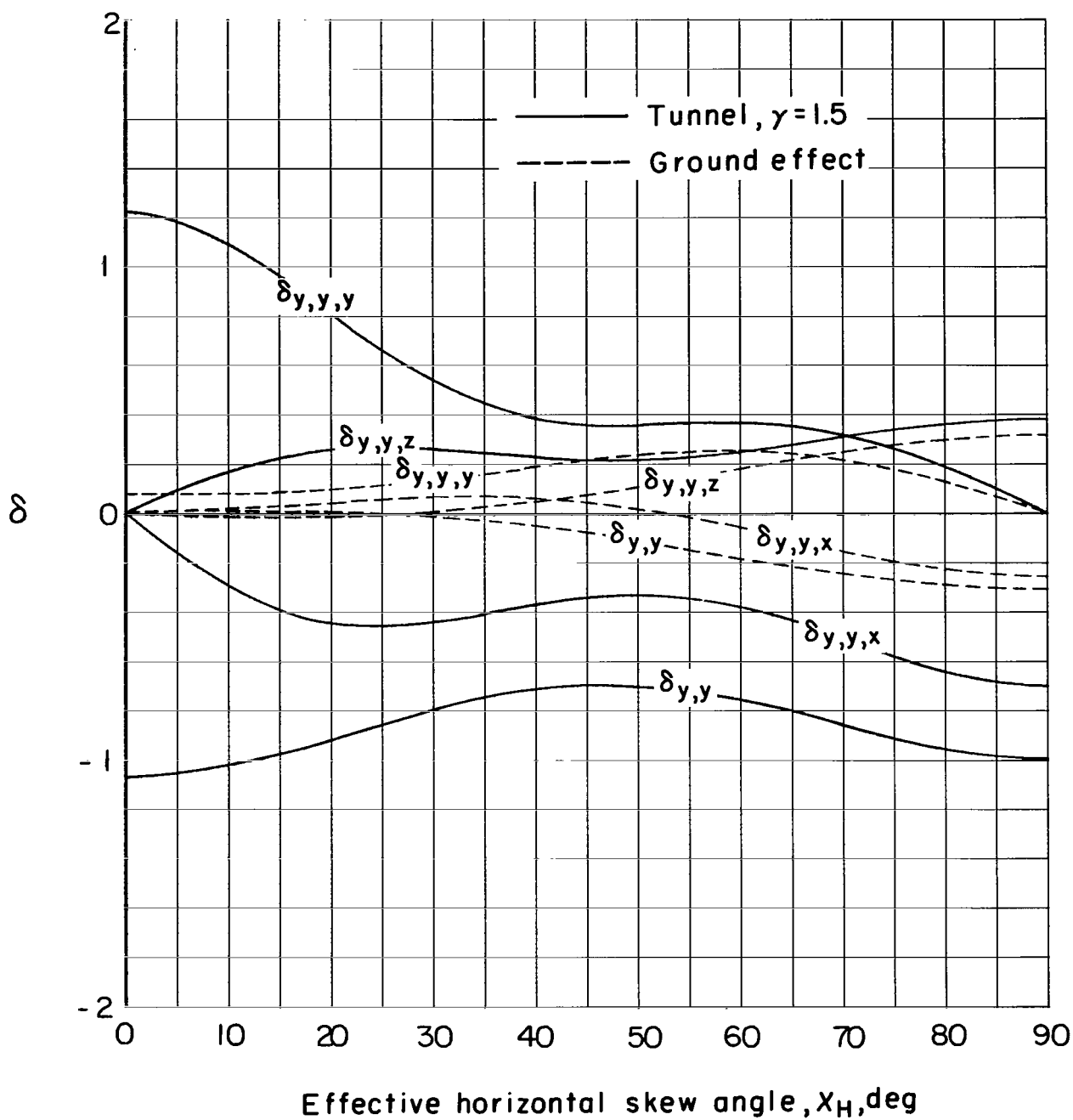


(c) $\delta_{x,z}$ and its gradients.



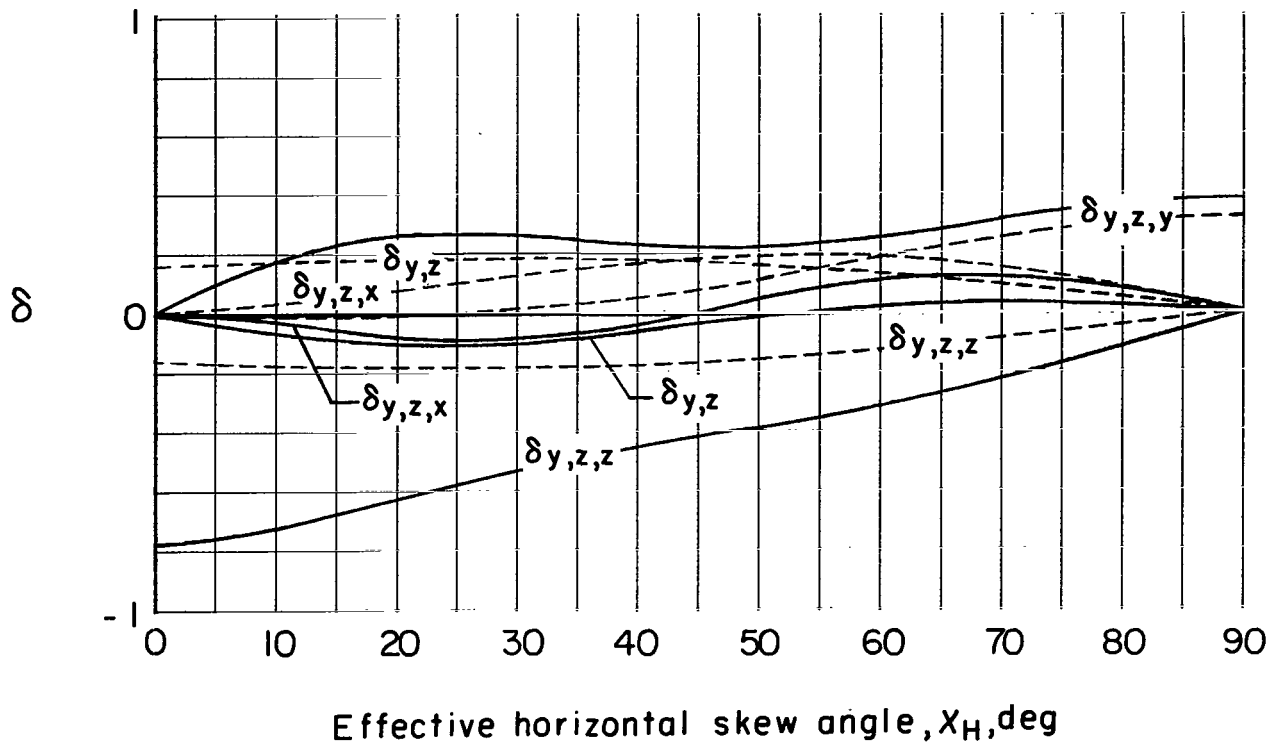
(d) $\delta_{y,x}$ and its gradients.

Figure 17.- Continued.

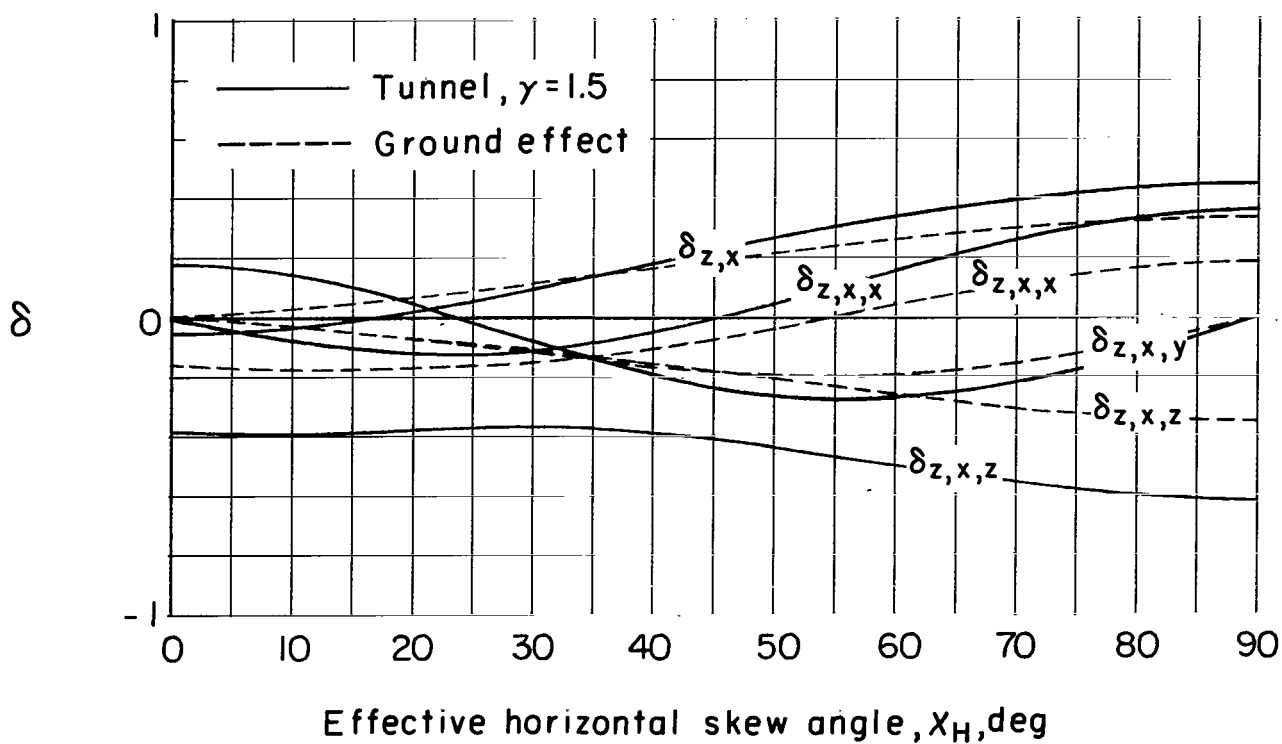


(e) $\delta_{y,y}$ and its gradients.

Figure 17.- Continued.

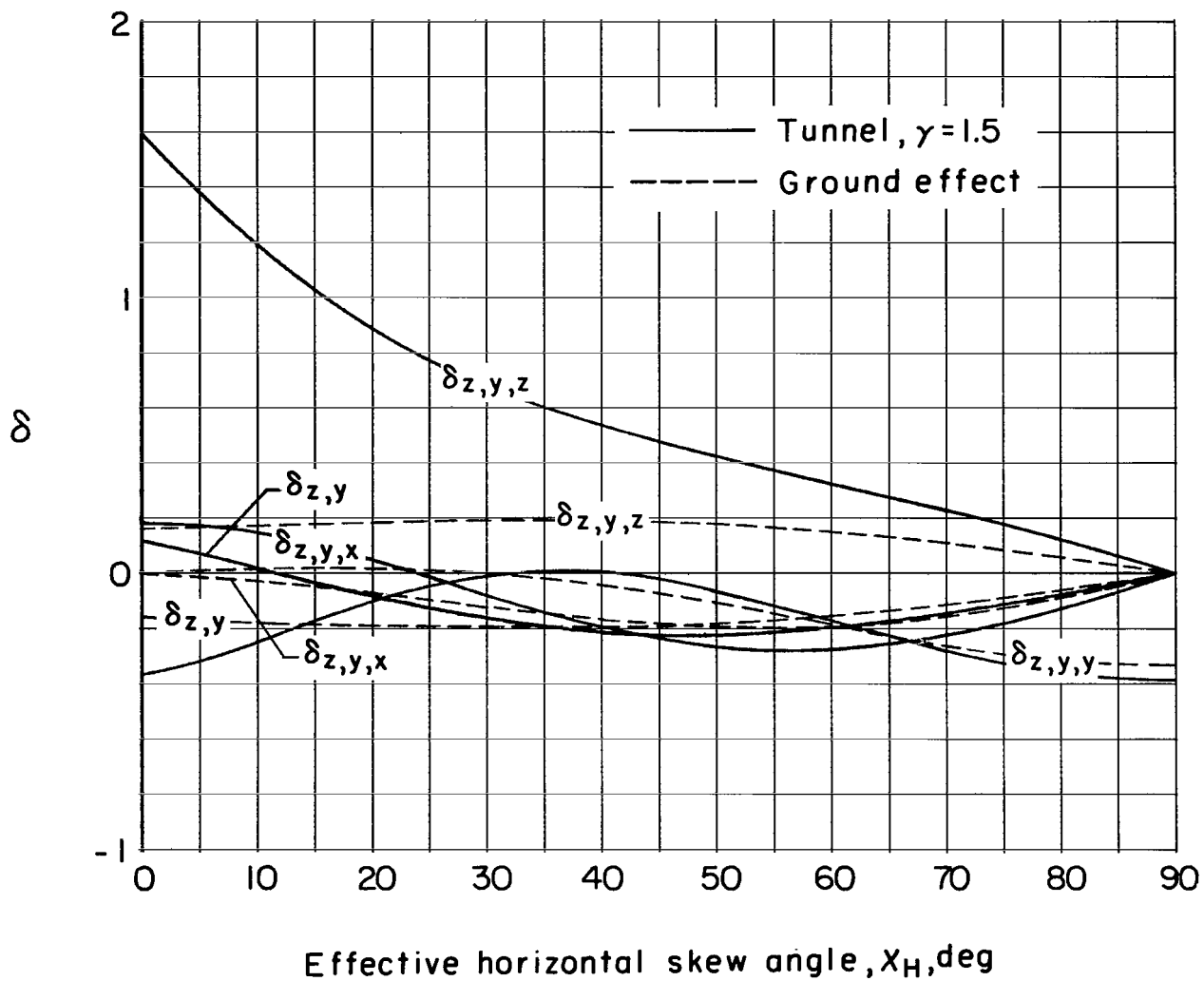


(f) $\delta_{y,z}$ and its gradients.



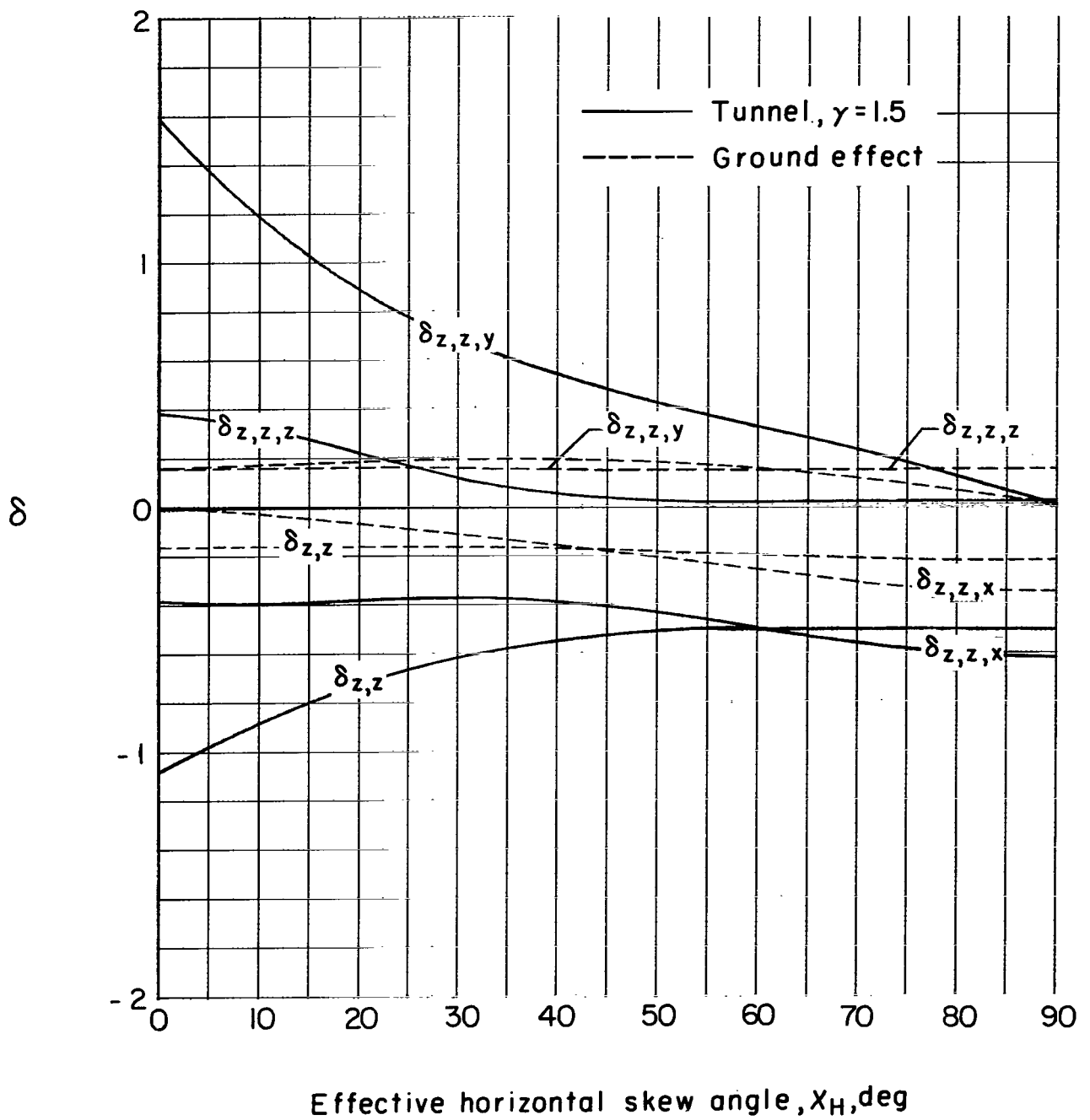
(g) $\delta_{z,x}$ and its gradients.

Figure 17.- Continued.



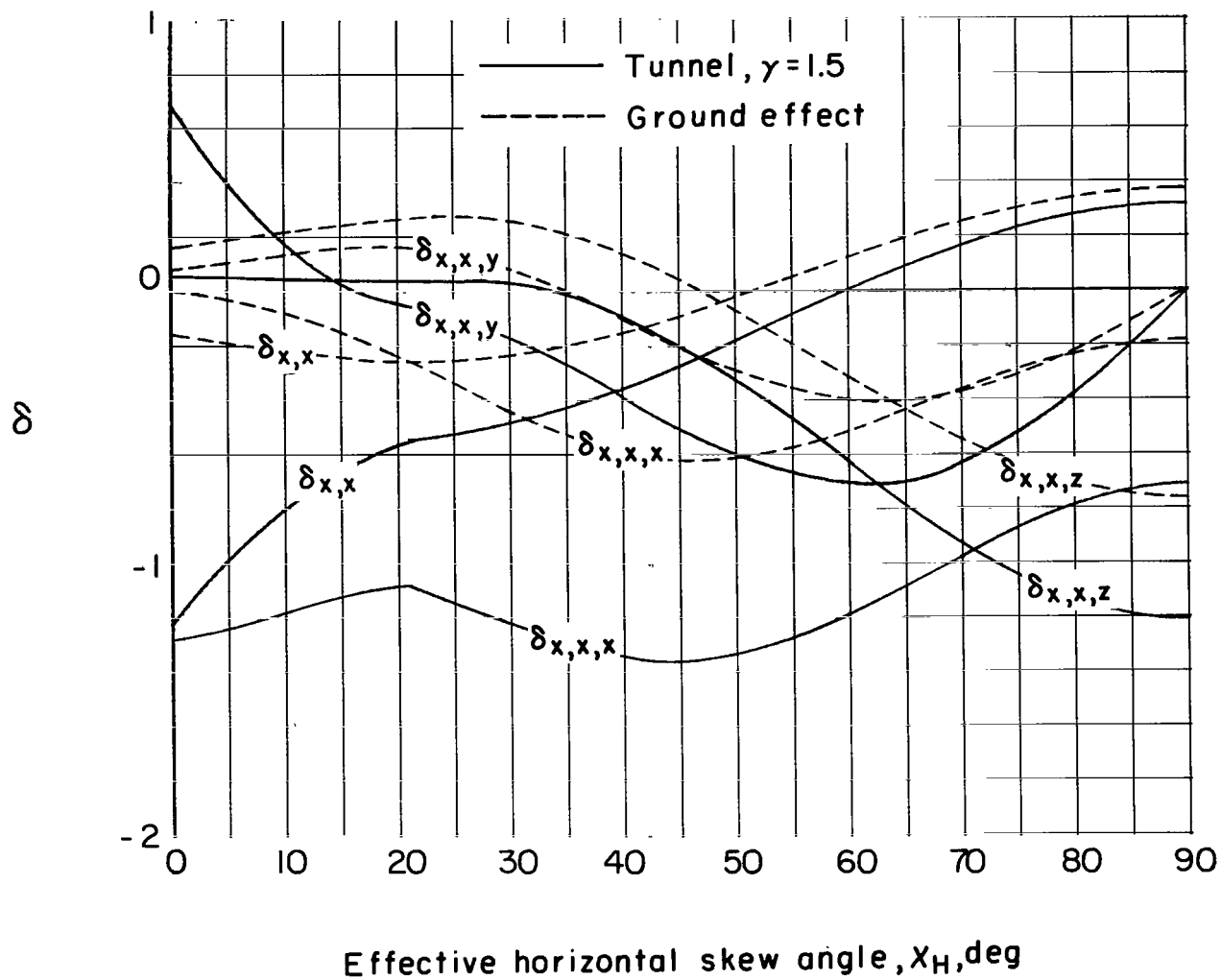
(h) $\delta_{z,y}$ and its gradients.

Figure 17.- Continued.



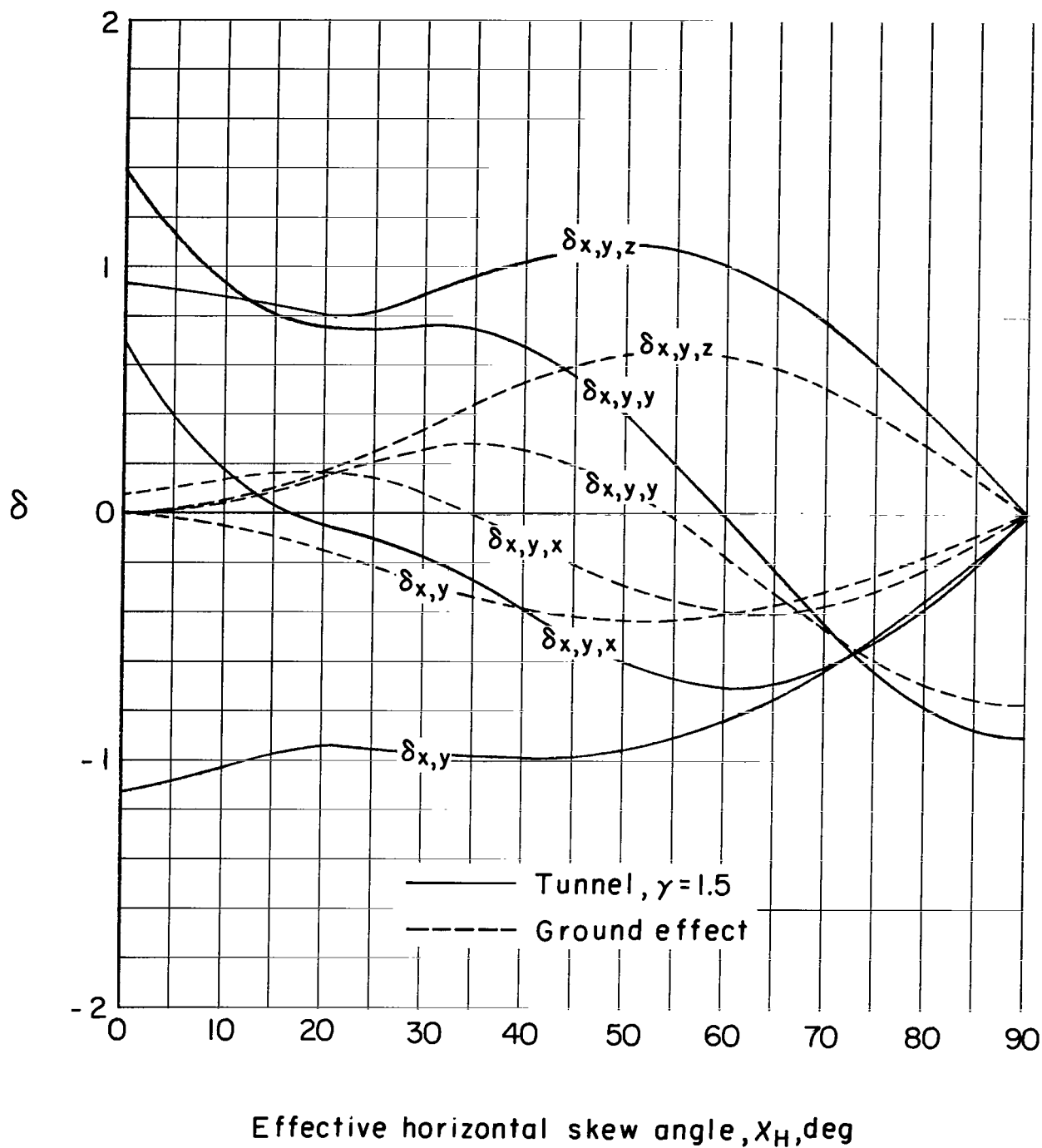
(i) $\delta_{z,z}$ and its gradients.

Figure 17.- Concluded.



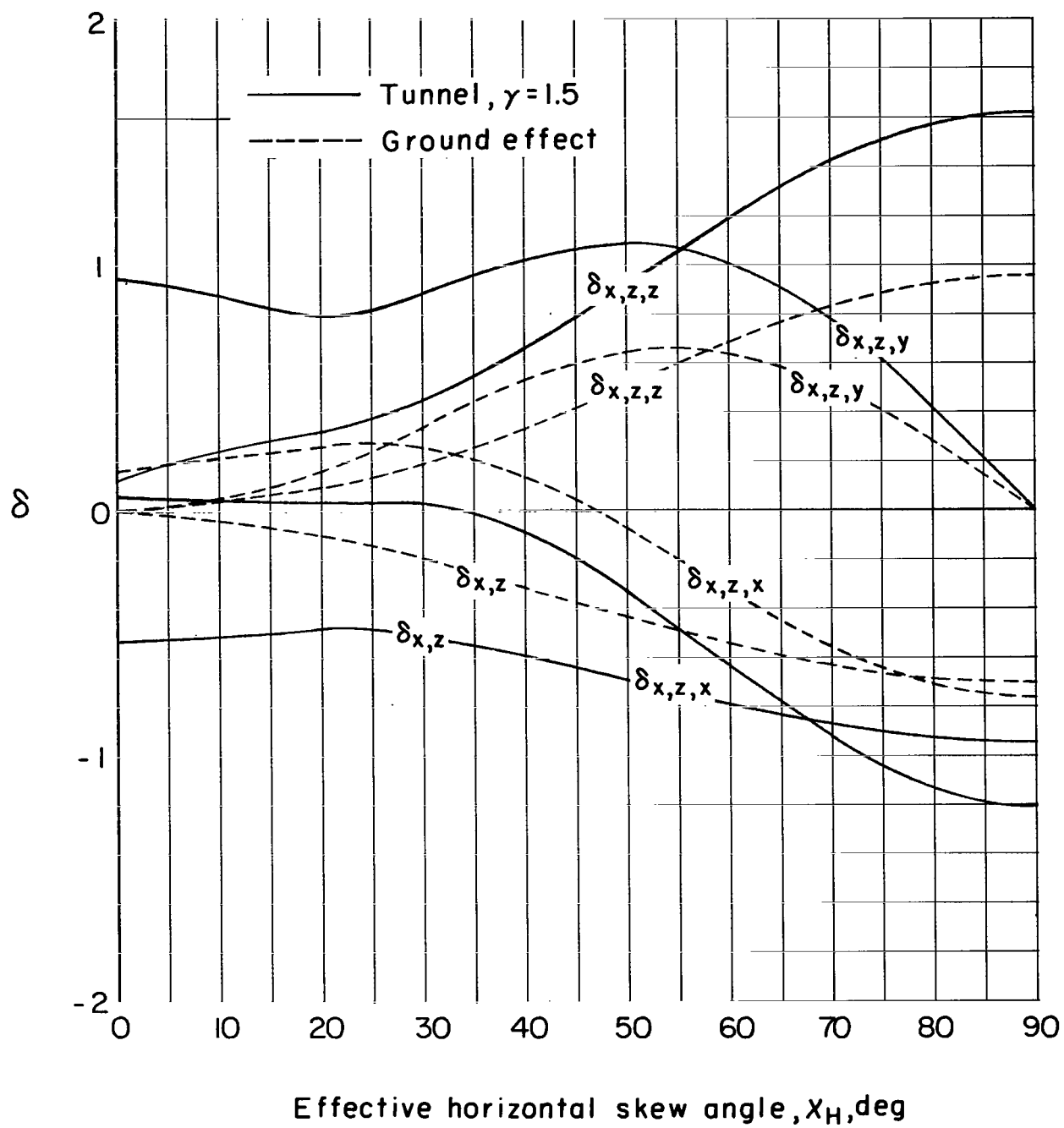
(a) $\delta_{x,x}$ and its gradients.

Figure 18.- Interference factors as a function of X_H for a vanishingly small model in ground effect and centered in a closed rectangular tunnel having a width-height ratio of 1.5. $X_V = 30^\circ$.



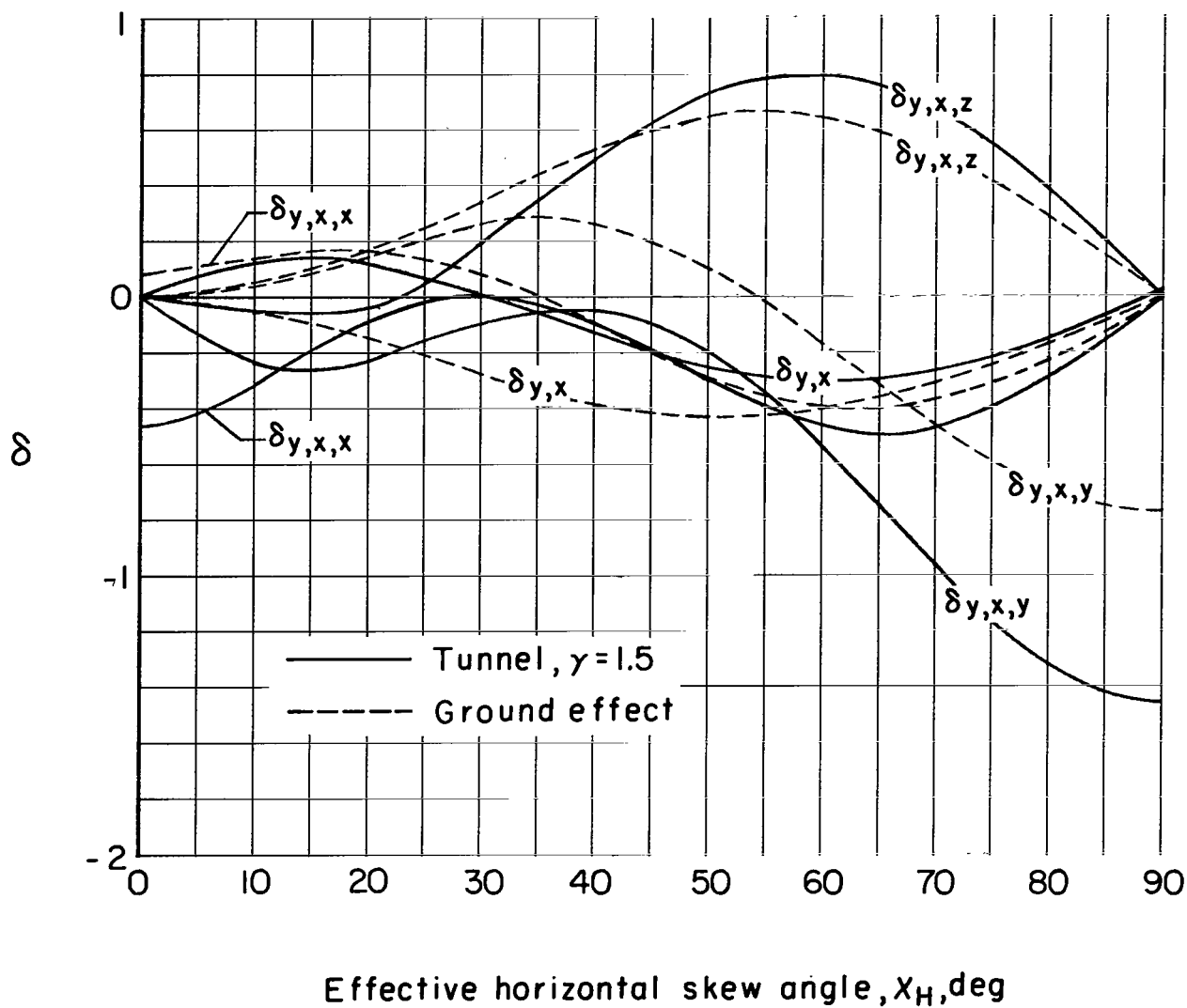
(b) $\delta_{x,y}$ and its gradients.

Figure 18.- Continued.



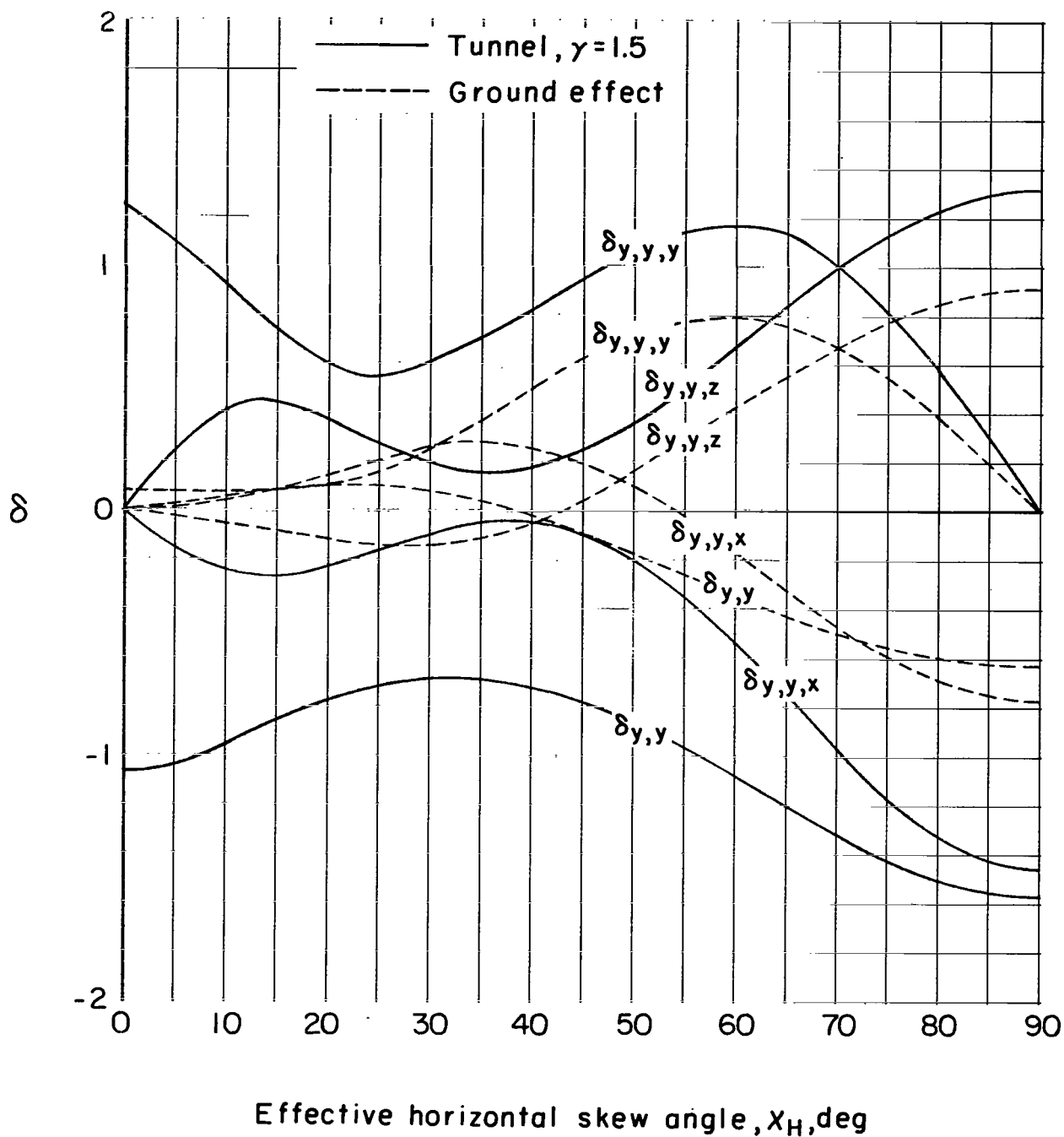
(c) $\delta_{x,z}$ and its gradients.

Figure 18.- Continued.



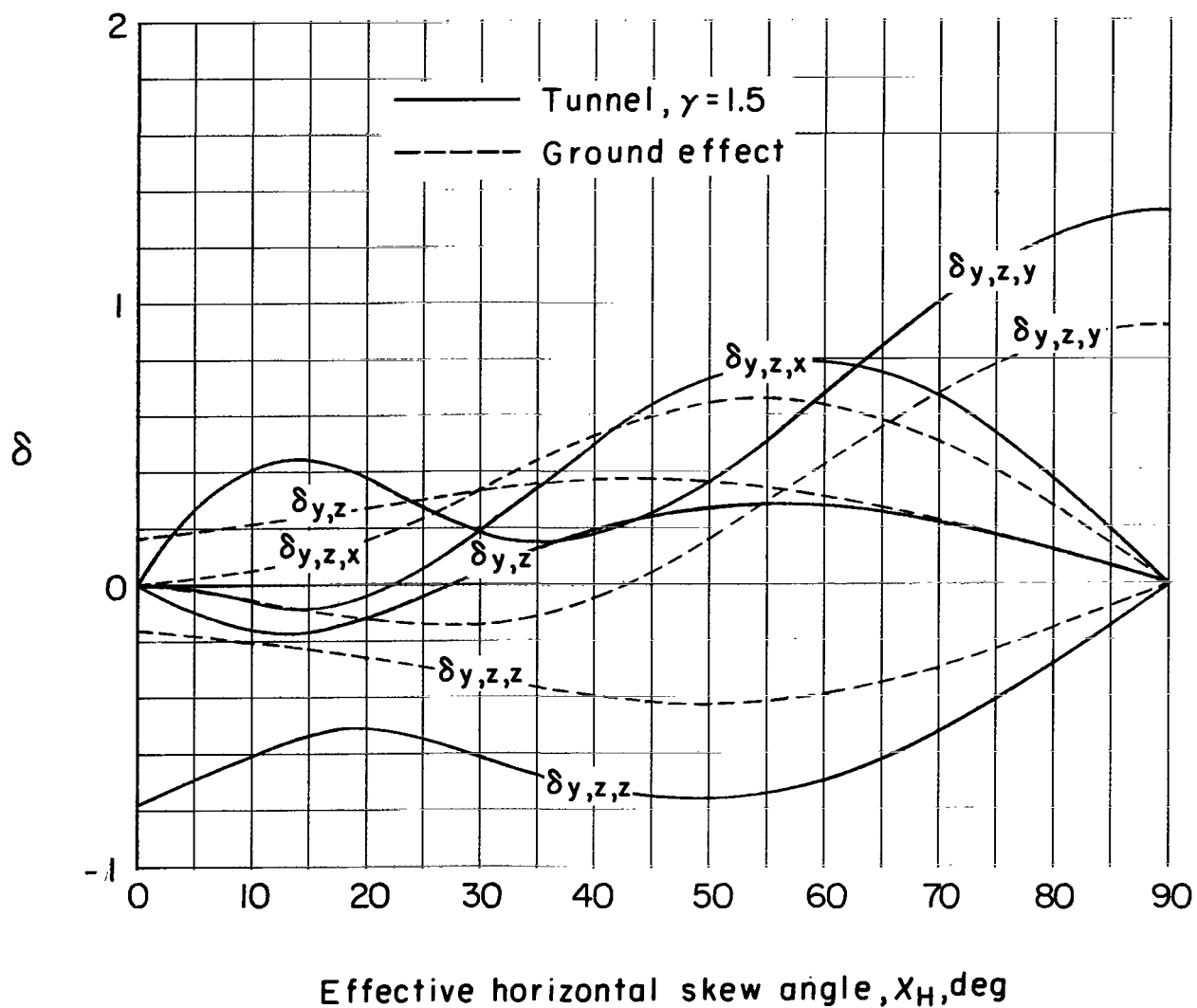
(d) $\delta_{y,x}$ and its gradients.

Figure 18.- Continued.



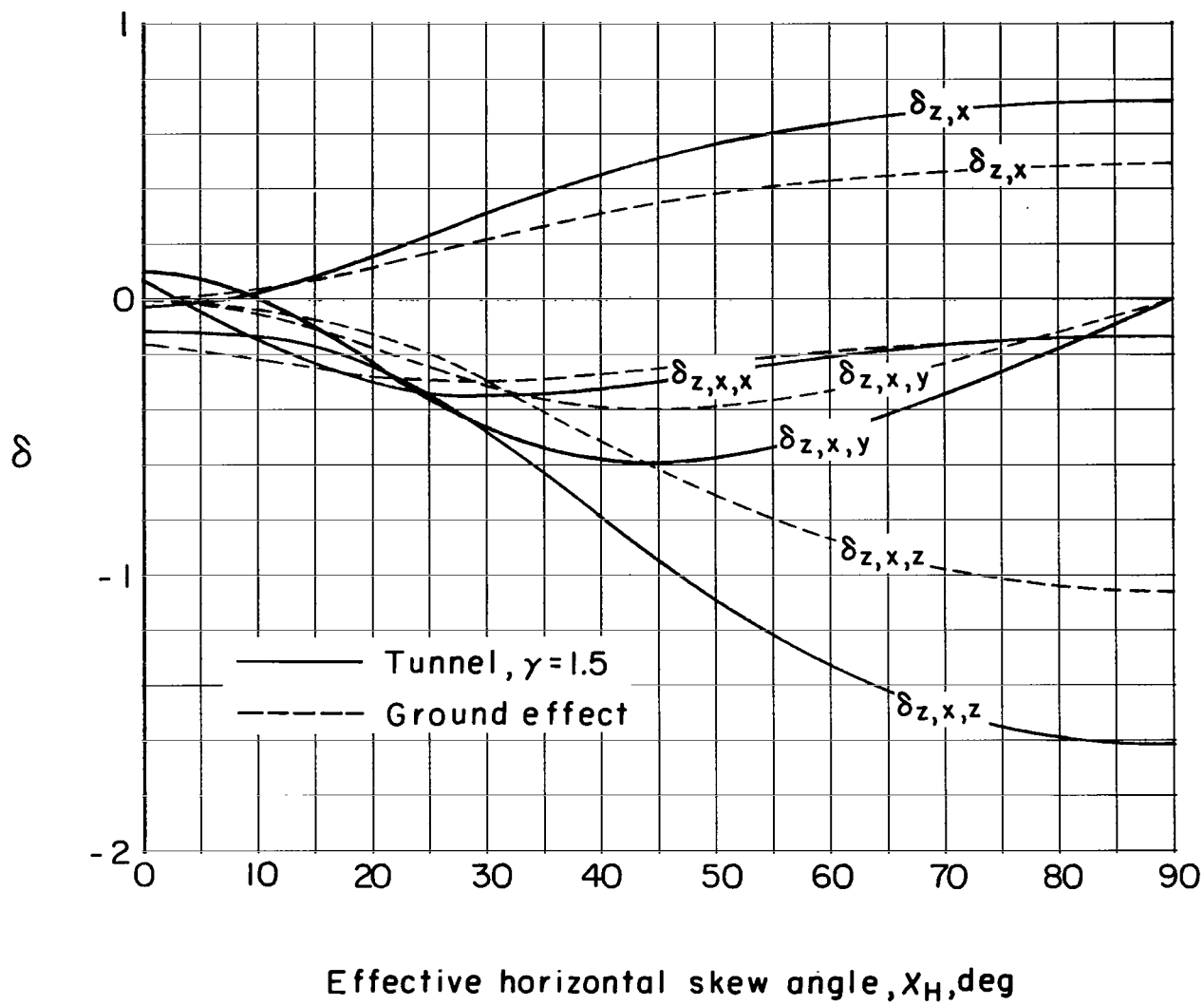
(e) $\delta_{y,y}$ and its gradients.

Figure 18.- Continued.



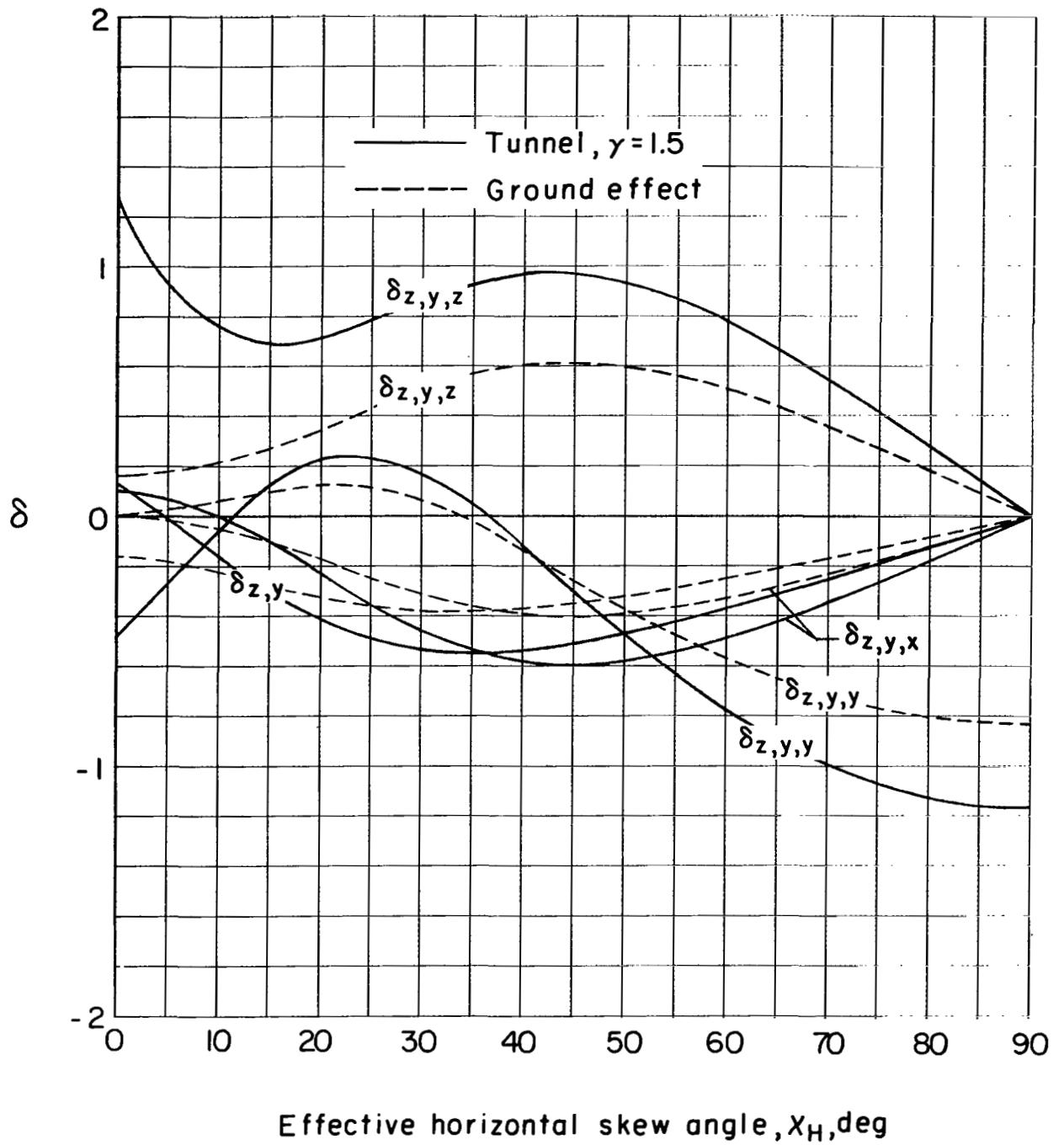
(f) $\delta_{y,z}$ and its gradients.

Figure 18.- Continued.



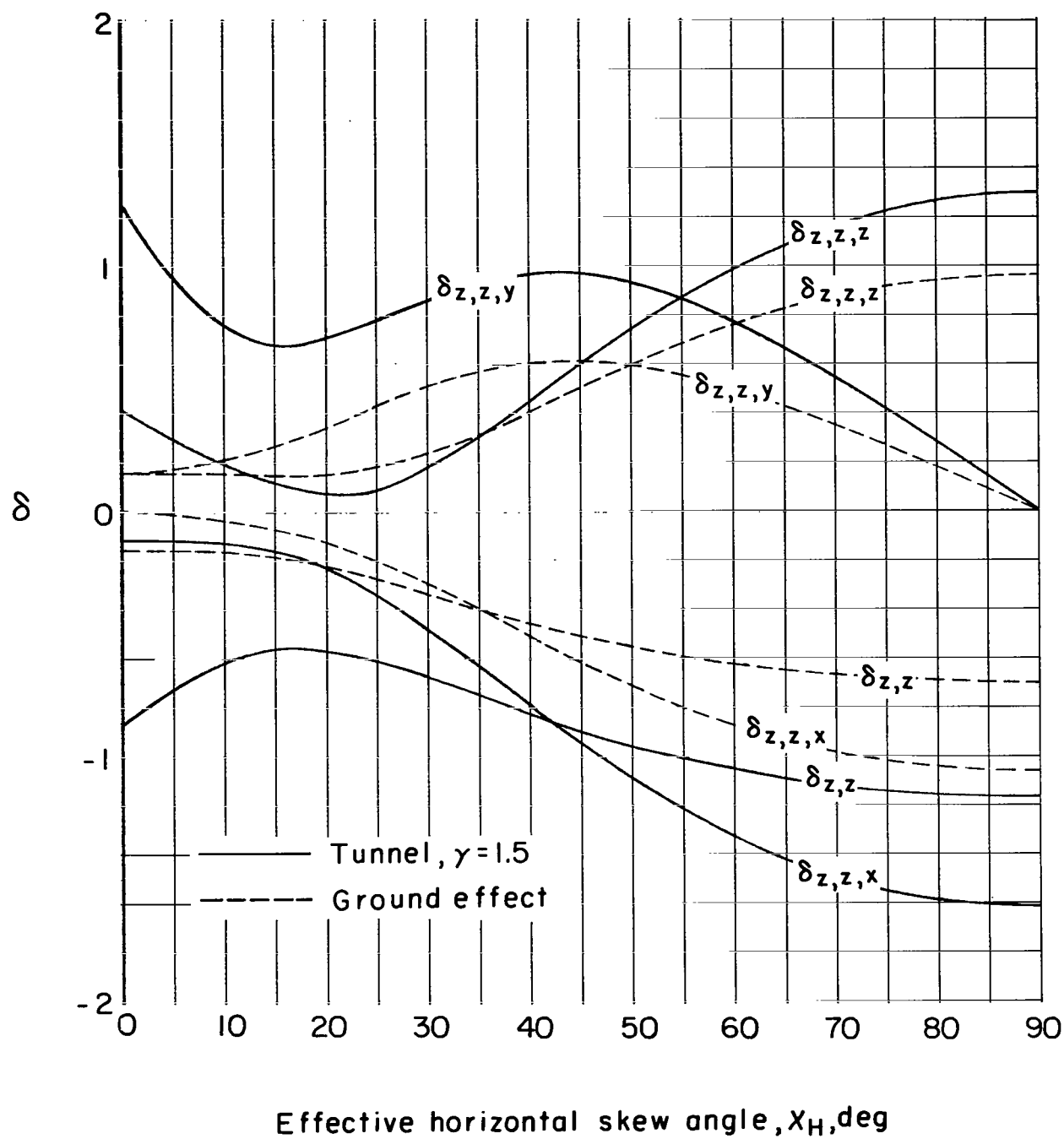
(g) $\delta_{z,x}$ and its gradients.

Figure 18.- Continued.



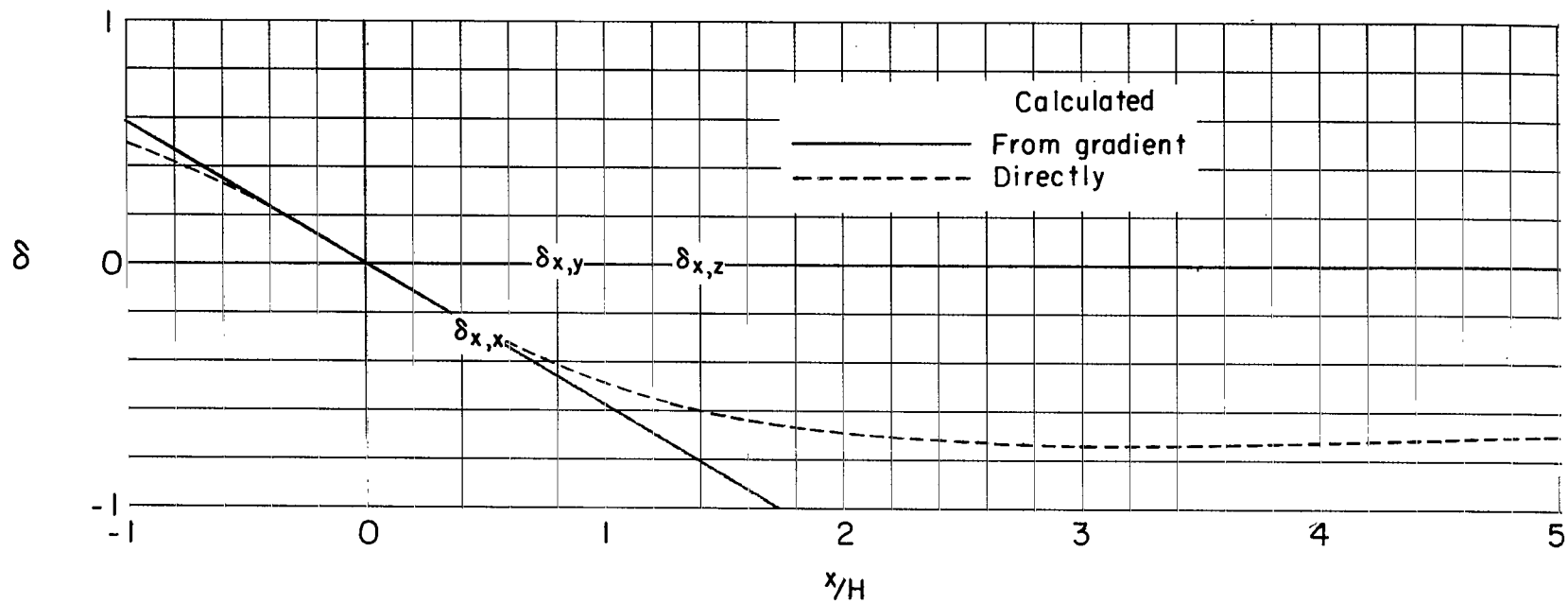
(h) $\delta_{z,y}$ and its gradients.

Figure 18.- Continued.



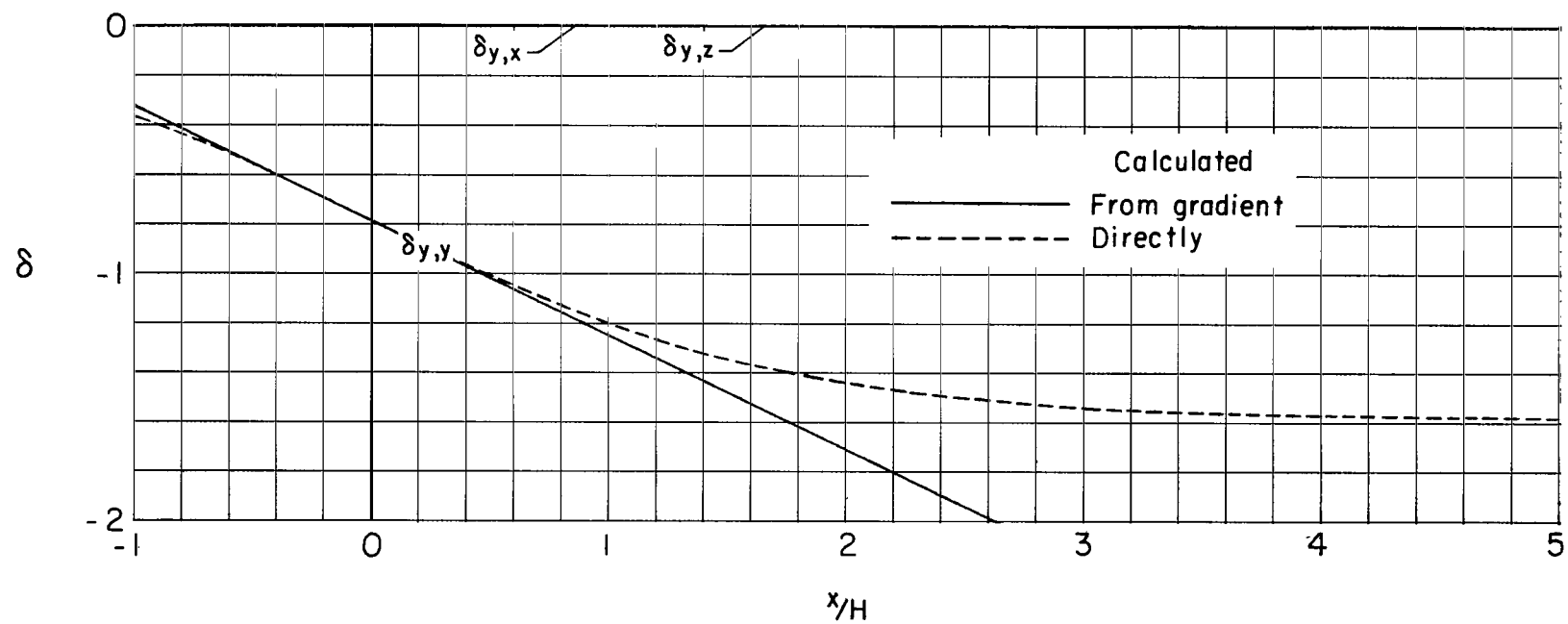
(i) $\delta_{z,z}$ and its gradients.

Figure 18.- Concluded.



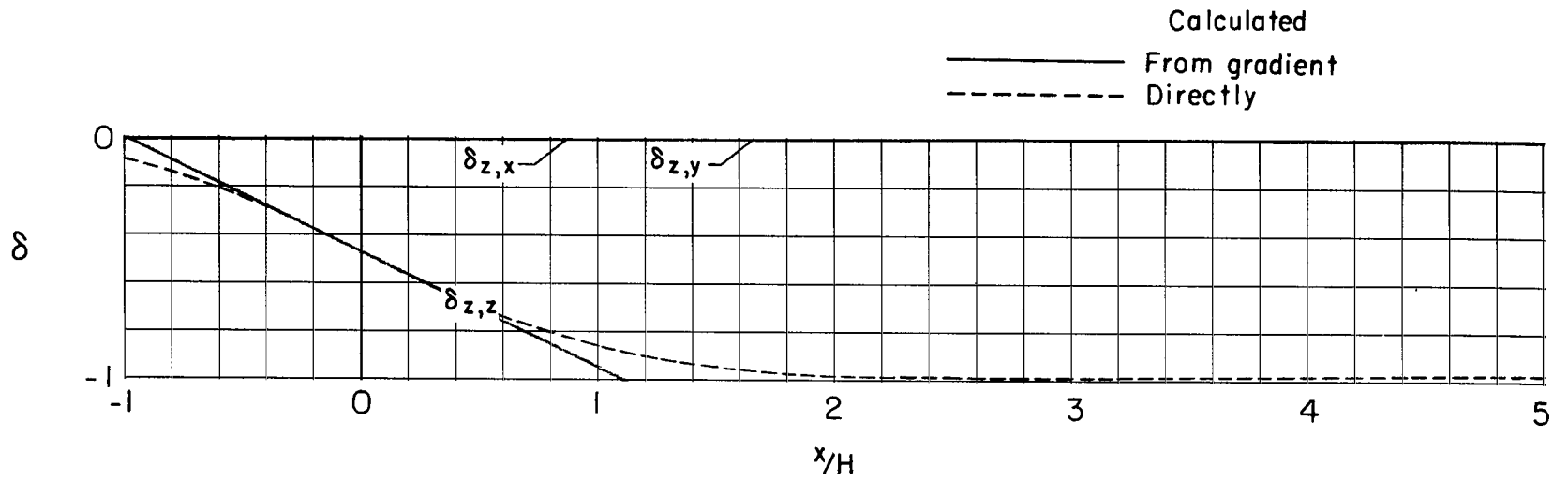
(a) Caused by forces in the X-direction.

Figure 19.- Distribution of interference factors along the longitudinal axis of the tunnel for a vanishingly small model centered in a closed rectangular tunnel having a width-height ratio of 1.5. $x_H = 90^\circ$; $x_V = 90^\circ$.



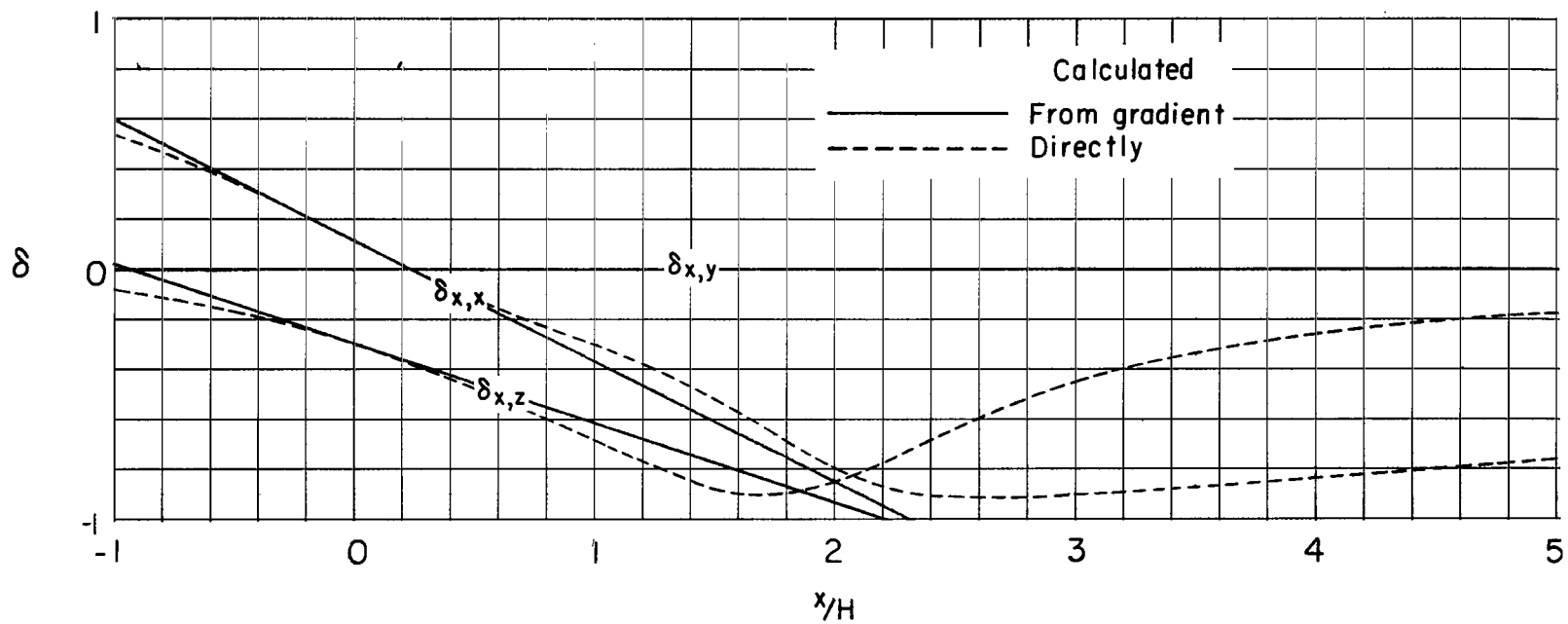
(b) Caused by forces in the Y-direction.

Figure 19.- Continued.



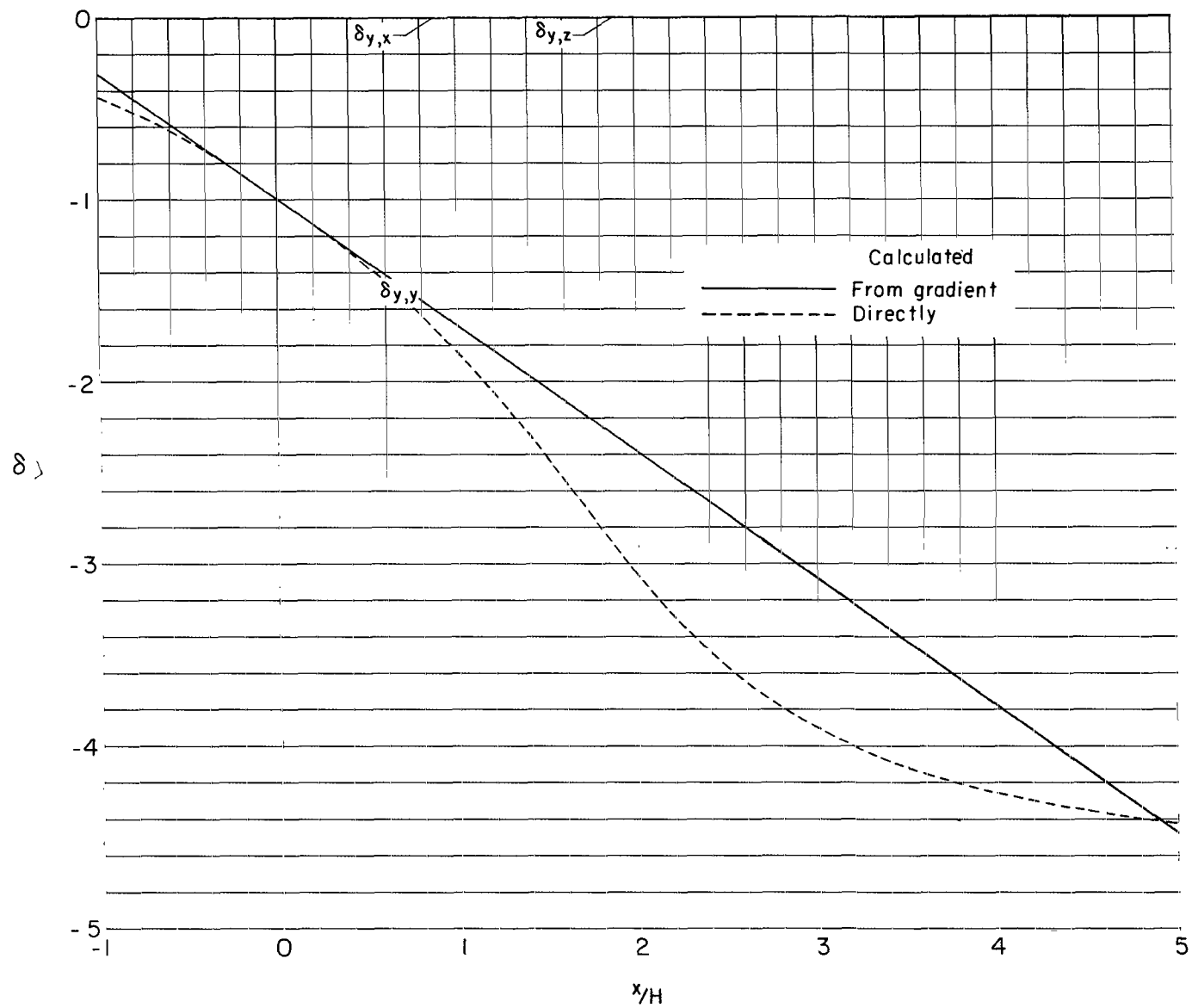
(c) Caused by forces in the Z-direction.

Figure 19.- Concluded.



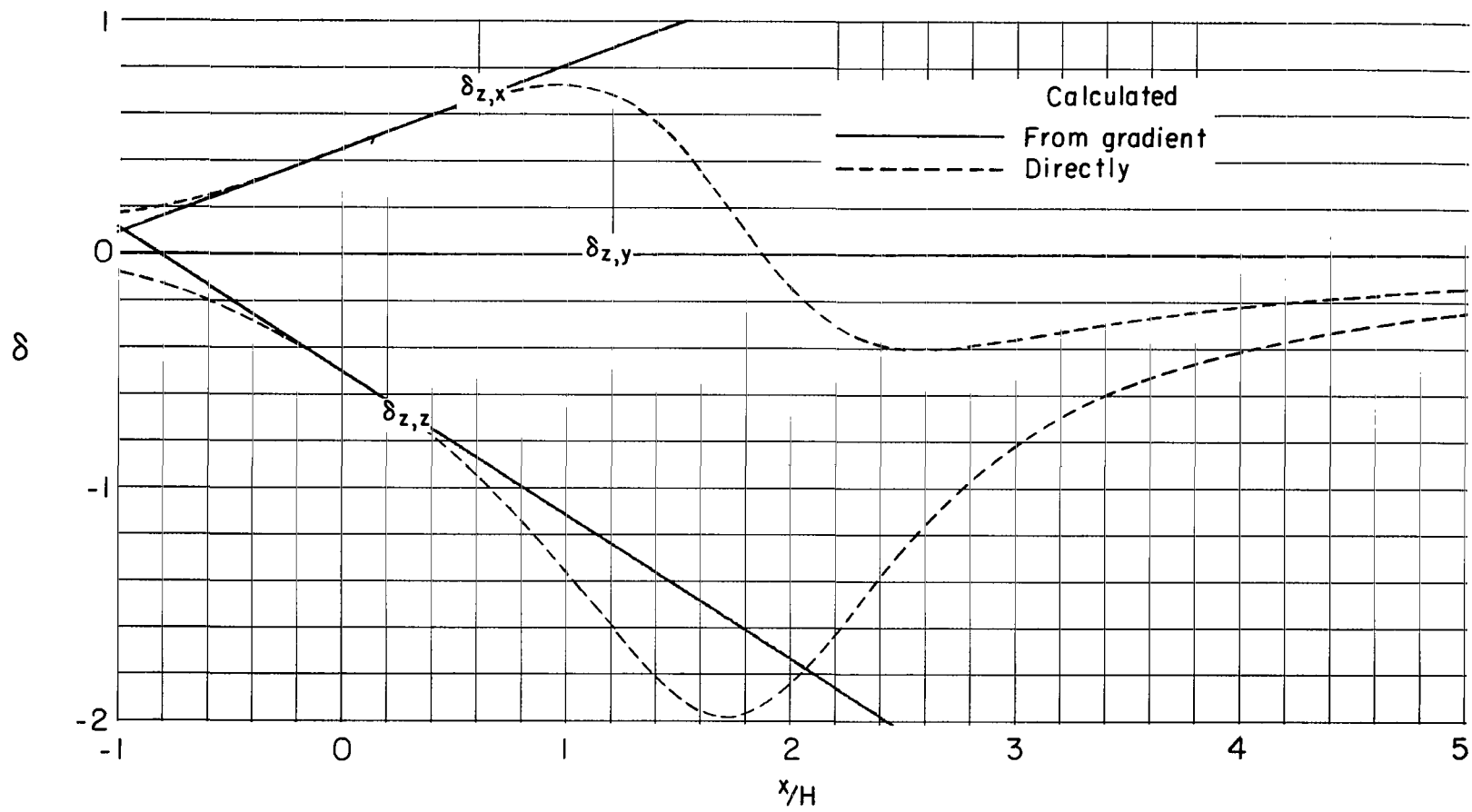
(a) Caused by forces in the X-direction.

Figure 20.- Distribution of interference factors along the longitudinal axis of the tunnel for a vanishingly small model centered in a closed rectangular tunnel having a width-height ratio of 1.5. $x_H = 90^\circ$; $x_V = 60^\circ$.



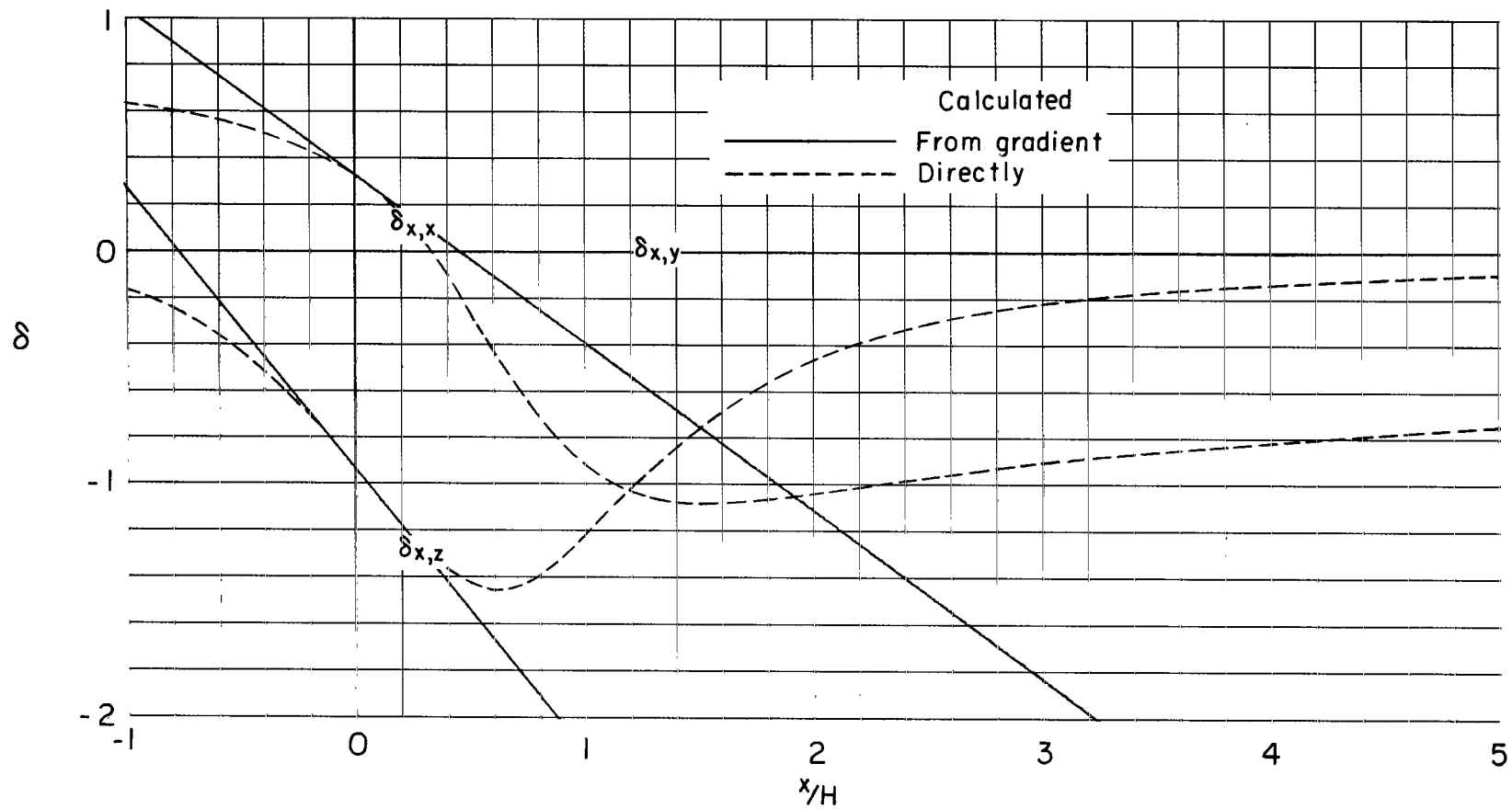
(b) Caused by forces in the Y-direction.

Figure 20.- Continued.



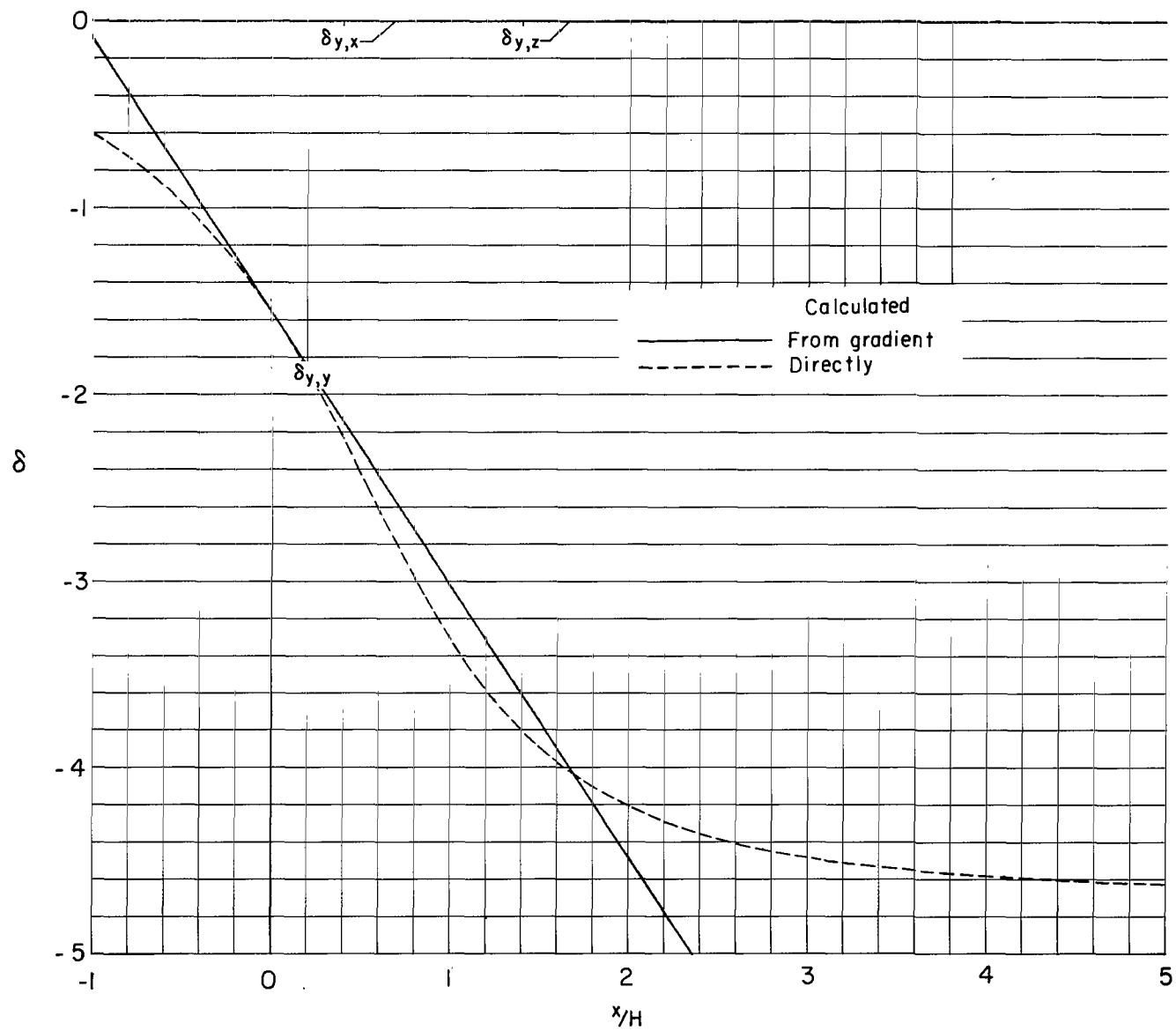
(c) Caused by forces in the Z-direction.

Figure 20.- Concluded.



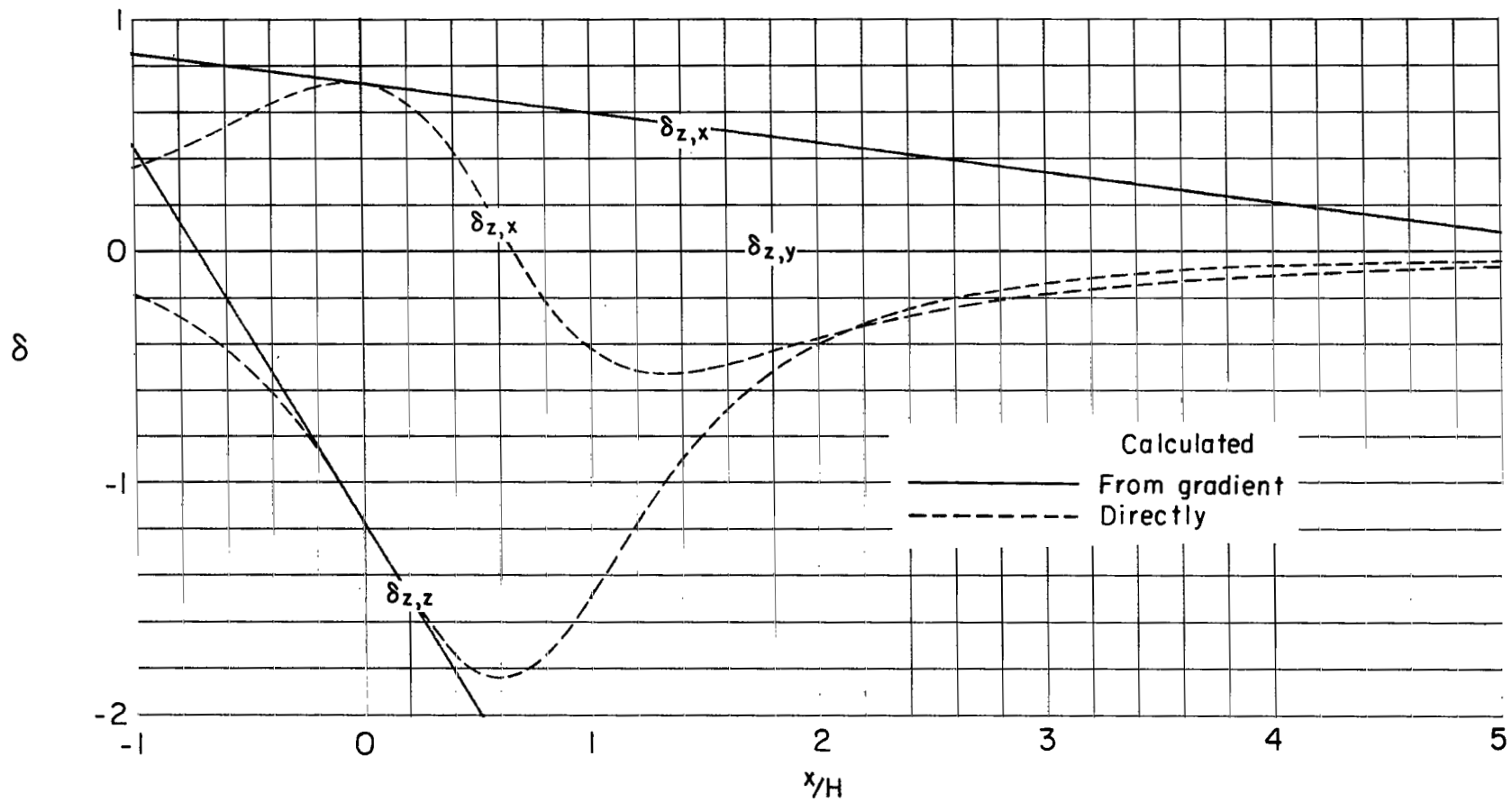
(a) Caused by forces in the X-direction.

Figure 21.- Distribution of interference factors along the longitudinal axis of the tunnel for a vanishingly small model centered in a closed rectangular tunnel having a width-height ratio of 1.5. $X_H = 90^\circ$; $X_V = 30^\circ$.



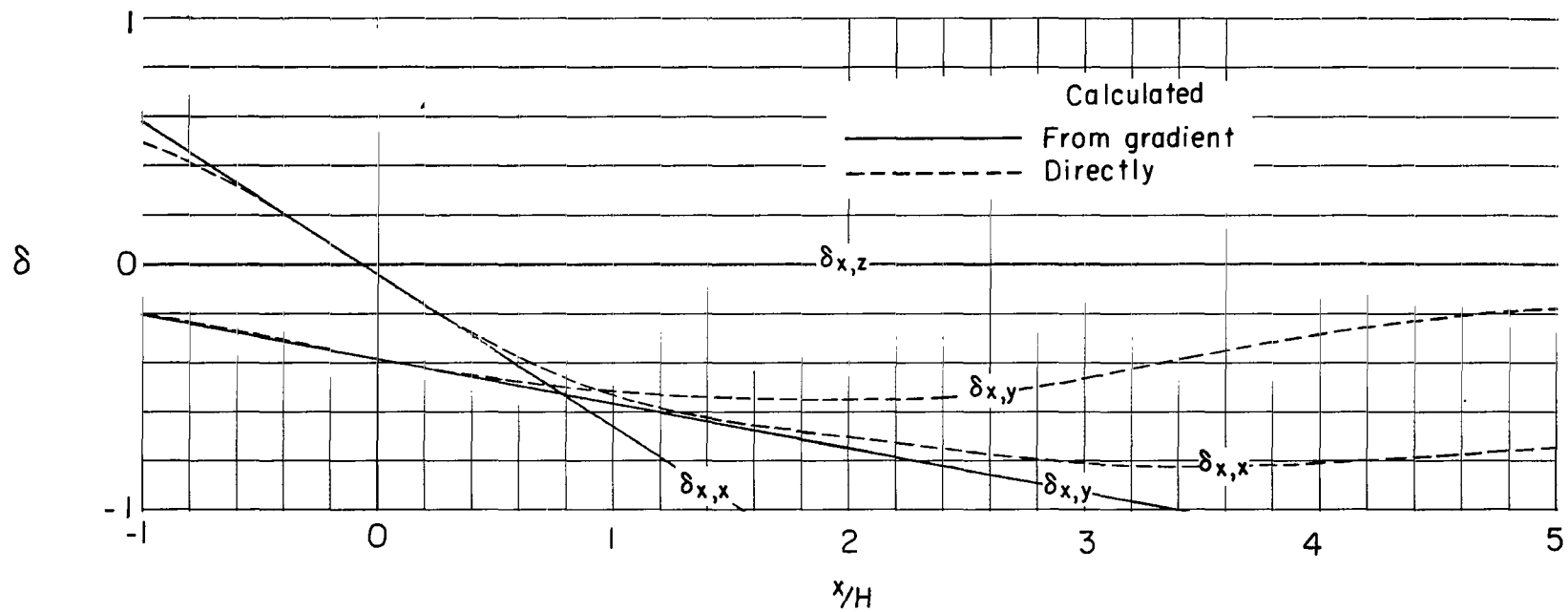
(b) Caused by forces in the Y-direction.

Figure 21.- Continued.



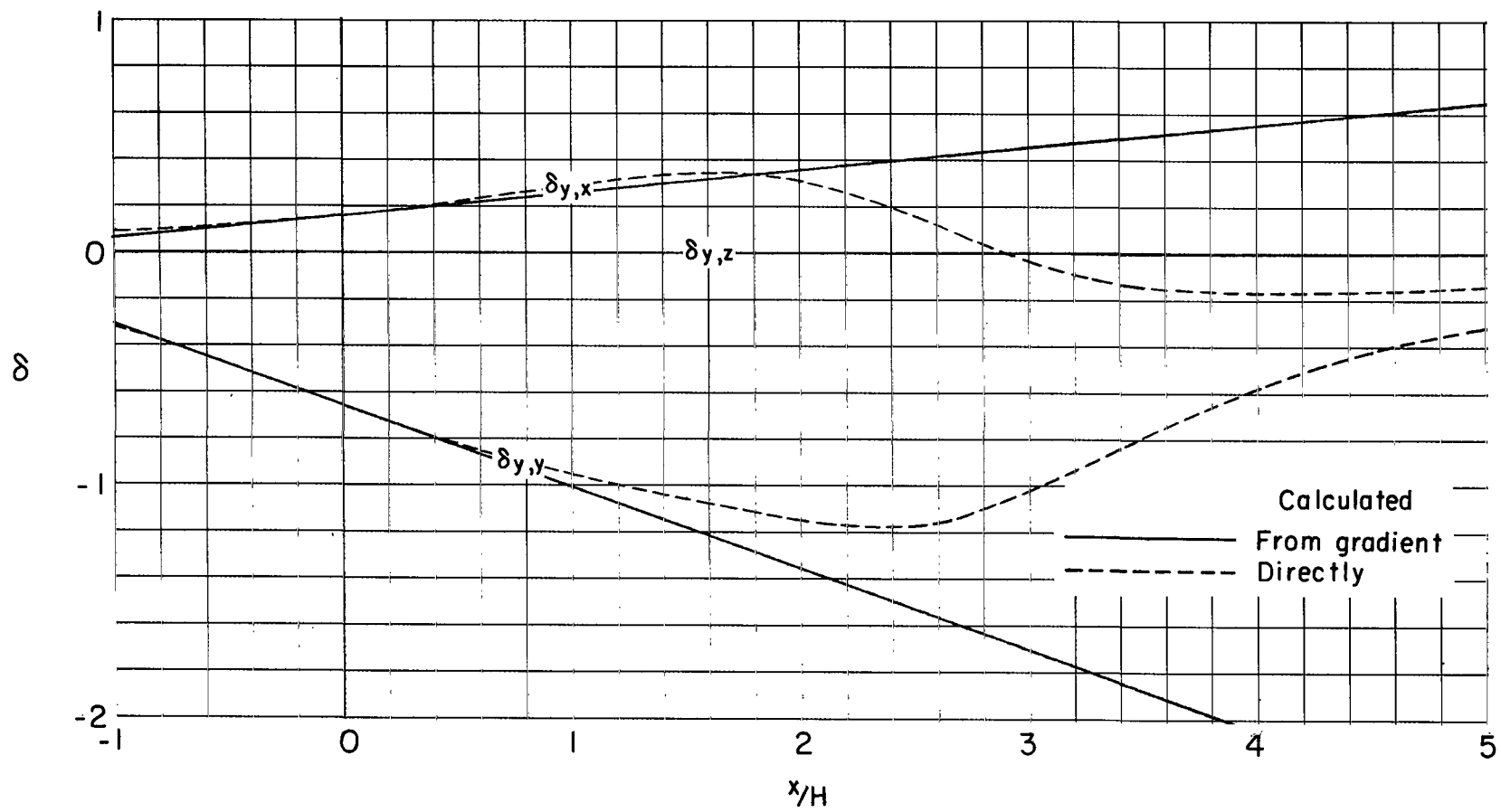
(c) Caused by forces in the Z-direction.

Figure 21.- Concluded.



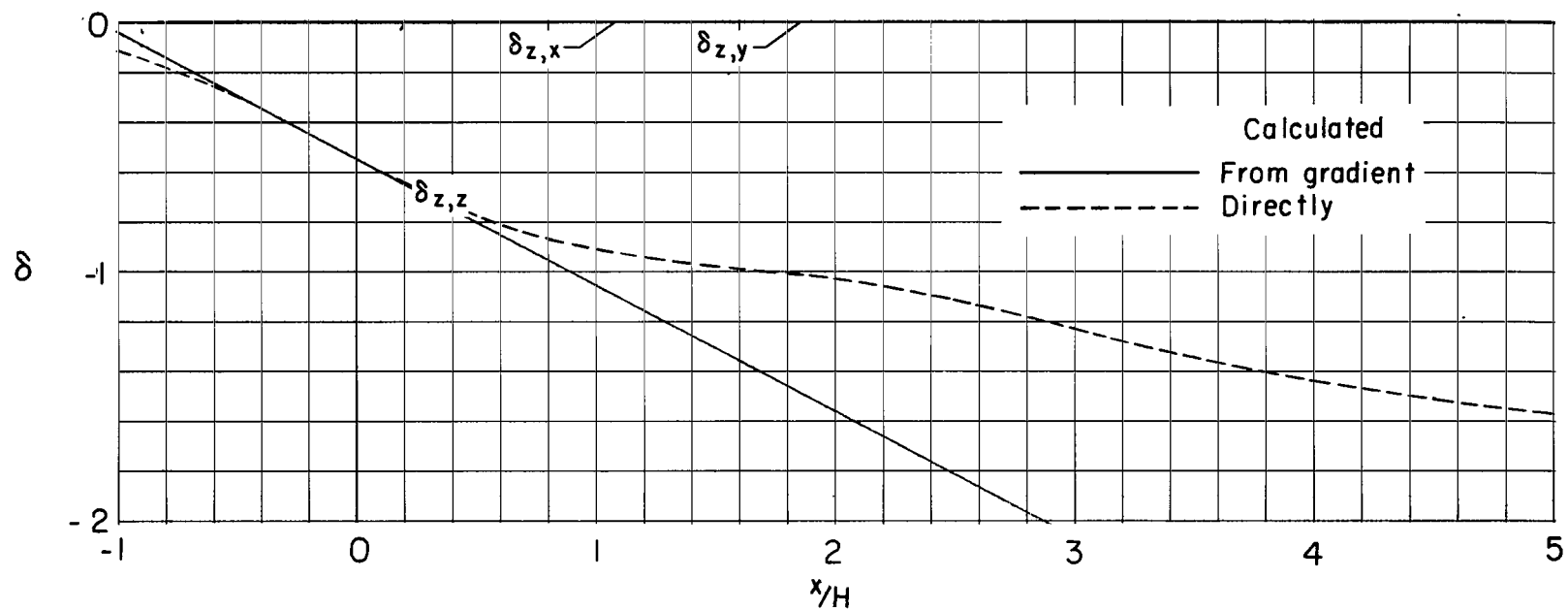
(a) Caused by forces in the X-direction.

Figure 22.- Distribution of interference factors along the longitudinal axis of the tunnel for a vanishingly small model centered in a closed rectangular tunnel having a width-height ratio of 1.5. $\chi_H = 60^\circ$; $\chi_V = 90^\circ$.



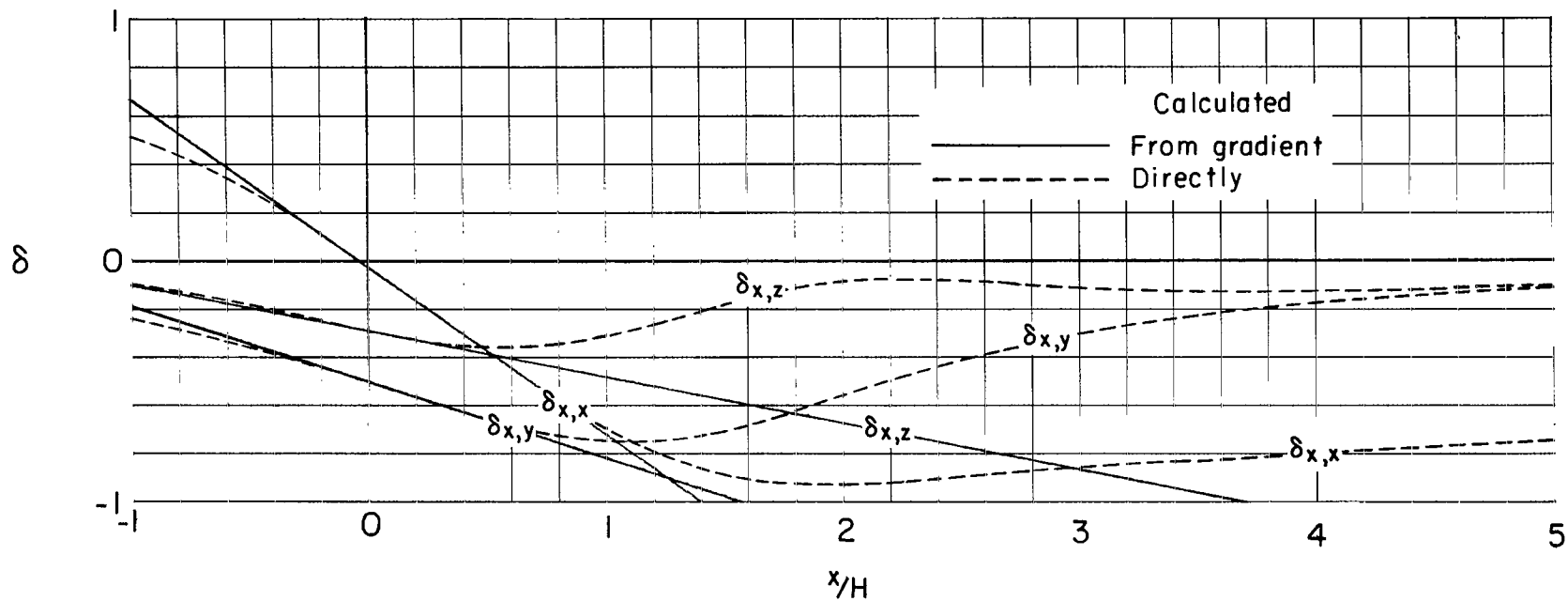
(b) Caused by forces in the Y-direction.

Figure 22.- Continued.



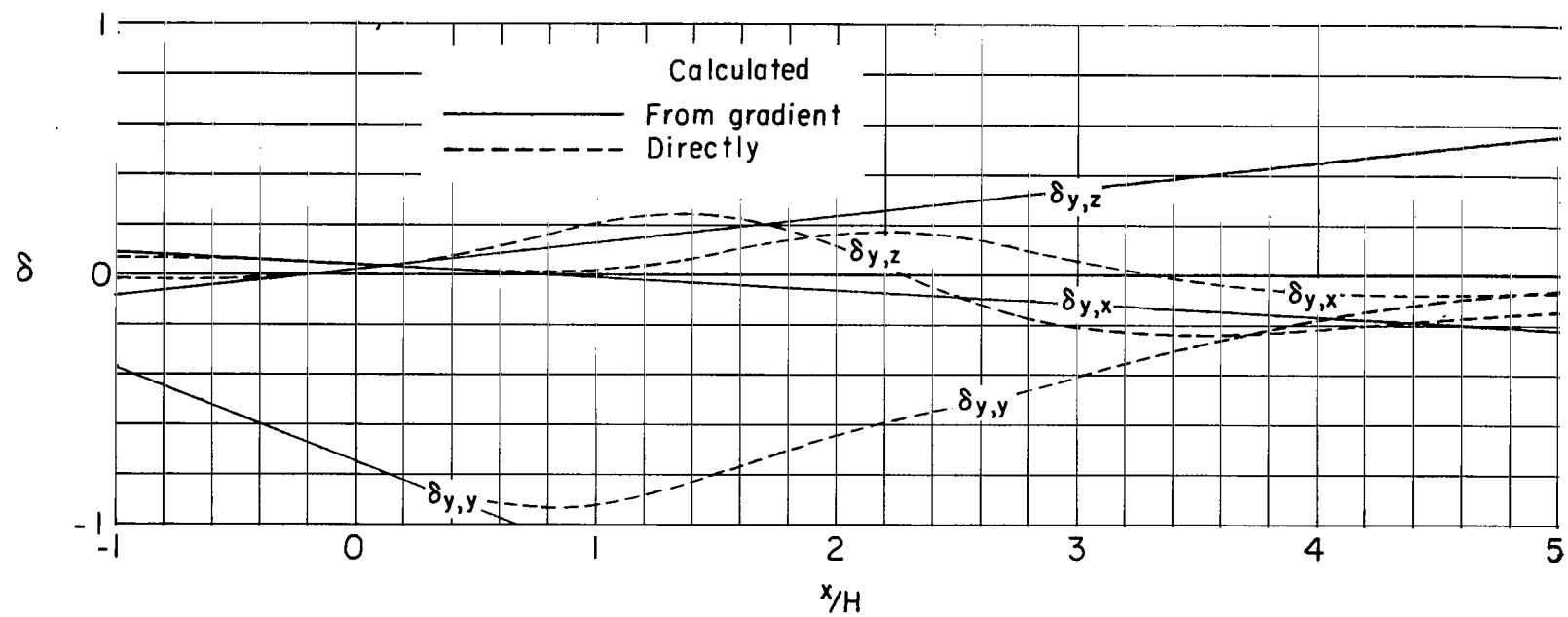
(c) Caused by forces in the Z-direction.

Figure 22.- Concluded.



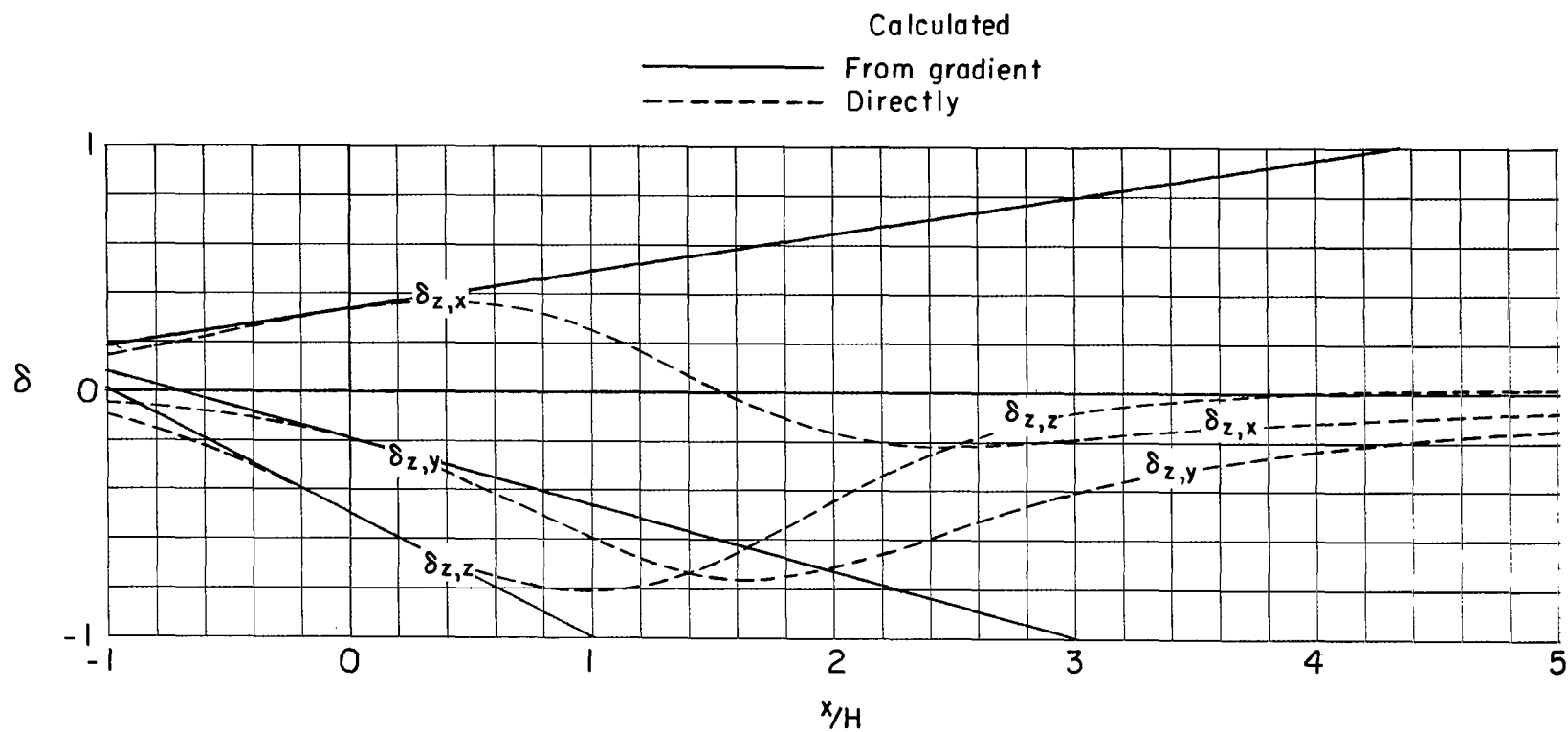
(a) Caused by forces in the X-direction.

Figure 23.- Distribution of interference factors along the longitudinal axis of the tunnel for a vanishingly small model centered in a closed rectangular tunnel having a width-height ratio of 1.5. $\chi_H = 60^\circ$; $\chi_V = 60^\circ$.



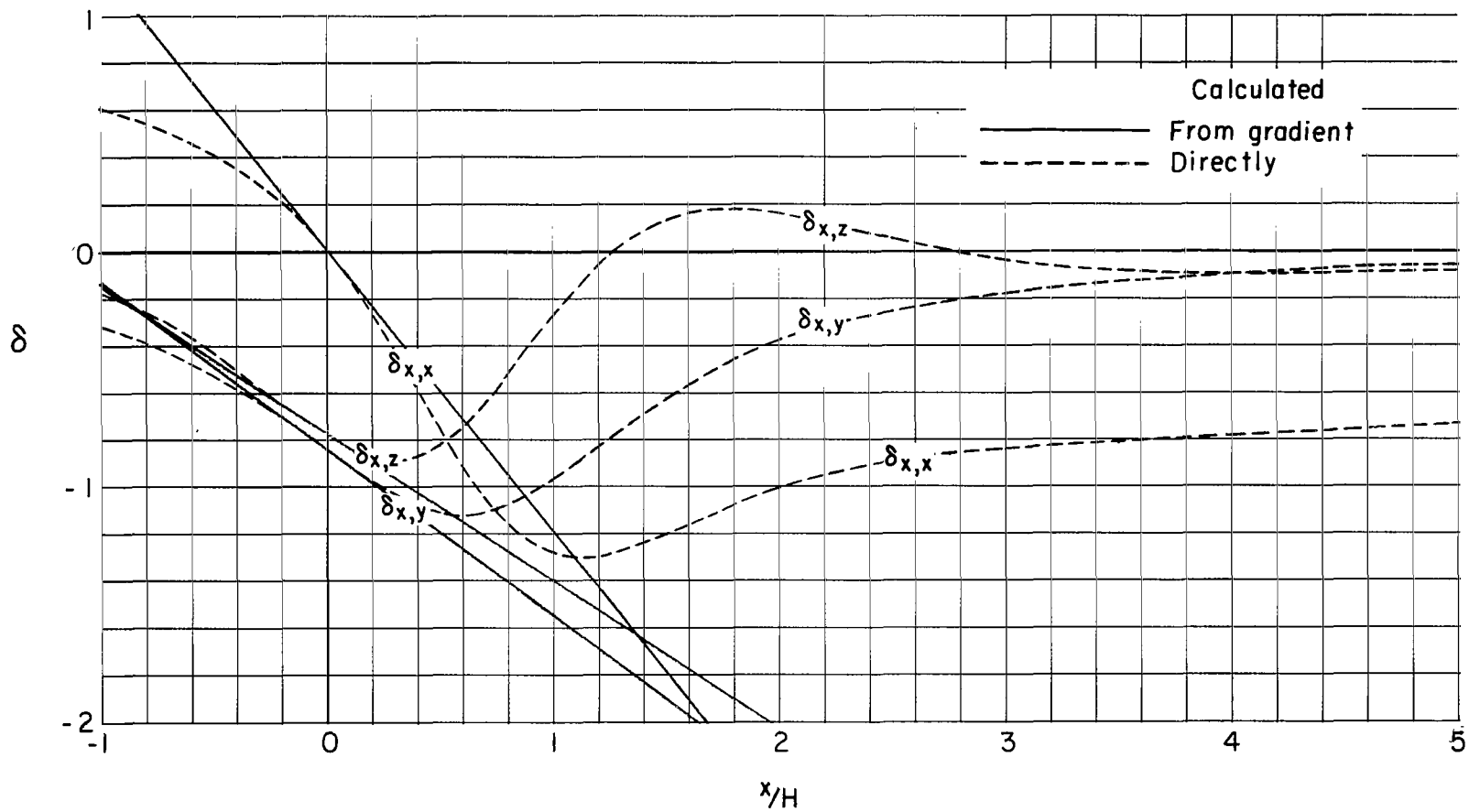
(b) Caused by forces in the Y-direction.

Figure 23.- Continued.



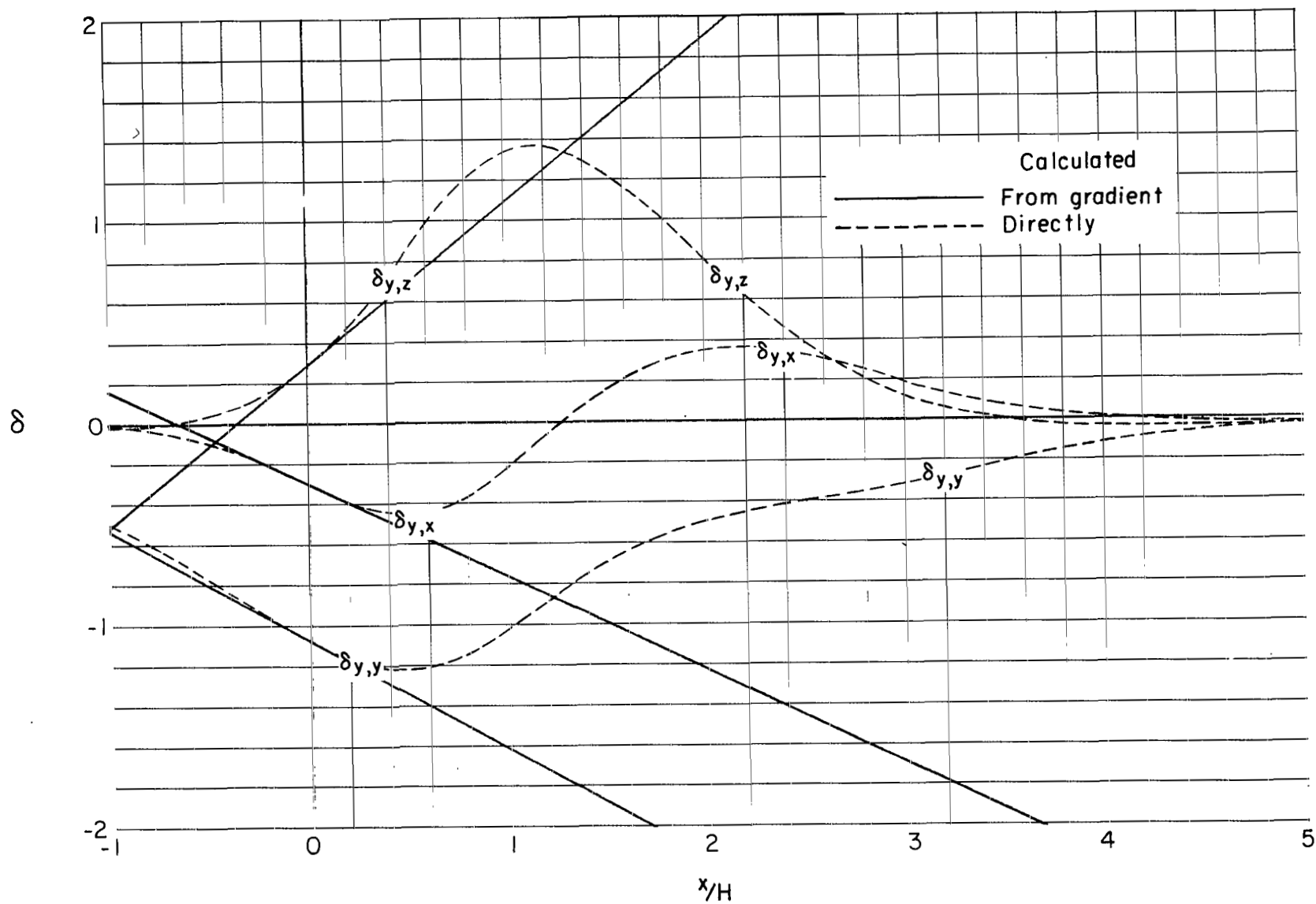
(c) Caused by forces in the Z-direction.

Figure 23.- Concluded.



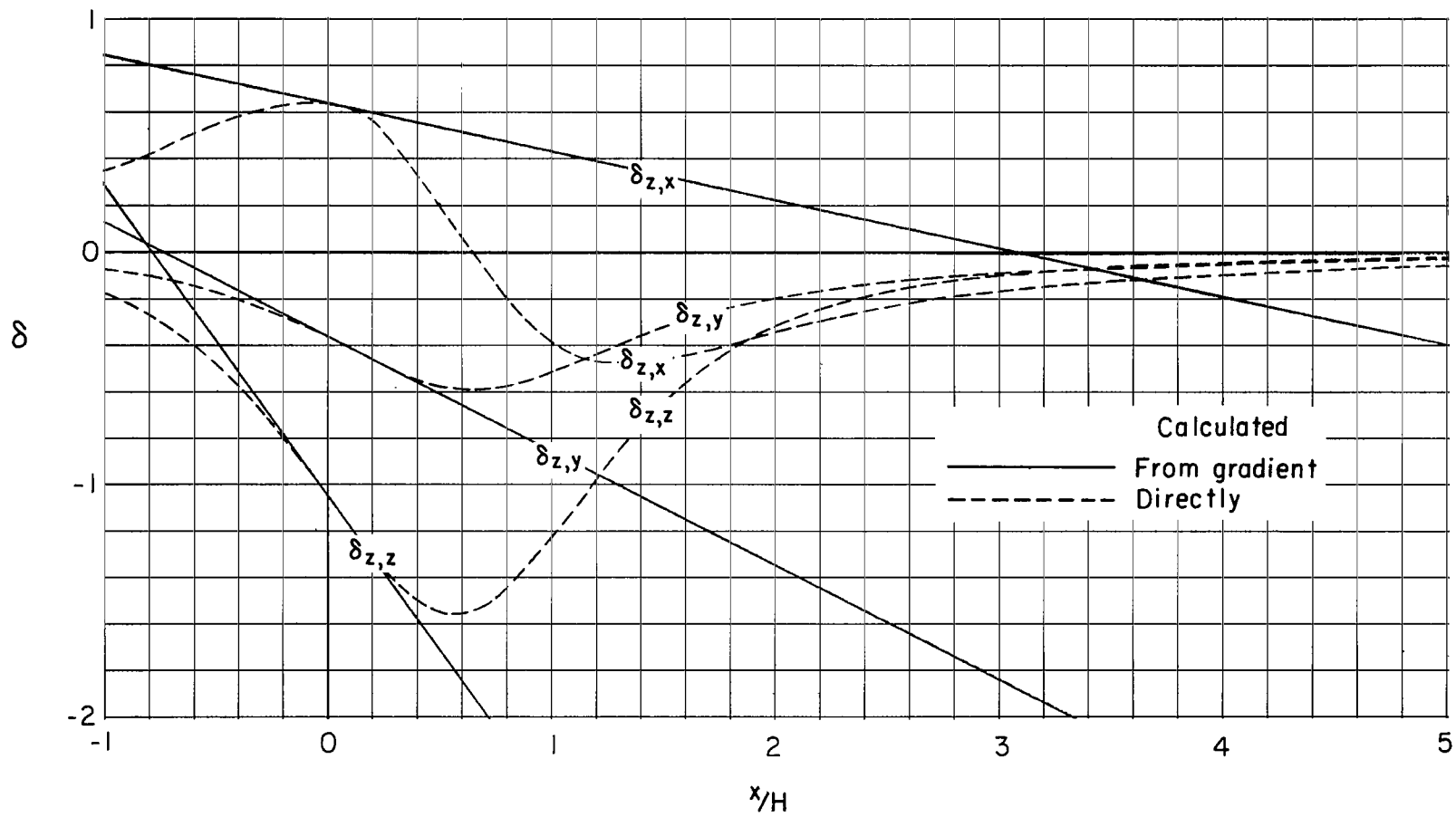
(a) Caused by forces in the X-direction.

Figure 24.- Distribution of interference factors along the longitudinal axis of the tunnel for a vanishingly small model centered in a closed rectangular tunnel having a width-height ratio of 1.5. $\chi_H = 60^\circ$; $\chi_V = 30^\circ$.



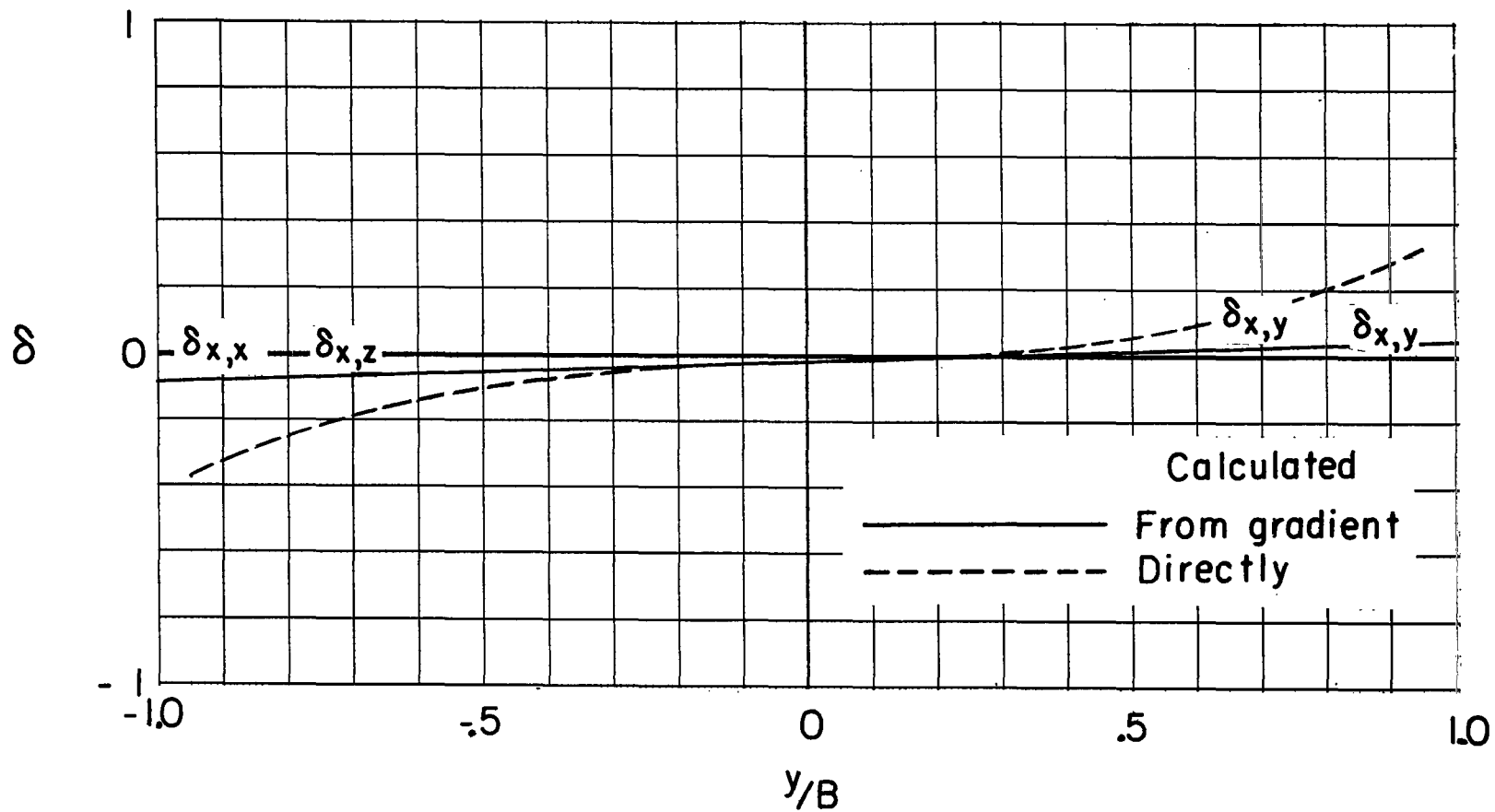
(b) Caused by forces in the Y-direction.

Figure 24.- Continued.



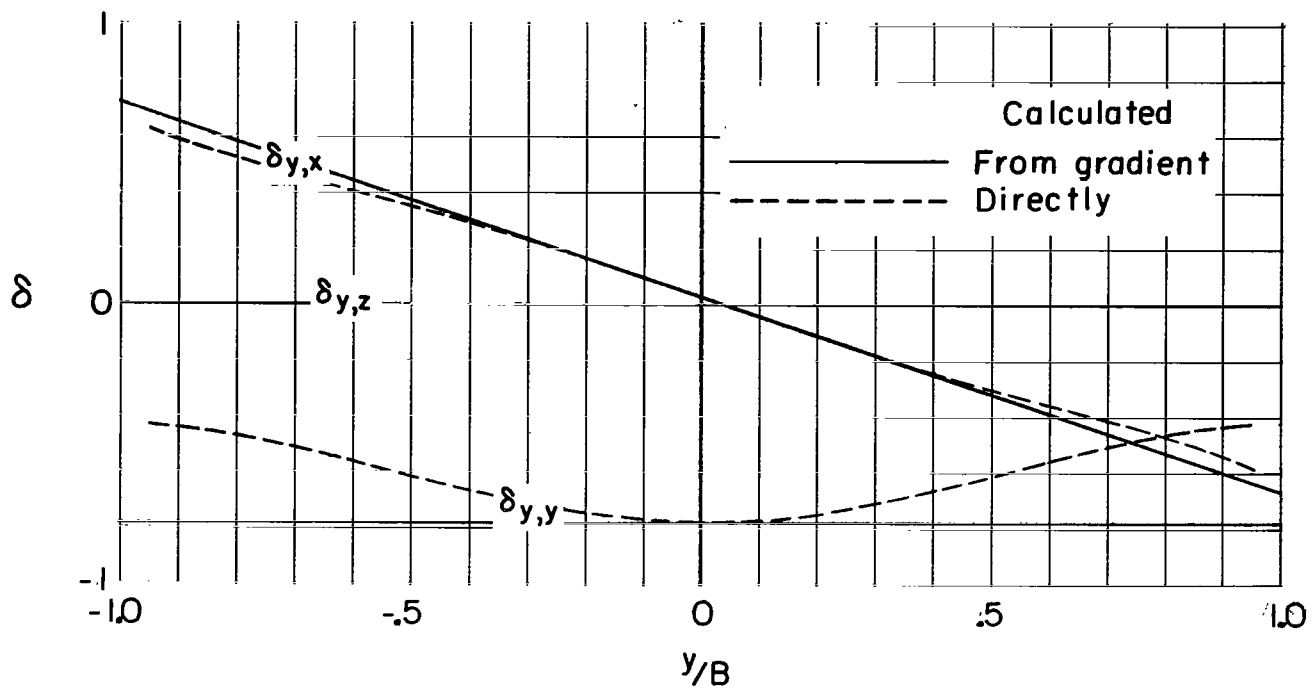
(c) Caused by forces in the Z-direction.

Figure 24.- Concluded.

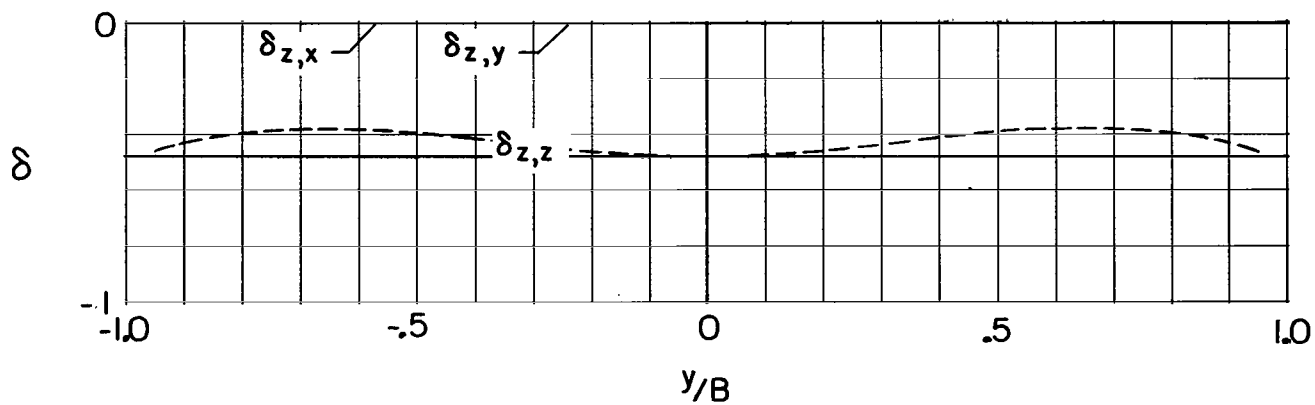


(a) Caused by forces in the X-direction.

Figure 25.- Distribution of interference factors along the lateral axis of the tunnel for a vanishingly small model centered in a closed rectangular tunnel having a width-height ratio of 1.5. $X_H = 90^\circ$; $X_V = 90^\circ$.

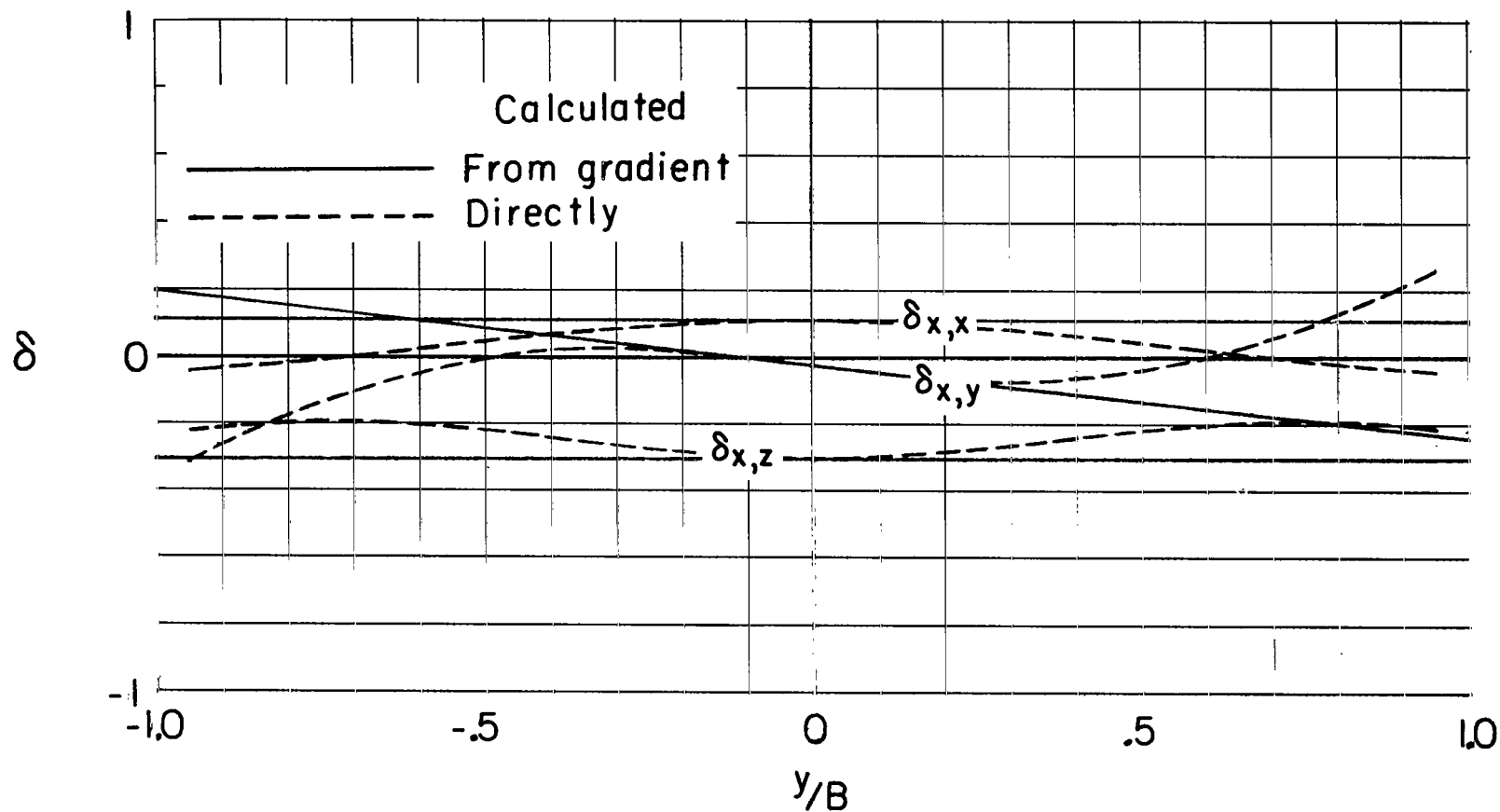


(b) Caused by forces in the Y-direction.



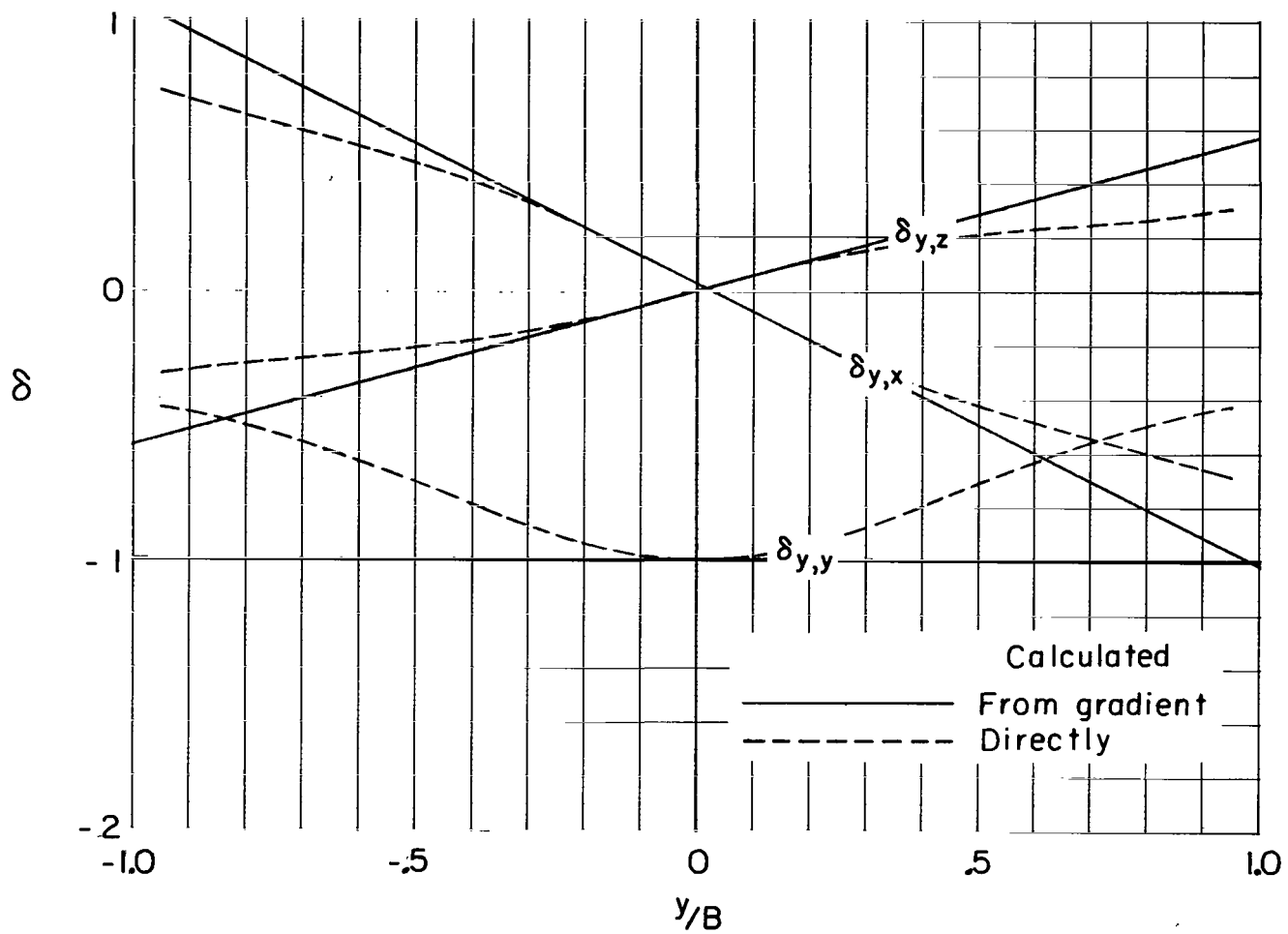
(c) Caused by forces in the Z-direction.

Figure 25.- Concluded.



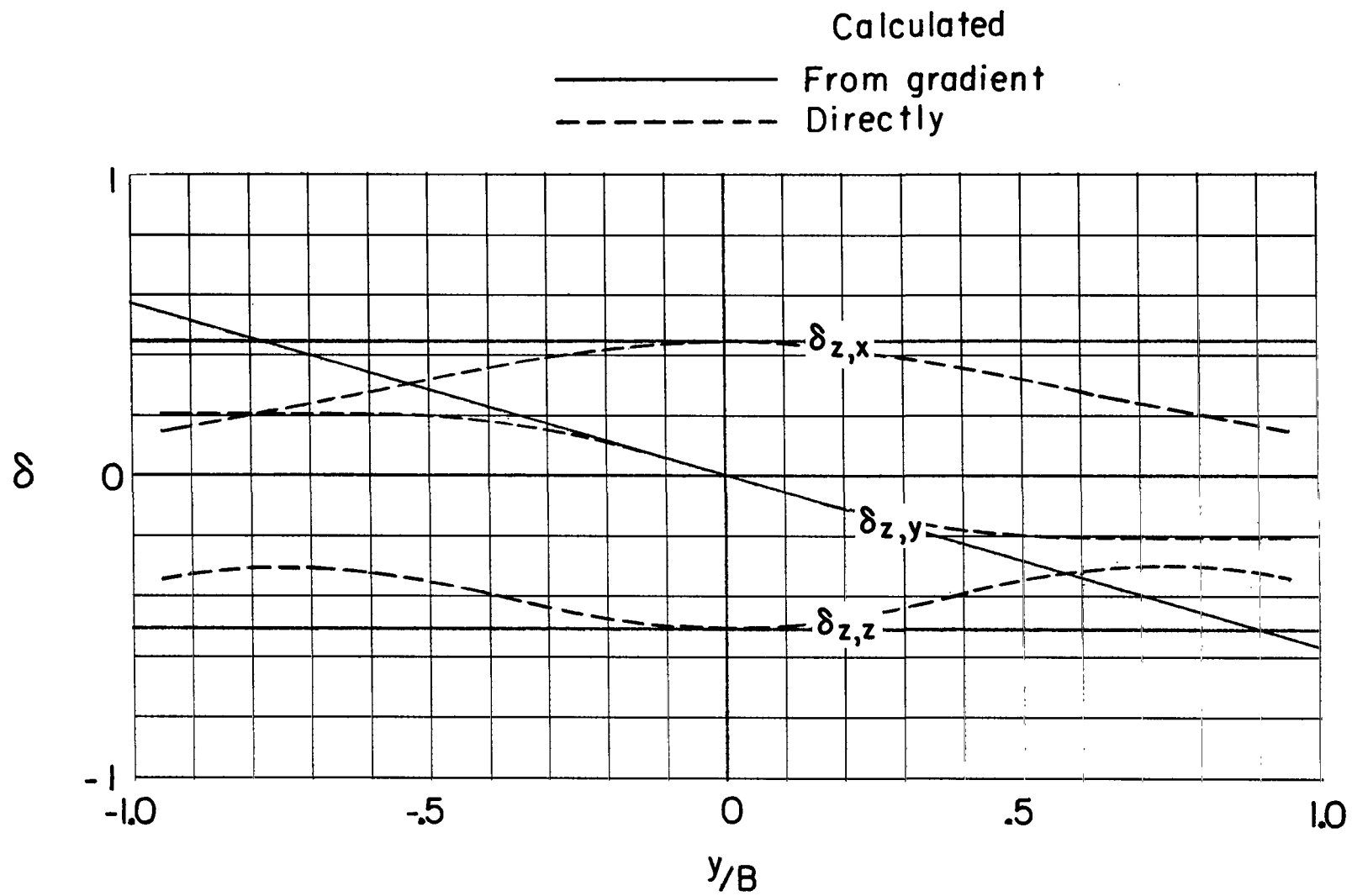
(a) Caused by forces in the X-direction.

Figure 26.- Distribution of interference factors along the lateral axis of the tunnel for a vanishingly small model centered in a closed rectangular tunnel having a width-height ratio of 1.5. $x_H = 90^\circ$; $x_V = 60^\circ$.



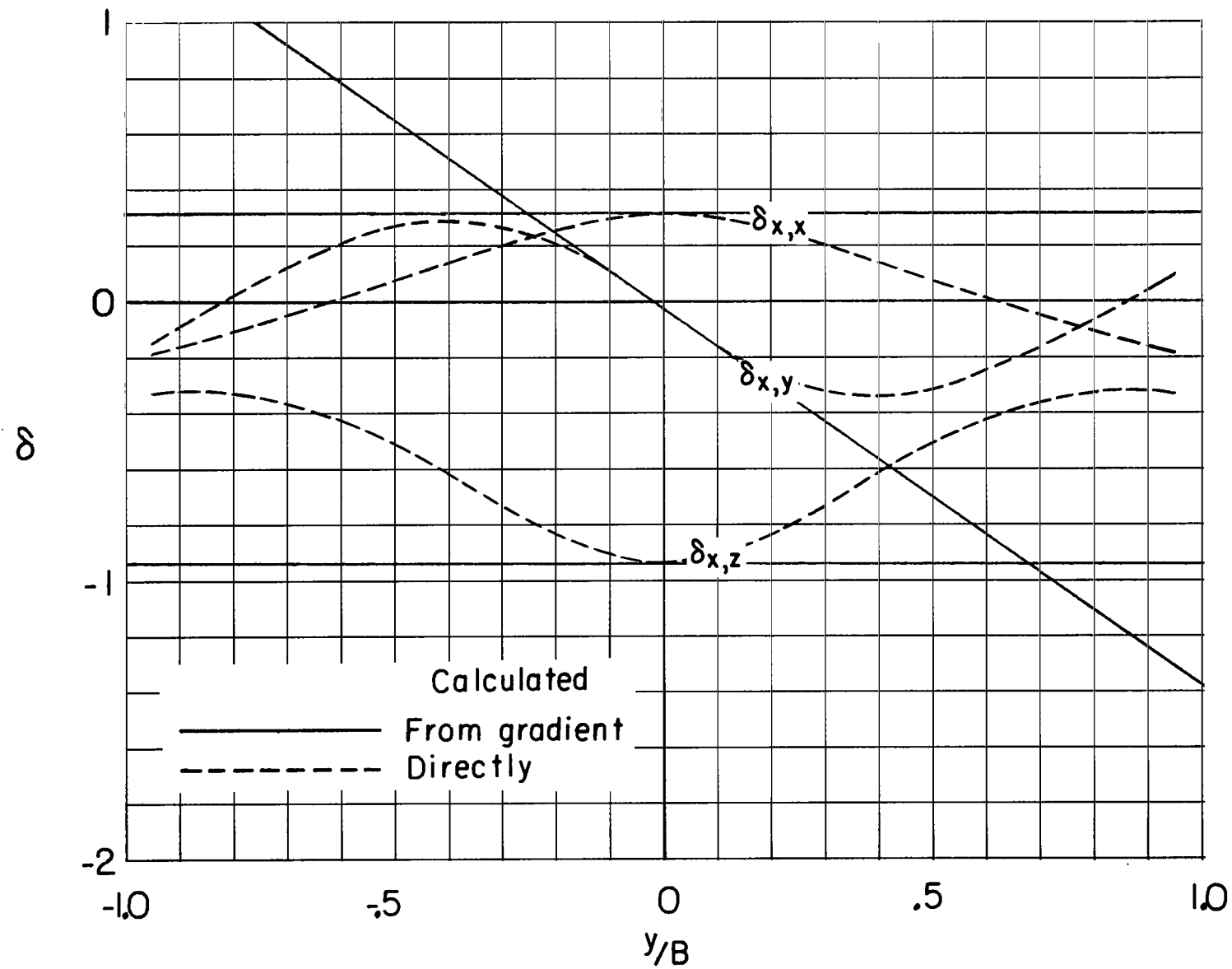
(b) Caused by forces in the Y-direction.

Figure 26.- Continued.



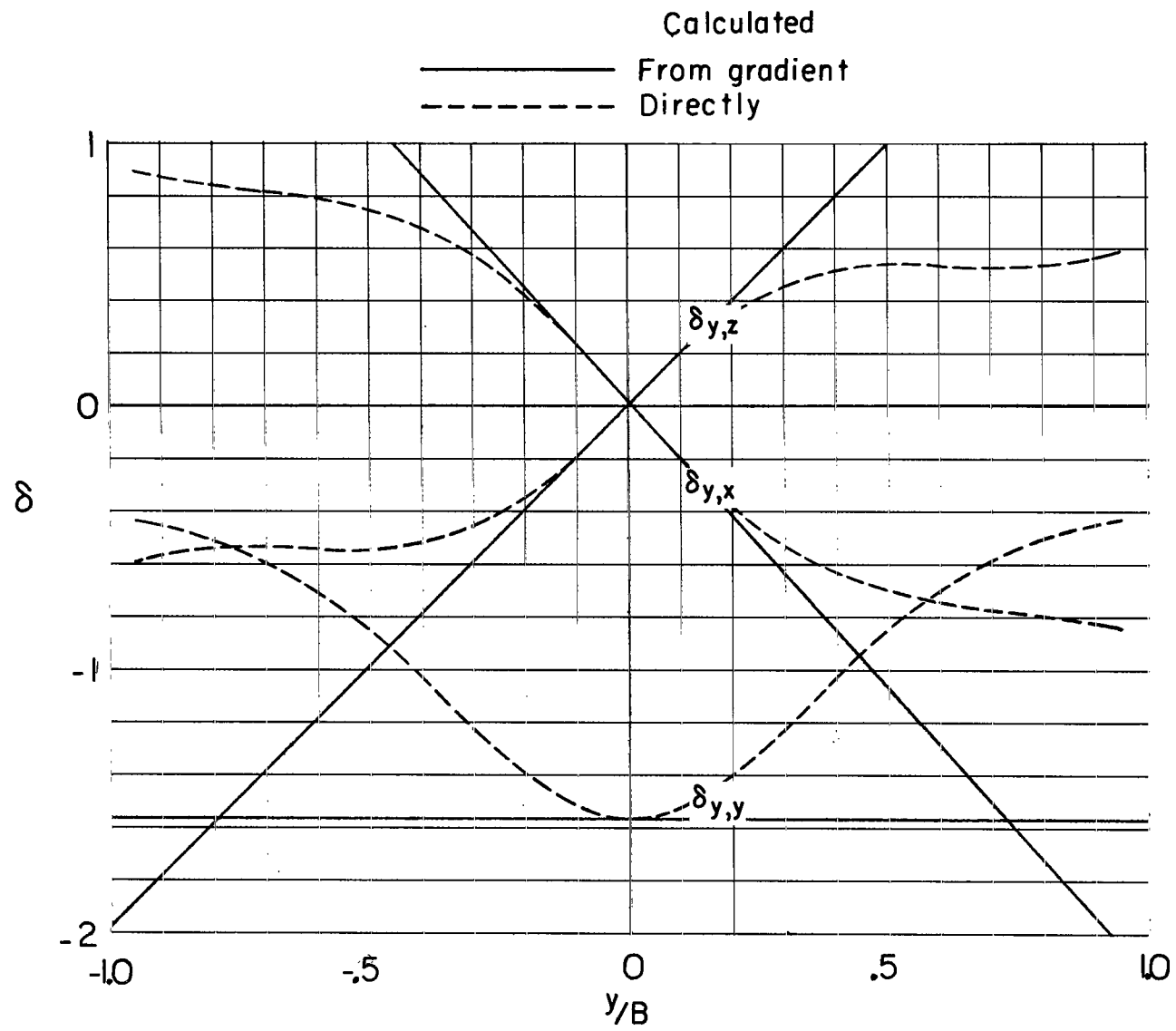
(c) Caused by forces in the Z-direction.

Figure 26.- Concluded.



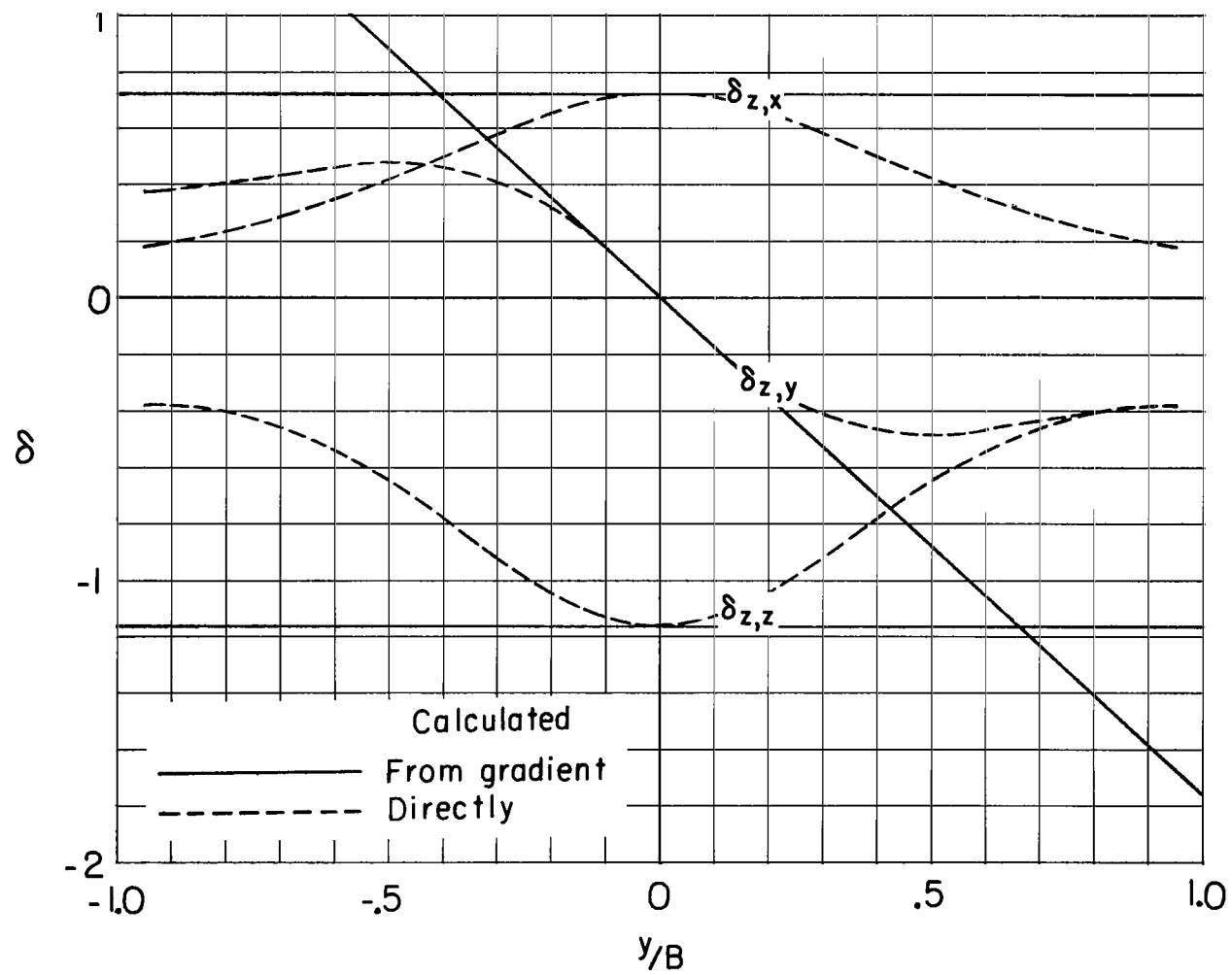
(a) Caused by forces in the X-direction.

Figure 27.- Distribution of interference factors along the lateral axis of the tunnel for a vanishingly small model centered in a closed rectangular tunnel having a width-height ratio of 1.5. $x_H = 90^\circ$; $x_V = 30^\circ$.



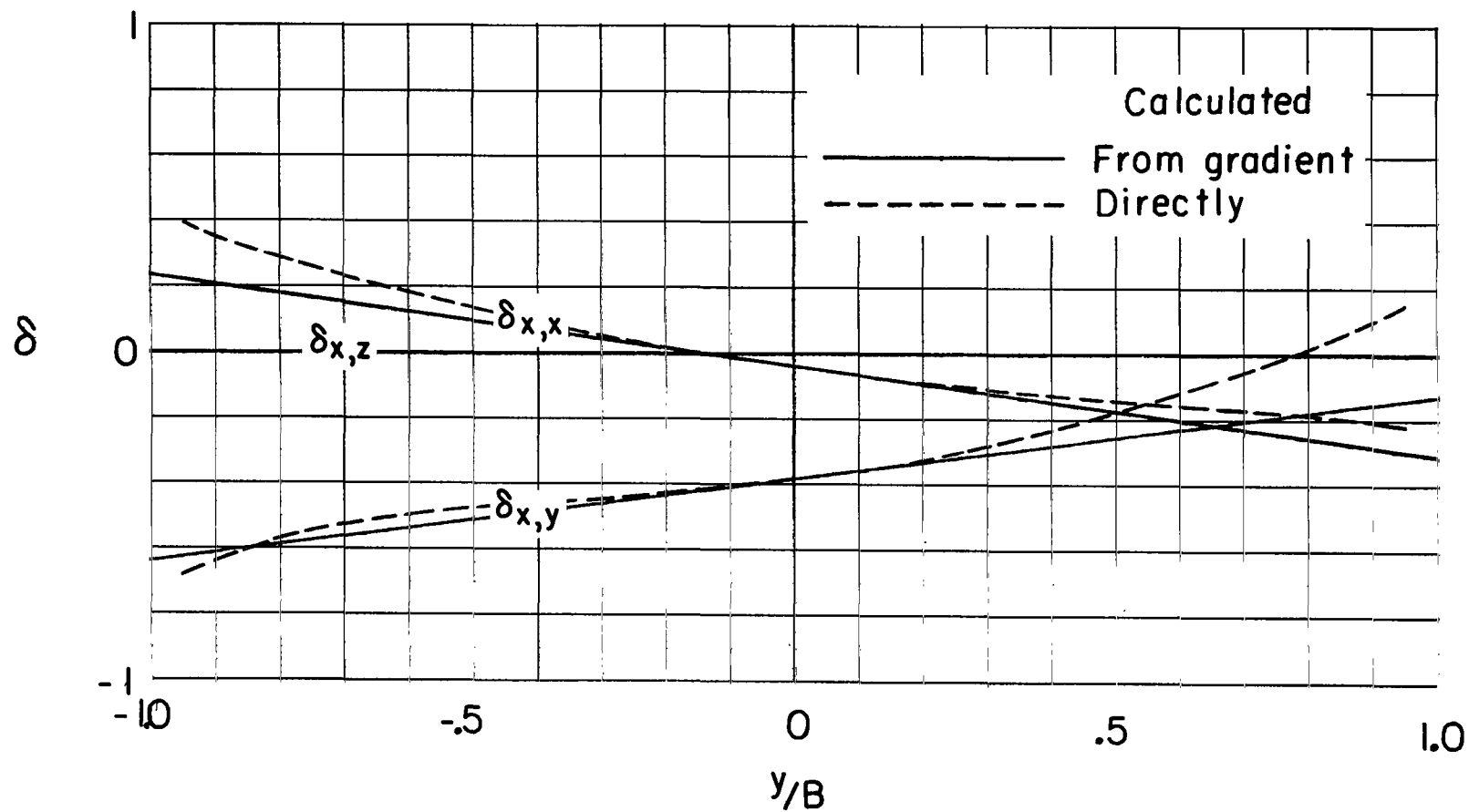
(b) Caused by forces in the Y-direction.

Figure 27.- Continued.



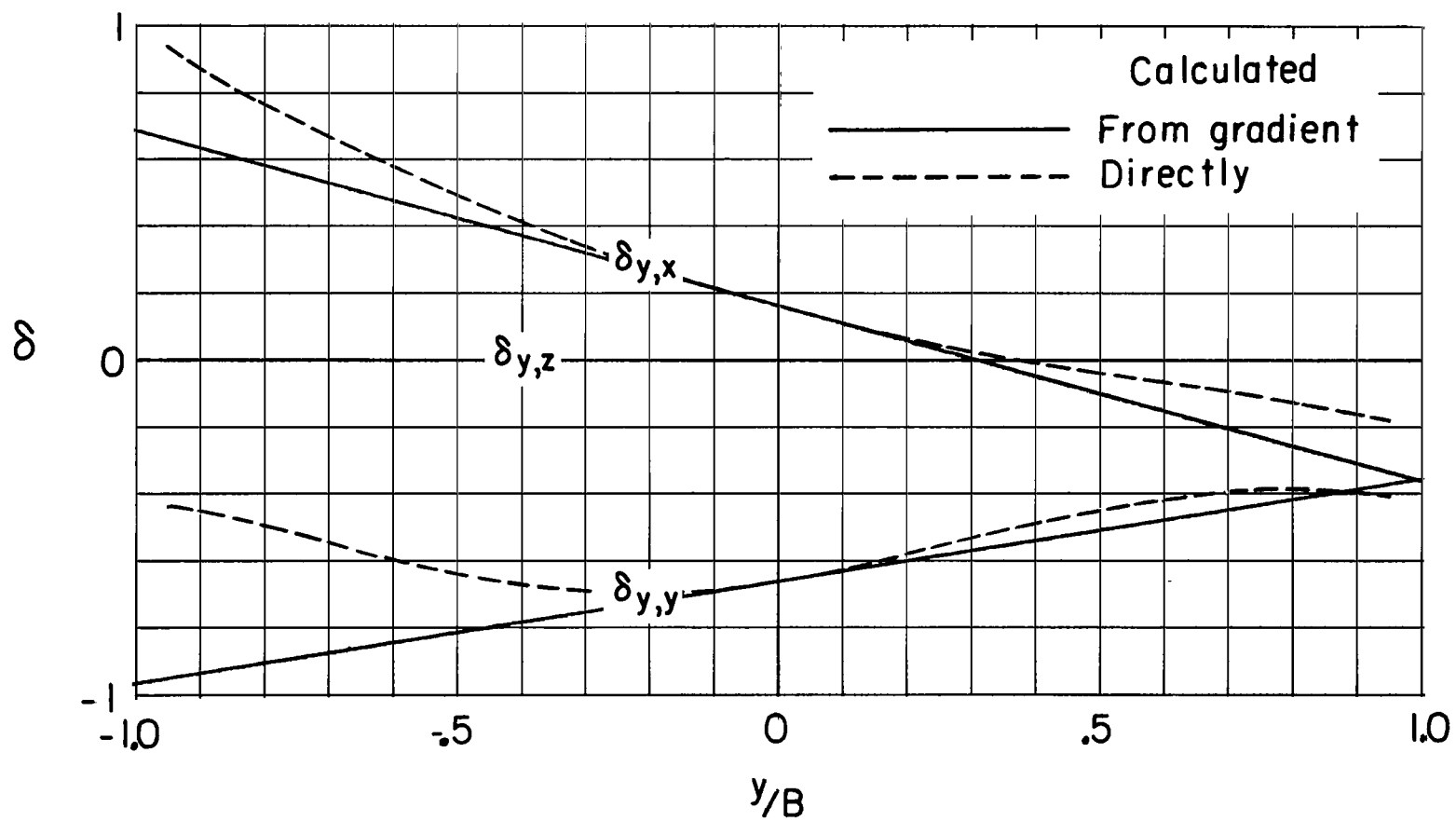
(c) Caused by forces in the Z-direction.

Figure 27.- Concluded.



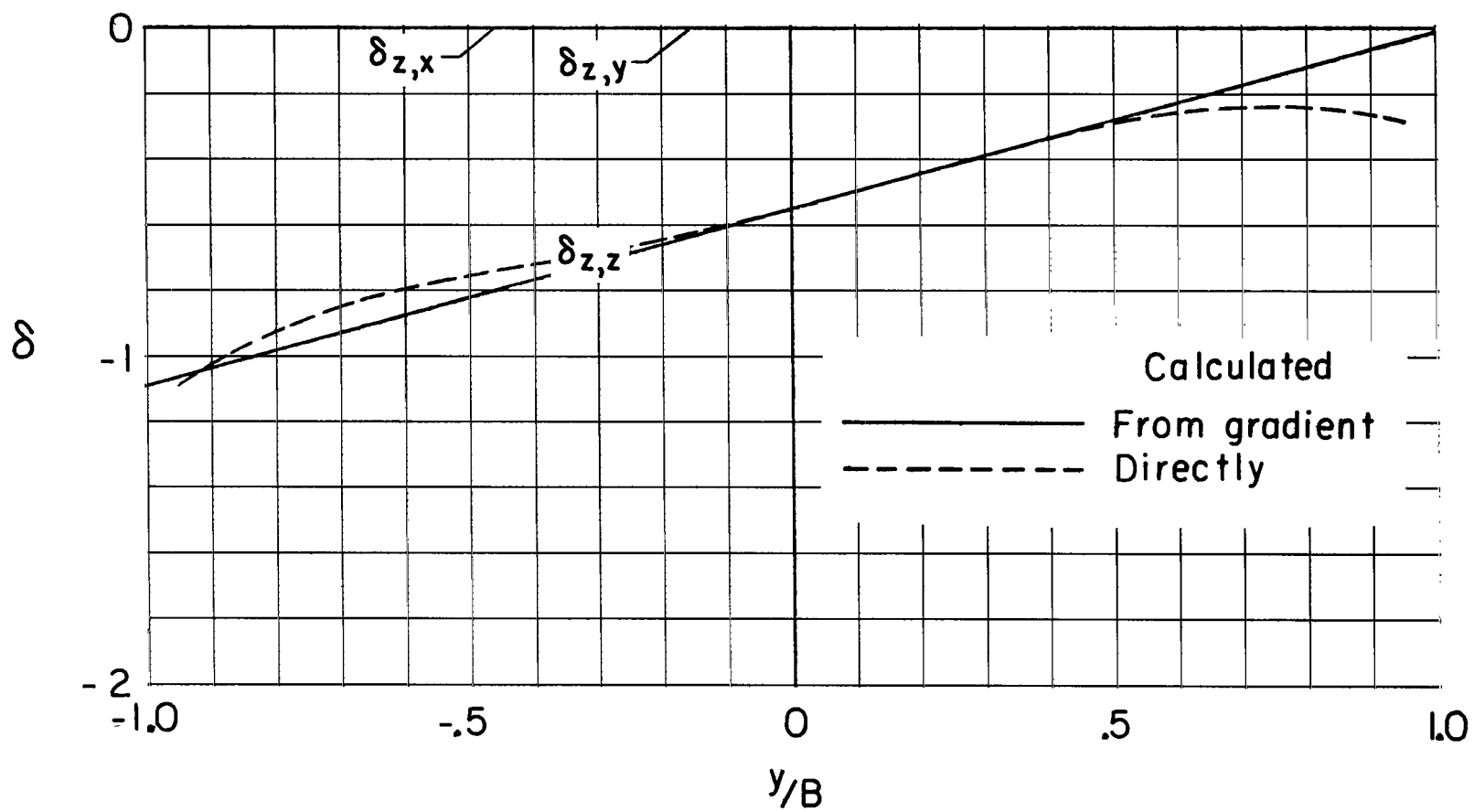
(a) Caused by forces in the X-direction.

Figure 28.- Distribution of interference factors along the lateral axis of the tunnel for a vanishingly small model centered in a closed rectangular tunnel having a width-height ratio of 1.5. $x_H = 60^\circ$; $x_V = 90^\circ$.



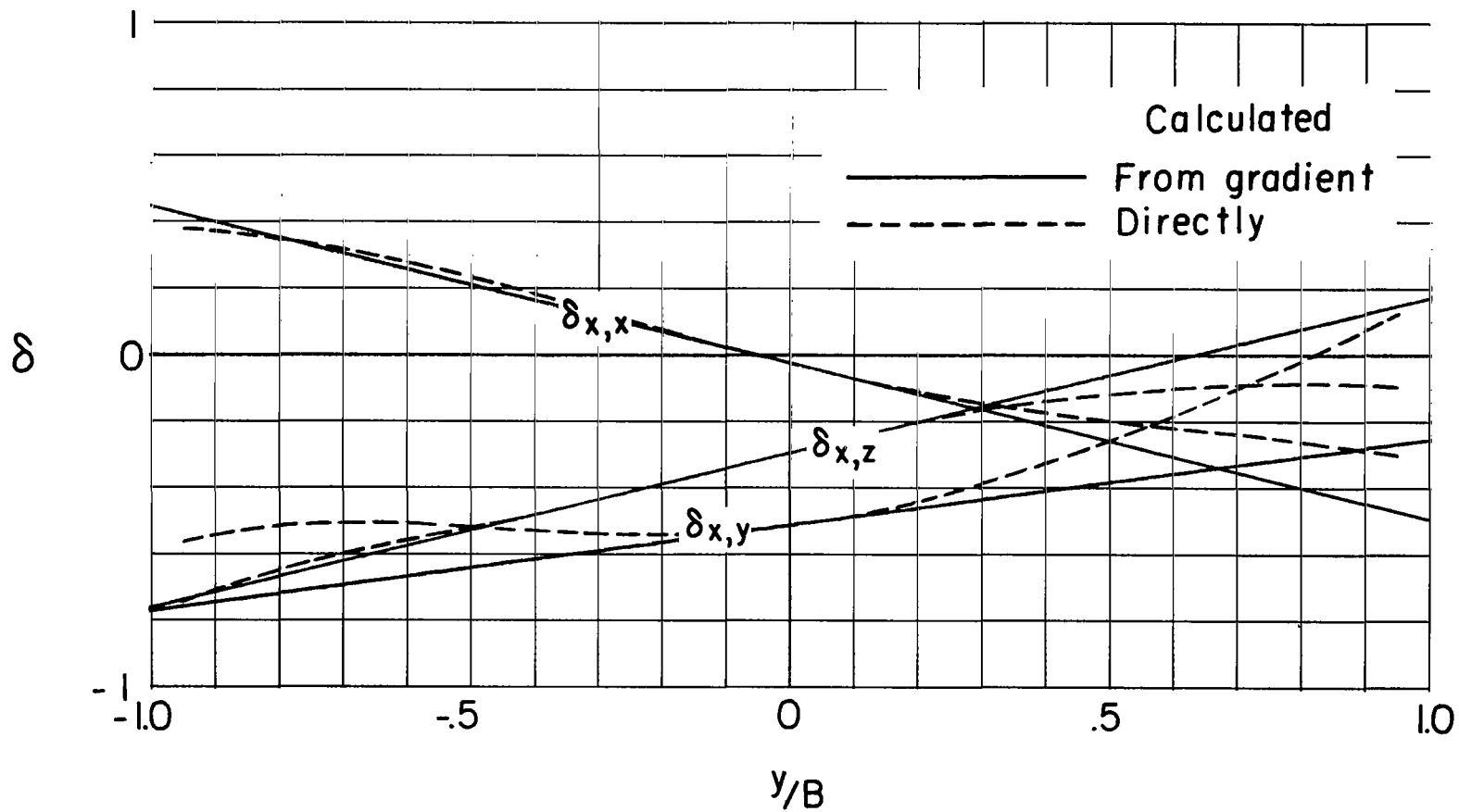
(b) Caused by forces in the Y-direction.

Figure 28.- Continued.



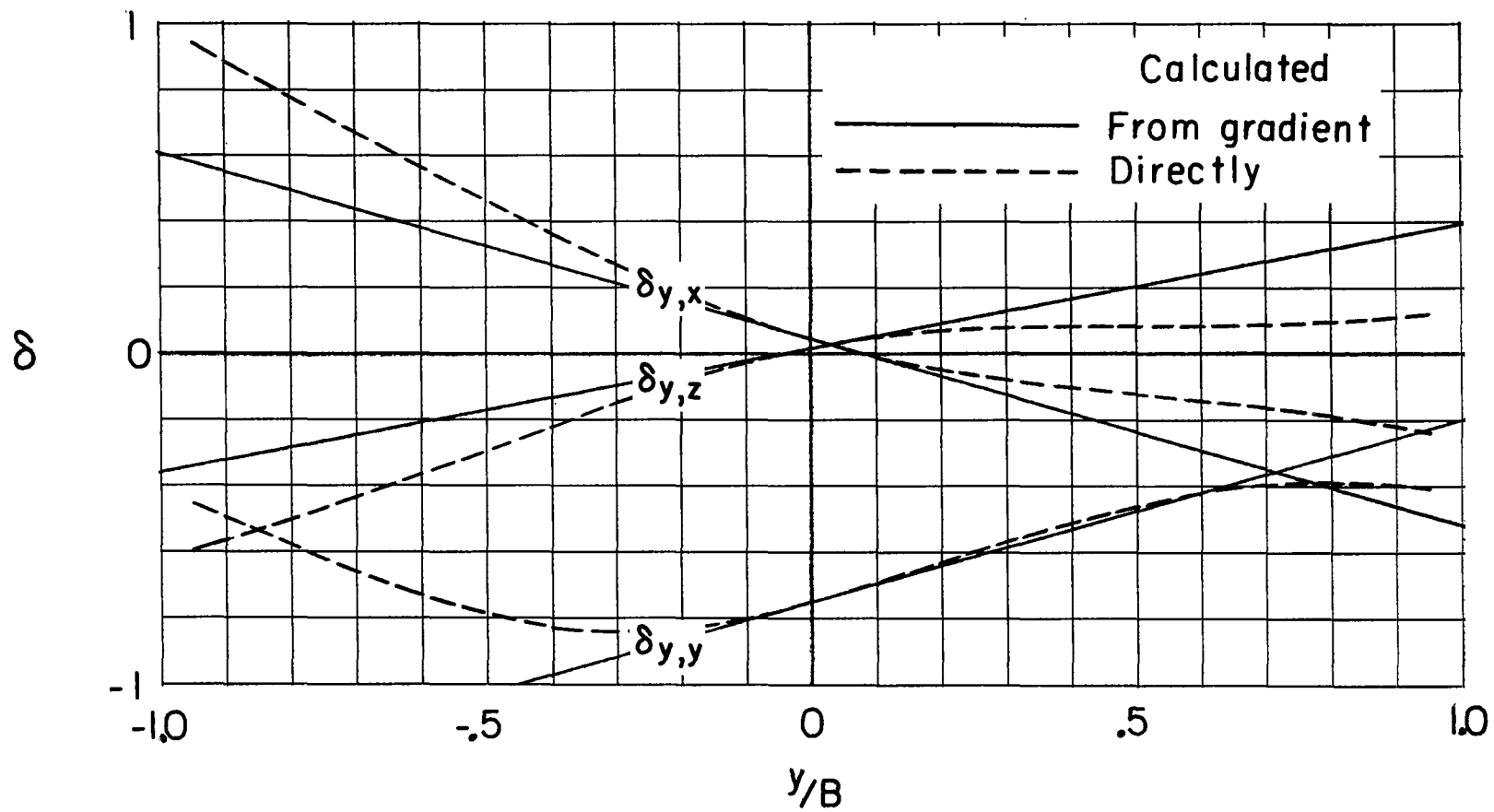
(c) Caused by forces in the Z-direction.

Figure 28.- Concluded.



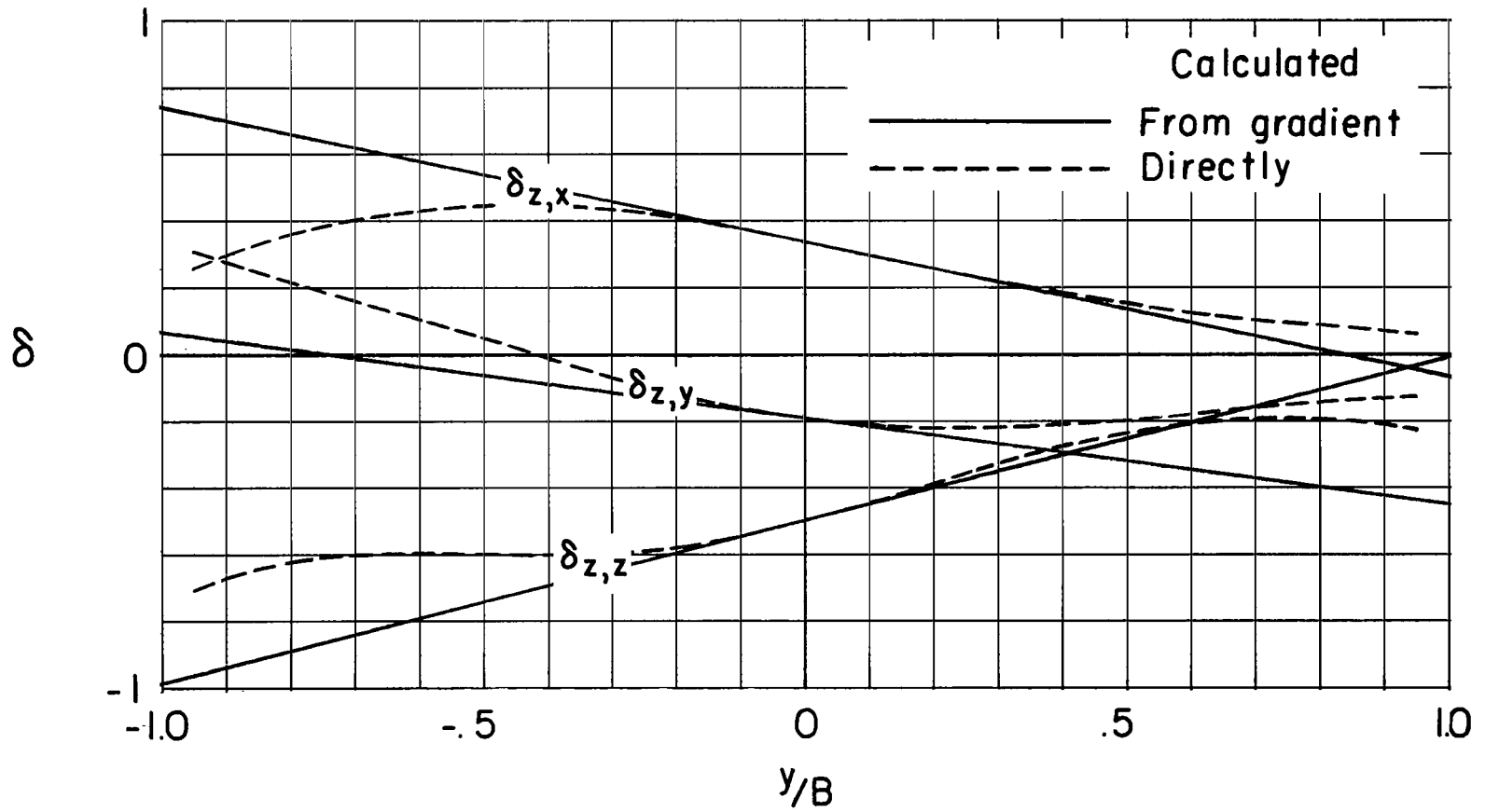
(a) Caused by forces in the X-direction.

Figure 29.- Distribution of interference factors along the lateral axis of the tunnel for a vanishingly small model centered in a closed rectangular tunnel having a width-height ratio of 1.5. $\chi_H = 60^\circ$; $\chi_V = 60^\circ$.



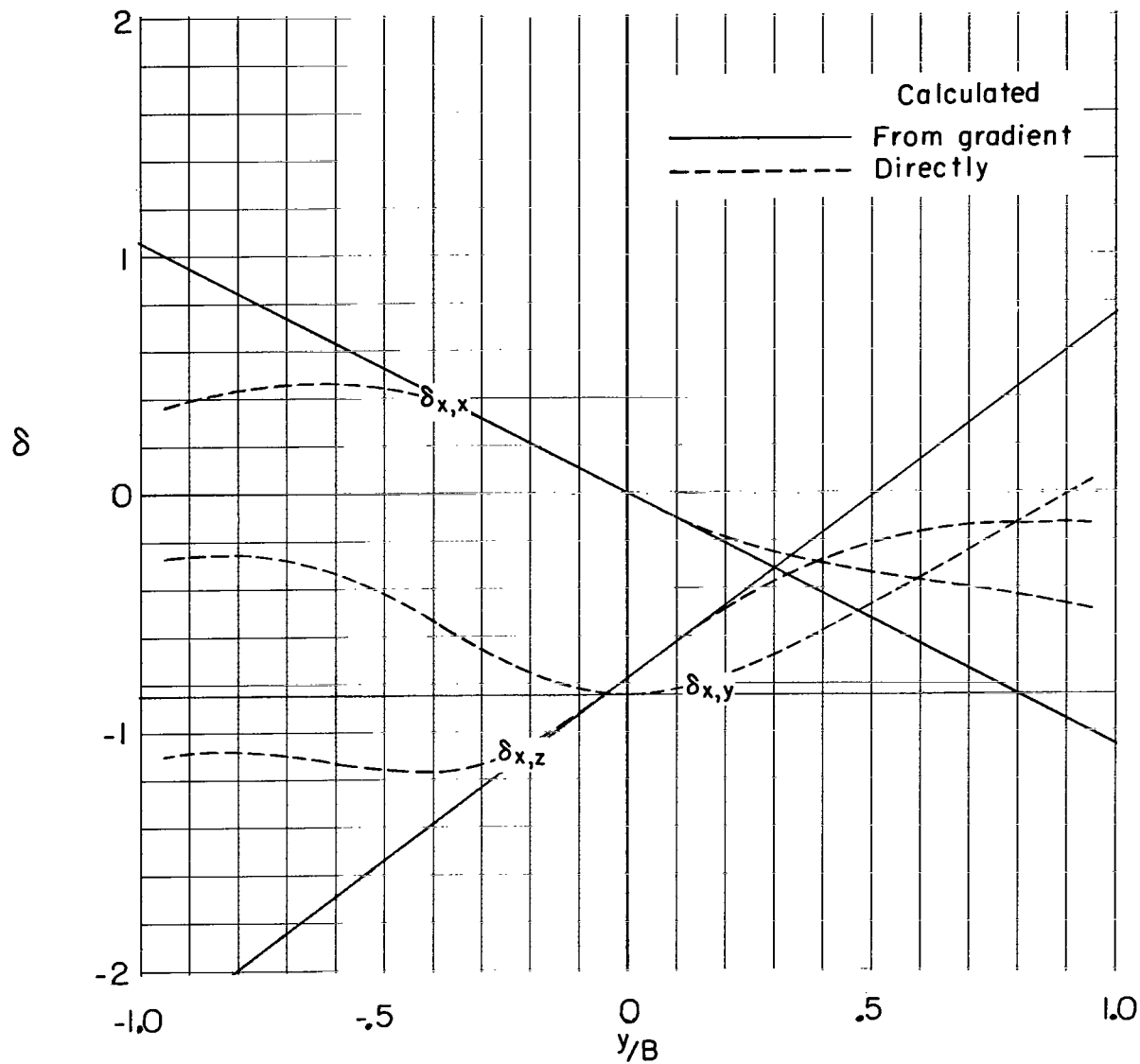
(b) Caused by forces in the Y-direction.

Figure 29.- Continued.



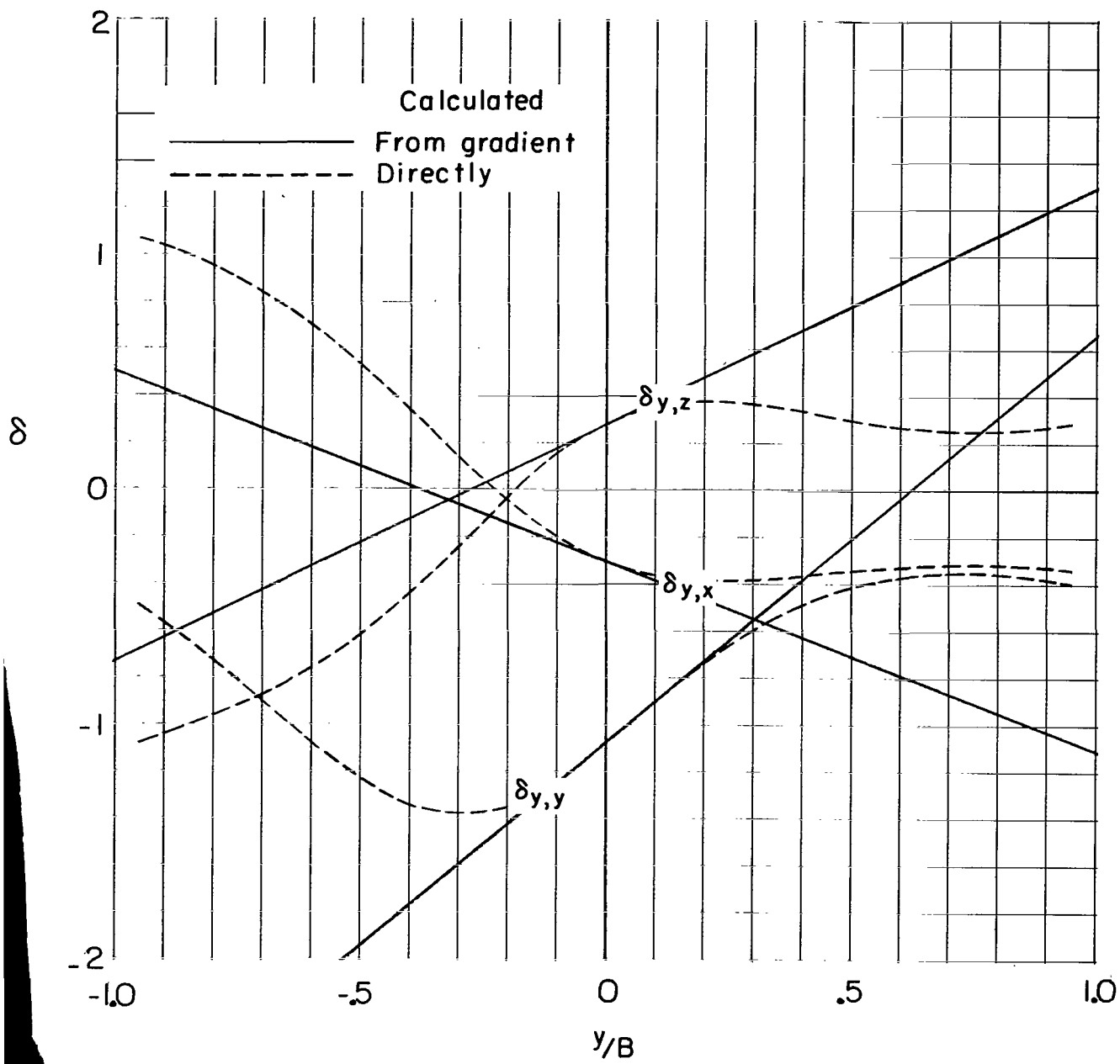
(c) Caused by forces in the Z-direction.

Figure 29.- Concluded.



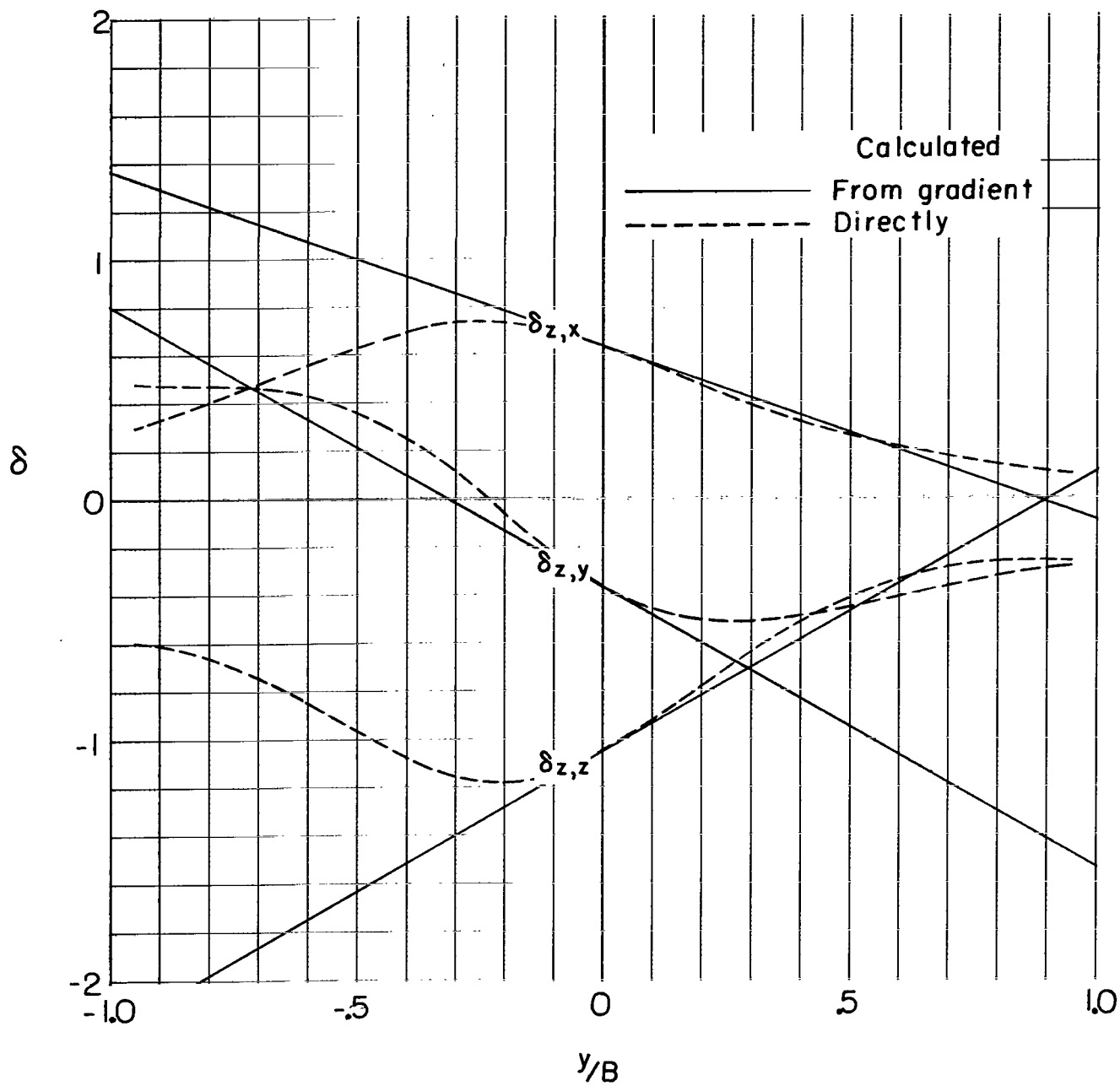
(a) Caused by forces in the X-direction.

Figure 30.- Distribution of interference factors over the lateral axis of the tunnel for a vanishingly small model centered in a closed rectangular tunnel having a width-height ratio of 1.5. $X_H = 60^\circ$; $X_V = 30^\circ$.



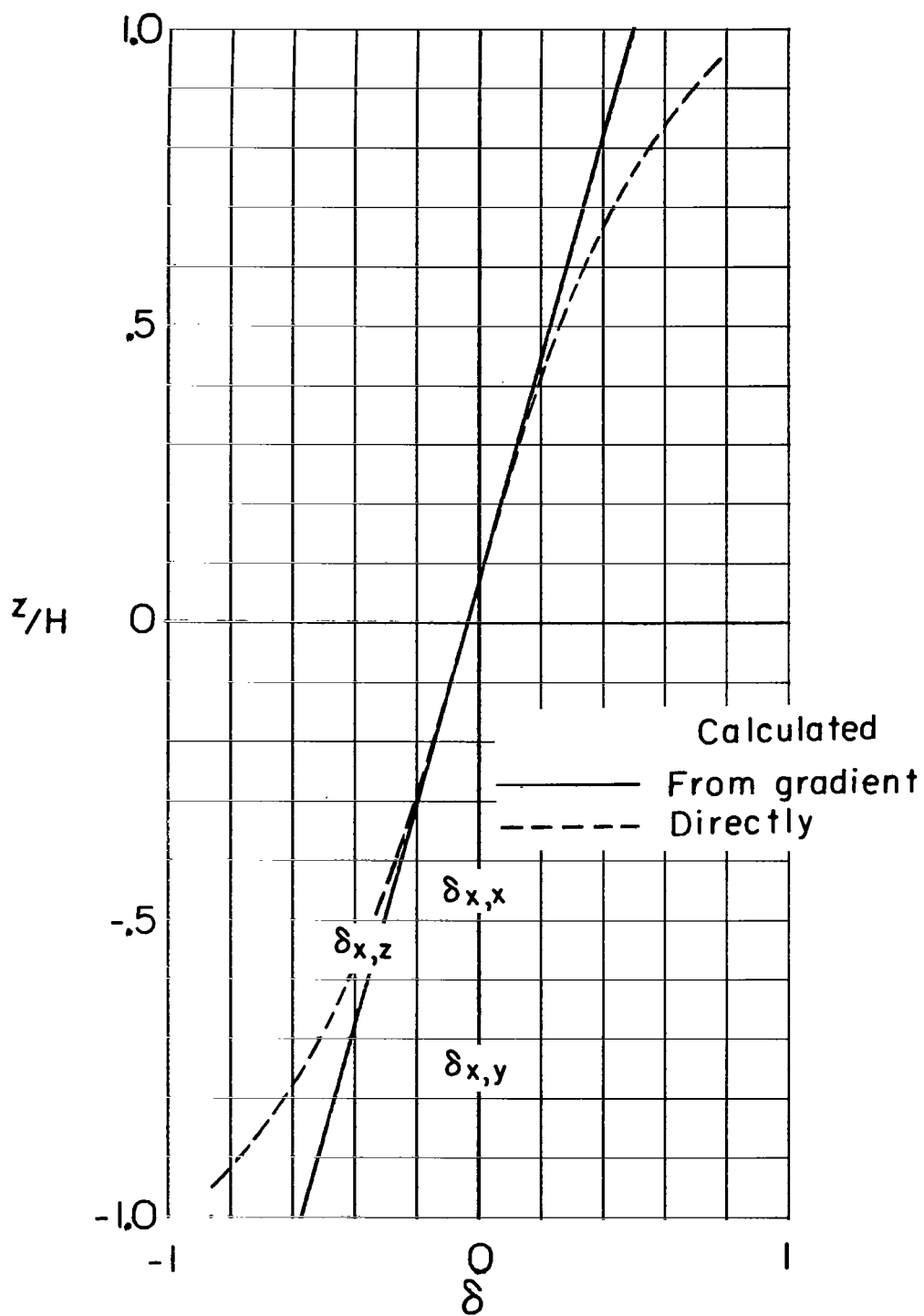
(b) Caused by forces in the Y-direction.

Figure 30.- Continued.



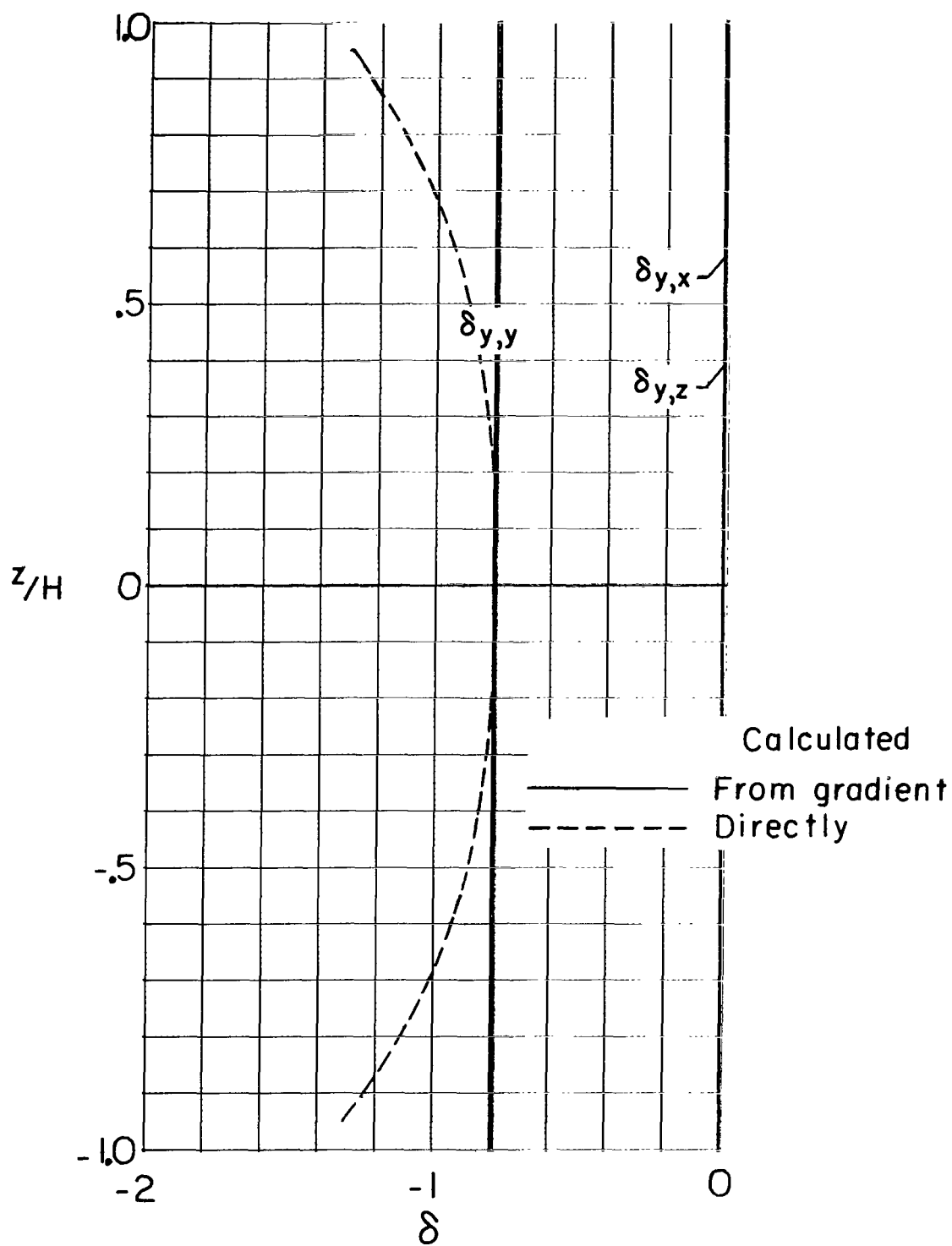
(c) Caused by forces in the Z-direction.

Figure 30.- Concluded.



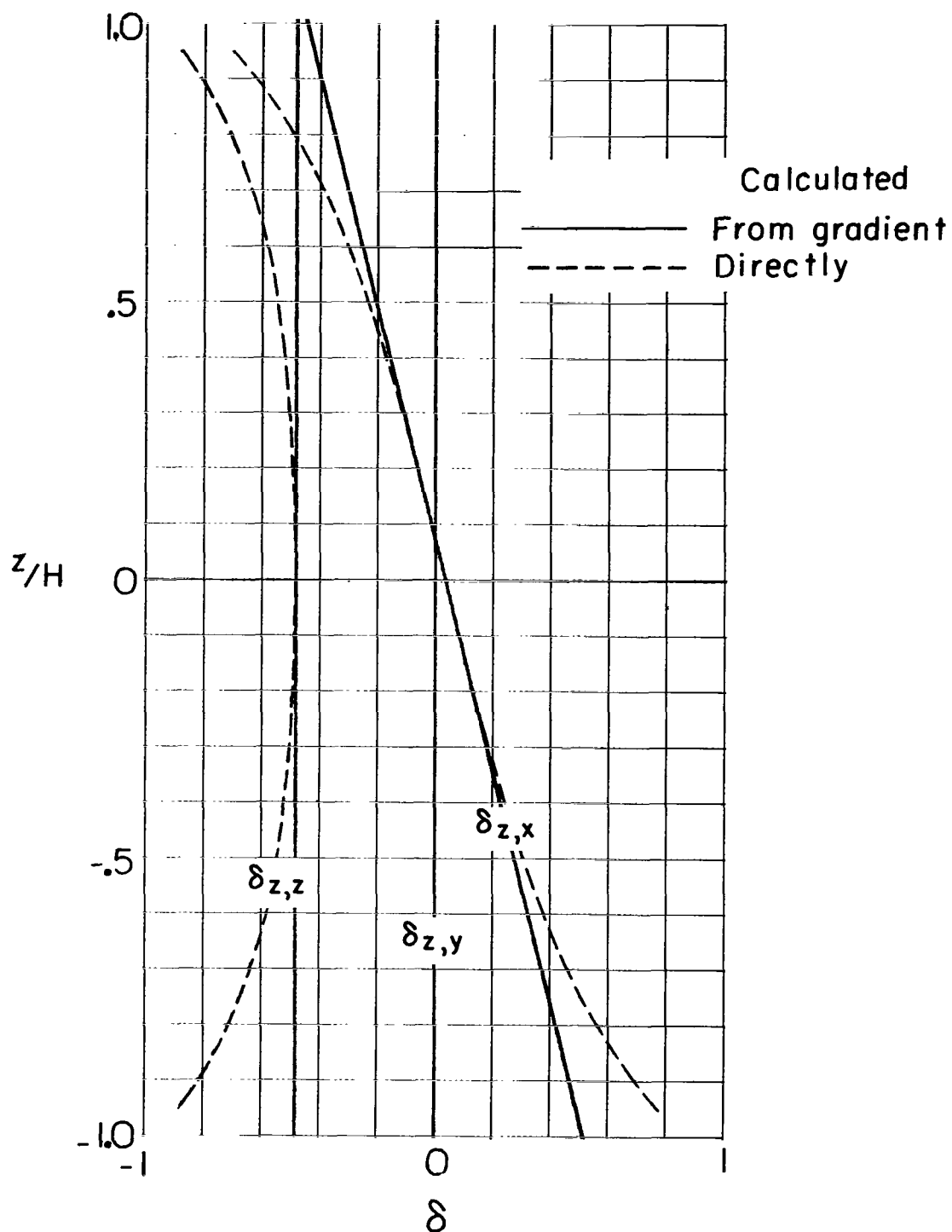
(a) Caused by forces in the X-direction.

Figure 31.- Distribution of interference factors over the vertical axis of the tunnel for a vanishingly small model centered in a closed rectangular tunnel having a width-height ratio of 1.5. $x_H = 90^\circ$; $x_V = 90^\circ$.



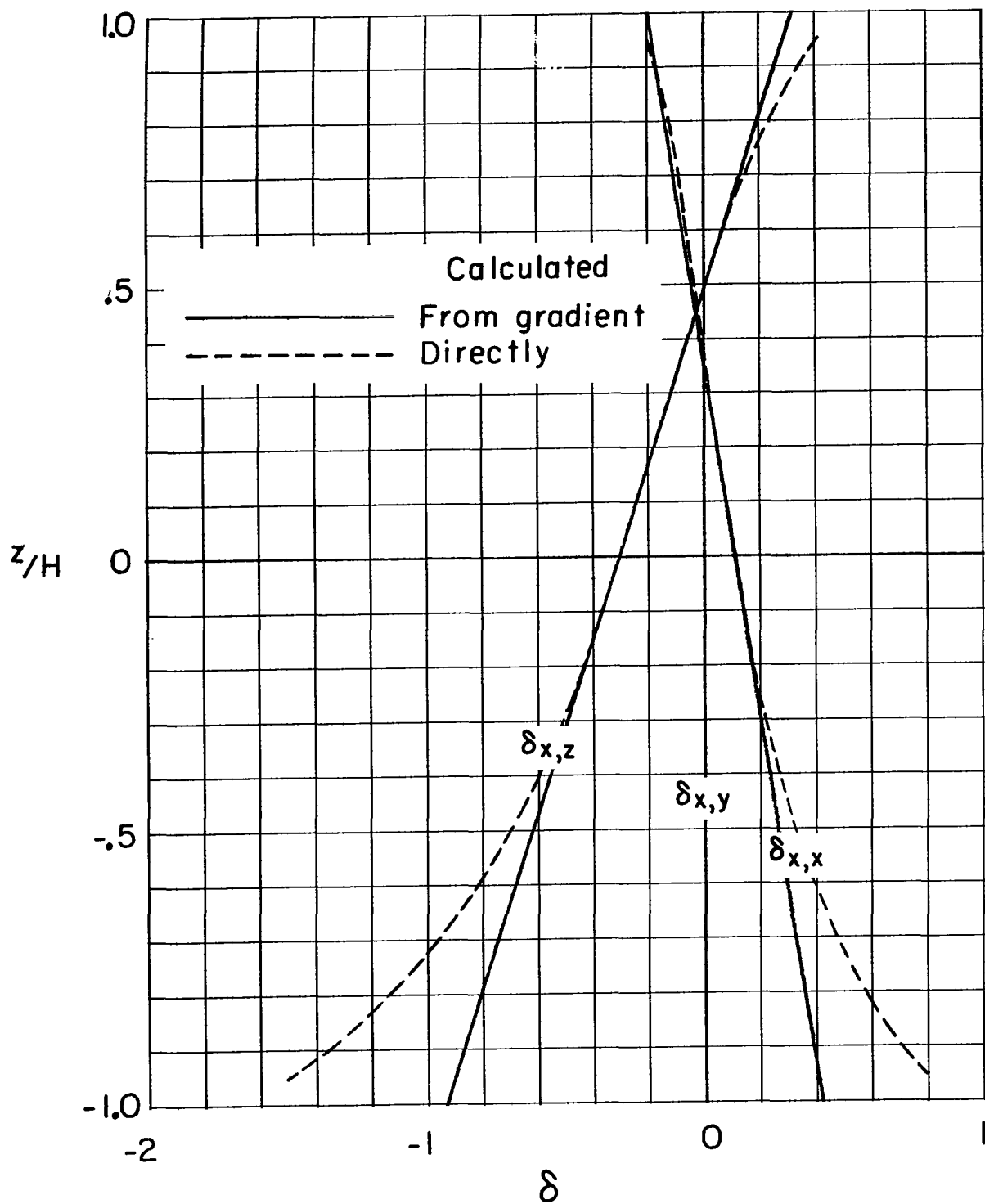
(b) Caused by forces in the Y-direction.

Figure 31.- Continued.



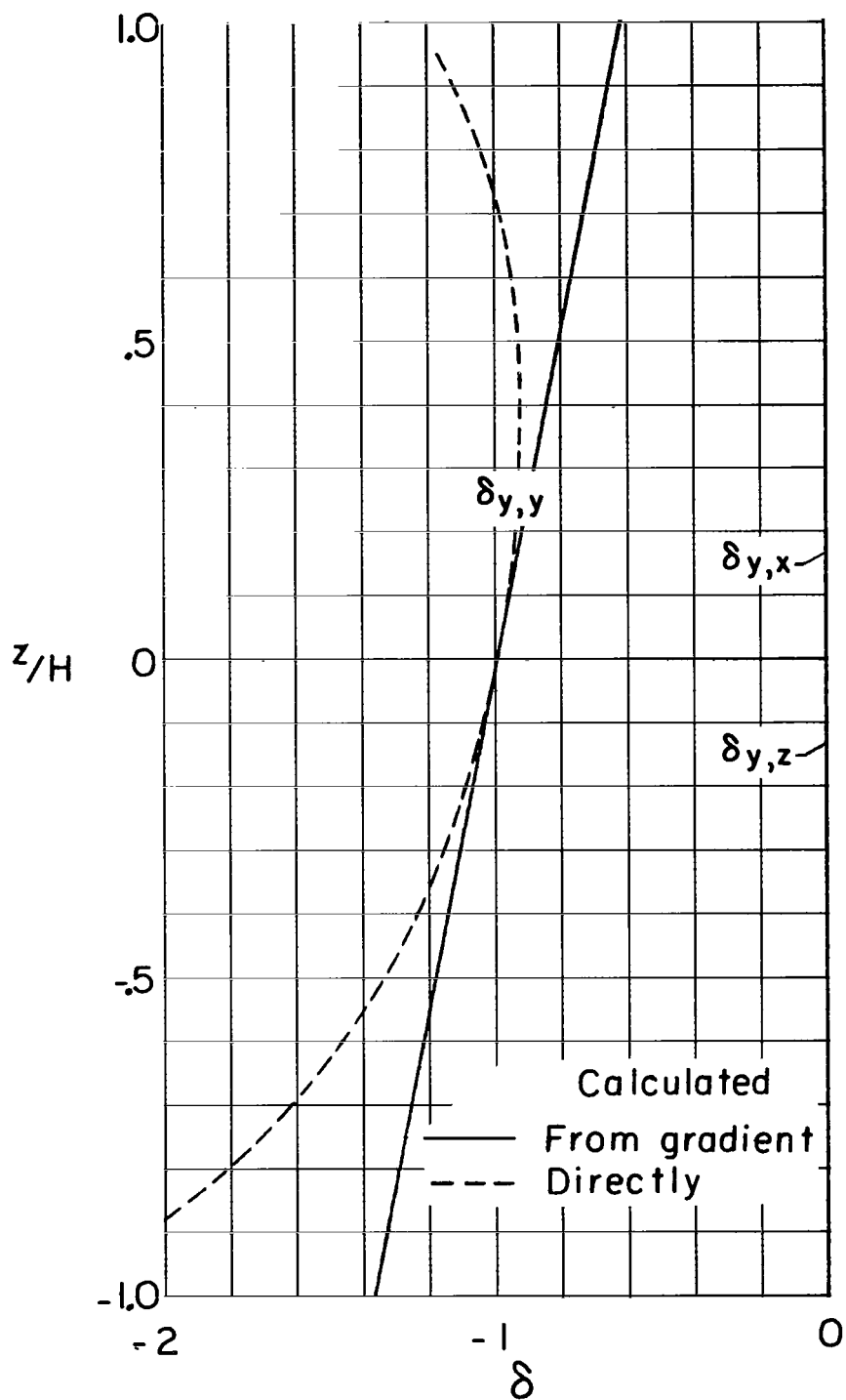
(c) Caused by forces in the Z-direction.

Figure 31.- Concluded.



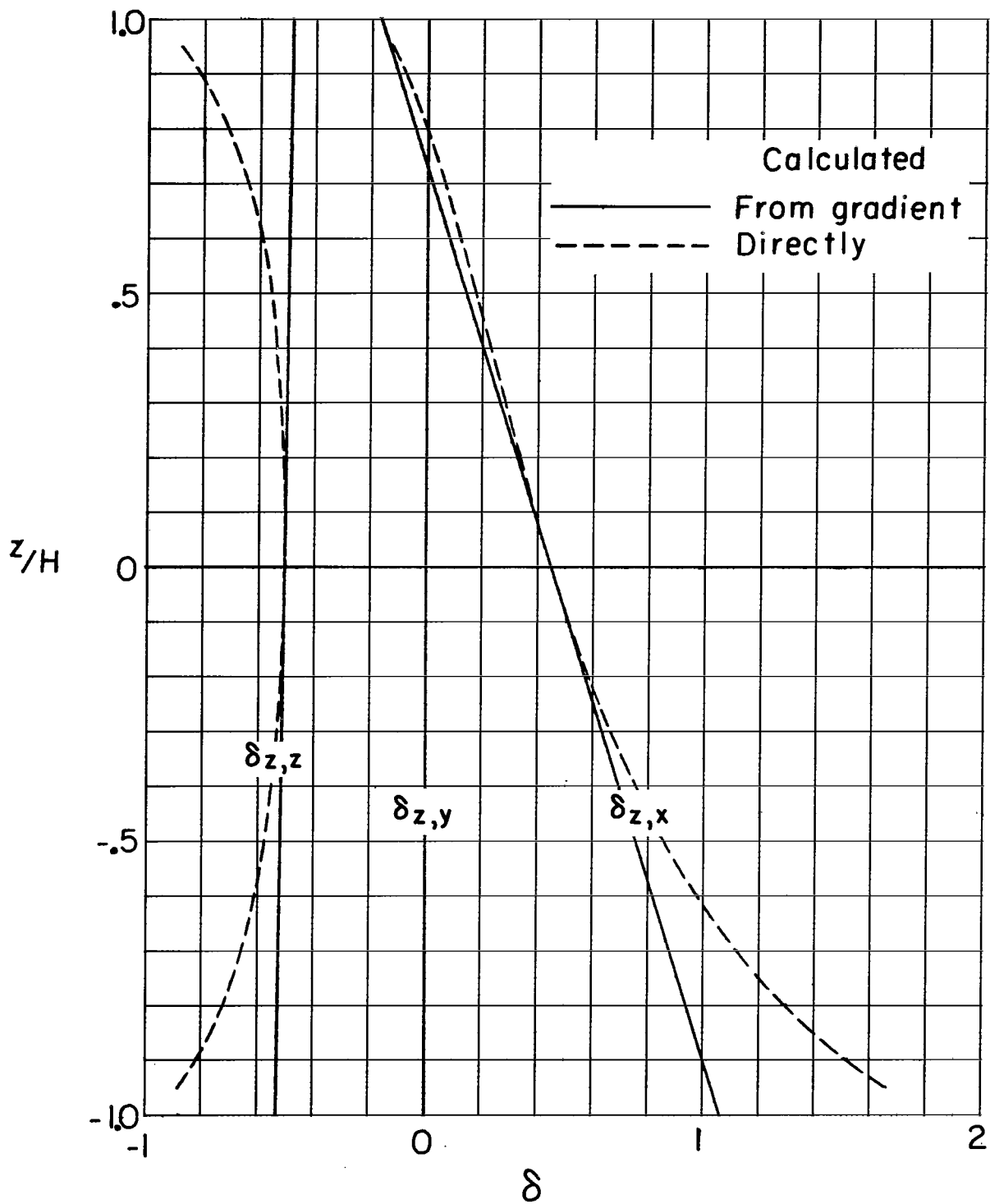
(a) Caused by forces in the X-direction.

Figure 32.- Distribution of interference factors over the vertical axis of the tunnel for a vanishingly small model centered in a closed rectangular tunnel having a width-height ratio of 1.5. $X_H = 90^\circ$; $X_V = 60^\circ$.



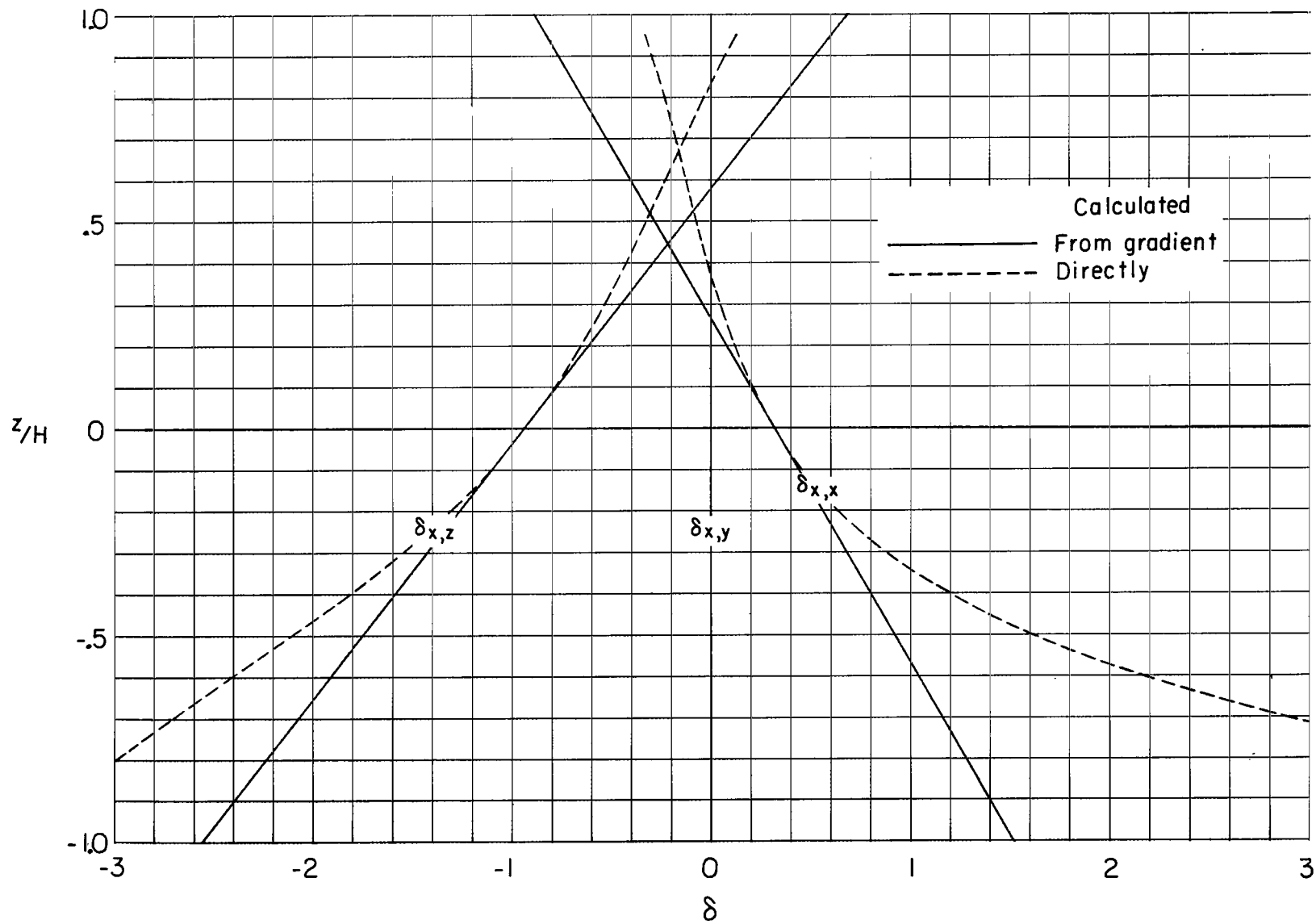
(b) Caused by forces in the Y-direction.

Figure 32.- Continued.



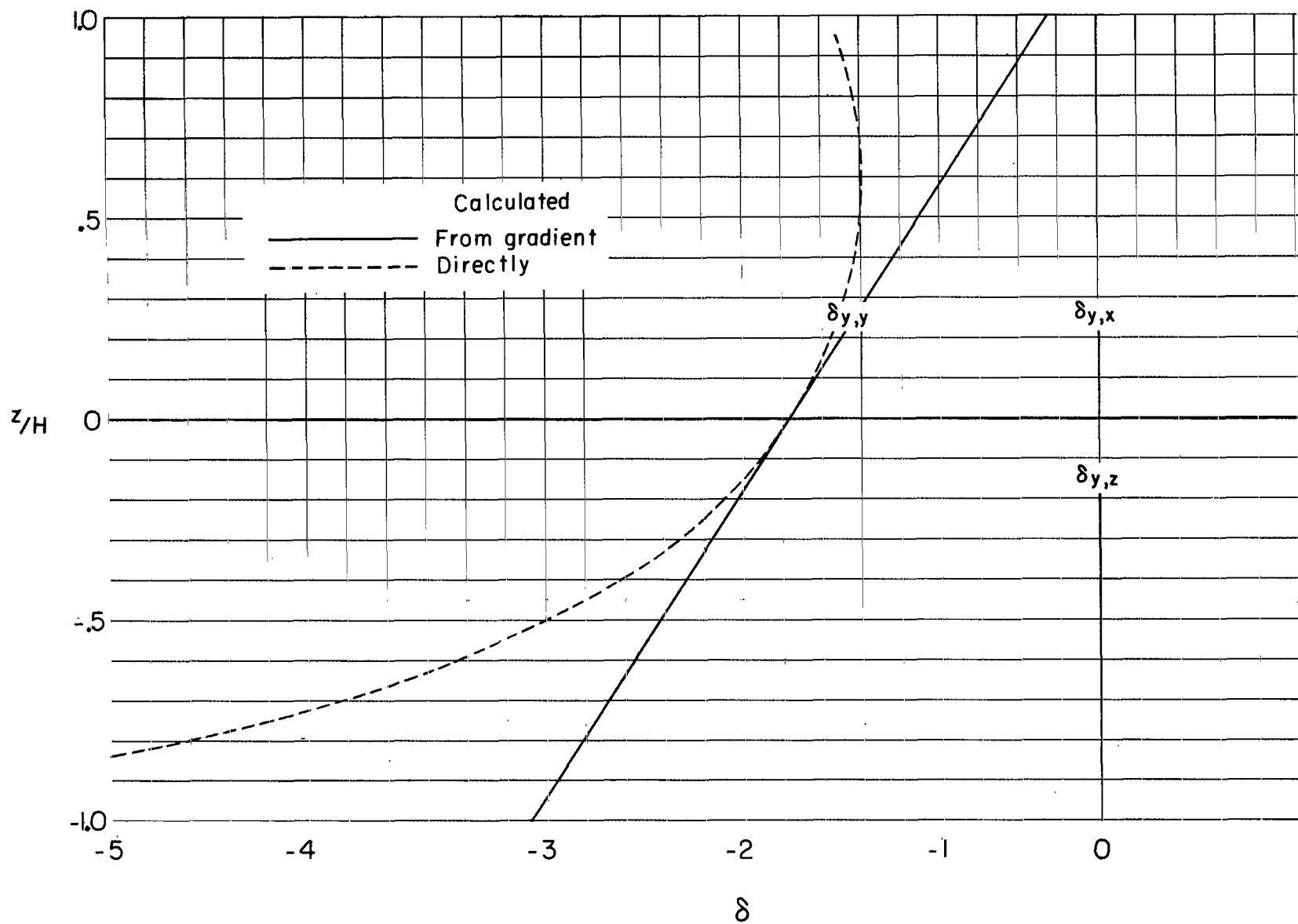
(c) Caused by forces in the Z-direction.

Figure 32.- Concluded.



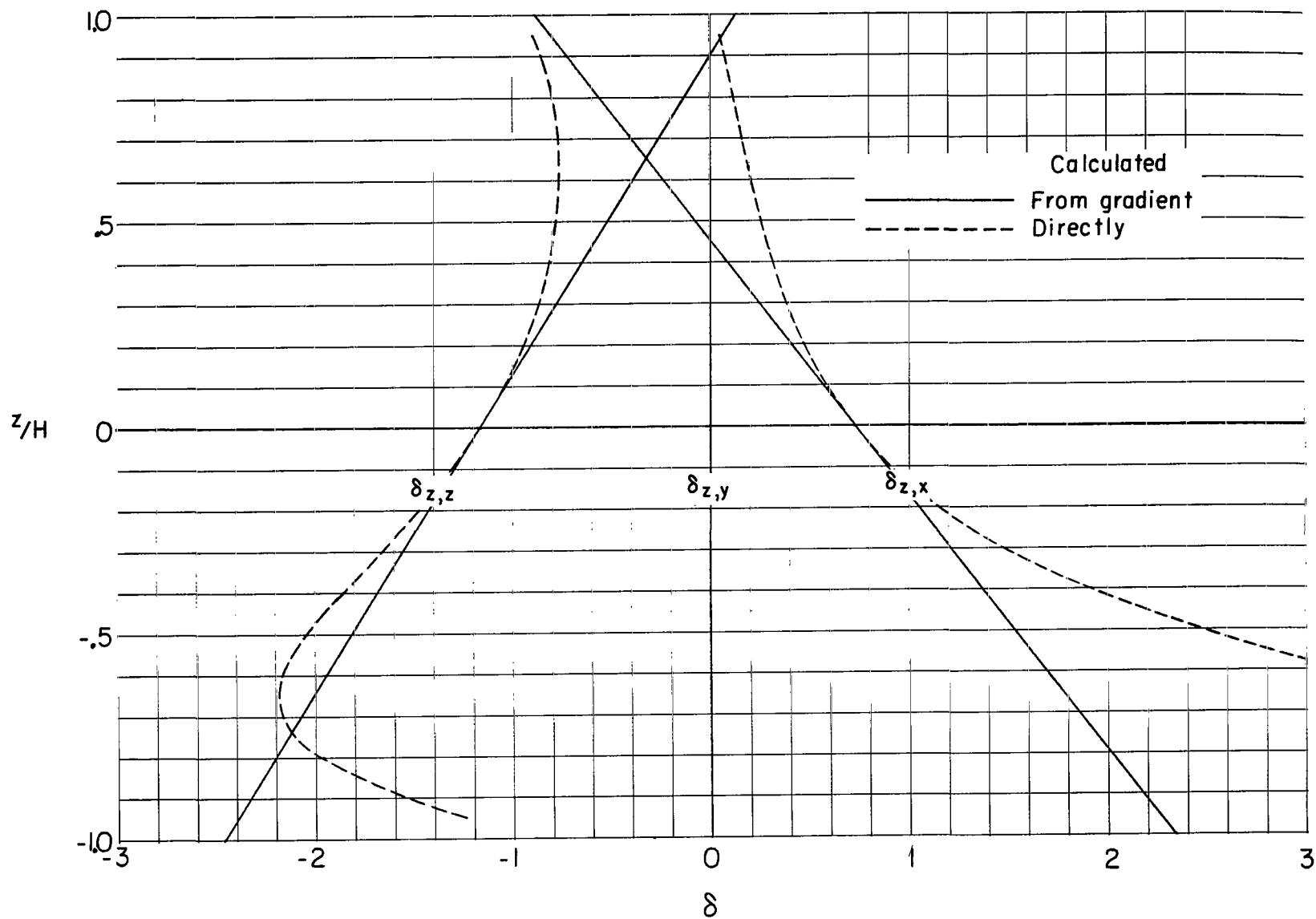
(a) Caused by forces in the X-direction.

Figure 33.- Distribution of interference factors over the vertical axis of the tunnel for a vanishingly small model centered in a closed rectangular tunnel having a width-height ratio of 1.5. $X_H = 90^\circ$; $X_V = 30^\circ$.



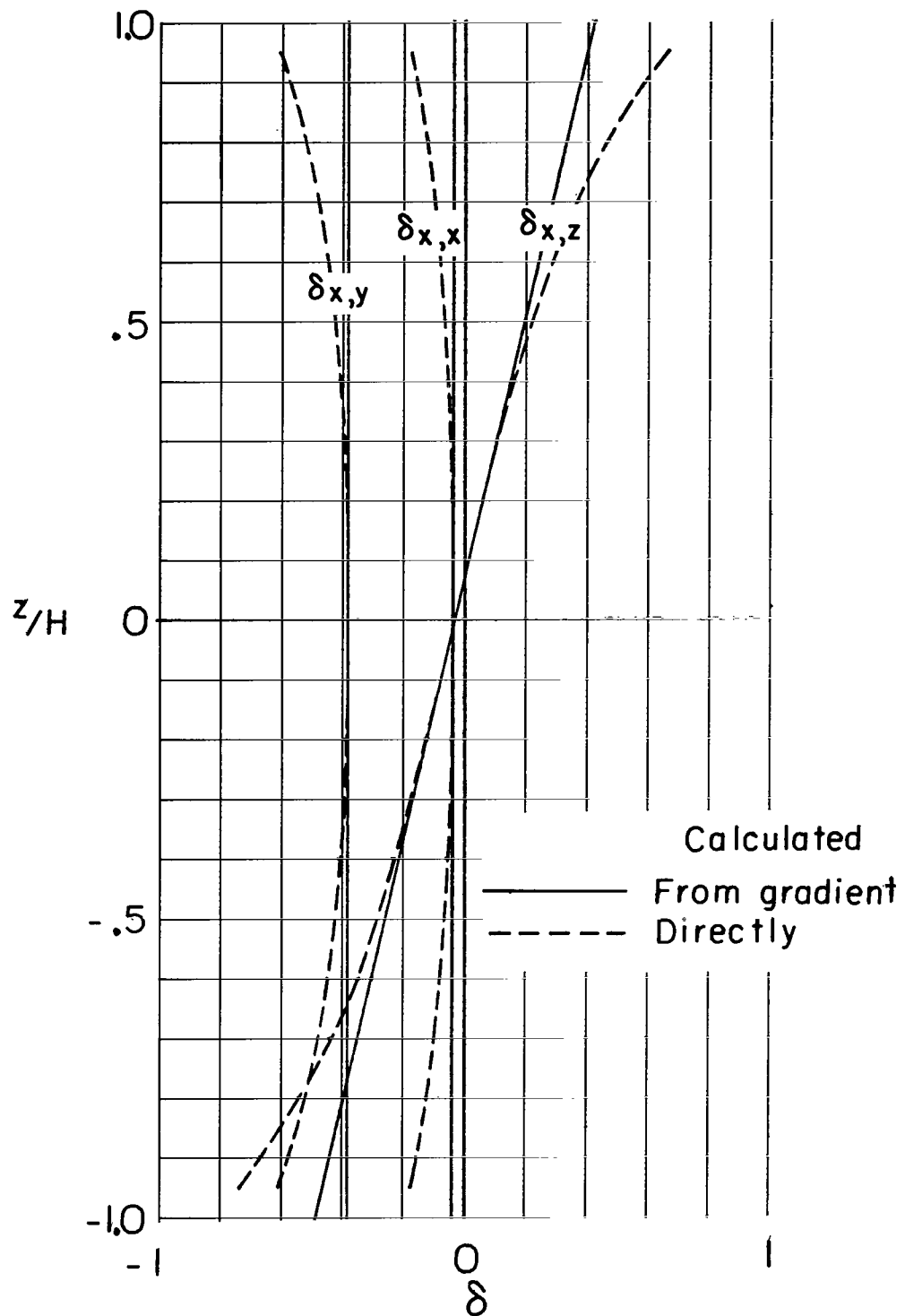
(b) Caused by forces in the Y-direction.

Figure 33.- Continued.



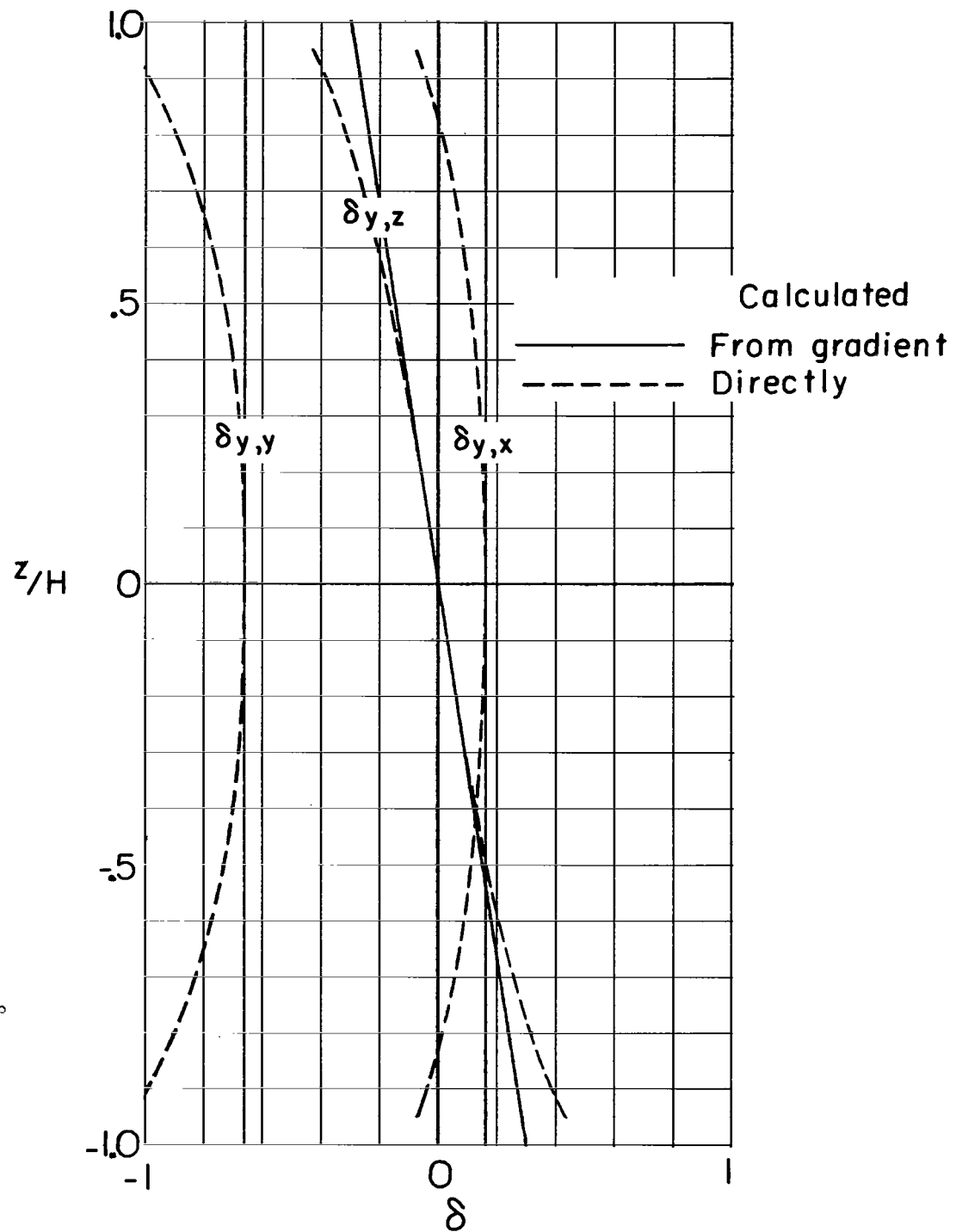
(c) Caused by forces in the Z-direction.

Figure 33,- Concluded.



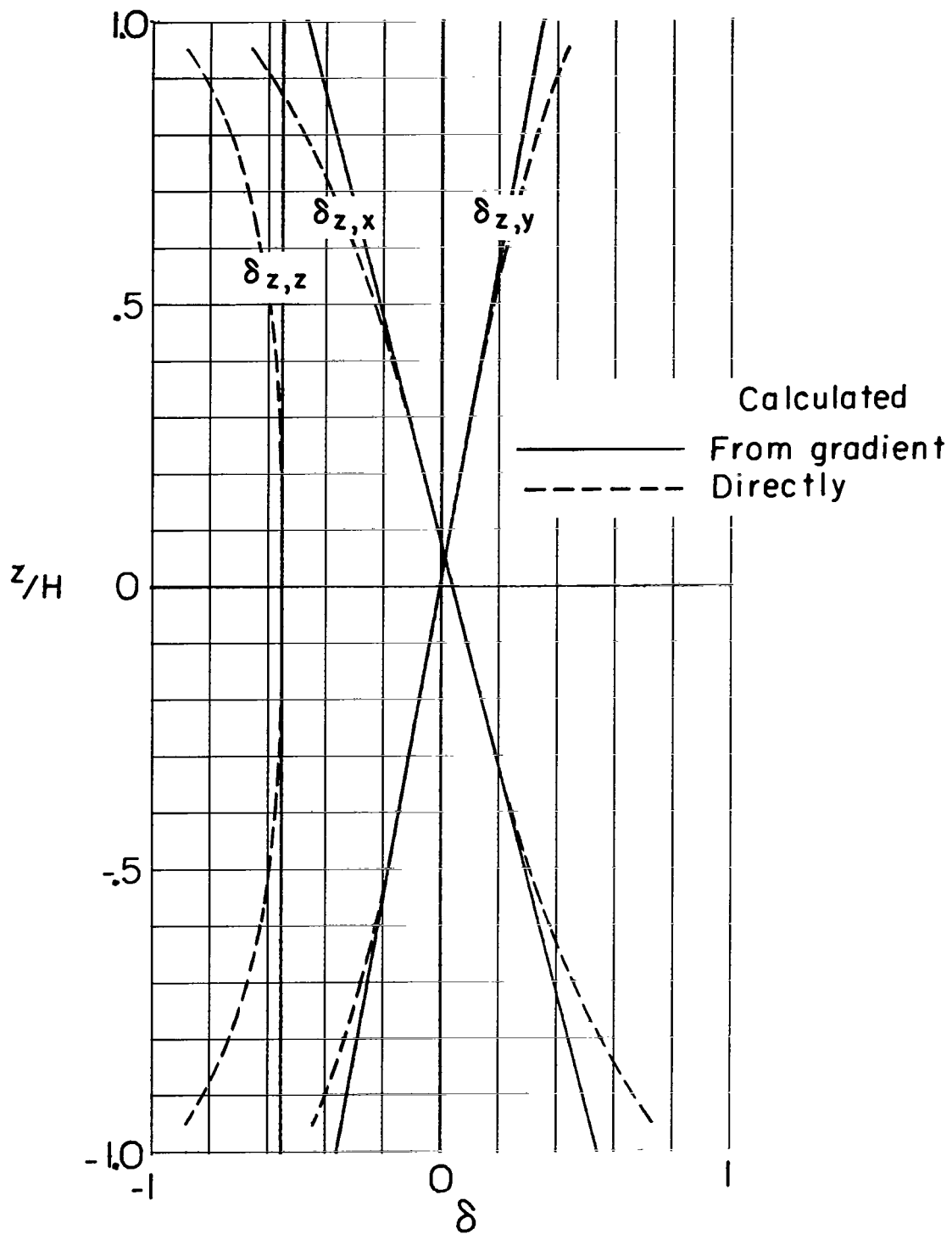
(a) Caused by forces in the X-direction.

Figure 34.- Distribution of interference factors over the vertical axis of the tunnel for a vanishingly small model centered in a closed rectangular tunnel having a width-height ratio of 1.5. $X_H = 60^\circ$; $X_V = 90^\circ$.



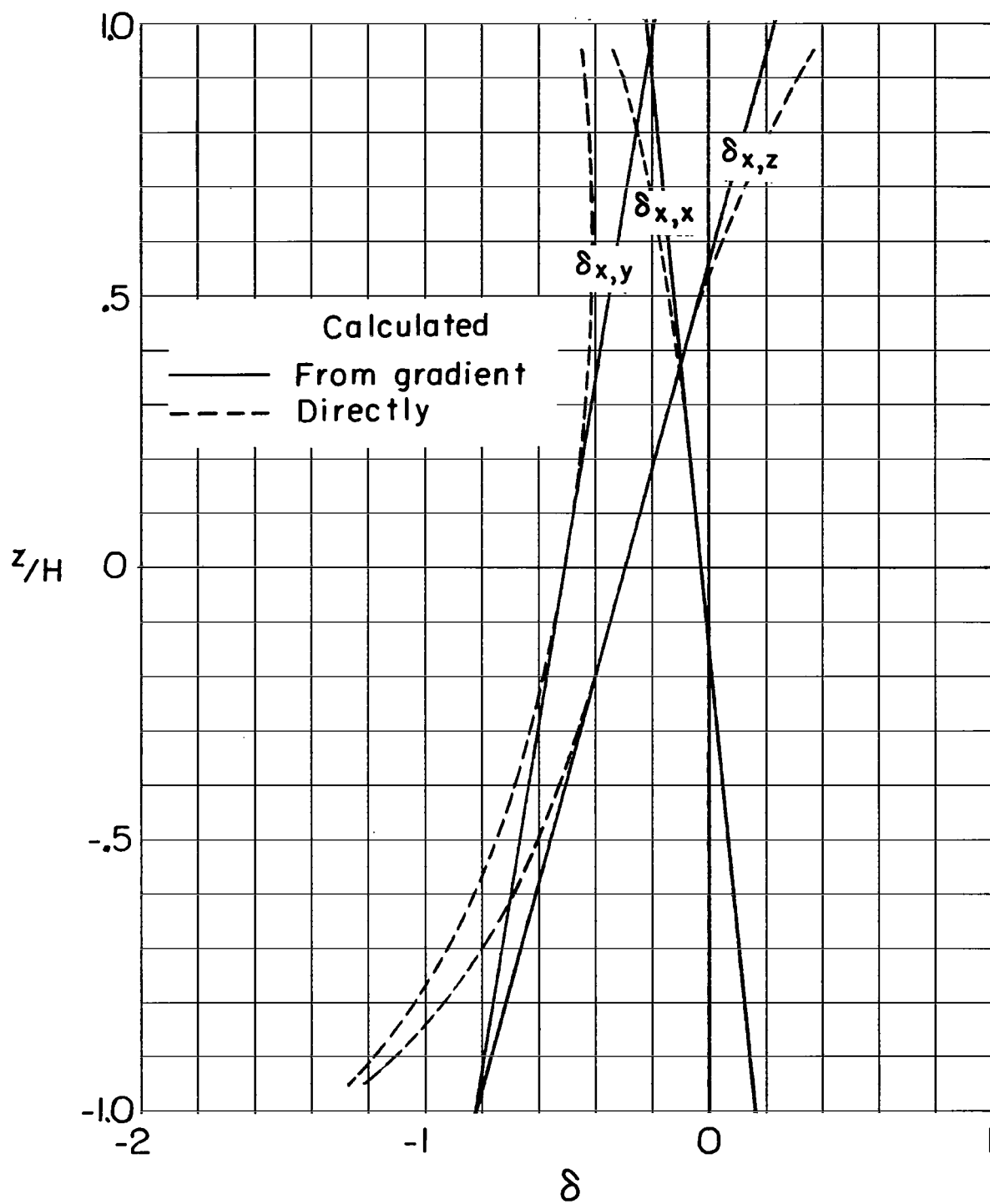
(b) Caused by forces in the Y-direction.

Figure 34.- Continued.



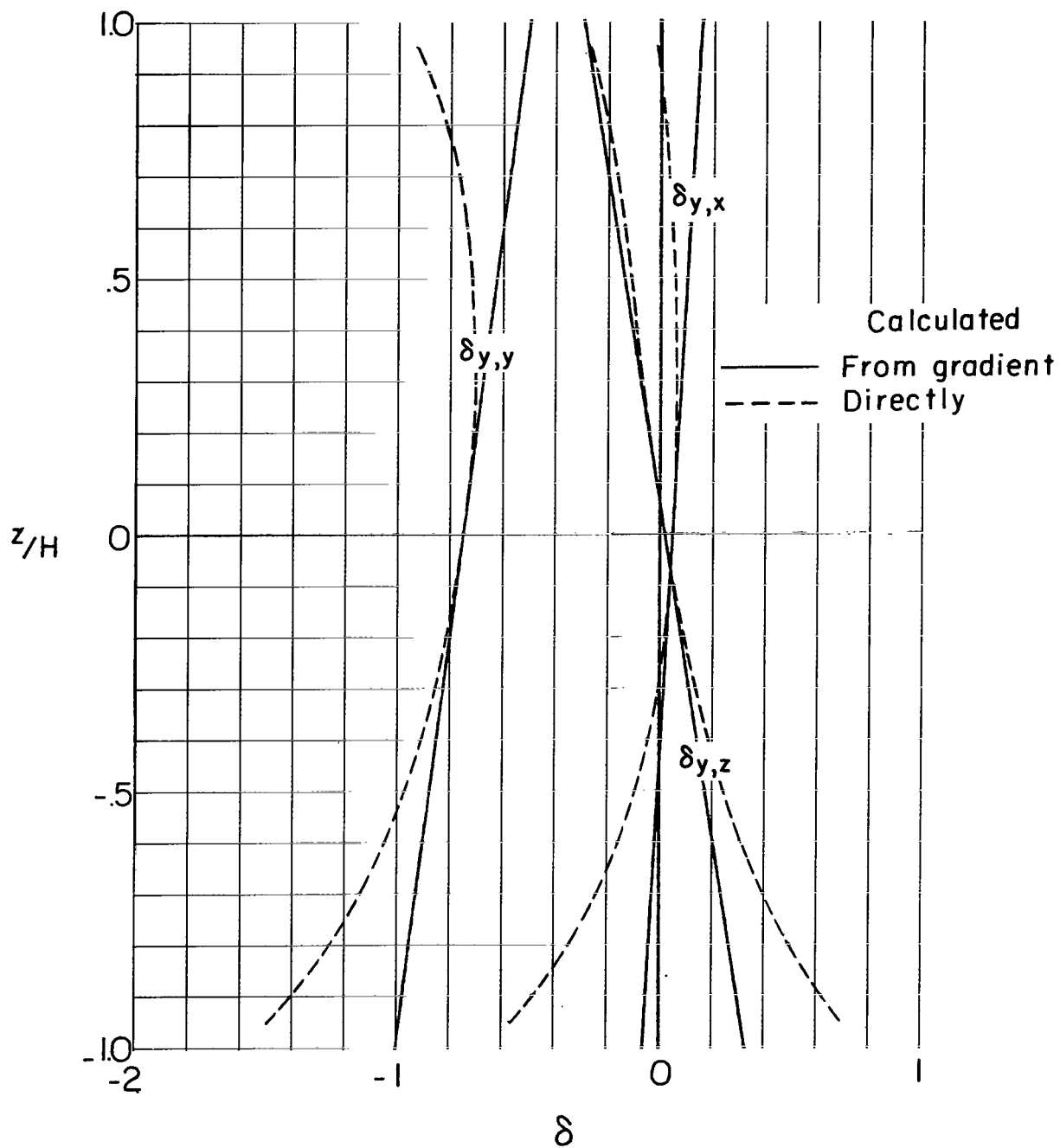
(c) Caused by forces in the Z-direction.

Figure 34.- Concluded.



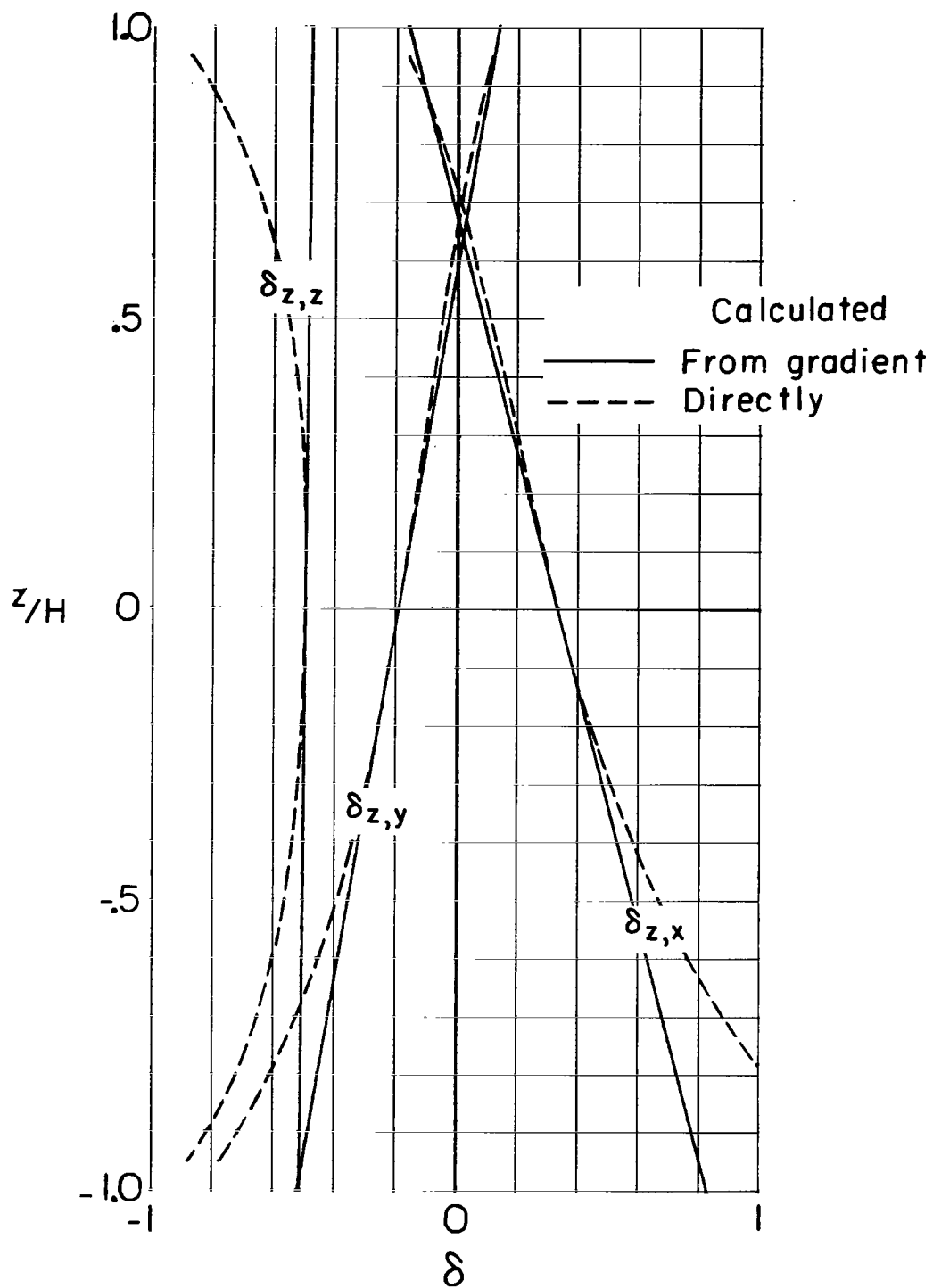
(a) Caused by forces in the X-direction.

Figure 35.- Distribution of interference factors over the vertical axis of the tunnel for a vanishingly small model centered in a closed rectangular tunnel having a width-height ratio of 1.5. $\chi_H = 60^\circ$; $\chi_V = 60^\circ$.



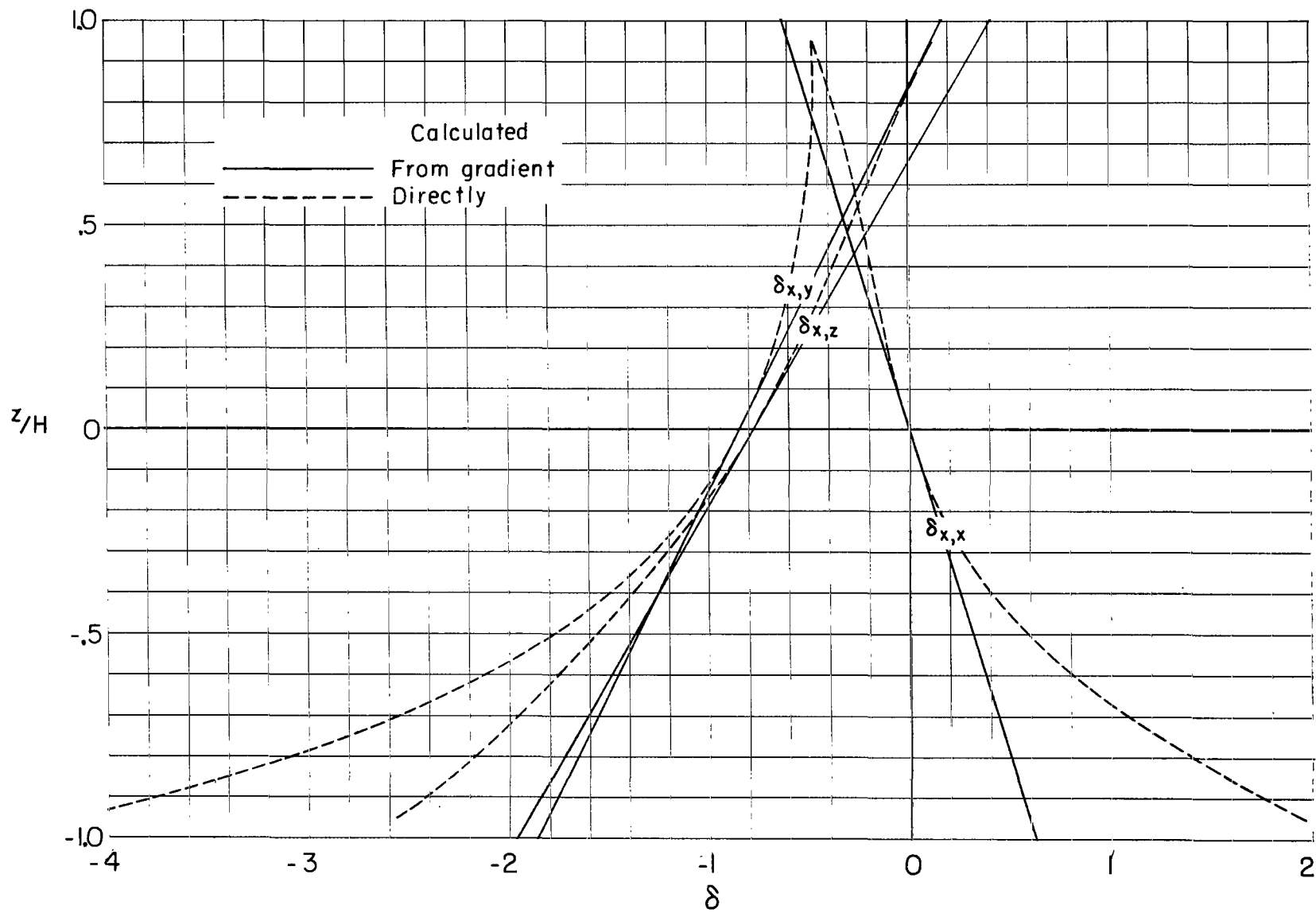
(b) Caused by forces in the Y-direction.

Figure 35.- Continued.



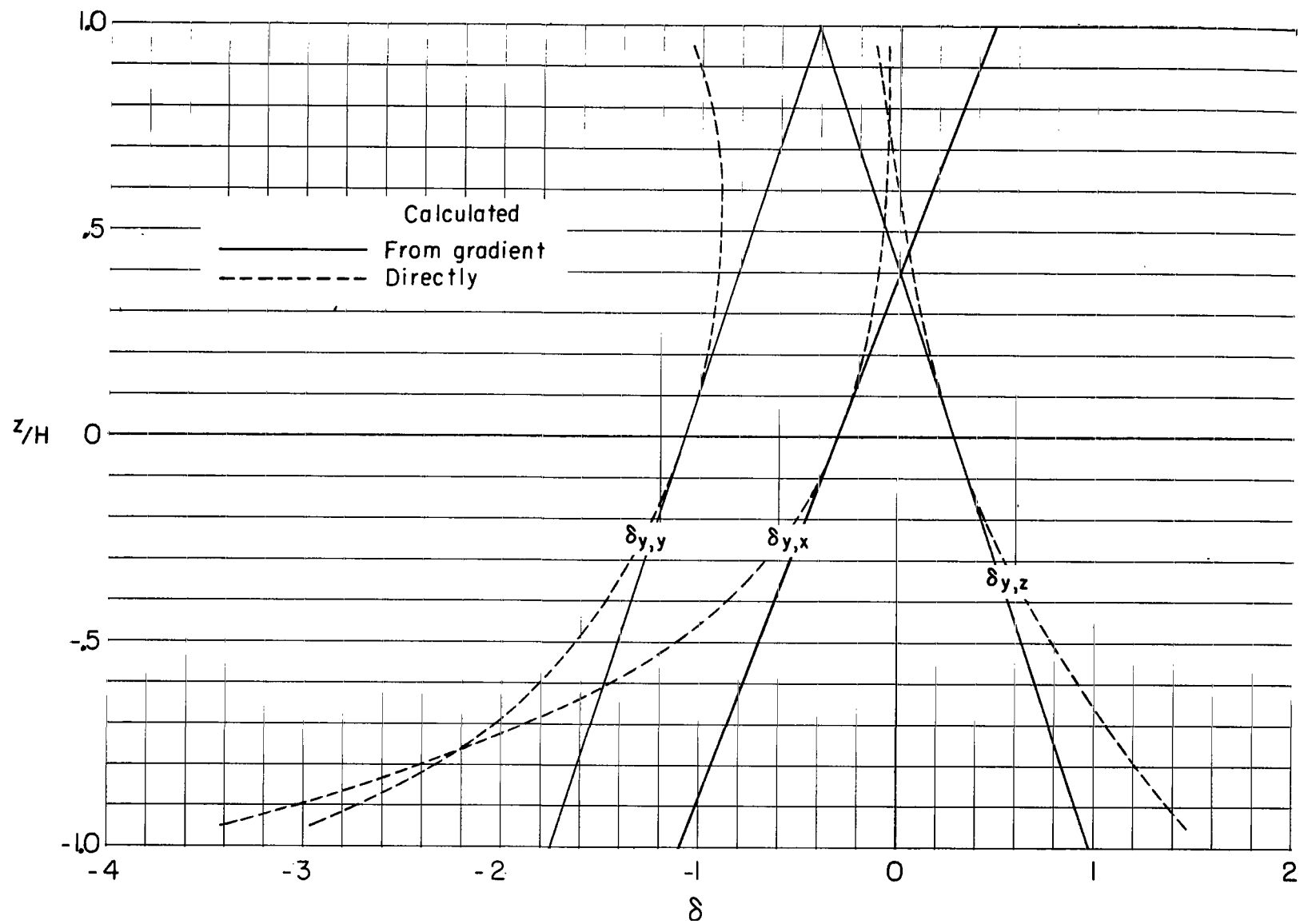
(c) Caused by forces in the Z-direction.

Figure 35.- Concluded.



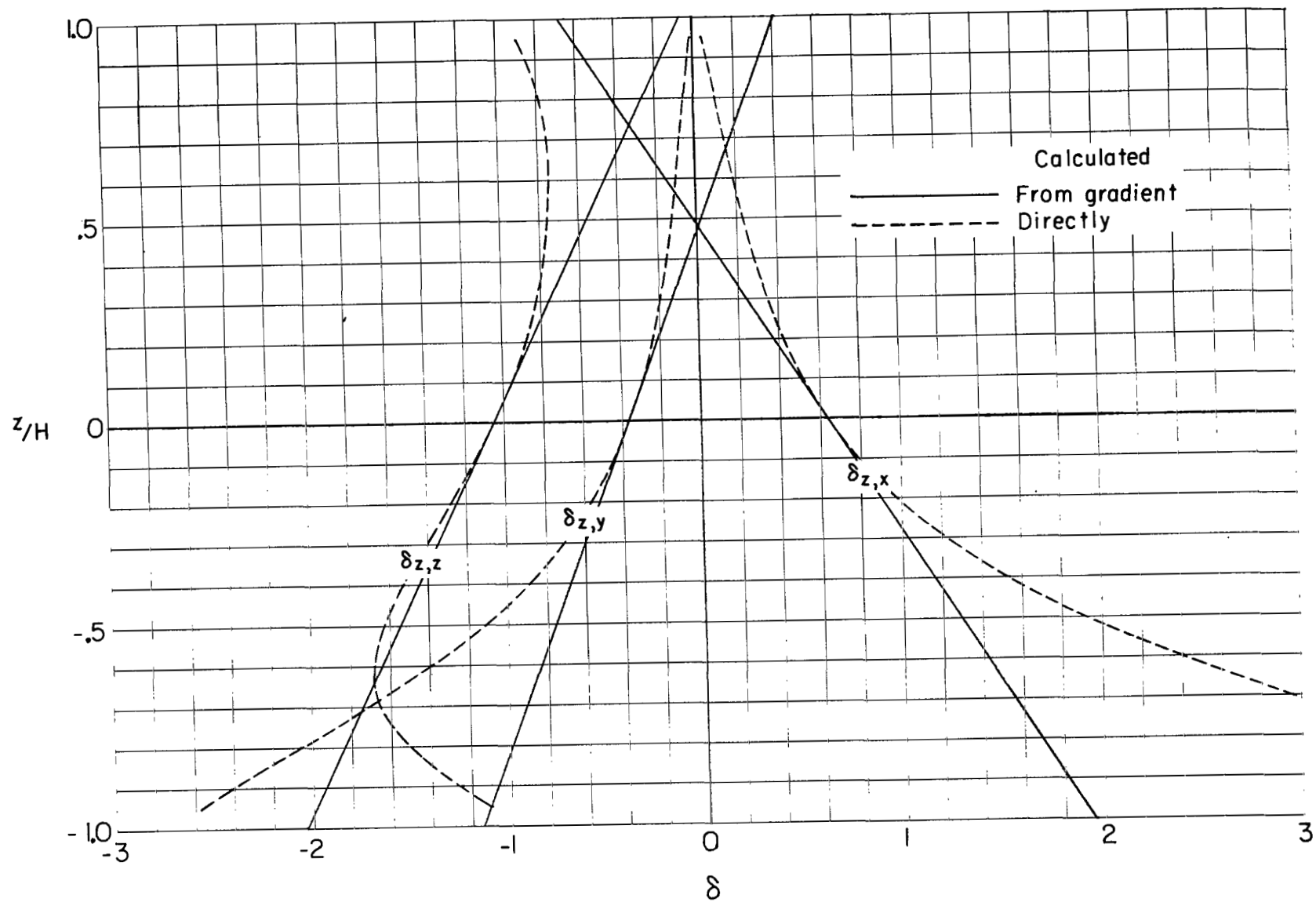
(a) Caused by forces in the X-direction.

Figure 36.- Distribution of interference factors over the vertical axis of the tunnel for a vanishingly small model centered in a closed rectangular tunnel having a width-height ratio of 1.5. $\chi_H = 60^\circ$; $\chi_V = 30^\circ$.



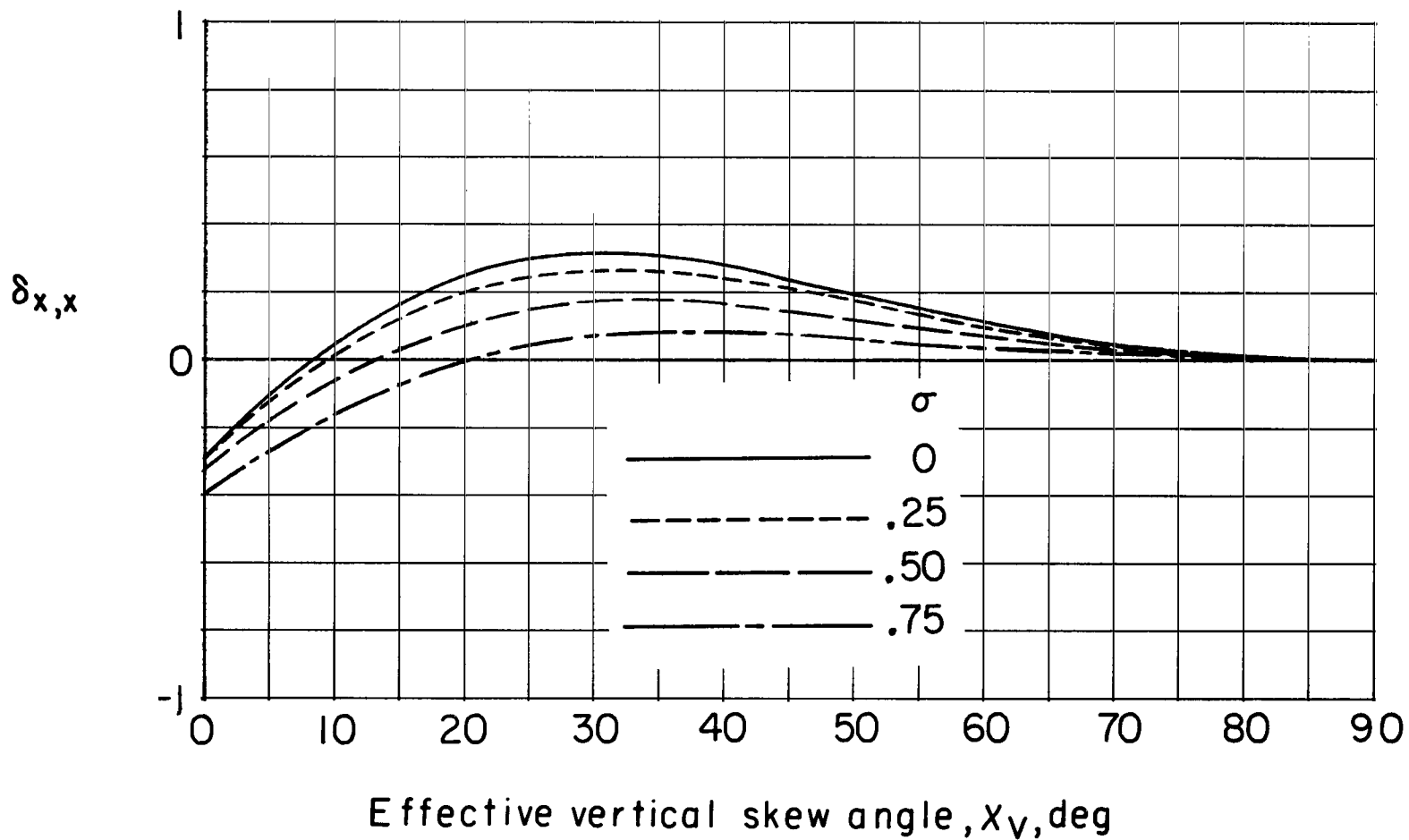
(b) Caused by forces in the Y-direction.

Figure 36.- Continued.



(c) Caused by forces in the Z-direction.

Figure 36.- Concluded.



(a) $\delta_{x,x}$.

Figure 37.- Effect of span-width ratio σ on interference velocity factors for unswept wings centered in a closed tunnel having a width-height ratio γ of 1.5. $X_H = 90^\circ$. Note that $\delta_{x,y} = \delta_{y,x} = \delta_{y,z} = \delta_{z,y} = 0$.

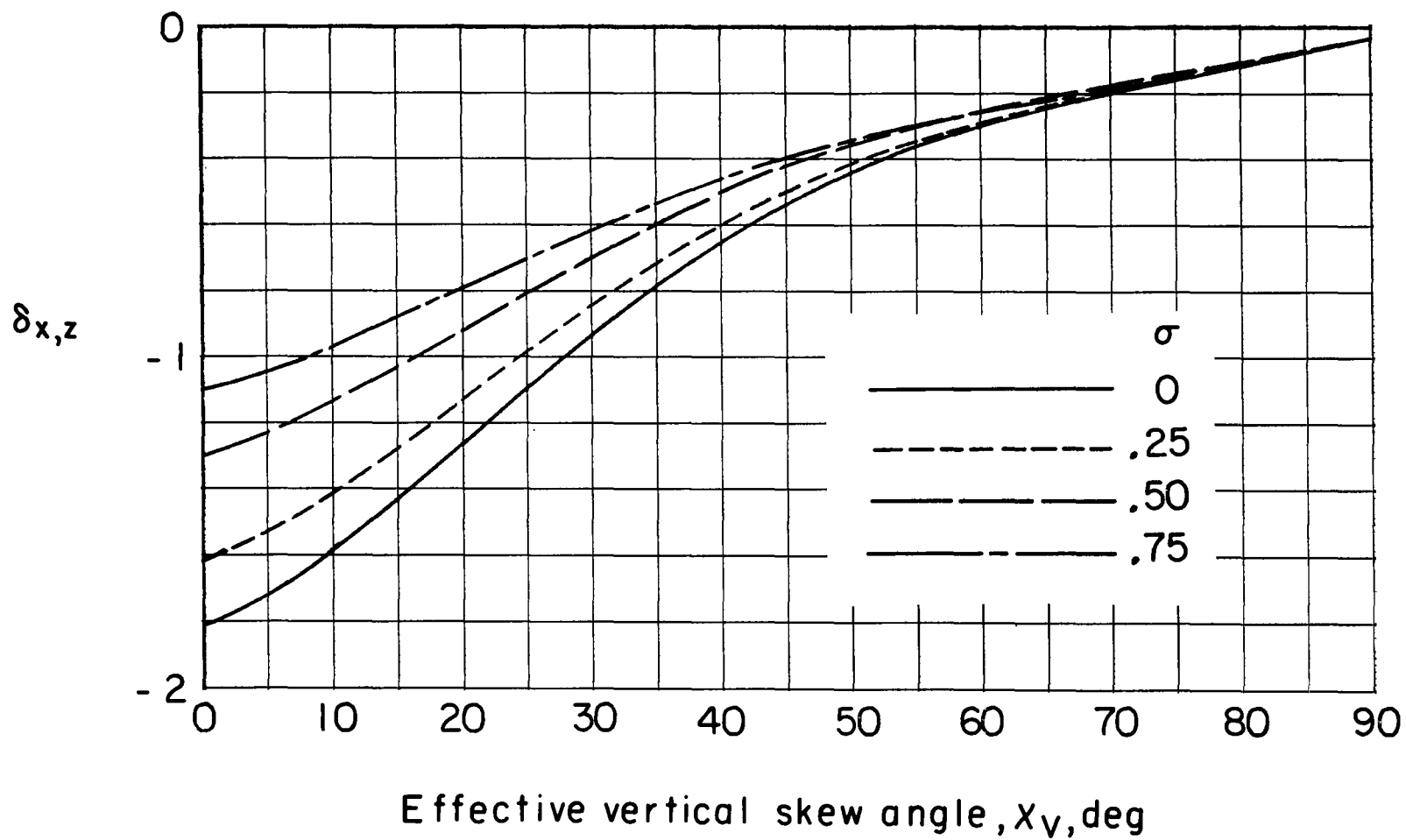
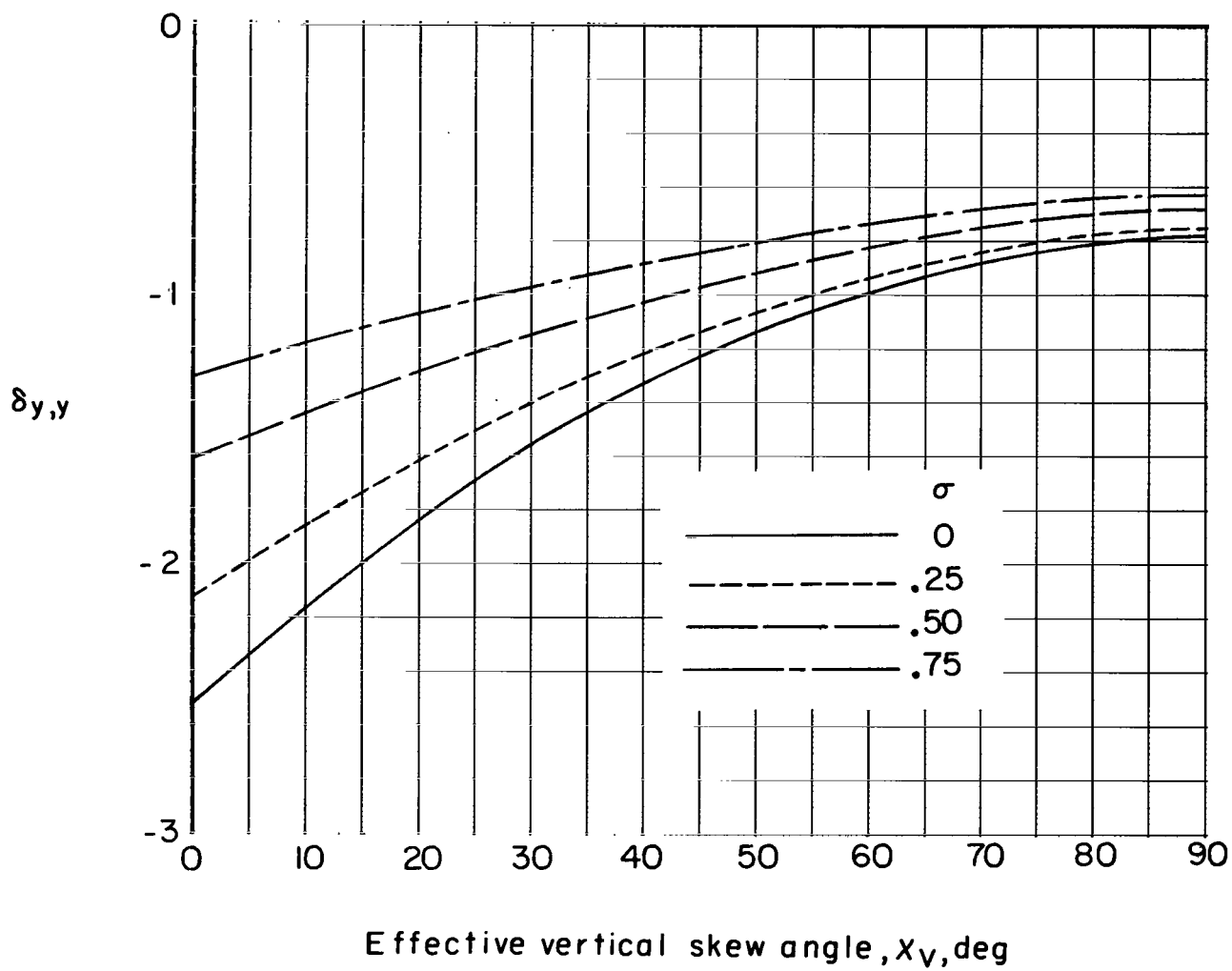
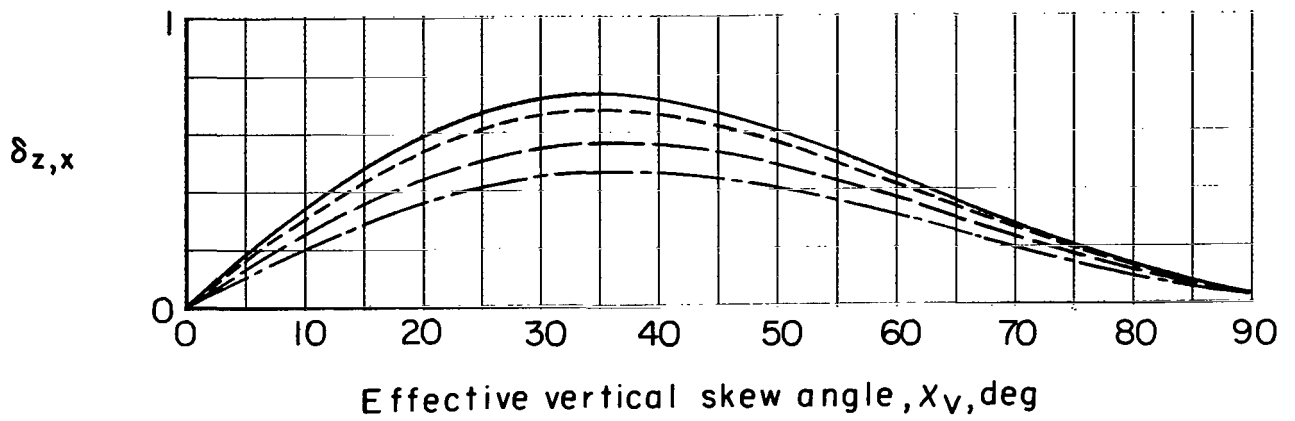
(b) $\delta_{x,z}$.

Figure 37.- Continued.

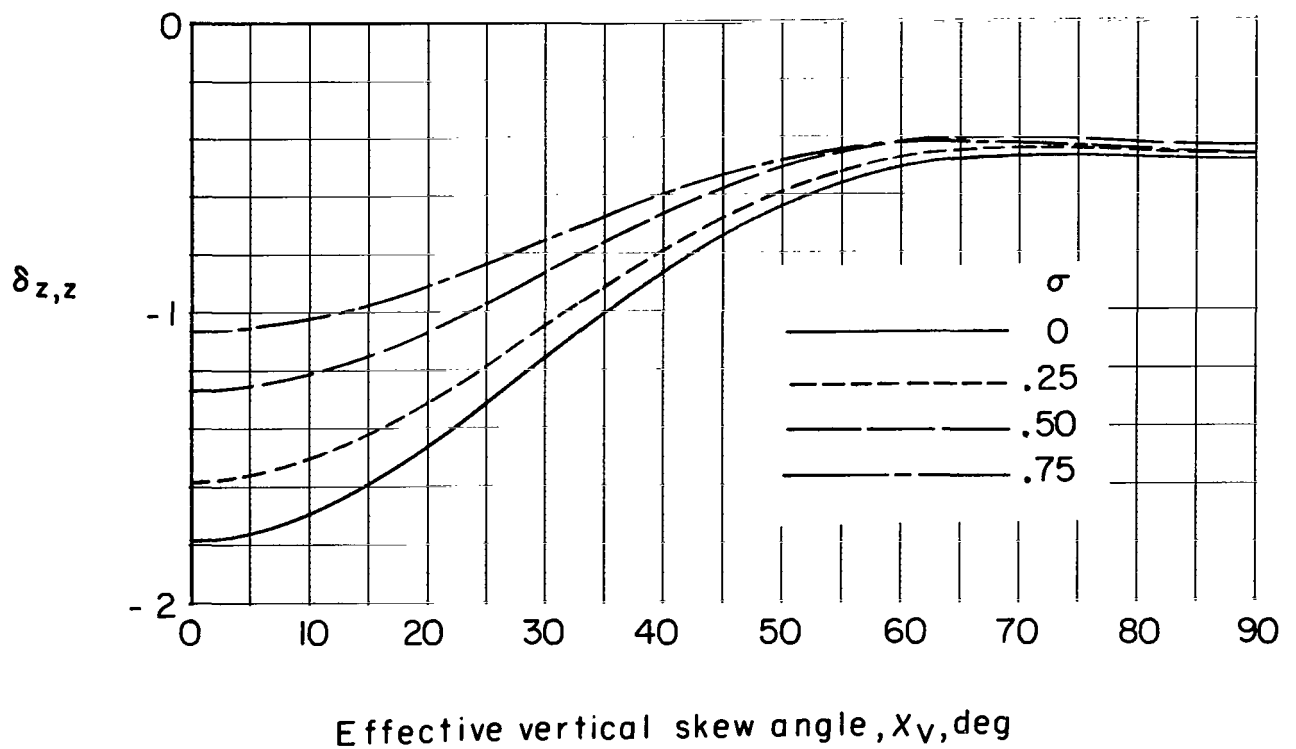


(c) $\delta_{y,y}$.

Figure 37.- Continued.

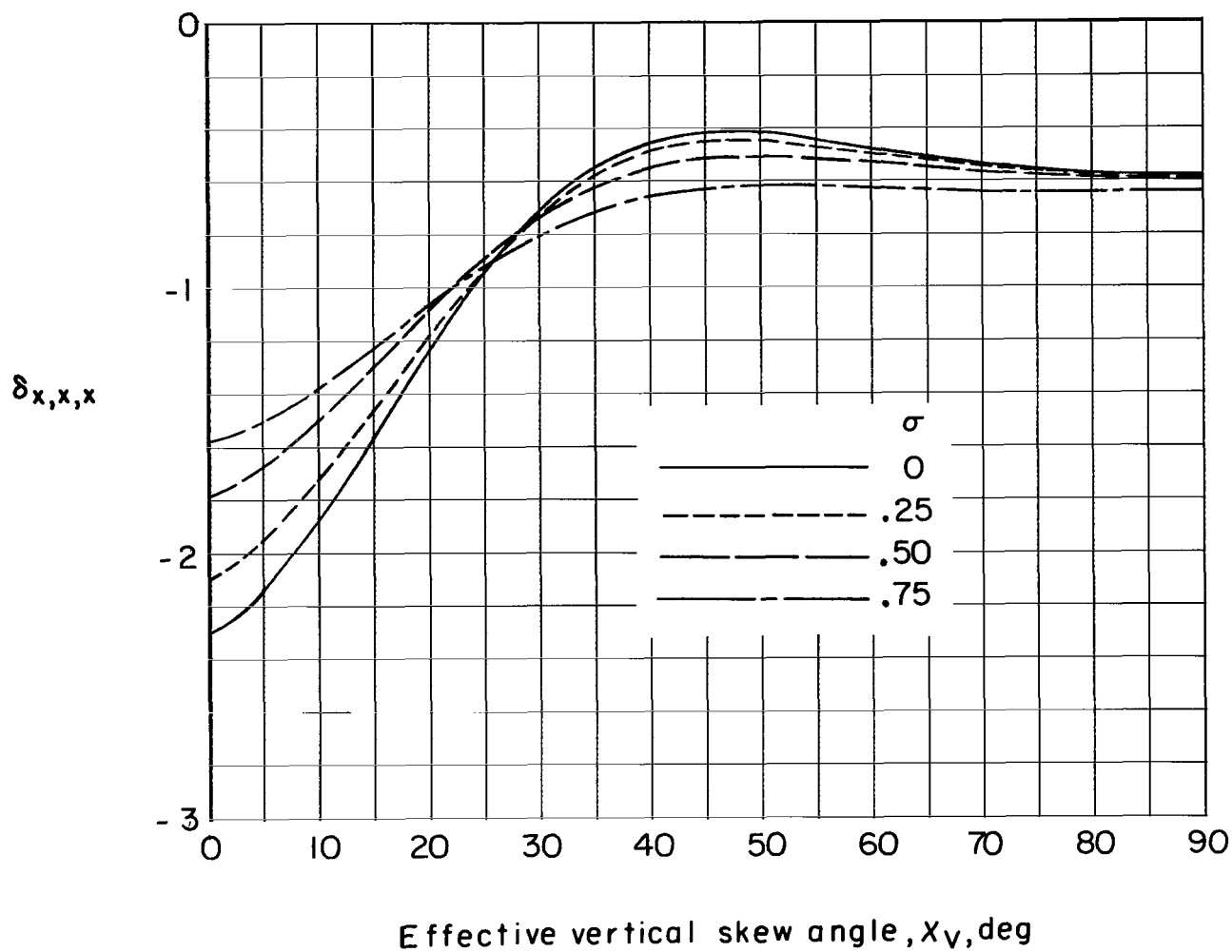


(d) $\delta_{z,x}$.



(e) $\delta_{z,z}$.

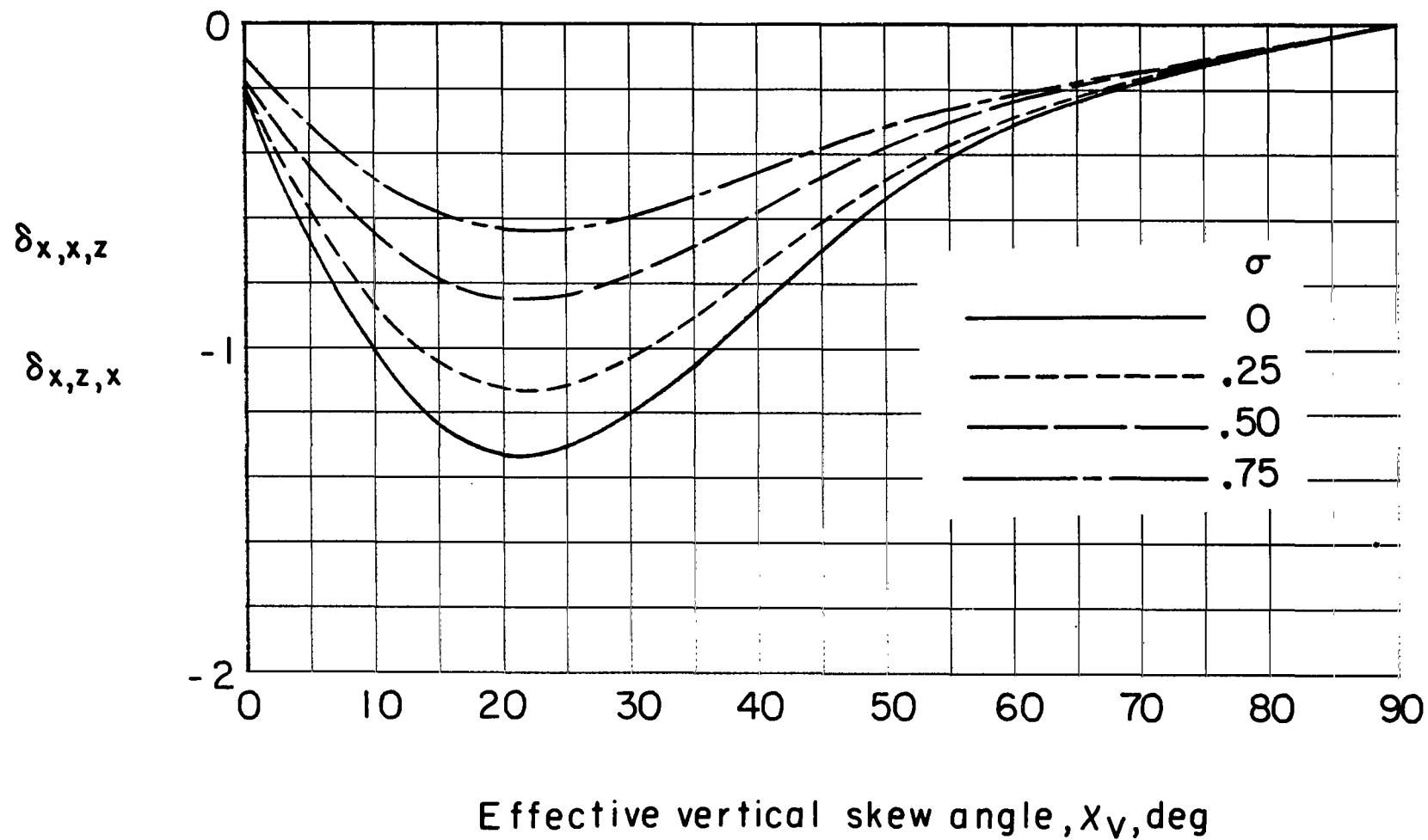
Figure 37.- Concluded.



(a) $\delta_{x,x,x}$.

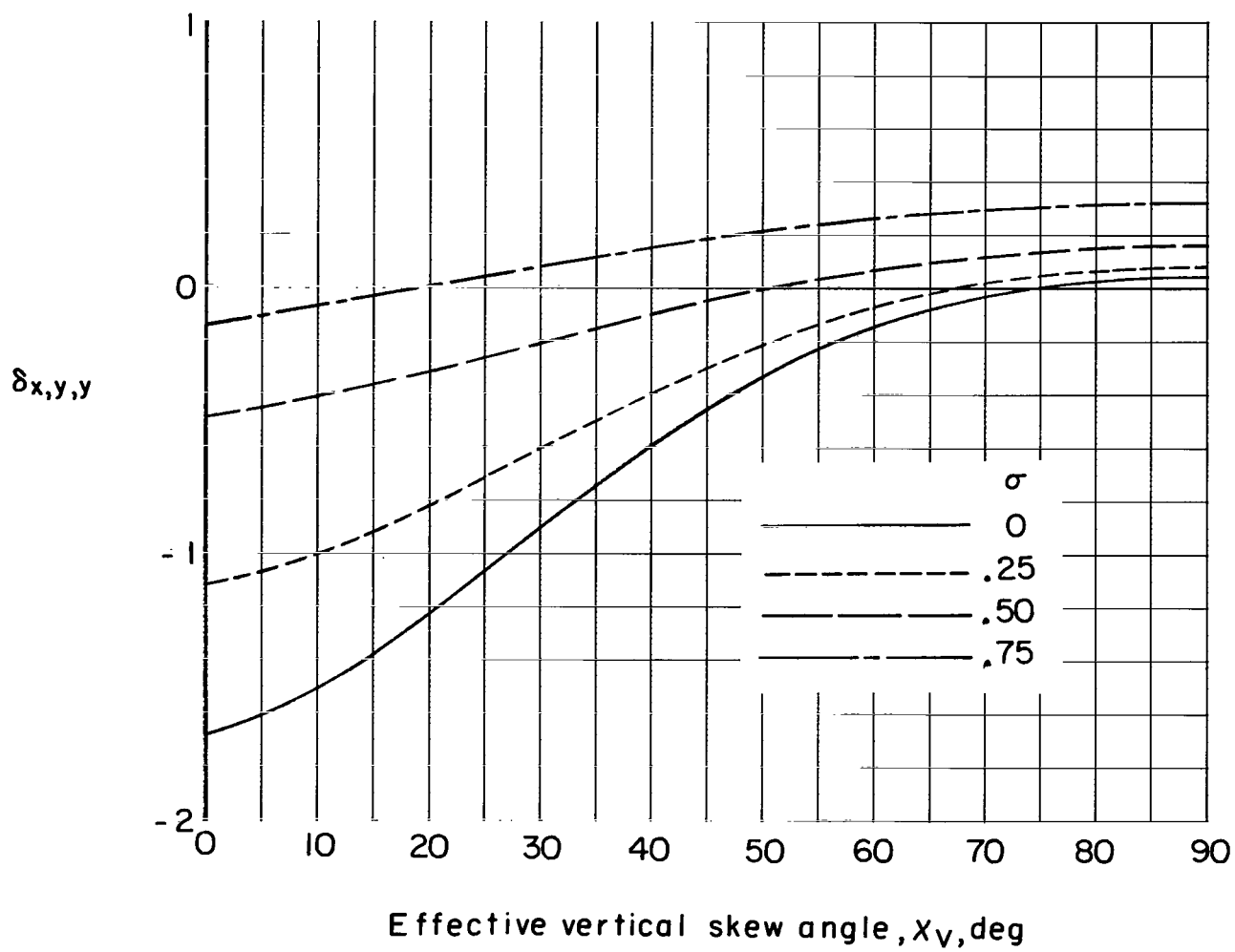
Figure 38.- Effect of span-width ratio σ on gradients of interference factors for unswept wings centered in a closed tunnel having a width-height ratio γ of 1.5. $X_H = 90^\circ$. Note that

$$\delta_{x,x,y} = \delta_{x,y,x} = \delta_{x,y,z} = \delta_{x,z,y} = \delta_{y,x,x} = \delta_{y,x,z} = \delta_{y,y,y} = \delta_{y,z,x} = \delta_{y,z,z} = \delta_{z,x,y} = \delta_{z,y,x} = \delta_{z,y,z} = \delta_{z,z,y} = 0.$$



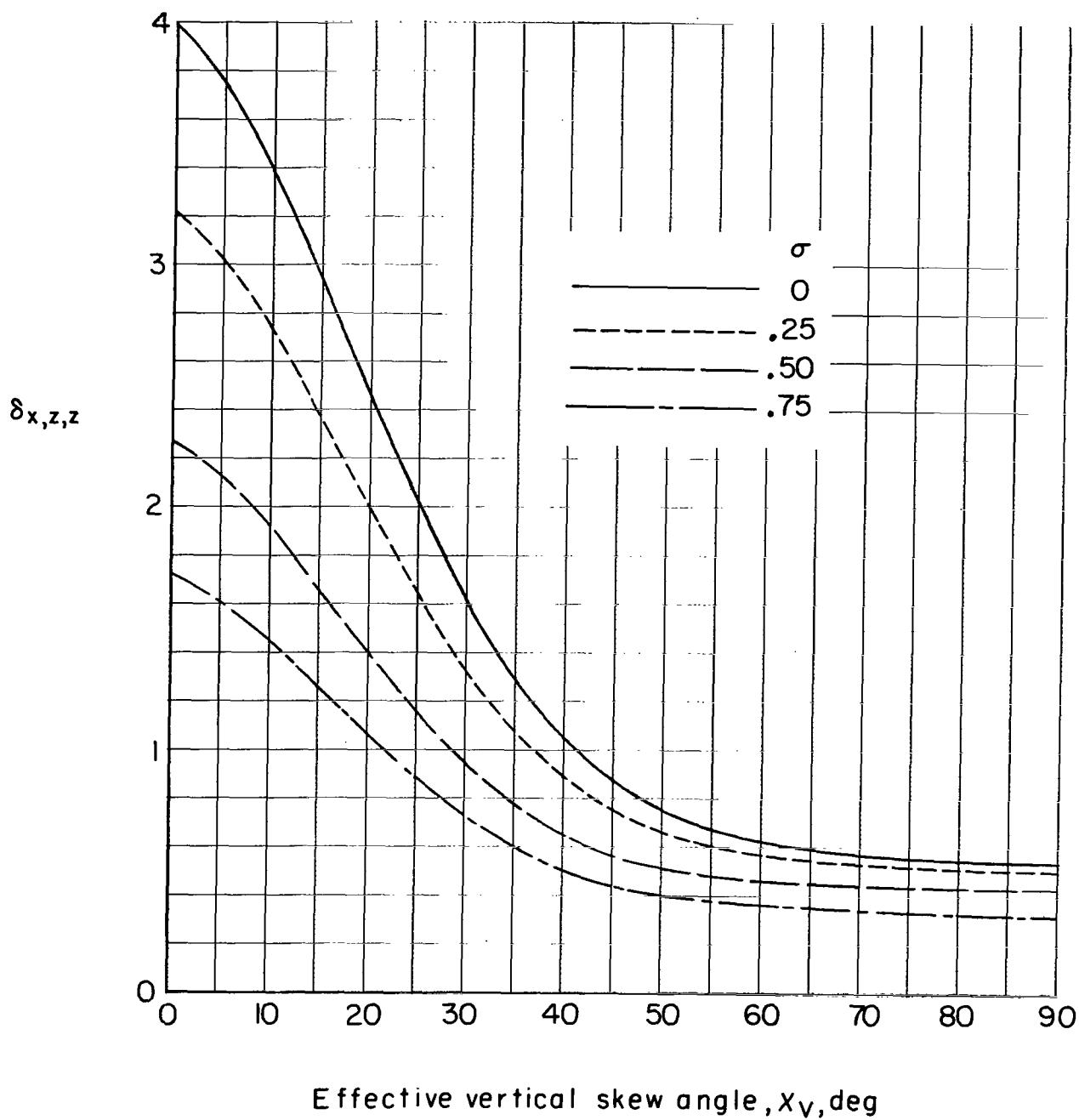
(b) $\delta_{x,x,z} = \delta_{x,z,x}$.

Figure 38.- Continued.



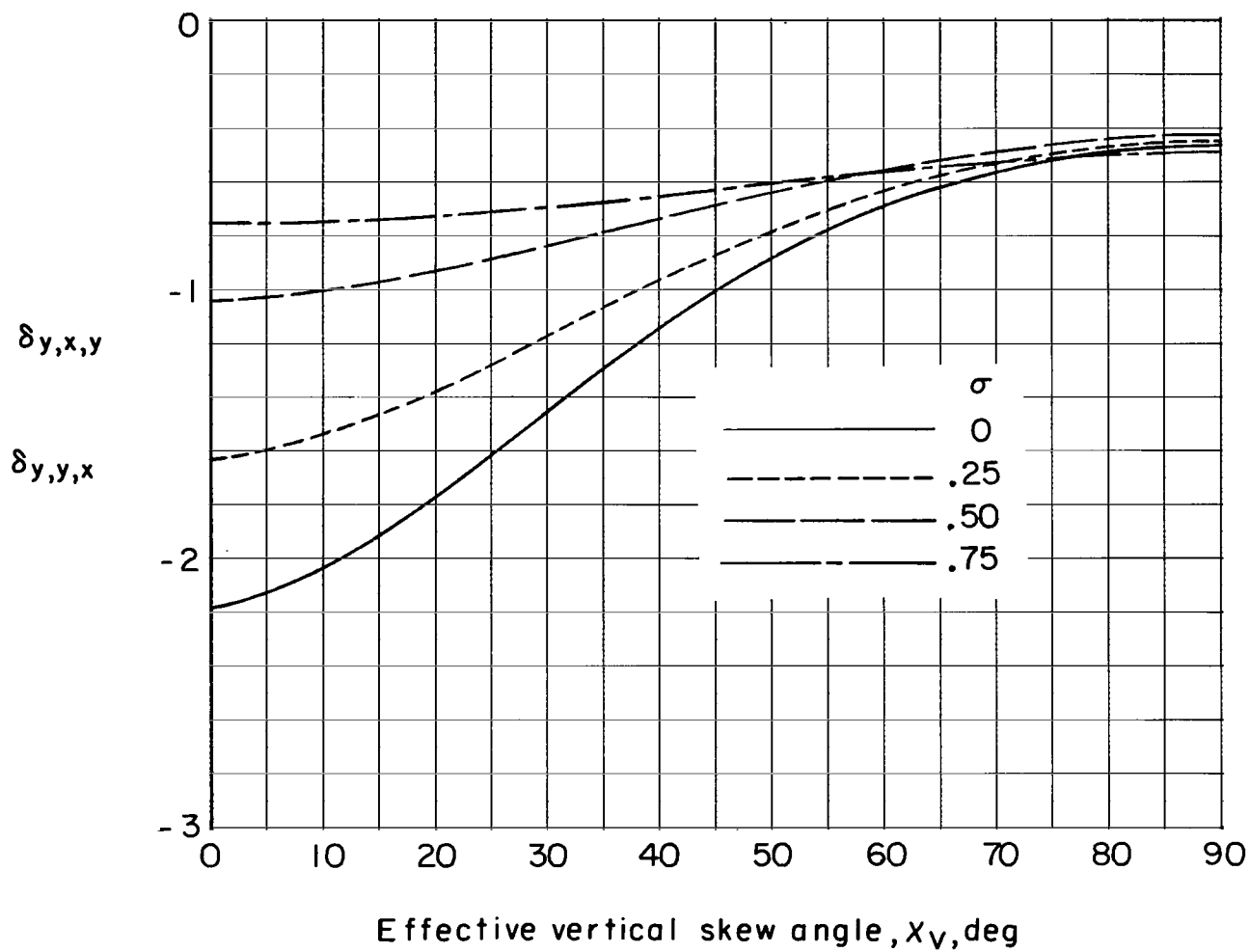
(c) $\delta_{x,y,y}$.

Figure 38.- Continued.



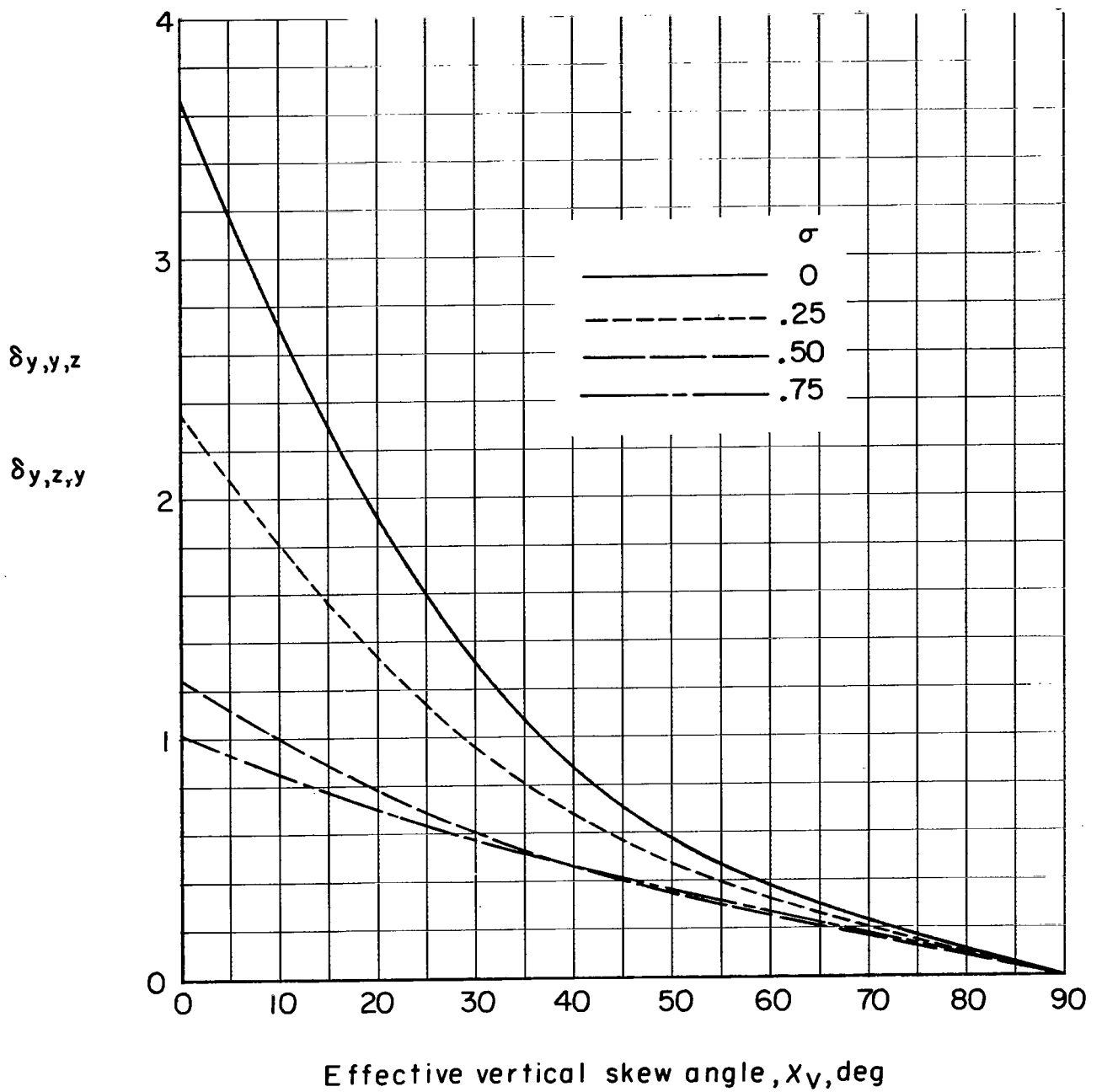
(d) $\delta_{x,z,z}$.

Figure 38.- Continued.



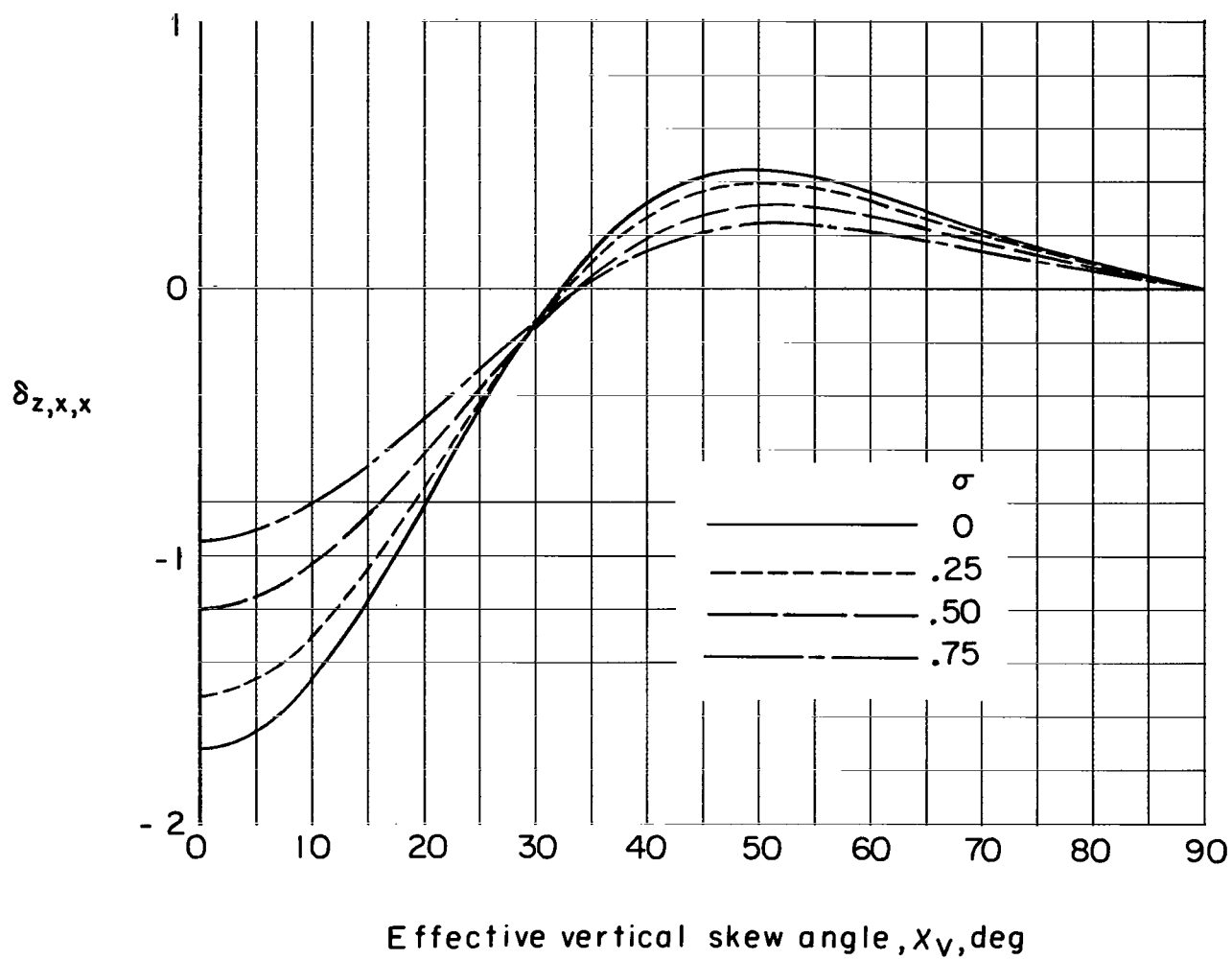
(e) $\delta_{y,x,y} = \delta_{y,y,x}$.

Figure 38.- Continued.



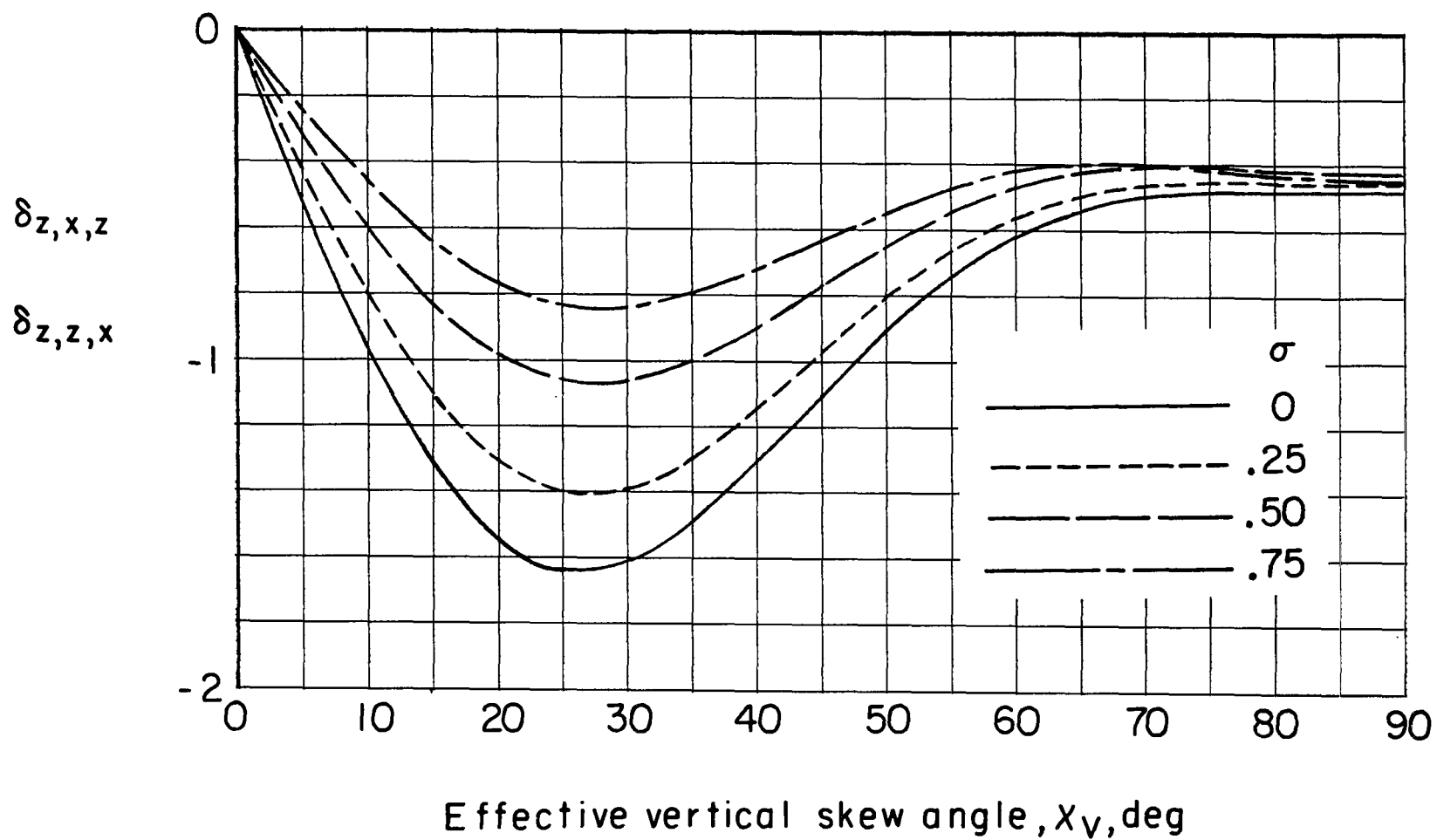
(f) $\delta_{y,y,z} = \delta_{y,z,y}$.

Figure 38.- Continued.



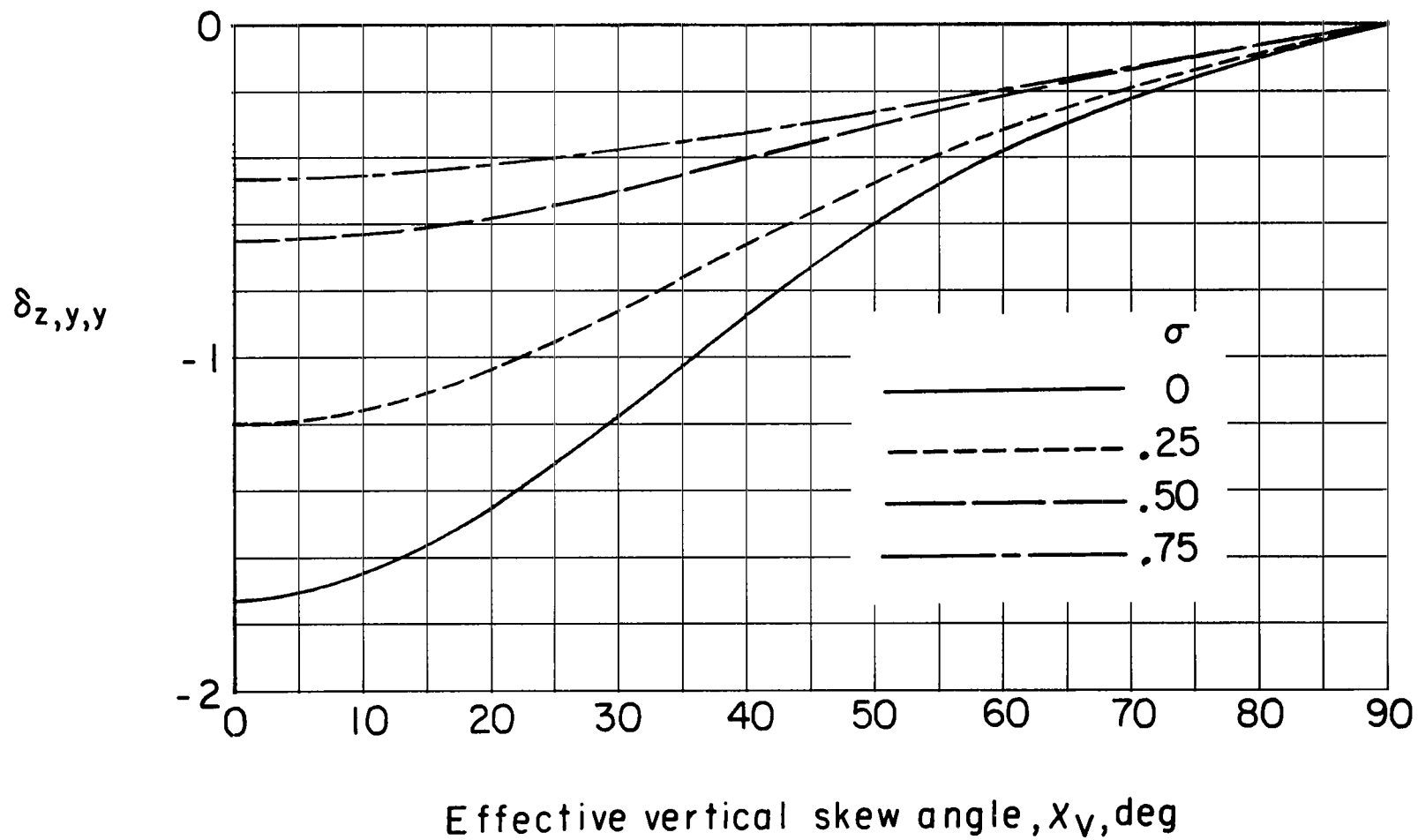
(g) $\delta_{z,x,x}$.

Figure 38.- Continued.



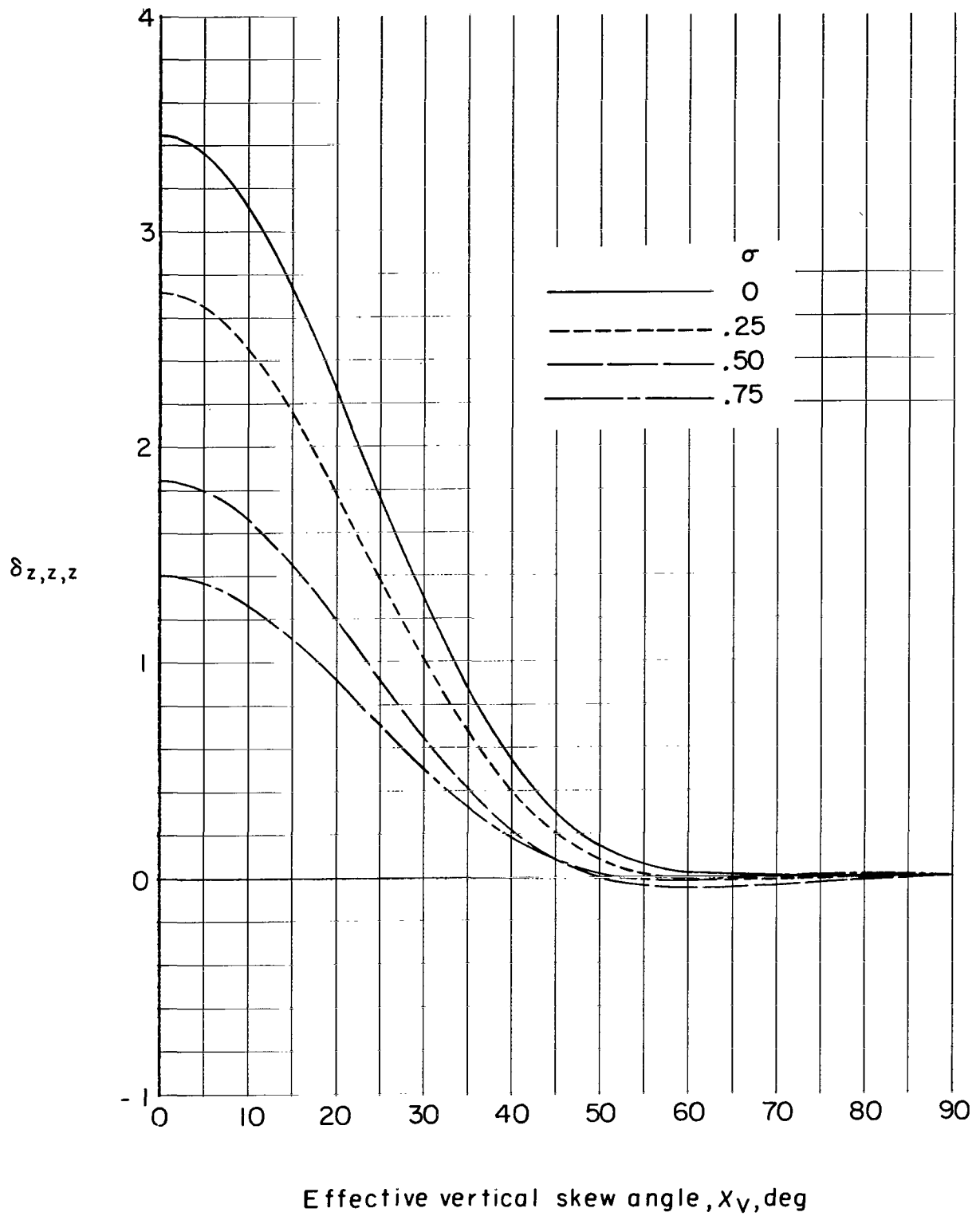
(h) $\delta_{z,x,z} = \delta_{z,z,x}$.

Figure 38.- Continued.



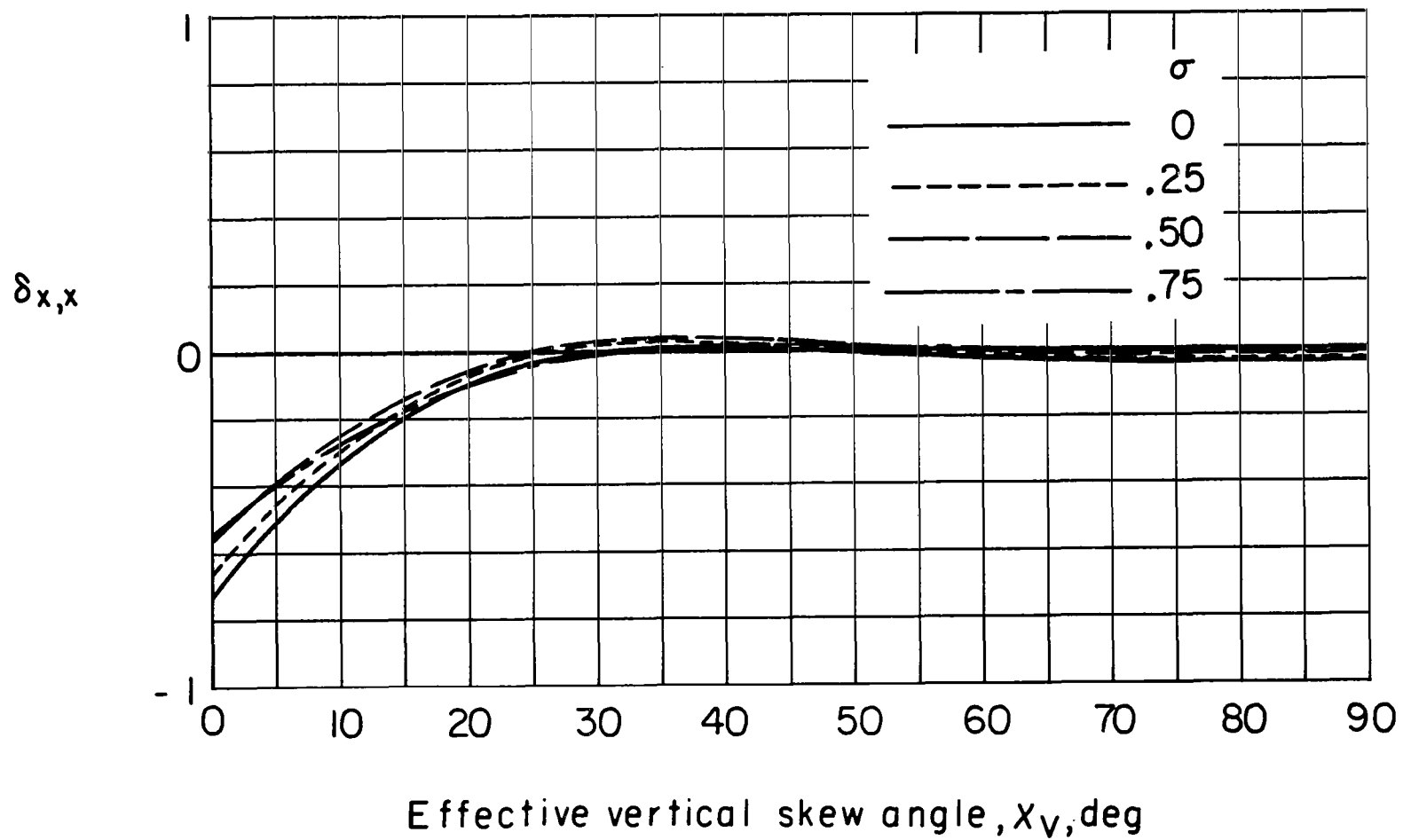
(i) $\delta_{z,y,y}$.

Figure 38.- Continued.



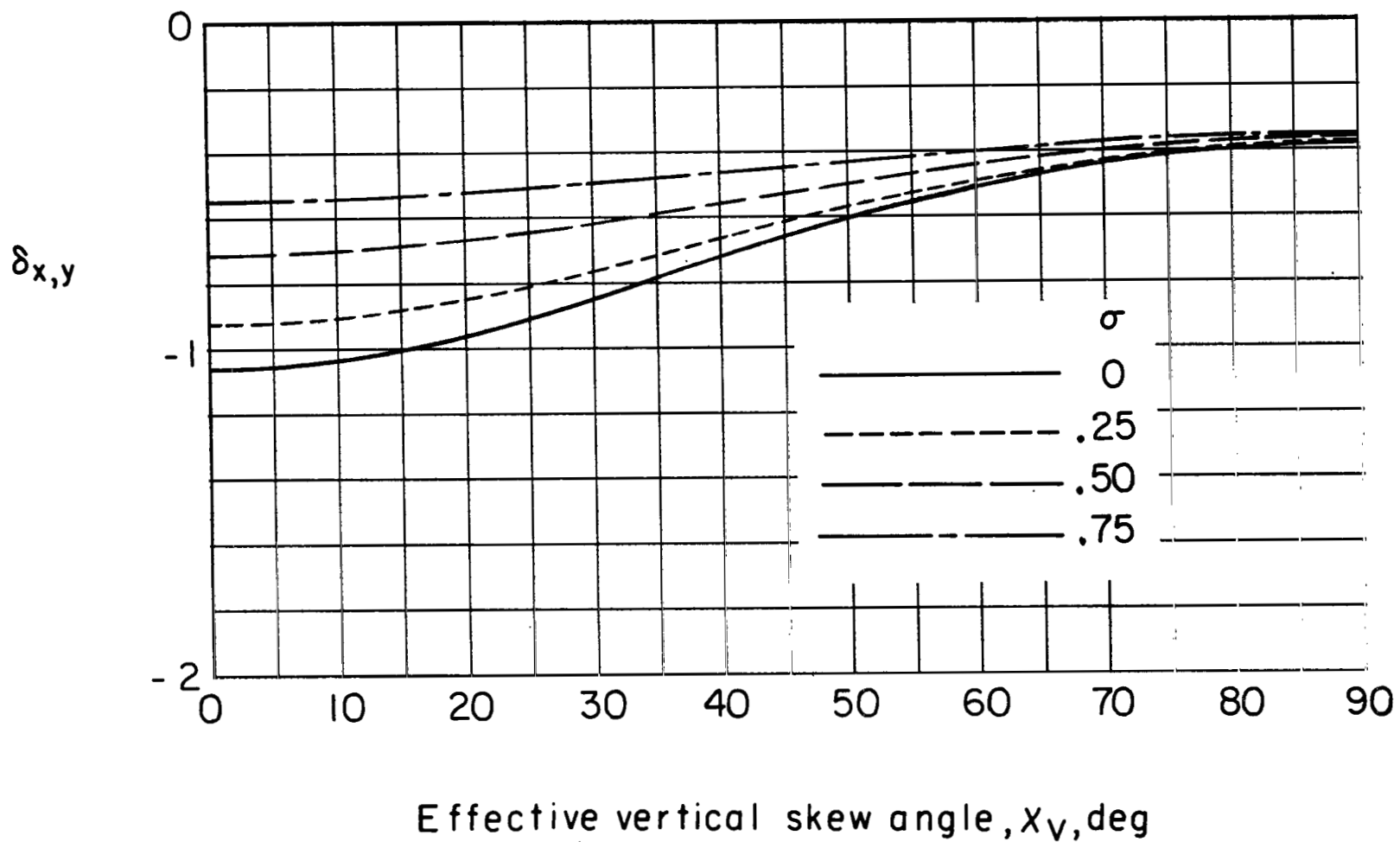
(j) $\delta_{z,z,z}$.

Figure 38.- Concluded.



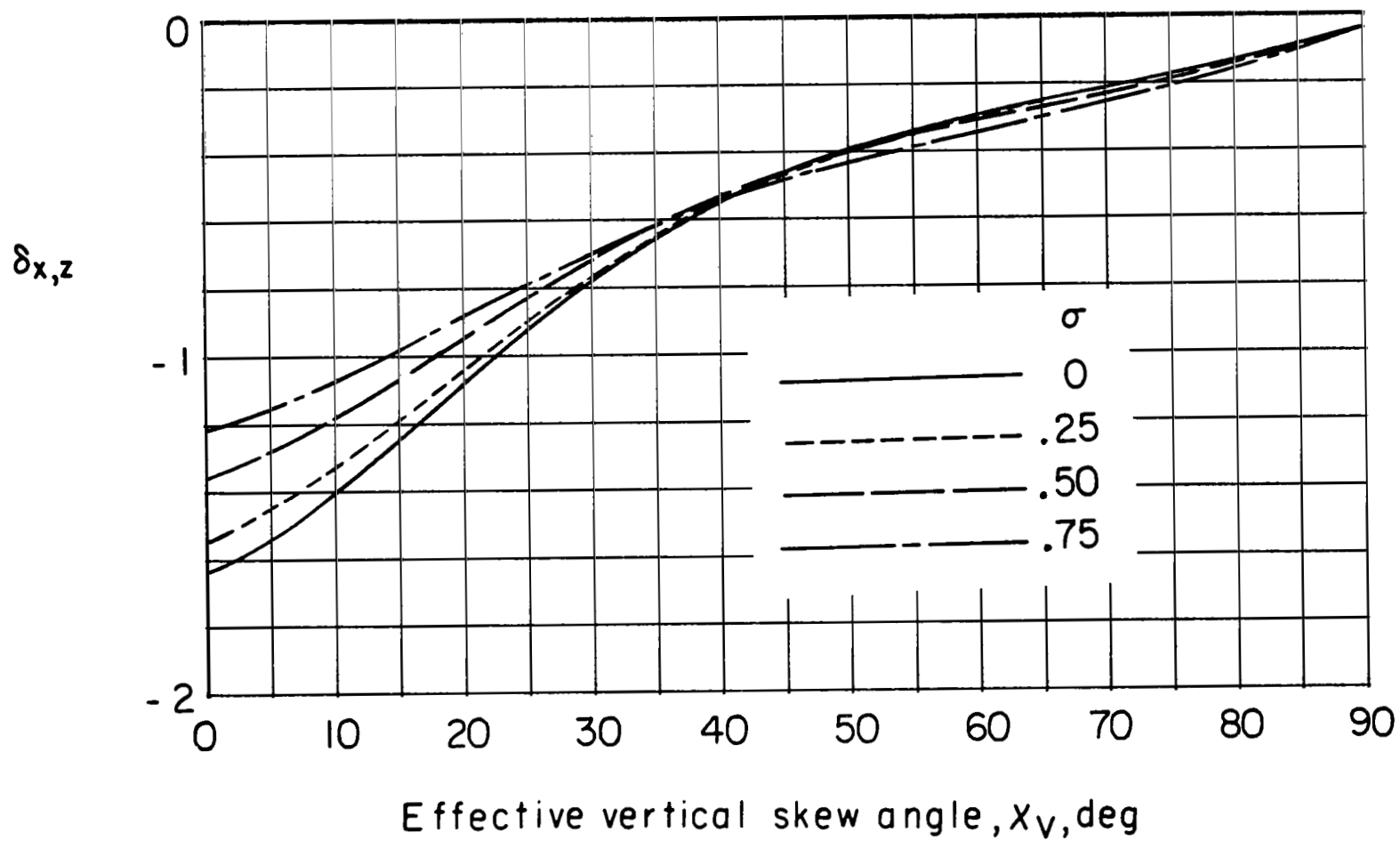
(a) $\delta_{x,x}$.

Figure 39.- Effect of span-width ratio σ on interference velocity factors for unswept wings centered in a closed tunnel having a width-height ratio γ of 1.5. $X_H = 60^\circ$.



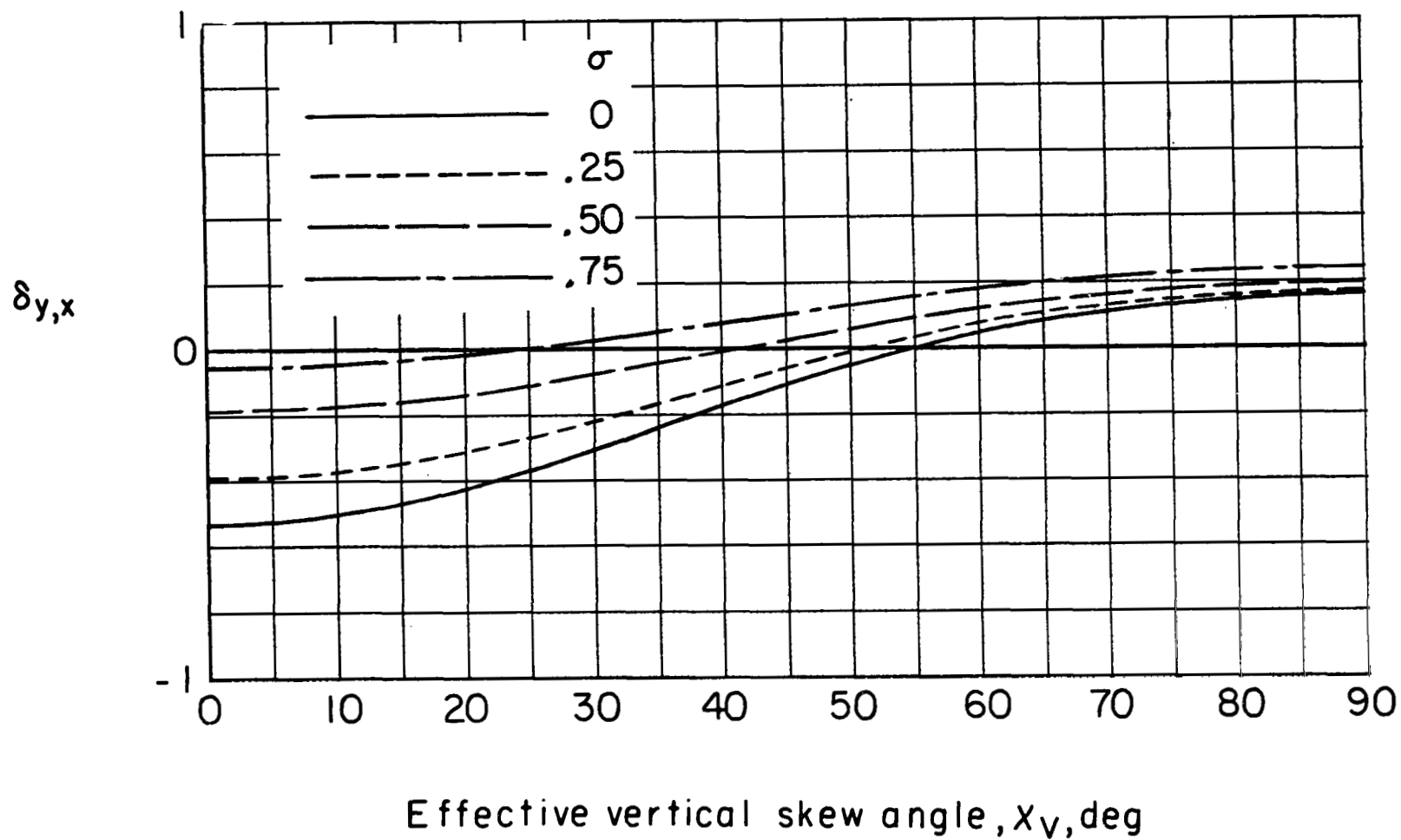
(b) $\delta_{x,y}$.

Figure 39.- Continued.



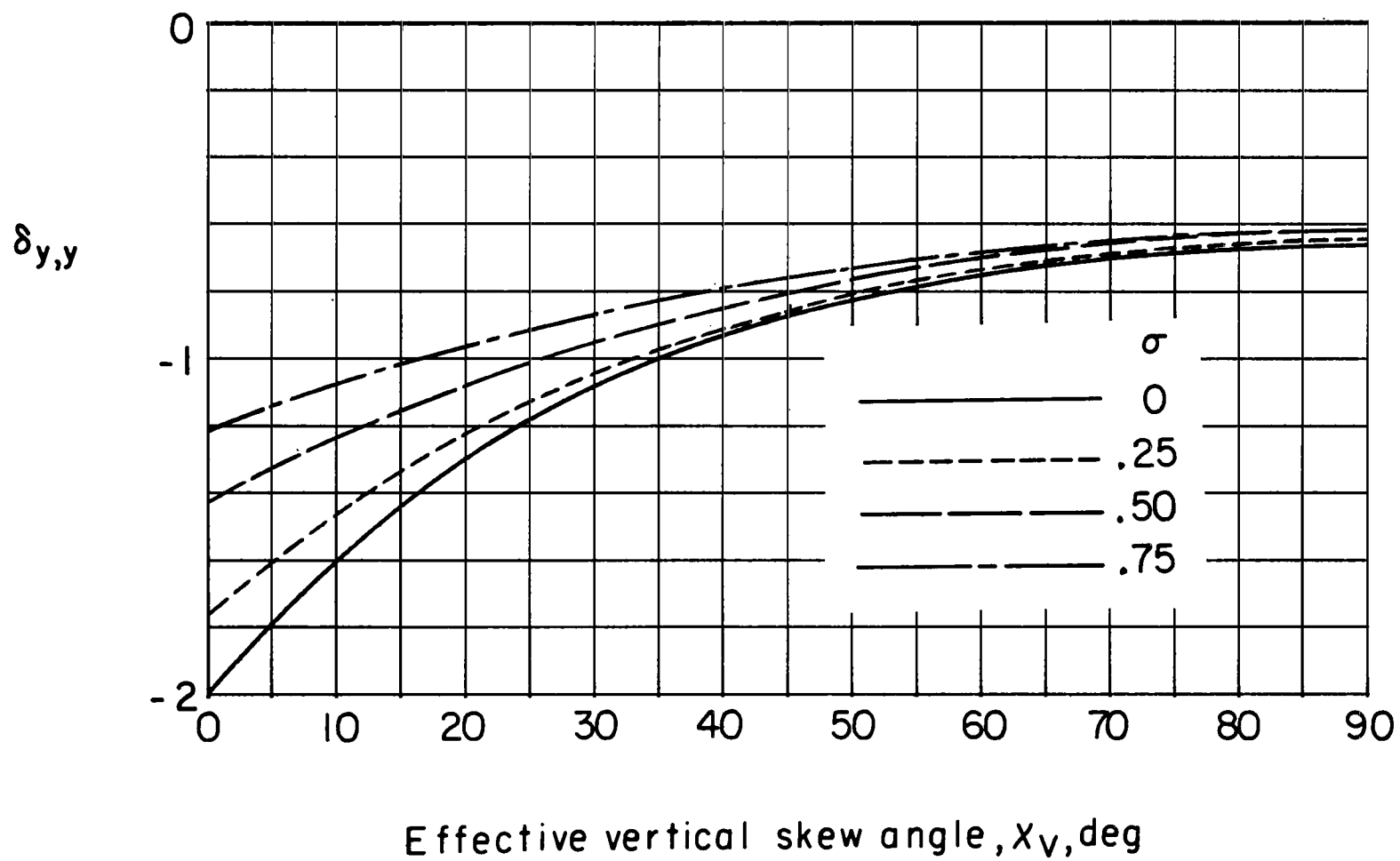
(c) $\delta_{x,z}$.

Figure 39.- Continued.



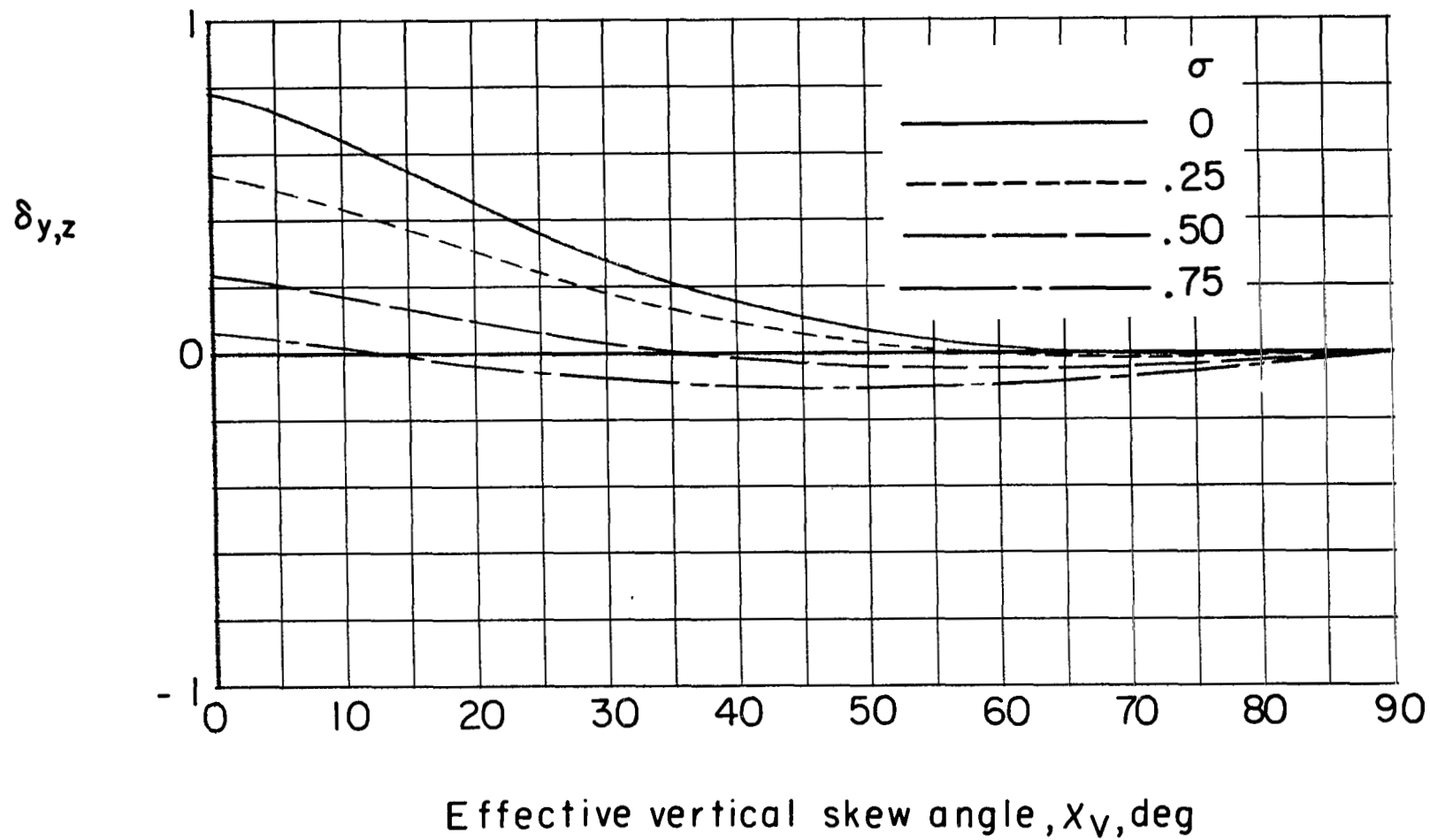
(d) $\delta_{y,x}$

Figure 39.- Continued.



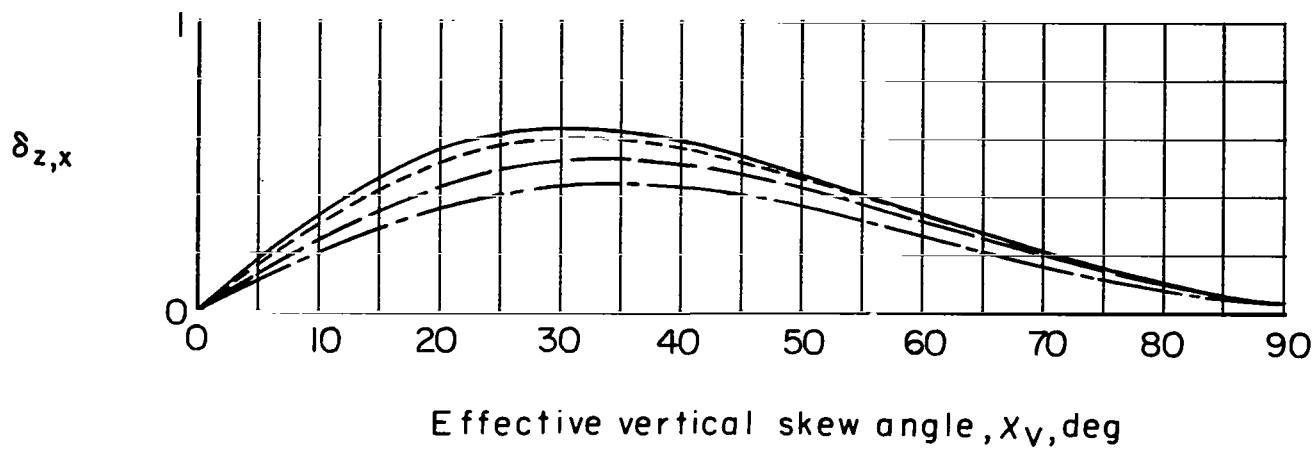
(e) $\delta_{y,y}$.

Figure 39.- Continued.

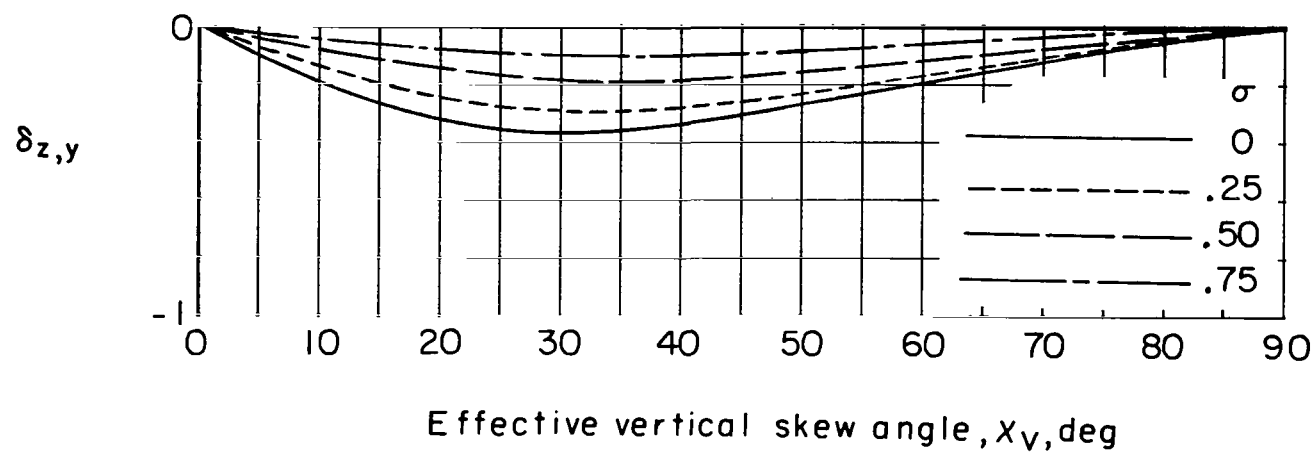


(f) $\delta_{y,z}$

Figure 39.- Continued.



(g) $\delta_{z,x}$.



(h) $\delta_{z,y}$.

Figure 39.- Continued.

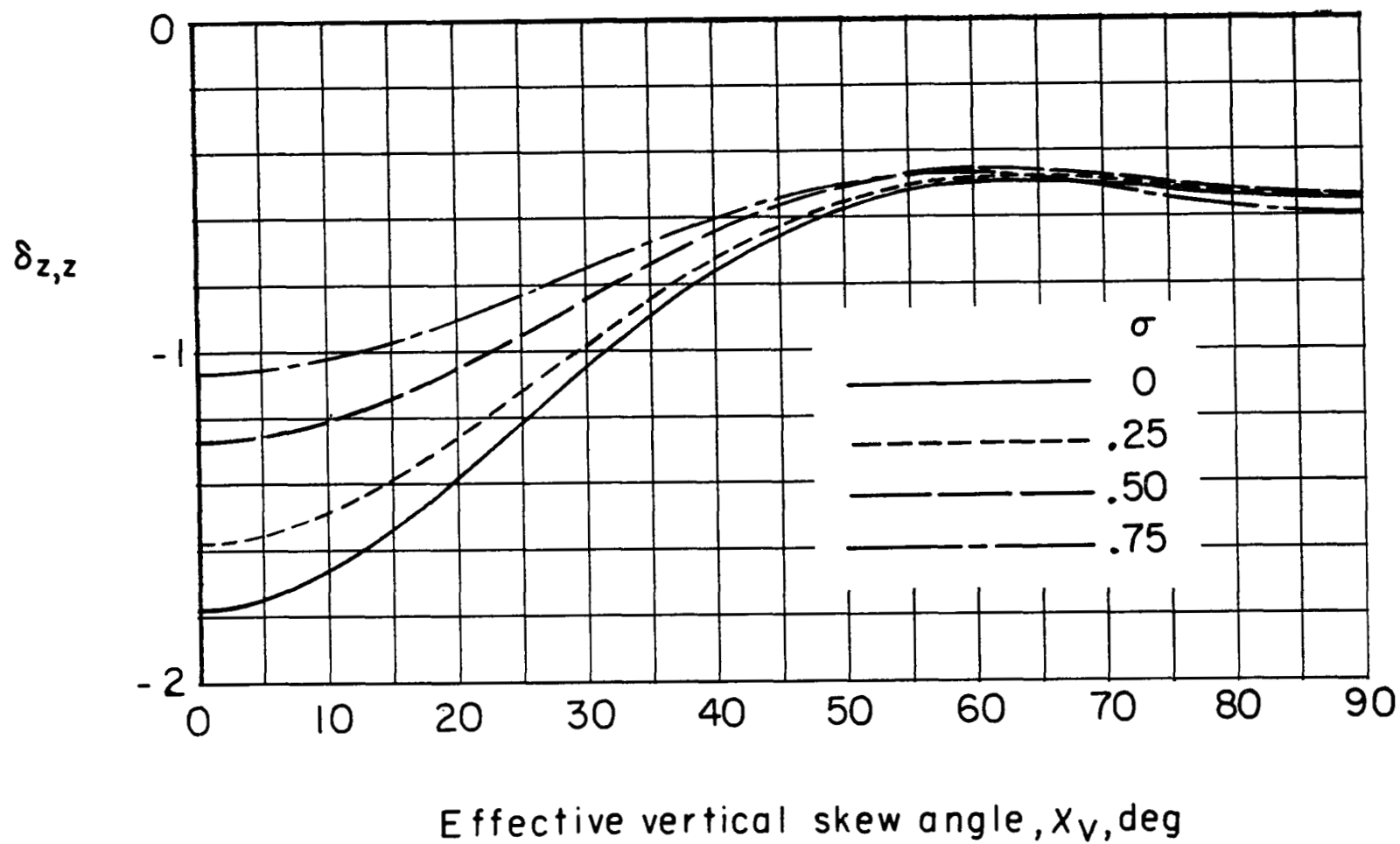
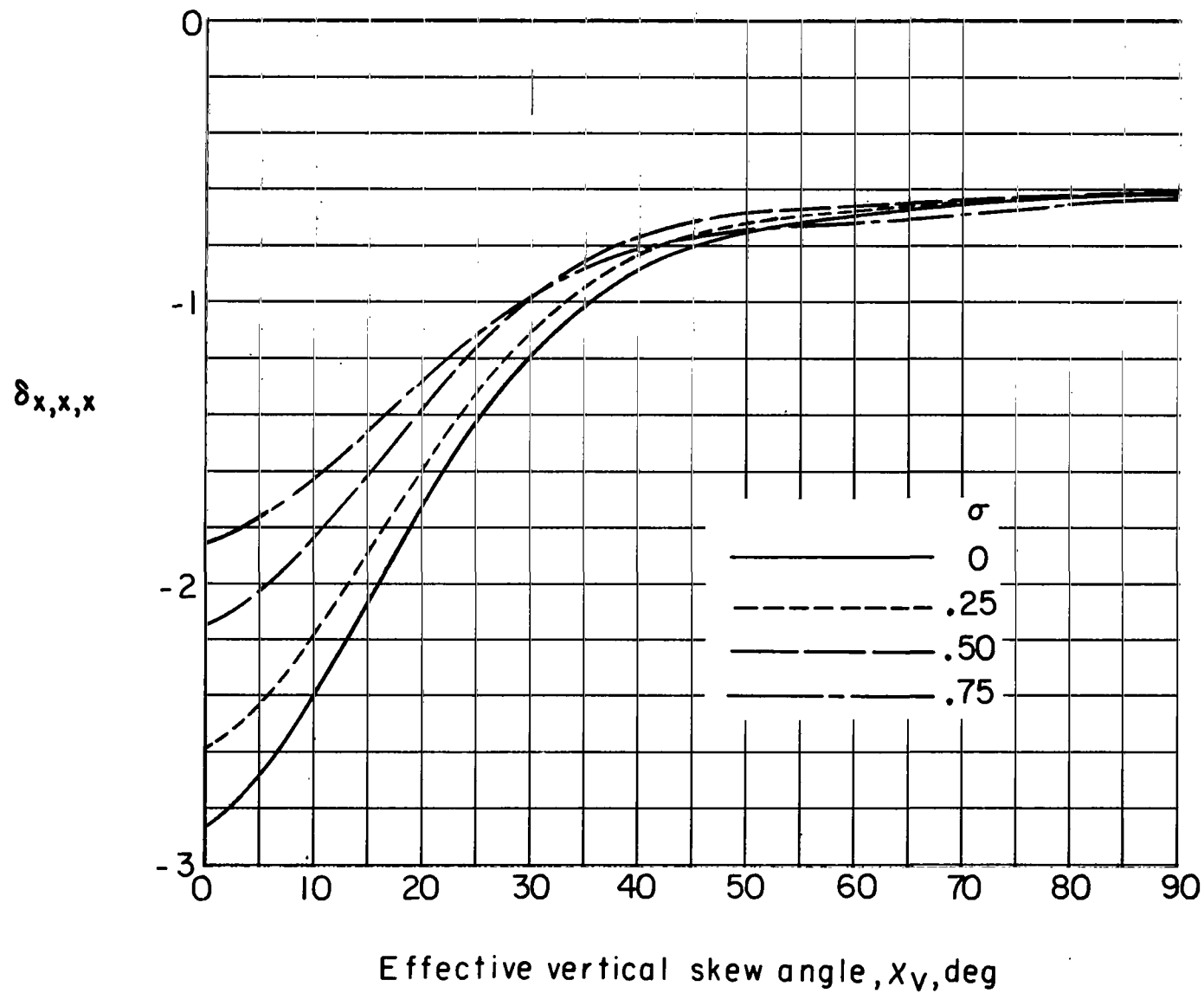
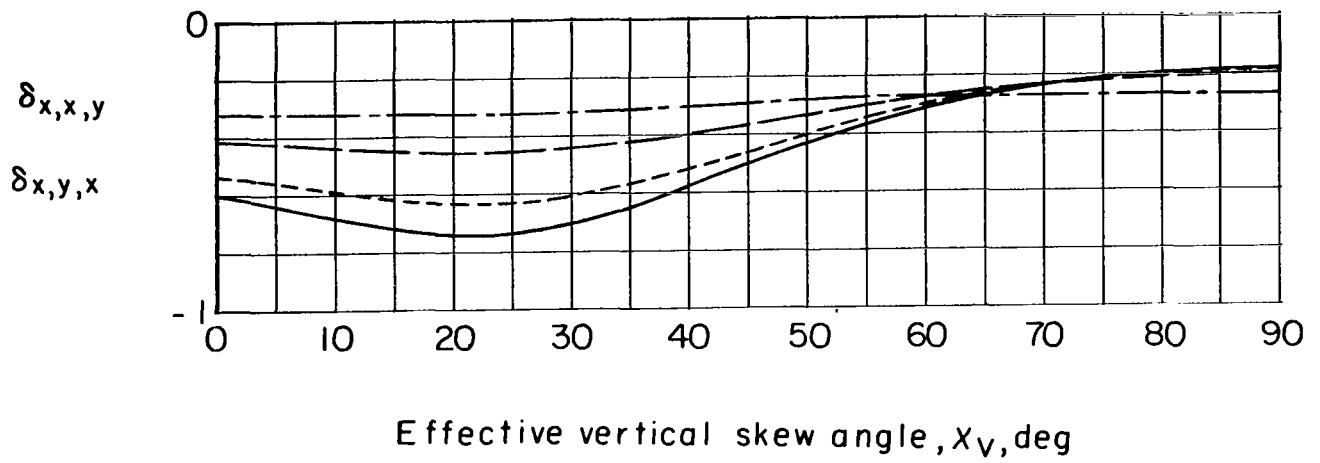
(i) $\delta_{z,z}$.

Figure 39.- Concluded.

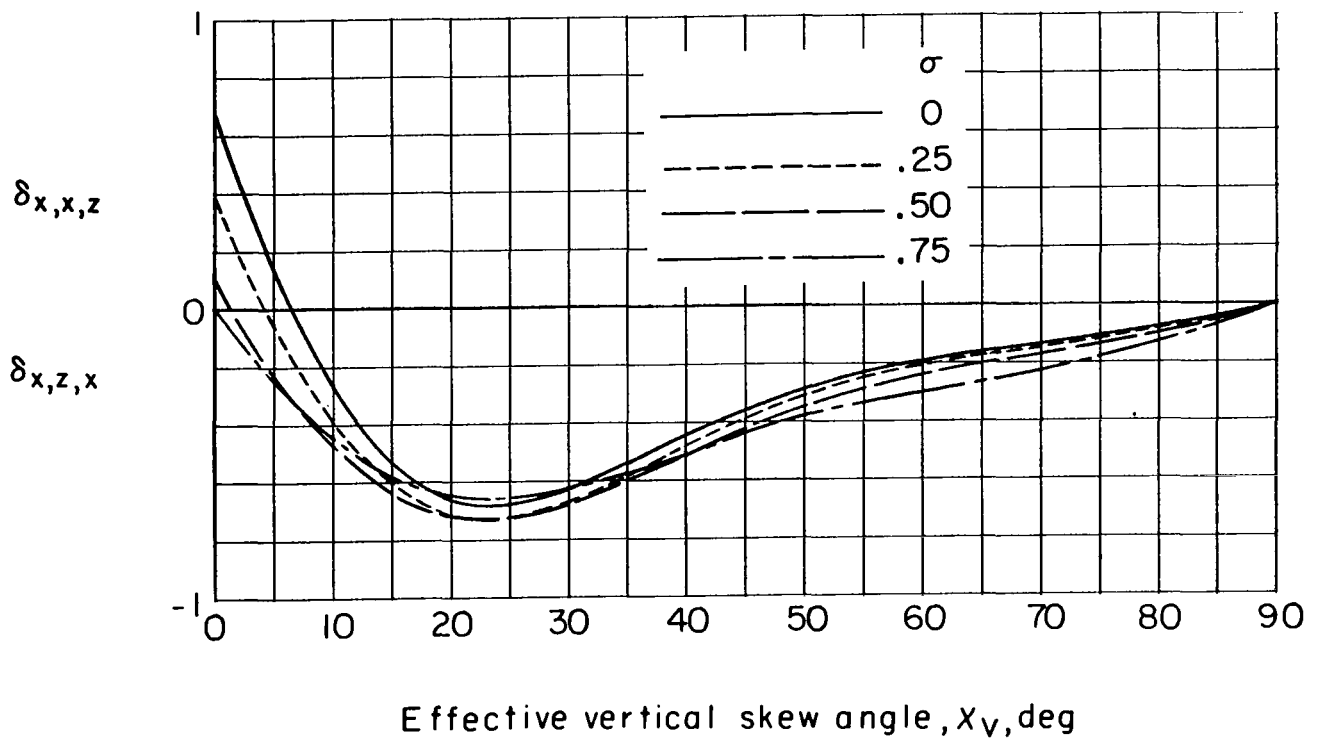


(a) $\delta_{x,x,x}$.

Figure 40.- Effect of span-width ratio σ on gradients of interference factors for unswept wings centered in a closed tunnel having a width-height ratio γ of 1.5. $\chi_H = 60^\circ$.

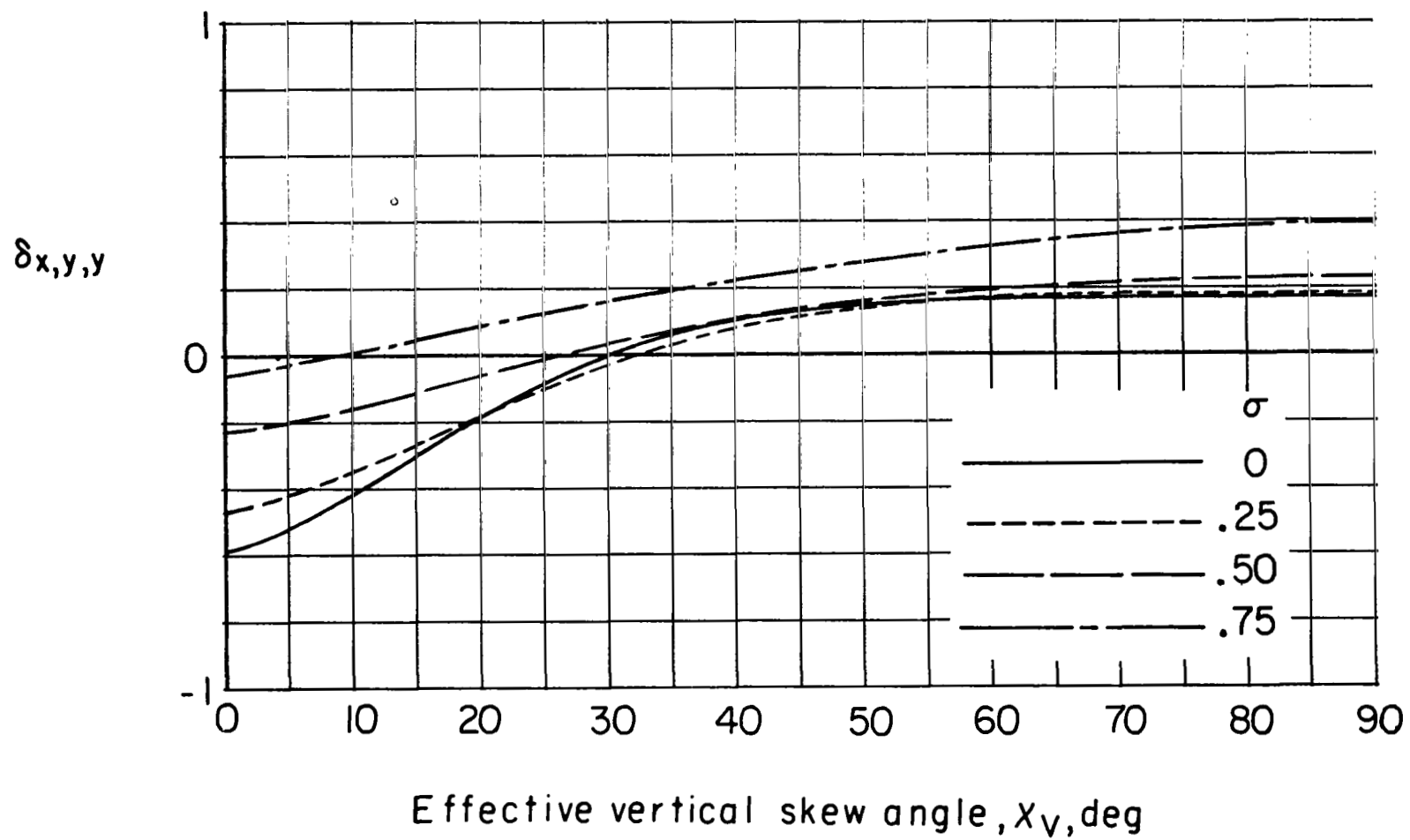


$$(b) \delta_{x,x,y} = \delta_{x,y,x}.$$



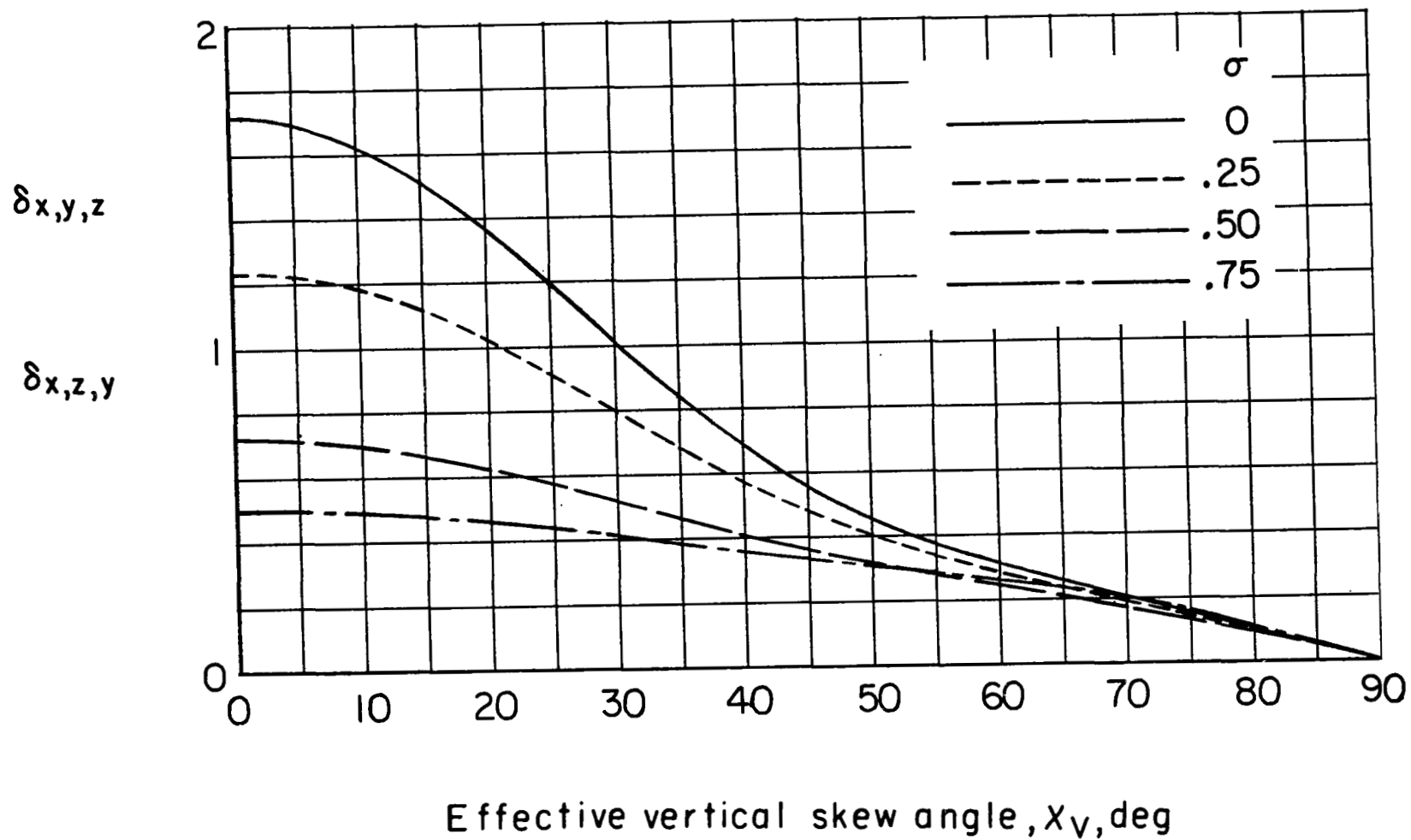
$$(c) \delta_{x,x,z} = \delta_{x,z,x}.$$

Figure 40.- Continued.



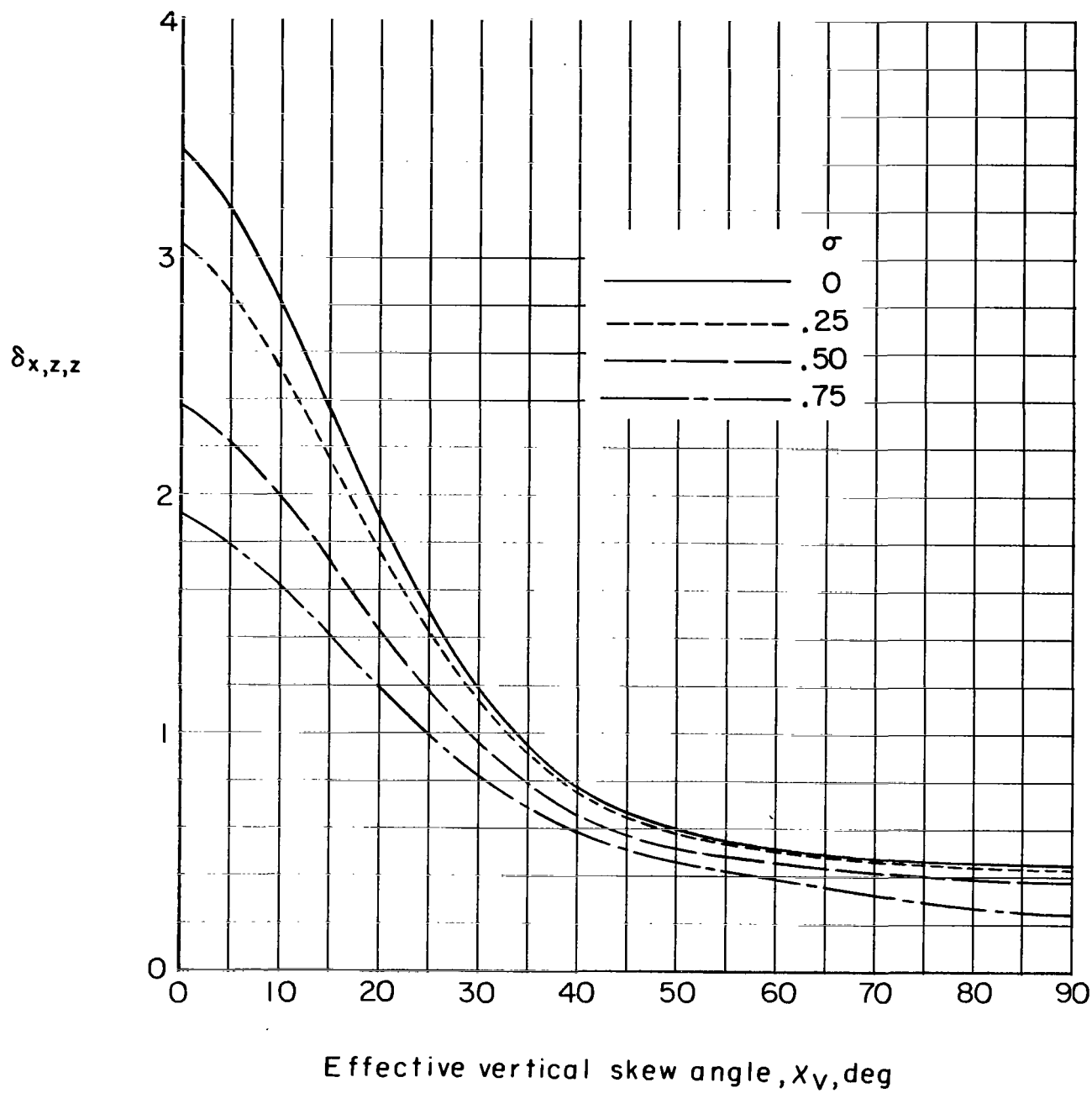
(d) $\delta_{x,y,y}$.

Figure 40.- Continued.



$$(e) \delta_{x,y,z} = \delta_{x,z,y}$$

Figure 40.- Continued.



(f) $\delta_{x,z,z}$.

Figure 40.- Continued.

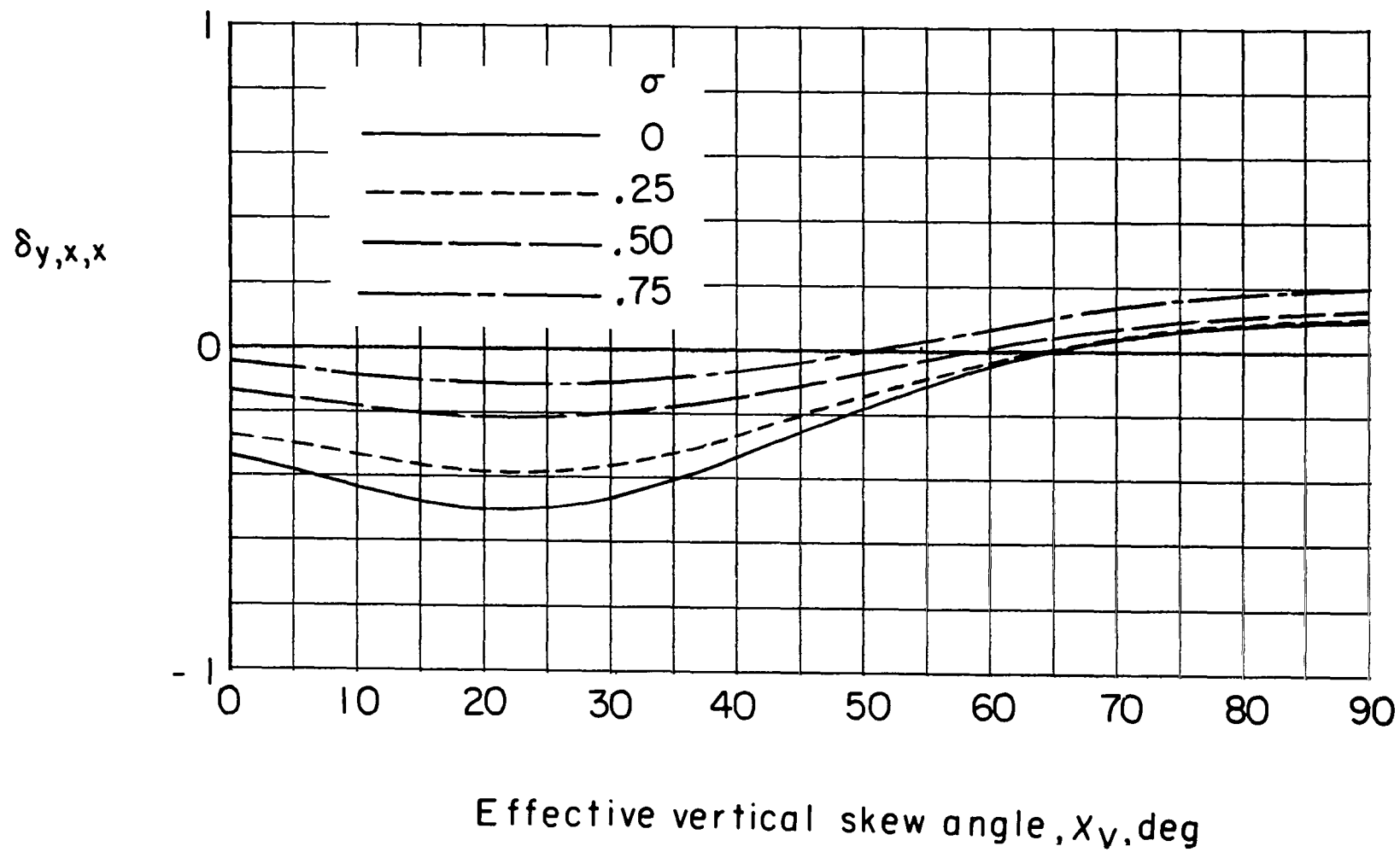
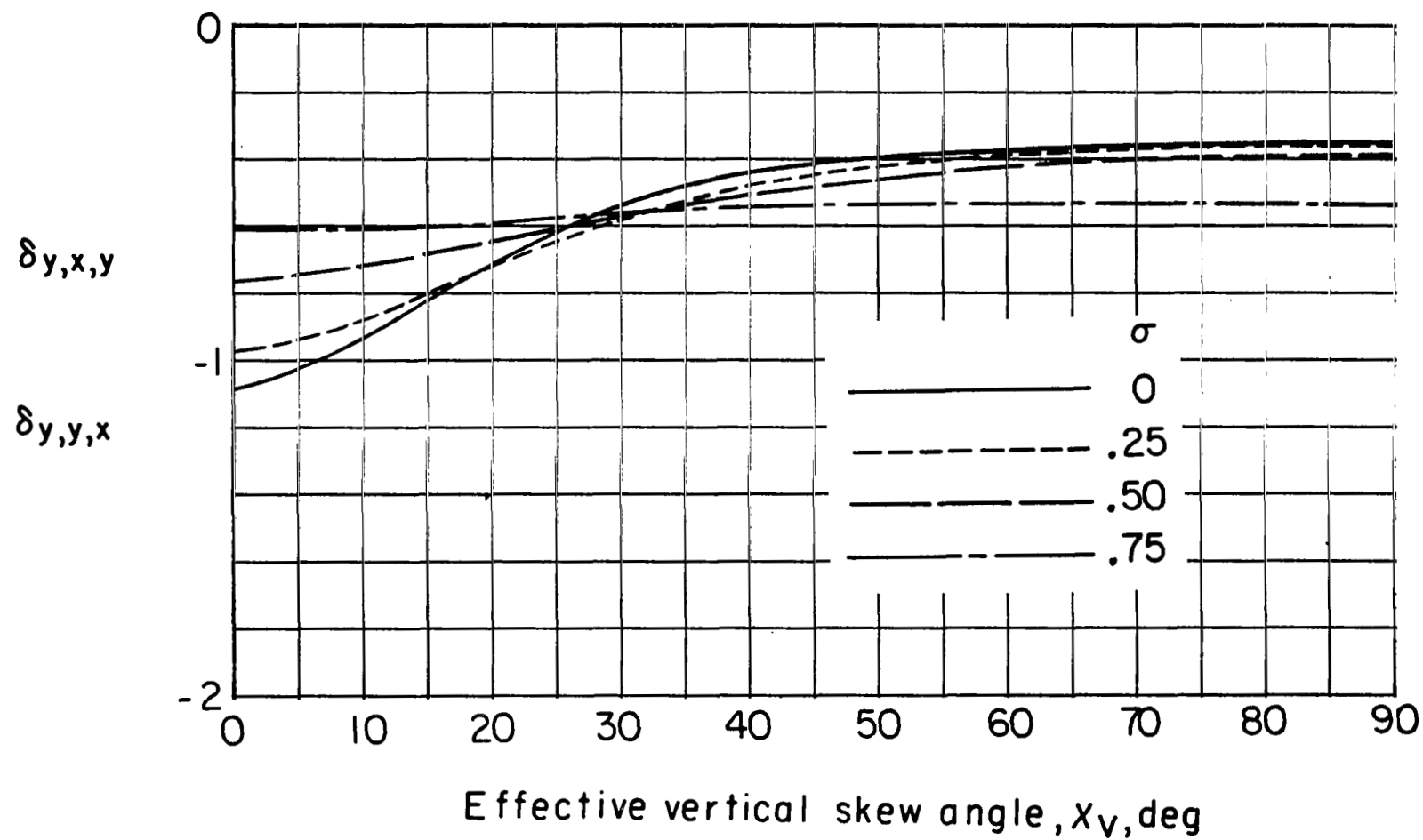
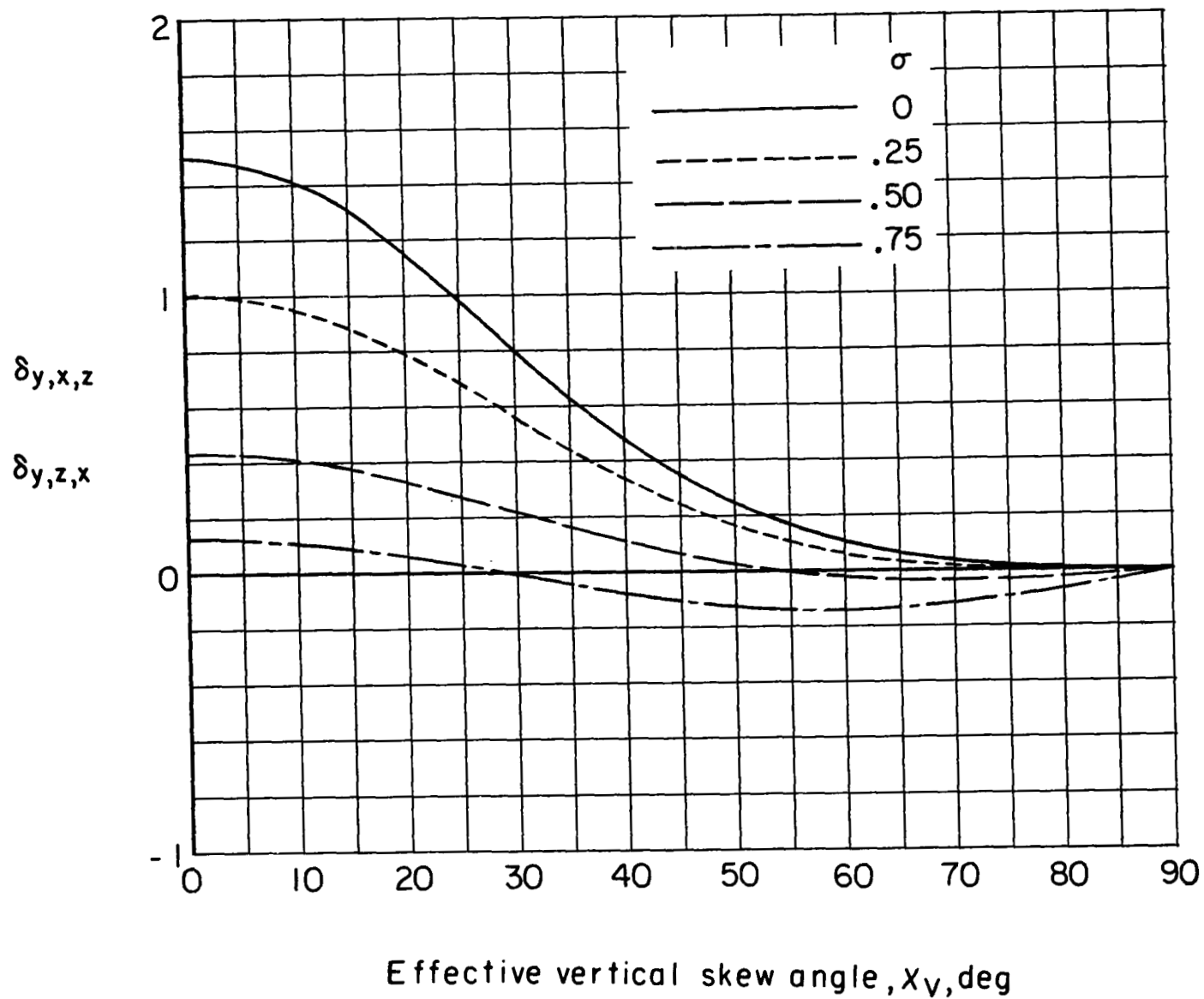
(g) $\delta_{y,x,x}$.

Figure 40.- Continued.



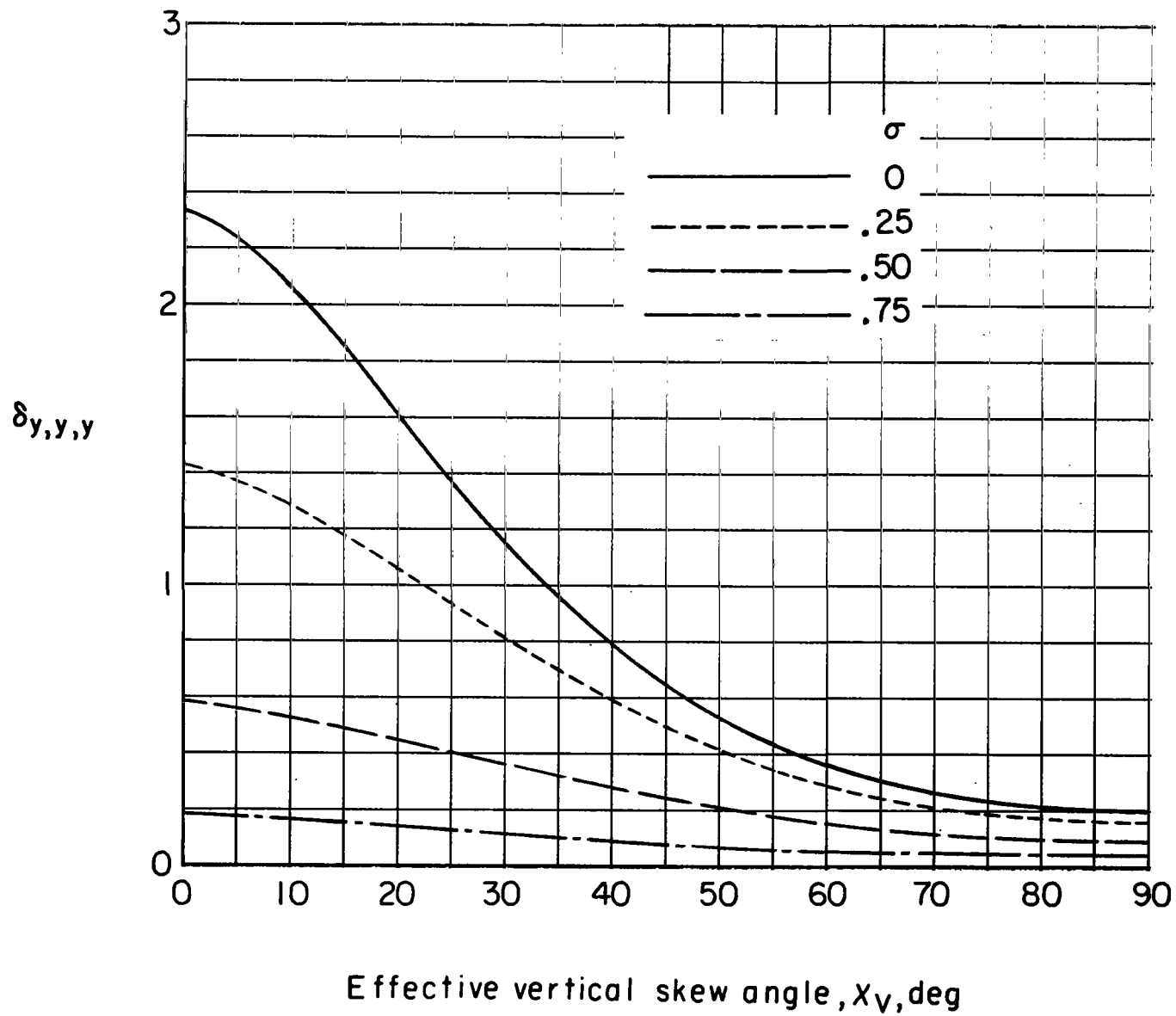
(h) $\delta_{y,x,y} = \delta_{y,y,x}$.

Figure 40.- Continued.



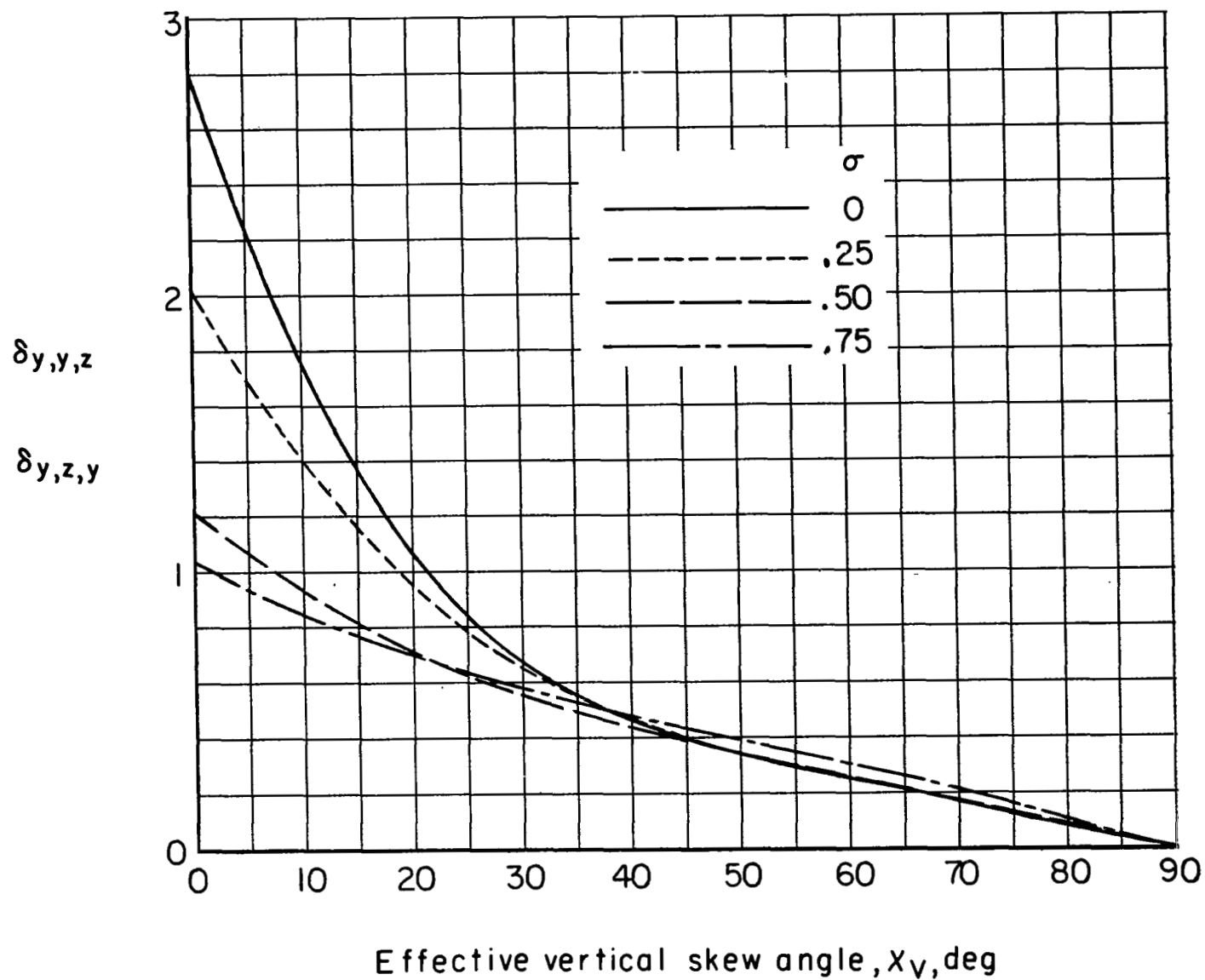
(i) $\delta_{y,x,z} = \delta_{y,z,x}$.

Figure 40.- Continued.



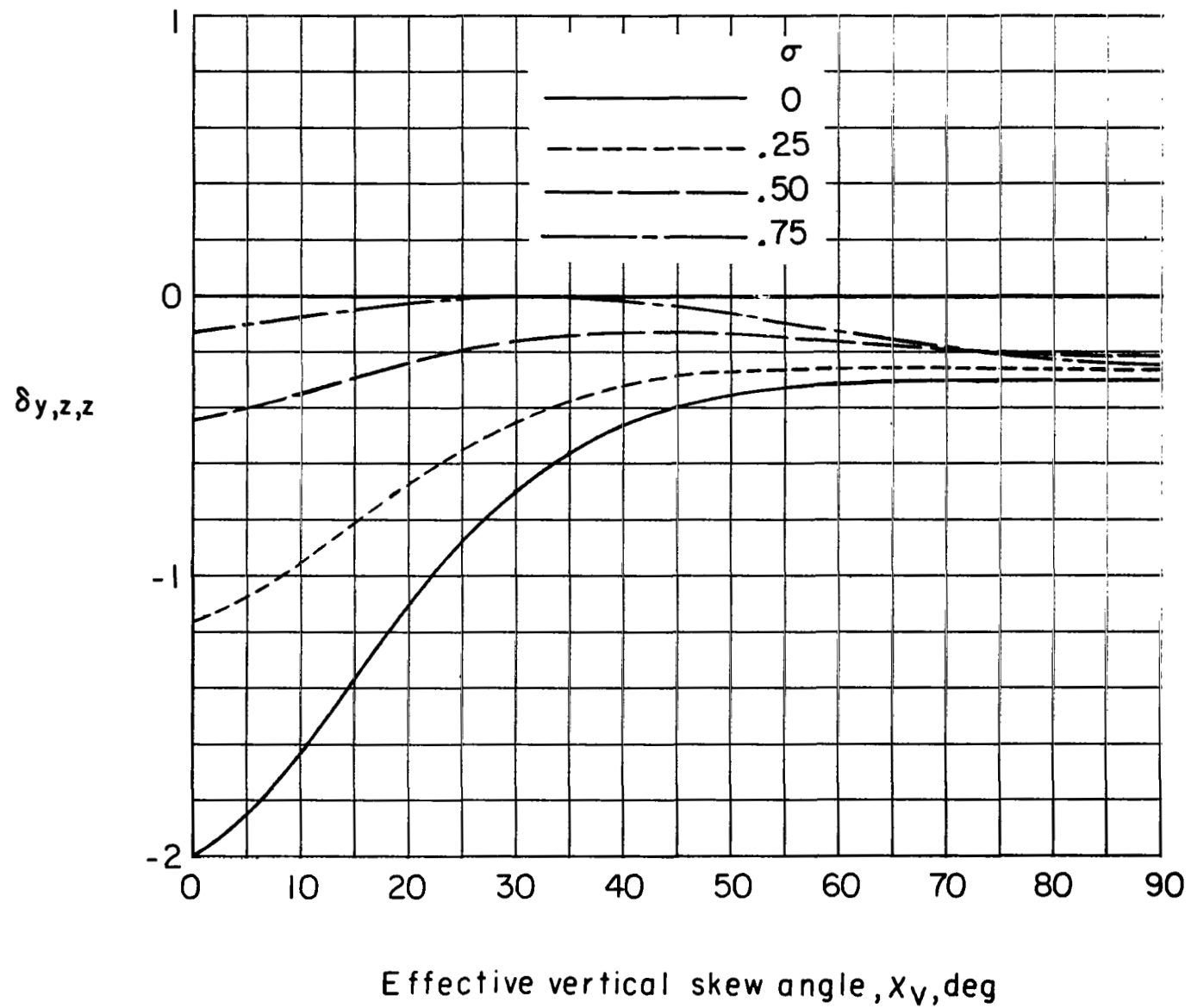
(j) $\delta_{y,y,y}$

Figure 40.- Continued.



(k) $\delta_{y,y,z} = \delta_{y,z,y}$.

Figure 40.- Continued.



(1) $\delta_{y,z,z}$.

Figure 40.- Continued.

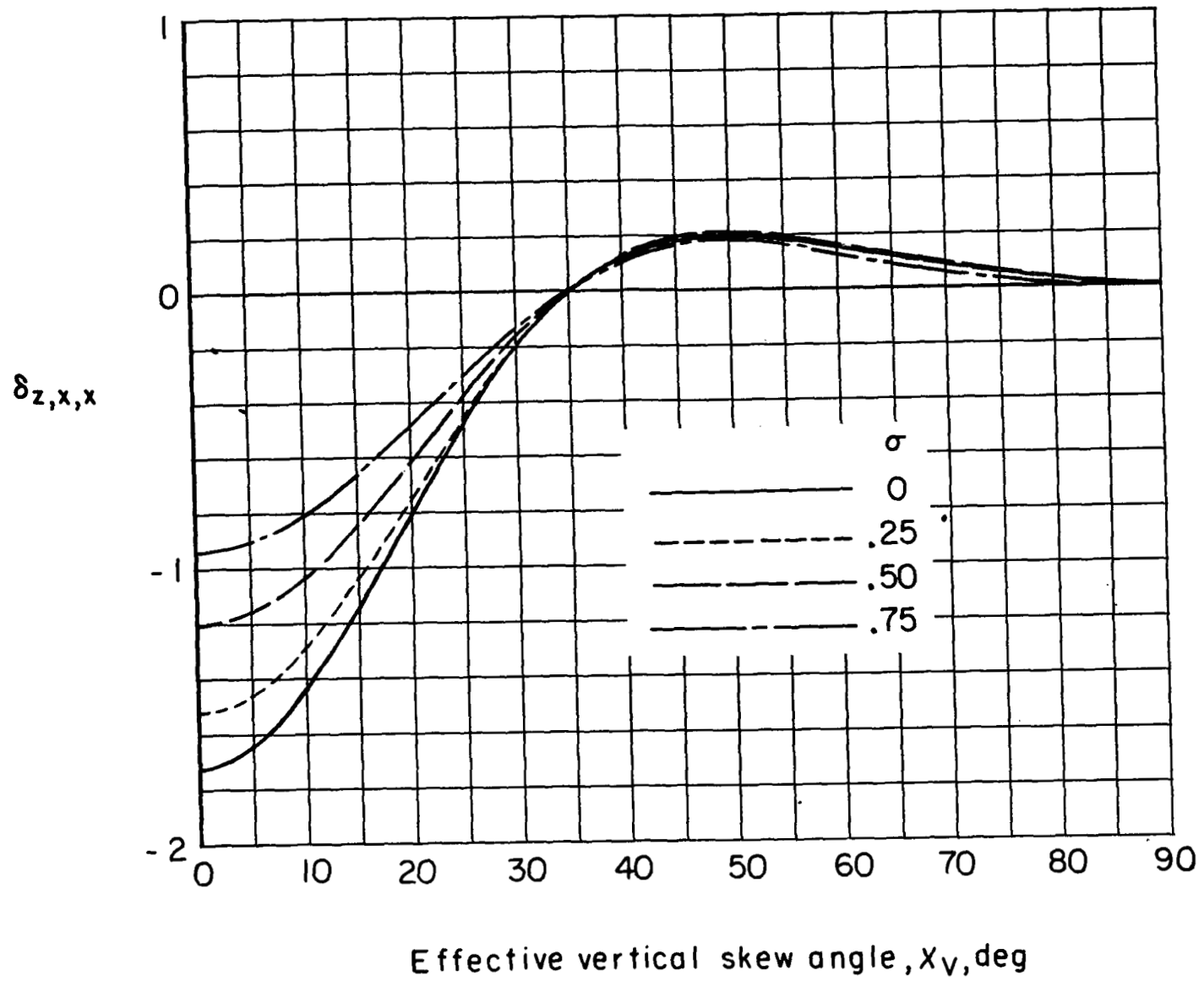
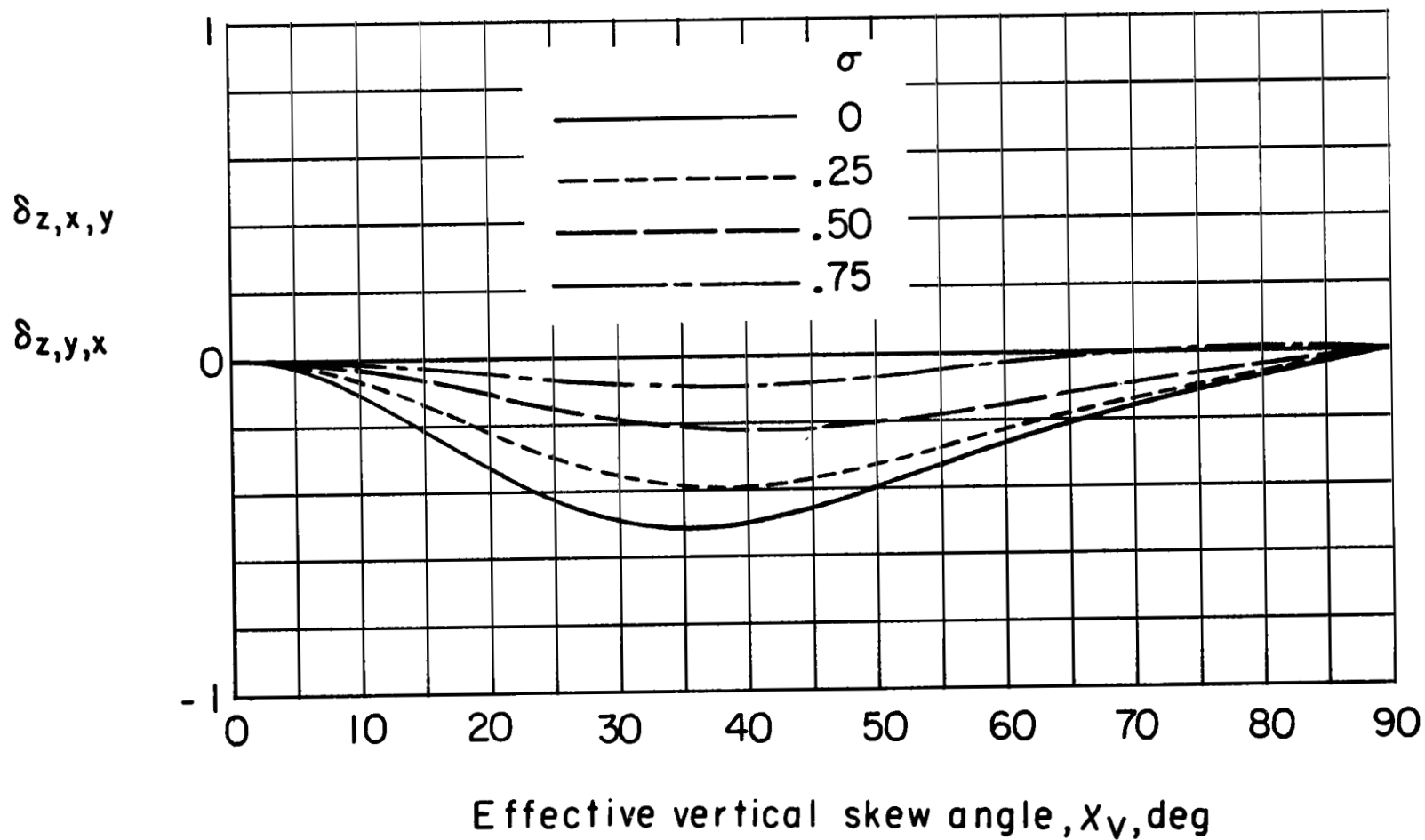
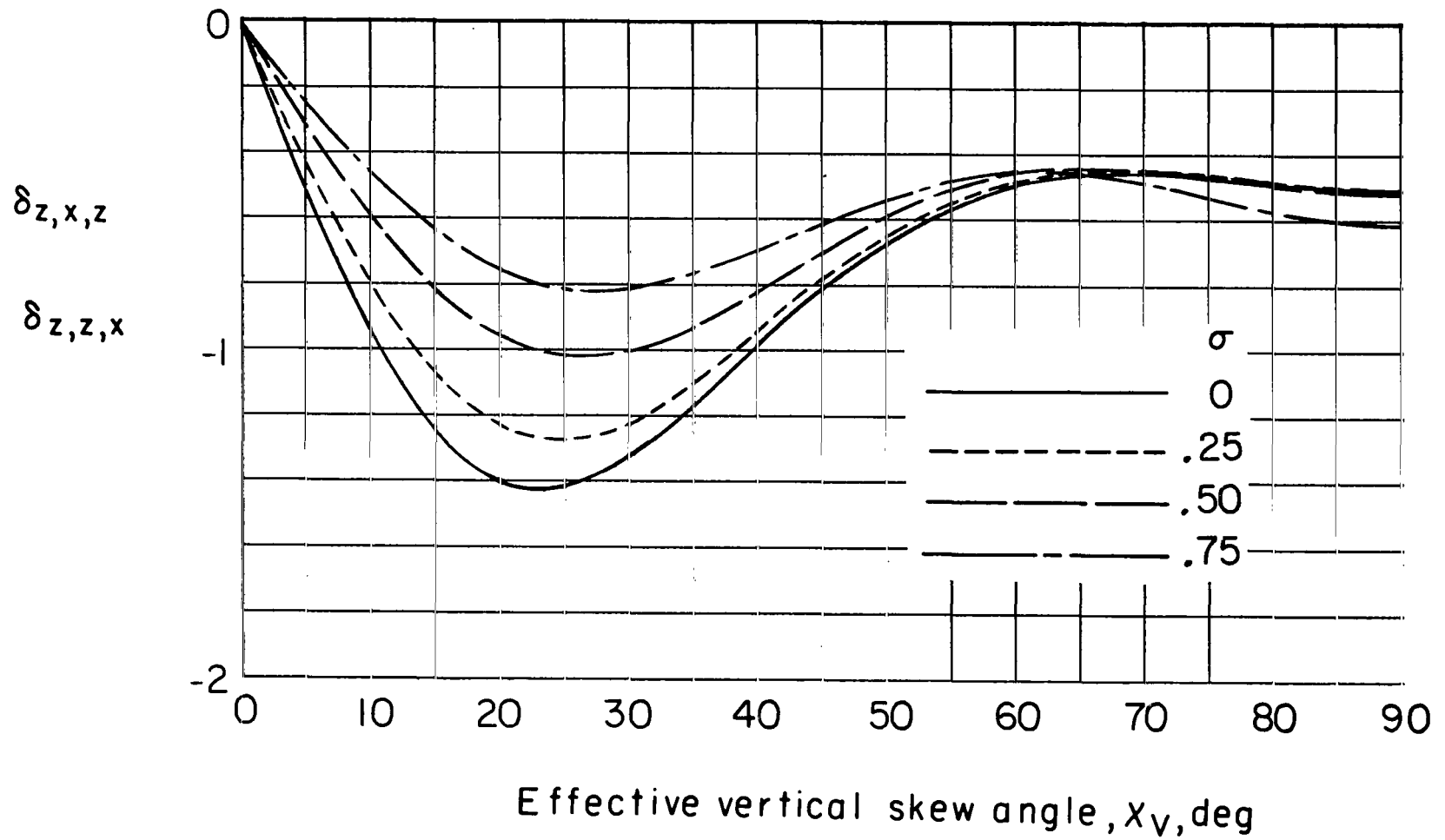
(m) $\delta_{z,x,x}$.

Figure 40.- Continued.



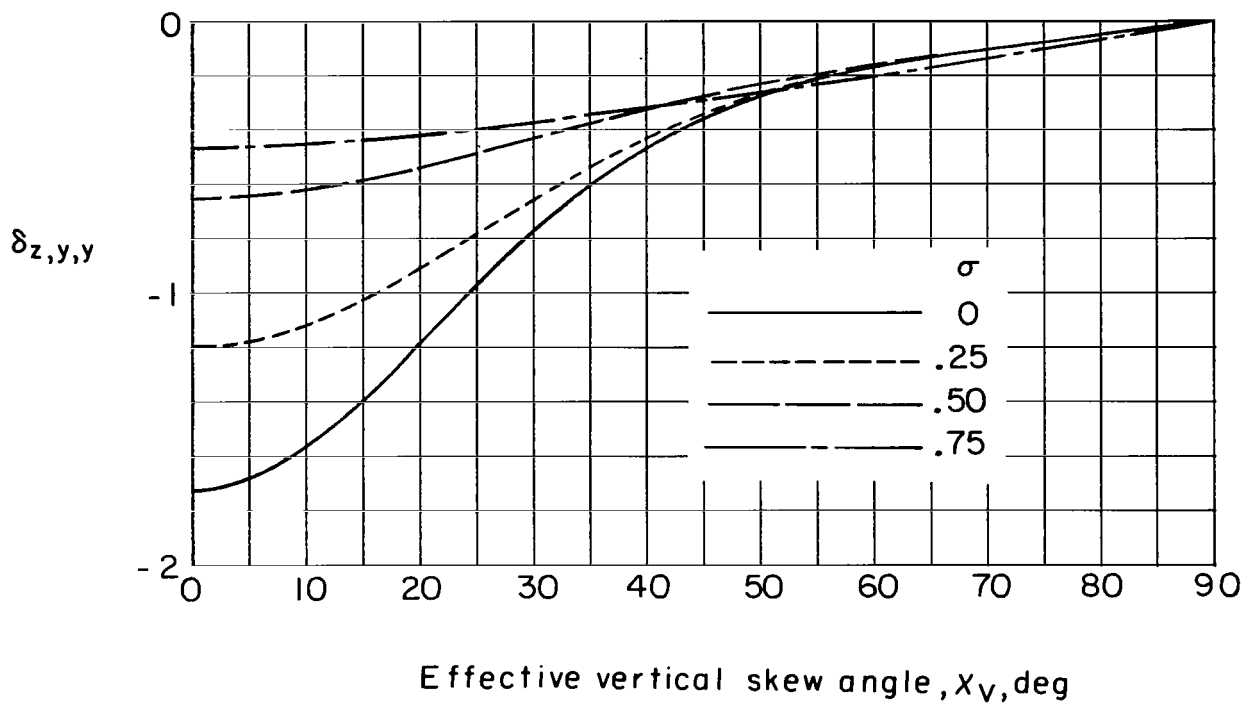
(n) $\delta_{z,x,y} = \delta_{z,y,x}$.

Figure 40.- Continued.

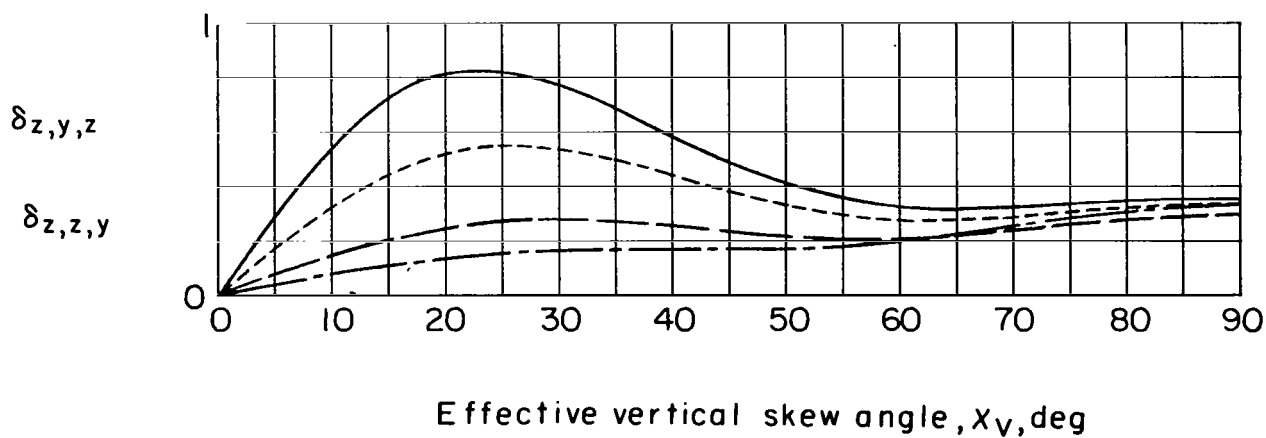


(a) $\delta_{z,x,z} = \delta_{z,z,x}$.

Figure 40.- Continued.

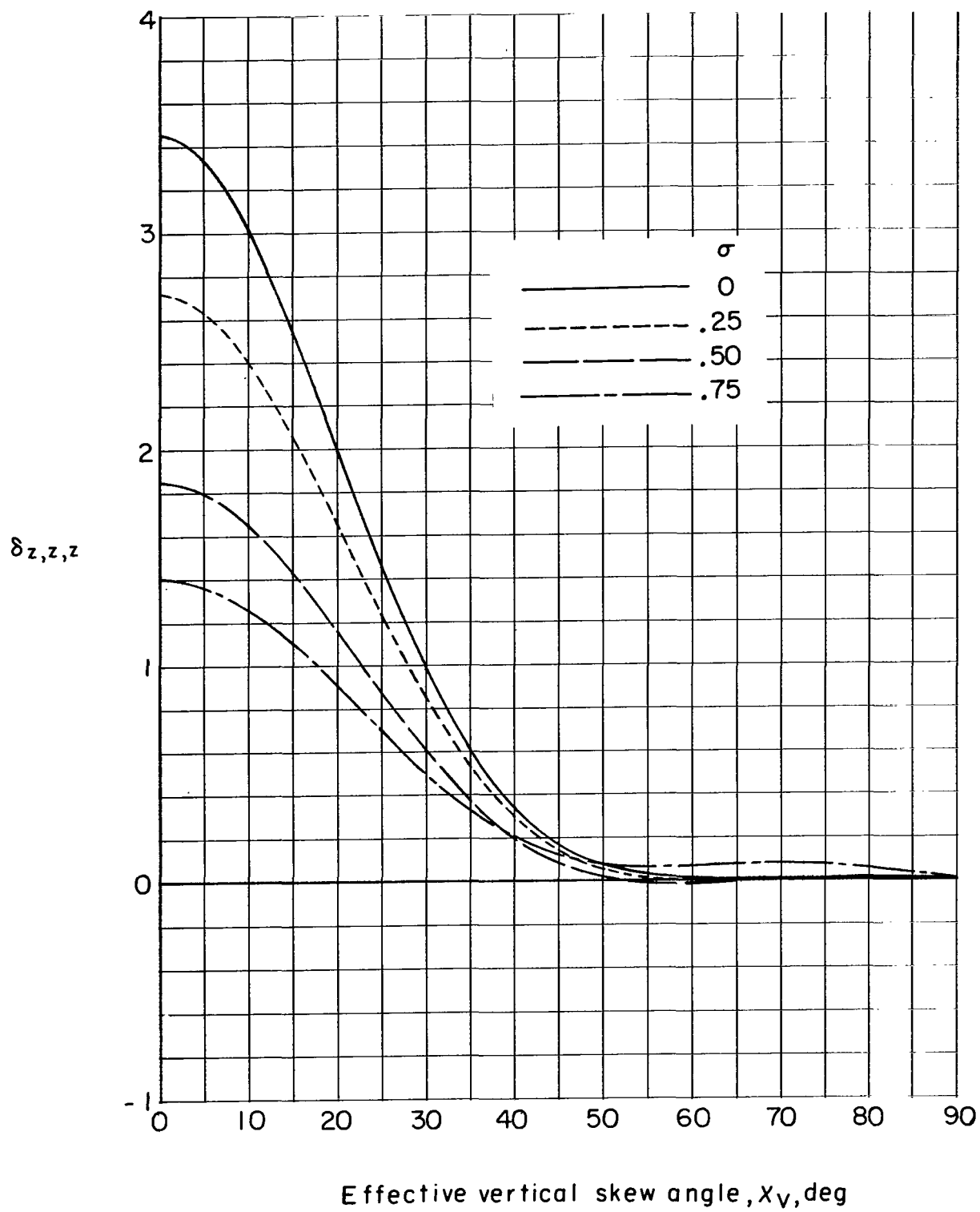


(p) $\delta_{z,y,y}$.



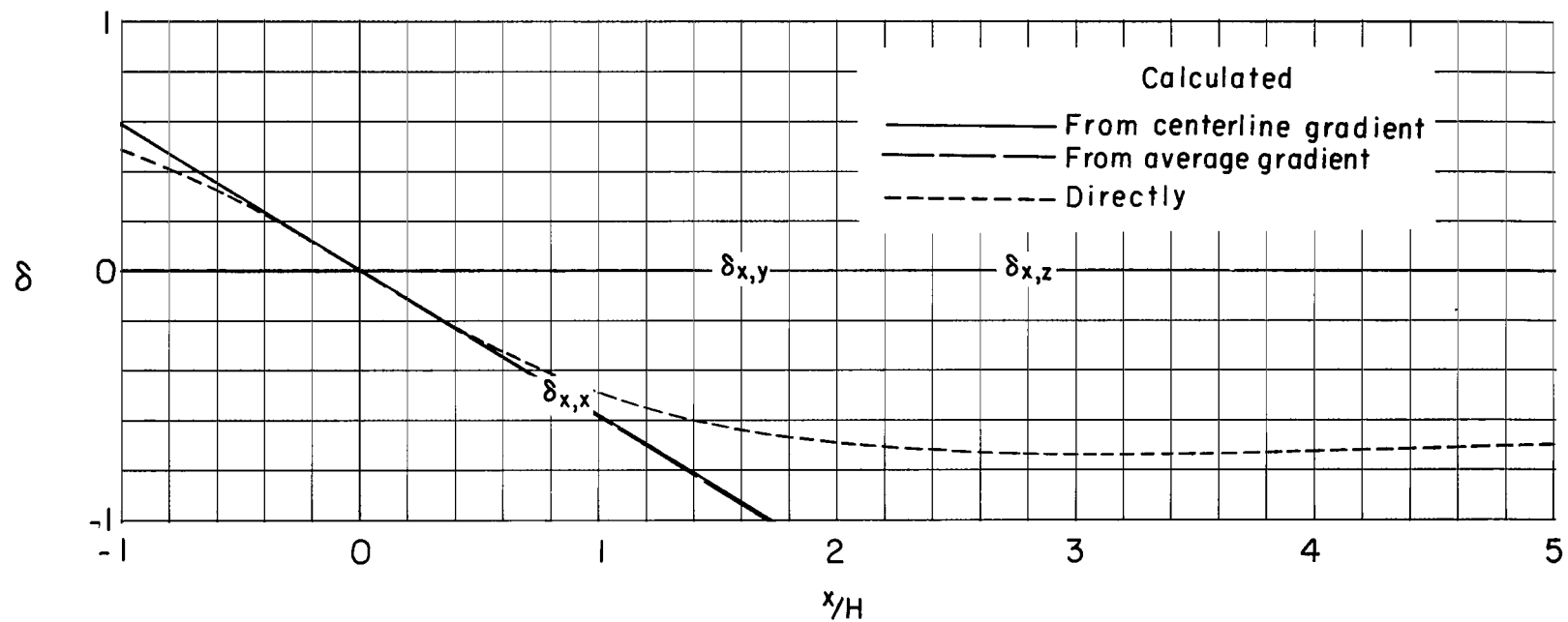
(q) $\delta_{z,y,z} = \delta_{z,z,y}$.

Figure 40.- Continued.



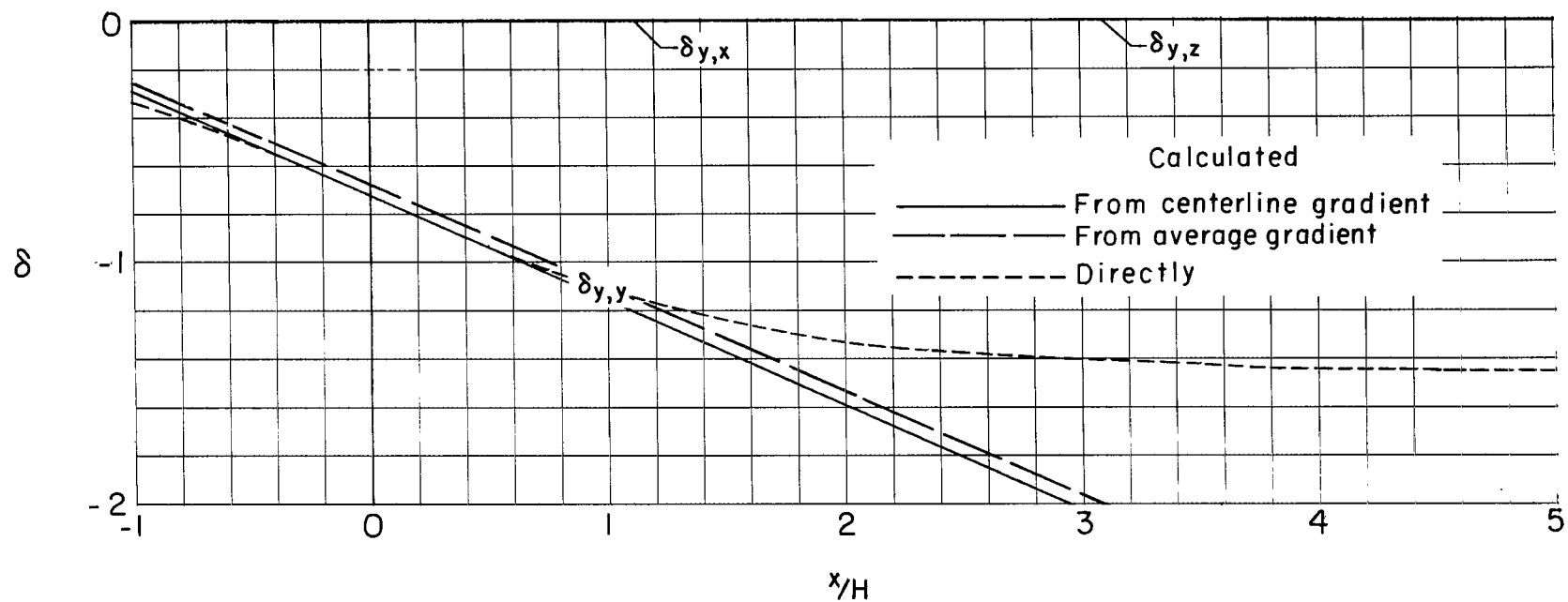
(r) $\delta_{z,z,z}$.

Figure 40.- Concluded.

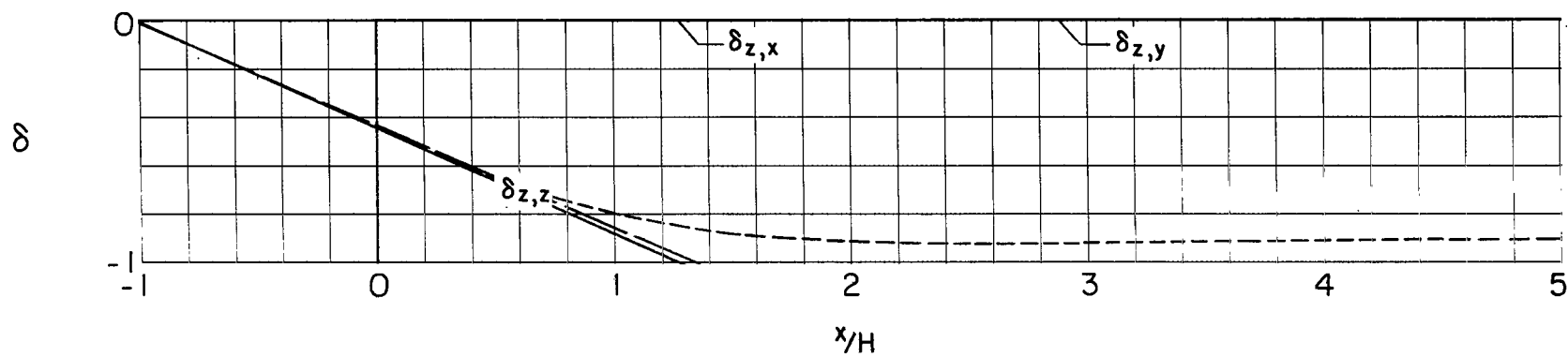


(a) Caused by forces in the X-direction.

Figure 41.- Distribution of interference factors over the longitudinal axis of the tunnel for a uniformly loaded unswept wing centrally located and spanning half the width of a closed rectangular tunnel having a width-height ratio of 1.5. $\chi_H = 90^\circ$; $\chi_V = 90^\circ$.

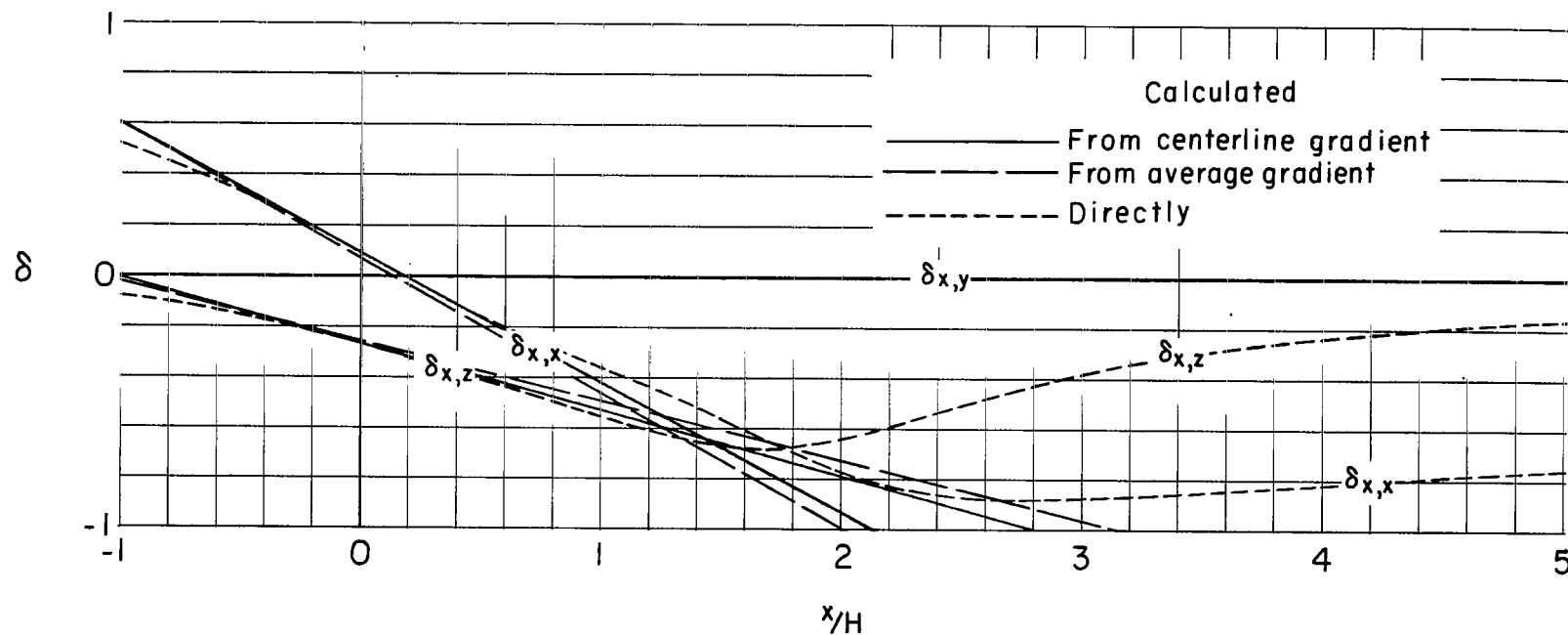


(b) Caused by forces in the Y-direction.



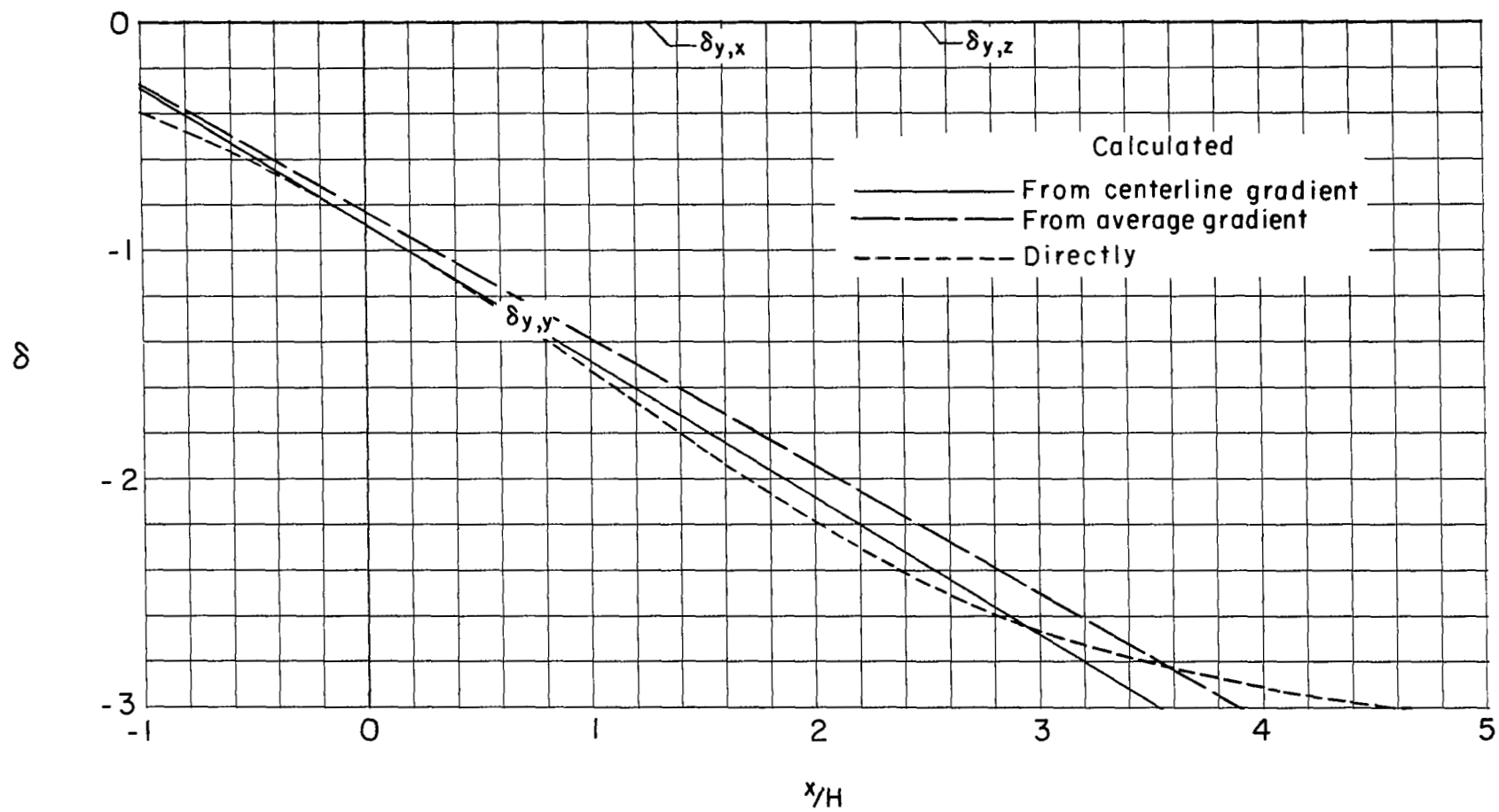
(c) Caused by forces in the Z-direction.

Figure 41.- Concluded.



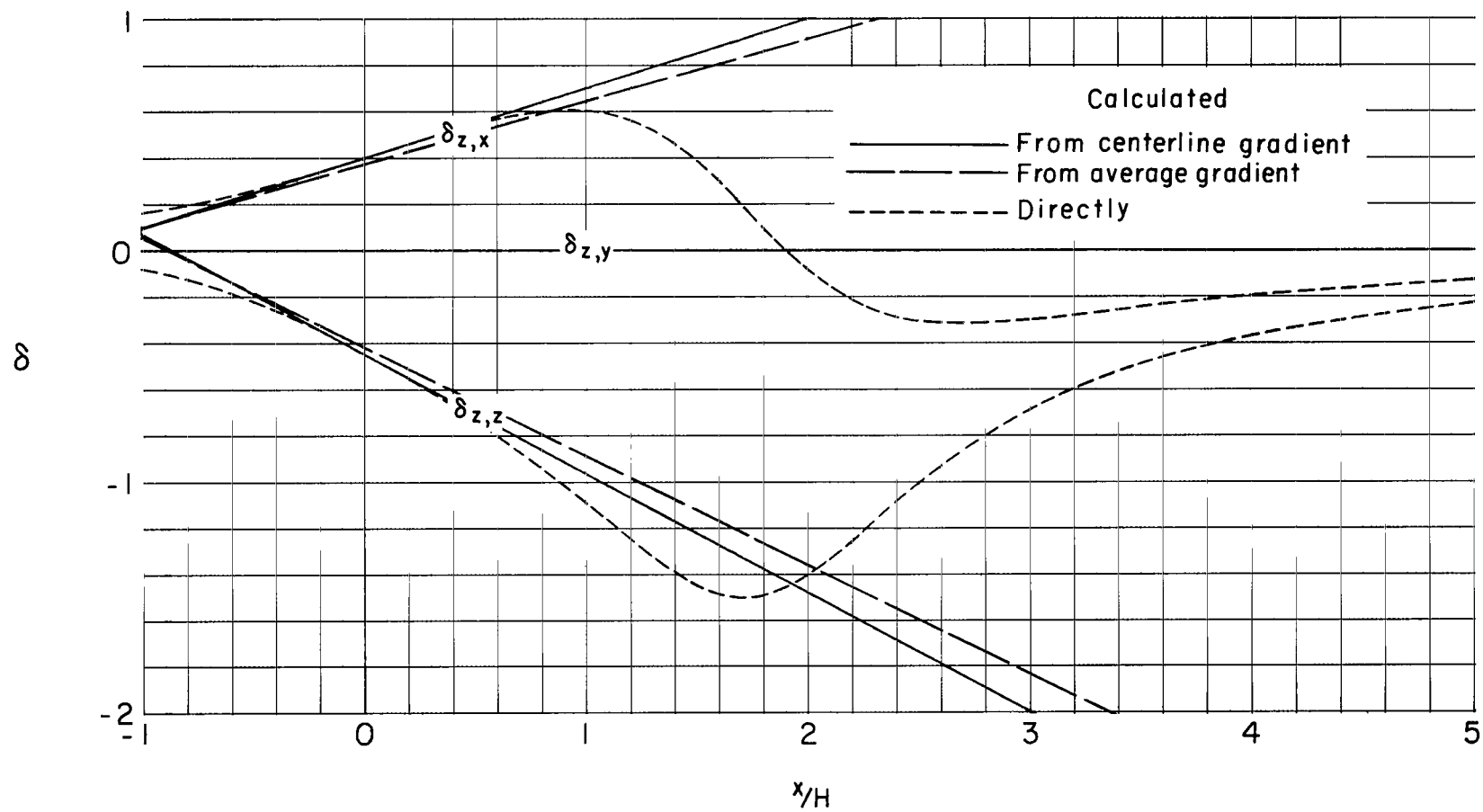
(a) Caused by forces in the X-direction.

Figure 42.- Distribution of interference factors over the longitudinal axis of the tunnel for a uniformly loaded unswept wing centrally located and spanning half the width of a closed rectangular tunnel having a width-height ratio of 1.5. $\chi_H = 90^\circ$; $\chi_V = 60^\circ$.



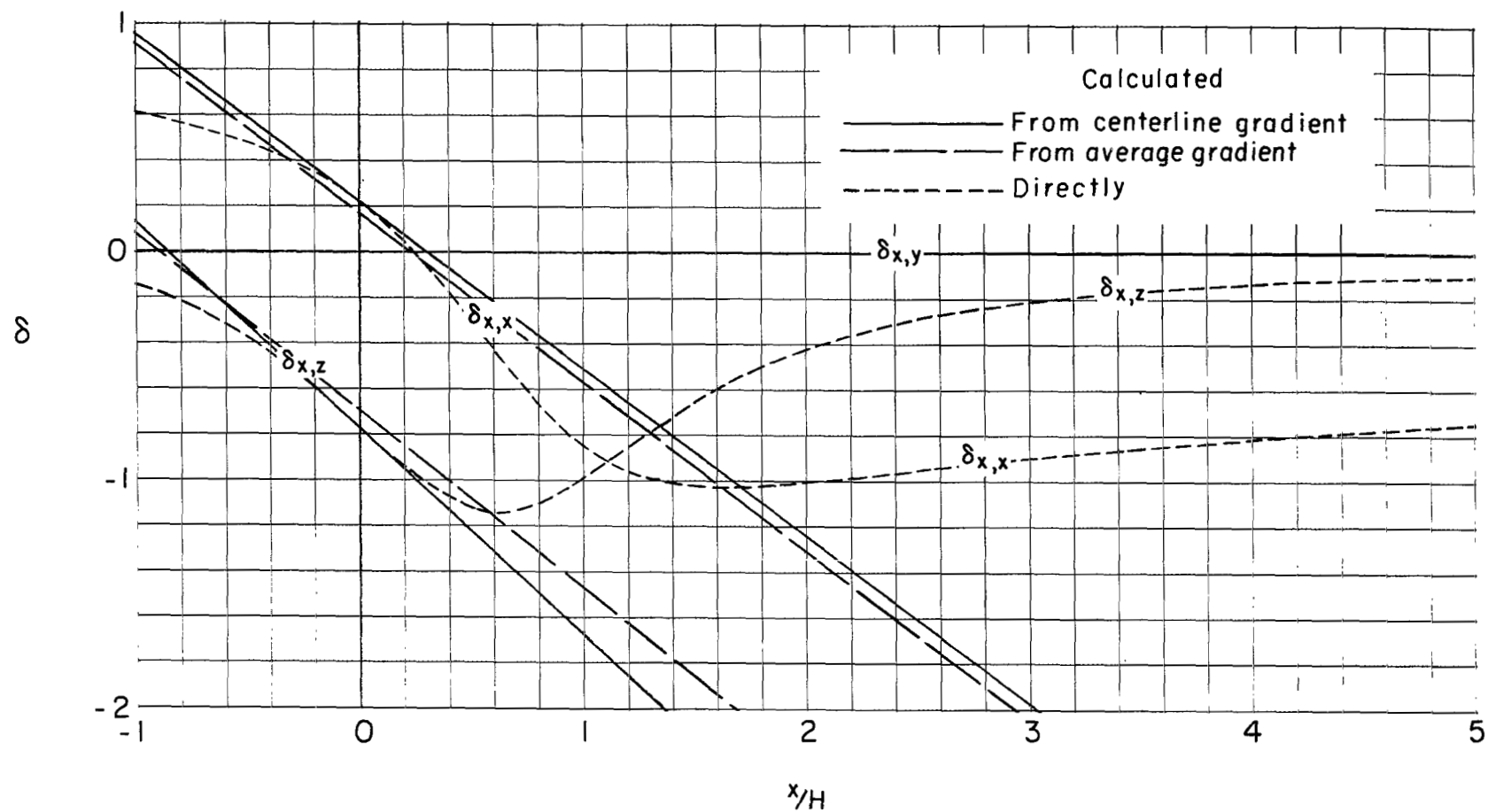
(b) Caused by forces in the Y-direction.

Figure 42.- Continued.



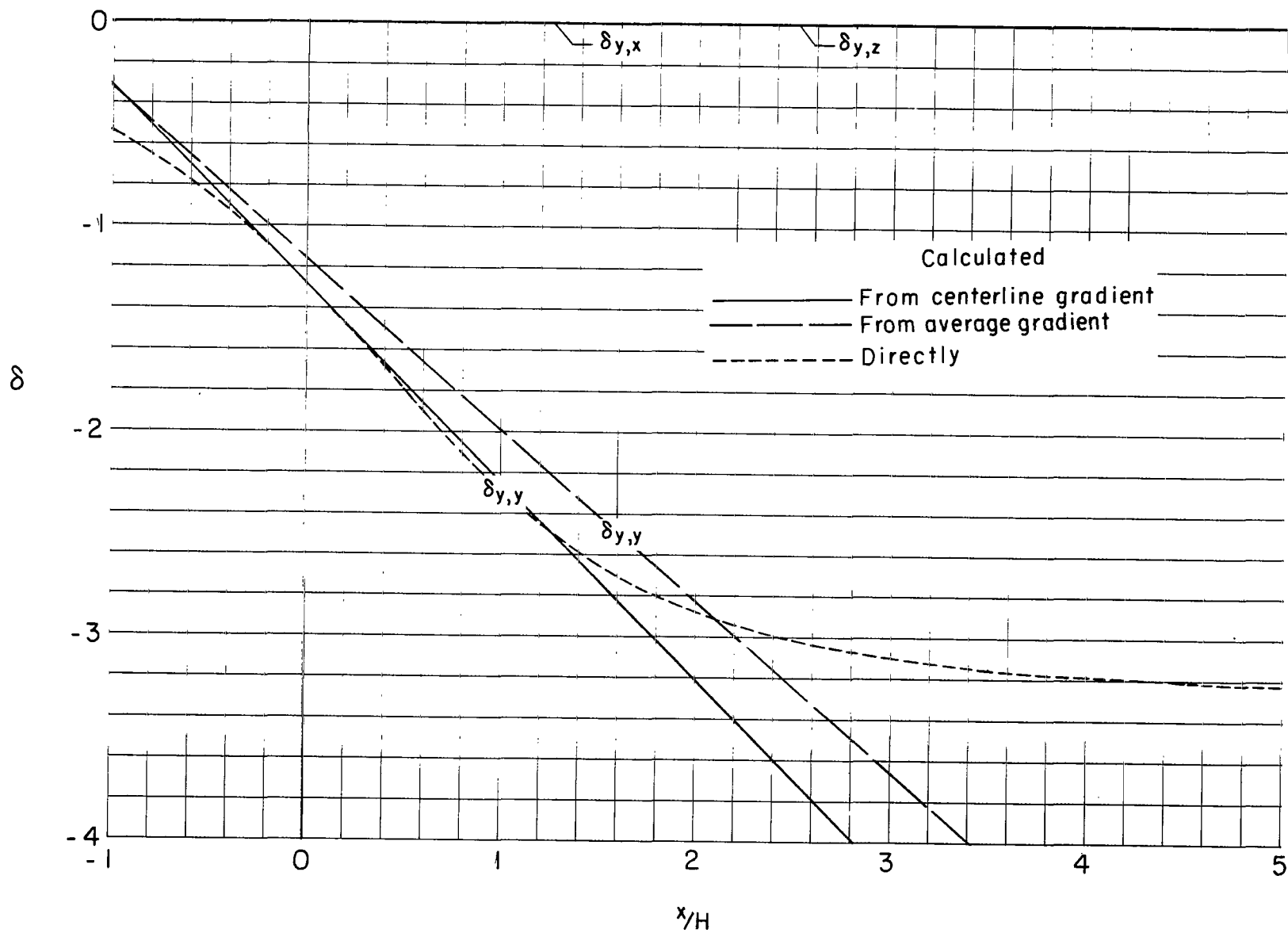
(c) Caused by forces in the Z-direction.

Figure 42.- Concluded.



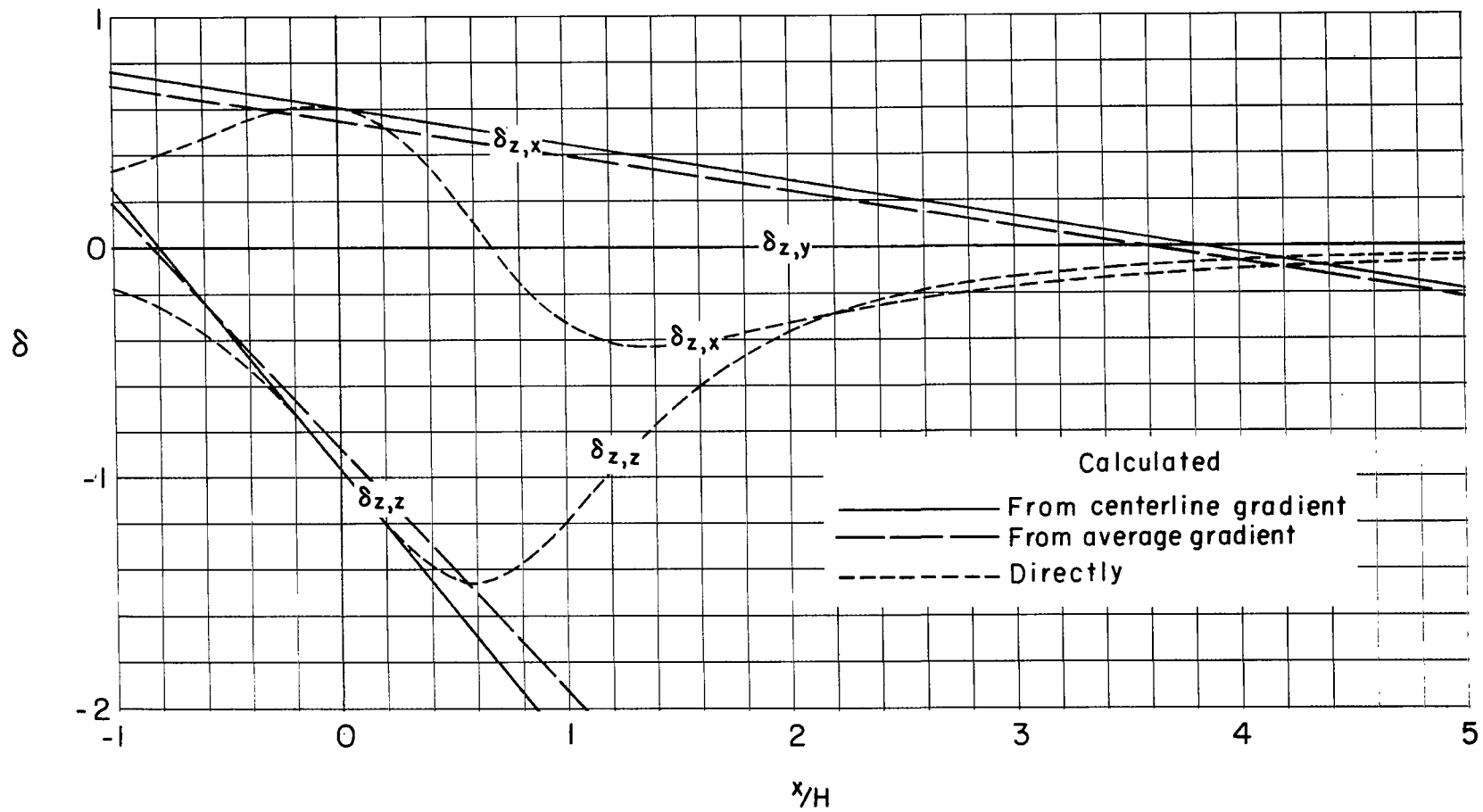
(a) Caused by forces in the X-direction.

Figure 43.- Distribution of interference factors over the longitudinal axis of the tunnel for a uniformly loaded unswept wing centrally located and spanning half the width of a closed rectangular tunnel having a width-height ratio of 1.5. $x_H = 90^\circ$; $x_V = 30^\circ$.



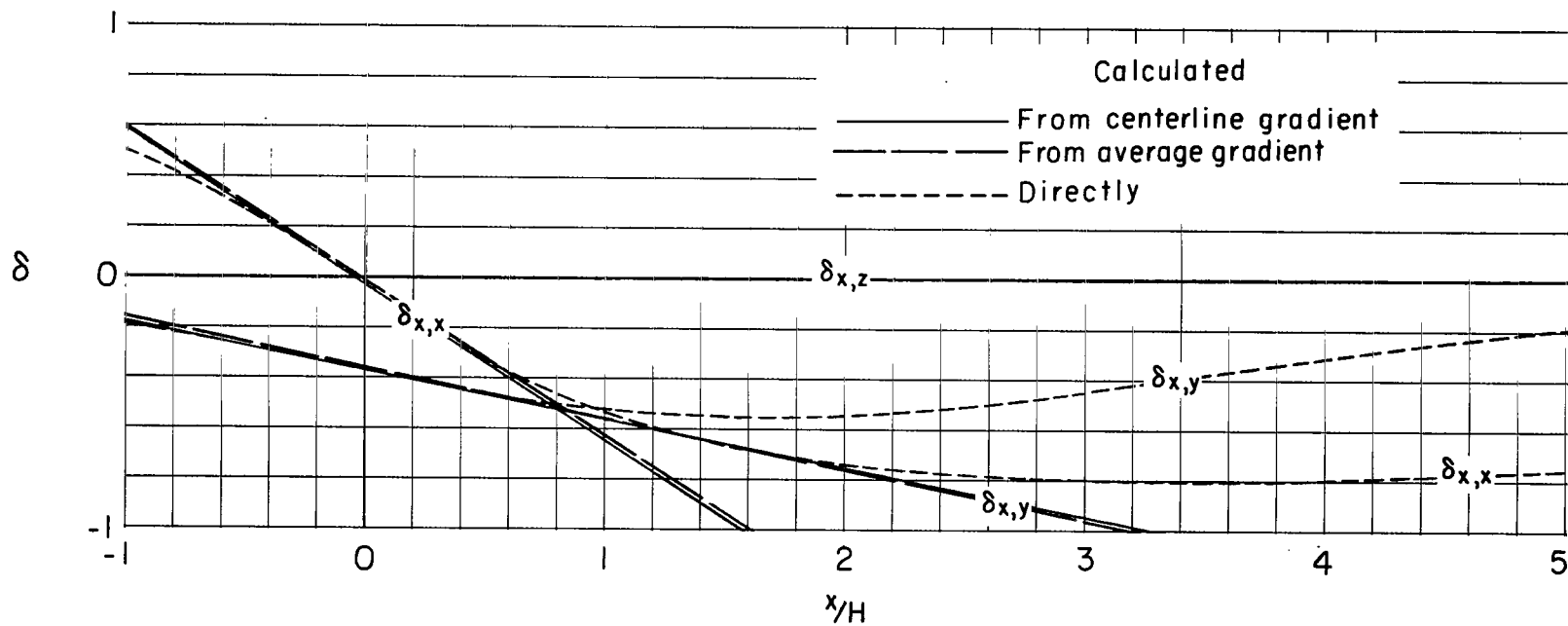
(b) Caused by forces in the Y-direction.

Figure 43.- Continued.



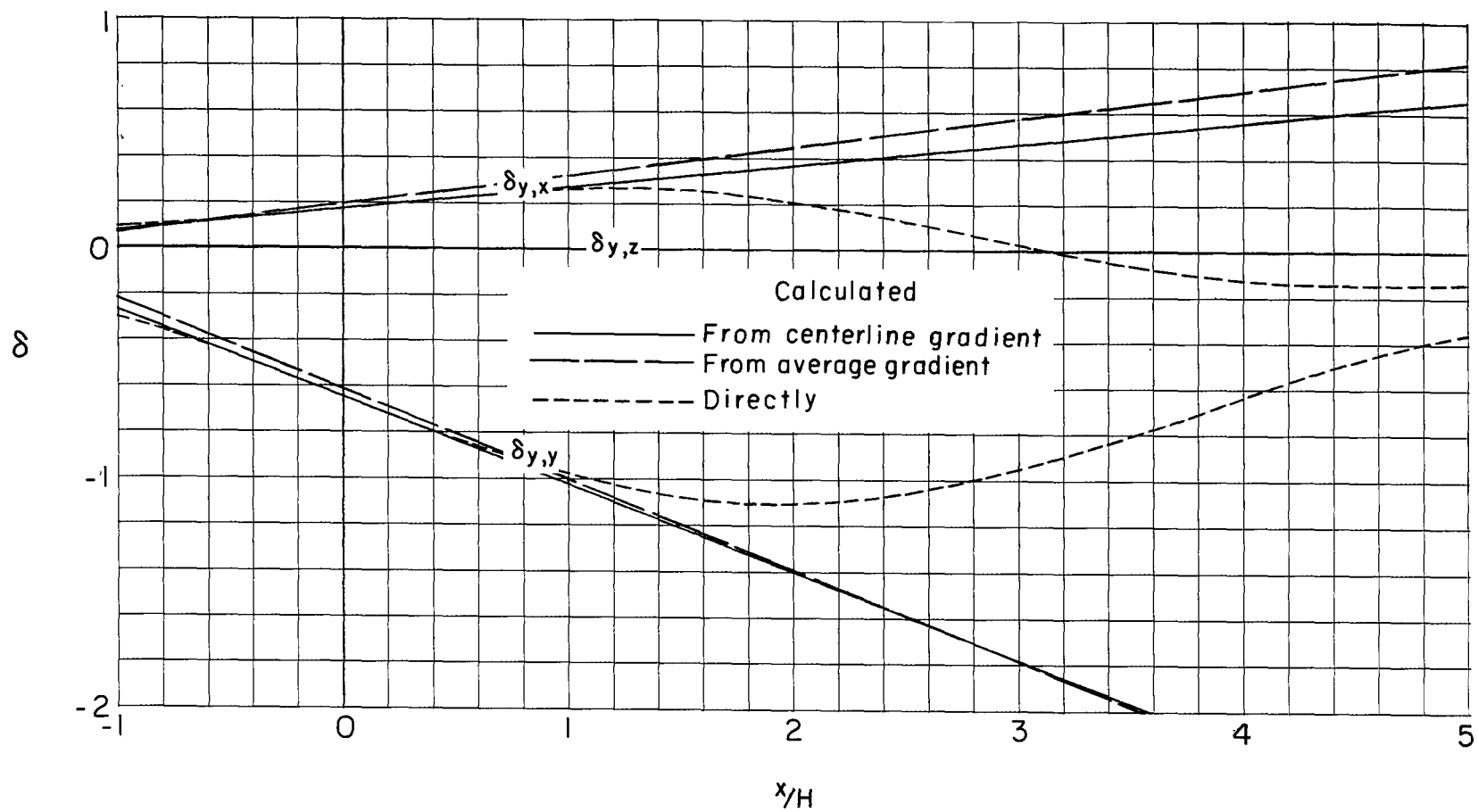
(c) Caused by forces in the Z-direction.

Figure 43.- Concluded.



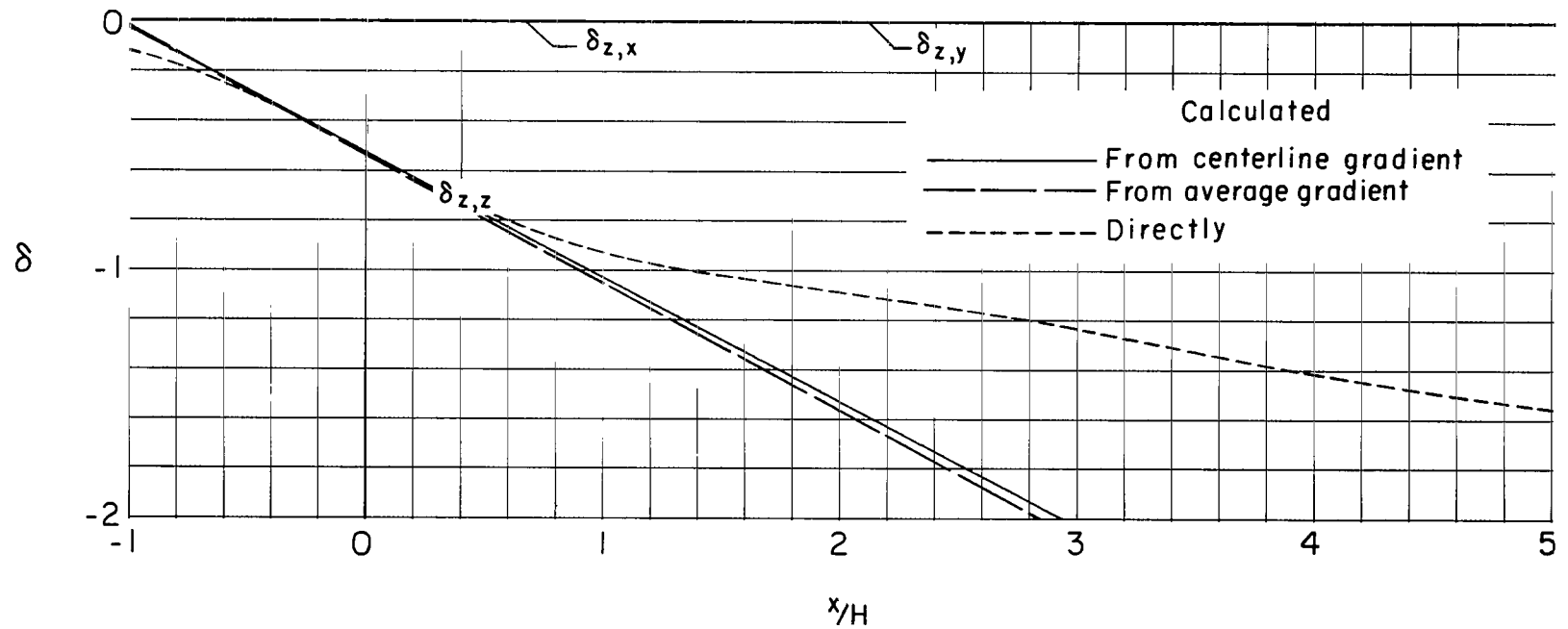
(a) Caused by forces in the X-direction.

Figure 44.- Distribution of interference factors over the longitudinal axis of the tunnel for a uniformly loaded unswept wing centrally located and spanning half the width of a closed rectangular tunnel having a width-height ratio of 1.5. $\chi_H = 60^\circ$; $\chi_V = 90^\circ$.



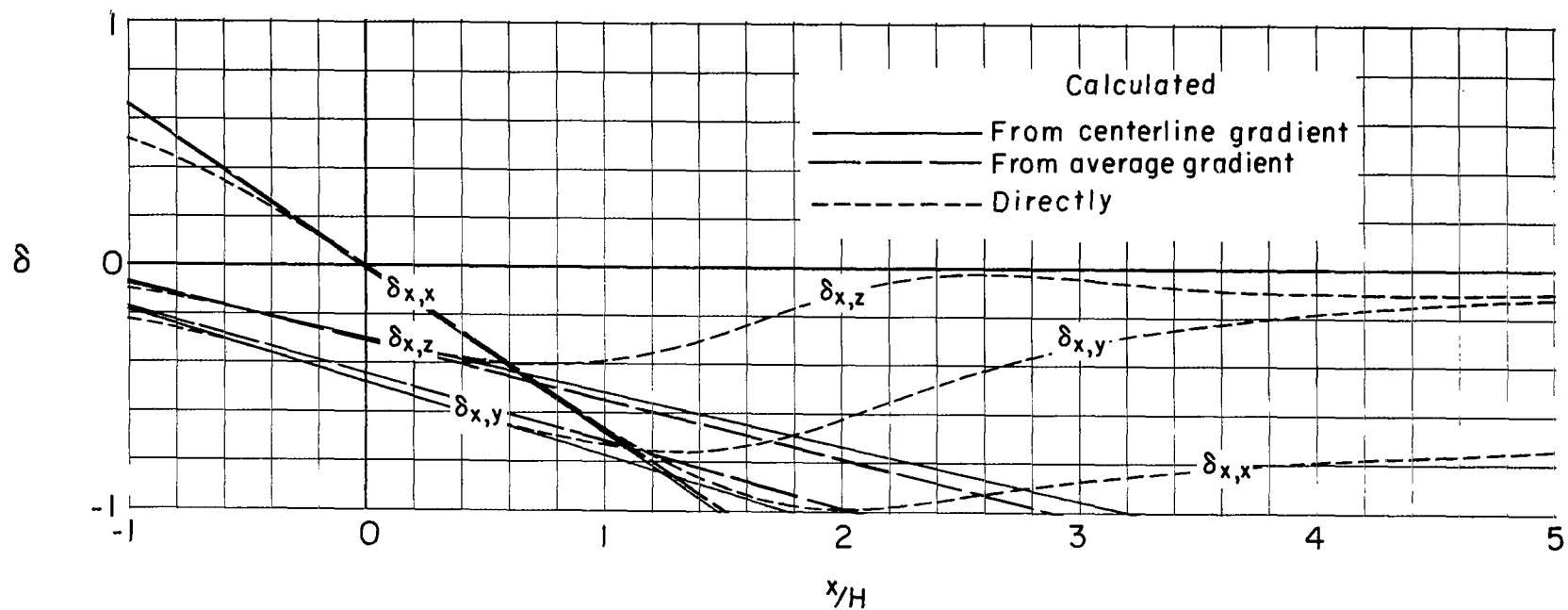
(b) Caused by forces in the Y-direction.

Figure 44.- Continued.



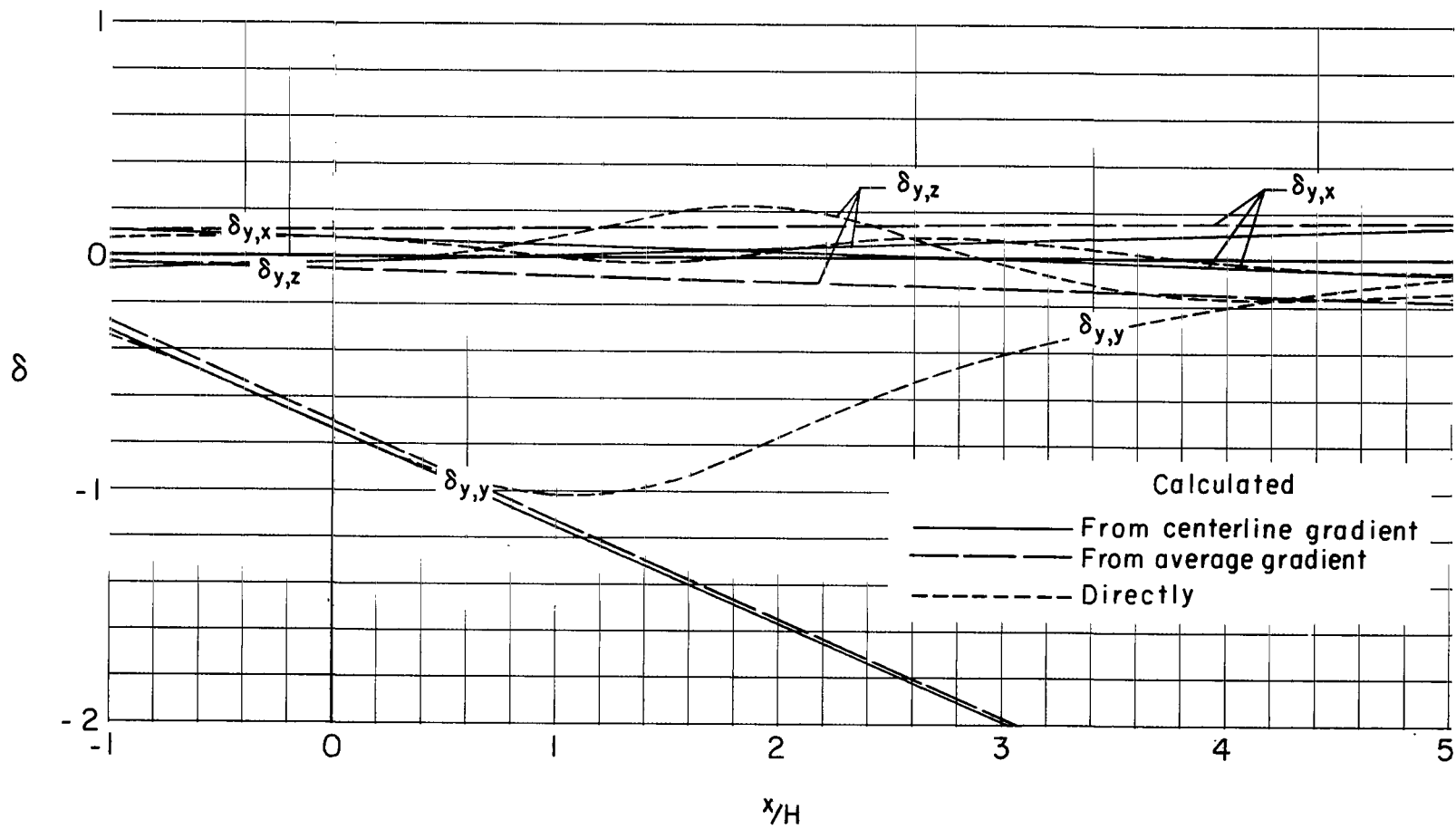
(c) Caused by forces in the Z-direction.

Figure 44.- Concluded.



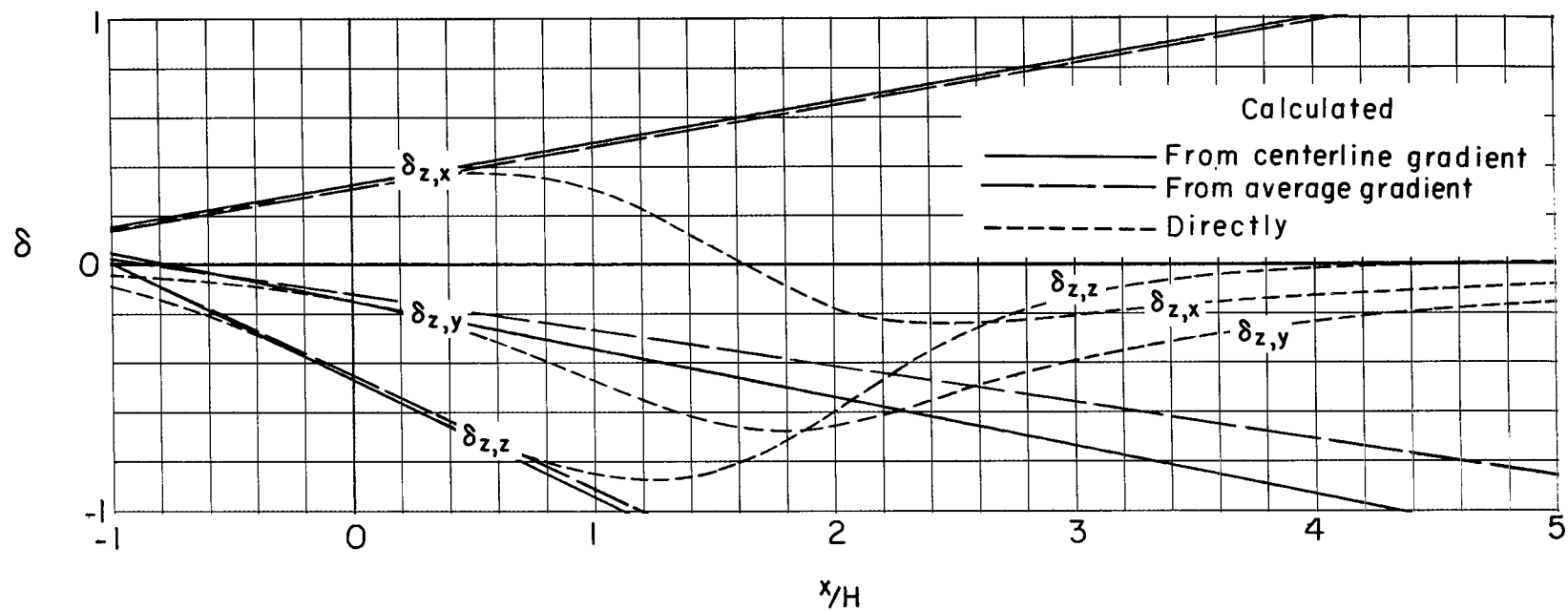
(a) Caused by forces in the X-direction.

Figure 45.- Distribution of interference factors over the longitudinal axis of the tunnel for a uniformly loaded unswept wing centrally located and spanning half the width of a closed rectangular tunnel having a width-height ratio of 1.5. $\chi_H = 60^\circ$; $\chi_V = 60^\circ$.



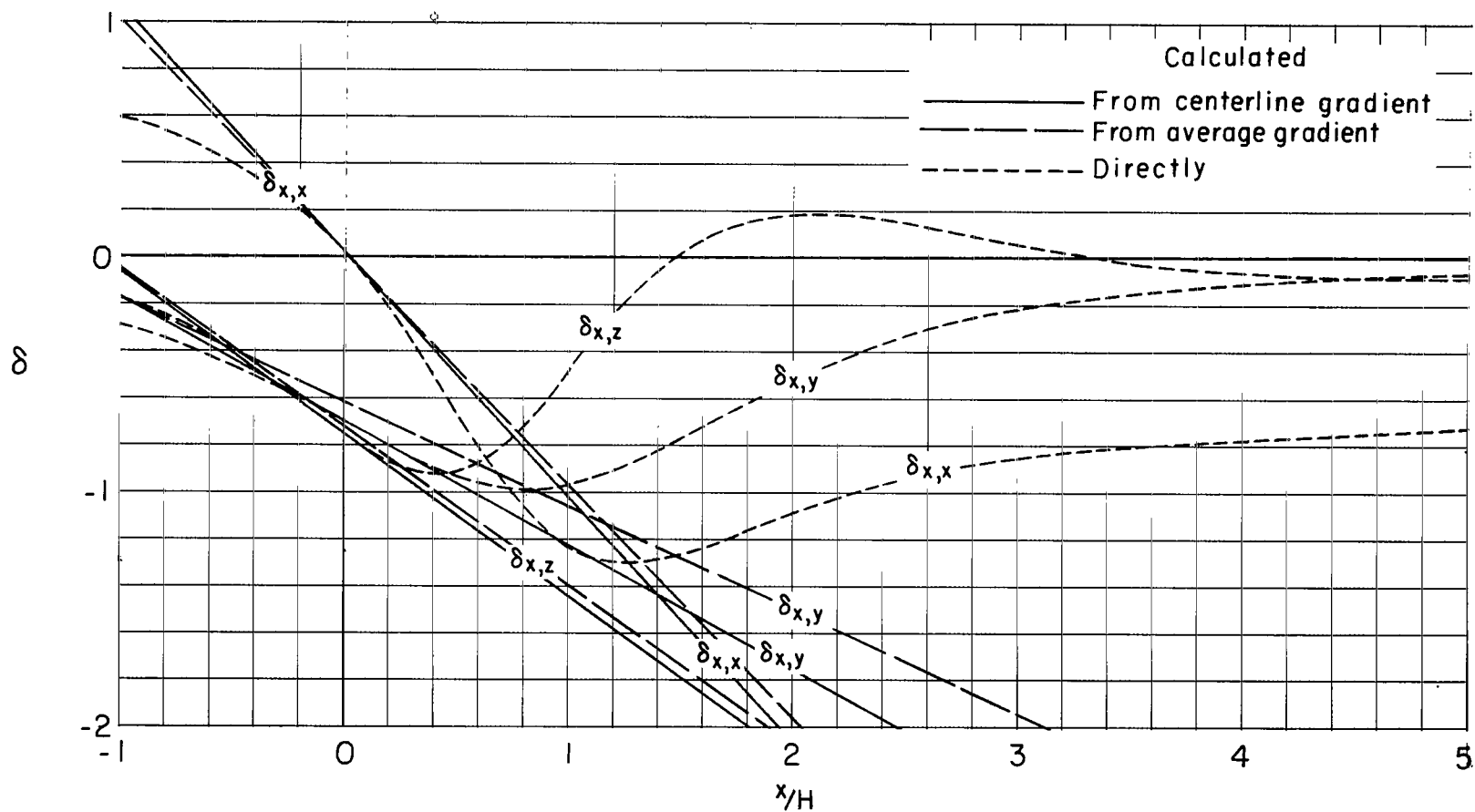
(b) Caused by forces in the Y-direction.

Figure 45.- Continued.



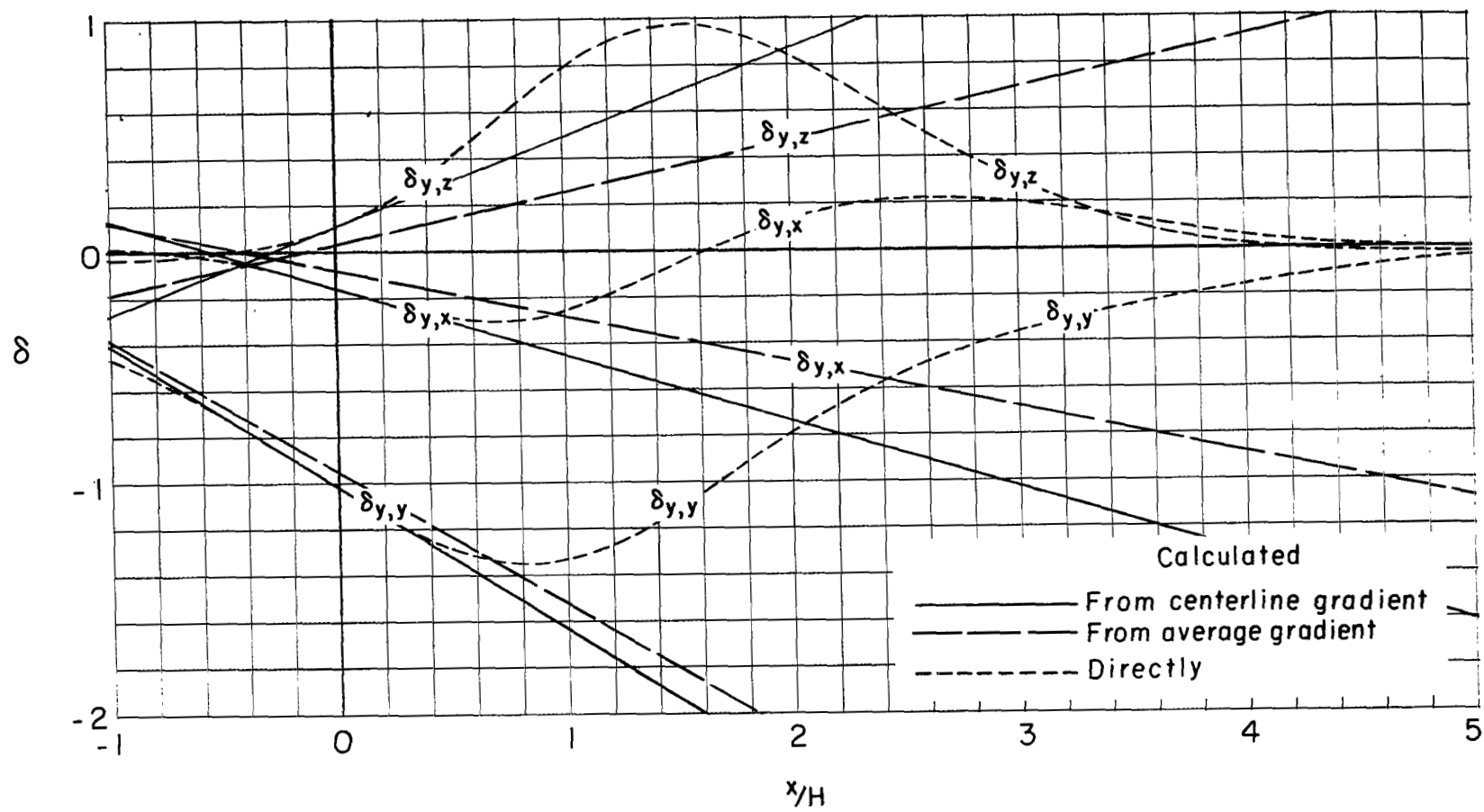
(c) Caused by forces in the Z-direction.

Figure 45.- Concluded.



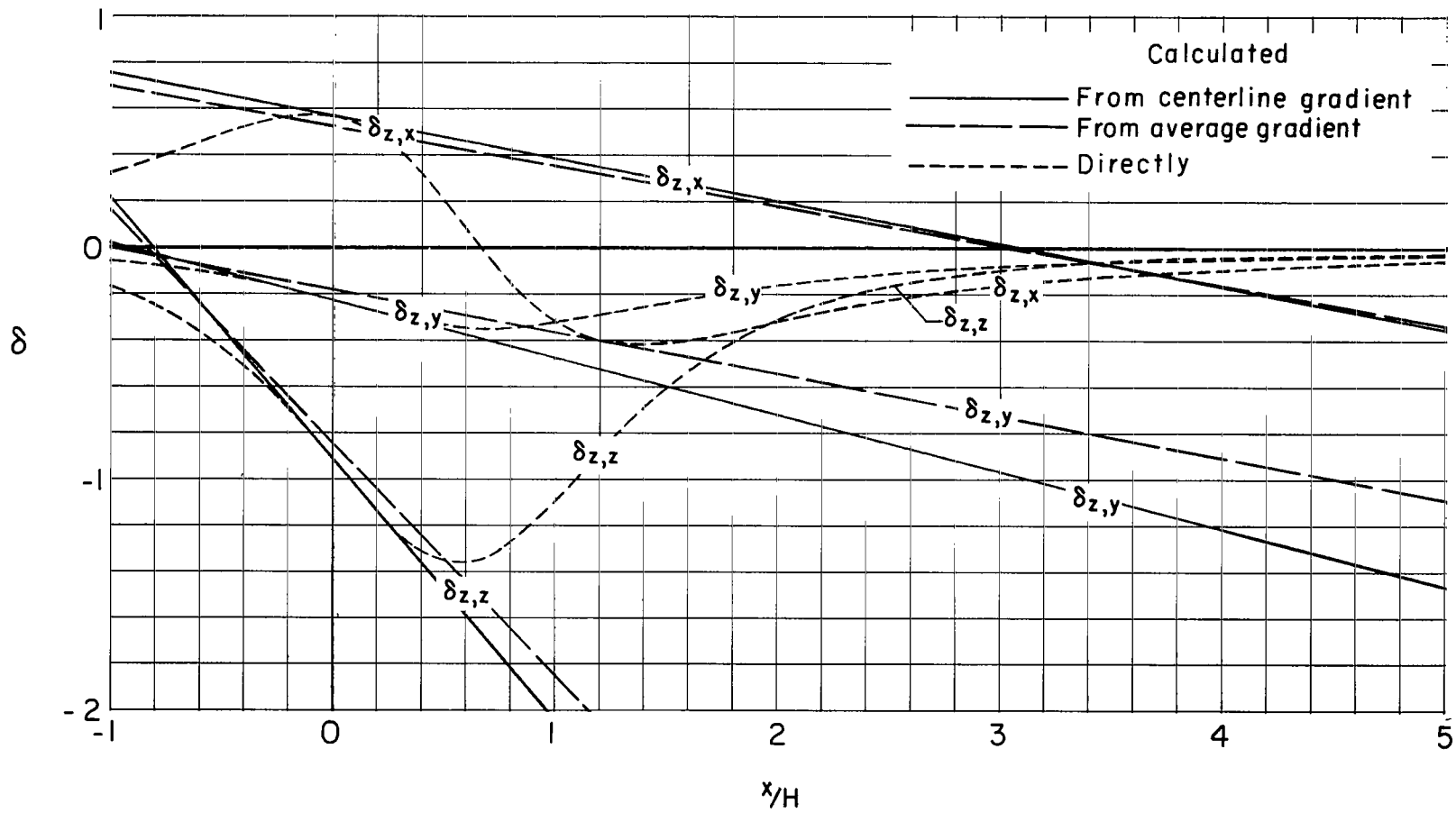
(a) Caused by forces in the X-direction.

Figure 46.- Distribution of interference factors over the longitudinal axis of the tunnel for a uniformly loaded unswept wing centrally located and spanning half the width of a closed rectangular tunnel having a width-height ratio of 1.5. $x_H = 60^\circ$; $x_V = 30^\circ$.



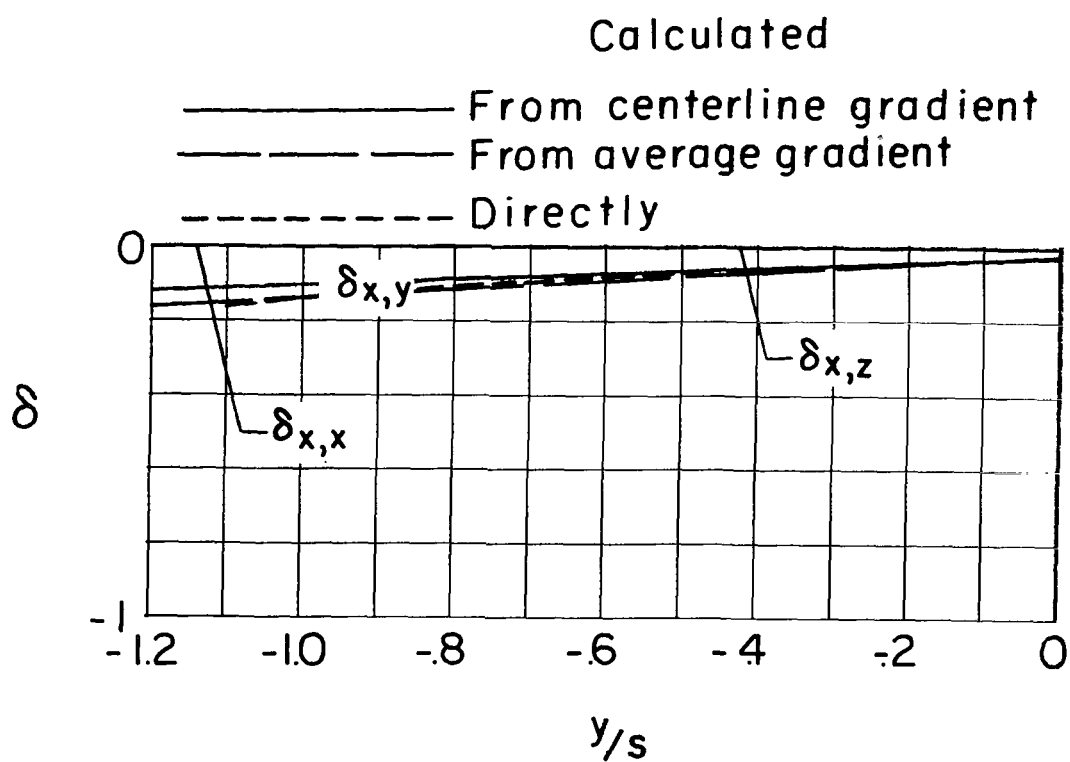
(b) Caused by forces in the Y-direction.

Figure 46.- Continued.



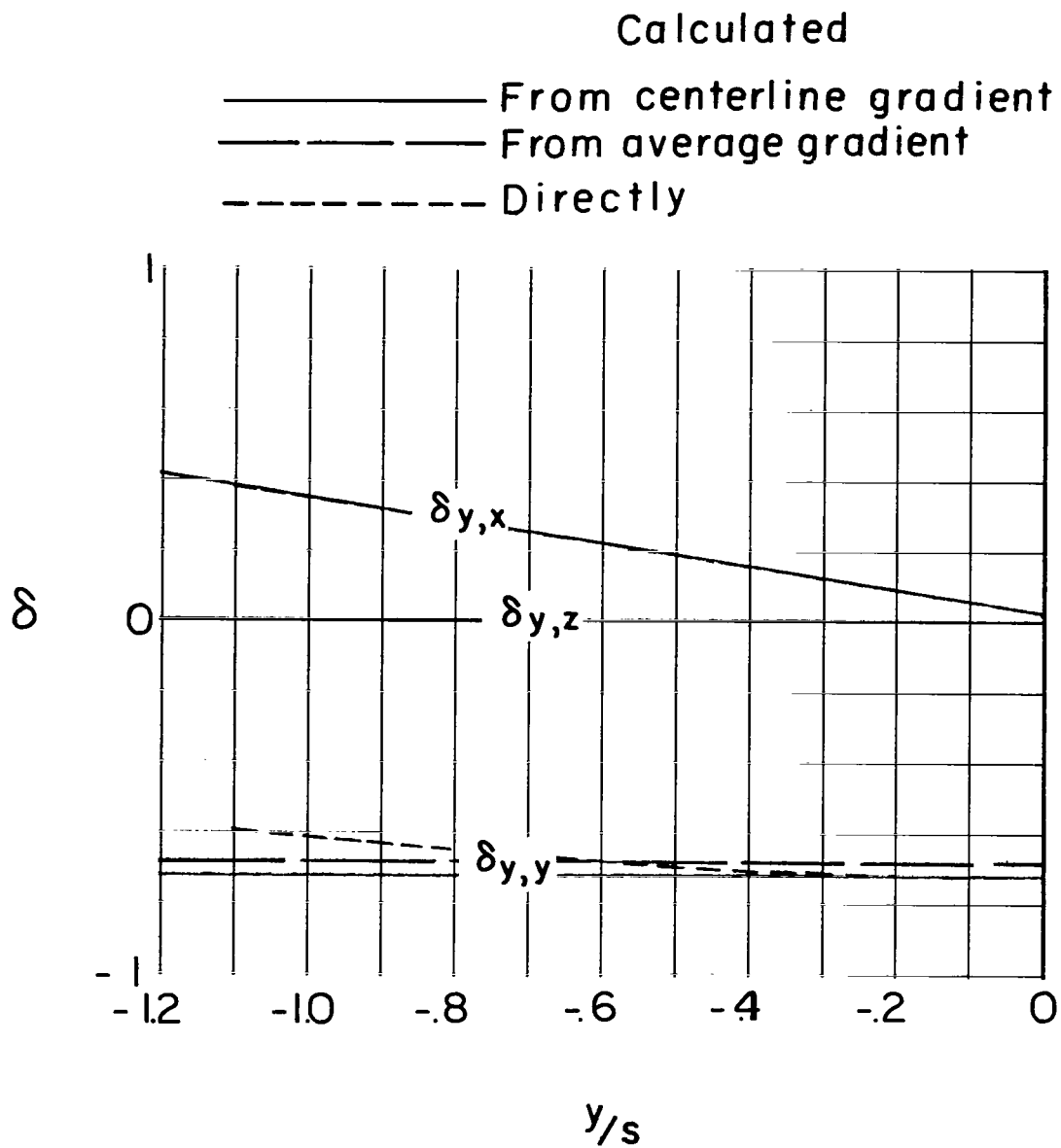
(c) Caused by forces in the Z-direction.

Figure 46.- Concluded.



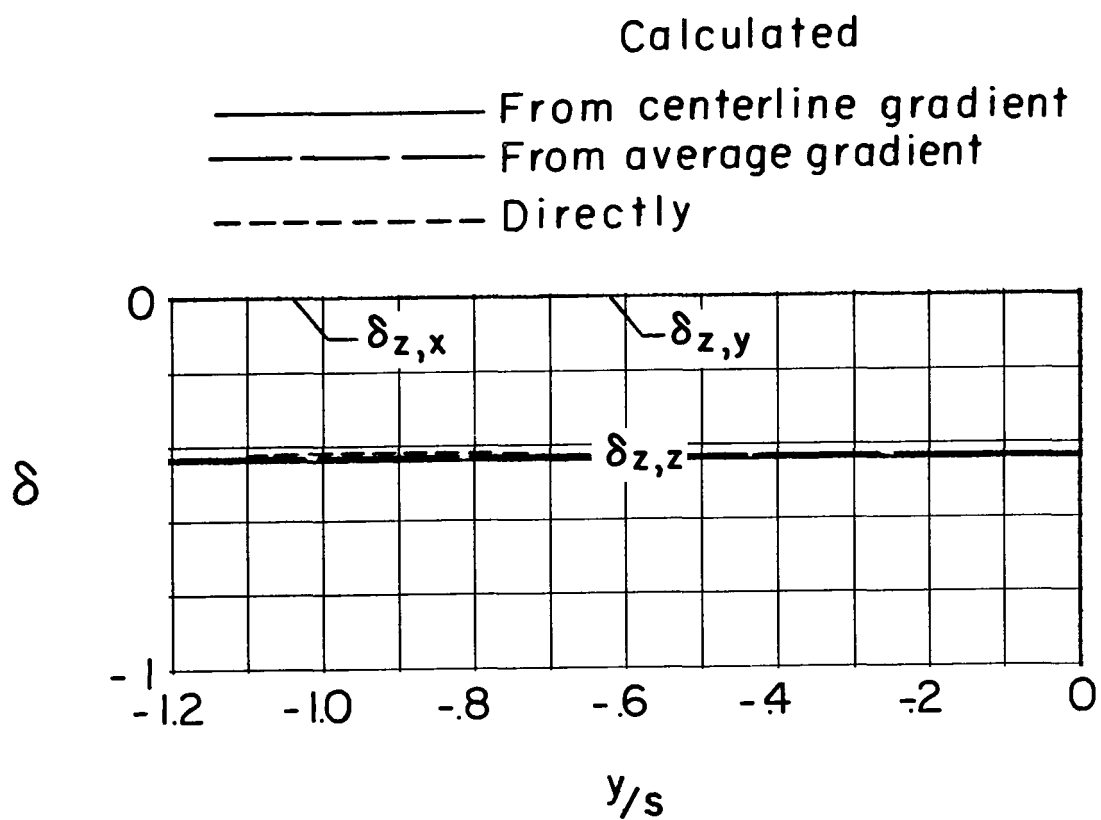
(a) Caused by forces in the X-direction.

Figure 47.- Spanwise distribution of interference factors for a uniformly loaded unswept wing centrally located and spanning half the width of a closed rectangular tunnel having a width-height ratio of 1.5. $\chi_H = 90^\circ$; $\chi_V = 90^\circ$.



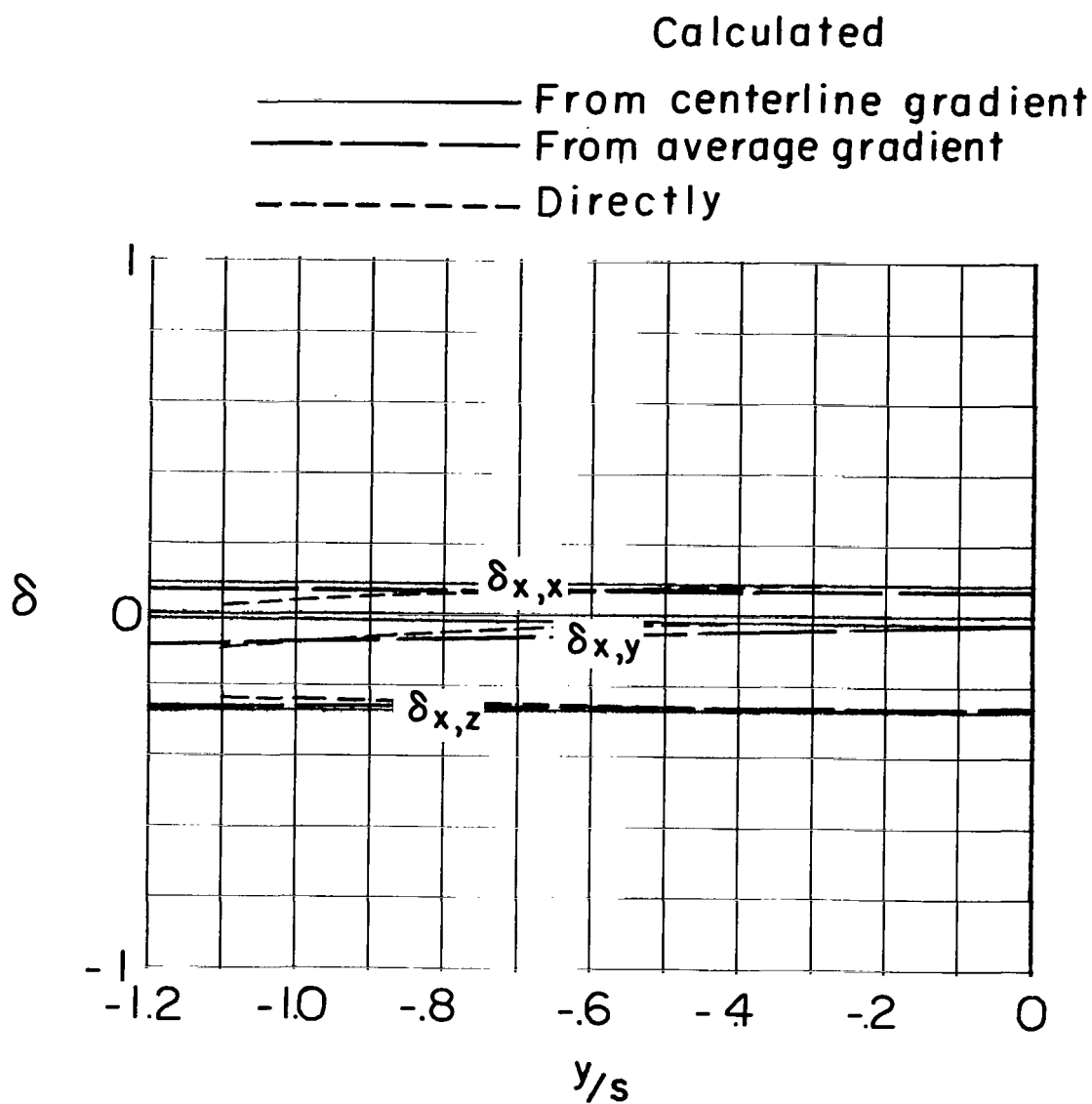
(b) Caused by forces in the Y-direction.

Figure 47.- Continued.



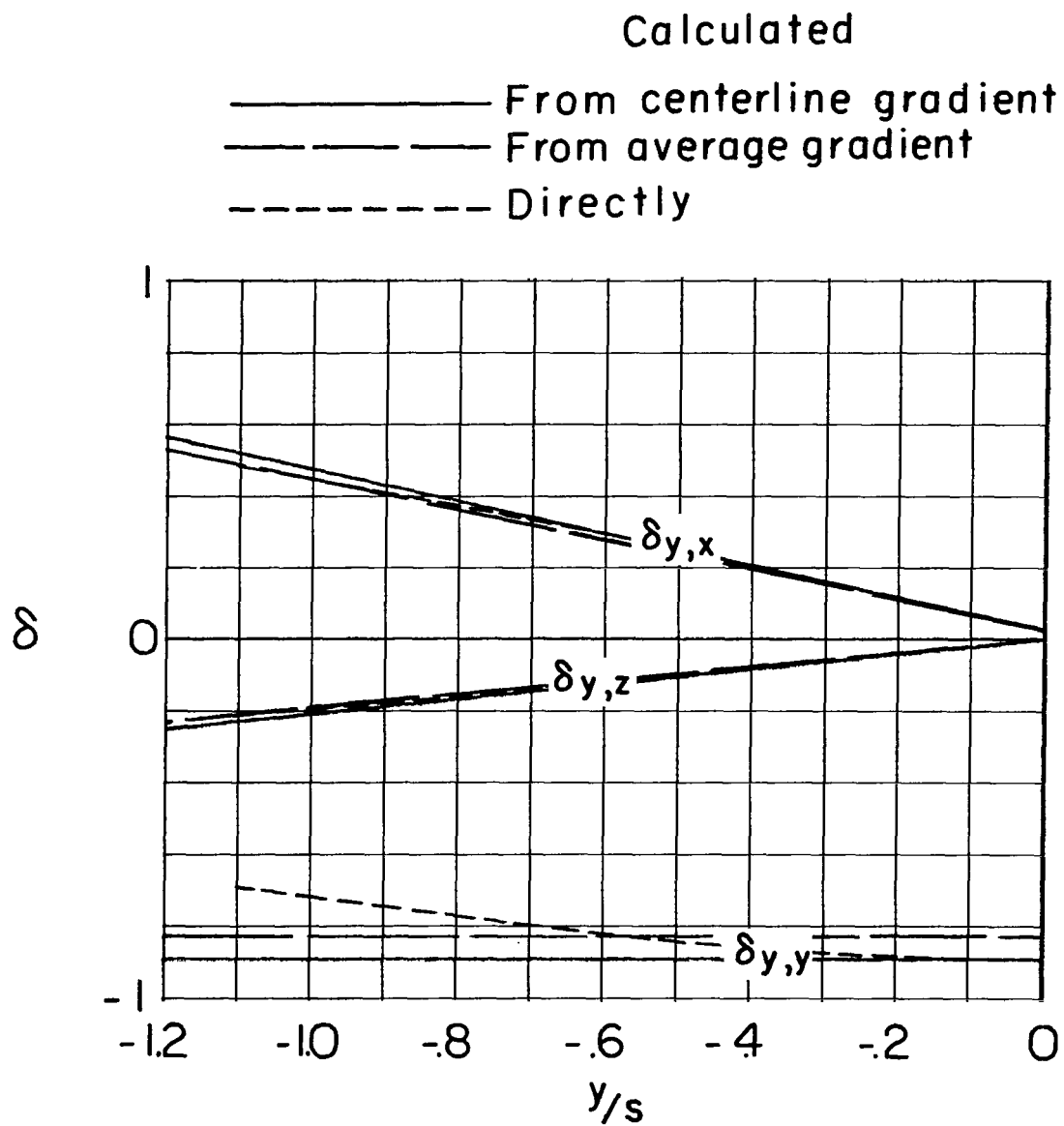
(c) Caused by forces in the Z-direction.

Figure 47.- Concluded.



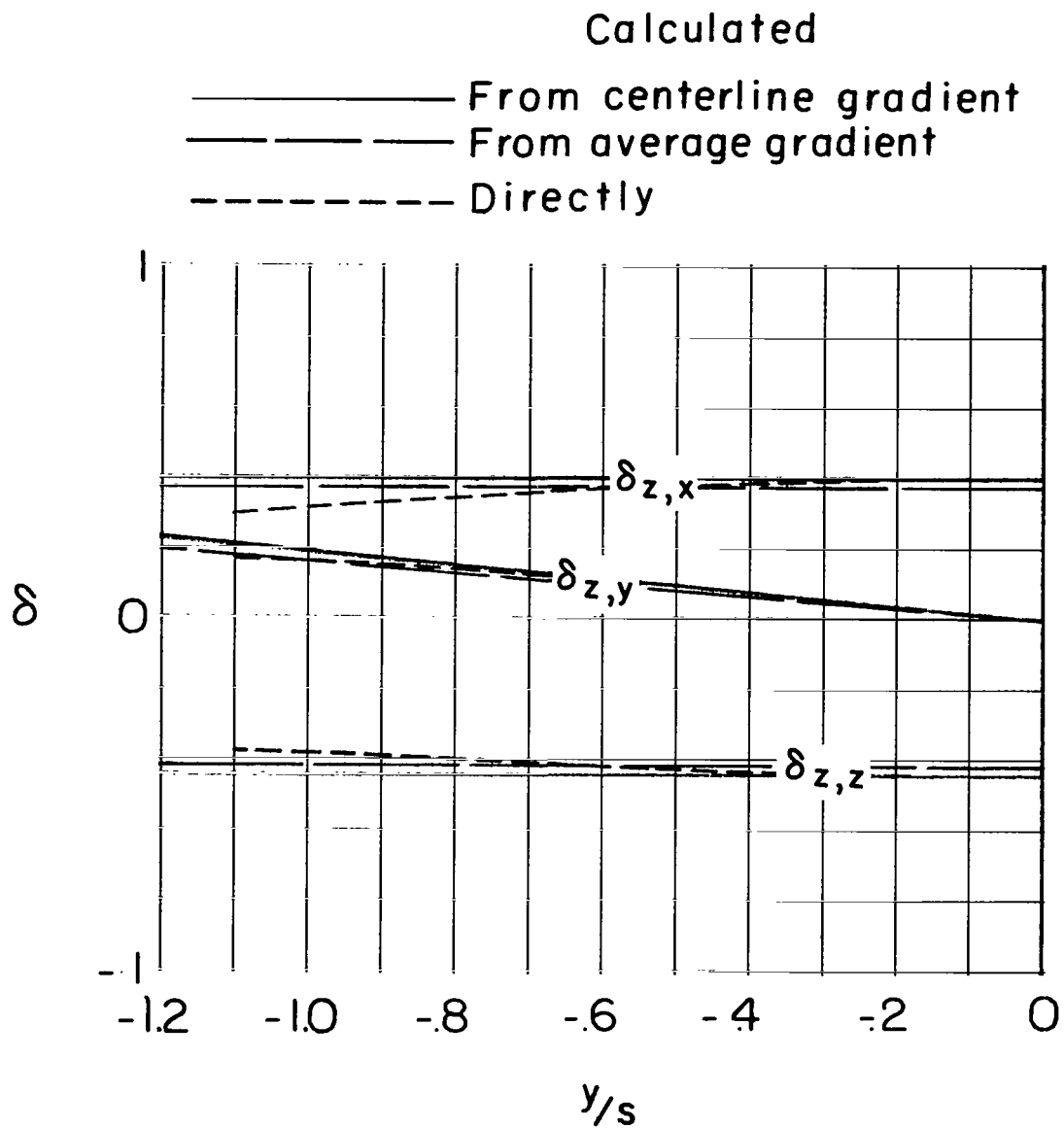
(a) Caused by forces in the X-direction.

Figure 48.- Spanwise distribution of interference factors for a uniformly loaded unswept wing centrally located and spanning half the width of a closed rectangular tunnel having a width-height ratio of 1.5. $\chi_H = 90^\circ$; $\chi_V = 60^\circ$.



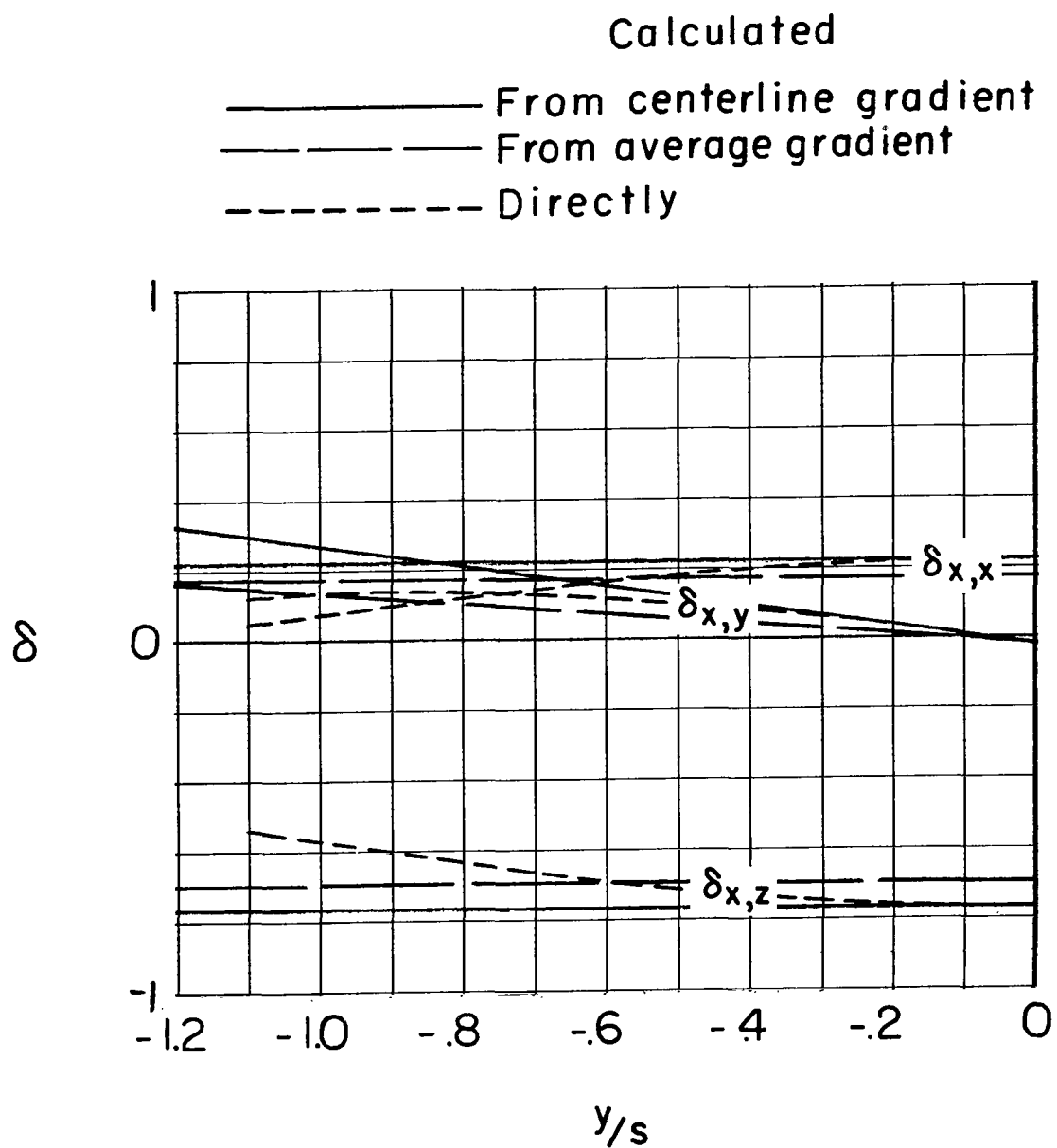
(b) Caused by forces in the Y-direction.

Figure 48.- Continued.



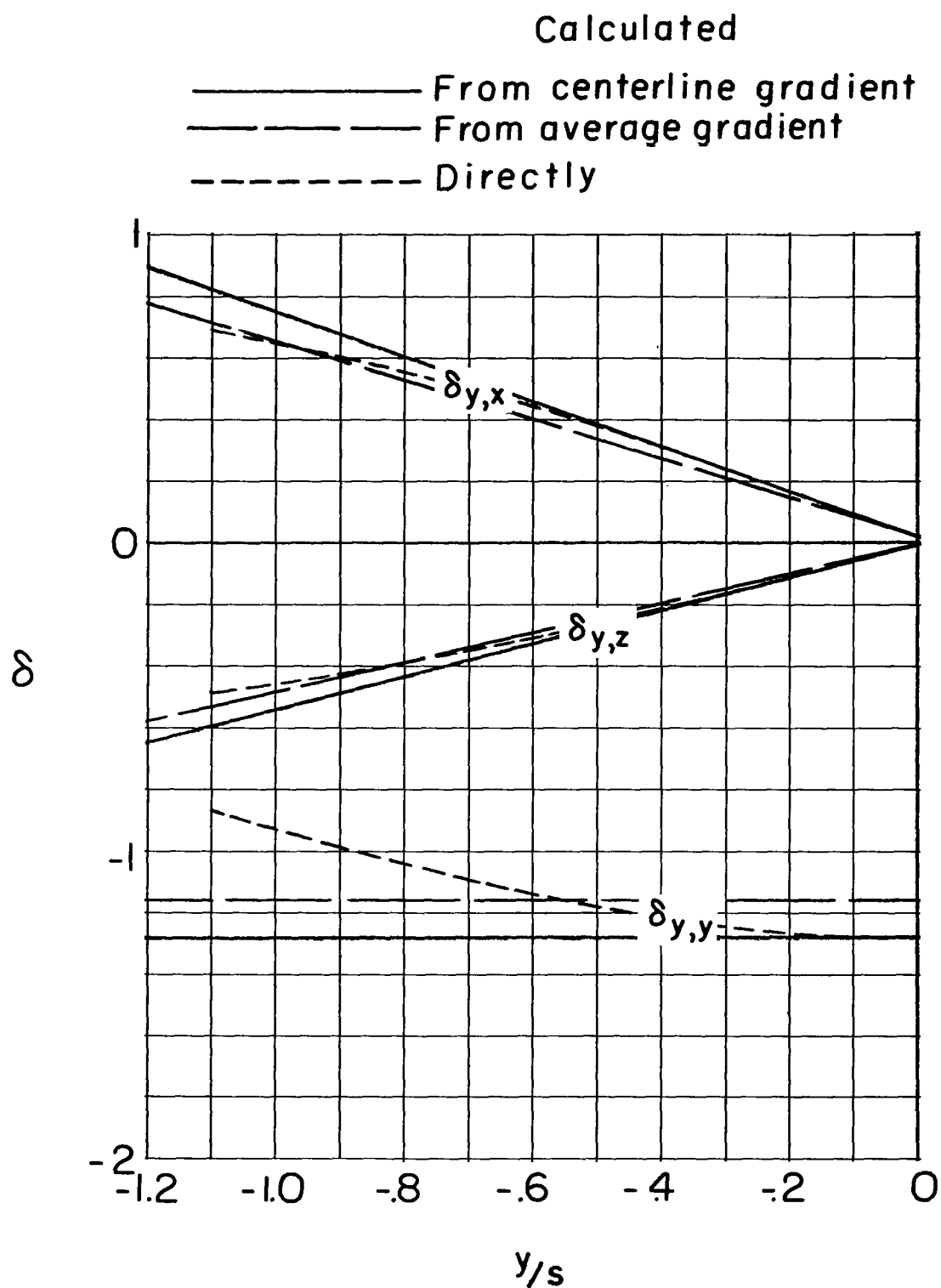
(c) Caused by forces in the Z-direction.

Figure 48.- Concluded.



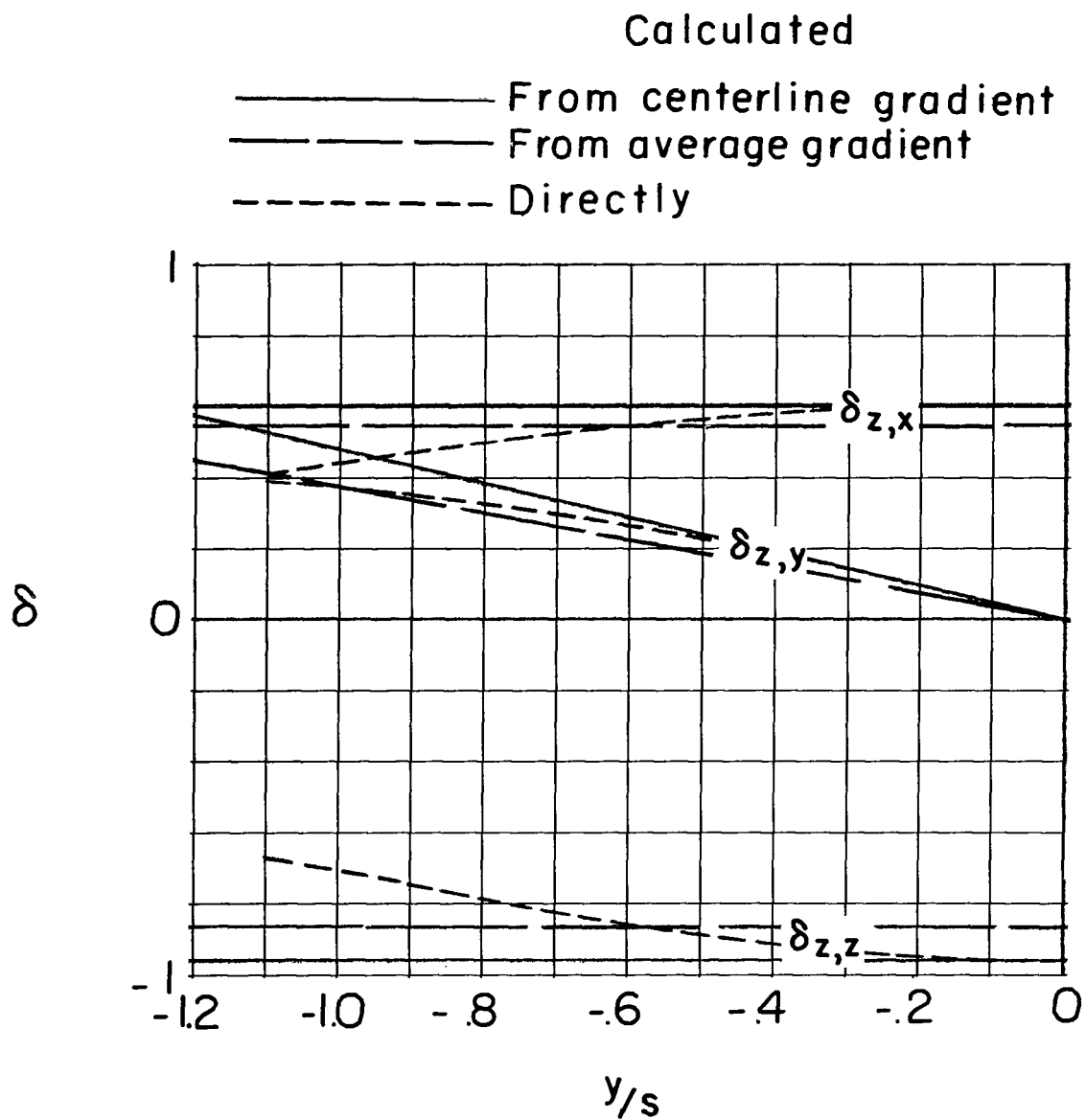
(a) Caused by forces in the X-direction.

Figure 49.- Spanwise distribution of interference factors for a uniformly loaded unswept wing centrally located and spanning half the width of a closed rectangular tunnel having a width-height ratio of 1.5. $X_H = 90^\circ$; $X_V = 30^\circ$.



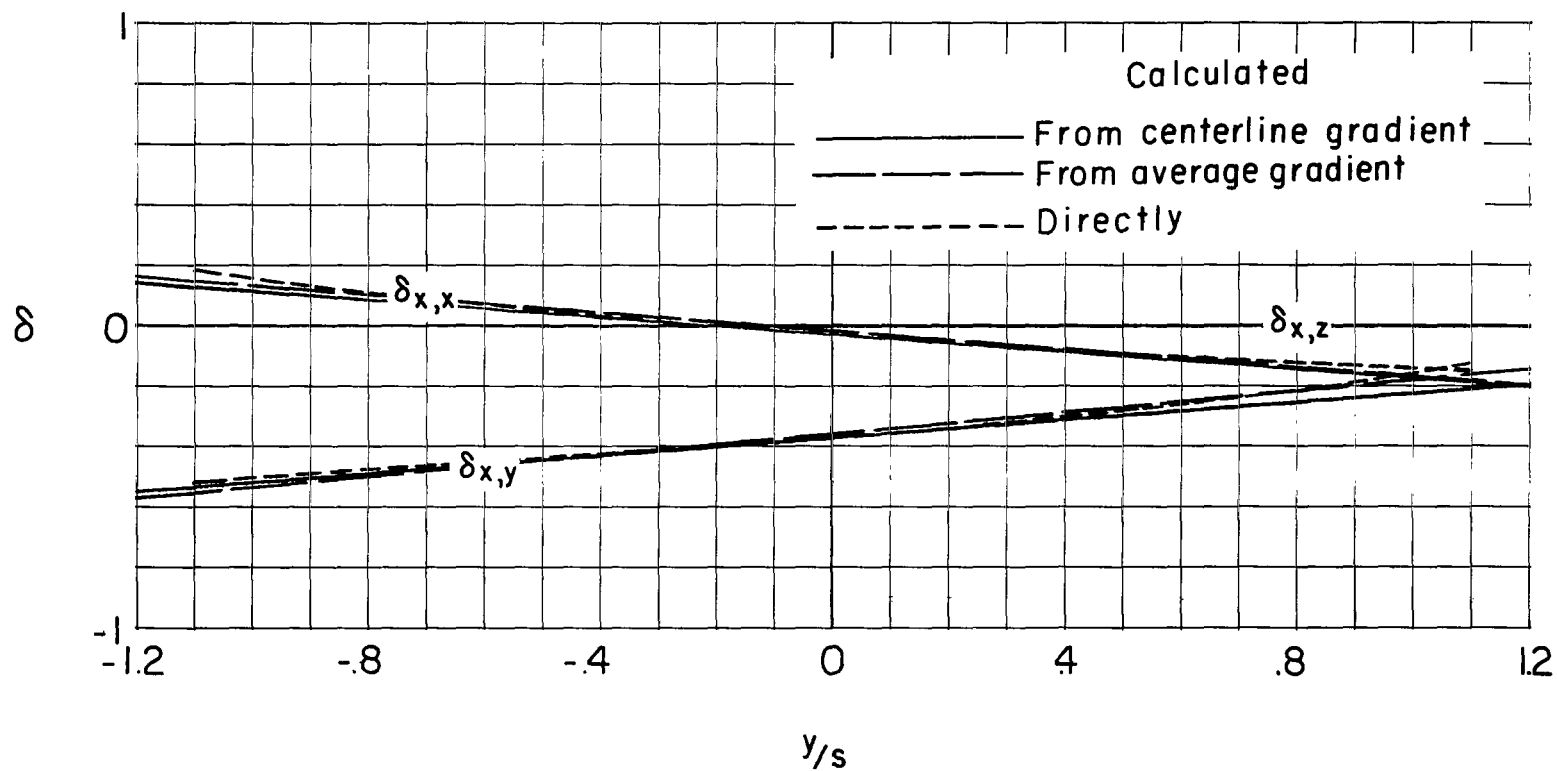
(b) Caused by forces in the Y-direction.

Figure 49.- Continued.



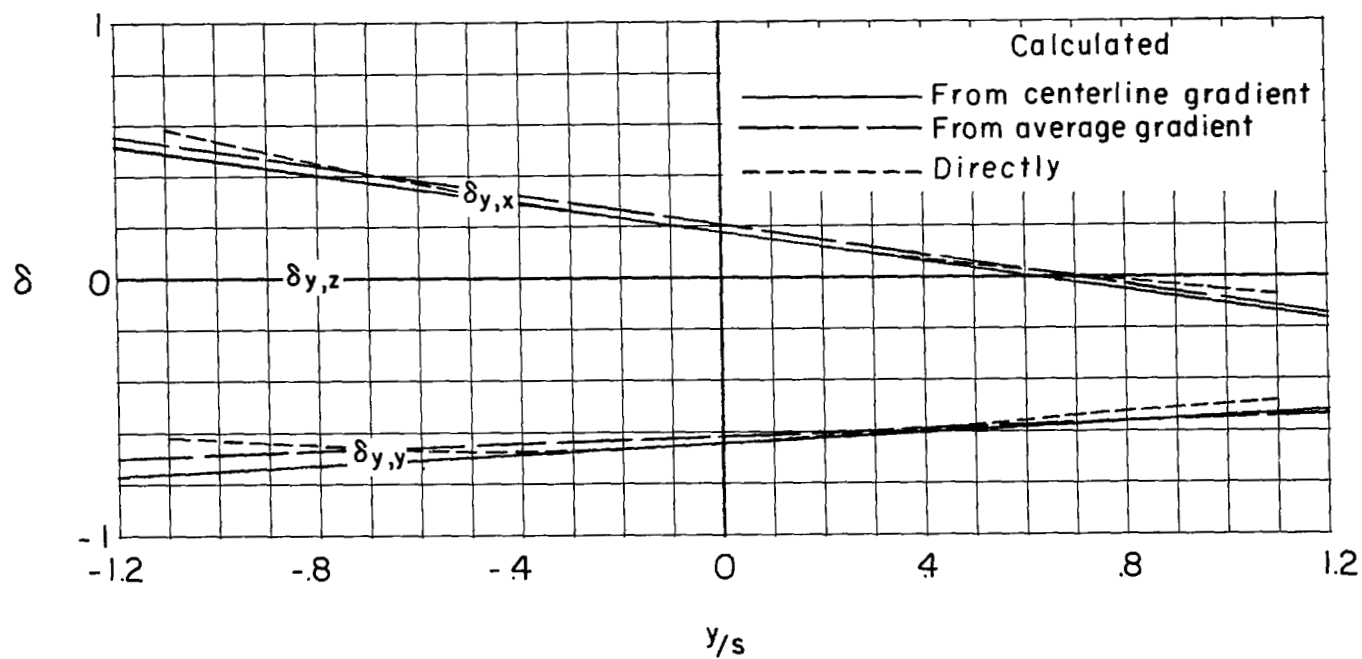
(c) Caused by forces in the Z-direction.

Figure 49.- Concluded.

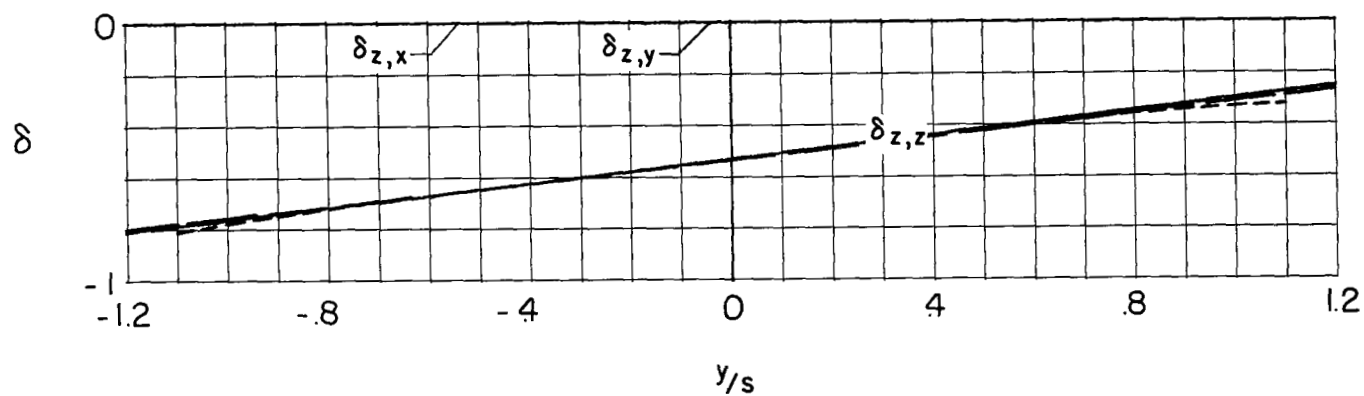


(a) Caused by forces in the X-direction.

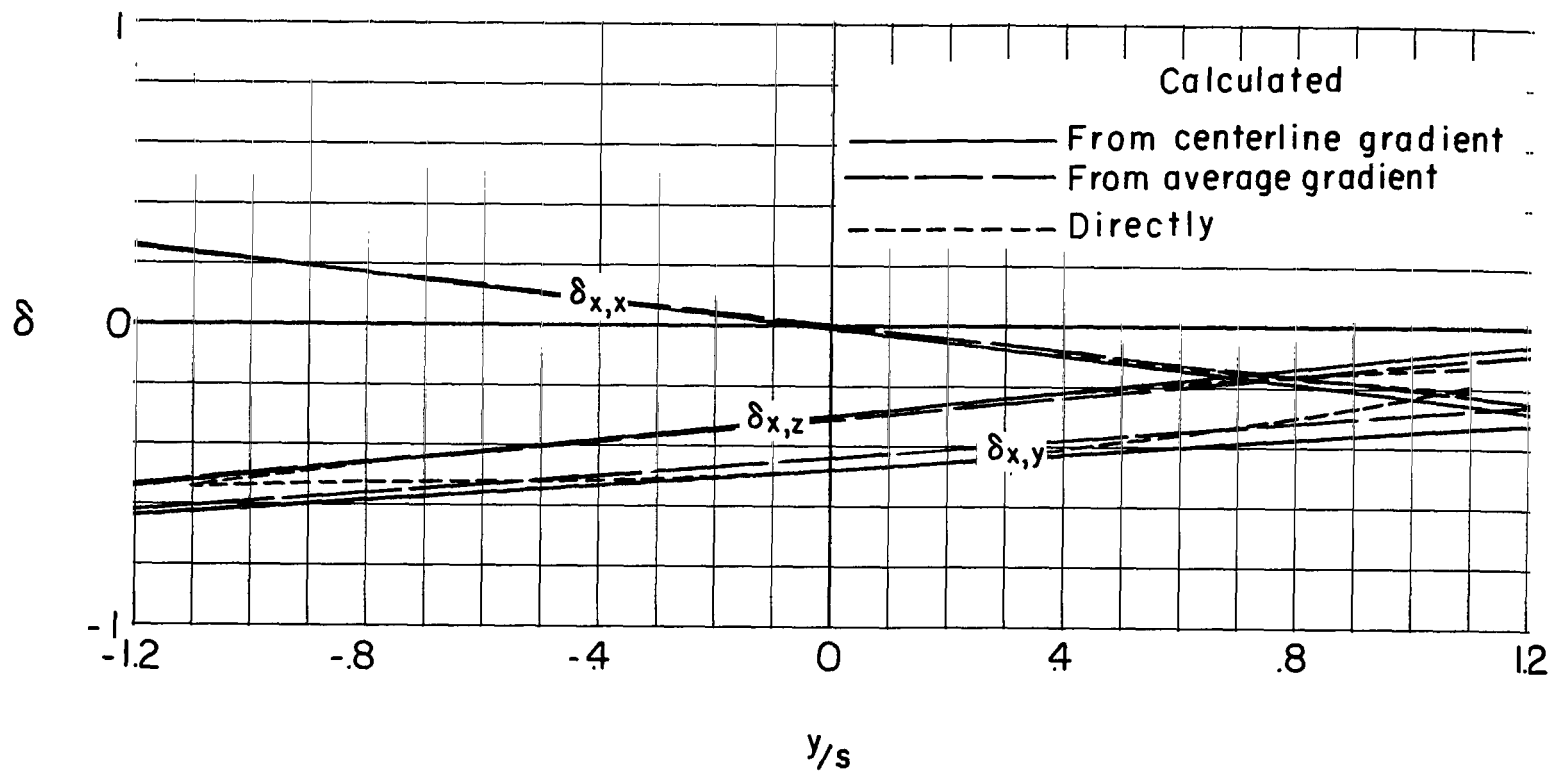
Figure 50.- Spanwise distribution of interference factors for a uniformly loaded unswept wing centrally located and spanning half the width of a closed rectangular tunnel having a width-height ratio of 1.5. $X_H = 60^\circ$; $X_V = 90^\circ$.



(b) Caused by forces in the Y-direction.

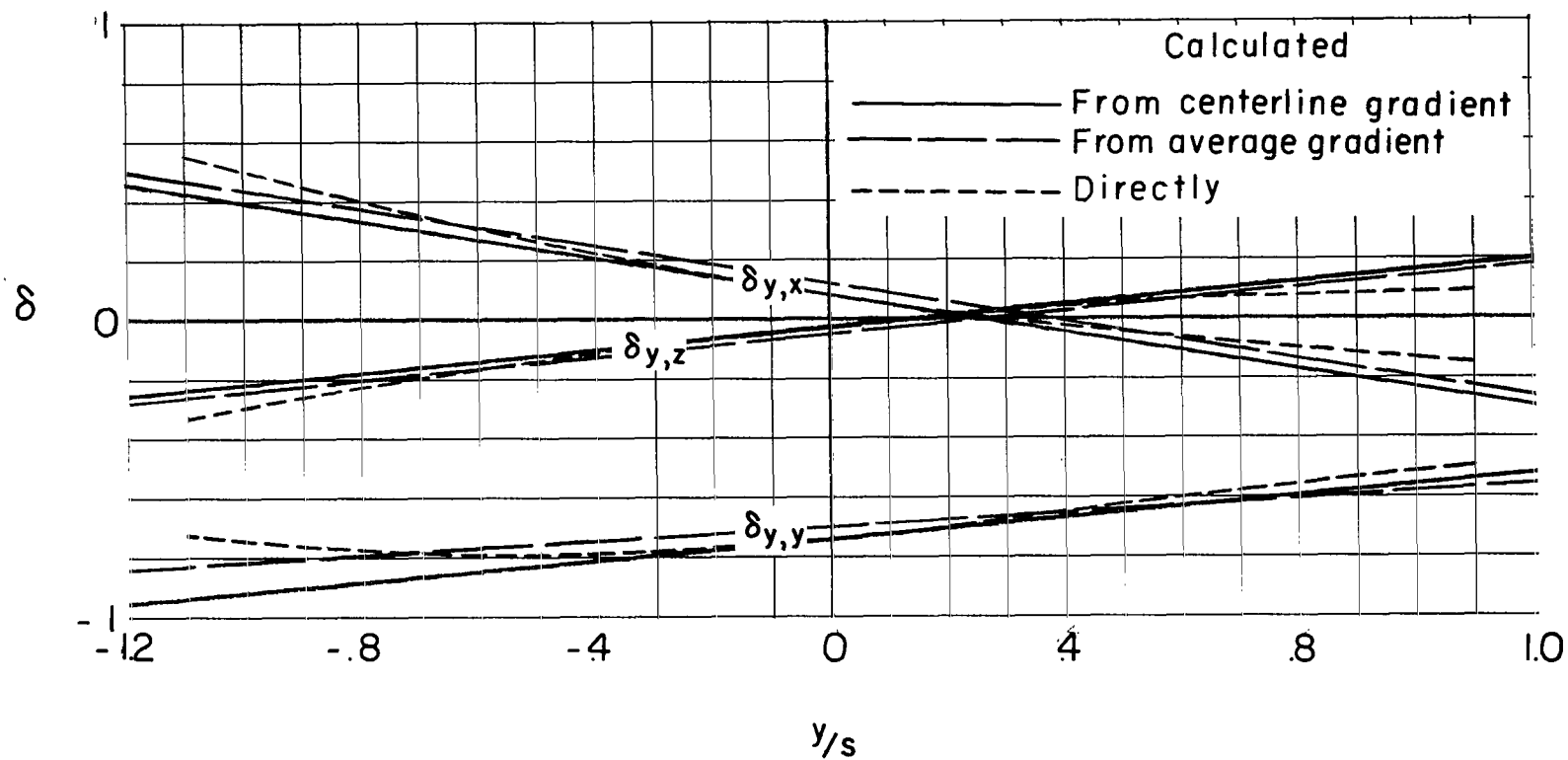


(c) Caused by forces in the Z-direction.



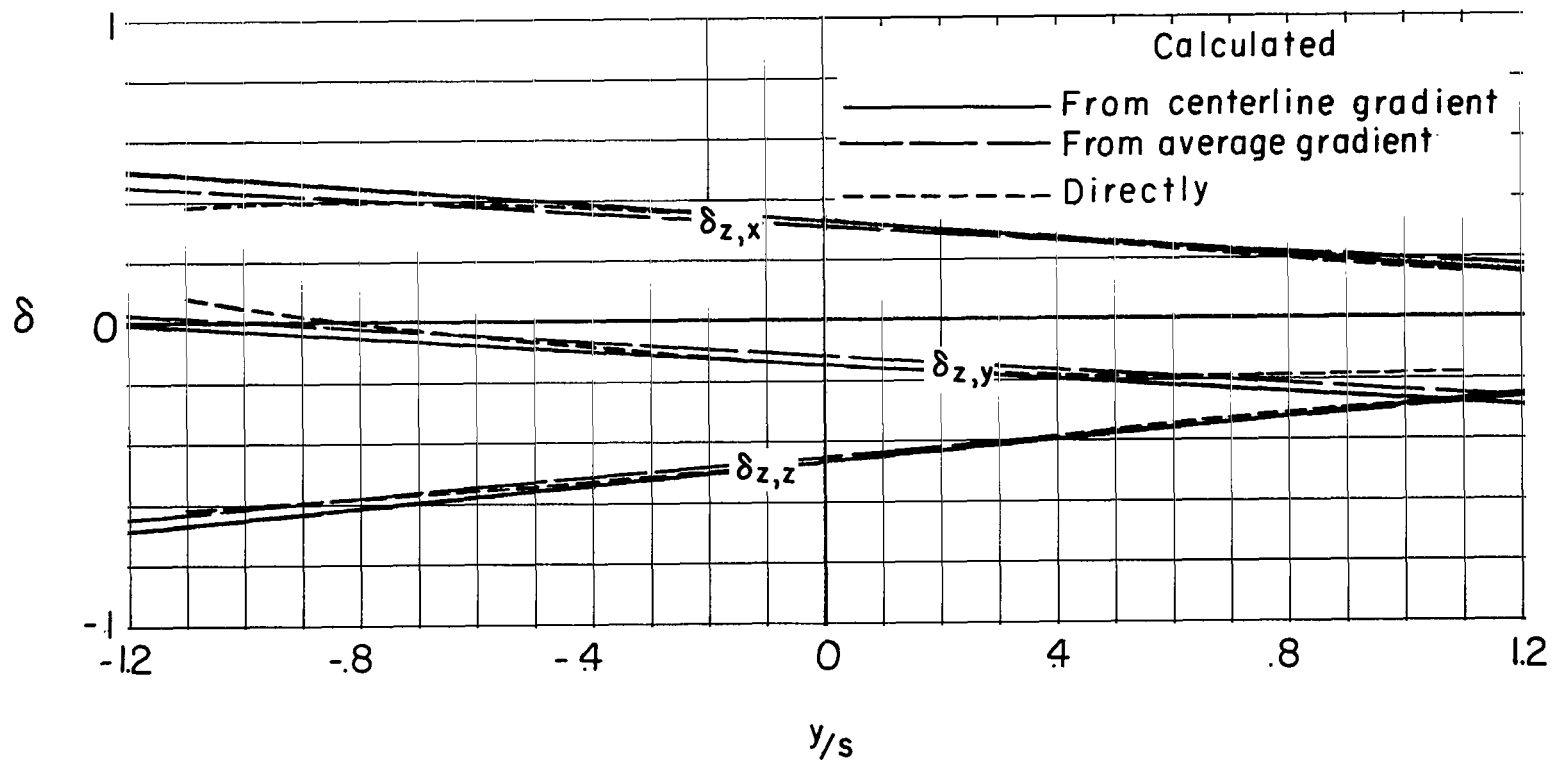
(a) Caused by forces in the X-direction.

Figure 51.- Spanwise distribution of interference factors for a uniformly loaded unswept wing centrally located and spanning half the width of a closed rectangular tunnel having a width-height ratio of 1.5. $\chi_H = 60^\circ$; $\chi_V = 60^\circ$.



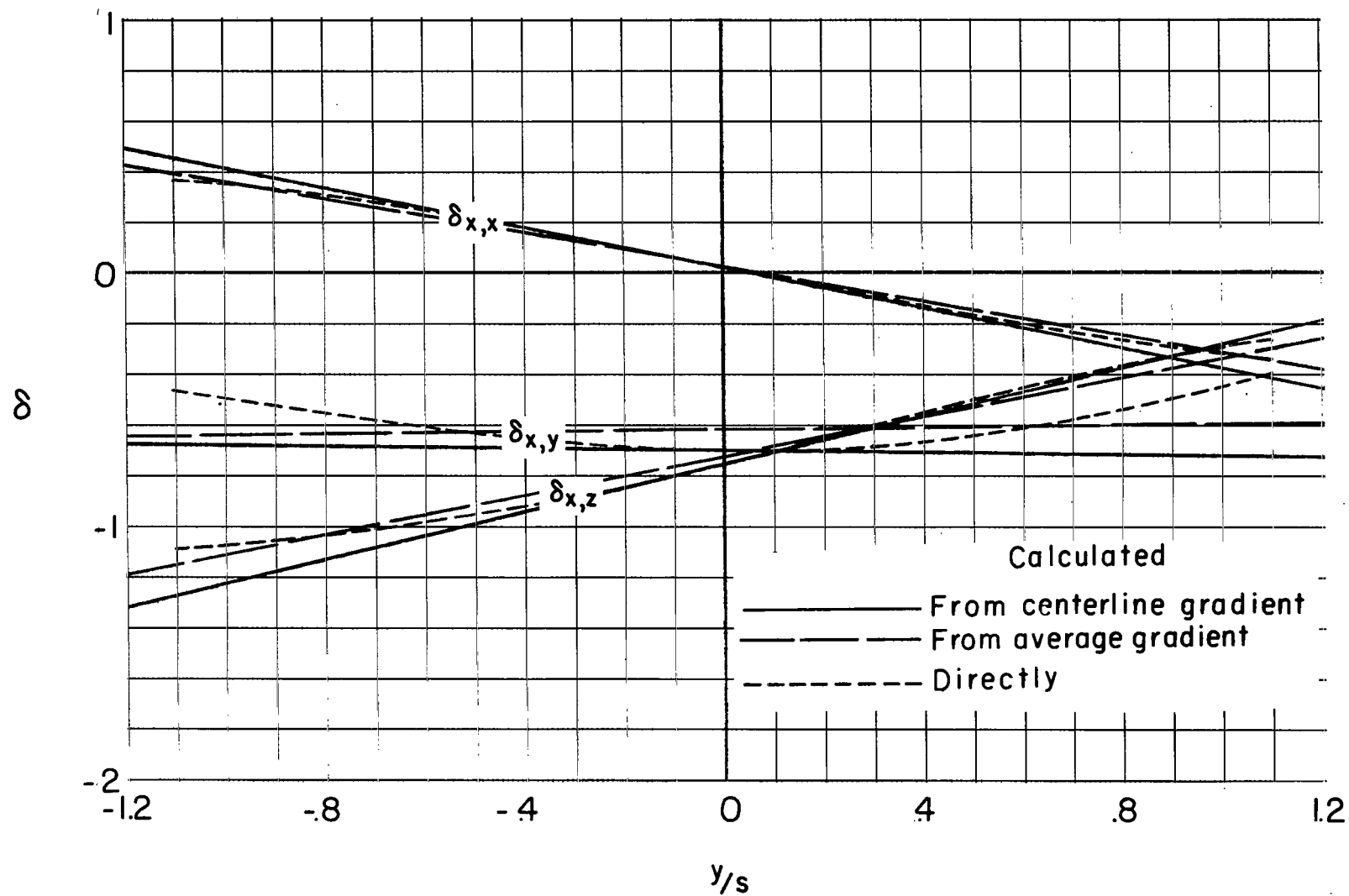
(b) Caused by forces in the Y-direction.

Figure 51.- Continued.



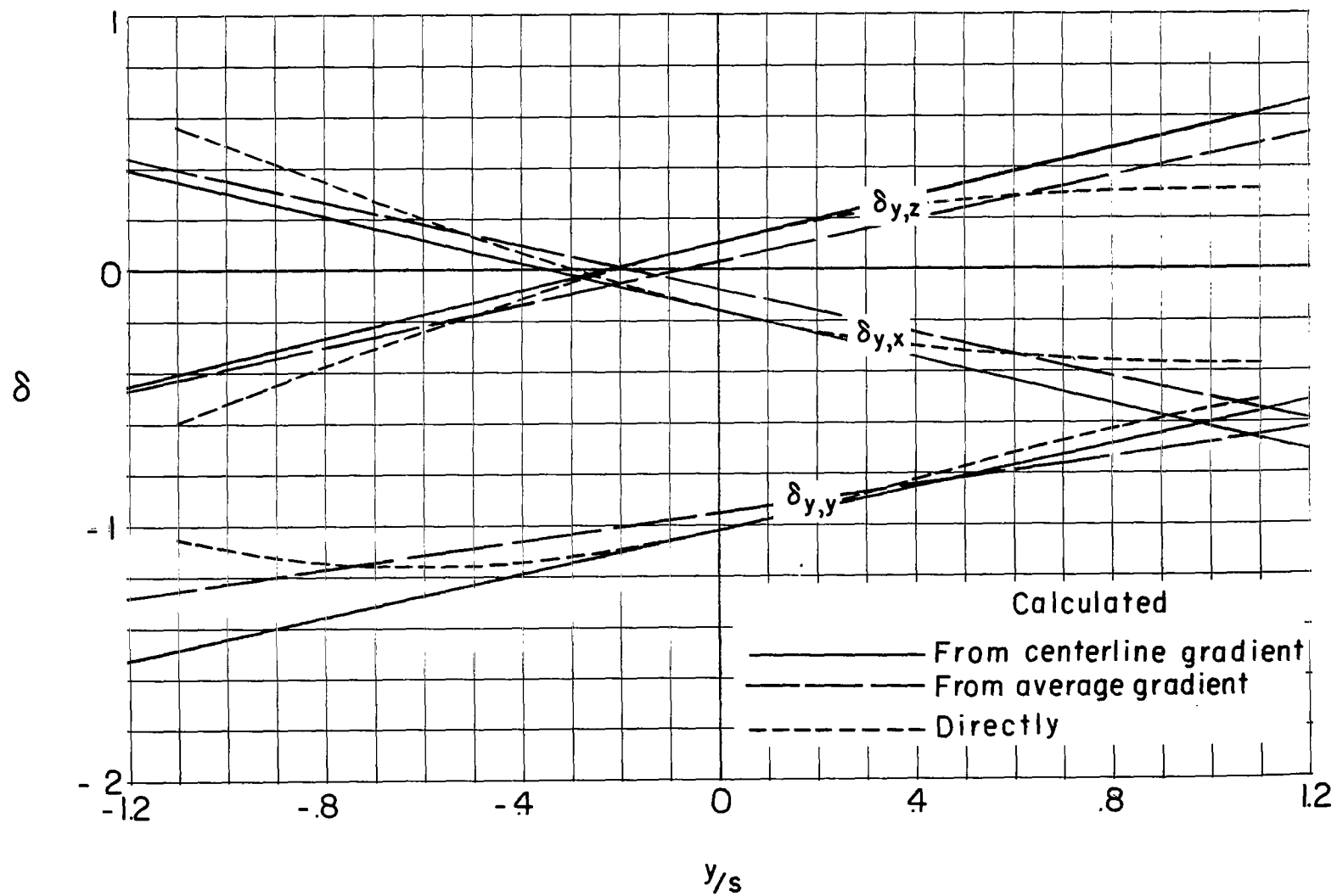
(c) Caused by forces in the Z-direction.

Figure 51.- Concluded.



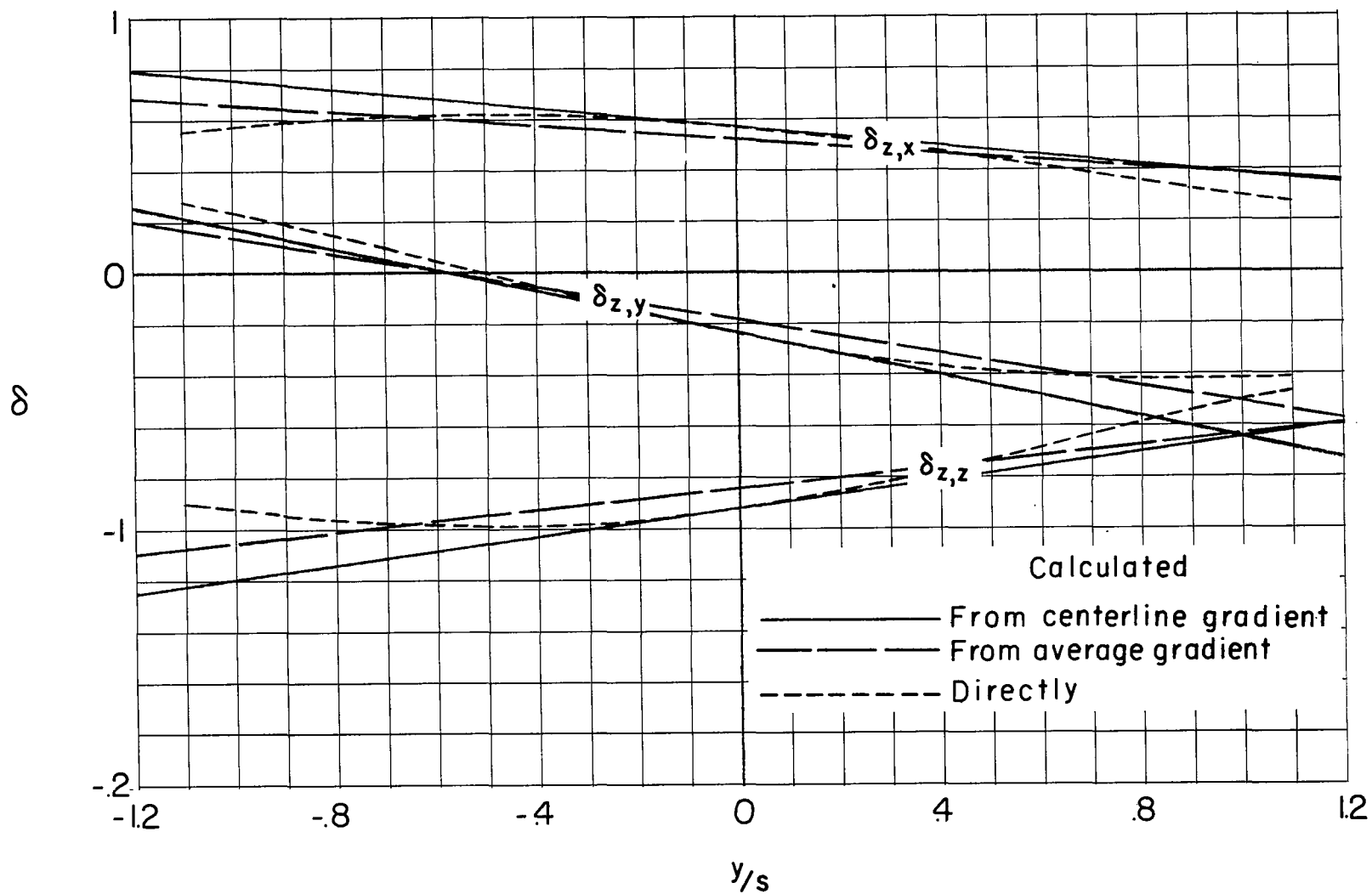
(a) Caused by forces in the X-direction.

Figure 52.- Spanwise distribution of interference factors for a uniformly loaded unswept wing centrally located and spanning half the width of a closed rectangular tunnel having a width-height ratio of 1.5. $\chi_H = 60^\circ$; $\chi_V = 30^\circ$.



(b) Caused by forces in the Y-direction.

Figure 52.- Continued.

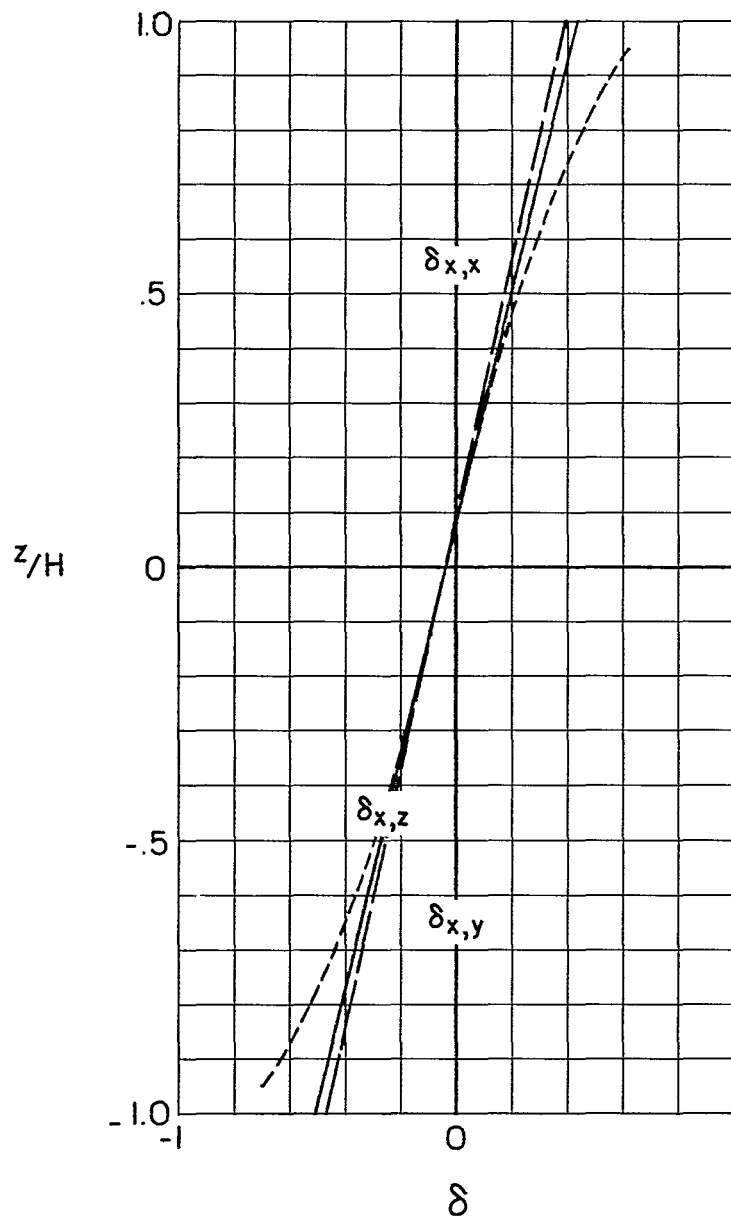


(c) Caused by forces in the Z-direction.

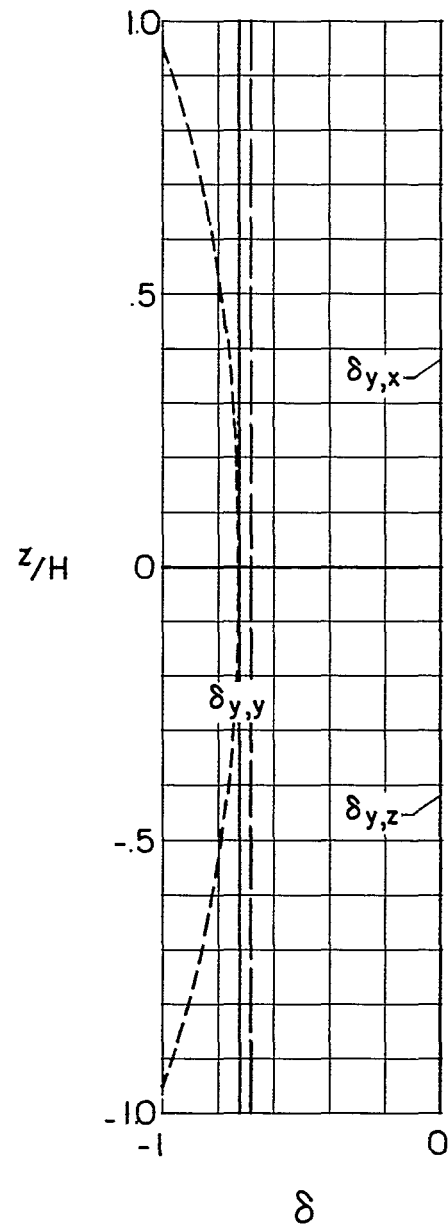
Figure 52.- Concluded.

Calculated

- From centerline gradient
- From average gradient
- Directly

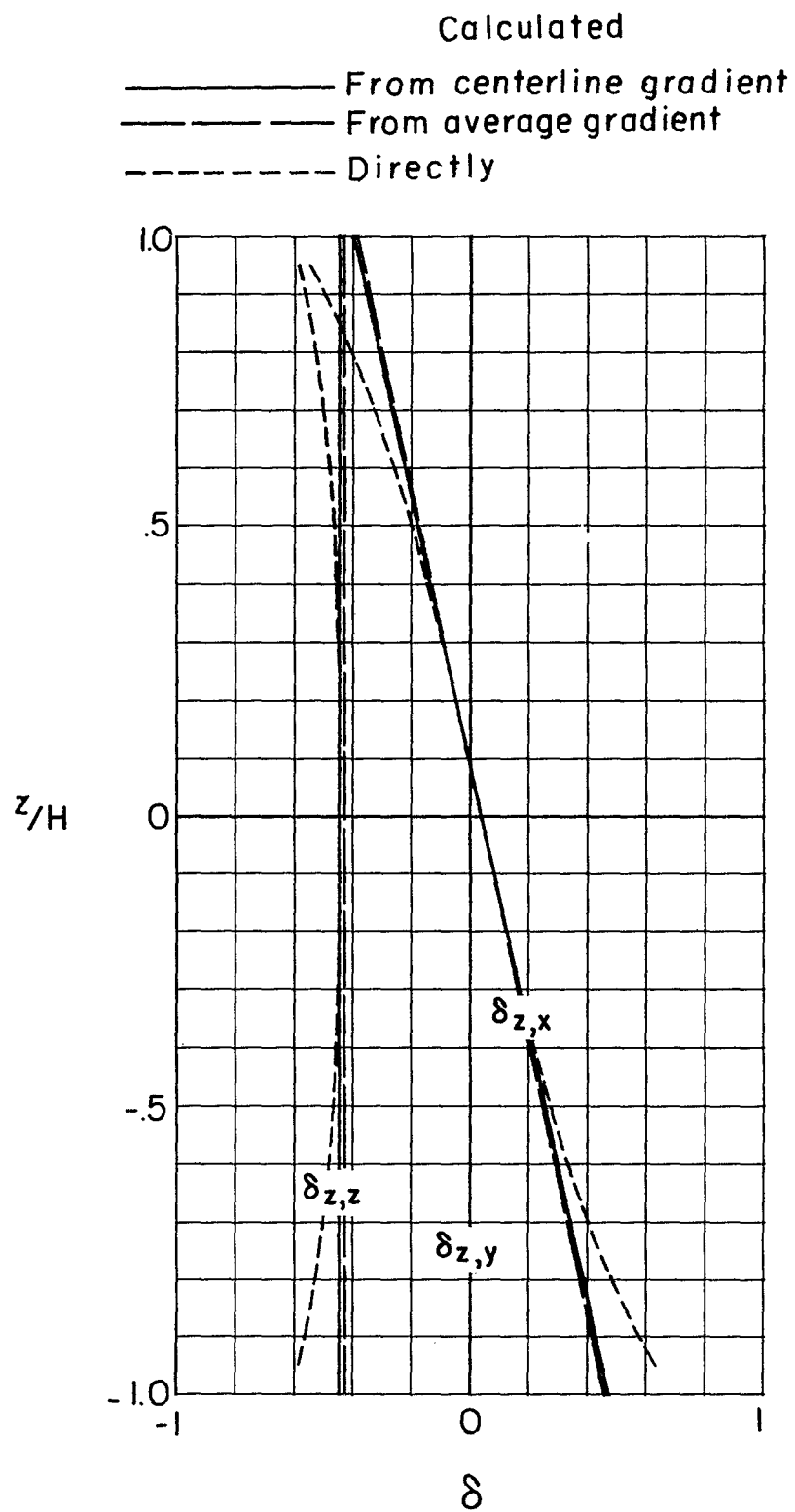


(a) Caused by forces in the X-direction.



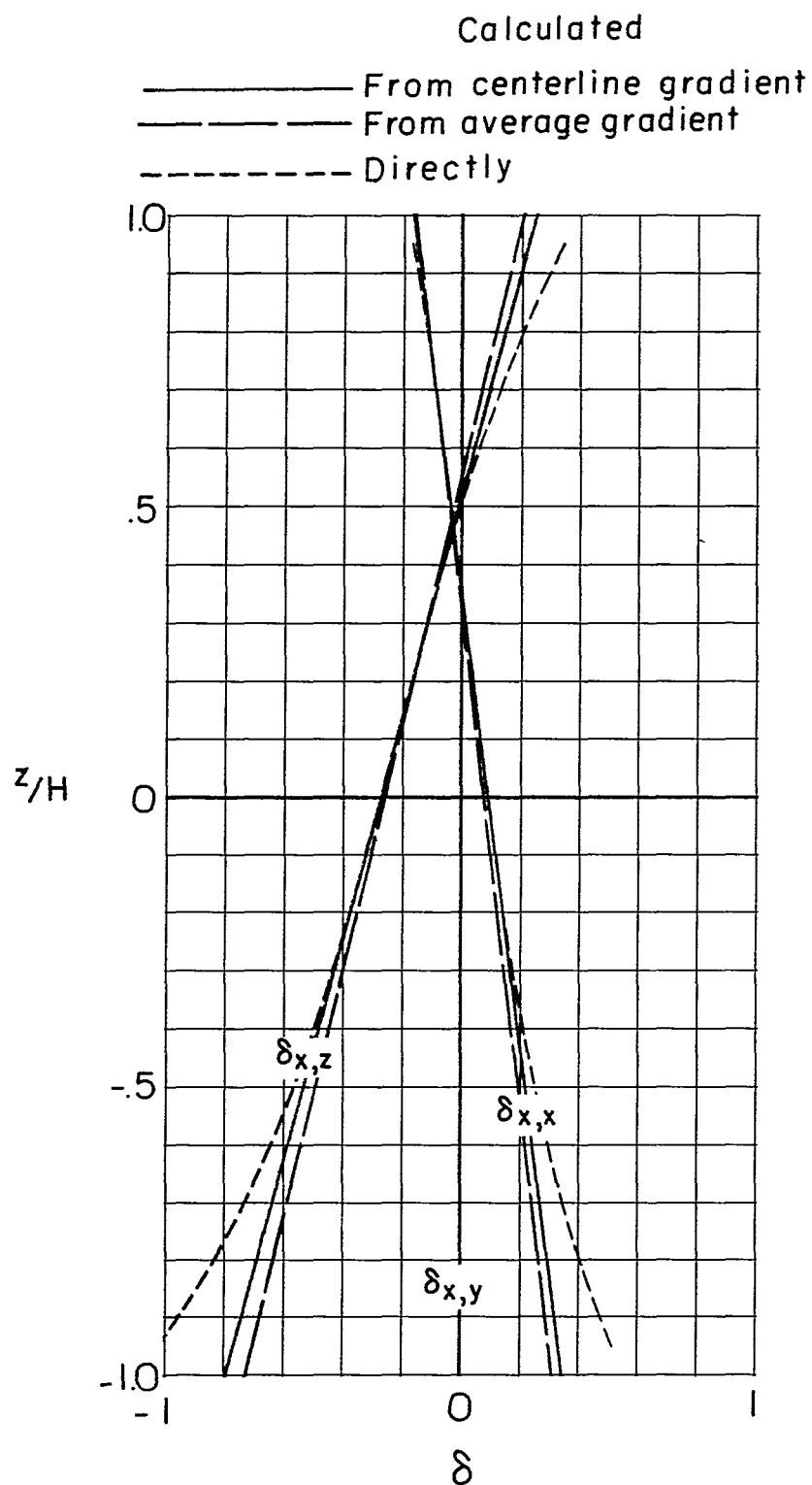
(b) Caused by forces in the Y-direction.

Figure 53.- Distribution of interference factors over the vertical axis of the tunnel for a uniformly loaded unswept wing centrally located and spanning half the width of a closed rectangular tunnel having a width-height ratio of 1.5. $\chi_H = 90^\circ$; $\chi_V = 90^\circ$.



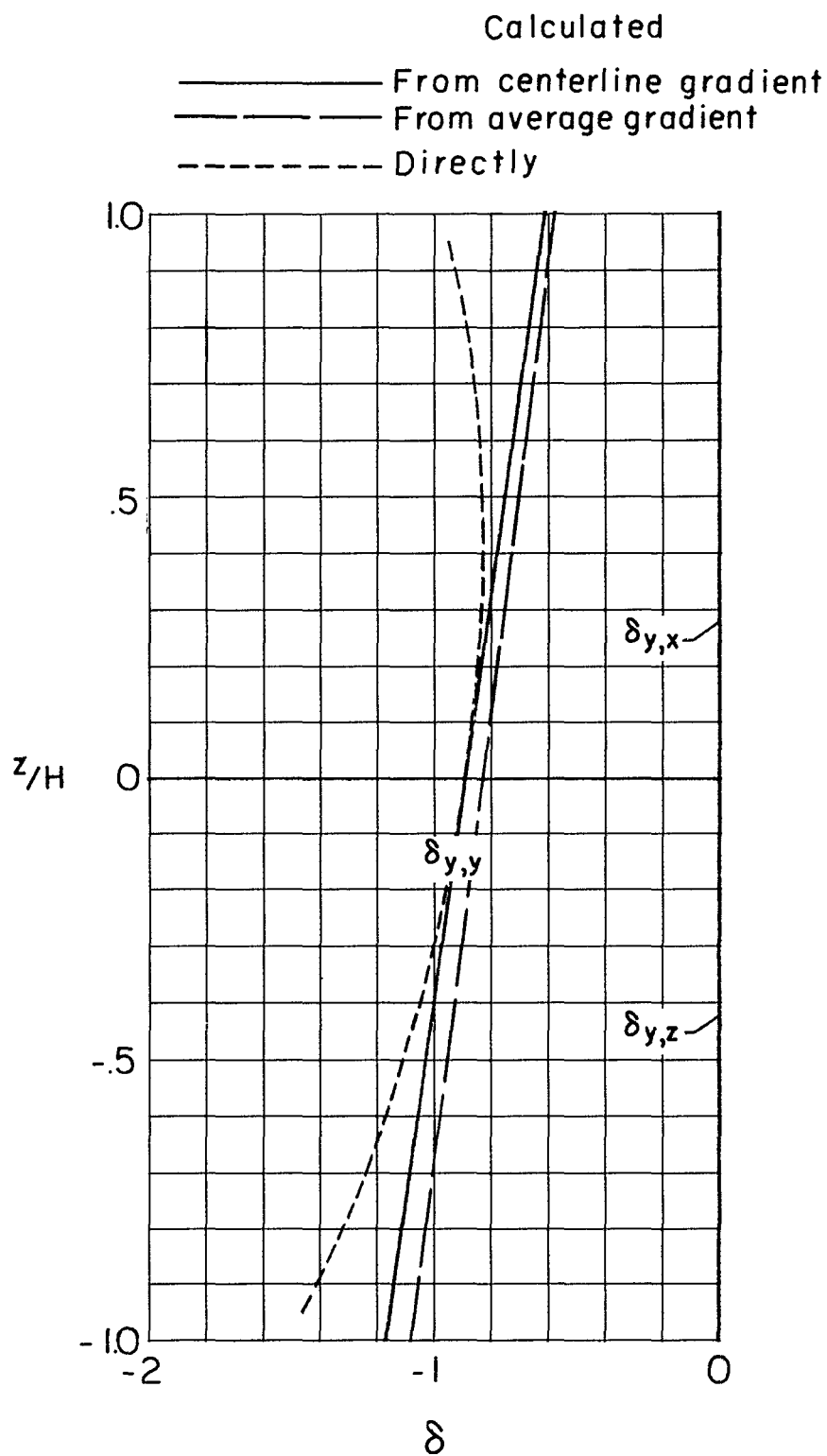
(c) Caused by forces in the Z-direction.

Figure 53.- Concluded.



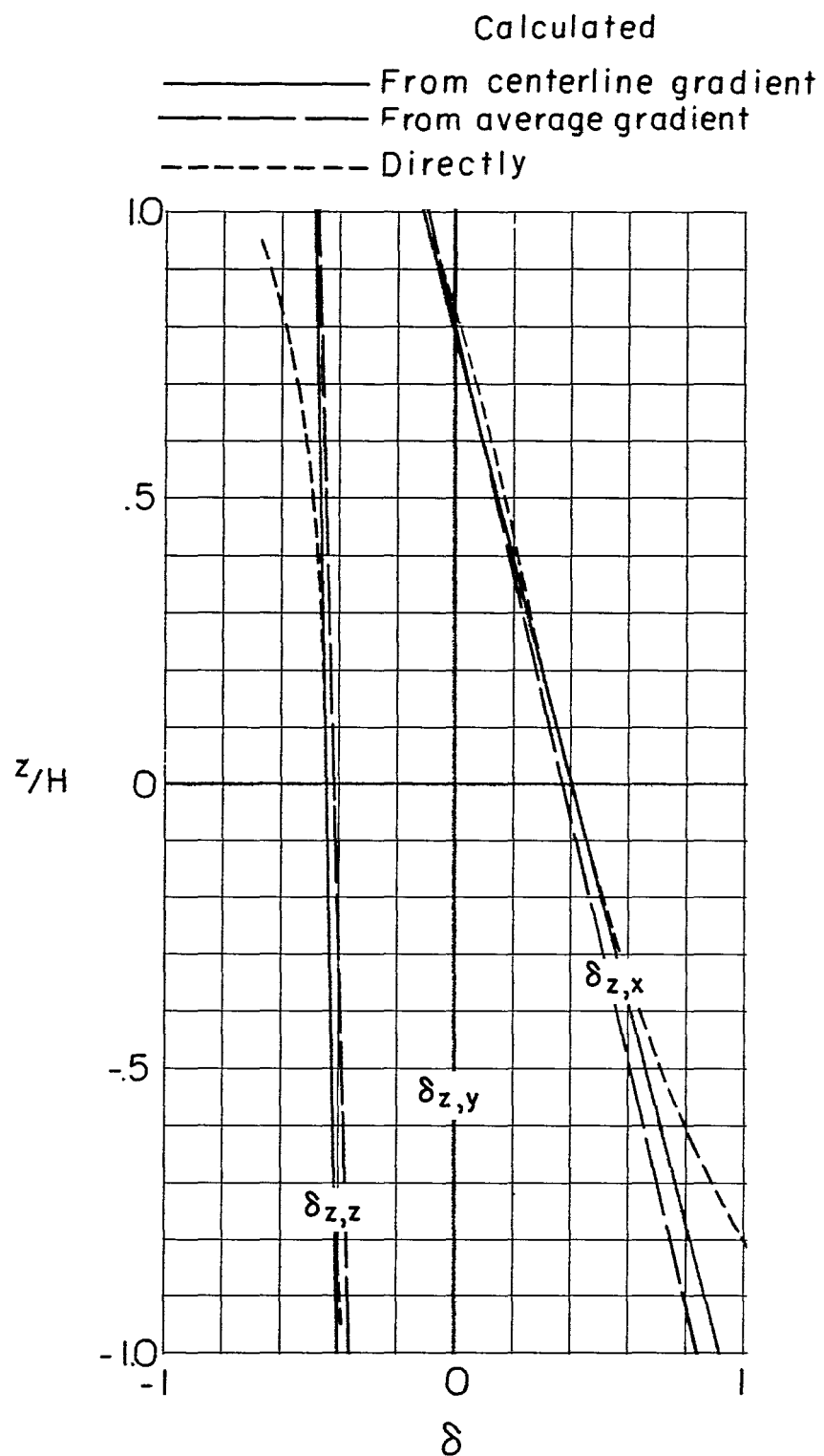
(a) Caused by forces in the X-direction.

Figure 54.- Distribution of interference factors over the vertical axis of the tunnel for a uniformly loaded unswept wing centrally located and spanning half the width of a closed rectangular tunnel having a width-height ratio of 1.5. $\chi_H = 90^\circ$; $\chi_V = 60^\circ$.



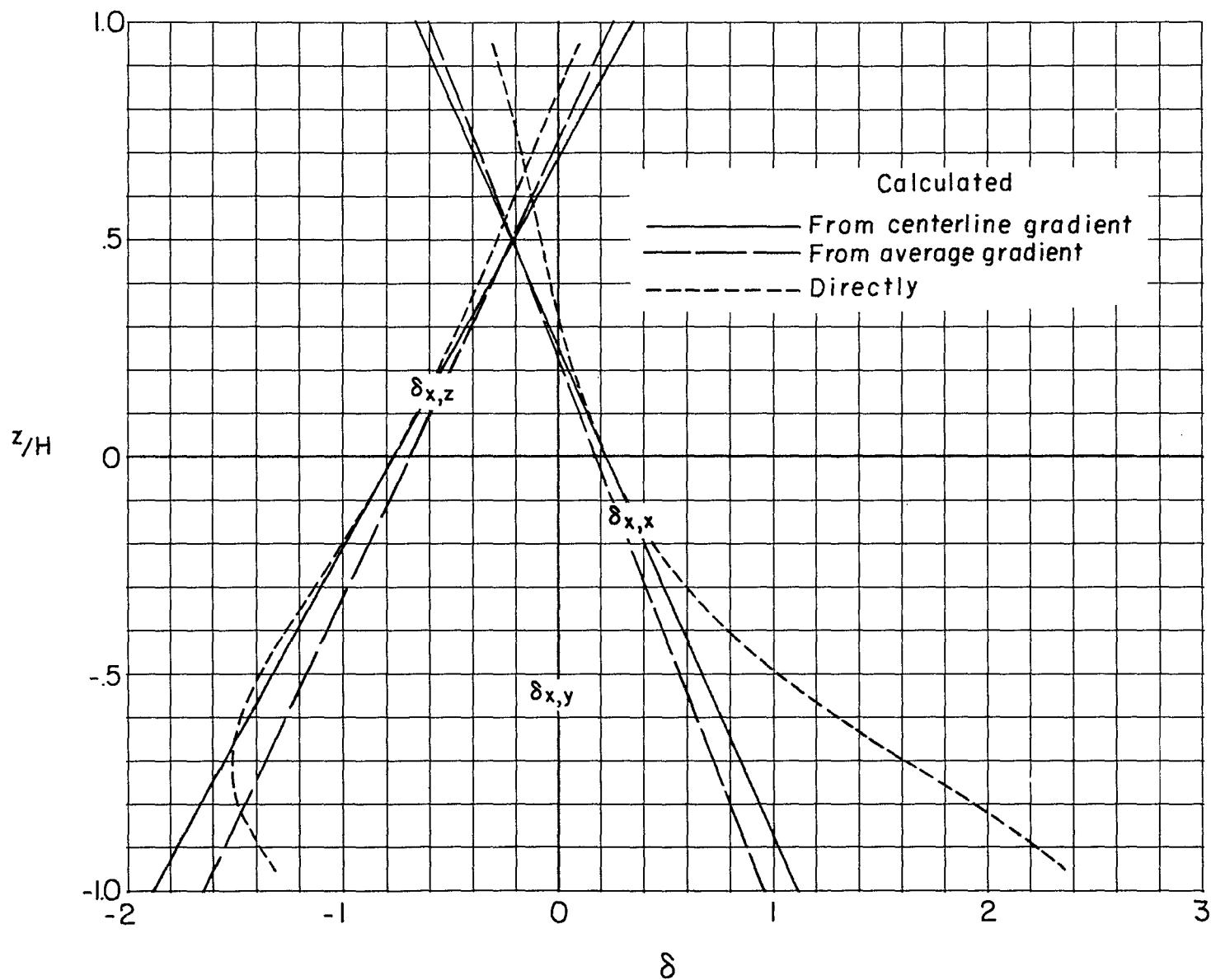
(b) Caused by forces in the Y-direction.

Figure 54.- Continued.



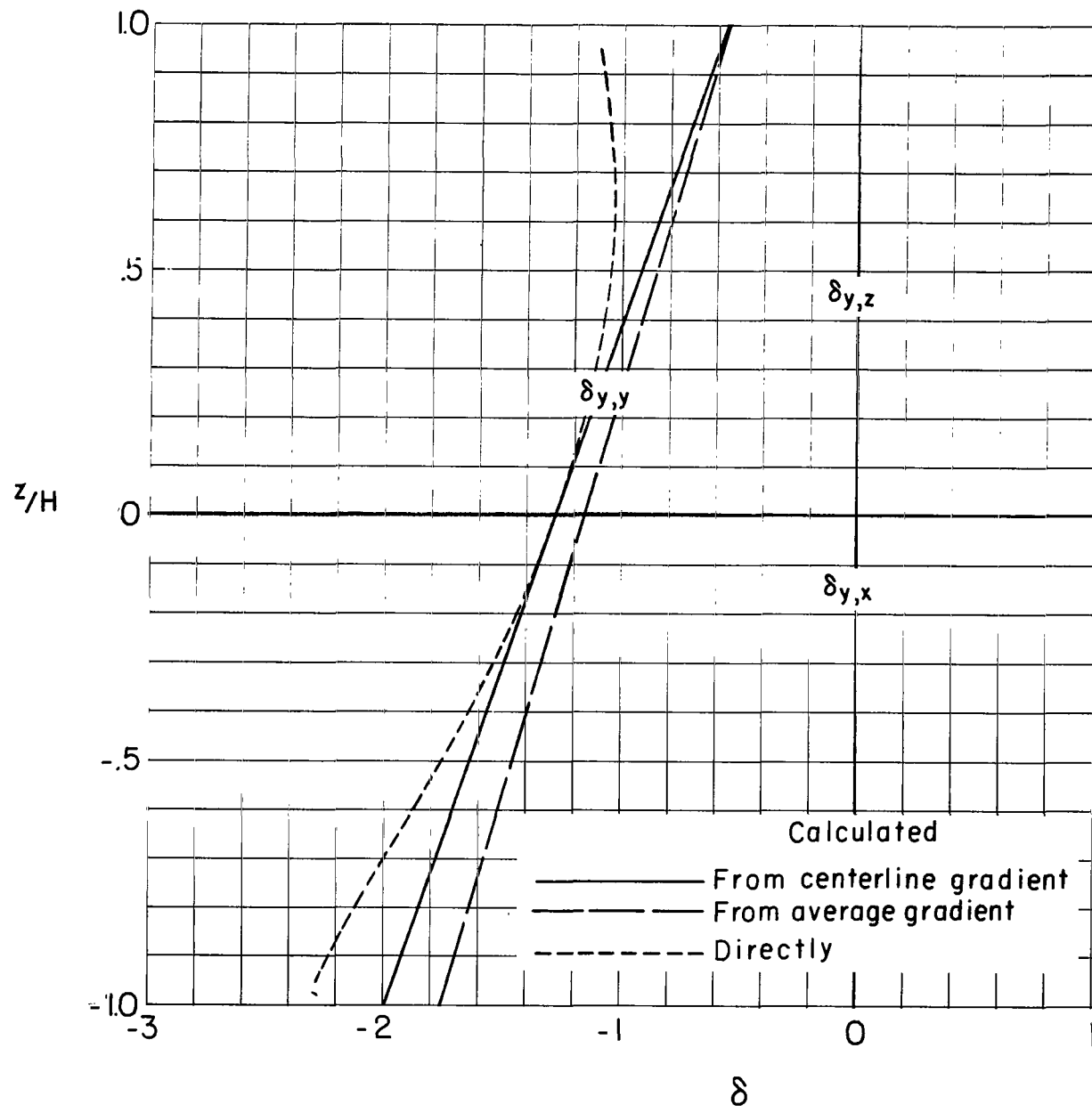
(c) Caused by forces in the Z-direction.

Figure 54.- Concluded.



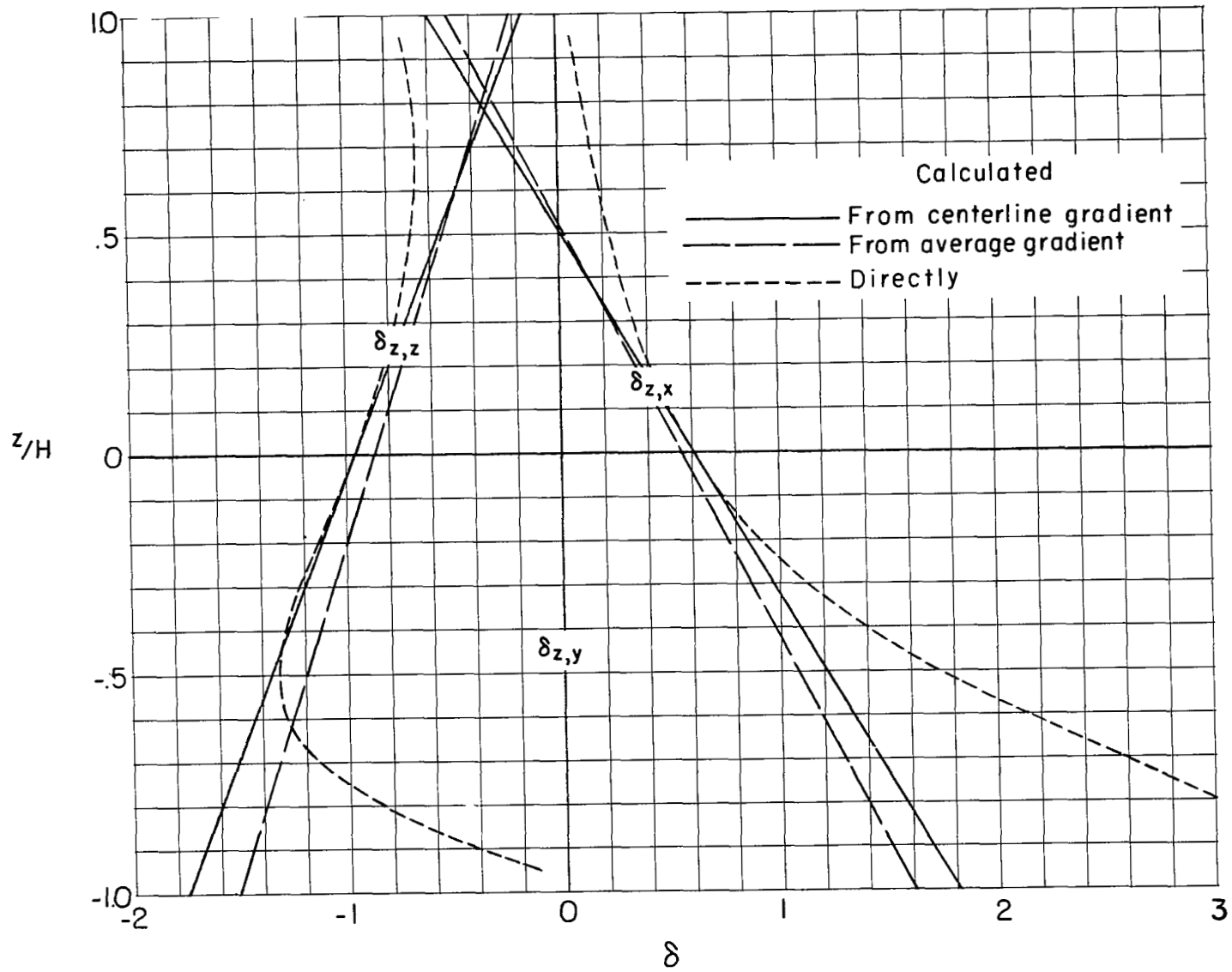
(a) Caused by forces in the X-direction.

Figure 55.- Distribution of interference factors over the vertical axis of the tunnel for a uniformly loaded unswept wing centrally located and spanning half the width of a closed rectangular tunnel having a width-height ratio of 1.5. $x_H = 90^\circ$; $x_V = 30^\circ$.



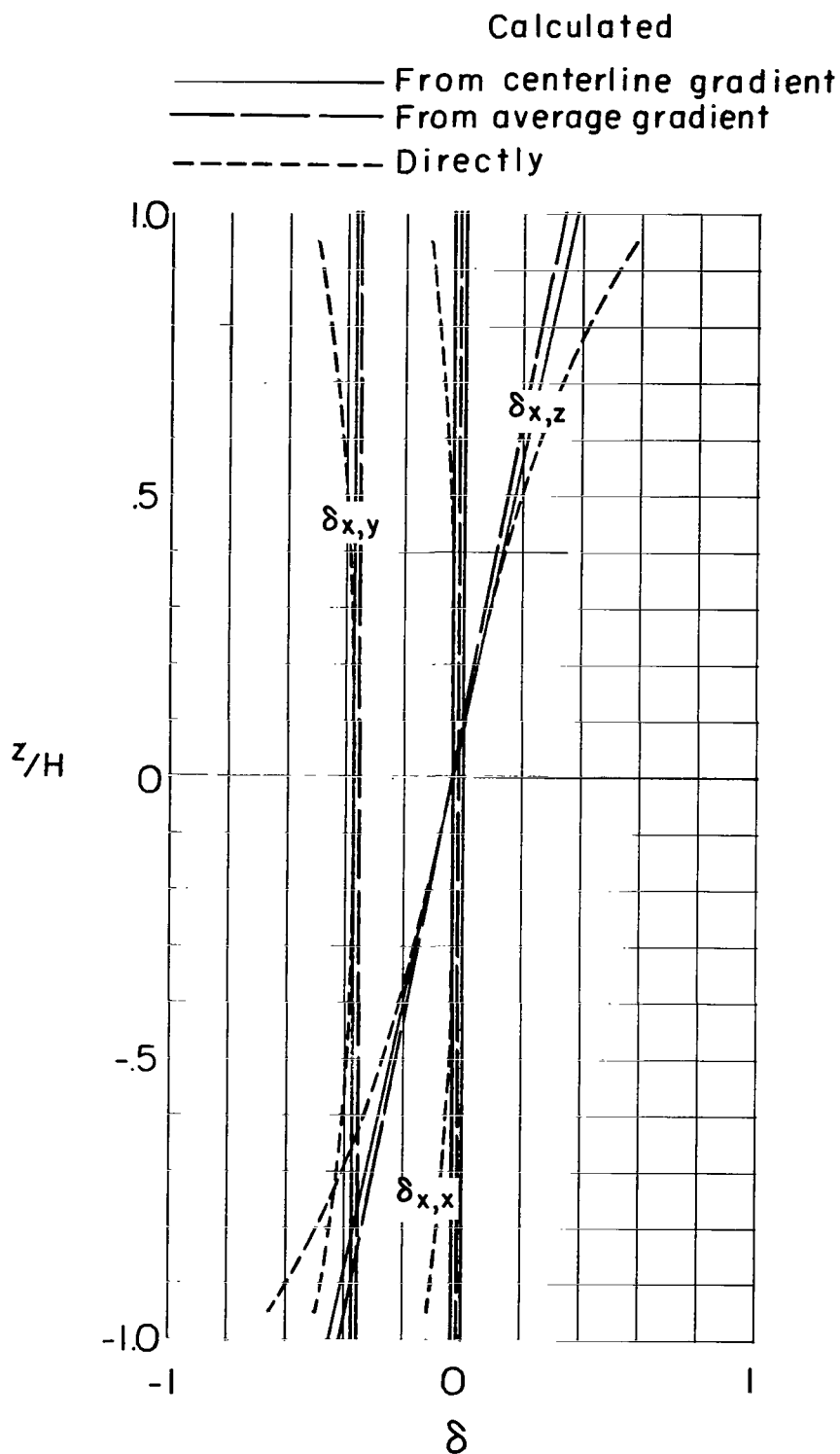
(b) Caused by forces in the Y-direction.

Figure 55.- Continued.



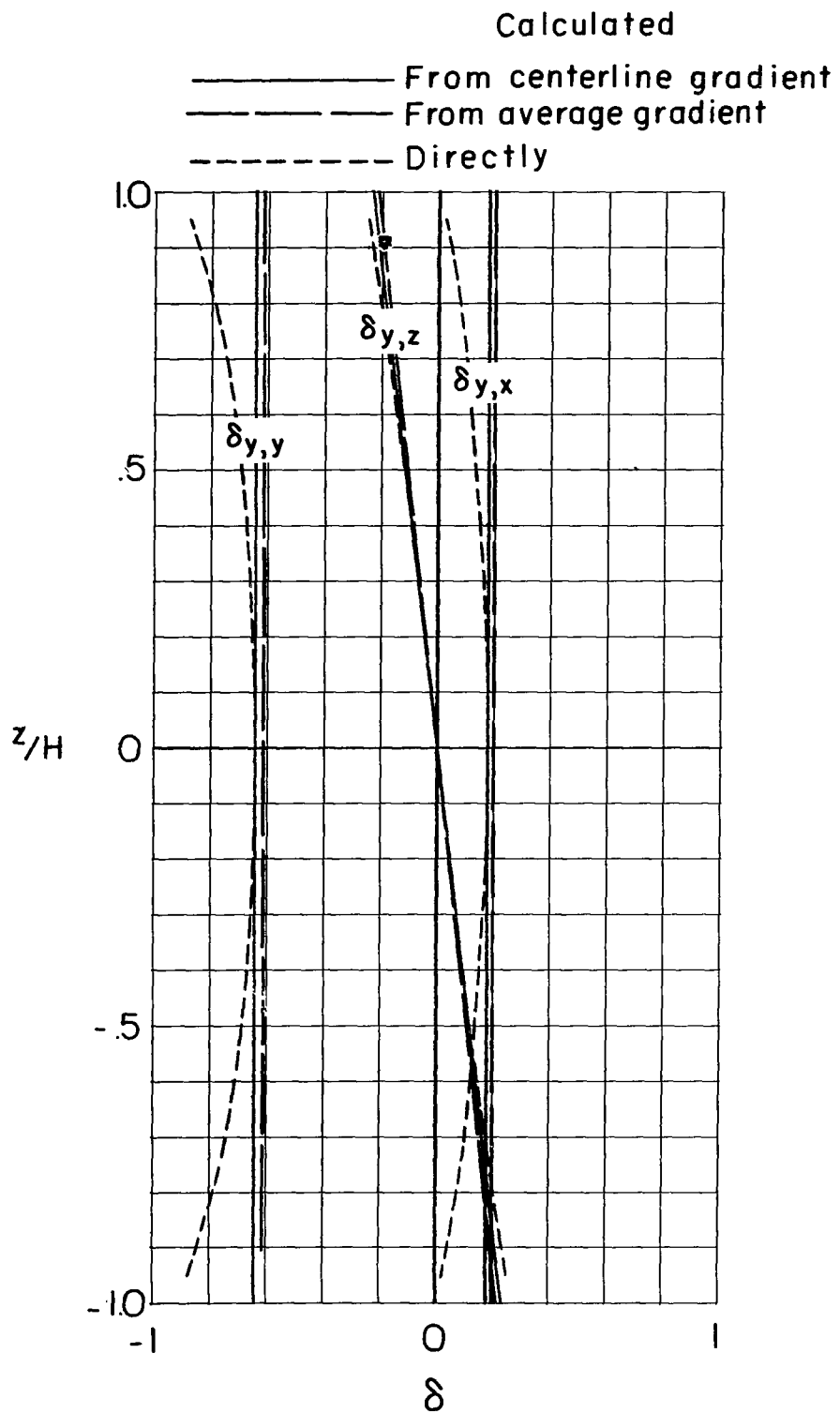
(c) Caused by forces in the Z-direction.

Figure 55.- Concluded.



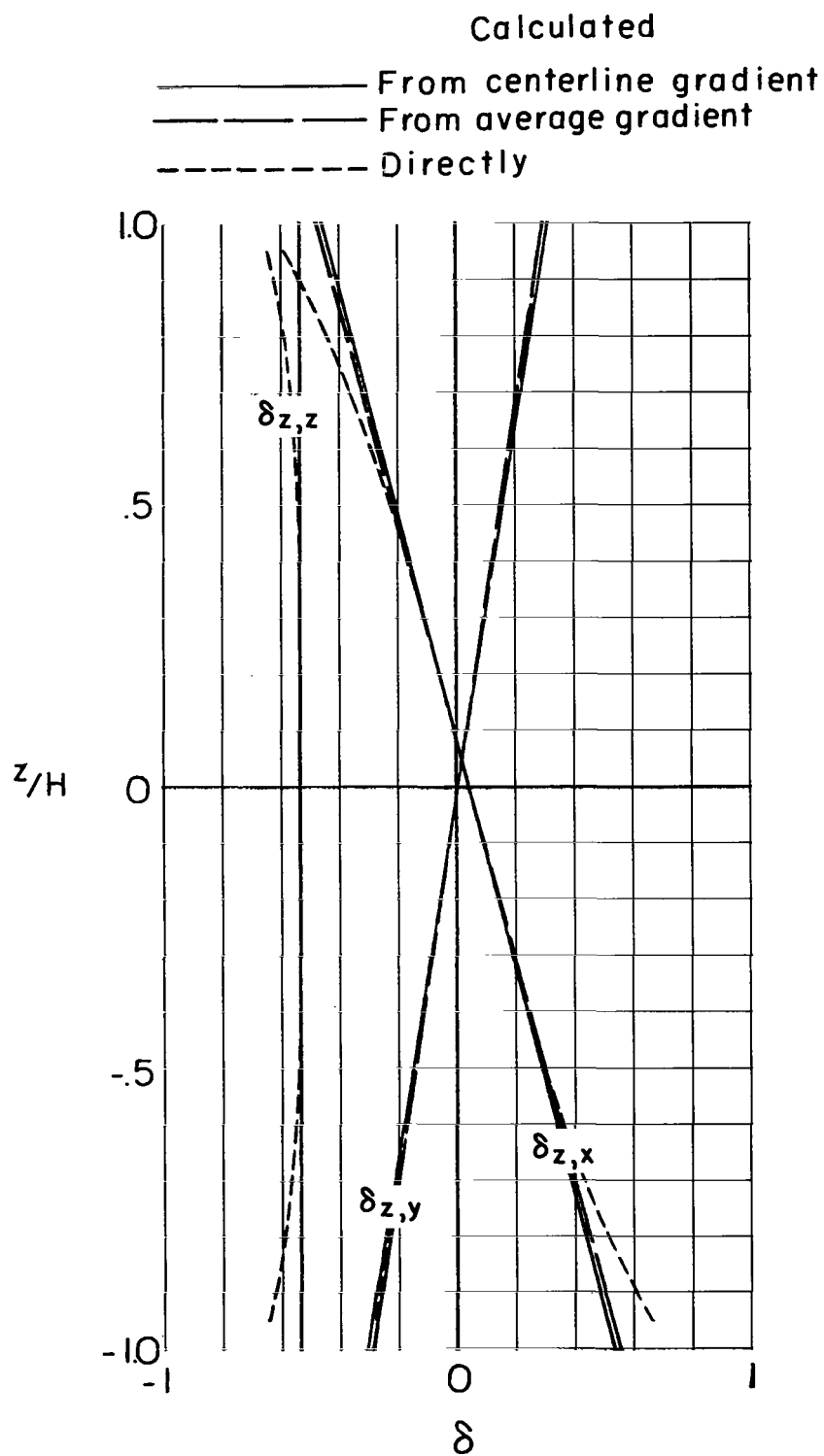
(a) Caused by forces in the X-direction.

Figure 56.- Distribution of interference factors over the vertical axis of the tunnel for a uniformly loaded unswept wing centrally located and spanning half the width of a closed rectangular tunnel having a width-height ratio of 1.5. $\chi_H = 60^\circ$; $\chi_V = 90^\circ$.



(b) Caused by forces in the Y-direction.

Figure 56.- Continued.



(c) Caused by forces in the Z-direction.

Figure 56.- Concluded.

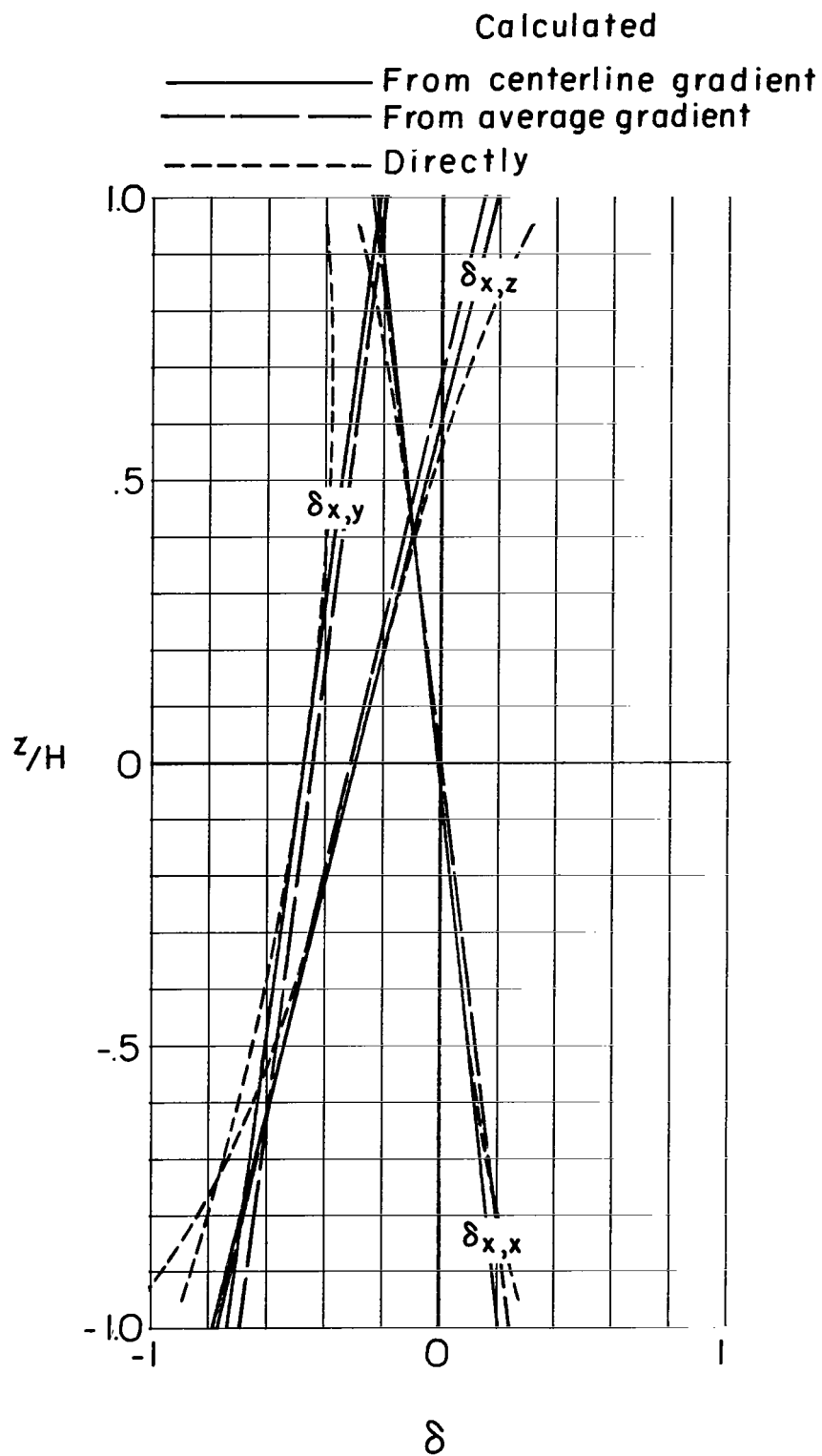
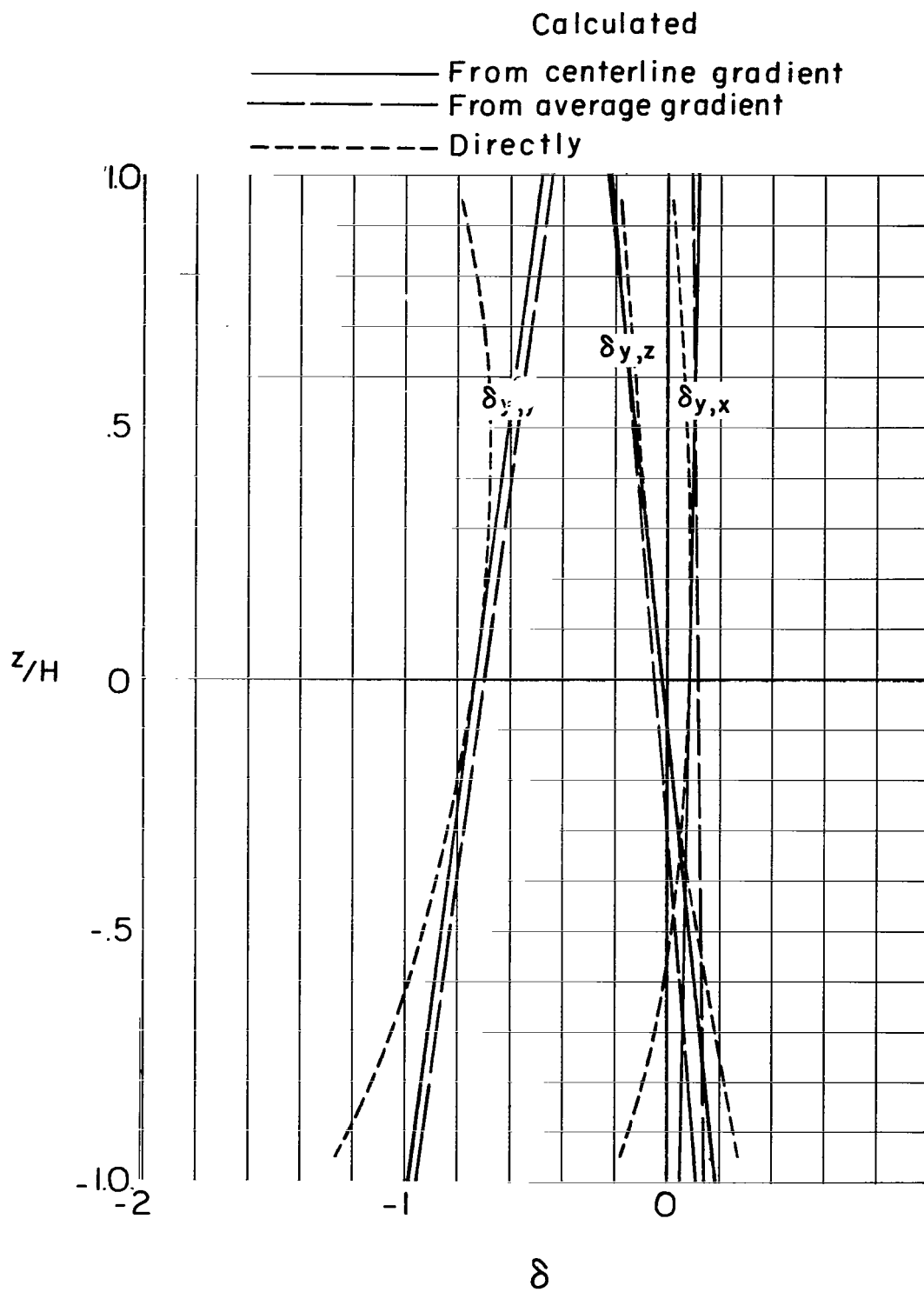
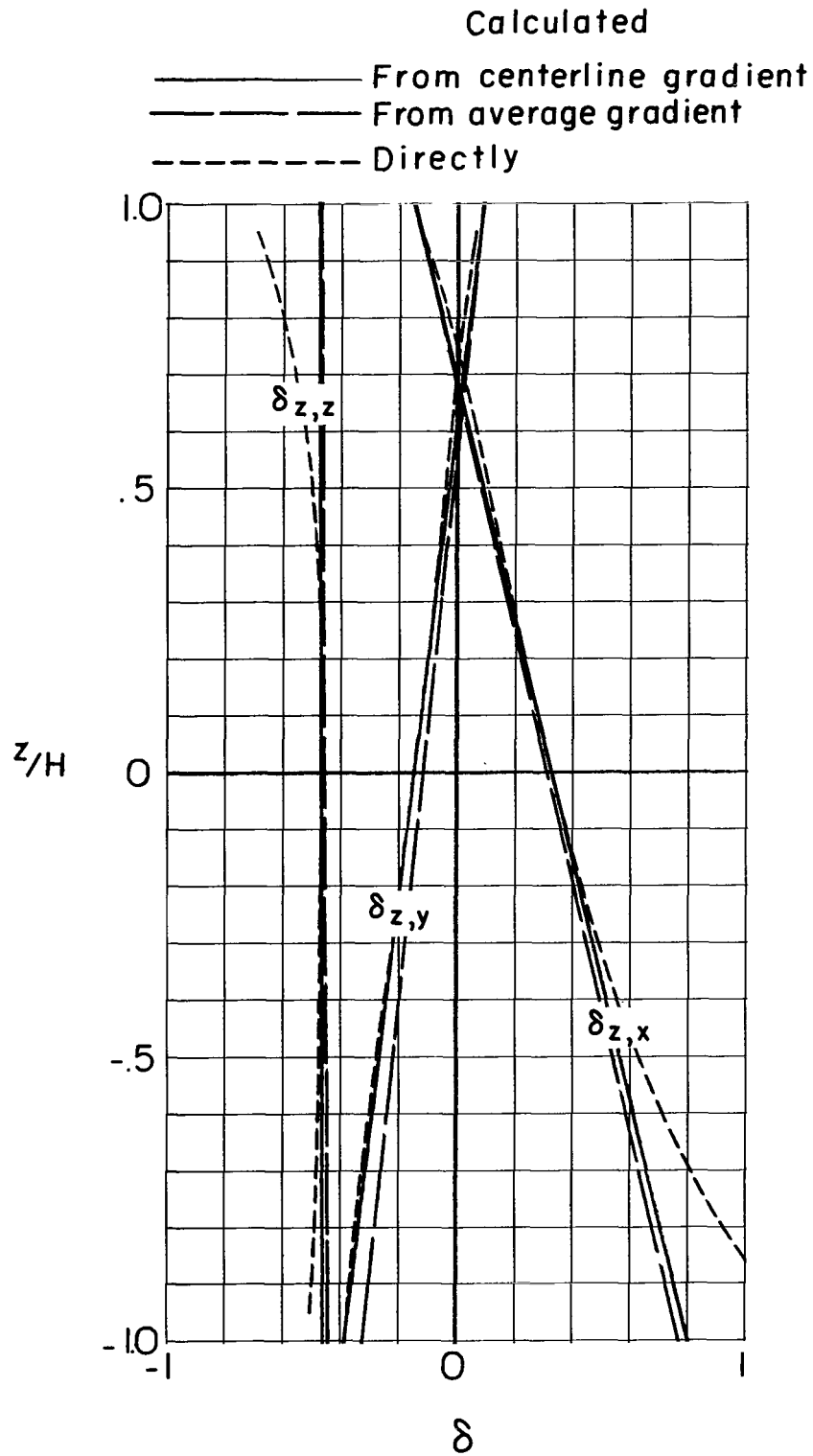


Figure 57.- Distribution of interference factors over the vertical axis of the tunnel for a uniformly loaded unswept wing centrally located and spanning half the width of a closed rectangular tunnel having a width-height ratio of 1.5. $X_H = 60^\circ$; $X_V = 60^\circ$.



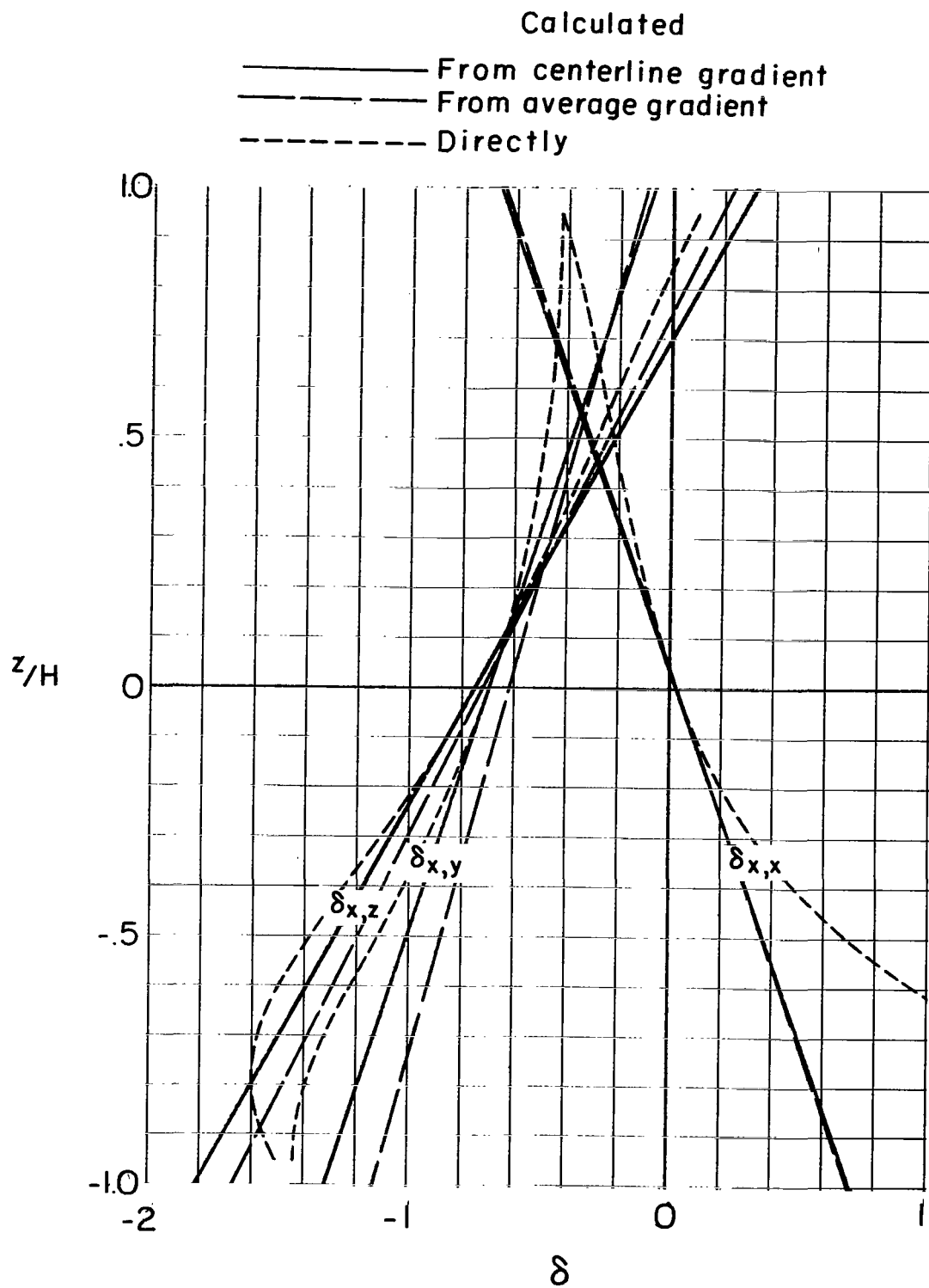
(b) Caused by forces in the Y-direction.

Figure 57.- Continued.



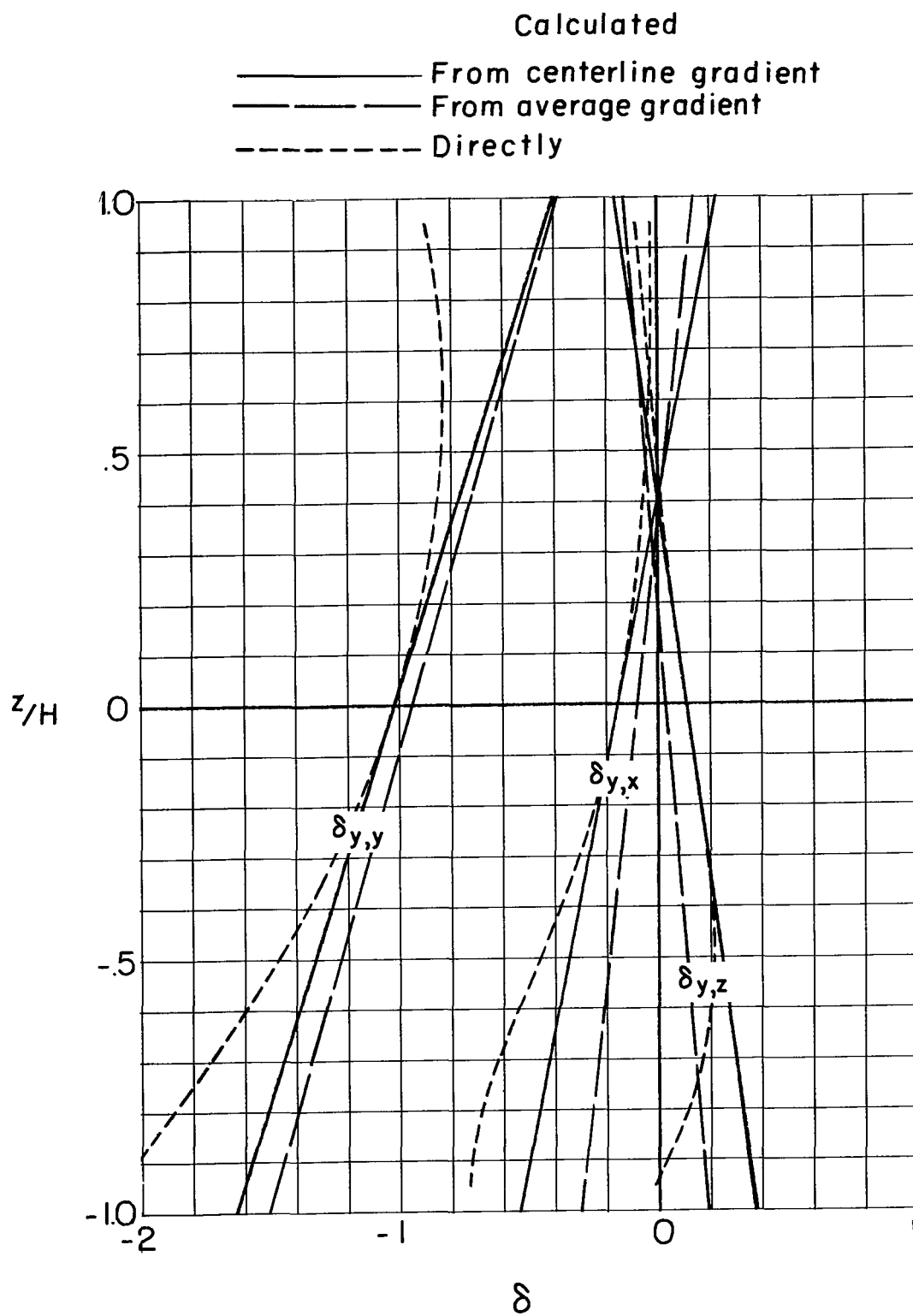
(c) Caused by forces in the Z-direction.

Figure 57.- Concluded.



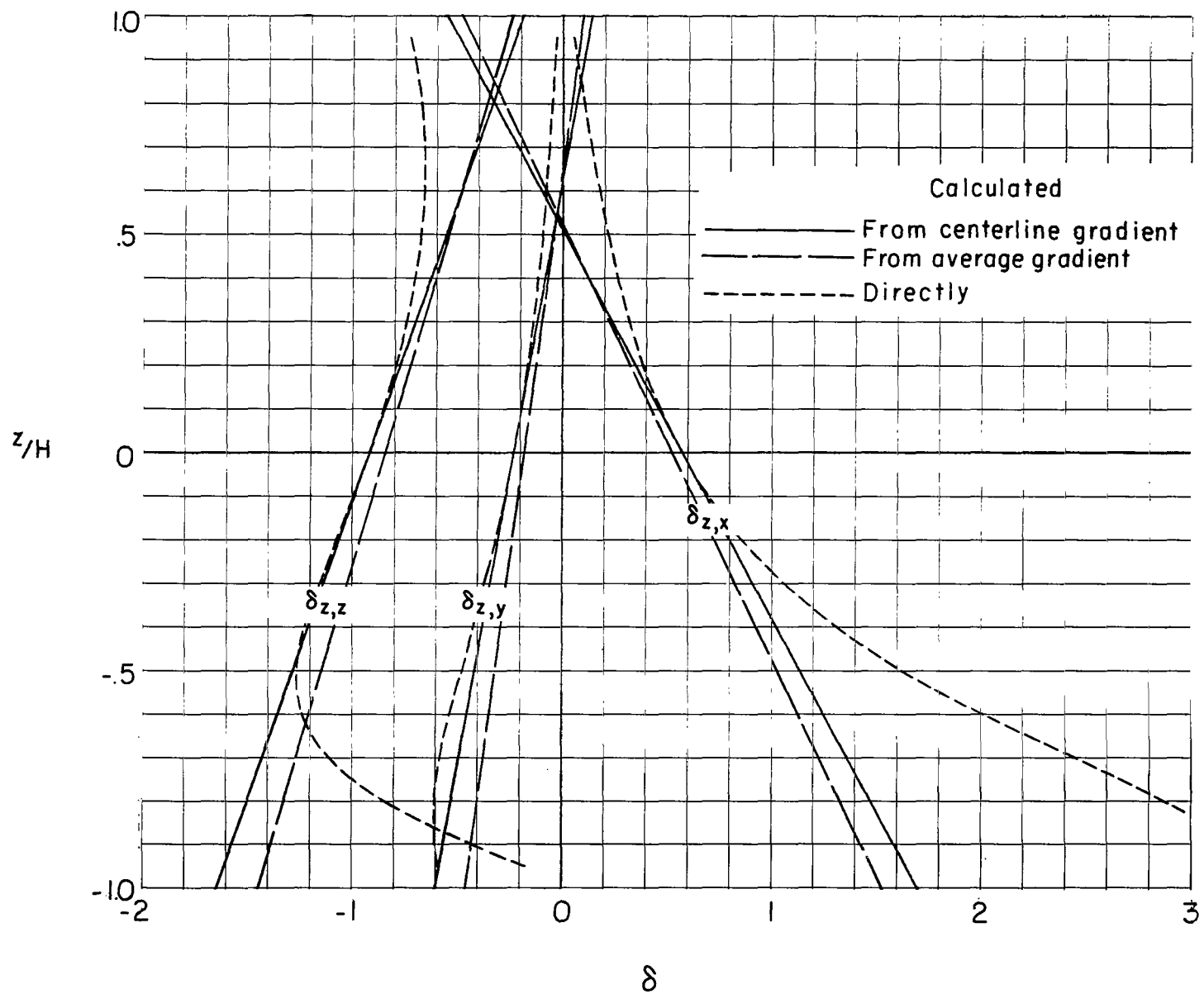
(a) Caused by forces in the X-direction.

Figure 58.- Distribution of interference factors over the vertical axis of the tunnel for a uniformly loaded unswept wing centrally located and spanning half the width of a closed rectangular tunnel having a width-height ratio of 1.5. $\chi_H = 60^\circ$; $\chi_V = 30^\circ$.



(b) Caused by forces in the Y-direction.

Figure 58.- Continued.



(c) Caused by forces in the Z-direction.

Figure 58.- Concluded.

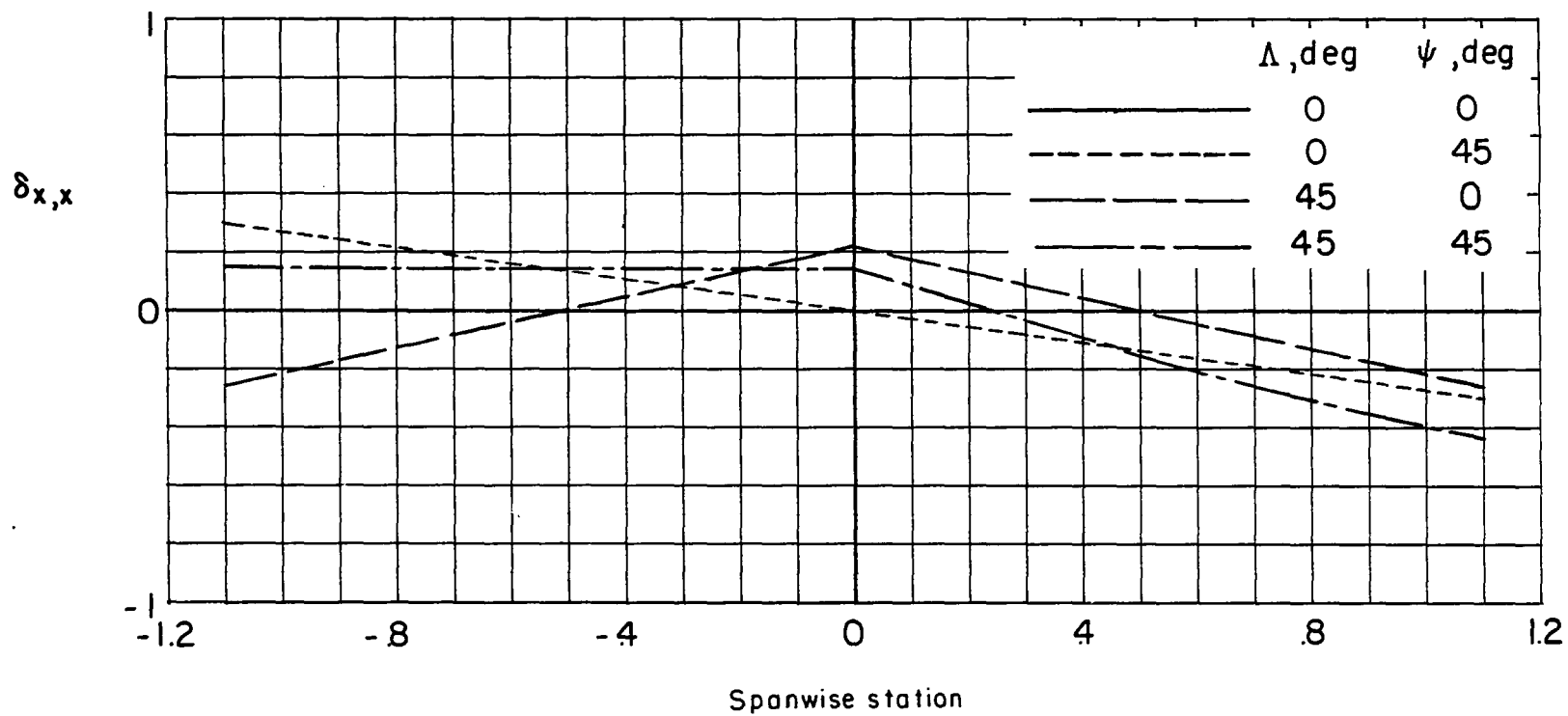
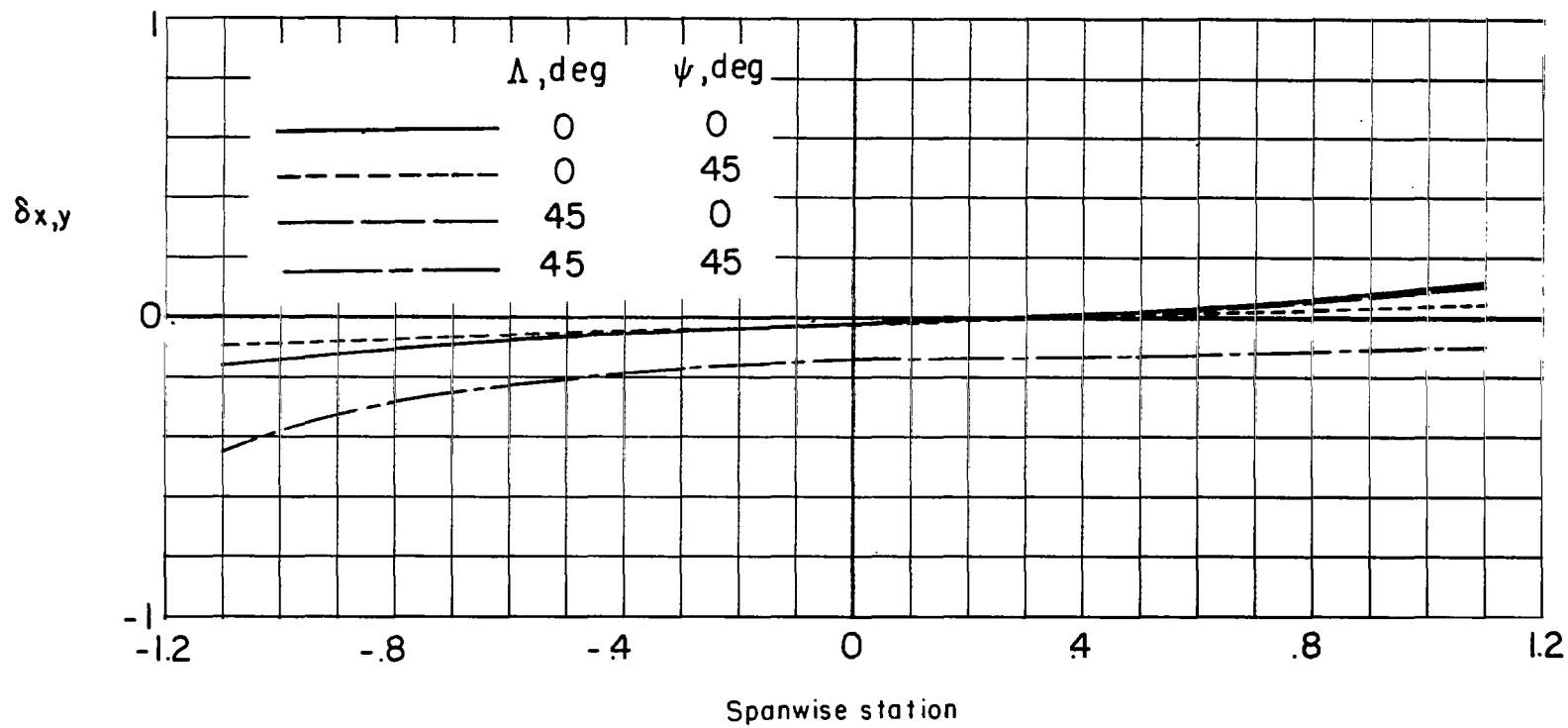
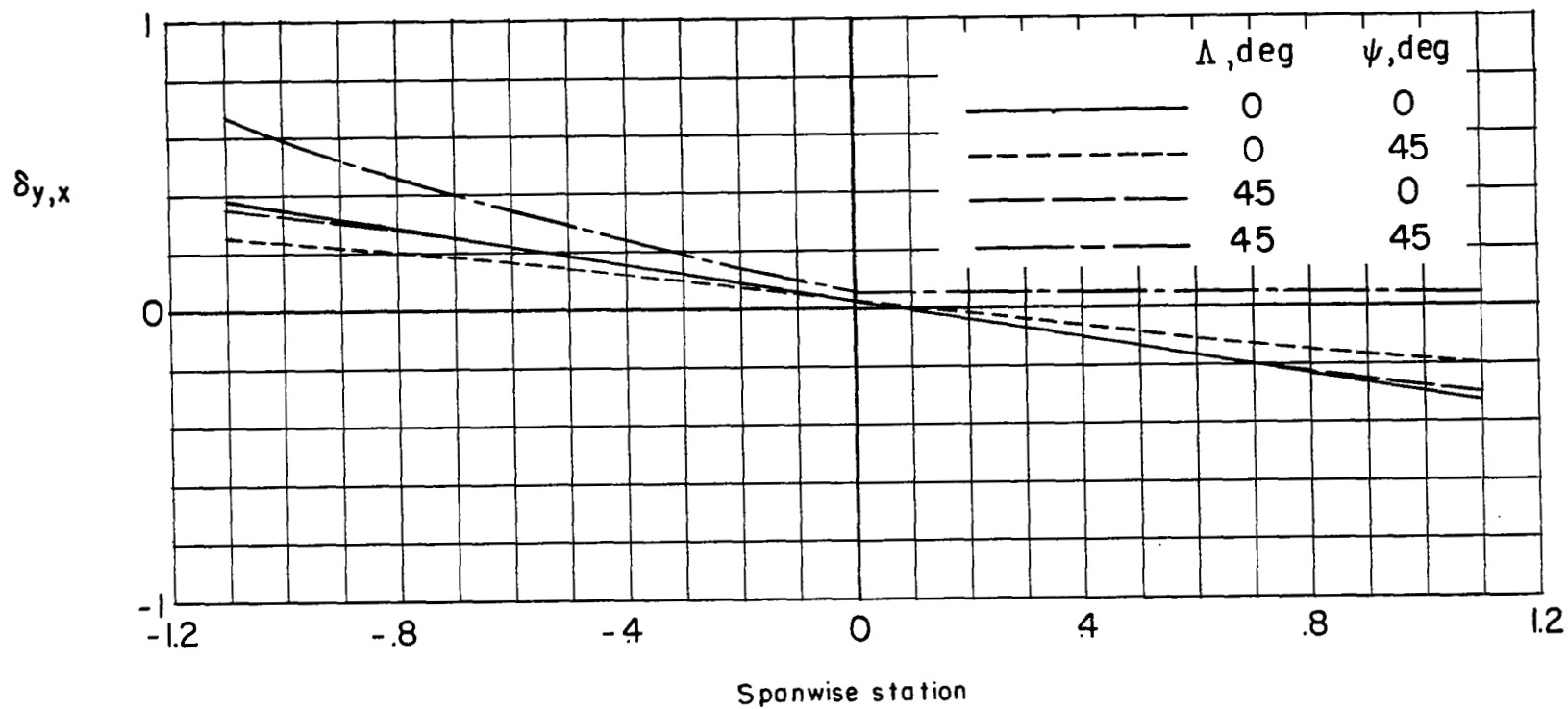
(a) $\delta_{x,x}$.

Figure 59.- Effect of sweep and yaw on the distribution of interference factors over the span of wings in a tunnel having a width-height ratio of 1.5. $\sigma = 0.5$; $\chi_H = 90^\circ$; $\chi_V = 90^\circ$. (Note that for these skew angles $\delta_{x,z} = \delta_{y,z} = \delta_{z,x} = \delta_{z,y} = 0$.) Apex of lifting line is fixed at center of the tunnel.



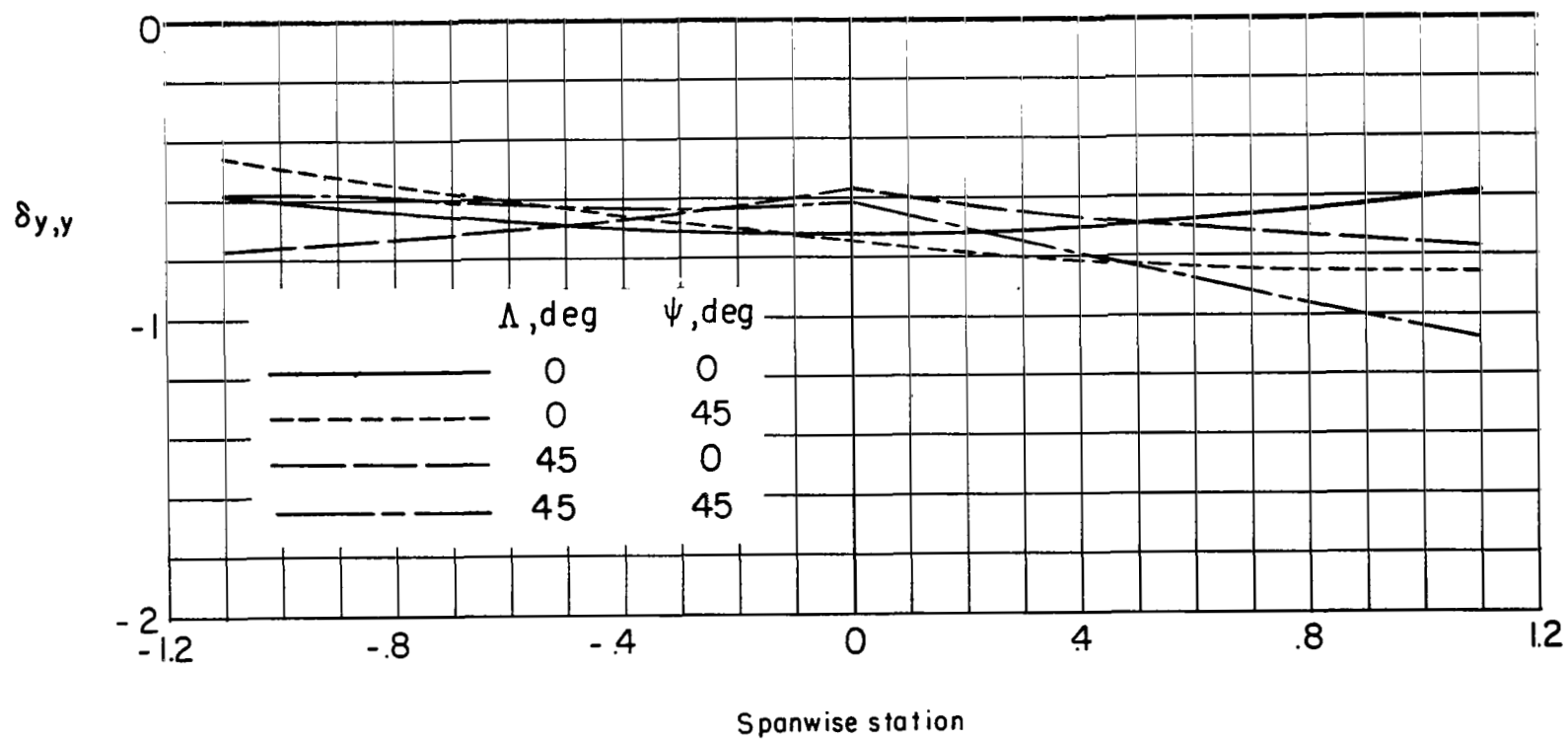
(b) $\delta_{x,y}$.

Figure 59.- Continued.



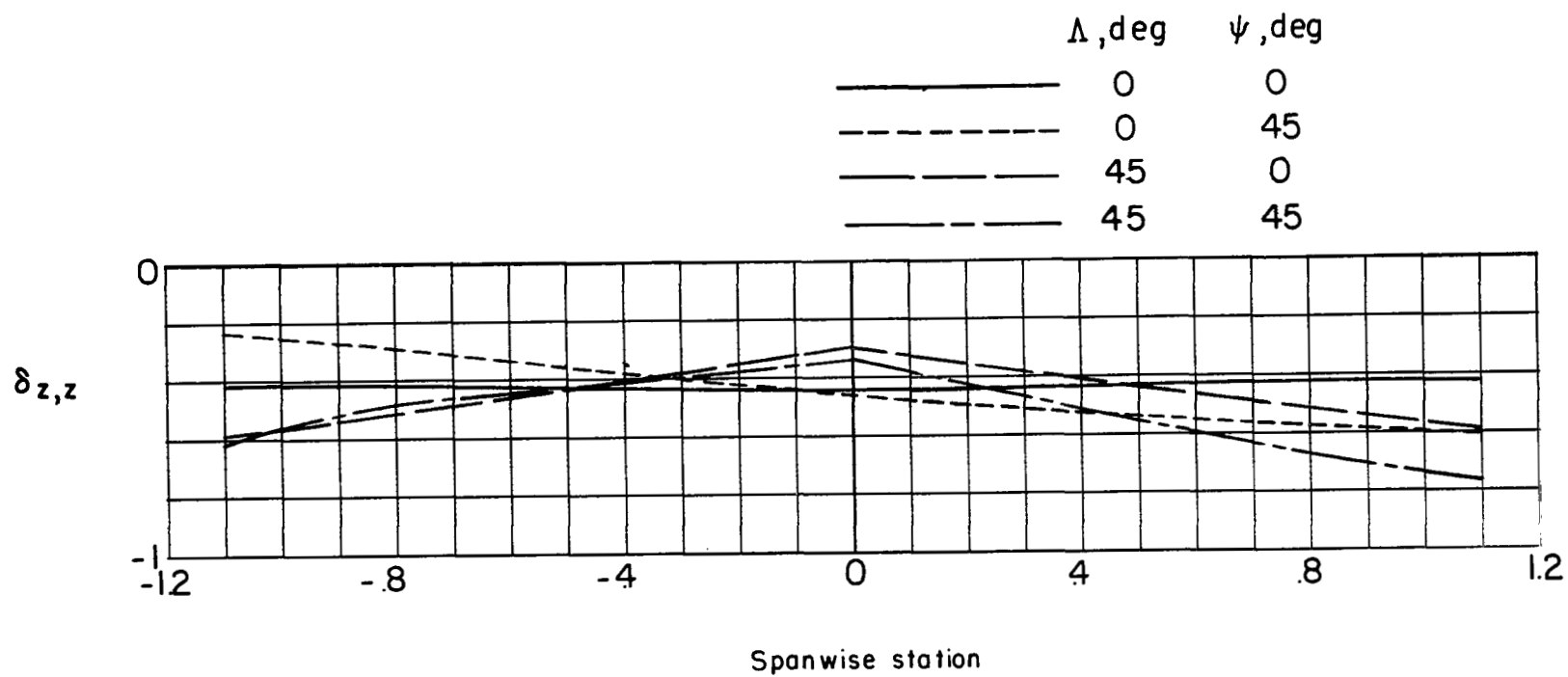
(c) $\delta_{y,x}$.

Figure 59.- Continued.



(d) $\delta_{y,y}$.

Figure 59.- Continued.



(e) $\delta_{z,z}$.

Figure 59.- Concluded.

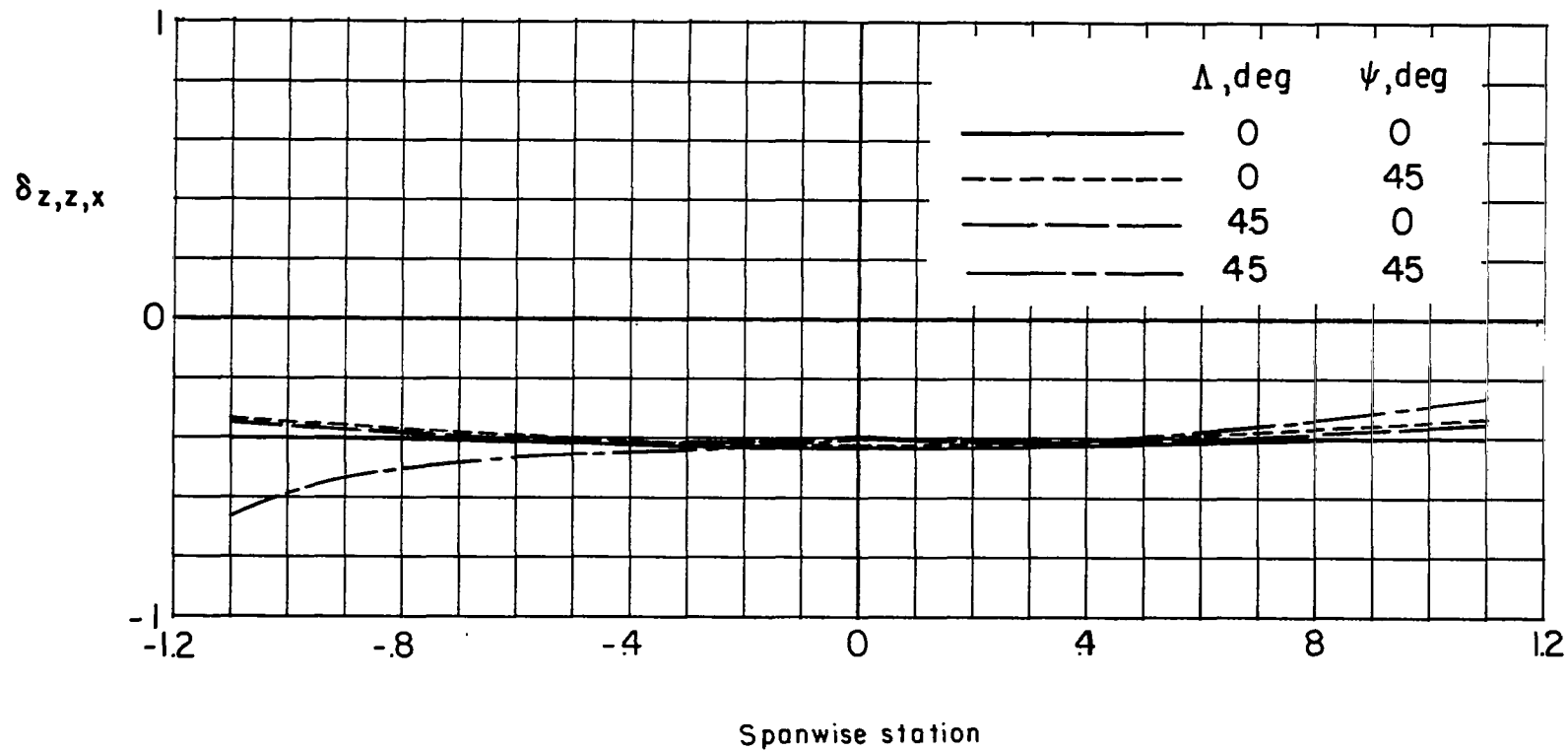


Figure 60.- Effect of sweep and yaw on the distribution of $\delta_{z,z,x}$ over the span of wings in a tunnel having a width-height ratio of 1.5. $\sigma = 0.5$; $X_H = 90^\circ$; $X_V = 90^\circ$. (Note that for these skew angles $\delta_{x,z,x}$ and $\delta_{y,z,x} = 0$.) Apex of lifting line is fixed at the center of the tunnel.

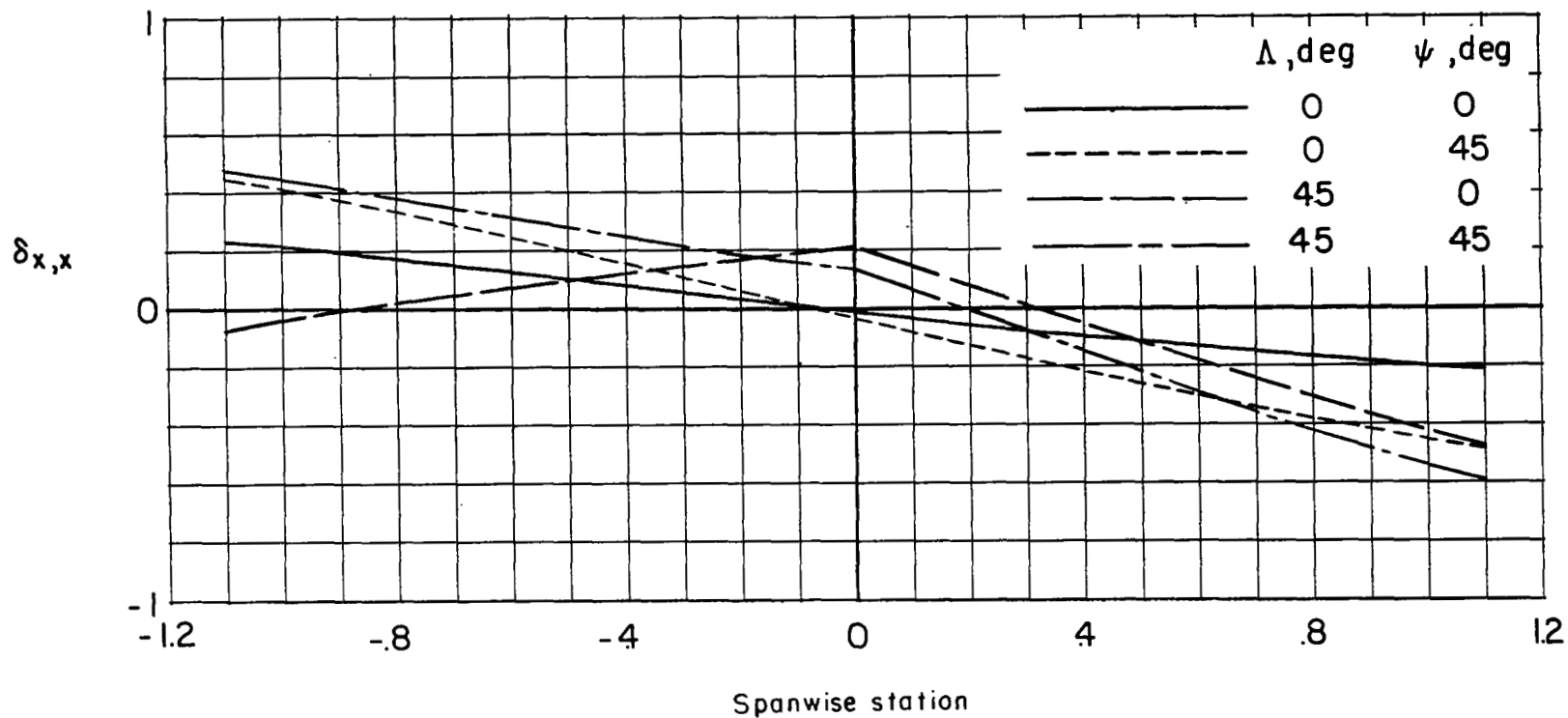
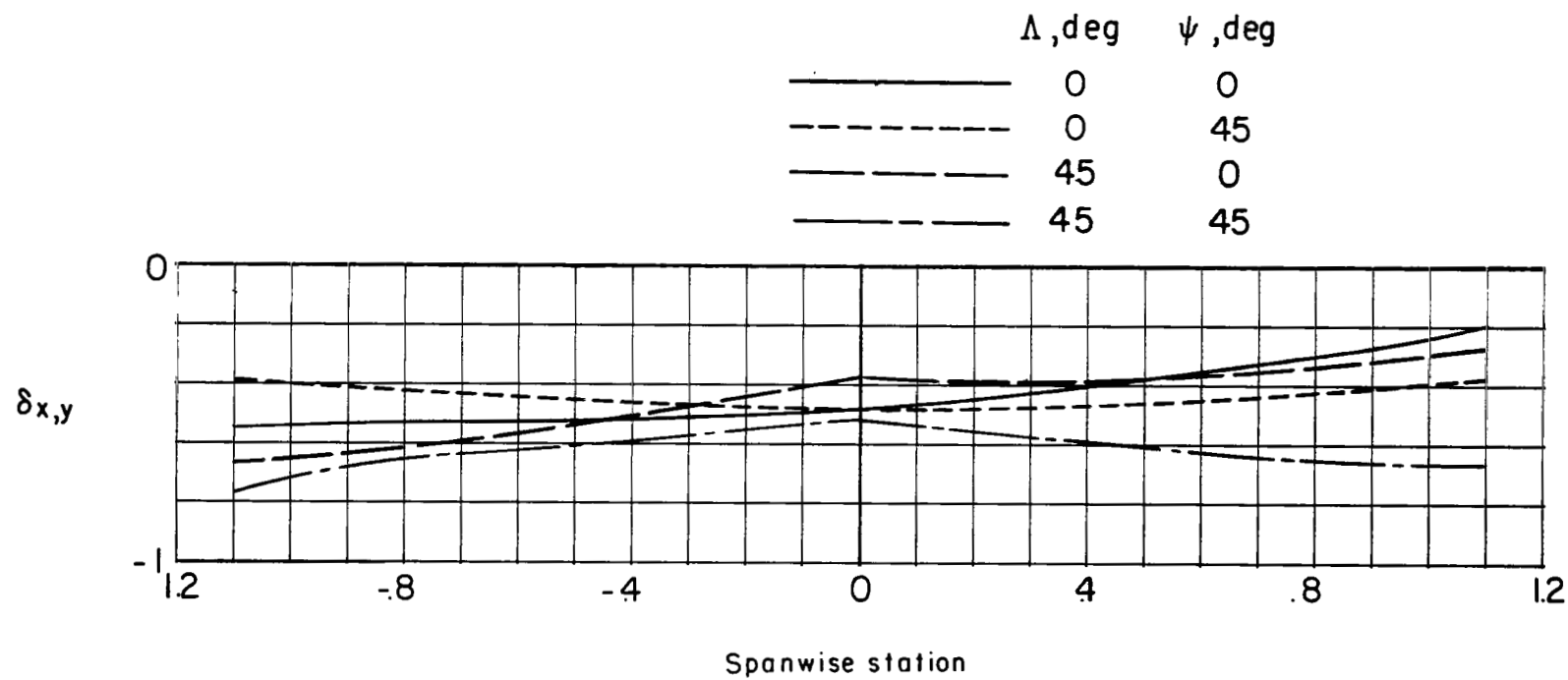
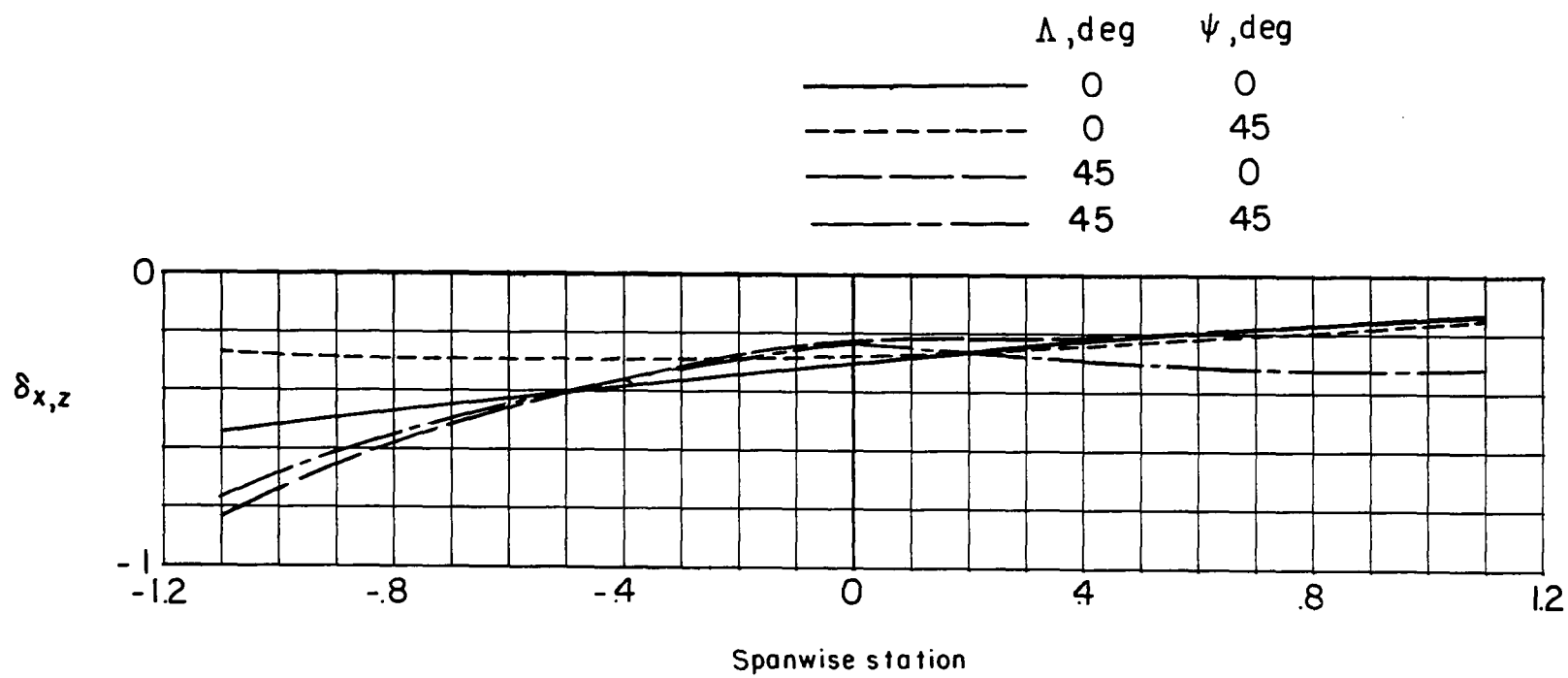
(a) $\delta_{x,x}$.

Figure 61.- Effect of sweep and yaw on the distribution of interference factors over the span of wings in a tunnel having a width-height ratio of 1.5.
 $\sigma = 0.5$; $X_H = 60^\circ$; $X_V = 60^\circ$. Apex of lifting line is fixed at center of tunnel.



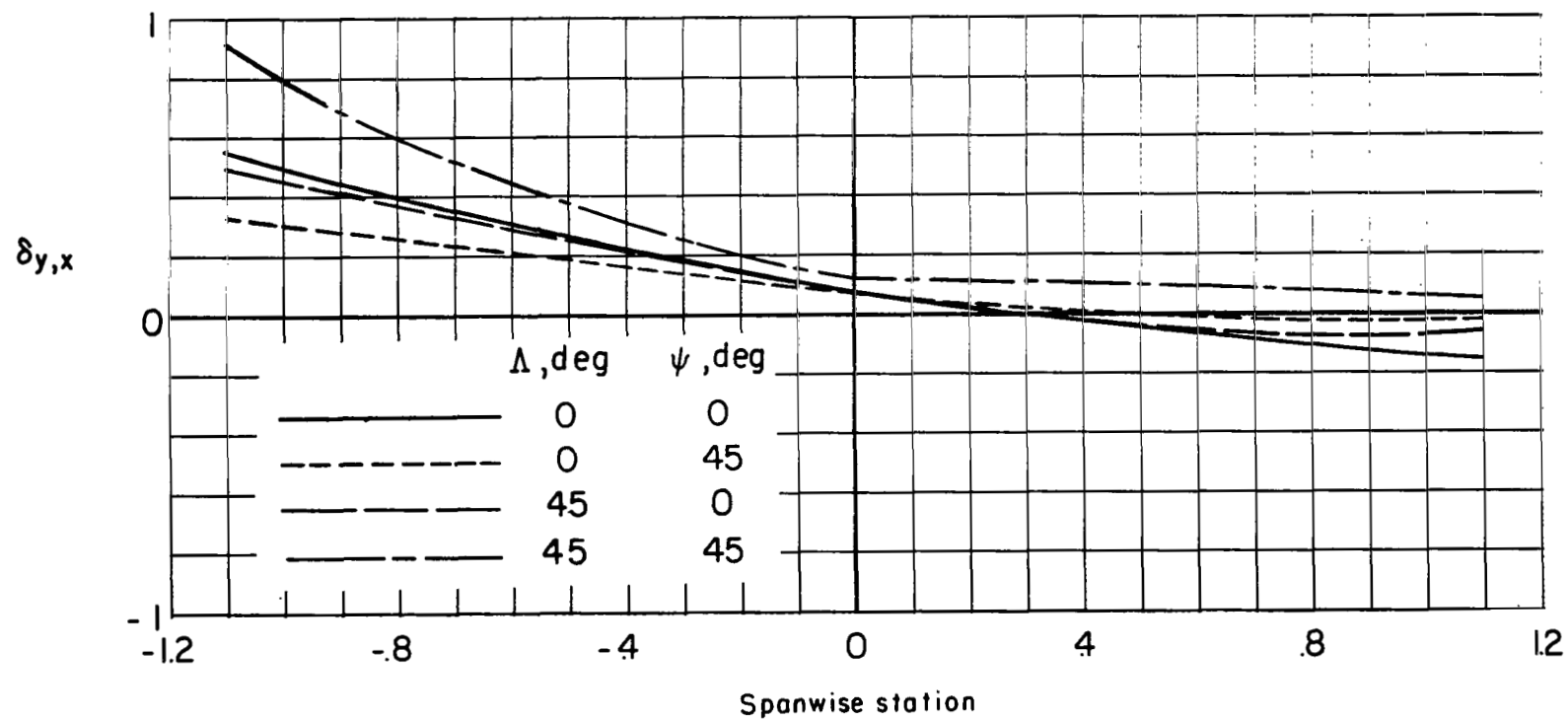
(b) $\delta_{x,y}$.

Figure 61.- Continued.



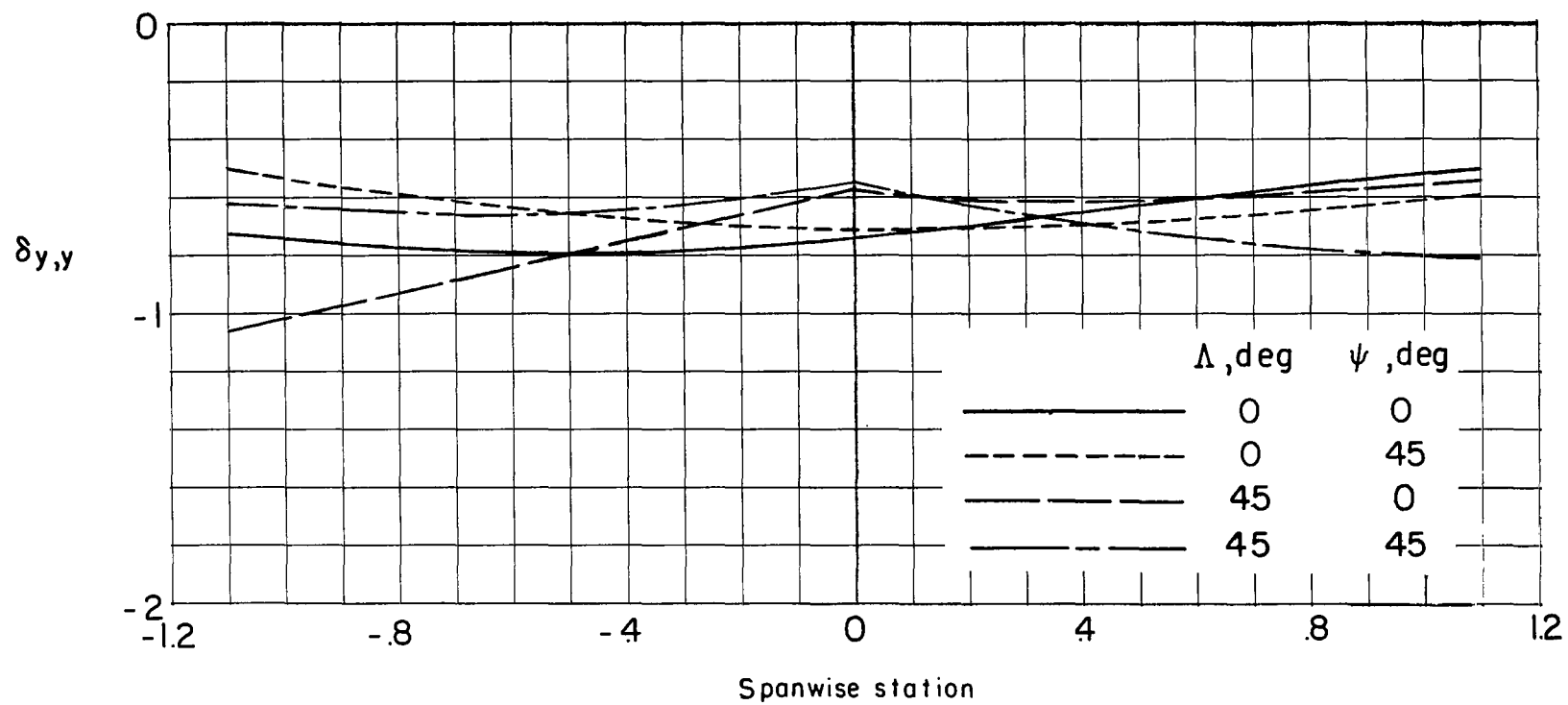
(c) $\delta_{x,z}$.

Figure 61.- Continued.



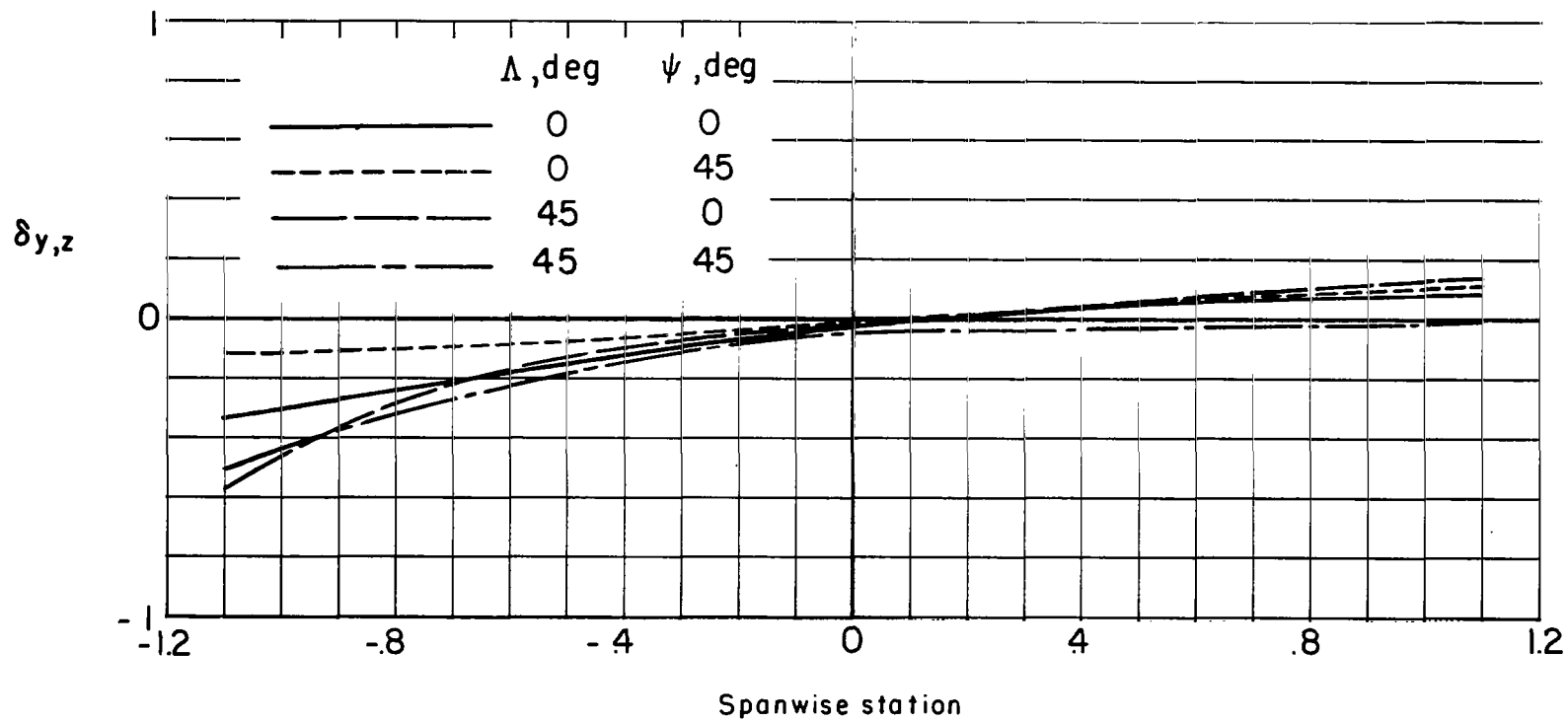
(d) $\delta_{y,x}$.

Figure 61.- Continued.



(e) $\delta_{y,y}$.

Figure 61.- Continued.



(f) $\delta_{y,z}$.

Figure 61.- Continued.

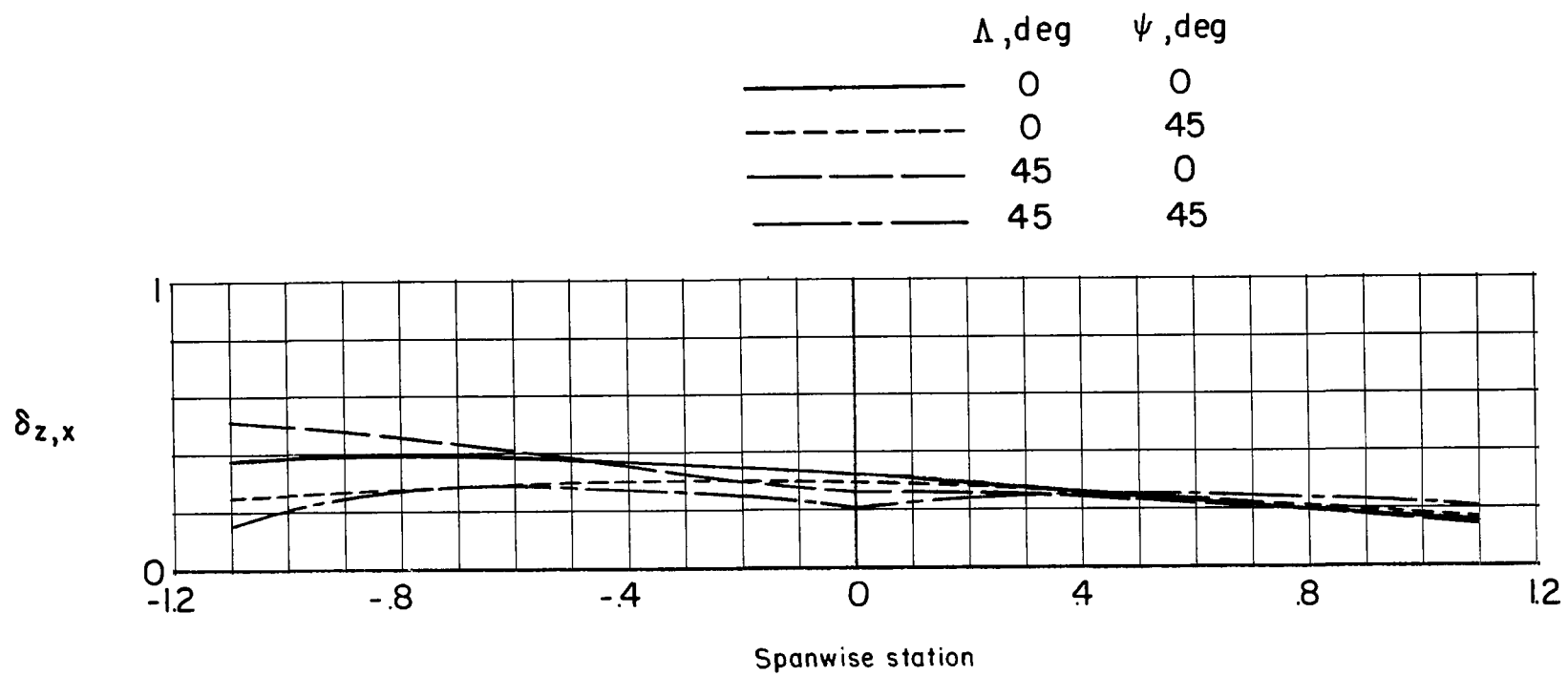
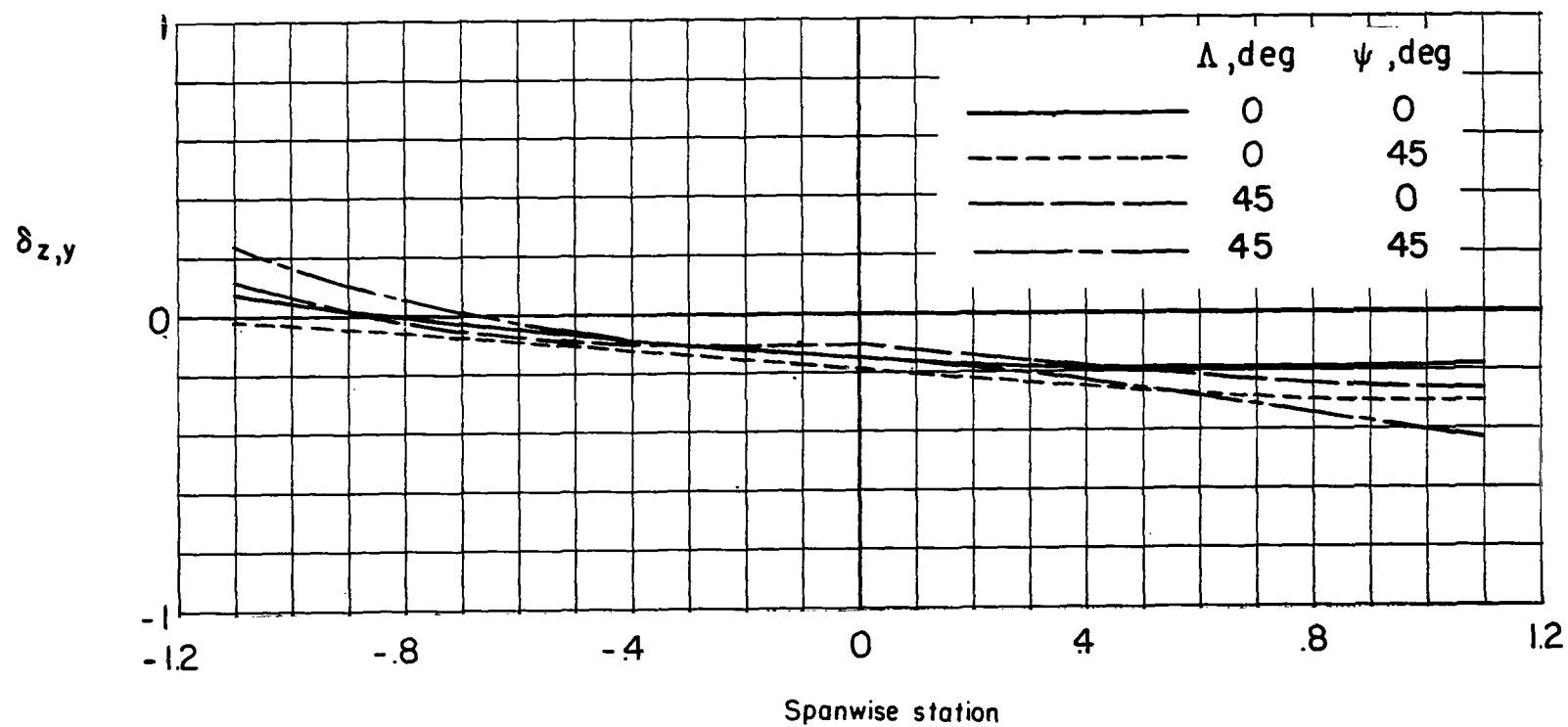
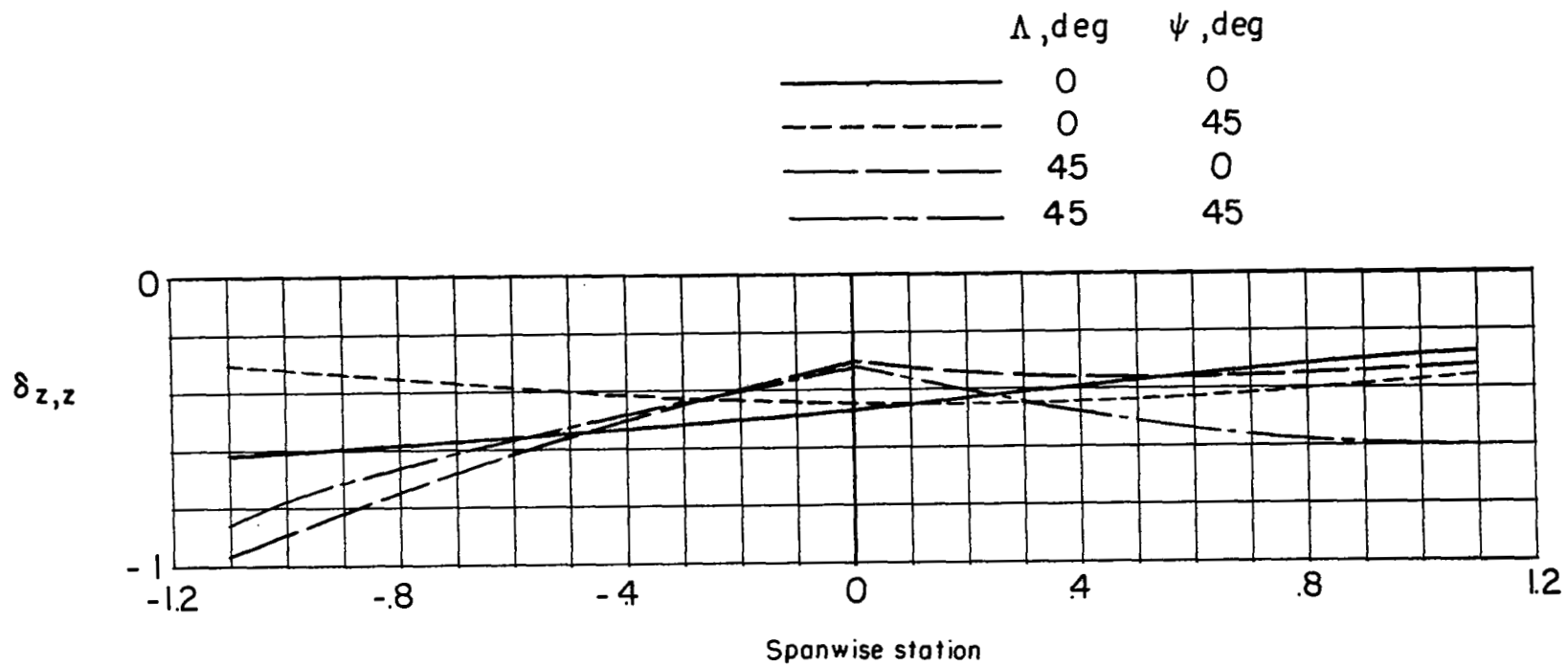
(g) $\delta_{z,x}$.

Figure 61.- Continued.



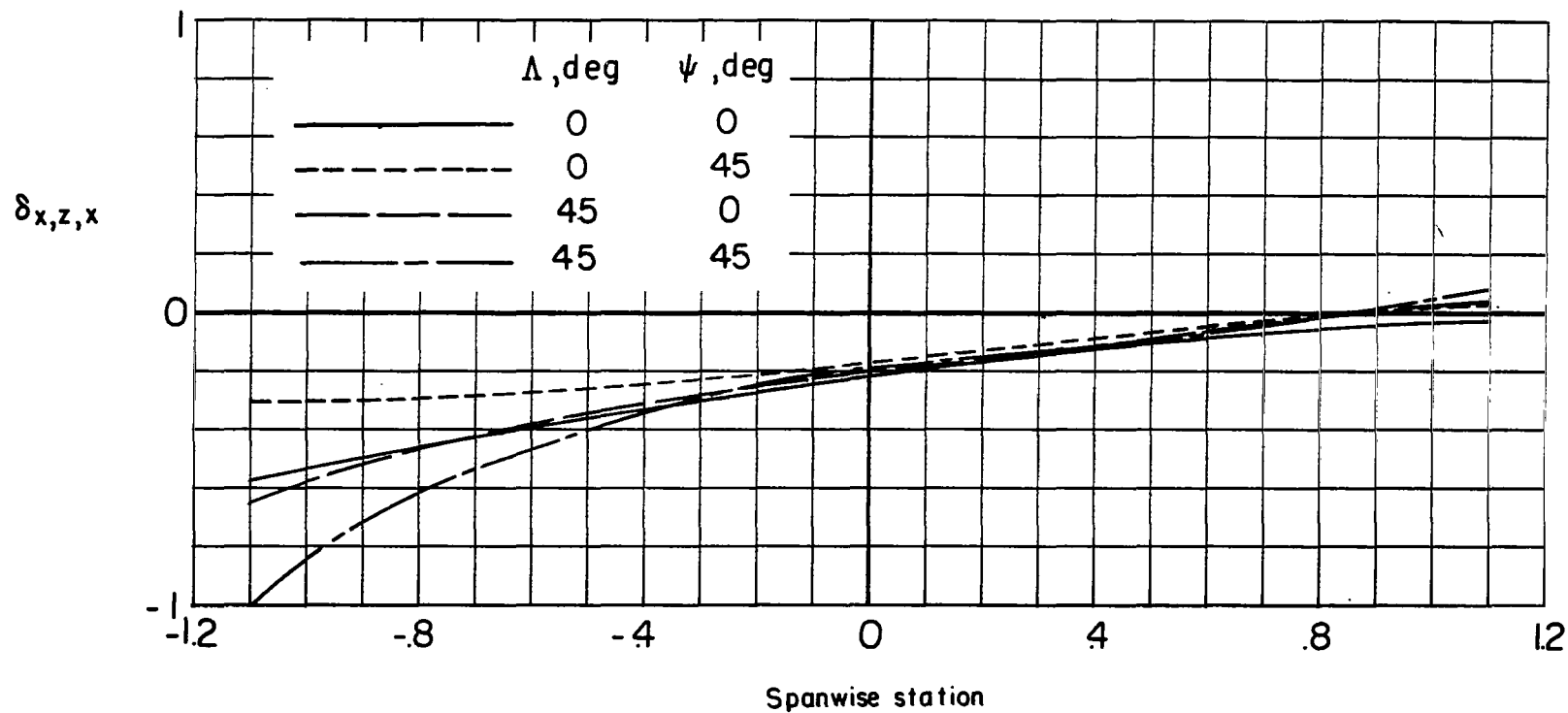
(h) $\delta_{z,y}$.

Figure 61.- Continued.



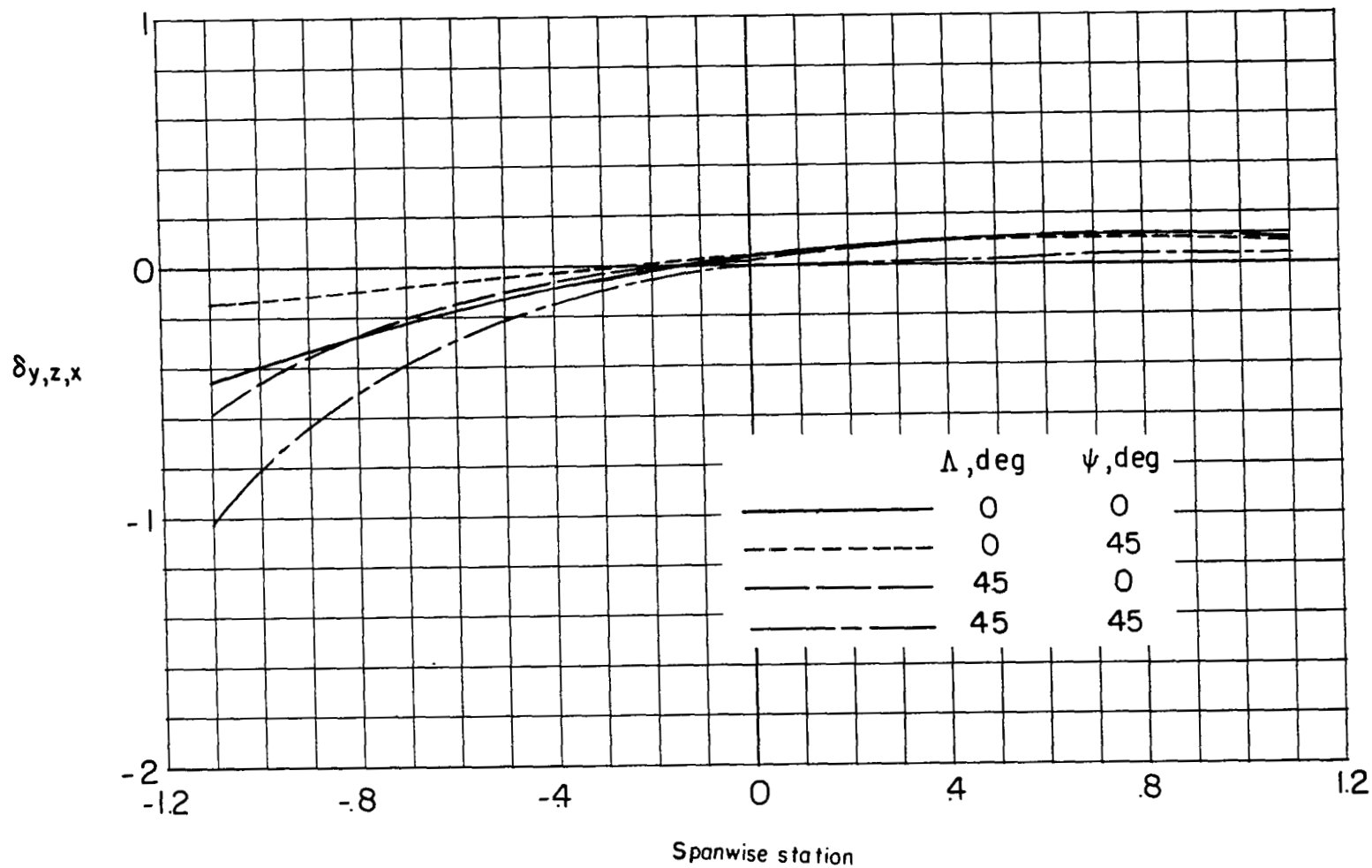
(i) $\delta_{z,z}$.

Figure 61.- Concluded.



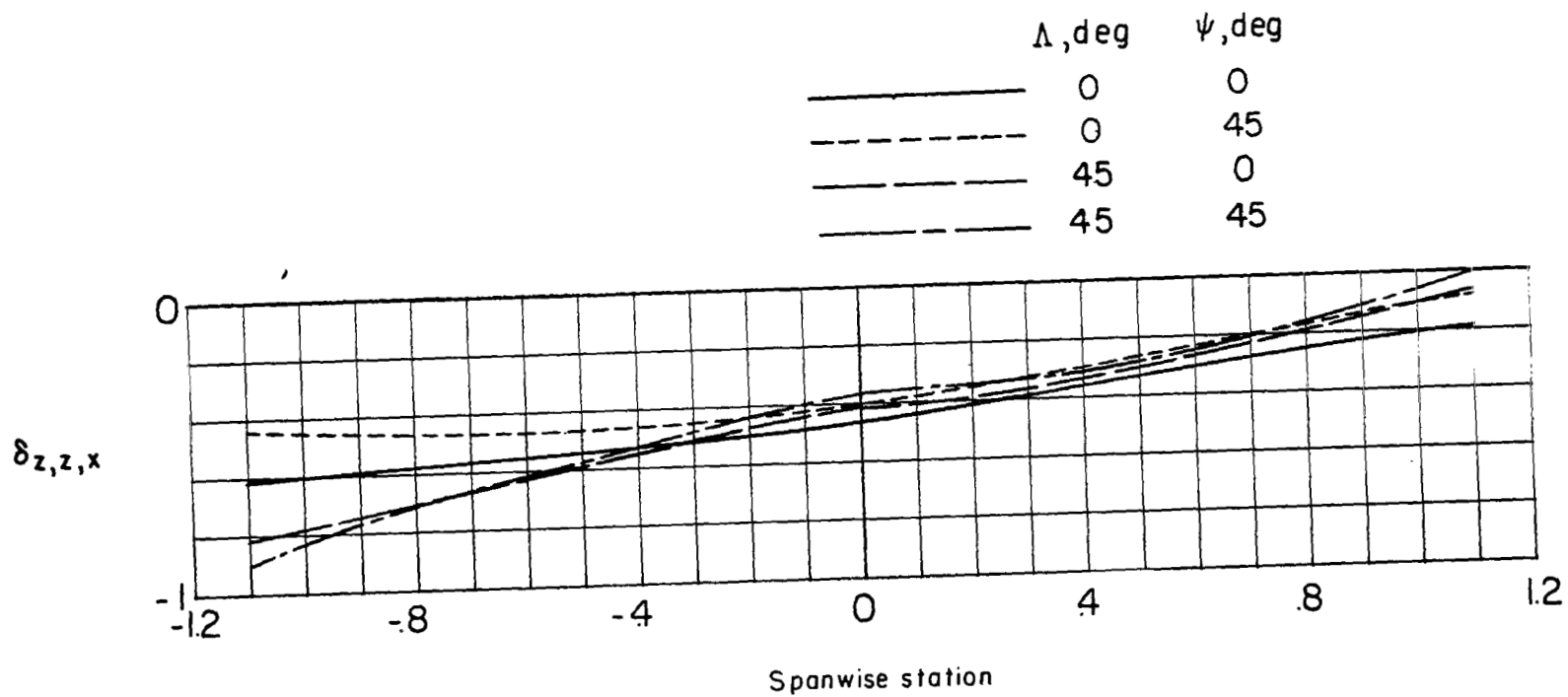
(a) $\delta_{x,z,x}$.

Figure 62.- Effect of sweep and yaw on the interference factor gradients related to the longitudinal distribution of vertical interference velocity. Distribution over the span of wings in a wind tunnel having a width-height ratio of 1.5. $\sigma = 0.5$; $\chi_H = 60^\circ$; $\chi_V = 60^\circ$. Apex of lifting line is fixed at center of tunnel.



(b) $\delta_{y,z,x}$.

Figure 62.- Continued.



(c) $\delta_{z,z,x}$.

Figure 62.- Concluded.